

School of Population Health

Elucidating and Utilising the Mechanisms Used by *Pseudomonas aeruginosa* to Develop Resistance to Bacteriophages to Aid Therapeutic Formulation and Application in Cystic Fibrosis

Andrew Vaitekenas

0000-0002-9935-5092



**This thesis is presented for the Degree of
Doctor of Philosophy of
Curtin University**

December 2023

Declaration

To the best of my knowledge and belief this thesis contains no material previously published by any other person except where due acknowledgment has been made.

This thesis contains no material which has been accepted for the award of any other degree or diploma in any university.

The research presented and reported in this thesis was conducted in accordance with the National Health and Medical Research Council National Statement on Ethical Conduct in Human Research (2007) – updated March 2014. The proposed research study received human research ethics approval from the Curtin University Human Research Ethics Committee (EC00262), Approval Number #2019-0086.

Signature: 

Date:15/12/2023.....

Copyright Statement

I have obtained permission from the copyright owners to use any third-party copyright material reproduced in the thesis (e.g. questionnaires, artwork, unpublished letters), or to use any of my own published work (e.g. journal articles) in which the copyright is held by another party (e.g. publisher, co-author).

Abstract

Antimicrobial resistance (AMR) is one of the greatest threats to human healthcare and caused almost 5 million deaths globally in 2019 [1]. Alarmingly, this figure is expected to rise to 10 million per annum by 2050, surpassing all other diseases [2]. Furthermore, AMR pathogens place a significant burden on the healthcare system and significantly impact the global economy. *Pseudomonas aeruginosa* is amongst the most deadly and costly AMR pathogens. It frequently causes hospital acquired pneumonia, burn wound, bloodstream, and pulmonary infections. Those with chronic lung diseases including Cystic Fibrosis (CF) are more at risk of infections with AMR pathogens. CF is a life-shortening genetic disease where frequent and life-long *P. aeruginosa* airway infections develop high levels of AMR and eventually cause respiratory failure. With very few antibiotics being developed to treat these AMR infections, there is now an urgent need for novel antimicrobials to be developed. One of the most promising alternatives to antibiotics utilise bacteriophages (phages). These are viruses that infect and kill bacteria and phage therapy has been demonstrated to be effective against AMR infections including those caused by *P. aeruginosa*. However, *P. aeruginosa* can also become resistant to phage therapy and how this occurs in CF clinical isolates is poorly studied which is a precursor to identify formulation strategies to prevent resistance emerging. The work in this thesis tested the hypothesis that identified phage cocktails and/or combination with antibiotics would suppress phage-resistance against planktonically growing *P. aeruginosa* compared to single phage preparations. Furthermore, identified effective formulations would not be inflammatory or cytotoxic to the host airway. Phages were initially isolated from wastewater and characterised and top phages were identified. These phages were then used to treat CF *P. aeruginosa* isolates, resistance evolution monitored, and phage resistant bacteria isolated. Mechanisms of phage resistance were evaluated, and antibiotic susceptibility determined to identify potential combinations. Finally, the ability of combinations to suppress phage resistance and elicit an inflammatory response from an airway primary epithelial cell model was measured.

Initial isolation and characterisation led to the selection of 20 phages that had the broadest host range against 94 diverse *P. aeruginosa* isolates. These phages all exhibited the myovirus morphotype and did not contain any temperate phage, bacterial AMR or virulence genes. Genomic and phylogenetic analyses allowed the selection of four phages

from distinct clades. Three of these (Kara-mokiny 8, 13 and 16) were from the *Pbunavirus* genus, bound the core of the LPS as their receptor, were stable over long-term storage, not degraded by a range of pHs and had burst sizes >130 phages per bacterium. The fourth phage was a *Phikzvirus*, used flagella as its binding receptor, was stable over long-term storage, stable at pHs > 3 and had a burst size of 59 phages per bacterium. Collectively, these results illustrated that phages could be successfully isolated that exhibited characteristics amenable for therapeutic application.

Next, three distinct CF isolates of *P. aeruginosa* (of varying AMR) were treated with phages at a range of multiplicities of infection (MOI) 10-0.01. Results generated showed variation according to phage-bacterial isolate pairing, and despite phage effectiveness bacterial resistance was observed and colonies isolated. In addition, frequency of resistance was mainly affected by bacterial isolate and the phage that was used. Kara-mokiny 16 treatment elicited the least amount of resistance. Those from phage treatments at MOI of 10 and 0.01 were then sequenced and analysed bioinformatically. Phage resistance was found to be due to alterations in phage receptors and not CRISPR-cas systems. Resistance did not seem to be affected by MOI and was similar between phages that used the same receptor. Despite there being some mutated genes common between the *P. aeruginosa* isolates, the bacterial genomic background influenced how resistance evolved. Furthermore, antibiotic resistance of isolated phage-resistant *P. aeruginosa* was halved to tobramycin. When investigated in more depth it was observed that the MIC of tobramycin was halved after Kara-mokiny 16 and 13 treatments. Collectively, findings supported the initial hypothesis that Kara-mokiny 16 and tobramycin in combination could be an effective strategy to prevent phage resistance.

To investigate how Kara-mokiny 16 and tobramycin should be paired, a synergism checkerboard assay was performed, and the fractional inhibitory concentration index calculated. Whilst no synergism was observed, an additive relationship was found between 10^6 or 10^7 PFU/mL with 2 μ g/mL of tobramycin. These were subsequently tested for their ability to prevent phage resistance and results were dependant on the *P. aeruginosa* isolate. Finally, primary airway epithelial cells were exposed to Kara-mokiny 16 (10^6 PFU/mL), tobramycin (2 μ g/mL) alone or combined as well as heat killed *P. aeruginosa* PAO1 and effects assessed included gross morphological changes, cell death (LDH), or inflammation (via IL-6 and IL-8 production). Results generated show that Kara-mokiny 16 and tobramycin alone/combined did not induce any morphological,

cytotoxicity, or inflammatory (IL-6 or IL-8) changes. Collectively, results supported the second hypothesis that phage therapy is safe and would not cause any harmful disruption to the airway environment.

Overall, work conducted in this thesis identified and characterised many phages that have therapeutic potential. Additionally, findings have broadened our understanding of how phage resistance develops in CF clinical isolates of *P. aeruginosa* and identified combinations that may suppress it evolving.

Table of Contents

Declaration	ii
Copyright Statement	iii
Abstract	iv
Table of Contents	vii
Declaration for Co-Authored Publications.....	xvi
List of Figures.....	xviii
List of Tables	xx
List of Abbreviations	xxii
Publications	xxv
Conference Presentations.....	xxvi
Awards	1
Acknowledgements	2
1. Literature Review	4
1.1 Introduction	4
1.2 The WHO Critical Priority Pathogens	7
1.3 <i>Pseudomonas aeruginosa</i> Antibiotic Resistance and Virulence	7
1.4 Cystic Fibrosis.....	9
1.4.1 CF Lung Disease and Infections	10
1.4.1.1 CF Viral Airway Infections.....	10
1.4.1.2 CF Fungal Airway Infections.....	11
1.4.1.3 CF Bacterial Airway Infections	11
1.4.1.3.1 <i>P. aeruginosa</i> Infections in CF.....	11
1.4.1.3.2 Anti- <i>P. aeruginosa</i> Antimicrobial Therapy in CF.....	12
1.4.1.3.3 Alternative Antimicrobial Strategies for <i>P. aeruginosa</i> Treatment.....	14
1.4.1.3.4 Novel Antimicrobial Strategies for <i>P. aeruginosa</i>	15
1.5 Bacteriophages	17
1.5.1 Phage Isolation and Characterisation for Therapy	19
1.5.2 Phage Therapy for the Treatment of <i>P. aeruginosa</i>	19
1.6 Phage Resistance.....	24
1.7 <i>P. aeruginosa</i> Phage Resistance	25
1.7.1 Receptor Mutations	25
1.7.2 Superinfection Systems	29
1.7.3 Masking Phage Receptors.....	29
1.7.4 CRISPR-cas.....	30

1.7.5	Restriction-Modification (RM) Systems	31
1.7.6	Other Phage Resistance Mechanisms	31
1.7.7	Phage evolution to Improve Therapeutic Potential	33
1.8	Preclinical models	34
1.9	Summary	36
1.10	Hypothesis and Aims	37
2.	Materials and Methods	38
2.1	General Materials	38
2.2	List of Bacteria Used in this Thesis	42
2.3	General Equipment	53
2.3.1	Autoclave	53
2.3.2	Balances	53
2.3.3	Biological Safety Cabinet (Biosafety Cabinet)	53
2.3.4	Centrifuges	53
2.3.5	Chemidoc	54
2.3.6	Primary airway epithelial cell sampling	54
2.3.7	Dry Oven	54
2.3.8	Electrophoresis	54
2.3.9	EVOM™	54
2.3.10	Gammacell Irradiation Units	54
2.3.11	Glassware	54
2.3.12	Heating Blocks	55
2.3.13	Incubators	55
2.3.14	Microscope	55
2.3.15	MinION Mk1C Nanopore Sequencer	55
2.3.16	NanoDrop 2000c	55
2.3.17	pH Meter	56
2.3.18	Pipettes	56
2.3.19	Plate Readers	56
2.3.20	Qubit™ fluorometer	56
2.3.21	Bacterial, tissue and general plasticware	56
2.3.22	Stirrers and Shakers	57
2.3.23	Spectrophotometer	57
2.3.24	Water Bath	57
2.4	General Buffers and Solutions	57
2.4.1	Bovine Serum Albumin (BSA)	57
2.4.2	Calcium chloride (CaCl₂; 1M) solution	57
2.4.3	Cefepime	58

2.4.4	Ceftazidime.....	58
2.4.5	Ciprofloxacin.....	58
2.4.6	Double Deionised Water (ddH ₂ O).....	58
2.4.7	Ethylenediaminetetraacetic Acid (EDTA).....	58
2.4.8	Ethylenediaminetetraacetic Acid Calcium Disodium Salt (CaEDTA).....	59
2.4.9	Ethanol (C ₂ H ₆ O; 80% v/v).....	59
2.4.10	Glycerol (50% v/v).....	59
2.4.11	Hank's Balanced Salt Solution (HBSS).....	59
2.4.12	4-2-hydroxyethyl_ -1-Piperazineethanesulfonic Acid (HEPES) Buffered Saline Solution.....	60
2.4.13	Hydrochloric Acid (HCl; 1M).....	60
2.4.14	Hydrochloric Acid (HCl; 4 mM).....	60
2.4.15	IL-6 Blocking Buffer.....	60
2.4.16	IL-6 Coating Buffer.....	61
2.4.17	IL-8 Assay Diluent.....	61
2.4.18	IL-8 Coating Buffer.....	61
2.4.19	IL-8 Wash Buffer.....	61
2.4.20	IL-8 Working Detector.....	61
2.4.21	Magnesium chloride (MgCl ₂ ; 1M) solution.....	61
2.4.22	Neutral Buffered Formalin (NBF).....	62
2.4.23	Piperacillin.....	62
2.4.24	1X PBS (ELISA).....	62
2.4.25	1X PBS (Cell culture).....	62
2.4.26	Sodium Deoxycholate Solution (C ₂₄ H ₃₉ NaO ₄).....	63
2.4.27	Sodium Hydroxide Solution (NaOH; 0.2M).....	63
2.4.28	Sodium Hydroxide Solution (NaOH; 1M).....	63
2.4.29	Sodium Orthovanadate Solution (Na ₃ VO ₄ ; 200 mM).....	63
2.4.30	Tazobactam.....	63
2.4.31	Tobramycin.....	64
2.4.32	Tris Buffered Saline (TBS).....	64
2.4.33	Tris(hydroxymethyl)aminomethane hydrochloride (Tris-HCl; 1M).....	64
2.4.34	Time Resolved Fluorescence (TRF) Wash Buffer.....	64
2.5	Bacteria and Bacteriophage Culture Solutions.....	65
2.5.1	Bacterial Culture Solutions.....	65
2.5.1.1	Luria-Bertani (Lennox) broth (LB broth).....	65
2.5.1.2	Luria-Bertani (Lennox) agar (LB agar).....	65
2.5.1.3	Cation-adjusted Mueller Hinton broth (CAMHB).....	65
2.5.2	Bacteriophage Culture Solutions.....	65

2.5.2.1	Luria-Bertani (Lennox) overlay (0.4% w/v) agar (LB overlay agar)	65
2.5.2.2	SM buffer	66
2.5.2.3	Double-strength Luria-Bertani (Lennox) broth (LB broth)	66
2.6	Cell Culture Solutions	66
2.6.1	Media Additives	66
2.6.1.1	Adenine	66
2.6.1.2	Cholera Toxin	66
2.6.1.3	Collagen Type 1 (rat tail)	66
2.6.1.4	Cryopreservation Solution for Conditionally Reprogrammed Cells	67
2.6.1.5	Foetal Calf Serum (FCS)	67
2.6.1.6	Cell Culture Medium (CCM)	67
2.6.1.7	FCS-based Trypsin Neutralising Solution (TNS)	67
2.6.1.8	Fibronectin coating buffer	68
2.6.1.9	NIH-3T3 Culture Growth Medium	68
2.6.1.10	Penicillin/Streptomycin	68
2.6.1.11	ROCK Inhibitor (Y-27632)	68
2.6.1.12	Subculture Reagents for Primary Cells	69
2.6.1.13	Trypan Blue Solution (0.05% v/v)	69
2.6.1.14	Primary Airway Epithelial Cell Growth Media	69
2.7	General Methodology	69
2.7.1	Bacterial Culture Techniques	69
2.7.1.1	Cryopreservation of Bacterial Isolates	69
2.7.1.2	Culture of Bacterial Stocks	70
2.7.1.3	Measuring Bacterial Optical Density at 600 nanometres (OD600nm)	70
2.7.1.4	Enumerating Viable Bacterial Load by Colony Forming Units per Millilitre (CFU/mL)	70
2.7.1.5	Antimicrobial and Synergy Testing	71
2.7.1.6	Bacterial DNA Extraction, Quality Control and Sequencing	71
2.7.1.7	Bacterial Short Paired-End Illumina Whole Genome Assembly	72
2.7.1.8	Bacterial Long Read Nanopore and Short Paired-End Illumina Whole Genome Hybrid Assembly	72
2.7.1.9	Bacterial Genome Annotation	73
2.7.1.10	Heat Killing <i>P. aeruginosa</i>	73
2.7.2	Bacteriophage Culture Techniques	73
2.7.2.1	Preparation of Overlay Agar	73
2.7.2.2	Phage Isolation from Wastewater Samples	74
2.7.2.3	Phage Purification	74
2.7.2.4	Miniaturised Phage Spot Test for Host Range	75
2.7.2.5	Overlay Agar Plate Determination of Host Range	75

2.7.2.6	Phage Propagation Using LB Agar	75
2.7.2.7	Phage Titre Enumeration in Plaque Forming Units per Millilitre (PFU/mL)	76
2.7.2.8	Efficiency of Plating (EOP)	76
2.7.2.9	Phage Time-Kill Assay.....	76
2.7.2.10	Phage Genome Extraction and Sequencing.....	77
2.7.2.11	Phage Genome Bioinformatic Analysis.....	77
2.7.2.12	Phage Phylogenetic Analysis.....	78
2.7.2.13	Transmission Electron Microscopy (TEM)	78
2.7.2.14	One-Step Growth Curve.....	79
2.7.2.15	Thermal and pH Stability.....	79
2.7.2.16	Endotoxin Removal from Phage Preparations.....	80
2.7.2.17	Endotoxin Quantification in Phage Preparations	80
2.7.3	Tissue Culture Methods	80
2.7.3.1.1	Cell Line Origins	80
2.7.3.1.2	Cell count and viability	81
2.7.3.1.3	Cell Line Recovery	81
2.7.3.1.4	Cell Line Subculture	81
2.7.3.1.5	Cell Line Cryopreservation	82
2.7.3.2	Paediatric primary airway epithelial cells	82
2.7.3.2.1	Ethics approval.....	82
2.7.3.2.2	Primary airway epithelial cell collection and processing.....	82
2.7.3.2.3	Irradiation of fibroblasts	83
2.7.3.2.4	Primary airway epithelial cells cryopreservation.....	83
2.7.3.2.5	Primary airway epithelial cells recovery.....	84
2.7.3.2.6	Primary airway epithelial cells subculturing.....	84
2.7.3.2.7	Primary airway epithelial cells maintenance.....	84
2.7.3.2.8	Air-liquid interface (ALI) cell culture	85
2.7.3.2.9	Trans-epithelial electrical resistance (TEER).....	85
2.7.3.2.10	Treatment conditions of established primary airway epithelial cells.....	86
2.7.3.2.11	Mycoplasma testing.....	86
2.7.4	Protein Expression Analyses.....	87
2.7.4.1	Cytotoxicity.....	87
2.7.4.2	IL-8 Enzyme Linked Immunosorbent Assay (ELISA)	87
2.7.4.3	IL-6 Enzyme Linked Immunosorbent Assay (ELISA)	87
2.7.4.4	Histology	87
2.7.4.5	Statistics	88
3.	Isolation and Characterisation of <i>Pseudomonas aeruginosa</i> Phages.....	90
3.1	Introduction	90
3.2	Materials and Methods.....	91

3.2.1	Materials	91
3.2.2	General Methodology	91
3.2.2.1	Bacterial Strains and Culture Conditions	91
3.2.2.2	Phage Isolation and Purification	92
3.2.2.3	Phage Host Range Analysis	93
3.2.2.4	Phage DNA Extraction	93
3.2.2.5	Extracted DNA Quality Evaluation and Whole Genome Sequencing	93
3.2.2.6	Phage Genome Assembly and Annotation	94
3.2.2.7	Transmission Electron Microscopy (TEM)	94
3.2.2.8	Phage Phylogenetic Analysis	95
3.2.2.9	Phage Receptor Identification	95
3.2.2.10	Bacterial DNA Extraction	96
3.2.2.11	Bacterial Genome Analysis	96
3.2.2.12	Thermal and pH Stability	97
3.2.2.13	One-step Growth Curve	98
3.2.2.14	Statistical Analysis	98
3.3	Results	98
3.3.1	Isolation, Purification and Macroscopic Characterisation	98
3.3.2	Phage Host Range	102
3.3.3	Phage Genomic Analysis	105
3.3.4	Phage TEM Analysis	108
3.3.5	Phage Phylogenetic Analysis	111
3.3.6	Phage Receptor Determination	117
3.3.7	Phage Storage Stability Over a Range of Temperatures	119
3.3.8	Phage pH Stability	121
3.3.9	One-Step Growth Curves	122
3.4	Discussion	123
4.	Phage Resistance Evolution in CF Isolates of <i>P. aeruginosa</i>	129
4.1	Introduction	129
4.2	Materials and Methods	130
4.2.1	Bacterial DNA Extraction, Quality Assessment and Sequencing	130
4.2.2	Bacterial Short Paired-End Illumina Whole Genome Assembly	133
4.2.3	Bacterial Long Read Nanopore and Short Paired-End Illumina Whole Genome Hybrid Assembly	133
4.2.4	Bacterial Genome Annotation	133
4.2.5	Phage Treatment of the Bacterial Isolates	134
4.2.6	Confirming Phage Resistance	136
4.2.7	Mutant Analysis	136
4.2.8	Statistical Analyses	136

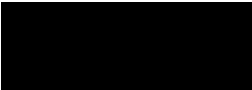

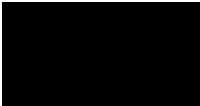

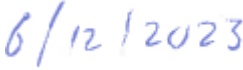
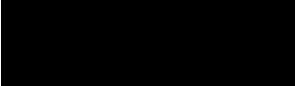
4.3	Results	137
4.3.1	Characteristics of <i>P. aeruginosa</i> Clinical isolates	137
4.3.2	Phage Infectivity Against Chosen <i>P. aeruginosa</i> Isolates	139
4.3.3	Phage Treatment of the <i>P. aeruginosa</i> Clinical Isolate M1C79	139
4.3.4	Phage Treatment of the <i>P. aeruginosa</i> Clinical Isolate AST154	144
4.3.5	Phage Treatment of the <i>P. aeruginosa</i> Clinical Isolate AST234	148
4.3.6	Frequency of Phage Resistance After Phage Treatment	152
4.3.7	Mechanisms of Phage Resistance in <i>P. aeruginosa</i> Isolate M1C79	155
4.3.8	Mechanisms of Phage Resistance in <i>P. aeruginosa</i> Isolate AST154	157
4.3.9	Mechanisms of Phage Resistance in <i>P. aeruginosa</i> Isolate AST234	159
4.3.10	Antibiotic Susceptibility After Phage Treatment	162
4.4	Discussion	162
5.	Phage-Antibiotic Cocktail Efficacy and Effects on Primary Airway Epithelial Cells	169
5.1	Introduction	169
5.2	Materials and Methods	170
5.2.1	Materials	170
5.2.2	General Methodology	170
5.2.2.1	Microbiology	170
5.2.2.2	Phage Propagation	171
5.2.2.3	Tobramycin	171
5.2.2.4	Synergism Checkerboard Assay	171
5.2.2.5	Evaluation of Suppression of Phage Resistance	171
5.2.2.6	Endotoxin Removal and Quantification	172
5.2.2.7	Cell Culture Ethics	172
5.2.2.8	Treatment Conditions of Established Primary Airway Epithelial Cells	173
5.2.2.9	Primary Airway Epithelial Cell Histology	174
5.2.2.10	Primary Airway Epithelial Cell Cytotoxicity	174
5.2.2.11	Primary Airway Epithelial Cell IL-8 Cytokine Quantification	175
5.2.2.12	Primary Airway Epithelial Cell IL-6 Cytokine Quantification	176
5.2.2.13	Statistics	177
5.3	Results	178
5.3.1	Kara-mokiny 16 and Tobramycin Combination Synergy	178
5.3.2	M1C79 Resistance Suppression by Kara-mokiny 16 and Tobramycin Combinations	179
5.3.3	AST154 Resistance Suppression by Kara-mokiny 16 and Tobramycin Combinations	183
5.3.4	AST234 Resistance Suppression by Kara-mokiny 16 and Tobramycin Combinations	187

5.3.5	Comparison of Phage Titres During Combination Treatments of the <i>P. aeruginosa</i> Isolates	191
5.3.6	Endotoxin Levels in Phage Preparations for Primary Airway Epithelial Exposures	194
5.3.7	Morphological Assessment of Differentiated Primary Airway Epithelial Cells	194
5.3.8	Assessment of Mucus Production by the Differentiated Primary Airway Epithelial Cells Following 24 Hrs of Exposure to Different Stimuli	196
5.3.9	Primary Airway Cytotoxicity Stimulated by Different Exposures	198
5.3.10	Assessment of IL-8 Produced by Primary Airway Cells Following Exposures to Different Treatments	200
5.3.11	Assessment of IL-6 Produced by Primary Airway Cells Following Exposures to Different Treatments	202
5.3.12	Phage Titres Following Exposure to ALI Cultured Primary Airway Epithelial Cells	204
5.4	Discussion	206
6.	Chapter 6: General Discussion	213
6.1	Summary of Findings	213
6.2	Is phage resistance a significant problem?	214
6.3	Is the model used to investigate phage resistance representative?	215
6.4	Increasing Phage Screening Throughput	216
6.4.1	Transposon Insertion Sequencing Libraries	216
6.4.2	Flow Cytometry	218
6.4.3	Artificial Intelligence Algorithms	218
6.5	How can phage preclinical safety be evaluated to be relevant to CF	220
6.6	Regulatory Roadblocks to Phage Therapy	222
6.7	Use phage products instead of whole phages	223
6.8	Conclusion	224
Appendix	225
Appendix A.1	225
Appendix Table B.1	<i>P. aeruginosa</i> Receptor Mutations Conferring Phage-Resistance	227
Appendix Table C.1	Ranked Host Range of all the Phages Isolated in this Thesis	236

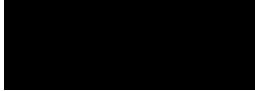

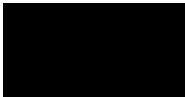
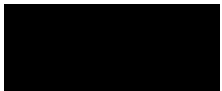
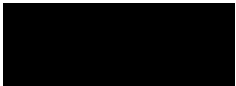
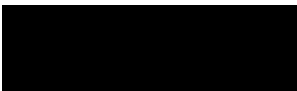
Appendix Table D.1 The Top 20 Phages Host Specificity	242
Appendix Table E.1 Effects of Phage Treatments at MOI 1 on M1C79 OD600nm and CFU/mL.....	243
Appendix Table E.2 Effects of Phage Treatments at MOI 0.1 on M1C79 OD600nm and CFU/mL.....	245
Appendix Table E.3 Effects of Phage Treatments at MOI 1 on AST154 OD600nm and CFU/mL.....	247
Appendix Table E.4 Effects of Phage Treatments at MOI 0.1 on AST154 OD600nm and CFU/mL.....	249
Appendix Table E.5 Effects of Phage Treatments at MOI 1 on AST234 OD600nm and CFU/mL.....	251
Appendix Table E.6 Effects of Phage Treatments at MOI 0.1 on AST234 OD600nm and CFU/mL.....	253
Appendix Table F.1 Selected Phage Treated Mutants EOP and Colony Morphology	255
Appendix Table G.1 Predicted Phage Spacers in M1C79 CRISPR-cas System	257
Appendix Table H.1 Filtered Mutations Identified in the M1C79 Mutants Following Phage Treatment.....	262
Appendix Table H.2 Filtered Mutations Identified in the AST154 Mutants Following Phage Treatment.....	263
Appendix Table H.3 Filtered Mutations Identified in the AST234 Mutants Following Phage Treatment.....	267
Appendix Table I.1 Statistics of 2-way ANOVA for Viable M1C79 at 6,12, 18 and 24 Hrs After the High Dose Combination Treatments.....	269
Appendix Table I.2 Statistics of 2-way ANOVA for Viable M1C79 at 6,12, 18 and 24 Hrs After Low Dose Combination Treatment.....	272
Appendix Table I.3 Statistics of 2-way ANOVA for Viable AST154 at 6,12, 18 and 24 Hrs After the High Dose Combination Treatments.....	274
Appendix Table I.4 Statistics of 2-way ANOVA for Viable AST154 at 6,12, 18 and 24 Hrs After Low Dose Combination Treatment.....	276
Appendix Table I.5 Statistics of 2-way ANOVA for Viable AST234 at 6,12, 18 and 24 Hrs After the High Dose Combination Treatments.....	278
Appendix Table I.6 Statistics of 2-way ANOVA for Viable AST234 at 6,12, 18 and 24 Hrs After Low Dose Combination Treatment.....	281
Appendix Table I.7 Statistics of 2-way ANOVA for Phage Titres After Combination Treatments of M1C79, AST154 and AST234 at 6,12, 18 and 24 Hrs.....	283

Declaration for Co-Authored Publications

This thesis contains work that has been published.

<p>Vaitekenas, A., Tai, A. S., Ramsay, J. P., Stick, S. M., & Kicic, A. (2021). <i>Pseudomonas aeruginosa</i> Resistance to Bacteriophages and Its Prevention by Strategic Therapeutic Cocktail Formulation. <i>Antibiotics</i>, 10(2), 145. doi:10.3390/antibiotics10020145</p>	
<p>Details of the work: This article reviewed the mechanisms of phage resistance in <i>Pseudomonas aeruginosa</i>. It also looked at methods to prevent resistance occurring so that phages are an effective treatment.</p>	
<p>Location in thesis: This manuscript constitutes Chapter One of this thesis</p>	
<p>Student contribution to work: AV (70%) was involved in literature collation, manuscript drafting, writing, incorporating co-authors feedback and final editing.</p>	
<p>Co-author signatures and dates:</p> <p>Anna Tai: </p> <p>Joshua Ramsay </p> <p>Stephen Stick: </p> <p>Anthony Kicic: </p>	<p>Date: 03/12/2023</p> <p>Date: </p> <p>Date: 03/12/2023</p> <p>Date: 03/12/2023</p>
<p>Student signature and date:</p> <p>Andrew Vaitekenas </p>	<p>Date: 15/12/2023</p>

This thesis contains work that has been published.

Vaitekenas, A., Tai, A. S., Ramsay, J. P., Stick, S. M., Agudelo-Romero, P., & Kicic, A. (2022). Complete Genome Sequences of Four Pseudomonas aeruginosa Bacteriophages: Kara-mokiny 8, Kara-mokiny 13, Kara-mokiny 16, and Boorn-mokiny 1. <i>Microbiology Resource Announcements</i> , 11(12), e00960-00922. doi:doi:10.1128/mra.00960-22	
Details of the work: This article is a genome announcement of four phages isolated from wastewater for this project. It summarises the bioinformatic methods and genomic characteristics. These characteristics make the four phages suitable for use in phage therapy.	
Location in thesis: This manuscript constitutes Chapter Three of this thesis	
Student contribution to work: AV (70%) was involved in conceptualisation, data generation, graphic illustration, manuscript preparation, writing, incorporating co-authors feedback and final editing.	
Co-author signatures and dates: Anna Tai:  Joshua Ramsay  Stephen Stick:  Patricia Agudelo-Romero  Anthony Kicic: 	 Date: 03/12/2023 Date: <i>6/12/2023</i> Date: 03/12/2023 Date: 05/12/2023 Date: 03/12/2023
Student signature and date: Andrew Vaitekenas 	 Date: 15/12/2023

List of Figures

- Figure 1. Common *Pseudomonas aeruginosa* Genetic Mutations that Prevent the Phage Receptors being Synthesised or Functioning**
- Figure 2. Methods to Prevent or Overcome Phage Resistance**
- Figure 3.1. Macroscopic Characterisation of Plaque Morphology**
- Figure 3.2. Host Range of the Top 20 Phages Against the Paediatric Derived CF *P. aeruginosa* Isolates**
- Figure 3.3. Phage Maximum Likelihood Phylogenetic Tree Calculated by MEGA v11 with 50 bootstraps and was annotated using iTOL**
- Figure 3.4. The Stability of the Top 4 Phages Across a Range of Temperatures**
- Figure 3.5. Stability of the Top 4 Phages at Different Acid-Base Concentrations (pH)**
- Figure 3.6. One-Step Growth Curves of Kara-mokiny 8, 13, 16 and Boorn-mokiny 1**
- Figure 4.1. Bacterial Sequencing and Analysis**
- Figure 4.2. Overview of the Method used to Treat the *P. aeruginosa* Isolates with Each Phage**
- Figure 4.3. The Effects of Phage Treatment on M1C79 Growth (OD600nm) and Culturable Bacteria**
- Figure 4.4. The Effects of Phage Treatment of M1C79 on Phage Titre**
- Figure 4.5. The Effects of Phage Treatment on AST154 Growth (OD600nm) and Culturable Bacteria**
- Figure 4.6. The Effects of Phage Treatment of AST154 on Phage Titre**
- Figure 4.7. The Effects of Phage Treatment on AST234 Growth (OD600nm) and Culturable Bacteria**
- Figure 4.8. The Effects of Phage Treatment of AST234 on Phage Titre**
- Figure 4.9. Mutations Identified in M1C79-Derived Mutants Surviving Phage Treatment**
- Figure 4.10. Mutations identified in AST154-derived mutants surviving phage treatment**
- Figure 4.11. Mutations Identified in AST234-Derived Mutants Surviving Phage Treatment**
- Figure 4.12. Fold-Change in Antibiotic Minimum Inhibitory (MIC) Concentrations in *P. aeruginosa* Surviving Phage Treatment**
- Figure 5.1. Synergistic Growth Suppression between Different Combinations of Kara-mokiny 16 and Tobramycin**
- Figure 5.2. Isolate M1C79 resistance suppression by additive combination of tobramycin and Kara-mokiny 16**
- Figure 5.3. Isolate M1C79 resistance suppression by additive combination of tobramycin and Kara-mokiny 16**

- Figure 5.4. Isolate AST154 resistance suppression of additive combination of tobramycin and Kara-mokiny 16**
- Figure 5.5. Isolate AST154 resistance suppression by additive combination of tobramycin and Kara-mokiny 16**
- Figure 5.6. Isolate AST234 resistance suppression of additive combination of tobramycin and Kara-mokiny 16**
- Figure 5.7. Isolate AST234 resistance suppression of additive combination of tobramycin and Kara-mokiny 16**
- Figure 5.8. Titre of Kara-mokiny 16 over time after different treatments of the *P. aeruginosa* isolates**
- Figure 5.9. Morphological assessment of treated ALI primary airway epithelial cell cultures**
- Figure 5.10. Mucus production visualisation after treatment of ALI primary airway epithelial cell cultures**
- Figure 5.11. Measurable LDH levels in apical (A) washings and basolateral (B) supernatants following 24 hrs exposure to phage, antibiotics and cocktail combinations**
- Figure 5.12. IL-8 produced ALI-cultured primary airway epithelial cells after 24 hrs of exposure to different treatments**
- Figure 5.13. IL-6 produced ALI-cultured primary airway epithelial cells after 24 hrs of exposure to different treatments**
- Figure 5.14. Phage titres in ALI-cultured primary airway epithelial cell cultures after 24 hrs of exposure to different treatments**

List of Tables

Table 1 WHO Priority Pathogens

Table 2 Different *P. aeruginosa* Antimicrobial Treatment Regimes

Table 3 Documented Compassionate Uses of Phage Therapy (as of September 2023)

Table 4 Clinical Trials of Phage Therapy Registered Through the National Library of Medicine Clinical Trials Registry (as of September 2023)

Table 5 Other Types of Phage Resistance Mechanisms Found in *P. aeruginosa* Genomes

Table 2.1 General Materials

Table 2.2 List of Bacteria Used in this Thesis

Table 3.1 Macroscopic Characterisation of Phage Plaque Morphologies

Table 3.2 Proportion of Phage Plaque Macroscopic Characteristics

Table 3.3 Host Range of the Top 20 Phages Against the CF and Non-CF *P. aeruginosa* Isolates

Table 3.4 General Genomic Characteristics of the Top 20 Putative Phages

Table 3.5 General Genome Characteristics of the Putative Temperate Phage Contaminants

Table 3.6 Representative Phage TEM Images and Morphology

Table 3.7 Average Nucleotide Identity of Isolated Phages from the *Pbunavirus* Genus

Table 3.8 Average Nucleotide Identity of Isolated Phages to Publicly Available *Pbunaviruses*

Table 3.9 *Phikzviruses* Average Nucleotide Identity to Publicly Available Phage

Table 3.10 Efficiency of Plating of the Top 20 Phages Against a PAO1 Phage Receptor Mutant Library

Table 3.11 Receptor Determination for Boorn-mokiny 1

Table 4.1 General Characteristics of the Clinical Isolates of *P. aeruginosa*

Table 4.2 Genome Characteristics of the *P. aeruginosa* Clinical Isolates

Table 4.3 Phage EOP Against the Clinical Isolates of *P. aeruginosa*

Table 4.4 Frequency of Resistance to Treating Phages in Surviving Bacteria

Appendix Table B.1 *P. aeruginosa* Receptor Mutations Conferring Phage-Resistance

Appendix Table C.1 Ranked Host Range of all the Phages Isolated in this Thesis

Appendix Table D.1 The Top 20 Phages' Host Specificity

Appendix Table E.1 Effects of Phage Treatments at MOI 1 on M1C79 OD600nm and CFU/mL

Appendix Table E.2 Effects of Phage Treatments at MOI 0.1 on M1C79 OD600nm and CFU/mL

Appendix Table E.3 Effects of Phage Treatments at MOI 1 on AST154 OD600nm and CFU/mL

Appendix Table E.4 Effects of Phage Treatments at MOI 0.1 on AST154 OD600nm and CFU/mL

Appendix Table E.5 Effects of Phage Treatments at MOI 1 on AST234 OD600nm and CFU/mL

Appendix Table E.6 Effects of Phage Treatments at MOI 0.1 on AST234 OD600nm and CFU/mL

Appendix Table F.1 Selected Phage Treated Mutants EOP and Colony Morphologies that was Used to Infer Diversity

Appendix Table G.1 Predicted Phage Spacers in M1C79 CRISPR-cas System

Appendix Table H.1 Filtered Mutations Identified in the M1C79 Mutants Following Phage Treatment Appendix Table

H.2 Filtered Mutations Identified in the AST154 Mutants Following Phage Treatment

Appendix Table H.3 Filtered Mutations Identified in the AST234 Mutants Following Phage Treatment

Appendix Table I.1 Statistics of 2-way ANOVA for Viable M1C79 at 6,12, 18 and 24 Hrs After the High Dose Combination Treatments

Appendix Table I.2 Statistics of 2-way ANOVA for Viable M1C79 at 6,12, 18 and 24 Hrs After Low Dose Combination Treatment

Appendix Table I.3 Statistics of 2-way ANOVA for Viable AST154 at 6,12, 18 and 24 Hrs After the High Dose Combination Treatments

Appendix Table I.4 Statistics of 2-way ANOVA for Viable AST154 at 6,12, 18 and 24 Hrs After Low Dose Combination Treatment

Appendix Table I.5 Statistics of 2-way ANOVA for Viable AST234 at 6,12, 18 and 24 Hrs After the High Dose Combination Treatments

Appendix Table I.6 Statistics of 2-way ANOVA for Viable AST234 at 6,12, 18 and 24 Hrs After Low Dose Combination Treatment

Appendix Table I.7 Statistics of 2-way ANOVA for Phage Titres After Combination Treatments of M1C79, AST154 and AST234 at 6,12, 18 and 24 Hrs

List of Abbreviations

AEC – Airway Epithelial Cells

ALI – Air Liquid Interface

AMR – Antimicrobial Resistance

ANI – Average Nucleotide Identity

ASL – Airway Surface Liquid

AST – American Thoracic Society

ATCC – American Type Culture Collection

AUC – Area Under the Curve

bp – Base Pairs

BREX – Bacteriophage Exclusion

BSA – Bovine Serum Albumin

CaEDTA – Ethylenediaminetetraacetic Acid Calcium Disodium Salt

CAMHB – Cation Adjusted Mueller Hinton Broth

CCM – Cell Culture Medium

CDS – Coding Sequences

CF – Cystic fibrosis

CFTR – Cystic Fibrosis Transmembrane Conductance Regulator

CFU/mL – Colony Forming Units per Millilitre

COGs – Cluster of Orthologous Genes

COPD – Chronic Obstructive Pulmonary Disease

CPA – Common Polysaccharide Antigen

CRISPR-cas – Clustered Regularly Interspaced Short Palindromic Repeat-cas

CRISPRi – CRISPR Interference

CRPA – Carbapenem-Resistant *P. aeruginosa*

crRNA – CRISPR RNA

ddH₂O – Double Deionised Water

DISARM – Defence Island Associated with RM

DMEM – Dulbecco's Modified Eagle Medium

DMSO – Dimethyl Sulfoxide

DND – DNA Degradation

Dub-seq – Dual-Barcoded Shotgun Expression Library Sequencing

EDTA – Ethylenediaminetetraacetic Acid

ELISA – Enzyme Linked Immunosorbant Assay
EOP – Efficiency of Plating
EPS – Exopolysaccharide
EU – Endotoxin Units
FICI – Fractional Inhibitory Concentration Index
G – Gauge
HBSS – Hank’s Buffered Salt Solution
HEPES – 4-(2-hydroxyethyl)-1-piperazineethanesulfonic Acid Buffered Saline Solution
HI-FCS – Heat Inactivate Foetal Calf Serum
HITS – High-Throughput Insertion Tracking
HRV – Human Rhinovirus
IL-6 – Interleukin 6
IL-8 – Interleukin 8
INPHARED – Infrastructure for a PHAge Reference Database
INSeq – Insertion Sequencing
LB – Luria-Bertani (Lennox)
LDH – Lactate Dehydrogenase
LPS – Lipopolysaccharide
LRI+ – Lower Respiratory Infections
MAEP – Mutated Antibiotic Efflux Pump
MI – Meconium Ileus
MIC – Minimum Inhibitory Concentration
MinYS – Mine Your Symbiont
M-LPS – Mutated LPS
MLST – Multilocus Sequence Type
MOI – Multiplicity of Infection
M-T4P – Mutated T4P
NATA – National Association of Testing Authorities
NBF – Neutral Buffered Formalin
OD600nm – Optical Density at 600nm
OGTR – Office of Gene Technology Regulator
OMV – Outer Membrane Vesicle
OSA – O-Specific Antigen
pAECs – Primary Airway Epithelial Cells
PBS – Phosphate Buffered Saline

PFU/mL – Plaque Forming Units per Millilitre
PHROGS – Prokaryotic Virus Remote Homology Groups
QS – Quorum Sensing
RAST – Radioallergosorbent Test
RBPs – Receptor Binding Proteins
RB-TnSeq – Random-Barcode Transposon Sequencing
RM – Repeated Measures
RM – Restriction Modification
ROCK – Rho-Associated Kinase
RSV – Respiratory Syncytial Virus
SMG – Submucosal Glands
SNPs – Single Nucleotide Polymorphisms
T4P – Type IV Pili
TBS – Tris Buffered Saline
TEM – Transmission Electron Microscopy
TNS – Trypsin Neutralising Solution
TraDIS – Transposon-Directed Sequencing
TRF – Time Resolved Fluorescence
WHO – World Health Organisation
WT – Wild-Type

Publications

Vaitekenas A., Tai A.S, Ramsay J.P, Stick S.M, Kicic A. 2021. *Pseudomonas aeruginosa* Resistance to Bacteriophages and Its Prevention by Strategic Therapeutic Cocktail Formulation. *Antibiotics* 10:145.

Vaitekenas A., Tai A.S., Ramsay J.P., Stick S.M., Agudelo-Romero P., Kicic A. 2022. Complete Genome Sequences of Four *Pseudomonas aeruginosa* Bacteriophages: Kara-mokiny 8, Kara-mokiny 13, Kara-mokiny 16, and Boorn-mokiny 1. *Microbiology Resource Announcements* 11:e00960-22.

Conference Presentations

Poster Presentations

Vaitekenas, A., Grey, L., Ng, R.N., Iszatt, J.J., Poh, M.W.P., Laucirica D.R., McLean S.A., Hillas, J., Tai, A.S., Ramsay J.P., Stick, S.M., Kicic A., WAERP & AREST CF. 2020. Strategic Phage Cocktail Formulation to Prevent the Evolution of *Pseudomonas aeruginosa* Resistance. Australian Society of Microbiology and the Australian Institute of Medical Scientists 2020 Annual Local Scientific Meeting, Perth, Australia.

Vaitekenas, A., Grey, L., Ng, R.N., Iszatt, J.J., Poh, M.W.P., Laucirica D.R., McLean S.A., Hillas, J., Tai, A.S., Ramsay J.P., Stick, S.M., Kicic A., WAERP & AREST CF (2020). “TP 073 Investigating pseudomonas aeruginosa phage-resistance to guide strategic therapy cocktail formulation.” *Respirology* 26(S2). Thoracic Society of Australia and New Zealand, Online, 2020.

Vaitekenas, A., Ng, R.N., Tai, A.S., Ramsay J.P., Kicic A., WAERP & AREST CF. 2021. Investigating Phage Resistance in CF Isolates of *Pseudomonas aeruginosa*. The World Microbe Forum (American Society of Microbiology and Federation of European Microbiological Societies) 2021 Annual Scientific Meeting, Online.

Vaitekenas, A., Ng, R.N., Tai, A.S., Ramsay J.P., Kicic A., WAERP & AREST CF. 2021. Understanding *Pseudomonas aeruginosa* Phage Resistance to Inform Phage Cocktail Formulation. Australasian Cystic Fibrosis 2021 Annual Scientific Meeting, Online.

Vaitekenas, A., Ng, R.N., Tai, A.S., Ramsay J.P., Kicic A., WAERP & AREST CF. 2021. Understanding *Pseudomonas aeruginosa* Phage Resistance to Guide Phage Cocktail Formulation. Thoracic Society of Australia and New Zealand 2021 Annual Local Scientific Meeting, Perth, Australia.

Andrew Vaitekenas, A. S. T., Joshua P. Ramsay and Anthony Kicic (2022). “TP095 *Pseudomonas aeruginosa* phage characterization for cystic fibrosis multi-drug resistant infections.” Respirology 27(S1): 88-220. Thoracic Society of Australia and New Zealand, Online, 2022.

Vaitekenas, A., Tai, A.S., Ramsay J.P., Agudelo-Romero, P., Kicic A., WAERP & AREST CF. 2022. Assessing resistance evolution dynamics between Cystic Fibrosis-derived *Pseudomonas aeruginosa* and targeted bacteriophage. BacPath 2022 Annual Scientific Meeting, Brisbane, Australia.

Vaitekenas, A., et al. (2022). “51: Assessing Phage Resistance Evolution by Distinct *Pseudomonas aeruginosa* Isolates from Individuals with Cystic Fibrosis.” Journal of Global Antimicrobial Resistance 31: S31. International Congress of Antimicrobials and Chemotherapy 2022 Annual Scientific Meeting, Perth, Australia.

Oral Presentations

Vaitekenas, A., Grey, L., Ng, R.N., Iszatt, J.J., Poh, M.W.P., Laucirica D.R., McLean S.A., Hillas, J., Tai, A.S., Ramsay J.P., Stick, S.M., Kicic A., WAERP & AREST CF. 2020. Strategic Phage Cocktail Formulation to Prevent the Evolution of *Pseudomonas aeruginosa* Phage-Resistance. Combined Biological Sciences Meeting 2020 Annual Local Scientific Meeting, Perth, Australia.

Vaitekenas, A., Grey, L., Ng, R. N., Iszatt, J. J., Poh, M. W., Laucirica, D. R., McLean, S. A., Hillas, J., Tai, A. S., Ramsay, J. P., Stick, S. M. and Kicic, A. (2021). “WS01.6 Exploring *Pseudomonas aeruginosa* phage resistance and prevention strategies.” Journal of Cystic Fibrosis 20: S3. 44th European Cystic Fibrosis Society 2021 Annual Scientific Meeting, Online.

Andrew Vaitekenas, Tai, A.S., Ramsay, J.P., Kicic, A., WAERP and AREST CF (2023). “Understanding phage-bacteria dynamics to formulate resistance- suppressing cocktails for pulmonary infections.” Respirology 28(S2). Thoracic Society of Australia and New Zealand 2023 Annual Scientific Meeting, Christchurch, New Zealand.

Vaitekenas, A., Tai, A.S., Ramsay J.P., Agudelo-Romero, P., Stick, S.M., Kicic A., WAERP & AREST CF. 2023. Understanding Phage-Bacteria Dynamics to Guide Resistance Suppressing Cocktail Formulation for Antibiotic Resistant Pulmonary Infections. Australian Society of Microbiology 2023 Annual Scientific Meeting, Perth, Australia.

Awards

- An Australian government Research Training Program (RTP) Fees Offset and Stipend (2020-2024)
- Australian Cystic Fibrosis Postgraduate Studentship Grant (2020-2021)
- Cystic Fibrosis Golf Classic Top-Up Scholarship (2021-2024)
- Wesfarmers Centre for Vaccines and Infectious Diseases and Wal-Yan Respiratory Research Centre (2021-2024)
- World Microbe Forum Student Travel Award (2021)
- Best Poster Award Thoracic Society of Australia and New Zealand WA Annual Scientific Meeting (2022)
- Thoracic Society of Australia and New Zealand Student Travel Award (2023)
- Finalist in the Ann Woolcock New Investigator Award at the Thoracic Society of Australia and New Zealand Annual Scientific Meeting (2023)

Acknowledgements

I would firstly like to acknowledge the participants and families who have donated to WAERP. Furthermore, I would also like to thank the doctors and the nurses of St John of God Subiaco who allowed us to work around them and collected our samples. I would like to thank the members of AREST CF Melbourne, especially Professor Sarath Ranganathan, Ms Rosemary Carzino and Ms Nadeene Clarke, who kindly collected and shared the *P. aeruginosa* that I have used so much. I would also like to thank Dr Anna Tai, Dr Papanin Putsathit, Professor Geoffrey Coombs, Ms Denise Daley and Professor Scott Bell who have also shared various clinical bacterial isolates. I would like to acknowledge Christopher Leigh from the University of Adelaide who did all the TEM in this thesis. I am also grateful to the Water Corporation of Western Australia who supplied us with the wastewater which we isolated phages from.

I would like to thank past and present members of the EPiC team who have all contributed in some form: Dr Angela Fuery, Dr Patricia Agudelo-Romero, Dr Elizabeth Kicic-Starceвич, Dr Nicole Shaw, Dr Katherine Landwehr, Dr Kelly Martinovich, Dr Luke Garratt, Dr Thomas Iosifidis, Dr Kevin Looi, Dr Daniel Laucirica, Dr Samuel Montgomery, Dr Matthew Wee-Peng Poh, Ms Lucinda Grey, Ms Samantha McLean, Ms Jessica Hillas, Ms Reanne Ho, Ms Rebecca Watkinson, Mr Luke Berry, Mr Craig Schofield, Mr Jack Canning, Mr Rohan Flint, Mr Sourav Shyam, Ms Rickie Fraser-Jones, Ms Emma Catchpole and Ms Alexia Foti. I would especially like to thank Mr Luke Berry who has helped at multiple points across my candidature whether it was ordering, organising couriers, making cell culture media or doing the histology. I would also like to give a special mention to Dr Samuel Montgomery who did the DNA extraction and sequencing of bacteria on the Nanopore machine. I would like to acknowledge Dr Patricia Agudelo-Romero for starting me on the winding path into bioinformatics. Thank you to Dr Renee Ng who laid the groundwork for much of the phage research that I have conducted.

To my supervisors I would like to express my gratitude. A/Professor Anthony Kicic you have worked tirelessly to support me on my PhD journey and this thesis is just as much yours as it is mine. Thank you to Dr Anna Tai and Dr Joshua Ramsay for being generous with their time and expertise and all the help you have given me. I regret not getting to speak to you all more often but still I couldn't have done it without you.

This research would not have been possible without the support of an Australian Government International Research Training Programme (RTP) Fees Offset Scholarship. I would also like to acknowledge that I was supported by a Cystic Fibrosis Australia Postgraduate Studentship Grant, Cystic Fibrosis Western Australia Golf Classic Top Up Scholarship and a Wesfarmers Centre of Vaccines and Infectious Diseases and Wal-Yan Respiratory Research Centre Top Up Scholarship.

Finally, I would like to thank all friends and family. You have supported me financially, physically and emotionally at different times. Thank you for putting up with my antics and moodiness. A special mention to Mr Joshua Iszatt for often being infuriating and frustrating but for showing me "This is the way" and helping to keep me sane. It is appreciated and this journey would not have been possible without you all.

The Bin Bandit

1. Literature Review

1.1 Introduction

Antimicrobials have traditionally been derived from secondary metabolites that microbes use to compete against each other for environmental niches [3]. As a result, bacteria have always naturally evolved antimicrobial resistance in order to overcome competitors [3]. Antimicrobial resistance (AMR) can be broadly grouped into intrinsic and acquired resistance. Intrinsic resistance mechanisms are innately present in a large group of bacteria, either a whole species or more, are independent of previous antimicrobial exposures [3, 4] and reduces the efficacy of antimicrobials or limits those available to treat a group of bacteria. One example is vancomycin which cannot pass through the outer membrane of Gram-negative bacteria [5]. Acquired AMR occurs when an initially susceptible microbial population evolves resistance due to the selection pressure placed on them by exposure to antimicrobials [3]. It can evolve through genetic mutation or horizontal gene transfer of mobile genetic elements carrying resistance genes, integrons, phages or plasmids [4]. Antimicrobial resistance can be achieved by; altering the antimicrobial molecule, preventing the intracellular accumulation of antimicrobials, changing or shielding an antimicrobial target, circumventing antimicrobial targets so that cellular function is maintained, or whole cell and community regulation [3, 4]. Bacteria are also capable of forming AMR communities called biofilms which are formed when they attach to a surface and propagate into communities [6, 7]. These communities are encapsulated by exopolysaccharides, proteins and DNA and the bacteria within are transcriptionally and metabolically distinct to their free-living counterparts [6-8]. Once biofilms have matured, bacteria can shed from it and disperse to setup new communities [6, 7]. Biofilms confer AMR through: causing bacteria to enter a starvation stress response; the formation of persister cells within that are metabolically dormant therefore they do not take up antibiotics; containing large concentrations of antibiotic destroying enzymes; greater frequency of horizontal gene transfer of antibiotic resistance genes; increased genetic diversity and the biofilm matrix itself often occludes antimicrobial penetration [8, 9]. Despite antimicrobial resistance being a natural process the rate of acquired resistance has been increased by anthropogenic practices that select resistant microbes [10, 11]. Increases in resistance have primarily been driven by antimicrobials being over prescribed, misused or exploited in industries such as animal care which then

release these into the environment [10, 11]. As a result, AMR has become a significant threat to healthcare globally [11, 12].

Antimicrobial resistant infections have been associated with 4.95 million deaths globally [1] and as a result, the World Health Organization (WHO) has developed a list of priority AMR bacterial species for whom alternative antimicrobials are urgently needed [12]. They have also ranked priority species based on healthcare burden and treatment difficulty with the current levels of resistance (Table 1). Certain nosocomial pathogens including *Enterococcus faecium*, *Staphylococcus aureus*, *Klebsiella pneumoniae*, *Acinetobacter baumannii*, *Pseudomonas aeruginosa*, and *Enterobacter* species (termed ESKAPE) have been identified to drive the majority of AMR infections [13] that have also been associated with lengthier hospital stays and increased risk of complications including death [14-17]. However, despite being a global healthcare priority, traditional antimicrobial discovery pipelines driven by pharmaceutical industries are waning and the lack of novel antimicrobials is more marked against the critical priority pathogens identified (Table 1) [18, 19]. If not addressed, AMR infections are predicted to be the leading cause of human death by 2050, killing 10 million people per year, and result in a USD\$100 trillion lost in gross domestic product [20]. It is also forecast that the highest number of deaths and healthcare burden will stem from lower respiratory infections (LRI+), since these account for over 30% of all AMR deaths currently [1].

Table 1: WHO Priority Pathogens

Assigned Priority Level	Bacteria
Critical	CR- <i>Acinetobacter baumannii</i>
	CR- <i>Pseudomonas aeruginosa</i>
	CR/3GCR-Enterobacteriaceae
High	VR- <i>Enterococcus faecium</i>
	VR/MR- <i>Staphylococcus aureus</i>
	CMR- <i>Helicobacter pylori</i>
	FQR- <i>Campylobacter</i> species
	FQR- <i>Salmonella</i> species
	3GCR/FQR- <i>Neisseria gonorrhoeae</i>
Medium	PNS- <i>Streptococcus pneumoniae</i>
	AR- <i>Haemophilus influenzae</i>
	FQR- <i>Shigella</i> species

CR-Carbapenem Resistant 3GCR-3rd Generation Cephalosporin Resistant VR-Vancomycin Resistant MR-Methicillin Resistant CMR-Clarithromycin Resistant FQR-Fluoroquinolone Resistant PNS-Penicillin Non-Susceptible AR-Ampicillin Resistant. Modified from [12].

1.2 The WHO Critical Priority Pathogens

Due to the increased threat posed by AMR bacterial infections and the lack of antibiotic development, there have been many efforts to monitor their epidemiology [1, 21-26]. There is particular interest in the surveillance of WHO critical priority pathogens (carbapenem-resistant *A. baumannii*, carbapenem-resistant *P. aeruginosa* and carbapenem/3rd generation cephalosporin-resistant Enterobacteriaceae; Table 1) because they have the most profound impact on healthcare and the fewest antibiotics available to treat them [12, 27-29]. One of these is Carbapenem-resistant *P. aeruginosa* (CRPA; Table 1). It has been listed as a critical priority pathogen because it is a major cause of hospital associated infections and predominantly infects wounds, the respiratory system, and the urinary tract [21, 22]. On a global scale, infections with CRPA have been associated with and attributable to 210,000 and 38,100 deaths respectively in 2019 [1]. In Australia, CRPA infections have a significant healthcare burden (~\$28 million) and cost the economy \$233.5 million in premature mortality [21]. The high mortality and costs associated with *P. aeruginosa* infections are due to a combination of its high virulence, intrinsic and acquired antibiotic resistance which warrants further consideration [28-30].

1.3 *Pseudomonas aeruginosa* Antibiotic Resistance and Virulence

P. aeruginosa is a Gram-negative ubiquitous bacterium [31]. It is an opportunistic pathogen capable of causing multiorgan infections including the skin, eyes, ears, lungs, and the blood stream [32]. It is also the leading cause of nosocomial pneumonia and ventilator-associated infections [33]. The prolific ability of this bacteria to survive in any environment is the product of its large genome and metabolic flexibility, stemming from genomic plasticity [34]. It also has high intrinsic antimicrobial resistance including low outer membrane permeability restricting antimicrobial intracellular passage [35-39], efflux proteins that actively excrete compounds [40-42] and enzymes that inactivate antimicrobial molecules [35, 43, 44]. The high genetic flexibility exhibited by *P. aeruginosa* means it is also adept at gaining acquired resistance through mutations that further decreases the passage of antimicrobials intracellularly [45, 46], upregulate efflux [47, 48], increase enzymatic activity [47, 49, 50] or change antimicrobial targets [51-53]. *P. aeruginosa* also forms biofilms which increase antibiotic tolerance via slowing down the metabolism of constituent bacteria, altering gene expression, concentrating

antimicrobial resistance enzymes, increasing horizontal gene transfer, reducing oxygen in the environment, reducing antimicrobial penetration, and allowing the formation of dormant persister cells [8, 54].

Interestingly, *P. aeruginosa* infections are associated with greater mortality compared to other Gram-negative bacteria that cannot be explained by AMR alone [30]. Evidence suggests that the expression of virulence factors which facilitate infection establishment and maintenance may explain this observation [55, 56]. *P. aeruginosa* also expresses two surface proteins that contribute to motility, namely flagella and type IV pili. The flagella are primarily responsible for swimming motility driven by chemotaxis [57-59] and is important in adhesion to surfaces and biofilm formation [60]. The type IV pili mediates twitching and swarming motility [58, 59, 61, 62]. It is also important for surface adhesion and biofilm formation [59, 62]. Another surface component is lipopolysaccharide (LPS) which mediates *P. aeruginosa* binding to host cells and stimulates the human immune system which can result in septic shock and death [63, 64]. Conversely in chronic infections, *P. aeruginosa* LPS appears to protect it from complement-mediated killing [65]. Work performed on this has shown that overproduced IgG2 antibodies bind the LPS forming a protective cloak which ultimately contributes to poorer lung function in chronic respiratory infections [65].

P. aeruginosa has six secretion systems that deliver a range of toxins. These can be broadly grouped into one step (type I, III, IV and VI) secretion systems and the two step (type II and V) secretion systems [66]. The type I secretion system secretes an alkaline protease, involved in haem and iron uptake [66-69]. The type II secretion system secretes a number of extracellular toxins including exotoxin A, phospholipase C, lipase A, lipase C elastase A and B that damage host tissue and protect the bacteria from the host immune system [66, 69-75]. The type III secretion system injects cytotoxins ExoS, ExoT, ExoY and ExoU into host cells, killing and disrupting them [66, 69, 76-79]. The virulence and lethality of *P. aeruginosa* is closely related to the function of the type III secretion system [69]. The type IV secretion system is used by bacteria for conjugation and facilitates *P. aeruginosa* horizontal gene transfer of virulence genes [80]. The type V secretion system

secretes EstA, TpsA and TpsB that are involved in bacterial adhesion, biofilm formation and immune escape [69].

P. aeruginosa also produces several factors called siderophores. Pyoverdine and pyochelin act to sequester iron and enable infection progression [81-83]. Pyocyanin enables anaerobic respiration, protects the bacteria from the host immune system and is cytotoxic [69, 81, 84]. The final two siderophores are less well studied and are thought to increase *P. aeruginosa* fitness in mixed microbial communities as well as function in iron sequestration [81, 85]. Collectively, virulence factors appear critical for *P. aeruginosa* infection establishment and chronic maintenance particularly in respiratory infections where infections begin intermittent and eventually become chronic. Those with chronic respiratory diseases, including chronic obstructive pulmonary disease, non-cystic fibrosis bronchiectasis and cystic fibrosis (CF) appear at greater risk of *P. aeruginosa* infection [10, 86-89] where infection is the major cause of morbidity and mortality [88, 90, 91].

1.4 Cystic Fibrosis

Cystic Fibrosis is an autosomal recessive genetic disease that affects 162,428 people globally [92]. Its incidence ranges from 1 in 1,353 – 6,000 in European descended populations [93] and here in Australia, 1 in 3,700 babies are born with CF [94]. Over 2,000 mutations in the Cystic Fibrosis Conductance Regulator (*CFTR*) gene results in the disease, whose function is to maintain osmotic homeostasis via the trafficking of ions across the apical membrane of epithelial cells. Whilst the disruption of *CFTR* function by CF affects multiple organs, the airways are the most affected and are where the most uncontrollable symptoms occur [95]. *CFTR* dysfunction leads to aberrant chloride [96] and bicarbonate ion transport from airway epithelial cells into the airway lumen, and sodium ion hyper-reabsorption [97, 98]. Furthermore, changes in the electrolyte composition within the airways causes the dehydration of the airway surface liquid (ASL) [99] which when combined with increased viscosity of fluids results in impaired mucociliary clearance [99]. Compromised mucociliary clearance, together with mucus hypersecretion [100] leads to the accumulation of mucus with steep oxygen gradients, an environment conducive to pathogenic microbial attachment and colonisation [101]. Breakthrough *CFTR* modulators are becoming increasingly available which restore some

chloride ion transport and vastly improve the symptoms of people with CF [102, 103]. CFTR modulators improve the structural lung disease and reduce inflammatory cytokines and immune cells [104, 105]. Modulators also reduce pathogen load and positivity in people with CF that are not chronically infected [106, 107]. However, established *P. aeruginosa* infections persist in those that are chronically infected [107, 108]. Recurrent infections drive progressive lung damage and lung function decline [109, 110] and as a result, respiratory failure remains the most common cause of death of people with CF [88, 90, 91].

1.4.1 CF Lung Disease and Infections

Lung disease begins in children with CF often before detectable infection and can include irreversible bronchiectasis, gas trapping and bronchial wall thickening [101, 111-114]. At this point, the airway microbiome is mostly normal and still diverse [115, 116]. Infections by viruses, fungi and bacteria in early life lead to a dysbiosis as the microbial diversity decreases [115]. As people with CF age, repeated infections drive airway inflammation causing further lung damage [101, 113, 114, 117, 118]. Eventually, the microbiota diversity decreases, and intermittent infections transition to colonisation which drives prolonged lung disease and lung function decline until respiratory failure [115, 118].

1.4.1.1 CF Viral Airway Infections

Viral airway infections are the most common early life infections in people with CF. Children with CF are infected with similar viral pathogens at a comparable frequency to those without the disease [119, 120]. Commonly detected viruses include human rhinovirus (HRV), followed by respiratory syncytial virus (RSV), adenovirus and influenza [120, 121]. In children with CF, viral infections cause greater morbidity [119, 120, 122] and increase neutrophilic infiltration, inflammatory cytokines [120, 122], airway obstruction [123] and functional decline [124]. The increased morbidity associated with viral infections in CF is in part due to altered innate immune responses of CF airway epithelial cells [125, 126]. Furthermore, these infections damage the airway epithelial cell barrier and alter the immune system allowing bacteria to subsequently begin airway colonisation [120].

1.4.1.2 CF Fungal Airway Infections

Fungal infections also begin early in life for those with CF, with *Aspergillus fumigatus* being recognised as one of the most common early life pathogens [127]. Historically, *Aspergillus fumigatus*, *Candida albicans* and other filamentous fungi have been isolated from adults with CF [128] and were only considered clinically significant when they caused allergic bronchopulmonary aspergillosis [128]. However, fungal infections are now being increasingly associated with worsening lung disease and outcomes [129]. Additionally, these infections appear to predispose individuals to bacterial infections [129, 130] and may also increase their virulence [131]. However, evidence about their importance and treatability in CF is still emerging [132].

1.4.1.3 CF Bacterial Airway Infections

Bacterial pulmonary infections can occur soon after birth in CF and are typically caused by *Staphylococcus aureus*, which is known to exacerbate airway inflammation and lung damage [133]. Interestingly, *P. aeruginosa* infections can also occur as early as three years of age, but are typically intermittent and chronic colonisation is prevented with antibiotic therapies [134]. Eventually, eradication fails at around six years of age when pathogens colonise the airways and become chronic [130, 134]. As individuals with CF age, prevalence of *S. aureus* decreases and *P. aeruginosa* increases, with over 70% of adults becoming chronically infected [88, 90]. In addition to *P. aeruginosa*, a number of rarer pathogens also cause severe infections and have high levels of intrinsic AMR [88, 90] including *Burkholderia cepacia* complex organisms, *Achromobacter xylosoxidans*, *Stenotrophomonas maltophilia* and non-tuberculosis mycobacterium [88, 135-139]. However, *P. aeruginosa* is still considered the most important pathogen in CF due to its prevalence and strong association with airway inflammation, lung disease progression and ultimately mortality [112, 133, 140-143].

1.4.1.3.1 *P. aeruginosa* Infections in CF

P. aeruginosa infections begin with a period of intermittent isolation in children, typically at 2-3 years of age, but can occur even earlier at 3 months of age [134, 144]. Early intermittent colonisations are typically caused by environmental *P. aeruginosa*

isolates [145], which commonly exhibit a non-mucoid colony morphology and are usually motile and virulent but still susceptible to antimicrobials [146, 147]. However, widespread *P. aeruginosa* strains (epidemic strains) are now known to be responsible for 60% of infections [148] and have greater antimicrobial resistance [149-155]. Eradication of *P. aeruginosa* following each infection is attempted to prevent chronic colonisation and airway damage [156-162], but despite vigilant detection, aggressive eradication, and infection control strategies, it appears to only delay, and not prevent, the eventual establishment of chronic infection in the CF airway [89, 163].

Once a person with CF is persistently colonised, they often form AMR *P. aeruginosa* biofilms [164] and despite arising from a clonal population, diversification occurs via mutation [165]. This process is frequently accelerated via hypermutable sub-populations of cells with deficits in DNA repair systems [166-169]. However, features typically exhibited by persistently infecting strains include high antimicrobial resistance with 32% of isolates exhibiting carbapenem resistance [148], mucoid colony morphology, and attenuated motility and virulence [170]. These adaptations likely contribute to *P. aeruginosa* being the most common persistently colonising pathogen in adults with CF [163]. Given that chronic *P. aeruginosa* is an important driver of lung disease antibiotic treatment regimens are fundamental to prolonging colonisation and preserving airway health.

1.4.1.3.2 Anti-*P. aeruginosa* Antimicrobial Therapy in CF

Antimicrobials are used to treat *P. aeruginosa* at every stage of infection in people with CF. Early eradication therapy is performed every time *P. aeruginosa* is isolated from the airways, with the aim of preventing chronic infection and airway damage. Once chronic infections are established antimicrobial management strategies are used (Table 2) to slow functional decline, prevent exacerbations and morbidity occurring [171-177]. When exacerbations inevitably occur, antimicrobials are again used, but it appears that lung function levels are never restored even once the exacerbation resolves [178]. It has also been found that use of multiple broad-spectrum antimicrobials courses over the lifetime of someone with CF drives the development of multi-drug resistant *P. aeruginosa* in 31% of individuals [179, 180]. In treating AMR infections, including *P.*

aeruginosa, clinicians typically use last resort antimicrobials, antibiotic cocktails, and high drug concentrations that present safety issues [181, 182]. Furthermore, long-term use of high concentrations of antibiotics can also lead to the development of allergies to drugs, ototoxicity, renal toxicity, and *Clostridium difficile* infections from gut dysbiosis [183-185]. Since current strategies are no longer viable long-term solutions, alternative antimicrobials are urgently required.

Table 2: Different *P. aeruginosa* Antimicrobial Treatment Regimes

Therapy	Class of Antibiotic	Route of Administration	Reference
Early Eradication	Aminoglycoside/Polymyxin	Inhalation	[156, 158, 160-162, 186, 187]
Early Eradication	AND Quinolone	Oral	[156, 161, 162]
Management	Quinolone	Oral	[188]
Management	OR Aminoglycoside	Inhalation	[171-176, 188, 189]
Management	OR Polymyxin	Inhalation	[188, 190]
Exacerbation	Beta-lactam AND Aminoglycoside	Intravenous	[188]

1.4.1.3.3 Alternative Antimicrobial Strategies for *P. aeruginosa* Treatment

Investment in conventional antimicrobial discovery pipelines has decreased resulting in the development of few compounds [19, 28]. Thus, clinicians are now exploiting old compounds as last line treatments of AMR infections including in CF [191]. However, such compounds including polymyxin B and colistin were shelved originally due to toxicity issues [191, 192]. Resistance has already emerged to polymyxin compounds and will increase with their use [193]. Similarly, resistance appears commonplace with beta-lactamase inhibitors, currently used to potentiate existing antibiotics [194, 195]. Although many other beta-lactamases inhibitors are being investigated, they are unlikely to be long term solutions given that resistance has developed to similar compounds [196-199]. A potent cephalosporin derivative, under development, also appears promising and may provide relief in the management of multi-drug resistant *P. aeruginosa* infections, but again, given it is related to other antibiotics, resistance will likely to eventuate [200]. Trials on a completely novel antimicrobial, Murepavadin, that blocks an outer membrane protein transporting LPS specifically in *P. aeruginosa*, were stopped due to renal toxicity concerns [191, 201].

A suite of broad-spectrum antimicrobial peptides with varying actions against planktonic *P. aeruginosa* and biofilm communities are currently being investigated pre-clinically but are still far from translation into clinic [202-204]. Inhaled novel formulations of existing antimicrobials either as dry powder [205, 206] or liposomal [207, 208], have shown promise as a treatment of chronic *P. aeruginosa* airway infections in people without CF. However, there have been issues with reproducibility of efficacy outcomes delaying their approval [205-207]. Liposomal amikacin that is able to penetrate airway mucus and *P. aeruginosa* biofilms was trialled for use in CF [209] but due to safety concerns was not approved for use in this setting [191]. Sequential administration of synergistic existing antimicrobials has also been proposed to be effective against *P. aeruginosa* biofilms in chronic CF infections [210, 211]. Although, a subsequent *in vitro* study showed that this strategy was ineffective at removing persister cells [212]. There also biofilm disrupting compounds being developed. One compound that is under investigation is sodium nitrite. *In vitro* sodium nitrite has been shown to facilitate biofilm dispersal and antibacterial activity [213, 214]. These results led to a phase 1 and 2 clinical trial (NCT02694393) whose results are yet to be published. Furthermore, the divalent cation chelator, EDTA, causes the dispersal of biofilms [215]. It is being investigated as an adjunct to antibiotics to increase bacterial susceptibility, however this has yet to be shown in a clinical trial [216]. Since most of the pipelines described above exploited existing or related compounds, many of which have safety concerns, there is a need to develop novel antimicrobial pipelines especially in children where antibiotics are often used outside recommended dosages, age and infection types [194].

1.4.1.3.4 Novel Antimicrobial Strategies for *P. aeruginosa*

Several novel treatment strategies have been trialled or investigated for the treatment of *P. aeruginosa* infections. Firstly, a vaccine against *P. aeruginosa* has been developed and trials in people with CF found it to be associated with lower levels of infection, However, once vaccine stocks were depleted it appears to have been discontinued [217]. *P. aeruginosa* antigens have also been investigated including LPS [218], flagella [219], O-antigen toxin A conjugate [217] and oprF-oprI fusion [220]. Administration routes of vaccines have varied between each formulation with oral, injection, nasal and a live attenuated *Salmonella* delivery being trialled [220] [219] [217]. No licensed therapy is available to date because a common finding is that those vaccinated become infected with

P. aeruginosa not covered by vaccine antigens [220] and a Cochrane review has found there is insufficient evidence to support the treatment [221]. Given the heterogeneity and uniqueness of CF isolates of *P. aeruginosa*, it is difficult to administer all the relevant antigens thus formulation is challenging [220].

Another alternative being investigated are virulence blockers whose function are to negate bacterial quorum-sensing (QS) that regulate virulence factors [222]. These may reduce the effect on the host and group behaviours of *P. aeruginosa* without killing them therefore preventing marked resistance selection. Azithromycin is known to block QS [223] and is routinely used in CF but does not eradicate the bacteria [191]. Other virulence reducers target the iron scavenging of *P. aeruginosa* by providing a similar ion (gallium; Ga³⁺) that cannot be used in biochemical reactions [224]. In a phase I clinical trial of those with CF lung infections, the disruption of iron scavenging using gallium was successful [224]. Inhibitors of *P. aeruginosa* *LasB* elastase and type III secretion systems are also under investigation [191]. Two of the anti-pseudomonal antimicrobials currently being clinically trialled are monoclonal antibodies [225, 226] that target the type III secretion system. However, CF clinical isolates typically downregulate or lose virulence factors so it is unclear how useful such inhibitors of virulence factors would be in this setting.

Finally, another type of novel antimicrobial utilises bacteriophages (phage) which has a long history, dating back more than 100 years [227]. Phage therapy also offers many benefits compared to conventional treatments. Principally, these include bactericidal action against multidrug-resistant strains, auto-dosing (increasing at site of infection due to phage replication), minimal disruption to the microbiota as they only target specific hosts, relatively low cost of isolation and production, activity against biofilms, ability to evolve or be engineered to increase effectiveness and causing minimal toxicity to mammalian cells [228, 229]. Phages also provide a source of antimicrobial enzymes that are being investigated for therapeutic use including endolysins (the enzymes phages use to break through the peptidoglycan layer from within bacteria), virion-associated peptidoglycan hydrolases (used by the virus to destroy the peptidoglycan layer and inject the genome) and polysaccharide depolymerases (the enzymes phages use to degrade the exopolysaccharides to access their receptors on bacteria) [230, 231]. However, the enzymes unless engineered are mainly active against Gram-positive bacteria where peptidoglycan plays a greater role in membrane stability [231] and thus, whole phages has been preferred in treating Gram-negative bacteria.

1.5 Bacteriophages

There are more than 10^{31} bacteriophages on the Earth, making them the most abundant life-form [232]. Originally discovered in 1915 by Frederick Twort, their antibacterial potential was not realised until 1917 by Felix d'Herelle [233, 234], but their use and research in Western medicine slowed after the discovery of antibiotics. Despite this, use continued in Eastern European countries where early proof of principle trials were performed, and routine therapeutic treatment is still practised [235]. Despite the early trials of phage therapy often being successful, there were also notable trial design, technological and knowledge limitations that restricted the useability of results [236]. Despite largely being forgotten as a therapeutic, phage research continued, and many early biology discoveries were made through studying phage infections of bacteria [237].

Phages, themselves are protein structures protecting a nucleic acid. The nucleic acid can be DNA or RNA and both can be either single or double stranded [238]. However, the majority of phages discovered to date are double stranded DNA, followed by single stranded DNA, unclassified, single stranded RNA and double stranded RNA [239]. Variation exists in their morphology, with most studied having a head (containing the genome), a tail of variable length and rigidity (which transports the genome into the bacteria) and occasionally tail fibres [240]. Regardless of structure, all phages have a complex of proteins that initiate contact with a specific bacterial molecule that acts as a receptor and facilitates irreversible binding [241]. This is followed by a conformational change that allows the baseplate protein (at the base of the tail) to contact the bacterial surface, the tail tip then extends and pierces the bacterial membrane and injects its genome into the periplasm [242]. Once within the bacterial host, there are two main lifecycles that the phage can follow, obligately lytic or temperate [243]. To describe these concepts, lambda phage of *Escherichia coli* can be used as an example as it is the most well characterised phage [244]. As a temperate phage, lambda can integrate into the host bacterial genome or undergo the lytic lifecycle [245]. There have been a number of cues discovered which lambda senses in order to choose whether to lyse or integrate that are related to resource availability such as, low temperatures, high phage to bacteria ratio or in dormant cells [246, 247]. There are many protein interactions that inform the decision to integrate, but once it has been made the integration genes are upregulated and lysis genes inhibited [245]. Lambda is then integrated into the host genome through

homologous recombination, and it is maintained by production of a protein that inhibits early lytic gene expression [245, 248] and the phage genome replicated with the hosts'. Temperate phages can contain genes that enhance bacterial fitness, so the phage's host is not out competed, such as proteins to prevent further phage infection, virulence or antimicrobial resistance genes [249]. Bacterial host stressors like UV, antibiotics and other phages' infection cause the lytic inhibitor to be repressed and the transcription of early lytic genes [245]. Early genes upregulate the middle lytic genes and repress lysogenic genes [244, 245]. Middle lytic genes are for DNA replication and excision [244, 245]. These in turn upregulate late genes which encode structural and packaging proteins [244, 245]. The temporal transcriptional regulation of these different genes is tightly controlled by many interactions [244, 245]. Upon entering the bacterial periplasm, obligately lytic phages follow the lytic cycle similar to lambda and efficiently transcribe their own genes and alter host bacterial transcription [250-253]. Phages typically upregulate bacterial energy, nucleotide and amino acid synthesis genes and downregulate genes involved in metabolic pathways that are not required to reproduce themselves [250-253]. Lytic phage infection has also been shown to change the transcription of integrated temperate phages, as these might sense the need to excise [254]. Phage-mediated bacterial lysis is performed by late proteins consisting of holins, which degrade the cell membrane, and endolysins, which destroy the peptidoglycan layer [255]. Given that temperate phages do not exhibit an exclusively bactericidal lifecycle, they are often discounted from use in therapy and only obligately lytic are used.

Although using single lytic phages for therapy has been successful, their specificity mean that they can only target a limited range of bacteria [256]. Furthermore, there is also the potential of bacterial developing resistance to the phage [257, 258]. This can be overcome by using phage cocktails, phage enzymes, and combination therapies, which have been reviewed previously [257, 258]. Therefore, phages are often administered as a cocktail with several phages targeting multiple strains of a single species or multiple species [257, 258]. In cases where a phage cocktail that targets multiple strains of a single species, combined phages are genetically diverse, target different receptors on the bacterial surface and have complimentary host ranges [259, 260].

1.5.1 Phage Isolation and Characterisation for Therapy

To overcome the shortfalls of past therapies and formulate a successful cocktail therapy, phages must be isolated and characterised. Phages are isolated where their host bacteria are found [256, 261]. Common sources include clinical infection samples, like sputum [262], or from wastewater, especially if collected in close proximity to hospitals [263, 264]. Isolation of phages active against different bacterial species have varied in success, but *P. aeruginosa* phages tend to be the most commonly found [265]. Characterisation of isolated phages is essential to ensure that they exclusively follow a lytic lifecycle by ensuring phage genomes are free of temperate lifestyle genes such as integrases, excisionases and transposases [266, 267]. Bioinformatic analysis can also determine if a phage can potentially improve a bacterium's fitness by identifying if it carries bacterial virulence or AMR genes [266, 267] and is the gold standard for phylogeny determination [268]. Whilst phylogenetic trees are typically still used, gene networks are considered more accurate due to pervasive mosaicism of phage genomes, whereby evolution does not occur linearly from a common ancestor but instead multiple recombination events between phages [268]. However, bioinformatically studying phages is insufficient in order to determine their usefulness in therapy [256]. Phages that have cleared bioinformatic checkpoints have their activity determined against clinically relevant bacteria and the evaluate which phages can be combined into cocktails with greater host range [256, 261]. Full phage characterisation will enable a greater chance of phage therapy effectiveness which is important to further the field.

1.5.2 Phage Therapy for the Treatment of *P. aeruginosa*

Numerous studies have demonstrated the effectiveness of phage against *P. aeruginosa* and eukaryotic tolerability *in vitro* and *in vivo* [269-282]. Individual phages only infect a specific subset of *P. aeruginosa* strains, so the effectiveness of phage therapy may vary greatly in settings where multiple strains or variants of *P. aeruginosa* have colonised such as CF [283, 284]. Therapy effectiveness has been shown to be improved by combining phages with a diversity of host ranges into cocktails [269, 280] and synergistic phage-antimicrobial cocktail therapy [275, 279, 285, 286]. However, it is important to determine the effects of antibiotic combination on phage infection empirically as antibiotics often impact bacterial pathways that are important for phage replication such as the ribosome and DNA synthesis [287-289].

Initial experimental successes have led to the compassionate use of phage therapy for treatment of AMR infections, including *P. aeruginosa* (Table 3). Most have been successful to those treated, and documented failures attributed to a participants advanced disease accompanying infection, or the develop of new infections [290-294]. Phage therapy has been well tolerated in all but one case, where 10^{11} PFU/mL was found to cause wheezing with an accompanying fever but when dosage was reduced to 10^{10} PFU/mL or new phages used, no adverse events were reported (Table 3; [293]. Despite the growing body of data from compassionate use applications, there have been limited clinical trials involving phage therapy (Table 4). Two of these trials have been successfully completed and published: a trial involving the treatment of *P. aeruginosa* ear [295] and burn infections [296]. Outcomes from these studies showed that phage therapy was effective [295] and safe [296]. Phage therapy has still not become routine clinical care necessitating additional future trials, however, how phage therapy is ultimately regulated will need to be informed by additional pre-clinical studies and open collaboration [297]. Despite progress made, one area requiring further investigation is the evolution of phage resistance and its suppression [298]. The importance of phage resistance has also been realised in the compassionate treatment of AMR infections and has necessitated rapid cocktail reformulation in order to prevent treatment failure [293, 299-302]. As a result, it is important to consider phage resistance in the context of *P. aeruginosa* AMR infection to ensure the efficacy of phage therapy in the long-term.

Table 3 Documented Compassionate Uses of Phage Therapy (as of September 2023).

	Bacteria	Condition	Outcome	Reference
CF <i>P. aeruginosa</i> Infections	<i>P. aeruginosa</i>	9 people with CF respiratory infections	Reduction in <i>P. aeruginosa</i> and increased lung function	[303]
	<i>P. aeruginosa</i>	CF airway infection	Infection resolution allowing successful lung transplant	[304]
	<i>P. aeruginosa</i>	CF airway infection	Infection resolution allowing successful lung transplant	[293]
Non-CF <i>P. aeruginosa</i> Infections	<i>P. aeruginosa</i>	Ventilator associated pneumonia	Infection resolution and eradication	[305]

	<i>P. aeruginosa</i>	Non-CF airway infections	Infection resolution	[302]
	<i>S. aureus, P. aeruginosa and E. faecium</i>	Heart surgery infection and airway infection	Infections resolved, but died due to new <i>E. coli</i> and <i>P. aeruginosa</i> infections	[290]
	<i>P. aeruginosa</i>	Lung transplant wound infection	Infection resolved	[290]
	<i>P. aeruginosa</i>	Spinal infection	Infection resolution	[306]
	<i>P. aeruginosa</i>	Heart surgery infection	Infection resolution	[307]
	<i>P. aeruginosa</i>	Heart device infection	No infection resolution	[293]
	<i>P. aeruginosa</i>	Nasal decolonisation	Nasal decolonisation	[308]
	<i>P. aeruginosa</i>	Heart surgery infection	Unclear	[309]
	<i>P. aeruginosa</i>	Pneumonia in lung transplant recipient	Infection resolved	[293]
	<i>P. aeruginosa</i>	Heart device infection	No infection resolution and fever and wheezing when given phages at 10^{11} PFU/mL	[293]
	<i>P. aeruginosa</i>	Heart surgery infection	Infection resolved	[293]
Non-<i>P. aeruginosa</i> CF Infections	<i>Burkholderia dolosa</i>	CF airway infection	Therapy failed and patient died	[302]
	<i>A. xylosoxidans</i>	CF respiratory infection	Patient stabilisation, no infection parameters	[310]
	<i>A. xylosoxidans</i>	CF respiratory infection	Infection resolved	[311]
	<i>A. xylosoxidans</i>	CF respiratory infection, post lung transplant	Infection resolved, but colonisation proceeded	[312]
	<i>M. abscessus</i>	chronic CF respiratory infection	Infection resolution	[313]
	<i>M. abscessus</i>	Disseminated infection post CF lung transplant	Infection resolution	[314]

Non-<i>P. aeruginosa</i> Non-CF Respiratory Infections	<i>A. baumannii</i>	COPD respiratory infection	<i>A. baumannii</i> infection resolved, but other species caused subsequent infections	[291]
	<i>A. baumannii</i>	Ventilator associated pneumonia	Infection control in four patients, however one died of another infection	[292]
	<i>A. baumannii</i>	Ventilator associated pneumonia	Infection resolution	[315]
	<i>M. abscessus</i>	chronic infection in non-CF bronchiectasis	Initial infection control but antibody response limited efficacy	[316]
Non-<i>P. aeruginosa</i> Non-CF Non- Respiratory Infections	<i>E. coli</i>	Urinary tract infection	Infection resolved	[293]
	<i>S. aureus</i>	Prosthetic joint infection	Infection resolved	[293]
	<i>S. aureus</i>	Heart device infection	Infection resolution allowing successful heart transplant	[293]
	<i>A. baumannii</i>	Cranial osteomyelitis	Unclear as infection resolved but no neurologic improvement	[293]
	<i>A. baumannii</i>	Disseminated infection	Infection resolved	[293]
	<i>K. pneumoniae</i>	Respiratory infection	Infection resolved	[290]
	<i>S. aureus</i>	Bloodstream infection	Infection resolved	[290]
	<i>S. aureus</i>	Heart device wound infection	Infection resolved	[290]
	<i>S. aureus</i>	Heart implant infection	Bacterial reduction but ultimately died of sepsis	[290]
	<i>S. aureus</i>	blood and catheter infection	Infection resolved	[290]
	<i>E. coli</i>	Heart device wound infection	Infection resolved	[290]
	<i>S. aureus</i>	Bloodstream infection	No response and treatment stopped	[294]

Table 4 Clinical Trials of Phage Therapy Registered Through the National Library of Medicine Clinical Trials Registry (as of September 2023).

NCT Trial Number	Study Status	Conditions
NCT04803708	COMPLETED	<i>P. aeruginosa</i> , <i>S. aureus</i> and <i>Acinetobacter</i> diabetic foot ulcer infection
NCT00663091	COMPLETED	Venous Leg Ulcers
NCT05498363	COMPLETED	Bacterial Infections
NCT05369104	RECRUITING	Infection of total hip joint prosthesis and total knee joint prosthesis
NCT05883995	RECRUITING	Bone infection
NCT05177107	RECRUITING	Diabetic foot osteomyelitis
NCT04650607	RECRUITING	Severe prosthetic Joint Infection
NCT05616221	RECRUITING	Non-cystic fibrosis bronchiectasis <i>Pseudomonas aeruginosa</i> lung infection
NCT05488340	RECRUITING	Urinary tract infections
NCT05453578	RECRUITING	Cystic fibrosis <i>P. aeruginosa</i> colonisation
NCT05184764	RECRUITING	<i>S. aureus</i> bacteraemia
NCT05010577	RECRUITING	Cystic fibrosis chronic <i>P. aeruginosa</i> infection
NCT05269134	RECRUITING	Prosthetic Joint Infection
NCT04596319	ACTIVE_NOT_RECRUITING	Cystic fibrosis <i>P. aeruginosa</i> lung infections
NCT05537519	ACTIVE_NOT_RECRUITING	Recurrent urinary tract infection
NCT04682964	ACTIVE_NOT_RECRUITING	Acute tonsillitis
NCT04684641	ACTIVE_NOT_RECRUITING	Cystic fibrosis
NCT05272579	NOT_YET_RECRUITING	Necrotizing enterocolitis
NCT04323475	NOT_YET_RECRUITING	<i>P. aeruginosa</i> and <i>E. coli</i> wound infection

NCT05269121	NOT_YET_RECRUITING	Prosthetic joint Infection bacterial infections
NCT04815798	NOT_YET_RECRUITING	Pressure ulcer
NCT05948592	NOT_YET_RECRUITING	Diabetic Foot Infection
NCT02664740	NOT_YET_RECRUITING	<i>S. aureus</i> diabetic foot ulcer
NCT00945087	UNKNOWN	Bacterial Infections
NCT02116010	UNKNOWN	<i>P. aeruginosa</i> burn wound infection
NCT04787250	WITHDRAWN	Prosthetic Joint Infection
NCT03395743	NO_LONGER_AVAILABLE	<i>P. aeruginosa</i> infections
NCT04636554	NO_LONGER_AVAILABLE	<i>P. aeruginosa</i> , <i>S. aureus</i> and <i>A. baumannii</i> septicemia and bacteraemia
NCT03395769	NO_LONGER_AVAILABLE	<i>S. aureus</i> infections
NCT04287478	TERMINATED	Urinary tract infection bacterial

1.6 Phage Resistance

Bacterial resistance to phages can occur at every stage of the phage lifecycle from: (i) receptor recognition and binding, (ii) genome injection, (iii) DNA replication, (iv) transcription and translation, (v) phage assembly, and (vi) phage release. The general bacterial phage-resistance mechanisms have been reviewed previously [317] and are still being discovered [318]. The evolution of bacterial resistance to phages is very rapid due to there being billions of bacteria in a single colony and the existence of resistant mutants. Likewise, phage evolution in response to bacterial changes is also rapid because 10 to >100 phages are released by productive infection of a host bacterium. The rapid reciprocal evolution of bacteria and phages has been explained by the Red Queen theory of evolution, where parasite and host are continually mutating, resulting in the relationship appearing static [319]. In the pursuit of understanding this host-parasite relationship, two of the most important genetic engineering technologies have been discovered, namely Clustered Regularly Interspaced Short Palindromic Repeat (CRISPR-cas) and restriction enzymes. However, in the context of phage therapy, the resistance predominantly occurs at the receptor recognition and binding stage through receptor mutations [320].

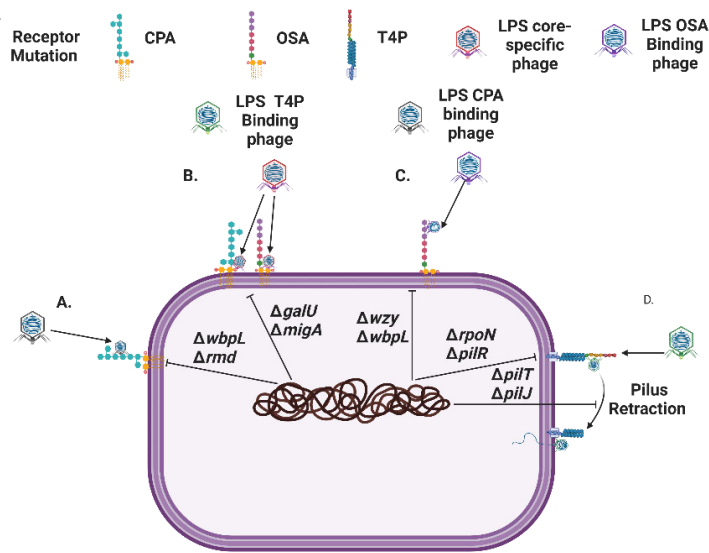


Figure 1: Common *Pseudomonas aeruginosa* Genetic Mutations that Prevent the Phage Receptors being Synthesised or Functioning. (A) CPA (Common Polysaccharide Antigen), (B) LPS core, (C) OSA (O-Specific Antigen) and (D) T4P (Type IV Pili). Created with BioRender.com.

1.7 *P. aeruginosa* Phage Resistance

P. aeruginosa has been found to have the highest diversity of intrinsic phage resistance mechanisms [321] and can evolve resistance in several ways. In the context of phage therapy where phages will be tested for activity against clinical isolates before being used, the predominant forms of resistance will be those that are evolved. There is growing evidence that bacteria, including *P. aeruginosa*, resist phage infection through mutating the receptors that phages recognise.

1.7.1 Receptor Mutations

Commonly identified receptors for *P. aeruginosa* phages are lipopolysaccharide and type IV pili (T4P) [322], with the phage OMKO1 using OprM, which is a key component of the MexAB-OprM antibiotic efflux pump [323]. Development of resistance to OMKO1 was shown to increase antimicrobial susceptibility in an initially multi-drug-resistant strain of *P. aeruginosa* [323]. This suggests that the effect of phage resistance may be beneficial in reducing antimicrobial resistance and that combined antimicrobial-phage therapy could prevent resistance evolving to either treatment. The phage resistance mutations identified in previous studies have been summarised in Appendix Table B.1.

LPS is composed of lipid A (membrane embedded domain), a core (domain connecting lipid A and O-antigen), and O-antigen (polysaccharide that extends extracellularly). *P. aeruginosa* expresses three types of O-antigen, which include the common polysaccharide antigen (CPA; homopolymer O-antigen), O-antigen specific (OSA; heteropolymer O-antigen), and uncapped antigen (no or one O-antigen sugar). Therefore, resistance mutations for LPS-exploiting phages vary according to which LPS component or type the phage specifically binds (Figure 1). Mutations to T4P can occur in genes encoding structural components, therefore preventing the receptor being created or those that drive pilus retraction for twitching motility (Figure 1). Retraction of T4P is required by pili-specific *P. aeruginosa* phages because it allows them to meet the host membrane and continue infection [324]. Additionally, receptor mutations range from single base-pair alterations to >100 kbp multi-gene deletions (refer to Appendix Table B.1). Receptor mutations can also have wider effects than the phage receptor through altering genes with multiple functions (refer to Appendix Table B.1). In some cases, large or regulatory gene mutations may be beneficial to *P. aeruginosa* by providing cross-resistance to other phages, they can also result in increased fitness costs [325]. Oechslin et al. (2016) found that a phage-resistant mutant carrying a large genomic deletion had increased susceptibility to ciprofloxacin and by exploiting this via combined phage-antimicrobial therapy, resistant bacterial mutants were suppressed. However, even small mutations to phage receptors, when phages are not present, have been shown to attenuate bacterial growth [282, 326], biofilm formation [327, 328], motility [275, 282, 328, 329], antimicrobial resistance [275, 323], virulence, and infectivity [275, 282, 330].

The strength of both phage resistance and the associated fitness cost is phage-specific [326]. Therefore, it is theoretically possible to combine phages into cocktails to provide multiple distinct selection pressures, which also comes with a maximum cost to fitness. Yang et. al. (2020) strategically formulated a cocktail of phages that successfully suppressed the evolution of resistance, but after prolonged incubation phage resistance was observed. Further suppression of phage resistance could be attained by using phages specific for more receptors, combining phages with antimicrobials, exploiting the fitness cost of phage resistance in therapeutic formulation, and including phages that kill specific resistant mutants of bacteria (escape mutants; Figure 2A). Moreover, the use of strains from non-CF origins in all but one of the studies of *P. aeruginosa* phage resistance [275] has neglected the contributions of the unique adaptations of CF clinical isolates of *P.*

aeruginosa on phage therapy and resistance. Therefore, this paucity limits the relevance of findings to the treatment of CF airway infections.

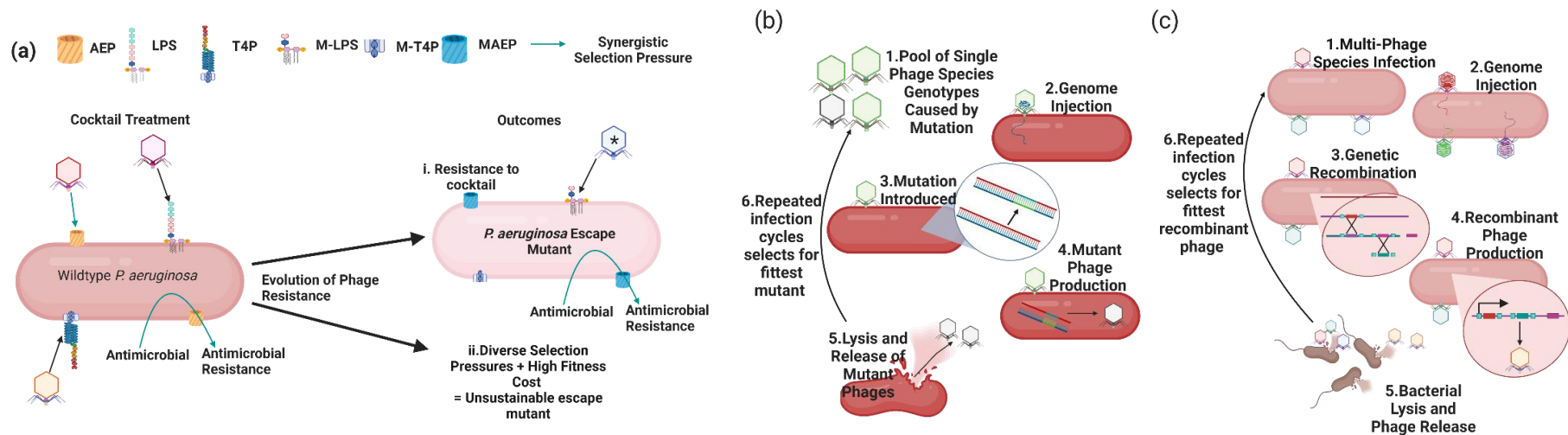


Figure 2. Methods to Prevent or Overcome Phage Resistance. (A) The Rationale for strategic cocktail formulation. Cocktails contain phages that use different receptors like lipopolysaccharide (LPS) or type IV pili (T4P) or antimicrobial resistant determinants (antibiotic efflux pumps; AEP) so that addition with antimicrobials provides opposite and synergistic selection pressures. This will result in outcome i. resistance arising to all the phages through mutations that alter the receptors for example resulting in mutated antibiotic efflux pump (MAEP), mutated LPS (M-LPS) and mutated T4P (M-T4P). This outcome can be prevented by adding a phage to the cocktail that specifically kills the escape mutant therefore forcing further different mutations in the bacteria which could result in outcome ii. Outcome ii. whereby the selection pressures are so diverse and come with a high fitness trade-off that resistance is unsustainable. (B) Phage evolution by spontaneous small mutation. (C) Phage evolution by genetic recombination between multiple phages. Created with BioRender.com.

1.7.2 Superinfection Systems

Temperate phages, capable of both lysis and integration into the host bacterial genome, are abundant in CF isolates of *P. aeruginosa* [331, 332]. Phages exhibiting temperate lifecycles are not used for phage therapy because integration into the host genome can increase *P. aeruginosa* virulence [331, 333, 334], antimicrobial resistance [331], and biofilm formation [332]. Temperate phages integrated into bacterial genomes can also increase host fitness by providing resistance to the subsequent phage infection, known as superinfection resistance. Mechanistically, this is achieved through the alteration of the two most common *P. aeruginosa* phage receptors (T4P and LPS) and production of repressors of phage infection [334, 335]. Superinfection resistance prevents the infection of a limited range of phages, which is determined by both the temperate phage and the *P. aeruginosa* host [335-338]. As phage therapy does not use temperate phages, superinfection resistance can be circumvented by conducting host range experiments. The host range experiments enable the identification of lytic phages that are not resisted by the temperate phages contained in a *P. aeruginosa* isolate. However, due to the mobile nature of temperate phages, these may become a problem *in vivo*, as they may transfer superinfection resistance between different *P. aeruginosa* strains. However, the chance of temperate phage mobility causing treatment failure can be minimised with an adequately diverse cocktail as superinfection resistance is only provided to a defined range of phages [335].

1.7.3 Masking Phage Receptors

The phenomenon of masking has been shown to be mediated by glycosylation of the T4P receptor on *P. aeruginosa*, providing it with resistance [339]. Unlike mutations to phage receptors, glycosylation does not affect the T4P-mediated twitching motility [339]. To overcome this mechanism of resistance, phages identified during host range characterisation could be selected or trained to be capable of infecting bacteria with a glycosylated T4P. Moreover, *P. aeruginosa* formation of biofilms and secretion of exopolysaccharide (EPS) can facilitate masking of receptors by preventing phage penetration and receptor binding [340]. However, some phages are more capable of penetrating biofilms due to the production of matrix degradative enzymes [341]. Outer membrane vesicles (OMVs) can provide *P. aeruginosa* with phage resistance [342].

OMVs possess LPS-specific phages' receptors which causes binding and neutralisation of the phages [342]. Unlike in other bacterial species, *P. aeruginosa* OMVs did not resensitise resistant bacteria by transfer of a phages' receptors [342]. OMV resistance could be overcome by using diverse phages that target different receptors.

1.7.4 CRISPR-cas

CRISPR-cas arrays are abundant in *P. aeruginosa* including CF isolates [343] and can mediate immunity to specific phages [344]. The CRISPR RNA (crRNA) component of the CRISPR-cas binds complementary phage-specific DNA sequences allowing cas nucleases to cleave the recognised invader's DNA. CRISPR-cas is also capable of adaptation so that a bacterium that survives an infection can incorporate a phage's DNA into its CRISPR-cas array. Adaptation allows a bacterium to recognise and prevent subsequent infections with the same phage. The CRISPR-cas found in *P. aeruginosa* falls into the subtype I-F, which has four cas-associated genes (that aid crRNA production and target recognition) and two cas nuclease genes (for cleavage of target and adaptation) [343]. However, phages are able to resist CRISPR-cas resistance [345, 346] and therapy uses cocktails of diverse phages, meaning it is unlikely to be the main form of resistance that evolves [320]. Increasingly, the complex interplay of phage, bacteria, and environment on CRISPR-cas phage resistance is being illuminated. CRISPR-cas phage resistance frequency is increased by any factor that reduces bacterial growth rate, including bacteriostatic antibiotics [347], reduced environmental temperature [348] and nutrient poor environments [349]. Reduced bacterial growth rate slows phage replication and maturation therefore leaving more time for bacteria to gain CRISPR-cas resistance [349]. Other factors that influence the frequency of CRISPR-cas phage resistance are the density of infecting phages [349] and bacterial mutation rate [350]. These two factors may hold relevance for phage therapy in CF where hypermutator phenotypes are common, which may favour receptor mutation resistance and unnaturally high doses of phages used for therapy may do the same. Nonetheless, recent *in vitro* work has shown that *P. aeruginosa* isolates develop CRISPR-cas resistance to single phages [320]. Recently, the complementation of phage therapy with QS inhibitors has been proposed to prevent CRISPR-cas resistance [351]. However, the QS inhibitor down regulated the phage's receptor causing antagonism, so interaction with phages that bind other receptors needs to be investigated [351].

1.7.5 Restriction-Modification (RM) Systems

Restriction-modification (RM) systems also provide immunity to phages by recognising and cleaving DNA sequence motifs [352]. Unlike CRISPR-cas systems, these motifs are less phage-specific and not adaptive. To prevent destruction of the bacterial genome, the nucleases are often associated with methylases or other nucleotide modifiers that mark the motifs on the self-DNA, thereby preventing its cleavage [352]. Two RM-associated systems have recently been characterised including Bacteriophage Exclusion (BREX) and Defence Island Associated with Restriction-Modification (DISARM) [318]. A third system called DNA Degradation (DND) denotes self-DNA via sulphur addition [353]. Identification and characterisation of these RM-associated systems and their role in *P. aeruginosa* have not been thoroughly explored. Although genome analysis has indicated BREX and DISARM components are present in *P. aeruginosa* genomes [318]. Similarly, other phage resistance mechanisms, like cell-signalling coupled with abortive infection and many unknown modes of action systems, have been predicted by *P. aeruginosa* genomic analysis, but are yet to be functionally verified [318].

1.7.6 Other Phage Resistance Mechanisms

Phage resistance mechanisms are continually being identified in genome sequences and validated. These are typically found in two core defence hotspots and are rich in mobile genetic elements to facilitate their dissemination [321] and have been summarised in Table 5.

Table 5 Other Types of Phage Resistance Mechanisms Found in *P. aeruginosa* Genomes

Mechanism	Type	Reference
AbiEii	Abortive infection	[354]
AVAST II	Abortive infection	[355]
Azaca	Nuclease activity	[356]
Borvo	Unknown mechanism. Proteolytic activity	[356]
BREX I	Phage DNA interference	[357]
BREX II	Phage DNA interference	[357]
BREX III	Phage DNA interference	[357]
Bunzi	Unknown mechanism	[356]

CBASS I	Abortive infection	[358]
CBASS II	Abortive infection	[358]
CBASS III	Abortive infection	[358]
CBASS III	Abortive infection	[358]
DarTG	Abortive infection	[359]
dCTPdeaminase	Destroys nucleotides and prevents phage DNA replication	[360]
DISARM 1	Phage DNA interference	[361]
DndABCDE	Phage DNA interference	[362]
DRT3	Unknown mechanism	[355]
Druantia I	Unknown mechanism	[363]
Druantia II	Unknown mechanism	[363]
Druantia III	Unknown mechanism	[363]
Dynamins	Lysis delay to reduce phage spread	[364]
Gabija	Unknown mechanism	[363]
GaoMza	Unknown mechanism	[355]
GaoQat	Unknown mechanism	[355]
GaoRL	Unknown mechanism	[355]
GaoUpx	Unknown mechanism	[355]
Hachiman	Unknown mechanism	[363]
Kiwa	Unknown mechanism	[363]
Lamassu	Abortive infection	[363]
Lamassu-Fam	Abortive infection	[363]
MokoshType I	Phage RNA degradation	[356]
PARISI	Prophage encoded abortive infection	[365]
PsyrTA	Abortive infection	[356]
RetronIC	Abortive infection	[355]
RosmerTA	Abortive infection	[356]
Septu	Unknown mechanism	[363]
Shango	Unknown mechanism	[321, 356]
Shedu	Unknown mechanism	[363]

SoFic	Unknown mechanism	[356]
SspBCDE	Damages phage DNA	[366]
ThoerisI	Abortive infection	[367]
ThoerisII	Abortive infection	[367]
Tiamat	Unknown mechanism	[356]
WadjetI	Unknown mechanism	[363]
WadjetII	Unknown mechanism	[363]
ZoryaType I	Abortive infection	[363]
ZoryaType II	Abortive infection	[363]

1.7.7 Phage evolution to Improve Therapeutic Potential

As previously mentioned, the relationship between bacteria and phages is reciprocal and the ability of phages to evolve alongside bacteria is an advantage compared to conventional antimicrobials. During DNA replication, phages undergo small mutations (Figure 2B). These are often in the receptor binding proteins, which are responsible for phage-host range and receptor recognition [368]. When multiple phages are present, as in a cocktail, evolution can occur through genome recombination (Figure 2C). Recombination creates a phage with a mosaic genome of its multiple ancestors (Figure 2C) [369]. Experimentally, evolution through recombination can produce a phage capable of infecting several initially resistant *P. aeruginosa* strains [369]. Evolution of phages can also be used to pre-adapt them to the bacterial host, suppressing the propagation of both receptor mutations [370, 371] and CRISPR-cas resistance [344]. Additionally, phages can be evolved (termed phage training) to overcome the resistance evolved by a *P. aeruginosa* strain [372]. Experimentally evolved phages require stringent genome characterisation to identify any that have picked up bacterial or temperate phage genes. Phages found to contain any deleterious genes can then be excluded from being considered in therapeutic formulation.

Phages have also evolved genes that encode proteins capable of overcoming other resistance mechanisms employed by *P. aeruginosa*. To overcome the resistance mediated by the masking of receptors, phages have evolved to carry biofilm-degrading enzymes

[341]. The enzymes breakdown the exopolysaccharide molecules in a biofilm matrix and allow more efficient penetration and phage infection [341]. Therefore, isolating and identifying phages with biofilm-degrading enzymes, through genome bioinformatic characterization, could provide preferential constituents of a cocktail for the treatment of *P. aeruginosa* biofilm infections. Additionally, phages can carry anti-CRISPR genes whose products circumvent CRISPR-cas resistance. Anti-CRISPRs can function through binding CRISPR-cas components, causing conformation changes that are non-functional; mimicking DNA to competitively bind CRISPR-cas, preventing recognition; binding cas nucleases, making them unable to interact and degrade phage sequences; and silencing the expression of CRISPR-cas genes [373]. Furthermore, co-operation between phages with anti-CRISPRs is integral to their infection success naturally so it may be an important consideration in cocktail formulation [374, 375]. Phage can also contain genes that disrupt QS systems which is an upstream regulator of phage resistance mechanisms including CRISPR-cas [376]. Therefore, phages found to contain anti-resistance genes like anti-CRISPRs or QS inhibitors, during characterisation, may be more applicable in a therapeutic cocktail formulation to prevent CRISPR-cas resistance arising against themselves and other phage constituents. To prevent RM system resistance, phages modify their nucleotide bases. Modified nucleotides in phage genomes, such as archeosine [261], queosine [377], hypermodified thymidine, and guanine bases [378], prevent DNA motif recognition and degradation. Phages more resistant to RM resistance can be found through genomic analysis identifying those with genes capable of modifying nucleotides [261].

1.8 Preclinical models

To ensure the translation of phage therapy, preclinical studies need to account for clinically relevant factors. Bacterial genetic factors are fundamental to phage therapy outcomes including the evolution of resistance [308, 379]. Since phage therapy is being proposed for CF airway infections it is especially important to use CF clinical isolates which are genotypically and phenotypically distinct to *P. aeruginosa* from other settings [379, 380]. Additionally, CF isolates of *P. aeruginosa* display high diversity, region specific genotypes [381] and intra-patient temporal genotypic and phenotypic changes [283, 382]. Therefore, to ensure accurate predictions of how phage resistance will evolve

and what therapeutic formulation may offer the most effective suppression, phage resistance needs to use a range of CF clinical isolates.

Furthermore, since phage therapy will be used to treat CF lungs infections, any potential effect on the human airways will also need to be assessed. Several animal models have been developed to enable the preclinical testing of CF therapies; however, many are limited in their ability to fully mimic CF lung infection pathology [383]. For example, although the CF porcine model successfully mimics several facets of the human disease including pancreatic deficiency, meconium ileus (MI) and similar airway epithelia and submucosal gland (SMG) activities. However, the model's use is limited due to its severe disease pathology and high mortality shortly after birth due to the gastrointestinal obstructions caused by MI [384-386]. Similarly, sheep models of CF have also been created but rarely used due to its severe disease pathology [387]. Although both the CF ferret model appears to overcome some of the difficulties in animal husbandry that larger CF animal models face, they also experience challenges in model longevity due to severe gastrointestinal manifestations [388]. Murine models of CF poorly reflect human CF disease due to difference in airway anatomy, disease manifestations and *CFTR* structure and expression [389-392]. However, there has been some success with *Scnn1b*-Transgenic mice which overexpress β -ENaC ion channels recapitulating a number of CF lung disease symptoms. These include reduced ASL, defective mucus clearance, mucus plugging, heightened inflammation and susceptibility to bacterial infection [393, 394]. Cell lines have also been used previously test the safety and efficacy of phage therapy [395-397]. These studies have not found any inflammation elicited by phage treatment and the therapy have been effective [395-397]. Rodent models of CF appear to more closely recapitulate human CF disease [398, 399], but since being only recently developed, the full extent of airway abnormalities still needs to be characterised [383].

In vitro CF cell lines, including CuFi or CFBE41o-, are commonly used in preclinical testing of therapies [383, 400, 401]. However, due to transformation, they behave differently and cannot fully differentiate into the cell types of the airway epithelium [402-404]. Primary airway epithelial cells (AEC; nasal and bronchial) can now be obtained from people with CF and cultured [125, 405-410]. Furthermore, these cells can undergo

differentiation at the air-liquid interface (ALI) which enables them to form a pseudostratified layer typically found in the airways, comprised of various cell types which are adhered to each other by tight junctional proteins [405, 411-416]. Although there are no reports assessing the preclinical safety of phages and/or combinations utilising primary AEC ALI cultures, studying the cell damage, and inflammatory markers stimulated by phage therapy in this model would provide great insight into its effects on the airway. However, the area of phage resistance remains severely understudied and by increasing its clinical relevance could lead to more effective and successful phage therapy formulations.

1.9 Summary

AMR bacterial infections pose a major threat to modern healthcare and is not being met by conventional development pipelines. Those most vulnerable to AMR bacterial infections are those living with chronic illnesses such as people with CF. These individuals are frequently infected by one of the most AMR bacterial pathogens, *P. aeruginosa*. Despite continued antimicrobial therapy chronic *P. aeruginosa* infections are common in people with CF, where they drive lung disease, functional decline and without transplantation eventually lead to death. Phage therapy has shown promise in treating AMR bacterial infections in people on a compassionate basis as shown in Table 1.3. However, fewer of these are for the treatment of *P. aeruginosa* infections in people with CF [293, 303, 304]. It has emerged that resistance to phages could potentially be a problem for the broader clinical translation of phage therapy. Whilst studying *P. aeruginosa* phage resistance has identified several mechanisms, it is predominantly caused by receptor mutation. Receptor mutations often come with bacterial fitness costs like antibiotic re-sensitisation, so it is possible to see how *P. aeruginosa* becomes resistant to phages and use this information to inform future cocktail/combination therapies. However, the majority of *P. aeruginosa* phage resistance studies have been done using laboratory strains which do not reflect clinical isolates, especially not those from CF. To ensure biological accuracy, it is essential that *in vitro* studies are performed using representative clinical isolates of *P. aeruginosa*. Information will facilitate the formulation of effective cocktails/combinations that prevent or suppress resistance which then need to be tested pre-clinically to ensure their safety.

1.10 Hypothesis and Aims

This study aimed to test the hypothesis that:

Identified phage cocktails and/or combination with antibiotics can suppress phage-resistance against planktonically growing *P. aeruginosa* compared to single phage preparations. Furthermore, identified effective formulations will not be inflammatory or cytotoxic to the host airway.

This was achieved through four aims:

1. To isolate and characterise phages with therapeutic potential against *P. aeruginosa* from wastewater.
2. To evolve and characterise resistance to phage treatment in CF clinical isolates of *P. aeruginosa*.
3. To formulate phage cocktails and test them for their ability to suppress phage resistance.
4. To test if the phage cocktail elicits inflammatory marker secretion or cytotoxicity in primary airway epithelial cells cultured at ALI.

2. Materials and Methods

2.1 General Materials

All general materials used in this thesis are listed in the table below.

Table 2.1 General Materials

Material Name	Supplier
0.22 µM syringe filter	Cytiva Whatman GmbH, Marlborough, Massachusetts, United States of America
0.22 µm bottle-top filter	Nalgene™ Rapid-Flow™, Thermo Fisher Scientific, Waltham, MA, USA
25, 27 and 28 G Needles	TERUMO, Macquarie Park, New South Wales, Australia
100kb Extended Ladder	New England Biolabs, Ipswich, Massachusetts, United States of America
6X Loading Dye	New England Biolabs, Ipswich, Massachusetts, United States of America
Acetic Acid	Sigma-Aldrich, St. Louis, Missouri, United States of America
Adenine	Sigma-Aldrich, St. Louis, Missouri, United States of America
Alcian Blue 8X	Sigma-Aldrich, St. Louis, Missouri, United States of America
Amphotericin B	Thermo Fisher Scientific, Waltham, Massachusetts, United States of America
Bacteriological Agar	Becton Dickinson Microbiology, Franklin Lakes, New Jersey, United States of America
Basal Epithelial BEBM™	Lonza, Basel, Switzerland
Biotin Conjugated Rat Anti-Human IL-6 2° Antibody	Becton Dickinson Biosciences, Franklin Lakes, New Jersey, United States of America
Bovine Serum Albumin (BSA)	Sigma-Aldrich, St. Louis, Missouri, United States of America
Bronchial epithelium Basal Medium (BEBM™)	Lonza, Basel, Switzerland
Calcium Chloride Hexahydrate (CaCl ₂ .6H ₂ O)	Sigma-Aldrich, St. Louis, Missouri, United States of America
Cefepime	Sigma-Aldrich, St. Louis, Missouri, United States of America
Ceftazidime	Sigma-Aldrich, St. Louis, Missouri, United States of America
Chloroform (>99.9%; CHCl ₃)	Sigma-Aldrich, St. Louis, Missouri, United States of America
Cholera Toxin	Sigma-Aldrich, St. Louis, Missouri, United States of America
Chromogenic Limulus Amebocyte Lysate Endotoxin Kit	Charles River, Marlborough, Massachusetts, United States of America
Ciprofloxacin	Sigma-Aldrich, St. Louis, Missouri, United States of America

Collagen Type 1 (rat tail)	Roche, Castle Hill, New South Wales, Australia
Cryo 1°C Freezing container “Mr Frosty”	Wessington Cryogenics, Houghtonle-Spring, Tyne & Wear, United Kingdom
Cryovials	Nunc, Roskilde, Denmark
Cuvettes	SARSTEDT AG & Co. KG, Nümbrecht, Germany
DELFIA [®] Assay Buffer	PerkinElmer, Waltham, Massachusetts, United States
DELFIA [®] Enhancement Solution	PerkinElmer, Waltham, Massachusetts, United States
Dimethyl sulfoxide (DMSO)	Sigma-Aldrich, St. Louis, Missouri, United States of America
DNase I 1 U/μL	New England Biolabs, Ipswich, Massachusetts, United States of America
DNase I 10X buffer	New England Biolabs, Ipswich, Massachusetts, United States of America
DNeasy Tissue and Blood Extraction Kit	Qiagen, Hilden, Germany
Dulbecco’s Modified Eagle Medium (DMEM)	Thermo Fisher Scientific, Waltham, Massachusetts, United States of America
Europium Labelled Streptavidin	PerkinElmer, Waltham, Massachusetts, United States
Endochrome-K limulus amoebocyte lysate kinetic chromogenic assay	Charles River Laboratories International, Inc., Wilmington, Massachusetts, United States of America
Epidermal growth factor (EGF) recombinant human	Sigma-Aldrich, St. Louis, Missouri, United States of America
Epinephrine hydrochloride	Sigma-Aldrich, St. Louis, Missouri, United States of America
Ethyl alcohol (C ₂ H ₆ O; Ethanol)	Sigma-Aldrich, St. Louis, Missouri, United States of America
Ethylenediaminetetraacetic Acid (EDTA)	Sigma-Aldrich, St. Louis, Missouri, United States of America
Ethylenediaminetetraacetic Acid calcium disodium salt (caEDTA)	Sigma-Aldrich, St. Louis, Missouri, United States of America
Foetal calf serum	Thermo Fisher Scientific, Waltham, Massachusetts, United States of America
Fibronectin	Sigma-Aldrich, St. Louis, Missouri, United States of America
Formalin (37%; w/v) aqueous formaldehyde	Sigma-Aldrich, St. Louis, Missouri, United States of America
Gentamicin	Thermo Fisher Scientific, Waltham, Massachusetts, United States of America
Glucose	Sigma-Aldrich, St. Louis, Missouri, United States of America
GlutaMAX	Thermo Fisher Scientific, Waltham, Massachusetts, United States of America
Glycerin (99.7%; Glycerol)	Univar, Ingleburn, New South Wales, Australia
Haematoxylin and Eosin	Sigma-Aldrich, St. Louis, Missouri, United States of America

Han's F-12 Nutrient Mix	Thermo Fisher Scientific, Waltham, Massachusetts, United States of America
Heparin Solution	Mayne Pharma, Mudgrave. Victoria, Australia
Heparin Sodium	Stem Cells Australia, Victoria, Australia
High Molecular Grade Agarose	BioRad Laboratories, Hercules, California, United States of America
Hydrochloric Acid (32%) (HCl)	Univar, Ingleburn, New South Wales, Australia
Hydrocortisone	Sigma-Aldrich, St. Louis, Missouri, United States of America
Hydrocortisone	Stem Cells Australia, Victoria, Australia
Inoculating Loop	COPAN Diagnostics, Murrieta, California, United States of America
Insulin	Sigma-Aldrich, St. Louis, Missouri, United States of America
Isopropyl alcohol (C ₃ H ₈ O)	Sigma-Aldrich, St. Louis, Missouri, United States of America
Lactate Dehydrogenase (LDH Cytotoxicity Assay: Cytotox 96 Non-Radioactive Assay)	Promega, Wisconsin, United States of America
L-Shaped Spreaders	COPAN Diagnostics, Murrieta, California, United States of America
Luria-Bertani (Lennox) Agar	Becton Dickinson Microbiology, Franklin Lakes, New Jersey, United States of America
Luria-Bertani (Lennox) Broth	Becton Dickinson Microbiology, Franklin Lakes, New Jersey, United States of America
Magnesium Chloride Hexahydrate (MgCl ₂ · 6H ₂ O)	Sigma-Aldrich, St. Louis, Missouri, United States of America
Magnesium Sulphate Heptahydrate (MgSO ₄ · 7H ₂ O)	Sigma-Aldrich, St. Louis, Missouri, United States of America
Minimum Essential Medium (MEM)	Thermo Fisher Scientific, Waltham, Massachusetts, United States of America
Mueller Hinton II Broth (Cation-Adjusted)	Becton Dickinson Microbiology, Franklin Lakes, New Jersey, United States of America
Non-essential amino acids (NEAA)	Thermo Fisher Scientific, Waltham, Massachusetts, United States of America
Normal goat serum	Thermo Fisher Scientific, Waltham, Massachusetts, United States of America
OptEIA Human IL-8 ELISA Set	Becton Dickinson Biosciences, Franklin Lakes, New Jersey, United States of America
Paraformaldehyde 16% Aqueous Solution EM Grade	Electron Microscopy Sciences, Hatfield, Philadelphia, United States of America
Phosphate Buffered Saline (PBS) Dehydrated Tablet	Sigma-Aldrich, St. Louis, Missouri, United States of America
Pasteur Pipettes	Corning, New York, United States of America
Penicillin-Streptomycin (Pen-Strep)	Thermo Fisher Scientific, Waltham, Massachusetts, United States of America
Phosphate-buffered saline (PBS)	Thermo Fisher Scientific, Waltham, Massachusetts, United States of America
Piperacillin	Sigma-Aldrich, St. Louis, Missouri, United States of America

PneumaCult™-ALI 10X Supplement	Stem Cells Australia, Victoria, Australia
PneumaCult™-ALI Basal Medium	Stem Cells Australia, Victoria, Australia
PneumaCult™-Ex Plus Medium	Stem Cells Australia, Victoria, Australia
PneumaCult™-ALI Maintenance Medium	Stem Cells Australia, Victoria, Australia
Potassium Chloride (KCl)	Sigma-Aldrich, St. Louis, Missouri, United States of America
Potassium Dihydrogen Phosphate (KH ₂ PO ₄)	Sigma-Aldrich, St. Louis, Missouri, United States of America
Proteinase K 10mg/mL	Thermo Fisher Scientific, Waltham, Massachusetts, United States of America
Purified Rat Anti-Human IL-6 1° Antibody	Becton Dickinson Biosciences, Franklin Lakes, New Jersey, United States of America
ReagentPack® Subculture Reagents	Lonza, Basel, Switzerland
RNase A	Invitrogen, Waltham, Massachusetts, United States of America
Rock Inhibitor (Y-27632)	Enxo Life Sciences, Farmingdale, New York, United States of America
RPMI-1640 Media	Thermo Fisher Scientific, Waltham, Massachusetts, United States of America
Sodium Azide (NaN ₃)	Sigma-Aldrich, St. Louis, Missouri, United States of America
Sodium Bicarbonate (NaHCO ₃)	Sigma-Aldrich, St. Louis, Missouri, United States of America
Sodium Carbonate (Na ₂ CO ₃)	Sigma-Aldrich, St. Louis, Missouri, United States of America
Sodium Chloride (NaCl)	Sigma-Aldrich, St. Louis, Missouri, United States of America
Sodium Deoxycholate (C ₂₄ H ₃₉ NaO ₄)	Sigma-Aldrich, St. Louis, Missouri, United States of America
Sodium Fluoride (NaF)	Sigma-Aldrich, St. Louis, Missouri, United States of America
Sodium Hydroxide (NaOH)	Sigma-Aldrich, St. Louis, Missouri, United States of America
Sodium Orthovanadate (Na ₃ VO ₄)	Sigma-Aldrich, St. Louis, Missouri, United States of America
Sodium phosphate dibasic (Na ₂ HPO ₄)	Sigma-Aldrich, St. Louis, Missouri, United States of America
Sodium pyrophosphate (Na ₄ P ₂ O ₇)	Sigma-Aldrich, St. Louis, Missouri, United States of America
Sodium Pyruvate (C ₃ H ₃ NaO ₃)	Sigma-Aldrich, St. Louis, Missouri, United States of America
Sulphuric Acid (2N; S ₂ SO ₄)	Univar, Ingleburn, New South Wales, Australia
Superfrost Slides	Waldemar Knittel Glasbearbeitungs GmbH, Braunschweig, Germany
Syringes (1 mL, 3 mL, 5 mL, 10 mL and 50 mL)	TERUMO, Macquarie Park, New South Wales, Australia
Sybr Safe	Invitrogen, Waltham, Massachusetts, United States of America

Tazobactam	Sigma-Aldrich, St. Louis, Missouri, United States of America
Tobramycin	Sigma-Aldrich, St. Louis, Missouri, United States of America
1-Step™ Ultra TMB-ELISA	Thermo Fisher Scientific, Waltham, Massachusetts, United States of America
Trans-Retinoic Acid	Sigma-Aldrich, St. Louis, Missouri, United States of America
Tris(hydroxymethyl)aminomethane base (C ₄ H ₁₁ NO ₃ ; Tris)	Univar, Ingleburn, New South Wales, Australia
Trizma Base (NH ₂ C(CH ₂ OH) ₃)	Sigma-Aldrich, St. Louis, Missouri, United States of America
Trypan Blue	Sigma-Aldrich, St. Louis, Missouri, United States of America
Trypsin	Sigma-Aldrich, St. Louis, Missouri, United States of America
Trypsin Ethylene Diamine Tetraacetic Acid (T-EDTA)	Sigma-Aldrich, St. Louis, Missouri, United States of America
Tween-20	Sigma-Aldrich, St. Louis, Missouri, United States of America
Qubit dsDNA High Sensitivity kit	Thermo Fisher Scientific, Waltham, Massachusetts, United States of America

2.2 List of Bacteria Used in this Thesis

Table 2.2 Bacterial Isolates

Microorganism	Laboratory Name	Source
<i>Pseudomonas aeruginosa</i>	AST11	Institute of Respiratory Health (Perth, Western Australia, Australia)
<i>Pseudomonas aeruginosa</i>	AST15	Institute of Respiratory Health
<i>Pseudomonas aeruginosa</i>	AST20	(Perth, Western Australia, Australia)
<i>Pseudomonas aeruginosa</i>	AST57	Institute of Respiratory Health
<i>Pseudomonas aeruginosa</i>	AST70	(Perth, Western Australia, Australia)
<i>Pseudomonas aeruginosa</i>	AST79	Institute of Respiratory Health
<i>Pseudomonas aeruginosa</i>	AST91	(Perth, Western Australia, Australia)
<i>Pseudomonas aeruginosa</i>	AST92	Institute of Respiratory Health
<i>Pseudomonas aeruginosa</i>	AST95	(Perth, Western Australia, Australia)

<i>Pseudomonas aeruginosa</i>	AST101	Institute of Respiratory Health
<i>Pseudomonas aeruginosa</i>	AST121	(Perth, Western Australia, Australia)
<i>Pseudomonas aeruginosa</i>	AST124	Institute of Respiratory Health
<i>Pseudomonas aeruginosa</i>	AST141	(Perth, Western Australia, Australia)
<i>Pseudomonas aeruginosa</i>	AST144	Institute of Respiratory Health
<i>Pseudomonas aeruginosa</i>	AST154	(Perth, Western Australia, Australia)
<i>Pseudomonas aeruginosa</i>	AST163	Institute of Respiratory Health
<i>Pseudomonas aeruginosa</i>	AST164	(Perth, Western Australia, Australia)
<i>Pseudomonas aeruginosa</i>	AST166	Institute of Respiratory Health
<i>Pseudomonas aeruginosa</i>	AST165	(Perth, Western Australia, Australia)
<i>Pseudomonas aeruginosa</i>	AST167	Institute of Respiratory Health
<i>Pseudomonas aeruginosa</i>	AST174	(Perth, Western Australia, Australia)
<i>Pseudomonas aeruginosa</i>	AST188	Institute of Respiratory Health
<i>Pseudomonas aeruginosa</i>	AST189	(Perth, Western Australia, Australia)
<i>Pseudomonas aeruginosa</i>	AST196	Institute of Respiratory Health
<i>Pseudomonas aeruginosa</i>	AST207	(Perth, Western Australia, Australia)
<i>Pseudomonas aeruginosa</i>	AST222	Institute of Respiratory Health
<i>Pseudomonas aeruginosa</i>	AST232	(Perth, Western Australia, Australia)
<i>Pseudomonas aeruginosa</i>	AST234	Institute of Respiratory Health
<i>Pseudomonas aeruginosa</i>	AST241	(Perth, Western Australia, Australia)
<i>Pseudomonas aeruginosa</i>	AST243	Institute of Respiratory Health
<i>Pseudomonas aeruginosa</i>	AST245	(Perth, Western Australia, Australia)
<i>Pseudomonas aeruginosa</i>	AST253	Institute of Respiratory Health
<i>Pseudomonas aeruginosa</i>	AST259	(Perth, Western Australia, Australia)
<i>Pseudomonas aeruginosa</i>	AST314	Institute of Respiratory Health

<i>Pseudomonas aeruginosa</i>	AST339	(Perth, Western Australia, Australia)
<i>Pseudomonas aeruginosa</i>	AST342	Institute of Respiratory Health
<i>Pseudomonas aeruginosa</i>	AST347	(Perth, Western Australia, Australia)
<i>Pseudomonas aeruginosa</i>	AST351	Institute of Respiratory Health
<i>Pseudomonas aeruginosa</i>	AST354	(Perth, Western Australia, Australia)
<i>Pseudomonas aeruginosa</i>	AST378	Institute of Respiratory Health
<i>Pseudomonas aeruginosa</i>	AST403	(Perth, Western Australia, Australia)
<i>Pseudomonas aeruginosa</i>	AST405	Institute of Respiratory Health
<i>Pseudomonas aeruginosa</i>	AST413	(Perth, Western Australia, Australia)
<i>Pseudomonas aeruginosa</i>	B302011628	Pathwest Laboratory Medicine Western Australia (Perth, Western Australia, Australia)
<i>Pseudomonas aeruginosa</i>	B102001197	Pathwest Laboratory Medicine Western Australia (Perth, Western Australia, Australia)
<i>Pseudomonas aeruginosa</i>	B106006516	Pathwest Laboratory Medicine Western Australia (Perth, Western Australia, Australia)
<i>Pseudomonas aeruginosa</i>	B208012237	Pathwest Laboratory Medicine Western Australia (Perth, Western Australia, Australia)
<i>Pseudomonas aeruginosa</i>	B105002205	Pathwest Laboratory Medicine Western Australia (Perth, Western Australia, Australia)
<i>Pseudomonas aeruginosa</i>	B203011236	Pathwest Laboratory Medicine Western Australia (Perth, Western Australia, Australia)
<i>Pseudomonas aeruginosa</i>	B802008986	Pathwest Laboratory Medicine Western Australia (Perth, Western Australia, Australia)
<i>Pseudomonas aeruginosa</i>	B103004365	Pathwest Laboratory Medicine Western Australia (Perth, Western Australia, Australia)

<i>Pseudomonas aeruginosa</i>	B115006074	Pathwest Laboratory Medicine Western Australia (Perth, Western Australia, Australia)
<i>Pseudomonas aeruginosa</i>	B113004743	Pathwest Laboratory Medicine Western Australia (Perth, Western Australia, Australia)
<i>Pseudomonas aeruginosa</i>	B101001656	Pathwest Laboratory Medicine Western Australia (Perth, Western Australia, Australia)
<i>Pseudomonas aeruginosa</i>	B201016028	Pathwest Laboratory Medicine Western Australia (Perth, Western Australia, Australia)
<i>Pseudomonas aeruginosa</i>	B317007211	Pathwest Laboratory Medicine Western Australia (Perth, Western Australia, Australia)
<i>Pseudomonas aeruginosa</i>	B122007587	Pathwest Laboratory Medicine Western Australia (Perth, Western Australia, Australia)
<i>Pseudomonas aeruginosa</i>	B206007549	Pathwest Laboratory Medicine Western Australia (Perth, Western Australia, Australia)
<i>Pseudomonas aeruginosa</i>	B202009799	Pathwest Laboratory Medicine Western Australia (Perth, Western Australia, Australia)
<i>Pseudomonas aeruginosa</i>	B206007542	Pathwest Laboratory Medicine Western Australia (Perth, Western Australia, Australia)
<i>Pseudomonas aeruginosa</i>	B102005558	Pathwest Laboratory Medicine Western Australia (Perth, Western Australia, Australia)
<i>Pseudomonas aeruginosa</i>	B105012186	Pathwest Laboratory Medicine Western Australia (Perth, Western Australia, Australia)
<i>Pseudomonas aeruginosa</i>	B106010593	Pathwest Laboratory Medicine Western Australia (Perth, Western Australia, Australia)
<i>Pseudomonas aeruginosa</i>	B523005052	Pathwest Laboratory Medicine Western

		Australia (Perth, Western Australia, Australia)
<i>Pseudomonas aeruginosa</i>	B104001777	Pathwest Laboratory Medicine Western Australia (Perth, Western Australia, Australia)
<i>Pseudomonas aeruginosa</i>	B304012656	Pathwest Laboratory Medicine Western Australia (Perth, Western Australia, Australia)
<i>Pseudomonas aeruginosa</i>	B208013006	Pathwest Laboratory Medicine Western Australia (Perth, Western Australia, Australia)
<i>Pseudomonas aeruginosa</i>	B201010513	Pathwest Laboratory Medicine Western Australia (Perth, Western Australia, Australia)
<i>Pseudomonas aeruginosa</i>	M1C4	Melbourne Pathology (Melbourne, Victoria, Australia)
<i>Pseudomonas aeruginosa</i>	M1C10	Melbourne Pathology (Melbourne, Victoria, Australia)
<i>Pseudomonas aeruginosa</i>	M1C14	Melbourne Pathology (Melbourne, Victoria, Australia)
<i>Pseudomonas aeruginosa</i>	M1C34	Melbourne Pathology (Melbourne, Victoria, Australia)
<i>Pseudomonas aeruginosa</i>	M1C37	Melbourne Pathology (Melbourne, Victoria, Australia)
<i>Pseudomonas aeruginosa</i>	M1C39	Melbourne Pathology (Melbourne, Victoria, Australia)
<i>Pseudomonas aeruginosa</i>	M1C50	Melbourne Pathology (Melbourne, Victoria, Australia)
<i>Pseudomonas aeruginosa</i>	M1C52	Melbourne Pathology (Melbourne, Victoria, Australia)
<i>Pseudomonas aeruginosa</i>	M1C54	Melbourne Pathology (Melbourne, Victoria, Australia)
<i>Pseudomonas aeruginosa</i>	M1C58	Melbourne Pathology (Melbourne, Victoria, Australia)
<i>Pseudomonas aeruginosa</i>	M1C64	Melbourne Pathology (Melbourne, Victoria, Australia)

<i>Pseudomonas aeruginosa</i>	M1C66	Melbourne Pathology (Melbourne, Victoria, Australia)
<i>Pseudomonas aeruginosa</i>	M1C67	Melbourne Pathology (Melbourne, Victoria, Australia)
<i>Pseudomonas aeruginosa</i>	M1C73	Melbourne Pathology (Melbourne, Victoria, Australia)
<i>Pseudomonas aeruginosa</i>	M1C74	Melbourne Pathology (Melbourne, Victoria, Australia)
<i>Pseudomonas aeruginosa</i>	M1C77	Melbourne Pathology (Melbourne, Victoria, Australia)
<i>Pseudomonas aeruginosa</i>	M1C79	Melbourne Pathology (Melbourne, Victoria, Australia)
<i>Pseudomonas aeruginosa</i>	M1C81	Melbourne Pathology (Melbourne, Victoria, Australia)
<i>Pseudomonas aeruginosa</i>	M1C86	Melbourne Pathology (Melbourne, Victoria, Australia)
<i>Pseudomonas aeruginosa</i>	M1C90	Melbourne Pathology (Melbourne, Victoria, Australia)
<i>Pseudomonas aeruginosa</i>	M1C93	Melbourne Pathology (Melbourne, Victoria, Australia)
<i>Pseudomonas aeruginosa</i>	M1C94	Melbourne Pathology (Melbourne, Victoria, Australia)
<i>Pseudomonas aeruginosa</i>	M1C100	Melbourne Pathology (Melbourne, Victoria, Australia)
<i>Pseudomonas aeruginosa</i>	M1C108	Melbourne Pathology (Melbourne, Victoria, Australia)
<i>Pseudomonas aeruginosa</i>	M1C123	Melbourne Pathology (Melbourne, Victoria, Australia)
<i>Pseudomonas aeruginosa</i>	M1C124	Melbourne Pathology (Melbourne, Victoria, Australia)
<i>Pseudomonas aeruginosa</i>	M1C130	Melbourne Pathology (Melbourne, Victoria, Australia)
<i>Pseudomonas aeruginosa</i>	M1C131	Melbourne Pathology (Melbourne, Victoria, Australia)

<i>Pseudomonas aeruginosa</i>	MIC141	Melbourne Pathology (Melbourne, Victoria, Australia)
<i>Pseudomonas aeruginosa</i>	PAO1	ATCC 15692; University of Western Australia, Department of Microbiology Culture Collection (MCC) [417]
<i>Pseudomonas aeruginosa</i>	mPAO1	Manoil Laboratory, University of Washington [418, 419]
<i>Pseudomonas aeruginosa</i>	PW1783 Δ oprM	Manoil Laboratory, University of Washington [418, 419]
<i>Pseudomonas aeruginosa</i>	PW4507 Δ galU	Manoil Laboratory, University of Washington [418, 419]
<i>Pseudomonas aeruginosa</i>	PW2279 Δ migA	Manoil Laboratory, University of Washington [418, 419]
<i>Pseudomonas aeruginosa</i>	PW2387 Δ mucA	Manoil Laboratory, University of Washington [418, 419]
<i>Pseudomonas aeruginosa</i>	PW10209 Δ wzt	Manoil Laboratory, University of Washington [418, 419]
<i>Pseudomonas aeruginosa</i>	PW9682 Δ rmlC	Manoil Laboratory, University of Washington [418, 419]
<i>Pseudomonas aeruginosa</i>	PW8621 Δ pilA	Manoil Laboratory, University of Washington [418, 419]
<i>Pseudomonas aeruginosa</i>	PW8623 Δ pilB	Manoil Laboratory, University of Washington [418, 419]
<i>Pseudomonas aeruginosa</i>	PW8767 Δ pilY1	Manoil Laboratory, University of Washington [418, 419]
<i>Pseudomonas aeruginosa</i>	PW5351 Δ oprH	Manoil Laboratory, University of Washington [418, 419]
<i>Pseudomonas aeruginosa</i>	PW8747 Δ oprJ	Manoil Laboratory, University of Washington [418, 419]
<i>Pseudomonas aeruginosa</i>	PW4134 voprF	Manoil Laboratory, University of Washington [418, 419]
<i>Pseudomonas aeruginosa</i>	PW2742 Δ oprD	Manoil Laboratory, University of Washington [418, 419]

<i>Pseudomonas aeruginosa</i>	PW1149 Δ clpV1	Manoil Laboratory, University of Washington [418, 419]
<i>Pseudomonas aeruginosa</i>	PW5186 Δ oprN	Manoil Laboratory, University of Washington [418, 419]
<i>Pseudomonas aeruginosa</i>	PW8407 Δ fliC	Manoil Laboratory, University of Washington [418, 419]
<i>Burkholderia cenocepacia</i> recA clade A	QLD001	Prince Charles Hospital, Brisbane, Queensland, Australia
<i>Burkholderia cenocepacia</i> recA clade A	QLD002	Prince Charles Hospital, Brisbane, Queensland, Australia
<i>Burkholderia cepacia</i>	QLD003	Prince Charles Hospital, Brisbane, Queensland, Australia
<i>Burkholderia multivorans</i>	QLD005	Prince Charles Hospital, Brisbane, Queensland, Australia
<i>Burkholderia cenocepacia</i> recA clade B (Aust. epid. strain)	QLD006	Prince Charles Hospital, Brisbane, Queensland, Australia
<i>Burkholderia arboris</i>	QLD007	Prince Charles Hospital, Brisbane, Queensland, Australia
<i>Burkholderia vietnamiensis</i>	QLD014	Prince Charles Hospital, Brisbane, Queensland, Australia
<i>Burkholderia multivorans</i>	QLD020	Prince Charles Hospital, Brisbane, Queensland, Australia
<i>Burkholderia cenocepacia</i> recA clade B	QLD022	Prince Charles Hospital, Brisbane, Queensland, Australia
<i>Burkholderia multivorans</i>	QLD023	Prince Charles Hospital, Brisbane, Queensland, Australia
<i>Burkholderia vietnamiensis</i>	QLD025	Prince Charles Hospital, Brisbane, Queensland, Australia
<i>Burkholderia ambifaria</i>	QLD027	Prince Charles Hospital, Brisbane, Queensland, Australia
<i>Burkholderia cepacia</i> complex indeterminate species	QLD028	Prince Charles Hospital, Brisbane, Queensland, Australia
<i>Burkholderia cepacia</i>	QLD032	Prince Charles Hospital, Brisbane, Queensland, Australia

<i>Burkholderia cenocepacia</i> recA clade A	QLD035	Prince Charles Hospital, Brisbane, Queensland, Australia
<i>Burkholderia cepacia</i> complex indeterminate species	QLD039	Prince Charles Hospital, Brisbane, Queensland, Australia
<i>Burkholderia cepacia</i> complex indeterminate species	QLD045	Prince Charles Hospital, Brisbane, Queensland, Australia
<i>Burkholderia latens</i>	QLD058	Prince Charles Hospital, Brisbane, Queensland, Australia
<i>Burkholderia contaminans</i>	QLD066	Prince Charles Hospital, Brisbane, Queensland, Australia
<i>Burkholderia cepacia</i>	QLD121	Prince Charles Hospital, Brisbane, Queensland, Australia
<i>Staphylococcus aureus</i>	SA1	Prince Charles Hospital, Brisbane, Queensland, Australia
<i>Staphylococcus aureus</i>	SA2	Prince Charles Hospital, Brisbane, Queensland, Australia
<i>Staphylococcus aureus</i>	SA3	Prince Charles Hospital, Brisbane, Queensland, Australia
<i>Staphylococcus aureus</i>	SA4	Prince Charles Hospital, Brisbane, Queensland, Australia
<i>Staphylococcus aureus</i>	SA5	Prince Charles Hospital, Brisbane, Queensland, Australia
<i>Staphylococcus aureus</i>	SA6	Prince Charles Hospital, Brisbane, Queensland, Australia
<i>Staphylococcus aureus</i>	SA7	Prince Charles Hospital, Brisbane, Queensland, Australia
<i>Staphylococcus aureus</i>	SA8	Prince Charles Hospital, Brisbane, Queensland, Australia
<i>Staphylococcus aureus</i>	SA9	Prince Charles Hospital, Brisbane, Queensland, Australia
<i>Staphylococcus aureus</i>	SA10	Prince Charles Hospital, Brisbane, Queensland, Australia
<i>Staphylococcus aureus</i>	SA11	Prince Charles Hospital, Brisbane, Queensland, Australia

<i>Staphylococcus aureus</i>	SA12	Prince Charles Hospital, Brisbane, Queensland, Australia
<i>Staphylococcus aureus</i>	SA13	Prince Charles Hospital, Brisbane, Queensland, Australia
<i>Staphylococcus aureus</i>	SA14	Prince Charles Hospital, Brisbane, Queensland, Australia
<i>Staphylococcus aureus</i>	SA15	Prince Charles Hospital, Brisbane, Queensland, Australia
<i>Staphylococcus aureus</i>	SA16	Prince Charles Hospital, Brisbane, Queensland, Australia
<i>Staphylococcus aureus</i>	SA17	Prince Charles Hospital, Brisbane, Queensland, Australia
<i>Staphylococcus aureus</i>	SA18	Prince Charles Hospital, Brisbane, Queensland, Australia
<i>Staphylococcus aureus</i>	SA19	Prince Charles Hospital, Brisbane, Queensland, Australia
<i>Staphylococcus aureus</i>	ATCC6538	Prince Charles Hospital, Brisbane, Queensland, Australia
<i>Escherichia coli</i>	ATCC25922	Pathwest Laboratory Medicine Western Australia (Perth, Western Australia, Australia)
<i>Enterococcus faecalis</i>	8094860T	Pathwest Laboratory Medicine Western Australia (Perth, Western Australia, Australia)
<i>Enterococcus faecium</i>	9047201T	Pathwest Laboratory Medicine Western Australia (Perth, Western Australia, Australia)
<i>Enterococcus faecium</i>	200610032	Pathwest Laboratory Medicine Western Australia (Perth, Western Australia, Australia)
<i>Enterococcus faecium</i>	200681636	Pathwest Laboratory Medicine Western Australia (Perth, Western Australia, Australia)
<i>Klebsiella pneumoniae</i>	ATCC700603	Pathwest Laboratory Medicine Western Australia (Perth, Western Australia, Australia)

<i>Klebsiella pneumoniae</i>	B104002730	Pathwest Laboratory Medicine Western Australia (Perth, Western Australia, Australia)
<i>Klebsiella pneumoniae</i>	B104009886	Pathwest Laboratory Medicine Western Australia (Perth, Western Australia, Australia)

2.3 General Equipment

2.3.1 Autoclave

Equipment, solution, and waste sterilization was carried out at 121°C for 15 mins using a Cyber Chipmunk (Atherton, Alphington, Victoria, Australia). Quality assurance was performed by BIONOVA BT220 biological indicators (manufactured by Terragene, Santa Fe, New Mexico, United States of America), steam penetration validation utilising the PMS Compact-PCD instrument (created by BMSS, Jandakot, Western Australia, Australia), and 3M Comply Steam Indicator Tape (supplied by Thermo Fisher Scientific, Waltham, Massachusetts, United States of America). Each of these measures was consistently employed to confirm successful sterilisation of each autoclave run.

2.3.2 Balances

OHAUS Explorer Balances were used to measure all reagents (OHAUS, Port Melbourne, Victoria, Australia).

2.3.3 Biological Safety Cabinet (Biosafety Cabinet)

Bacterial and cell cultures were conducted in a National Association of Testing Authorities (NATA) certified biological safety cabinet, Labculture® Class II Type A2 biosafety cabinet (Esco Micro Pte. Ltd, Singapore), compliant with the Office of the Gene Technology Regulator (OGTR) regulations.

2.3.4 Centrifuges

A benchtop Eppendorf® 5415D mini centrifuge (Eppendorf, Hamburg, Hamburg, Germany) was used to centrifugate solutions in microcentrifuge tubes. All buffers, solutions, and suspensions in larger volumes were centrifuged using a benchtop Eppendorf® 5810R swing-bucket rotor centrifuge (Eppendorf, Hamburg, Hamburg, Germany).

2.3.5 Chemidoc

Bacterial plates were and DNA electrophoresis gels were images using a BioRad ChemiDoc XRS+ (BioRad Laboratories, Hercules, California, United States of America).

2.3.6 Primary airway epithelial cell sampling

Samples of primary airway epithelial cells were obtained using paro® isola long interdental brushes featuring an outer diameter of 2.5 mm, provided (Esro AG, Kilchberg, Switzerland).

2.3.7 Dry Oven

Sterilised bacterial culture media was kept molten at 55°C in a Memmert UL30 dry oven (Mettler-Toledo GmbH + Co. KG, Schwabach, Germany).

2.3.8 Electrophoresis

A PowerPac™ basic power supply (Bio-Rad Laboratories, Hercules, California, United States of America) was used for DNA gel electrophoresis.

2.3.9 EVOM™

The EVOM™ was used to measure Trans-epithelial electrical resistance to ensure tight junction formation and barrier integrity (World Precision Instruments, Sarasota, Florida).

2.3.10 Gammacell Irradiation Units

The NIH-3T3 cell line was irradiated with 3000cGy γ -radiation using a Gammacell 3000 Elan (Nordion, Oxfordshire, United Kingdom).

2.3.11 Glassware

Laboratory glassware was from Schott (Frenchs Forest, New South Wales, Australia). Glassware was initially soaked overnight in Liquid Pyroneg (Diversey Australia, Smithfield, New South Wales, Australia) and then cleaned in an INNOVA® M5/M5-ISO

glassware washer (BHT Hygienetechnik GmbH, Gersthofen, Germany). Cleaned glassware was autoclave sterilised prior to use (refer to 2.3.1).

2.3.12 Heating Blocks

Heating of samples and buffers was performed using a Ratek 1 Block Digital Dry Block Heater (Ratek Instruments Pty Ltd, Boronia, Victoria, Australia).

2.3.13 Incubators

Bacterial cultures were incubated and maintained in a Heratherm™ incubator (Thermo Fisher Scientific, Waltham, Massachusetts, United States of America) that was not humidified. Cell cultures were maintained in a Heracell™ VIOS 160i CO₂ (Thermo Fisher Scientific, Waltham, Massachusetts, United States of America) humidified incubator with a 5% CO₂/ 95% air atmosphere.

2.3.14 Microscope

Visual assessment of cell cultures was performed with a Leica Microsystem GmbH biphasic microscope (Wetzlar, Hesse, Germany).

2.3.15 MinION Mk1C Nanopore Sequencer

Long read bacterial libraries were loaded onto MinION flow cells (Oxford Nanopore Technologies, Oxford Science Park, Oxford, United Kingdom) and sequenced using the MinION Mk1C Nanopore (Oxford Nanopore Technologies, Oxford Science Park, Oxford, United Kingdom).

2.3.16 NanoDrop 2000c

Preliminary assessments of extracted DNA were performed with a NanoDrop 2000c (Eppendorf, Hamburg, Hamburg, Germany). A 1 µL aliquot of DNA elute was assessed spectrophotometrically at 260 and 280nm wavelengths. This provided an estimate of DNA concentration as well as the quality by the 260/280nm absorbance ratio of 1.8-2.0.

2.3.17 pH Meter

The pH of buffers and solutions were measured with an edge® Dedicated pH/ORP Meter (Hanna Instruments Inc., Woonsocket, Rhode Island, United States of America) that was regularly calibrated with solutions purchased from Scharlau (Barcelona, Catalonia, Spain).

2.3.18 Pipettes

Aliquots of solutions between 1 and 25 mL were measured with S1 Pipet Fillers (Thermo Fisher Scientific, Waltham, Massachusetts, United States of America). Single channel Pipetman L (Gilson Inc., Middleton, Wisconsin, United States of America) pipettes were used to measure volumes less than 1000 µL. Where multichannel delivery was required a Pipetman L multichannel pipette (Gilson Inc., Middleton, Wisconsin, United States of America) or F1-ClipTip™ multichannel pipette (Thermo Fisher Scientific, Waltham, Massachusetts, United States of America) were used.

2.3.19 Plate Readers

Spectrophotometric readings of 96-well plates were performed with a CLARIOstar® Plus machine (BMG Labtech GmbH, Ortenberg, Germany).

2.3.20 Qubit™ fluorometer

Confirmation of extracted DNA quantity was performed using the High Sensitivity dsDNA kit and a Qubit 4 fluorometer (Thermo Fisher Scientific, Waltham, Massachusetts, United States of America).

2.3.21 Bacterial, tissue and general plasticware

Disposable Petri dishes used for bacterial culture were obtained from Greiner Bio-One (Kremsmünster, Austria). General use and cell culture disposable plasticware was obtained from Nunc™ (Thermo Fisher Scientific, Waltham, Massachusetts, United States of America).

2.3.22 Stirrers and Shakers

Mixing and agitation of solutions was performed with magnetic stirrers (Industrial Equipment and Control Pty Ltd, Melbourne, Victoria, Australia), Ratek shakers (Ratek Instruments Pty Ltd, Boronia, Victoria, Australia) or Stuart® rocking platform (Barloworld Scientific Laboratory Group, Rochester, New York, United States of America).

2.3.23 Spectrophotometer

All bacterial optical density was measured using an Eppendorf Fluorescent BioSpectrometer® (Eppendorf, Hamburg, Hamburg, Germany).

2.3.24 Water Bath

To maintain or heat solutions, buffers and freeze-thawing of cryopreserved cell cultures were performed using a heated water bath (Ratek Instruments Pty Ltd, Boronia, Victoria, Australia).

2.4 General Buffers and Solutions

2.4.1 Bovine Serum Albumin (BSA)

Bovine serum albumin (BSA; 1mg/mL) was made by dissolving 100 mg of BSA powder (Sigma-Aldrich, St. Louis, Missouri, United States of America) in 100 mL of 1X Phosphate buffered saline (PBS; refer to 2.4.25). The prepared solution was filter-sterilised using a 0.22 µm syringe filter filter (Cytivas Whatman™ Uniflo™ PES membrane, Massachusetts, United States of America) and stored at 4°C until use.

2.4.2 Calcium chloride (CaCl₂; 1M) solution

A 1M CaCl₂ solution was made by dissolving 11.098 g of CaCl₂·6H₂O (Sigma Aldrich, North Ryde, New South Wales, Australia) in 100 mL of ddH₂O. CaCl₂ solution. The solution was then filter-sterilised by passing it through a 0.22 µm syringe filter (Cytivas Whatman™ Uniflo™ PES membrane, Massachusetts, United States of America) and stored at room temperature prior to use.

2.4.3 Cefepime

A 50 mg/mL stock solution was made by dissolving cefepime (Sigma-Aldrich, St. Louis, Missouri, United States of America) in ddH₂O. The solution was filtered with a 0.22 µm syringe filter (Cytivas Whatman™ Uniflo™ PES membrane, Massachusetts, United States of America) and stored in 500 µL aliquots at -20°C until use.

2.4.4 Ceftazidime

A 50 mg/mL stock solution was made by dissolving ceftazidime (Sigma-Aldrich, St. Louis, Missouri, United States of America) in ddH₂O. The solution was filtered with a 0.22 µm syringe filter (Cytivas Whatman™ Uniflo™ PES membrane, Massachusetts, United States of America) and stored in 500 µL aliquots at -20°C until use.

2.4.5 Ciprofloxacin

A 50 mg/mL stock solution was made by dissolving ciprofloxacin (Sigma-Aldrich, St. Louis, Missouri, United States of America) in ddH₂O. The solution was then filtered using a 0.22 µm syringe filter (Cytivas Whatman™ Uniflo™ PES membrane, Massachusetts, United States of America) stored as 500 µL aliquots at -20°C until use.

2.4.6 Double Deionised Water (ddH₂O)

Distilled water was passed through a Milli-Q water purification system (Purelab® Ultra, Elga Veolia, Kewdale, Western Australia, Australia) to produce double-deionised water.

2.4.7 Ethylenediaminetetraacetic Acid (EDTA)

A 500 mM stock solution was made by dissolving 18.71 g of EDTA (Sigma-Aldrich, St. Louis, Missouri, United States of America) in 100 mL of 3 M NaOH and stored at room temperature until use.

2.4.8 Ethylenediaminetetraacetic Acid Calcium Disodium Salt (CaEDTA)

A 200 mM stock solution was made by dissolving 374.27 mg of CaEDTA (Sigma-Aldrich, St. Louis, Missouri, United States of America) in 5 mL of ddH₂O, filtered using a 0.22 µm syringe filter (Cytivas Whatman™ Uniflo™ PES membrane, Massachusetts, United States of America) and stored at room temperature until required.

2.4.9 Ethanol (C₂H₆O; 80% v/v)

Ethanol (80% v/v) was made by mixing 700 mL of absolute ethyl alcohol (Sigma-Aldrich, St. Louis, Missouri, United States of America) with 300 mL of ddH₂O, which was stored at room temperature until required.

2.4.10 Glycerol (50% v/v)

Glycerol solution (50% v/v) was made by mixing 50 mL of glycerol stock solution (Univar, Ingleburn, New South Wales, Australia) with 50 mL of ddH₂O. The solution was autoclaved and stored at room temperature until use.

2.4.11 Hank's Balanced Salt Solution (HBSS)

Hank's balanced salt solution was made by dissolving 0.185 g of CaCl₂ (Sigma-Aldrich, St. Louis, Missouri, United States of America), 0.097 g of MgSO₄ (Sigma-Aldrich, St. Louis, Missouri, United States of America), 0.4g of KCl (Sigma-Aldrich, St. Louis, Missouri, United States of America), 0.06 g of KH₂PO₄ (Sigma-Aldrich, St. Louis, Missouri, United States of America), 8 g of NaCl (Sigma-Aldrich, St. Louis, Missouri, United States of America), 0.047 g of Na₂HPO₄ (Sigma-Aldrich, St. Louis, Missouri, United States of America) and 1 g of glucose (Sigma-Aldrich, St. Louis, Missouri, United States of America) in 900 mL of ddH₂O. The resulting solution was adjusted to pH 7.4 with 1M HCl (refer to 2.4.13), made up to 1 L with ddH₂O, autoclaved and stored at room temperature until use.

2.4.12 4-2-hydroxythyl_1-Piperazineethanesulfonic Acid (HEPES) Buffered Saline Solution

A 10X stock of HBSS solution was made by dissolving 47.6 g of HEPES, 70.7 g of NaCl (Sigma-Aldrich, St. Louis, Missouri, United States of America), 2 g of KCl (Sigma-Aldrich, St. Louis, Missouri, United States of America), 1.7 g of glucose (Sigma-Aldrich, St. Louis, Missouri, United States of America) and 10.2 g of Na₂HPO₄ (Sigma-Aldrich, St. Louis, Missouri, United States of America) in 800 mL of ddH₂O. The resulting solution was adjusted to pH 7.4 with 1M HCl (refer to 2.4.13), made up to 1 L with ddH₂O, autoclaved and stored at room temperature until use. When used a 1X solution was made by diluting 10X 1:10 with ddH₂O.

2.4.13 Hydrochloric Acid (HCl; 1M)

A 1M HCl solution was made by mixing 10 mL of 32% HCl (Univar, Ingleburn, New South Wales, Australia) with 90 mL of ddH₂O, which was stored at room temperature until used.

2.4.14 Hydrochloric Acid (HCl; 4 mM)

A 4 mM HCl solution was made by adding 17 µL of 32% HCl (Univar, Ingleburn, New South Wales, Australia) to 49.98 mL of ddH₂O, which was stored at room temperature until used.

2.4.15 IL-6 Blocking Buffer

The IL-6 blocking buffer was prepared by dissolving 6.05 g Tris (Univar, Ingleburn, New South Wales, Australia), 9g Na₂CO₃ (Sigma-Aldrich, St. Louis, Missouri, United States of America), 0.25 g NaN₃ (Sigma-Aldrich, St. Louis, Missouri, United States of America) to the water 800mL of ddH₂O. The pH of the solution was adjusted to 7.4 with 1M HCl (refer to 2.4.13) and 5 g of BSA (Sigma-Aldrich, St. Louis, Missouri, United States of America) dissolved in it before being topped up to 1 L with ddH₂O.

2.4.16 IL-6 Coating Buffer

The IL-6 ELISA coating buffer was made by dissolving 1.59 g of Na₂CO₃ (Sigma-Aldrich, St. Louis, Missouri, United States of America) and 2.93 g of NaHCO₃ (Sigma-Aldrich, St. Louis, Missouri, United States of America) in ddH₂O. The pH of the solution was adjusted to 9.6 with 1M NaOH (refer to 2.4.28) and the solution was topped up to 1 L with ddH₂O.

2.4.17 IL-8 Assay Diluent

IL-8 assay diluent was made by mixing 1X PBS (refer to 2.4.25) with 10% (v/v) HI-FCS (refer to 2.6.1.5).

2.4.18 IL-8 Coating Buffer

IL-8 coating buffer was prepared by dissolving 7.13 g of NaHCO₃ (Sigma-Aldrich, St. Louis, Missouri, United States of America), 1.59 g of Na₂CO₃ (Sigma-Aldrich, St. Louis, Missouri, United States of America) in ddH₂O. The pH was adjusted to 9.5 with 1M NaOH (refer to 2.4.28) and the solution was made up to 1 L with ddH₂O.

2.4.19 IL-8 Wash Buffer

IL-8 wash buffer was prepared by mixing 1 L of 1X PBS (refer to 2.4.25) with 0.05% (v/v) Tween-20 (Sigma-Aldrich, St. Louis, Missouri, United States of America).

2.4.20 IL-8 Working Detector

The IL-8 working detector was made by diluting the detection antibody and horseradish peroxidase enzyme (Becton Dickinson Biosciences, Franklin Lakes, New Jersey, United States of America) 1:250 in assay diluent (refer to 2.4.17) 15 mins prior to use in the ELISA.

2.4.21 Magnesium chloride (MgCl₂; 1M) solution

A 1M MgCl₂ solution was made by dissolving 9.5211 g of MgCl₂·6H₂O (Sigma Aldrich, North Ryde, New South Wales, Australia) in 100 mL of ddH₂O. The MgCl₂ solution was

sterilised by filtering through a 0.22 µm syringe filter (Cytivas Whatman™ Uniflo™ PES membrane, Massachusetts, United States of America). The solution was stored at room temperature until used.

2.4.22 Neutral Buffered Formalin (NBF)

A 10% (v/v) NBF was made by mixing 100 mL of formalin (Sigma-Aldrich, St. Louis, Missouri, United States of America), 900 mL of ddH₂O and then dissolving 4 g of NaH₂PO₄ (Sigma-Aldrich, St. Louis, Missouri, United States of America) and 6.5 g of Na₂HPO₄ (Sigma-Aldrich, St. Louis, Missouri, United States of America) in the solution. The NBF solution was then stored away from direct light at 4°C until required.

2.4.23 Piperacillin

A 50 mg/mL stock solution was made by dissolving piperacillin (Sigma-Aldrich, St. Louis, Missouri, United States of America) in ddH₂O. The solution was filtered with a 0.22 µm syringe filter (Cytivas Whatman™ Uniflo™ PES membrane, Massachusetts, United States of America) and stored in 500 µL aliquots at -20°C until use.

2.4.24 1X PBS (ELISA)

A 10X PBS stock was made by dissolving 80 g of NaCl (Sigma-Aldrich, St. Louis, Missouri, United States of America), 2 g of KCl (Sigma-Aldrich, St. Louis, Missouri, United States of America), 14.4 g of NaH₂PO₄ (Sigma-Aldrich, St. Louis, Missouri, United States of America) and 2.4 g of KH₂PO₄ (Sigma-Aldrich, St. Louis, Missouri, United States of America) in 1 L of ddH₂O. The pH of the solution was then adjusted to pH 7.0 with 1M HCl (refer to 2.4.13). Prior to use a 1X solution was made by diluting the 10X stock 1:10 with ddH₂O. The solution was stored at room temperature until used.

2.4.25 1X PBS (Cell culture)

A 1X solution of PBS for cell culture was made by dissolving a dehydrated PBS tablet (Sigma-Aldrich, St. Louis, Missouri, United States of America) in 1 L of ddH₂O. Prior to use the solution was autoclaved and stored at room temperature.

2.4.26 Sodium Deoxycholate Solution (C₂₄H₃₉NaO₄)

A 10% (w/v) sodium deoxycholate solution was made by dissolving 10 g of sodium deoxycholate (Sigma-Aldrich, St. Louis, Missouri, United States of America) in 100 mL of ddH₂O, which was passed through a 0.22 µm syringe filter (Cytivas Whatman™ Uniflo™ PES membrane, Massachusetts, United States of America) and stored at room temperature until use.

2.4.27 Sodium Hydroxide Solution (NaOH; 0.2M)

A 0.2M sodium hydroxide (NaOH) solution was made by dissolving 80 mg of NaOH tablets (Sigma-Aldrich, St. Louis, Missouri, United States of America) in 10 ml of ddH₂O, which was subsequently stored at room temperature until needed.

2.4.28 Sodium Hydroxide Solution (NaOH; 1M)

A 1M sodium hydroxide (NaOH) solution was made by dissolving 40 g of NaOH (Sigma-Aldrich, St. Louis, Missouri, United States of America) in 1 L of ddH₂O and was stored at room temperature until required.

2.4.29 Sodium Orthovanadate Solution (Na₃VO₄; 200 mM)

A 200 mM sodium orthovanadate solution was made by dissolving 1.85 g of sodium orthovanadate in 50 ml of ddH₂O, which was filter-sterilised through a 0.22 µm syringe filter (Cytivas Whatman™ Uniflo™ PES membrane, Massachusetts, United States of America) and stored at room temperature until needed.

2.4.30 Tazobactam

A 50 mg/mL stock solution was made by dissolving tazobactam (Sigma-Aldrich, St. Louis, Missouri, United States of America) in ddH₂O. The solution was filtered with a 0.22 µm syringe filter (Cytivas Whatman™ Uniflo™ PES membrane, Massachusetts, United States of America) and stored in 500 µL aliquots at -20°C until use.

2.4.31 Tobramycin

A 50 mg/mL stock solution was made by dissolving tobramycin (Sigma-Aldrich, St. Louis, Missouri, United States of America) in ddH₂O. The solution was filtered with a 0.22 µm syringe filter (Cytivas Whatman™ Uniflo™ PES membrane, Massachusetts, United States of America) and stored in 500 µL aliquots at -20°C until use.

2.4.32 Tris Buffered Saline (TBS)

A 10X stock solution of Tris Buffered Saline (TBS) was prepared by dissolving 80 g of NaCl, 2 g of KCl and 30 g of Trizma base (Sigma-Aldrich, St. Louis, Missouri, United States of America) in 800 mL of ddH₂O. The pH was adjusted to 7.4 with 1M HCl (refer to 2.4.13) and the final solution was stored at room temperature. Prior to use the 10X solution was diluted to 1X by mixing 1:10 in ddH₂O.

2.4.33 Tris(hydroxymethyl)aminomethane hydrochloride (Tris-HCl; 1M)

To make 500 mL of 1M Tris-HCl, 60.57 g of Tris (Univar, Ingleburn, New South Wales, Australia) was reconstituted in 400 mL of ddH₂O. The prepared solution was adjusted to a pH of 7.4, adding approximately 70 mL of 1M HCl (refer to 2.4.13) and subsequently adjusting to a final volume of 500 mL. The 1M Tris-HCl was filter-sterilised by passing through a 0.22 µm syringe filter (Cytivas Whatman™ Uniflo™ PES membrane, Massachusetts, United States of America) and dispensed into aliquots of 50 mL and stored at room temperature until required.

2.4.34 Time Resolved Fluorescence (TRF) Wash Buffer

A 10X solution of TRF wash buffer was prepared by dissolving 60.5 g of Tris (Univar, Ingleburn, New South Wales, Australia), 90 g NaCl (Sigma-Aldrich, St. Louis, Missouri, United States of America), 2.5 g of NaN₃ (Sigma-Aldrich, St. Louis, Missouri, United States of America) in 800 mL of ddH₂O. The pH was adjusted to 7.8 with 1M HCl (refer to 2.4.13) and the solution topped up to 1 L. This was stored at room temperature until required when it was diluted 1:10 with ddH₂O to make 1X TRF wash buffer and 0.05%

(v/v) of Tween-20 (Sigma-Aldrich, St. Louis, Missouri, United States of America) was added.

2.5 Bacteria and Bacteriophage Culture Solutions

2.5.1 Bacterial Culture Solutions

2.5.1.1 Luria-Bertani (Lennox) broth (LB broth)

Luria-Bertani broth was prepared by adding 10 g of LB broth powder (BD Micro, New Jersey, United States of America) to 500 mL of ddH₂O, which was autoclaved to sterilise (refer to 2.3.1).

2.5.1.2 Luria-Bertani (Lennox) agar (LB agar)

Luria-Bertani agar was made by adding 17.5 g of LB agar powder (BD Micro, New Jersey, United States of America) to 500 mL of ddH₂O. The solution was sterilised by autoclave (refer to 2.3.1). LB agar plates were made by pouring 18 mL of sterile molten LB agar into Petri dishes (refer to 2.3.21) in the biosafety cabinet and allowed to dry for 60 mins. Prepared LB agar plates were then bagged and kept at 4°C for up to 3 months.

2.5.1.3 Cation-adjusted Mueller Hinton broth (CAMHB)

To make 500 mL of cation-adjusted Mueller Hinton broth, 11 g of dehydrated media powder (BD Micro, New Jersey, United States of America) was rehydrated with 500 mL of ddH₂O. Sterilisation of media was then performed in an autoclave (refer to 2.3.1) at 121°C for 40 mins.

2.5.2 Bacteriophage Culture Solutions

2.5.2.1 Luria-Bertani (Lennox) overlay (0.4% w/v) agar (LB overlay agar)

To make overlay agar, 2 g of bacteriological agar (BD Micro, New Jersey, United States of America) was mixed with 10 g of LB broth media powder and 500 mL of ddH₂O. The solution was supplemented with 500 µL of both 1M CaCl₂ (refer to 2.4.2) and 1M MgCl₂ (refer to 2.4.21) to give a final concentration of 1 mM. Sterilisation of media was then

performed in an autoclave (refer to 2.3.1). Autoclaved overlay agar was kept molten in the dry oven at 55°C.

2.5.2.2 SM buffer

SM buffer was prepared by dissolving 5.8 g of NaCl (Sigma-Aldrich, St. Louis, Missouri, United States of America), 0.96 g of MgSO₄ (Sigma-Aldrich, St. Louis, Missouri, United States of America) in 950 mL of ddH₂O and adding 50 mL of 1M Tris-HCl (refer to 2.4.33). Reconstituted SM buffer was then autoclaved (refer to 2.3.1).

2.5.2.3 Double-strength Luria-Bertani (Lennox) broth (LB broth)

To make double strength LB broth, 20 g of LB powder (BD Micro, New Jersey, United States of America) was mixed with 500 mL of ddH₂O. The solution was sterilised via autoclave (refer to 2.3.1).

2.6 Cell Culture Solutions

2.6.1 Media Additives

2.6.1.1 Adenine

A 10 mg/mL stock of adenine was made by dissolving 200 mg of powdered adenine powder (Sigma-Aldrich, St. Louis, Missouri, United States of America) in 20 mL of 1M HCl (refer to 2.4.13). The solution was then filter-sterilised by passing through a 0.22 µm syringe filter and stored as 5 mL aliquots at -20°C.

2.6.1.2 Cholera Toxin

A 200 µg/mL stock of cholera toxin was made by dissolving 2 mg of powdered cholera toxin (Sigma-Aldrich, St. Louis, Missouri, United States of America) in 10 mL of ddH₂O, which was filtered through a 0.22 µm syringe filter and stored as 5 mL aliquots at -20°C.

2.6.1.3 Collagen Type 1 (rat tail)

Type 1 rat tail collagen (Roche, Castle Hill, New South Wales, Australia) was diluted to 0.03 µg/mL in 1X PBS (refer to 2.4.25) to use as a coating buffer for air-liquid interface

cell culture inserts. The solution was made fresh as required and 200 μL used per 24-well inserts.

2.6.1.4 Cryopreservation Solution for Conditionally Reprogrammed Cells

Conditionally reprogrammed primary airway epithelial cells were cryopreserved in a solution that contained 90% (v/v) HI-FCS (refer to 2.6.1.5), 10% (v/v) DMSO (Sigma-Aldrich, St. Louis, Missouri, United States of America) and 1 μL of ROCK inhibitor (refer to 2.6.1.11).

2.6.1.5 Foetal Calf Serum (FCS)

Heat inactivated FCS (HI-FCS) was prepared by heating commercially purchased low endotoxin FCS (Thermo Fisher Scientific, Waltham, Massachusetts, United States of America) at 56°C for 2 h.

2.6.1.6 Cell Culture Medium (CCM)

Base CCM was made by mixing Han's F-12 Nutrient Mix (Thermo Fisher Scientific, Waltham, Massachusetts, United States of America) 2:1 with DMEM (Thermo Fisher Scientific, Waltham, Massachusetts, United States of America). The base media was then supplemented with 5% (v/v) HI-FCS (refer to 2.6.1.5), 24 $\mu\text{g}/\text{mL}$ adenine (refer to 2.6.1.1), 8.4 ng/mL cholera toxin (refer to 2.6.1.2), 0.4 $\mu\text{g}/\text{mL}$ hydrocortisone (Sigma-Aldrich, St. Louis, Missouri, United States of America), 0.5 $\mu\text{g}/\text{mL}$ insulin (Sigma-Aldrich, St. Louis, Missouri, United States of America), 10 ng/mL EGF (Sigma-Aldrich, St. Louis, Missouri, United States of America) and 10 $\mu\text{M}/\text{L}$ Rock inhibitor (refer to 2.6.1.11). Media was prepared in a biological safety cabinet and filtered with a 0.22 μm bottle-top filter (Nalgene™ Rapid-Flow™, Thermo Fisher Scientific, Waltham, MA, USA). Sterilised CCM was stored out of direct light at 4 °C until required.

2.6.1.7 FCS-based Trypsin Neutralising Solution (TNS)

During passage of primary airway epithelial cells trypsin activity needed to be neutralised once it has facilitated NIH 3T3 cell line monolayer detachment. To prepare TNS, DMEM

(Thermo Fisher Scientific, Waltham, Massachusetts, United States of America) was mixed with 5% (v/v) HI-FCS (refer to 2.6.1.5), which was then stored at 4°C until needed.

2.6.1.8 Fibronectin coating buffer

To prepare the fibronectin coating buffer that facilitates primary airway epithelial cell attachment to plastic cell culture flasks, 1 mg of fibronectin (Sigma-Aldrich, St. Louis, Missouri, United States of America) was added to 10 mL of BEBM™ (Lonza, Basel, Switzerland) at 37°C for 1 hour to allow complete dissolution. Subsequently, 1 mL of collagen type 1 (rat tail; refer to 2.6.1.3), 10 mL of BSA stock (refer to 2.4.1), 0.2% (v/v) gentamicin (Thermo Fisher Scientific, Waltham, Massachusetts, United States of America) and 0.125 µg/mL amphotericin B (Thermo Fisher Scientific, Waltham, Massachusetts, United States of America) were added to the buffer. The final solution was filter-sterilised using 0.22 µm syringe filters and stored at 4 °C until use and away from direct light exposure.

2.6.1.9 NIH-3T3 Culture Growth Medium

The feeder cell line used, NIH 3T3, were passaged in DMEM (Thermo Fisher Scientific, Waltham, Massachusetts, United States of America), with 10% HI-FCS (v/v; refer to 2.6.1.5) and 1% penicillin/streptomycin (v/v; refer to 2.6.1.10). Media was prepared in a biological safety cabinet, filter-sterilised through a 0.22 µm filter and stored at 4°C until required.

2.6.1.10 Penicillin/Streptomycin

Penicillin/streptomycin (Thermo Fisher Scientific, Waltham, Massachusetts, United States of America) with 10000 units/mL of penicillin and 10000 µg/mL of streptomycin was added to cell culture media to prevent contamination.

2.6.1.11 ROCK Inhibitor (Y-27632)

A 10 mM rho-associated protein kinase (ROCK) inhibitor (Y-27632) stock solution was prepared by dissolving 25 mg of ROCK inhibitor (Enxo Life Sciences, Farmingdale, New York, United States of America) in 7.8 mL of ddH₂O. This solution was filtered through

a 0.22 µm syringe filter (Cytivas Whatman™ Uniflo™ PES membrane, Massachusetts, United States of America) and stored as 50 µL aliquots at -20°C until required.

2.6.1.12 Subculture Reagents for Primary Cells

Primary cell subculture reagents (including HEPES buffered saline solution, Trypsin-EDTA and TNS; ReagentPack® subculture reagents, Lonza, Basel, Switzerland) were thawed upon receipt and stored at -20°C as 10 mL aliquots. When aliquots were required, they were thawed and subsequently stored at 4°C until finished.

2.6.1.13 Trypan Blue Solution (0.05% v/v)

For counting of primary airway epithelial cells, a 0.05% (v/v) Trypan Blue solution was made by diluting 5 mL Trypan Blue 0.4% (w/v; Sigma-Aldrich, St. Louis, Missouri, United States of America) in 35 mL of 1X PBS (refer to 2.4.25.). Solutions were filtered with a 0.22 µm syringe filter (Cytiva Whatman™ Uniflo™ PES membrane, Massachusetts, United States of America) and kept at room temperature until needed.

2.6.1.14 Primary Airway Epithelial Cell Growth Media

For culturing, passaging, and maintaining primary airway epithelial cell monolayer cultures Pneumacult™-Ex Plus was purchased (Stem Cells Australia, Victoria, Australia). For culturing cells at the air-liquid interface (ALI) Pneumacult™-ALI was purchased (Stem Cells Australia, Victoria, Australia). Prior to exposure experiments, primary airway epithelial cells grown at ALI were switched to Pneumacult™-ALI starvation which has penicillin/streptomycin and hydrocortisone omitted which can affect immune signalling outputs.

2.7 General Methodology

2.7.1 Bacterial Culture Techniques

2.7.1.1 Cryopreservation of Bacterial Isolates

Bacterial isolates were cryopreserved by mixing 900µL of 50% v/v glycerol (refer to 2.4.10) with 900µL of overnight bacterial culture (refer to 2.7.1.2). These were mixed

thoroughly by pipetting and left at room temperature for at least 30 mins before being transferred to -80 °C.

2.7.1.2 Culture of Bacterial Stocks

Cryopreserved bacterial stocks were removed -80 °C and kept in an esky with dry ice. A 10 µL loop (COPAN Diagnostics, Murrieta, California, United States of America) was used to streak glycerol stocks onto agar plates which were subsequently incubated statically in a non-humidified incubator. A single colony from agar plates was picked with a 10 µL loop (COPAN Diagnostics, Murrieta, California, United States of America) and resuspended in LB broth (refer to 2.5.1.1) before incubation overnight at 37 °C with 120 rpm of shaking.

2.7.1.3 Measuring Bacterial Optical Density at 600 nanometres (OD600nm)

Overnight cultures of bacteria (refer to 2.7.1.2) were diluted 1:10 with LB broth (refer to 2.5.1.1) in a cuvette (SARSTEDT AG & Co. KG, Nümbrecht, Germany). The OD600nm was then measured by an Eppendorf Fluorescent BioSpectrometer® (Eppendorf, Hamburg, Hamburg, Germany).

2.7.1.4 Enumerating Viable Bacterial Load by Colony Forming Units per Millilitre (CFU/mL)

Bacterial overnight cultures were established (refer to 2.7.1.2) and after overnight incubation, bacterial OD600nm was measured (refer to 2.7.1.3). Bacterial OD600nm was adjusted to 1.0, 0.1 and 0.01. Each of these bacterial densities were serially ten-fold diluted to 10^{-7} in LB broth (refer to 2.5.1.1). Then 100 µL of each dilution was spread on LB agar plates (refer to 2.5.1.2) using L-shaped spreaders (COPAN Diagnostics, Murrieta, California, United States of America). Once these had dried at room temperature the plates were incubated overnight at 37 °C in a non-humidified incubator. Bacterial colonies were then counted, and the CFU/mL calculated by the equation below.

$$\text{colony} \times \text{dilution} \times \text{dilution factor (to make it in millilitres)}$$

A line of best fit was made correlating the CFU/mL with OD600nm and the equation used in subsequent experiments to adjust a bacterial overnight culture's OD600nm to one corresponding to the desired OD600nm.

2.7.1.5 Antimicrobial and Synergy Testing

The details of experimental conditions can be found in Chapter 5 (refer to 5.2.2.3). *P. aeruginosa* isolates were treated singularly with antibiotics, phages, or combinations. A 50 µL volume of ten-fold dilutions of Kara-mokiny 16 (10^7 - 10^1 PFU/mL) and two-fold dilutions of tobramycin (128 - 0.25 µg/mL) were then added to each well. Wells were topped up with LB broth (Becton Dickinson Microbiology, Franklin Lakes, New Jersey, United States of America) to a total volume of 200 µL and plates incubated for 24 hrs at 37°C. Bacterial growth in all wells were then measured via turbidity (at OD600nm) using a CLARIOstar® Plus machine (BMG Labtech GmbH, Ortenberg, Germany). Where multiple antimicrobials were mixed, their fractional inhibitory concentration index (FICI) was calculated using the equation below. The antimicrobial relationship was then classified as synergistic (≤ 0.5), indifferent ($0.5 \leq 1$) or antagonistic (> 1).

$$\text{FICI} = \left(\frac{\text{Combination OD600nm}}{\text{Kara - mokiny 16 OD600nm}} \right) + \left(\frac{\text{Combination OD600nm}}{\text{Tobramycin OD600nm}} \right)$$

2.7.1.6 Bacterial DNA Extraction, Quality Control and Sequencing

For Illumina 150bp paired-end sequencing, bacteria were cultured on LB agar (refer to 2.5.1.2) overnight and then a single colony was cultured overnight in LB broth (refer to 2.5.1.1 and 2.7.1). Genomic DNA was then extracted using the DNeasy Tissue and Blood Extraction Kit (Qiagen, Hilden, Germany). Here, a 1 mL aliquot of the overnight culture was initially centrifuged at 4,000 xg for 10 mins at room temperature and resuspended in 180 µL of ATL buffer and 20 µL of Proteinase K (Qiagen, Hilden, Germany). Solutions were then incubated at 56 °C for 1 hour. Following this, 4 µL of RNase A (Invitrogen, Waltham, Massachusetts, United States of America) was added before a 15-minute incubation at room temperature. The process of washing and eluting the DNA was performed as per provided instructions in the kit (Qiagen, Hilden, Germany). overnight and then a single colony was cultured overnight growth in LB broth (Becton Dickinson, Franklin Lakes, New Jersey, United States of America; refer to 2.7.1.2).

DNA quality was initially checked using a Nanodrop 2000c (Thermo Fisher Scientific, Waltham, Massachusetts, United States of America) to ensure the 260/280 ratio was between 1.8-2.0. Concentration was then measured using the Qubit dsDNA High Sensitivity kit (Thermo Fisher Scientific, Waltham, Massachusetts, United States of America). Genomic DNA was Nextera XT library prepared and sequenced on the

NovaSeq 6000 Illumina (Illumina, San-Diego, California, United States of America) next generation sequencing platform that generated 150 bp paired-end reads. Library preparation and sequencing was performed by the Australian Genomic Research Facility (Monash University, Melbourne, Victoria, Australia).

Long bacterial reads were sequenced courtesy of Dr Samuel Montgomery (UWA, Perth Australia), where high molecular weight DNA was initially extracted [420] from overnight cultures of bacteria (refer to 2.7.1) and subsequently sequenced on Nanopore MinION flow cells using a Mk1C MinION sequencer (Oxford Nanopore Technologies, Oxford Science Park, Oxford, United Kingdom).

2.7.1.7 Bacterial Short Paired-End Illumina Whole Genome Assembly

Bacterial 150-bp paired-end Illumina reads were quality controlled and assembled using a docker container created as part of this thesis called Orange (<https://hub.docker.com/r/mantistobogan/orange>). Briefly, the assembly pipeline of this docker image uses a number of packages from BBmap v39.01 [421] to: trim reads with bbdduk, remove duplicate reads with dedupe, normalise coverage to 100X with bbnorm and merge reads to create longer ones with bbmerge. Reads were assembled with SPAdes v3.15.4 [422], and assembly gaps filled with Mind the Gap v2.3.0 [423] and utility scripts from Mine Your Symbiont v1.1 (MinYS) [424]. Species contamination was checked for by Kraken v1.0 [425].

2.7.1.8 Bacterial Long Read Nanopore and Short Paired-End Illumina Whole Genome Hybrid Assembly

MinION Nanopore long reads were QC and assembled through a custom bash script. Quality control of short reads was performed as above in 2.7.1.8 except these were not merged at the end. The long reads were filtered by length (>1000 bp), quality (Q10), 140bp head cropped and 40bp tail cropped with chopper v0.6.0 [426]. Hybrid assemblies were then made using unicycler v0.4.8 [427]. Long read only assemblies were also created by unicycler v0.4.8 [427] and flye v2.8.1-b1676 [428]. A consensus assembly was then created from each of the long read drafts and the hybrid using tricycler v0.5.4 [429]. The consensus assembly was then polished using medaka v 1.7.2 [430], BWA v 0.7.17-r1188 [431], and polypolish v0.5.0 [432].

2.7.1.9 Bacterial Genome Annotation

The Orange docker image (<https://hub.docker.com/r/mantistobogan/orange>) also has an annotation pipeline. The annotation pipeline determines the species of bacteria that was input via Kraken v1.0 [425], annotates general genomic features with Bakta v1.7.0 [433], phage resistance mechanisms by PADLOC v1.1.0 [434], multilocus sequence type (MLST) by the mlst v2.23.0 package [435] which uses the PubMLST database [436], it then uses abricate v1.0.1 [437] to find antibiotic resistance genes and virulence genes by searching a number of databases [438-444] and finally searches for prophages using DBSCAN-SWA [445] which makes use of both diamond [446], prokka v1.14.6 [447] and blast software [448].

2.7.1.10 Heat Killing *P. aeruginosa*

P. aeruginosa PAO1 (refer to Table 2.2) was grown overnight in LB broth (refer to 2.5.1.1 and 2.7.1.2). The OD_{600nm} of the overnight culture was then measured and adjusted to a value corresponding to 10⁸ CFU/mL in LB broth (refer to 2.7.1.3). The adjusted culture was centrifuged at 4000 rpm for 10 mins and the supernatant decanted. Then 5 mL of 1X PBS (refer to 2.4.25) was used to resuspend the cell pellet and this was centrifuged again at 4000 rpm for 10 mins. This process was repeated once more to wash the cell pellet before the cells were resuspended in 1X PBS (refer to 2.4.25) and left at 90 °C for one hour on a heat block.

2.7.2 Bacteriophage Culture Techniques

2.7.2.1 Preparation of Overlay Agar

LB overlay agar (refer 2.5.2.1) inoculated with bacteria was used for phage isolation, propagation, and enumeration. Molten 3 mL aliquots of LB overlay agar (refer to 2.5.2.1) were inoculated with 100 µL of bacterial culture grown overnight (refer to 2.7.1.2). Bacterial inoculated LB overlay agar was poured onto LB agar (refer to 2.5.1.2), evenly distributed across the surface and dried in a biosafety cabinet. Plates were statically incubated at 37°C overnight in non-humidified.

2.7.2.2 Phage Isolation from Wastewater Samples

Wastewater samples were enriched and screened for phages with activity against the panel of 29 *P. aeruginosa* clinically derived isolates or PAO1 (refer to Table 2.2)[449]. Wastewater was initially filtered through a 0.22 µm bottle-top filter (Nalgene™ Rapid-Flow™, Thermo Fisher Scientific, Waltham, MA, USA). The supernatant was collected and supplemented with 1M CaCl₂ (refer to 2.4.2) and 1M MgCl₂ (refer to 2.4.21) to a final concentration both of 0.1M. Double strength LB broth (refer to 2.5.2.3) was supplemented with CaCl₂ (refer to 2.4.2) and MgCl₂ (refer to 2.4.21) to final concentrations of 1 mM each. Enrichment was performed by combining 5 mL of supplemented double-strength LB broth (refer to 2.5.2.3), 200 µL of overnight *P. aeruginosa* cultures (refer to 2.7.1.2) and supplemented wastewater filtrate. Enrichment cultures were then incubated with 50 rpm of shaking for 24 and 48 hrs at 37 °C in ambient air. Bacteria and debris in enriched LB broth was pelleted by centrifugation at 4000 rpm (3220 xg) for 10 mins at room temperature, and the supernatants were filtered through 0.22 µm syringe filters (Cytiva Whatman™ Uniflo™ PES membrane, USA). Overnight cultures of each of the *P. aeruginosa* isolates (refer to 2.7.1.2) used as hosts in the enrichment were streaked in lines across LB agar plates (refer to 2.5.1.2) using 10 µL microbiological loops (COPAN Diagnostics, Murrieta, California, United States of America) and allowed to dry at room temperature in biological safety cabinets. Five microlitres of filtered enrichments were then spot tested (drop-on-plate) on the *P. aeruginosa* isolates' streaks they were enriched with to identify lytic activity. These spots were allowed to dry at room temperature in a biological safety cabinet before being incubated in non-humidified incubators at 37 °C overnight. The presence of phages and successful enrichment was determined via visualisation of clearance on the bacterial streaks.

2.7.2.3 Phage Purification

Isolated phages were purified through three rounds of plaque purification. Prior to purification, filtered enriched cultures where lysis was observed (refer to 2.7.2.2) were titrated (refer to 2.7.2.7). Double agar overlay inoculated with bacterial overnight culture (refer to 2.7.2.1) and enrichments at the dilution determined to be optimal for individual plaque formation were incubated overnight at 37 °C. Subsequently, plates were removed and inspected for individual plaques and morphological heterogeneity. A maximum of nine plaques per bacterial host with different morphologies were selected. The overlay

agar within selected plaques was aspirated with a sterile Pasteur pipette (Corning, New York, United States of America) and resuspended in 1 mL of SM buffer (refer to 2.5.2.2). Overlay agar was then broken up by vortexing and the solution filtered through a 0.22 µm syringe filter (Cytiva Whatman™ Uniflo™ PES membrane, USA). This process of plating, picking, and filtering was repeated three times per plaque. After the third round, phages were stored in the SM buffer (refer to 2.5.2.2) at 4 °C for further analysis.

2.7.2.4 Miniaturised Phage Spot Test for Host Range

To save on time and costs a miniaturised host range assay was initially performed on the isolated and purified phages [450]. Briefly, this involved inoculating 3 mL of LB overlay agar per plate with 100 µL of bacterial culture grown overnight (refer to 2.7.1.2). Then 350 µL of the inoculated overlay was added to wells of 24 well plates and allowed to dry at room temperature for 15 mins. Subsequently 2 µL of isolated and purified phages was added to the surface of overlay agar in the wells and allowed to dry at room temperature before being incubated at 37 °C in a non-humidified incubator. The following day wells containing phage spots were visualised for plaques and scored as either complete, partial or no lysis.

2.7.2.5 Overlay Agar Plate Determination of Host Range

To confirm phage host range in a smaller subset of phages the experiment was repeated on whole LB agar plates (refer to 2.5.1.2). LB overlay was inoculated with bacterial overnight cultures (refer to 2.7.2.1), poured on LB agar plates (refer to 2.5.1.2) and allowed to dry at room temperature. Then 10 µL of phages were spotted in duplicate onto sections of the surface. These were allowed to dry at room temperature before overnight incubation at 37 °C in a non-humidified incubator. Plates were visualised for complete, turbid or no lysis.

2.7.2.6 Phage Propagation Using LB Agar

To propagate phages 3 mL of molten LB overlay agar (refer to 2.7.2.1) was inoculated with equal 100 µL volumes of both *P. aeruginosa* and phage. This was inverted to mix, poured onto a LB agar plate (refer to 2.5.1.2) and allowed to dry at room temperature for 15 mins. Plates were incubated overnight at 37 °C in a non-humidified incubator.

Subsequently, 5 mL of SM buffer (refer to 2.5.2.2) was dispensed onto each agar plate and incubated for 15 mins on a platform orbital shaker at 50 rpm. The SM buffer (refer to 2.5.2.2) was collected, dispensed into 15 mL conical tubes, and centrifuged at 4000 rpm for 10 mins to pellet debris. Supernatants were passed through 0.22 µm syringe filters (Cytiva Whatman™ Uniflo™ PES membrane, USA) into a new conical tube. Filtered phage suspensions were enumerated (refer to 2.7.2.7) and stored at 4°C.

2.7.2.7 Phage Titre Enumeration in Plaque Forming Units per Millilitre (PFU/mL)

To determine phage concentrations, the phage solutions in were diluted ten-fold serially in SM buffer (refer to 2.5.2.2). LB agar plates (refer to 2.5.1.2) marked with different sections for dilutions from neat to 10⁻⁸. Inoculated LB overlay agar (refer to refer to 2.7.2.1) with the host bacteria was spread on the LB agar plates (refer to 2.5.1.2) and 10 µL of the phage serial dilutions were spotted onto their corresponding section. Spots were allowed to dry in for up to 30 mins and then incubated overnight at 37 °C in a non-humidified incubator. Dilutions with single plaques were counted and phages enumerated via the equation below.

$$CFU/mL = \text{Plaques} \times \text{Dilution} \times \text{Dilution Factor (make it per millilitre)}$$

2.7.2.8 Efficiency of Plating (EOP)

To determine the efficiency of plating, phages were enumerated (refer to 2.7.2.7) using both a wild-type (WT) and a mutant. EOP was then calculated by dividing the average PFU/mL on mutant by the average PFU/mL on the WT. This was performed in triplicate. The determined average EOP value for a particular phage-bacterium combination was then classified as infective when $EOP \geq 0.1$, weak infection when $EOP < 0.1$, and no infection when $EOP = 0$ as previously described [451].

2.7.2.9 Phage Time-Kill Assay

Detailed experimental conditions are described in Chapter 4 (refer to 4.2.5). Briefly, 100 µL of phages were added at varying concentrations to 100 µL *P. aeruginosa* cultures that had been adjusted to 10⁸ CFU/mL (refer to 2.7.1.3). Overall bacterial growth was measured using OD600nm at one hour time intervals. The lytic activity of the phages was

confirmed by enumerating viable bacterial load (CFU/mL; refer to 2.7.1.4) and phages (PFU/mL; refer to 2.7.2.7) every six hrs.

2.7.2.10 Phage Genome Extraction and Sequencing

Phage DNA was extracted as previously described with minor modifications [452]. Briefly, 900 μ L of filtered phage lysate was added to 100 μ L DNase I 10X buffer (New England Biolabs, Ipswich, MA, USA), 2 μ L of 1 U/ μ L DNase I (New England Biolabs, Ipswich, MA, USA), 1 μ L of 10 mg/mL RNase A (Thermo Fisher Scientific, Waltham, MA, USA) and incubated at 37 °C for two hrs. Following this, 24 μ L of 0.4 M EDTA (Sigma-Aldrich, St. Louis, MO, USA) and 1.25 μ L of 10 mg/mL Proteinase K was added (Invitrogen, Waltham, MA, USA) and the solution left to incubate for two hrs at 56 °C. The resulting solution was then purified through a DNeasy Blood and Tissue kit following the associated protocol (Qiagen, Hilden, Germany).

2.7.2.11 Phage Genome Bioinformatic Analysis

Phage reads were quality controlled and assembled by Phanatic v2.2.0 using the default settings [453]. Briefly, this package uses bbduk, bbmerge and bbnorm from BBmap v38.18 [421] to prepare reads for assembly by SPAdes v3.15.4 [422]. Assemblies were checked for completeness and contamination by CheckV v1.0.1 and its corresponding database v0.11.9 [454]. Sequences determined to be complete, meaning they were ranked at least high quality by CheckV based on completeness and contamination scores, were standardised and annotated using PhageOrder [455]. Specifically this package annotates genome assemblies using Prokka v1.14.6 [447] with the Prokaryotic Virus Remote Homologous Groups (PHROGS) database [456]. The package then utilised Biopython modules [457] to order assembled genomes relative to either the small or large terminase subunit (preferentially using the small subunit) and reannotates the reordered genome using prokka as already described. Specialist annotation was performed using tRNAscan-SE v1.3.1 [458] and abricate v1.0.1 (Seemann T, *Abricate*, <https://github.com/tseemann/abricate>).

2.7.2.12 Phage Phylogenetic Analysis

Closest relatives to isolated phage genomes were found in the 1st of July 2023 upload to the Infrastructure for a PHAge REference Database (INPHARED)[239] using PhindersKeepers [459]. These reference phages were reordered by PhageOrder [455] as above before being aligned with the isolated phages using Mafft [460], which determined the FFT-NS-2 fast progressive method was optimal. The multiple sequence alignment was then used to generate a maximum likelihood phylogenetic tree in MEGA v11 with 100 bootstraps [461]. Phylogenetic trees were then annotated using the online software Interactive Tree of Life [462] and 1st of July 2023 INPHARED data [239]. A BLAST database of the INPHARED data was made and each isolated phage was searched against it. Phusion [463] was used to obtain putative family, sub-family, genus and species of each of the phages by comparing them to a blast database of the 1st of May 2023 INPHARED data [239], extracting the top hits and creating a consensus for each of these categories. The average nucleotide identity (ANI) was compared between the phages isolated here and the closest relatives from INPHARED (that were downloaded from above) using VIRIDIC v1.1 [464].

2.7.2.13 Transmission Electron Microscopy (TEM)

Chloroform (Sigma-Aldrich, St. Louis, Missouri, United States of America) at a 1% (v/v) concentration was added to 10 mL of propagated phages (refer to 2.7.2.6 and 2.7.2.7), vortexed and incubated for 15 mins at room temperature with inverting every five mins. The mixture was then centrifuged at 4,000 xg for 10 mins at room temperature. Tubes were pierced with a 28 G needle (TERUMO, Macquarie Park, NSW, Australia) just above the aqueous-organic interface and the aqueous phase aspirated. Phages were titred (refer to 2.7.2.7) prior to shipping to ensure that they were still active and present. These were stored at 4 °C until they were shipped to the University of Adelaide (Adelaide, South Australia, Australia) where TEM imaging was performed by Mr Christopher Leigh. Samples were initially fixed with paraformaldehyde (Electron Microscopy Sciences, Hatfield, PA, USA) to a final concentration of 2% (v/v) and diluted 1:10 in SM buffer (refer to 2.5.2.2). Glow discharged Carbon/formvar coated grids (Gatan Solarus Plasma System, Pleasanton, CA, USA) were loaded with 5 µL of sample and left for 2 mins. Grids were dried with filter paper and washed with 5 µL of ddH₂O water for 30 sec before drying again. The grid was then stained with 5 µL of 2% (v/v) uranyl acetate for 2 mins at room temperature and dried again. Acceleration voltage was set at 100 kV and grids

were then visualised on a Tecnai G2 Spirit 120 kV TEM (FEI Company, Hillsboro, OR, USA) and imaged with an AMT Nanosprint 15 digital camera and software v7.0.1 (AMT Imaging, Woburn, MA, USA). Five images taken at 68,000 X magnification were used to measure phage dimensions (head diameter, head length, tail length and tail width) with ImageJ [465].

Based on their appearance, phages were named in consultation with the Noongar language centre in the language of the traditional owners of the land from where they were isolated. The smaller phages were therefore named Kara-mokiny kep-wari Wadjak which translates to good spider (from) still water pond Wadjak and will now be referred to as their shorter name Kara-mokiny followed by a number. The larger phages were called Koomba boorn-mokiny kep-wari Wadjak which translates to big tree-like (from) still water pond Wadjak. Again, with permission these have been referred to as Boorn-mokiny followed by a number.

2.7.2.14 One-Step Growth Curve

A one-step growth curve was performed as previously described with minor modifications [466]. Briefly, an overnight culture of PAO1 was adjusted to an OD_{600nm} of 1.0 (refer to 2.7.1.3). PAO1 was then mixed with 10⁸ PFU/mL of each phage so there was a multiplicity of infection (MOI) of 1. Phages were allowed to adsorb for five mins at 37 °C (non-humidified) with 50 rpm of shaking. A 100 µL aliquot was removed and used to enumerate phages (refer to 2.7.2.7) and the adsorbed solution was then diluted 1:10,000 and replaced in the incubator with 50 rpm of shaking. Every 10 mins 100 µL was removed and used to enumerate phages (refer to 2.7.2.7). Plates were incubated overnight at 37 °C in a non-humidified incubator and plaques were counted. Plaque counts were used to determine the phages produced per infected bacterium (burst size) using the formula below:

$$\text{Burst size} = \left(\frac{\text{PFU}}{\text{mL}} \text{ at plateau of phage infection} \right) / \left(\frac{\text{PFU}}{\text{mL}} \text{ at during latent period} \right)$$

2.7.2.15 Thermal and pH Stability

The thermal stability of each of the phages was determined by storing 1 mL of propagated phage (refer to 2.7.2.6) at 25 °C (room temperature), 4 °C, -20 °C and -80 °C. Phages were enumerated after one week, one month, three months, six months, and a year of

storage using their host *P. aeruginosa* (refer 2.7.2.7). Stability of phages at pH 3, 5, 7, 9 and 11 was also measured by changing the pH of SM buffer (refer to 2.5.2.2) to the desired level using 1M HCl (Univar, Ingleburn, NSW, Australia) or 1M NaOH (Sigma-Aldrich, St. Louis, MO, USA). Phages were propagated, titred (refer to 2.7.2.6 and 2.7.2.7) and diluted 1 in 100 in each of the different pH SM buffers (refer to 2.5.2.2). These were left at 37 °C in a non-humidified incubator for one hour and 24 hrs before being enumerated again (refer to 2.7.2.7). All experiments were performed in triplicate with duplicate enumerations at each time point.

2.7.2.16 Endotoxin Removal from Phage Preparations

Phages were propagated (refer to 2.7.2.6) and enumerated (refer to 2.7.2.7). The lysate was then passed through twice Cytiva Acrodisc™ Units with Mustang E membrane (Cytiva, Marlborough, Massachusetts, United States of America).

2.7.2.17 Endotoxin Quantification in Phage Preparations

To measure the endotoxin level in the different exposures to the primary airway epithelial cells the chromogenic Limulus Amebocyte Lysate (LAL) assay was performed as per the manufacturer's protocol (Charles River, Willmington, Massachusetts, United States of America).

2.7.3 Tissue Culture Methods

Detailed descriptions of experimental exposures can be found in Chapter 5 (refer to 5.2.2.7). Briefly, primary AECs were exposed to phages or antibiotics alone or combined. They were also exposed to heat killed PAO1 and a PBS vehicle control. This was done to determine any phenotypical and cytokine induction differences in response to phage exposure.

2.7.3.1.1 Cell Line Origins

The mouse fibroblast, NIH-3T3 cell line was obtained from the American Type Culture Collection (ATCC; Manassas, Virginia, United States of America) and are feeder cells used to establish and maintain conditionally reprogrammed primary airway epithelial cell

cultures. The NIH-3T3 cell line originated from desegregated NIH Swiss mouse embryo fibroblasts [467, 468].

2.7.3.1.2 Cell count and viability

Total cell count and viability were calculated by trypan blue (refer to 2.6.1.13) staining of primary airway epithelial cells and visualisation on a haemocytometer. Cell suspension and trypan blue (refer to 2.6.1.13) were mixed in equal 10 μ L volumes. Then 10 μ L of the solution was added to the haemocytometer chamber and visualised with a microscope. Viable cells were counted across the four grids of the chamber, followed by the non-viable cells. Non-viable cells were stained darker blue due to trypan blue permeating through damaged cell membranes, while viable cells remained impermeable to the dye and unstained. The total cell count was performed by averaging the cell numbers of four grids and multiplying it by the dilution factor and the density of the suspension. Cell viability was represented by dividing the viable cells by total (viable and non-viable) and representing this as a percentage.

2.7.3.1.3 Cell Line Recovery

To revive NIH-3T3 cells cryopreservation in DMSO they were rapidly thawed in a 37 °C water bath and diluted 1:10 in RPMI-1640 (v/v; Thermo Fisher Scientific, Waltham, Massachusetts, United States of America). The solution was centrifugated at 500 xg for 7 mins at 4 °C, then the cell pellet was resuspended in 1 mL of the growth medium (refer to 2.6.1.9). The total cell count and viability (refer to 2.7.3.1.2) were performed using trypan blue solution (refer to 2.6.1.13) and a haemocytometer. The revived cells were then seeded into a 25 cm² tissue culture flask in 5 mL of growth medium (refer to 2.6.1.9). The cell culture was maintained at 37 °C in 5% CO₂/ 95% air in a cell line dedicated Heracell™ VIOS 160i incubator. Cell cultures were regularly tested and certified as mycoplasma free (refer to 2.7.3.2.11).

2.7.3.1.4 Cell Line Subculture

When NIH-3T3 cells were observed to be ~90% confluent under microscope, they were passaged. Briefly, cells were washed once with 1X PBS (refer to 2.4.25) and detached from the flask by incubation with 0.25% Trypsin-EDTA (Sigma-Aldrich, St. Louis, Missouri, United States of America) solution for 7 mins at 37 °C in 5% CO₂/95% air. The

flask was washed with FCS-based TNS-neutralised trypsin (refer to 2.6.1.7), followed by 1X PBS (refer to 2.4.25) and this was collected in a 15 mL tube. The cell suspension was centrifuged at 500 xg for 7 mins at 4 °C, and the cell pellet was resuspended in 1 mL of growth medium (refer to 2.6.1.9). A total cell and viability count was performed (refer to 2.7.3.1.2) before cells were seeded into a new tissue culture flask at a density of 5,000 cells per cm². Cultures were maintained at 37 °C in 5% CO₂/ 95% air in a cell line dedicated Heracell™ VIOS 160i incubator.

2.7.3.1.5 Cell Line Cryopreservation

Cell lines were cryopreserved in liquid nitrogen at -196°C (refer to 2.6.1.4). Briefly, the cells were passaged (refer to 2.7.3.1.4) and cell count and viability were performed (refer to 2.6.1.13). Cells were stored in cryovials in 1 mL of cryopreservation solution (refer to 2.6.1.4) with a minimum concentration of 0.5x10⁶ cells/mL with. Cryovials were then stored for 24 hrs at -80°C with isopropanol in Mr Frosty cryo-containers (Thermo Fisher Scientific, Waltham, Massachusetts, United States of America) to allow freezing at a rate of -1°C/ minute before being transferred to liquid nitrogen at -196°C.

2.7.3.2 Paediatric primary airway epithelial cells

2.7.3.2.1 Ethics approval

The current study was approved by St. John of God (Subiaco) Hospital and Curtin Human Research Ethic Committee. Permission was granted to collect paediatric primary airway epithelial cells from patients undergoing elective surgery for non-respiratory conditions by St. John of God Hospital (Subiaco; WAERP #901) and Curtin Human Research Ethics Committee (2019-0086; refer to Appendix A.1).

2.7.3.2.2 Primary airway epithelial cell collection and processing

Primary airway epithelial cells from children that did not have a history of atopy were used in this study. Participants were verified to be free of respiratory symptoms such as bacterial or viral chest infection at the time of recruitment. Parents gave written consent for their children to participate in the programme, and ISAAC and American Thoracic Society (ATS) respiratory questionnaires were used to verify the children's health status or respiratory conditions reported by parents or guardians. The allergy status of all children was determined by a radioallergosorbent test (RAST) against common allergens.

The collection of primary airway epithelial cells was performed through blind brushing of one nostril with a sterile interdental brush (refer to 2.3.6) after the child was anaesthetised. Once completed, the brushes were inserted into sterile CCM (refer to 2.6.1.6) with 20% HI-FCS (v/v; refer to 2.6.1.5). This process with a second brush in the adjacent nostril and put into the same collection tube. Samples were stored on ice until they could be taken to the laboratory for processing. In the laboratory cells were dislodged from the brush by vortexing, and brushes were transferred into a new collection tube and the process repeated to remove as many cells as possible. The cell suspensions from both tubes were pooled and centrifuged at 500 xg for 7 mins at 4 °C. The cell pellet was resuspended in 1 mL of CCM (refer to 2.6.1.6). A single cell suspension was then made by passing the solution through two syringe needles of 25 G, 1-inch length, followed by 27 G, ½-inch length (TERUMO, Macquarie Park, New South Wales, Australia). Total cell count and viability were then performed (refer to 2.7.3.1.2). Cells were cryopreserved (refer to 2.7.3.2.4) in cryopreservation media (refer to 2.6.1.4).

2.7.3.2.3 Irradiation of fibroblasts

Before using fibroblasts to establish a primary airway epithelial cell culture, NIH-3T3 fibroblasts were subcultured (refer to 2.7.3.1.4) and γ -irradiated with 3000 cGy γ -radiation (refer to 2.3.10). A total cell count and viability were performed (refer to 2.7.3.1.2). Prior to primary airway epithelial cells being seeded, irradiated fibroblasts were seeded at a density of 5,000 cells per cm² into a fibronectin-coated tissue culture flask (refer to 2.6.1.8).

2.7.3.2.4 Primary airway epithelial cells cryopreservation

Primary airway epithelial cells were cryopreserved in 1 mL of cryopreservation media (refer to 2.7.3.2.4 and 2.6.1.4) with at least 0.5×10^6 cells/mL in cryovials. These were stored for at least 24 hrs at -80°C with isopropanol in Mr Frosty cryo-containers (Thermo Fisher Scientific, Waltham, Massachusetts, United States of America) to allow freezing at a rate of -1 °C/minute before being transferred to liquid nitrogen at -196 °C.

2.7.3.2.5 Primary airway epithelial cells recovery

Cryopreserved airway epithelial cells were revived by rapid thawing of cryovials at 37 °C in a water bath. The solution was diluted 1:10 in Pneumacult™-EX Plus (refer to 2.6.1.14) and centrifuged at 500 xg for 7 mins at 4 °C. The cell pellet was resuspended in 3 mL of Pneumacult™-EX Plus (refer to 2.6.1.14) before total and viable cell counts were performed (refer to 2.7.3.1.2). Irradiated fibroblasts were seeded at 5000 cells per cm² to tissue culture flasks before primary airway cells were also added at 5000 cells per cm². The media in the flask was topped up to 5 mL of Pneumacult™-EX Plus (refer to 2.6.1.14) and cells were maintained at 37 °C in 5%CO₂/95% air in a primary cell Heracell™ VIOS 160i incubator.

2.7.3.2.6 Primary airway epithelial cells subculturing

Primary AECs were revived (refer to 2.7.3.2.5) and established. Once cells were observed to reach ~80% confluence under a microscope, passage was performed using a commercial subculture reagent pack (refer to 2.6.1.12). Cells were washed with reagent subculture pack HEPES buffered saline solution, followed by incubation with trypsin-EDTA solution for 5 mins at 37 °C to remove NIH3T3 cells. To neutralise trypsin-EDTA an equal amount of TNS (refer to 2.6.1.7) was added. To dislodge primary airway epithelial cells 1:100 trypsin (Sigma-Aldrich, St. Louis, Missouri, United States of America) in 1X PBS (refer to 2.4.25) was incubated with the cells at 37 °C for at least five mins or until the cells were observed to come off the plastic. The flask was washed with HI-FCS (refer to 2.6.1.5) and this cell suspension was collected and centrifuged at 500 xg for 7 mins at 4 °C. The cell pellet was resuspended in Pneumacult™-EX Plus (refer to 2.6.1.14) and transferred to another fibronectin (refer to 2.6.1.8) precoated tissue culture flask or Transwell® permeable inserts for experimentation (refer to 2.7.3.2.8). All primary cell cultures were maintained at 37 °C in 5%CO₂/95% air in a primary cell dedicated Heracell™ VIOS 160i incubator. Primary cell cultures were certified as mycoplasma free using the supernatants collected during subculture (refer to 2.7.3.2.11).

2.7.3.2.7 Primary airway epithelial cells maintenance

Primary airway epithelial cell cultures were maintained every Monday, Wednesday, and Friday. Briefly, cultures were visually inspected for contamination and confluence under a microscope. When cultures were not confluent media was aspirated and changed.

2.7.3.2.8 Air-liquid interface (ALI) cell culture

Transwell® permeable 24 well plate inserts were coated with 200 µL of collagen type I (rat tail; refer to 2.6.1.3) and incubated at 4 °C overnight. The collagen was aspirated, and the inserts washed with 200 µL 1X PBS (refer to 2.4.25). Primary airway epithelial cells were subcultured (refer to 2.7.3.2.6) and 750,000 cells/mL seeded onto each insert. The basal compartment was filled with 500 µL of Pneumacult™-EX Plus (refer to 2.6.1.14). The ALI cultured cells were maintained at 37°C in 5%CO₂/95% air in a primary cell dedicated Heracell™ VIOS 160i incubator. For the first week the apical and basal media was aspirated and changed, and inserts were inspected for cell confluence. After a week, the apical media was aspirated and not replaced, and the basal media was changed to Pneumacult™-ALI (refer to 2.6.1.14). After this the basal media was only changed every Monday, Wednesday and Friday. Trans-epithelial electrical resistance (TEER; refer to 2.7.3.2.9) was performed on day 7, 14 and 28 post-airlift to indicate tight junction formation and barrier integrity.

2.7.3.2.9 Trans-epithelial electrical resistance (TEER)

Primary airway epithelial cells cultured at the ALI were prepared for TEER by washing with 1X PBS (refer to 2.4.25) to remove mucus. Any culture media was removed from the inserts and 200 µL 1X PBS (refer to 2.4.25) added to the apical side. This was left for 5 mins at 37 °C in 5%CO₂/95% air before aspiration. Then to take TEER measurements 200 µL and 300 µL 1X PBS (refer to 2.4.25) was added to the apical and basal sections of the inserts respectively. The two prongs of the EVOM electrode were submerged in the apical and basal 1X PBS (refer to 2.4.25) until the current stopped on a number and this was recorded. Three readings per insert were taken and five inserts per participants cells were used for TEER. After this was complete the PBS was aspirated and replaced with 500 µL Pneumacult™-ALI (refer to 2.6.1.14). Cell cultures were put back into a primary cell dedicated Heracell™ VIOS 160i incubator at 37 °C in 5%CO₂/95% air.

2.7.3.2.10 Treatment conditions of established primary airway epithelial cells

At 28 days post-airlift primary airway epithelial cell ALI culture basal media was switched to Pneumacult™-ALI starvation (refer to 2.6.1.14). At 31 days post-airlift the apical side of the cells were washed with 200 µL 1X PBS (refer to 2.4.25) and incubated with this at 37°C in 5%CO₂/95% air for five mins. Then the 1X PBS (refer to 2.4.25) was aspirated and the basal Pneumacult™-ALI starvation (refer to 2.6.1.14) changed. All the solutions exposed to the cells were diluted in 1X PBS (refer to 2.4.25). Then, 10 µL of 10⁶ PFU/mL Kara-mokiny 16, 2 µg/mL of tobramycin, 10⁶ PFU/mL Kara-mokiny 16 combined with 2 µg/mL of tobramycin, 10⁶ CFU/mL of heat killed PAO1, or PBS was added to the apical surface of the cells. Exposures were performed in triplicate wells, and they were maintained at 37°C in 5%CO₂/95% air in a primary cell dedicated Heracell™ VIOS 160i incubator. After 24 hrs of exposure to these conditions 200 µL of 1X PBS (refer to 2.4.25) was added to the apical surface of the cells for five mins at room temperature. This was collected and 180 µL frozen at -80 °C, whilst the remaining 20 µL was kept at 4 °C. The basal media was equally divided between -80 °C and 4 °C storage. The -80 °C stored samples were for inflammation marker and cytotoxicity assays (refer to 2.7.4.1, 2.7.4.2 and 2.7.4.3) whilst the samples kept at 4 °C were used for phage enumeration (refer to 2.7.2.7).

2.7.3.2.11 Mycoplasma testing

Cell cultures were routinely tested for mycoplasma contamination using the MycoAlert™ PLUS assay (Lonza, Basel, Switzerland). Cell culture supernatant was collected during subculture (refer to 2.7.3.2.6 and 2.7.3.1.4) after centrifugation to ensure that there was no eukaryotic cell contamination. Cell supernatants were stored at -80 °C until tested. Reagents and samples were equilibrated to room temperature prior to testing. Samples and the positive control were diluted 1:10 (v/v) with MycoAlert™ PLUS assay buffer. All dilutions were transferred to a 96 half-area white plate (Perkin Elmer, Massachusetts, United States of America). An equivalent amount of MycoAlert™ PLUS substrate was added to each well, incubated at room temperature for 30 mins and luminescence measured by the CLARIOstar® Plus machine (BMG Labtech GmbH, Ortenberg, Germany). The result of this was referred to as Reading A. The process was repeated with the samples again to get Reading B. The ratio of Reading B/Reading A was then

determined and ratios >1.0 were indicative of the presence of mycoplasma. All cell cultures used in this study were tested and verified to be mycoplasma contamination-free.

2.7.4 Protein Expression Analyses

2.7.4.1 Cytotoxicity

Briefly, the cytotoxicity to primary airway epithelial cells caused by different stimuli was measured by the concentration of lactate dehydrogenase (LDH) using the CytoTox 96® Non-Radioactive Cytotoxicity Assay (Promega Corporation, Madison, Wisconsin, United States of America) according to manufacturer's instructions. The full methodology can be found in Chapter 5 (refer to 5.2.2.9).

2.7.4.2 IL-8 Enzyme Linked Immunosorbent Assay (ELISA)

Briefly, the inflammatory cytokine (interleukin-8; IL-8) secreted by the primary airway epithelial cells was measured with a commercial ELISA kit following the manufacturer's instructions (Becton Dickinson Biosciences, Franklin Lakes, New Jersey, United States of America). The full methodology can be found in Chapter 5 (refer to 5.2.2.10).

2.7.4.3 IL-6 Enzyme Linked Immunosorbent Assay (ELISA)

Briefly, the inflammatory cytokine (interleukin-6; IL-6) secreted by the primary airway epithelial cells was measured with an in-house developed TRF ELISA [469]. The full methodology can be found in Chapter 5 (refer to 5.2.2.11).

2.7.4.4 Histology

To confirm full differentiation of primary airway epithelial cell ALI cultures, one insert per participant per treatment was prepared for histology staining and microscopy. Here, inserts were cut in half and placed in NBF (refer to 2.4.22) at 4 °C for 24 hrs and then 95% (v/v) ethanol at 4 °C for 24 hrs. Inserts were then embedded in paraffin blocks, sliced into 5 µm sections and mounted on glass slides. The sections were then de-paraffin and rehydrated prior to the staining with haematoxylin and eosin (Sigma-Aldrich, St. Louis, Missouri, United States of America) to visualise the morphology or Alcian blue (Sigma-Aldrich, St. Louis, Missouri, United States of America) for mucous production.

2.7.4.5 Statistics

All statistical tests were performed in GraphPad Prism v9.3.1 (GraphPad Software, La Jolla, CA). Normality was tested for using the Shapiro-Wilk normality test. This informed the statistical tests that were performed and the specifics of these are described in the relevant chapters. A $p < 0.05$ was considered statistically significant.

This page is intentionally left blank.

3. Isolation and Characterisation of *Pseudomonas aeruginosa* Phages

3.1 Introduction

The use of phages as an alternative therapy to treat AMR infections has regained popularity in recent years with the successful treatment of those most critically ill [293, 296, 302, 304]. Being readily isolated from the environment [470], they coinhabit niches with their host bacteria and can be sourced from clinical samples, soil, farmyard slurries and wastewater [256, 265, 471]. Once isolated, phages must then be characterised by scrutinising their activity and genome to ensure their safety and applicability for therapeutic use [256, 267, 472, 473]. The foremost aspect to establish is the phage's lifestyle. Temperate phages are not applicable for therapy because they integrate into the bacterium and do not obligately kill it [256, 267, 472, 473]. Additionally, they transduce genes at high frequency into the bacterial host which can increase its virulence or antibiotic resistance [474]. For therapy, obligately lytic phages are sought because they have to kill their host bacteria and transduce genes at a low frequency [267, 472-474]. This is typically determined via bioinformatic analysis of phage genomes, identifying the absence of integrases, bacterial virulence, and antibiotic resistance genes [267, 472, 473]. Bioinformatics can also be used to determine if a sample contains more than one phage by identifying the presence of multiple contigs and investigating these for phage and bacterial genes [267]. Secondly, determining phage host range establishes species specificity as well as the breadth of strain activity [256, 471, 475]. Other non-essential phage characteristics that are often determined include stability over a spectrum of pH and temperatures [256, 475, 476] as well as morphological assessment via transmission electron microscopy (TEM) [476, 477].

Phages vary widely in their host range, stability, and their ability to transduce DNA as mentioned above. To establish a translational pipeline for phage therapy a repository of well-characterised bacteriophage is needed for which these parameters are known and can be used to select the most appropriate bacteriophage for treatment. Work conducted in this chapter tested the hypothesis that phages active against *P. aeruginosa* could be isolated from suburban wastewater. Work conducted successfully isolated and purified

252 phages active against this pathogen. Host range was then determined before those with broadest activity were sequenced. Phage genomes were inspected for temperate phage, antibiotic resistant and bacterial virulence genes. Sequencing samples were also scrutinised for multiple phage contigs, indicating temperate phage contamination. Phages whose genome passed this quality control were then evaluated morphologically TEM, before being phylogenetically compared to other isolated phages and well as those publicly available. Distinct phages identified from the phylogenetic investigation, then had their receptor, cryo-stability, pH stability and one-step growth parameters determined to complete their characterisation.

3.2 Materials and Methods

3.2.1 Materials

All reagents and chemical utilised in this chapter are listed in Chapter 2.

3.2.2 General Methodology

3.2.2.1 Bacterial Strains and Culture Conditions

The *P. aeruginosa* laboratory reference strain (PAO1; ATCC 15692) was obtained from the Department of Microbiology Culture Collection at the University of Western Australia [417]. Respiratory clinical isolates of *P. aeruginosa* (n=29) from children with CF were obtained from Melbourne Pathology (Melbourne, Victoria, Australia) and de-identified (refer to Table 2.2). Clinical isolates were also obtained from adults with CF (n=73; courtesy of Dr Anna Tai, Institute of Respiratory Health, Perth, Western Australia) and from other types of infection (n=40; courtesy of Prof. Geoffrey Coombs, PathWest Laboratory Medicine, Perth, Western Australia, Australia; refer to Table 2.2). A mutant PAO1 library (n=27; refer to Table 2.2) was also obtained from the Manoil Laboratory (University of Washington, USA). These had putative phage receptors knocked out by transposon insertion into the mPAO1 (wild type; WT) genome [418, 419, 478]. Knockouts were created using either the *lacZ* or *phoA* reporter sequences [418, 419, 478]. Each mutant had a gene knocked out that was suspected of being a phage receptor such as those involved in LPS biosynthesis (*wzt*, *galU*, *rmlC* and *migA*), type IV pilus formation and function (*pilA*, *pilB* and *pilY1*), flagellum structure (*fliC*), outer membrane

proteins (*oprM*, *oprD*, *oprJ*, *oprF*, *oprH* and *oprN*) and type VI secretion system (*clpVI*). *P. aeruginosa* were maintained using LB agar or broth (Becton Dickinson, Franklin Lakes, NJ, USA) and propagated as previously described [479] (refer to 2.7.1.2).

For host specificity studies, several bacterial species were used including *Burkholderia cepacia* complex (n=20) and *Staphylococcus aureus* (n=20) courtesy of Prof. Scott Bell (QIMR Berghofer Medical Research Institute, Brisbane, Queensland, Australia) and *Escherichia coli* (n=1), *Enterococcus faecalis* (n=1), *Enterococcus faecium* (n=2) and *Klebsiella pneumoniae* (n=3) kindly provided by Prof. Geoffrey Coombs (PathWest Laboratory Medicine, Perth, Western Australia, Australia; refer to Table 2.2). All bacterial species were maintained as previously described [480-484] and isolate stocks maintained in 25% (v/v) glycerol at -80 °C (refer to 2.7.1.1).

3.2.2.2 Phage Isolation and Purification

Phages were isolated from wastewater samples collected at a suburban wastewater treatment plant (Shenton Park, Western Australia, Australia). Unenriched and enriched isolation was performed using 30 *P. aeruginosa* isolates as hosts (PAO1 and 29 paediatric CF isolates; refer to Table 2.2, 2.7.2.2 and 2.7.2.3). Samples were then screened for lytic activity against each of the 30 *P. aeruginosa* by streaking 10 µL loopfuls of overnight cultures onto LB agar plates (refer to 2.5.1.2) and allowing them to dry before spotting 5 µL of the samples onto them (refer 2.7.2.2). Samples were visually inspected and those that were positive for lysis were then supplemented with 1M CaCl₂ (refer to 2.4.2) and 1M MgCl₂ (refer to 2.4.21). Samples were then mixed with 100 µL of the bacterial isolation host and 3 mL of overlay agar (refer to 2.7.2.2) and poured onto an LB agar plate (refer to 2.5.1.2). Plates were then incubated overnight in a 37 °C non-humidified incubator before single plaques were picked and resuspended in SM buffer (refer to 2.5.2.2). Phages were preferentially picked from unenriched samples to conserved diversity by reducing the amount of selection on the phage population. The process of purifying each isolated phage was repeated three times (refer to 2.7.2.3). Plaque morphologies were then categorised according to size (<1mm [pinpoint], 1-2mm [medium] and >2mm [large]), shape (round or irregular), presence of halo (absent or present) and turbidity (turbid or clear). After the final round of purification, phages were filtered and suspended in SM buffer (refer 2.5.2.2) and stored at 4 °C. For each experiment, phages were propagated on LB agar (refer to 2.5.1.2) using their isolation

host (refer to 2.7.2.6) and the resulting titre of the solution determined through dilution and spot test (refer to 2.7.2.7).

3.2.2.3 Phage Host Range Analysis

Host range of phages were initially tested using a previously described methodology (refer to 2.7.2.4) against PAO1, paediatric (n=29) and adult (n=73) CF *P. aeruginosa* clinical isolates (refer to Table 2.2). The host range of the 20 phages capable of lysing the highest proportion of clinical isolates was confirmed using whole plate overlay (refer to 2.7.2.5) and included 25 *P. aeruginosa* clinical isolates (refer to Table 2.2) derived from non-CF respiratory (n=5), tissue/sterile (n=6), blood cultures (n=3), wounds (n=10) and urine infection sites (n=1). Phage E79 was included as a reference comparison phage [262]. In all host range experiments, zones of clearance were visually inspected, after overnight incubation at 37 °C in a non-humidified incubator, and classified as complete, partial, or negative for lysis.

3.2.2.4 Phage DNA Extraction

Phage DNA was extracted as previously described with minor modifications [452]. Briefly, 900 µL of filtered phage lysate was added to 100 µL DNase I 10x buffer (New England Biolabs, Ipswich, MA, USA), 2 µL of 1 U/µL DNase I (New England Biolabs, Ipswich, MA, USA), 1 µL of 10 mg/mL RNase A (Thermo Fisher Scientific, Waltham, MA, USA) and incubated at 37 °C for 2 hrs. Following this, 24 µL of 0.4M EDTA (Sigma-Aldrich, St. Louis, MO, USA) and 1.25 µL of 10 mg/mL Proteinase K was added (Invitrogen, Waltham, MA, USA) and the solution left to incubate for two hrs at 56 °C. The resulting solution was then purified through a DNeasy Blood and Tissue kit following the associated protocol (Qiagen, Hilden, Germany).

3.2.2.5 Extracted DNA Quality Evaluation and Whole Genome Sequencing

DNA quality was initially checked using a Nanodrop 2000c (Thermo Fisher Scientific, Waltham, MA, USA) to ensure that the 260/280 ratio was between 1.8-2.0. Concentration was then measured using the Qubit dsDNA High Sensitivity kit (Thermo Fisher Scientific, Waltham, MA, USA). Genomic DNA was Nextera XT library prepared and sequenced on the NovaSeq 6000 Illumina (Illumina, San-Diego, CA, USA) next

generation sequencing platform that generated 150 bp paired-end reads. Library preparation and sequencing was performed by the Australian Genomic Research Facility (Monash University, Melbourne, Vic, Australia).

3.2.2.6 Phage Genome Assembly and Annotation

Phage reads were quality controlled and assembled by Phanatic v2.2.0 using the default settings [453]. Briefly, this package uses bbdduk, bbmerge and bbnorm from BBmap v38.18 [421] to prepare reads for assembly by SPAdes v3.15.4 [422]. Assemblies were checked for completeness and contamination by CheckV v1.0.1 and its corresponding database v0.11.9 [454]. Assembled sequences only passed if there was a single contig ranked as at least high quality by CheckV based on completeness and contamination scores. Any other contigs >1,000 bp were annotated and checked for intergrases, excisionases and transposases to ascertain if these were temperate phage contaminants [267]. Assemblies that did not contain multiple phage genomes were standardised and annotated using PhageOrder [455]. Specifically this package annotates genome assemblies using Prokka v1.14.6 [447] with the Prokaryotic Virus Remote Homologous Groups (PHROGS) database [456]. The package then utilised Biopython modules [457] to order assembled genomes relative to either the small or large terminase subunit (preferentially using the small subunit) and reannotates the reordered genome using prokka as already described. Specialist annotation was performed using tRNAscan-SE v1.3.1 [458] and abricate v1.0.1 (Seemann T, *Abricate*, <https://github.com/tseemann/abricate>).

3.2.2.7 Transmission Electron Microscopy (TEM)

Chloroform (Sigma-Aldrich, St. Louis, MO, USA) at a 1% (v/v) concentration was added to 10 mL of propagated phages (refer to 2.7.2.6 and 2.7.2.13), vortexed and incubated for 15 mins at room temperature with inverting every 5 mins. The mixture was then centrifuged at 4,000 xg for 10 mins at room temperature. Tubes were pierced with a 28 G needle (TERUMO, Macquarie Park, NSW, Australia) just above the aqueous-organic interface and the aqueous phase contain phage aspirated out. Phages were titred (refer to 2.7.2.7) to ensure that they were still active and present and stored at 4 °C until TEM imaging was performed (Mr Christopher Leigh, University of Adelaide, Adelaide, South Australia, Australia). Briefly, samples were initially fixed with paraformaldehyde

(Electron Microscopy Sciences, Hatfield, PA, USA) to a final concentration of 2% (v/v) and diluted one in ten in SM buffer (refer to 2.5.2.2). Glow discharged Carbon/formvar coated grids (Gatan Solarus Plasma System, Pleasanton, CA, USA) were loaded with 5 μ L of sample and left for 2 mins. Grids were dried with filter paper and washed with 5 μ L of ddH₂O water for 30 sec before drying again. The grid was then stained with 5 μ L of 2% (v/v) uranyl acetate for two mins at room temperature and dried again. Acceleration voltage was set at 100 kV and grids were then visualised on a Tecnai G2 Spirit 120 kV TEM (FEI Company, Hillsboro, OR, USA) and imaged with an AMT Nanosprint 15 digital camera and software V7.0.1 (AMT Imaging, Woburn, MA, USA). Five images taken at 68,000X magnification were used to measure phage dimensions (head diameter, head length, tail length and tail width) with ImageJ [465].

3.2.2.8 Phage Phylogenetic Analysis

Closest relatives to isolated phage genomes were found in the 1st of July 2023 upload to the INfrastructure for a PHAge REference Database (INPHARED) [239] using PhindersKeepers [459]. These reference phages were reordered by PhageOrder [455], before being aligned with the isolated phages using Mafft [460], and the FFT-NS-2 fast progressive method. Multiple sequence alignment was then used to generate a maximum likelihood phylogenetic tree in MEGA v11 with 100 bootstraps [461]. These were then annotated using the online software Interactive Tree of Life [462] and 1st of July 2023 INPHARED data [239]. A BLAST search of the INPHARED data (1st of May, 2023; Cook et al. 2021) was also performed and Phusion [463] used to obtain putative family, sub-family, genus and species of each isolated phage. The average nucleotide identity (ANI) was compared between the phages isolated and to the closest relatives identified using VIRIDIC v1.1 [464].

3.2.2.9 Phage Receptor Identification

To determine the receptor binding of phages, efficiency of plating (EOP) was performed using the transposon knockout mutants and WT mPAO1 (refer to Table 2.2). Briefly, EOP is performed by diluting phages and enumerating them on various mutant and WT PAO1 (refer to 2.7.2.8). Phage titres on mutants were then divided by their titre on the WT giving an EOP score which indicates how well a phage can infect the mutant (refer to 2.7.2.7). Where a phages' receptor was present the $EOP \geq 0.1$, where a receptor that was

missing contributes to phage infection the $0.1 > EOP > 0$ and the main receptor was missing when the $EOP = 0$ [451]. Phage E79 was included as a reference comparison phage [262].

An additional step was needed for phages whose receptor was unable to be identified by the PAO1 mutant panel. These phages and PAO1 were plated together as described for phage propagation (refer to 2.7.2.6). After overnight incubation, five colonies (escape mutants) were picked with a bacterial loop, streaked onto fresh LB agar (refer to 2.5.1.2) and incubated overnight at 37 °C in a non-humidified incubator. Repeated picking of single colonies and replating was performed another five times to remove any possibility of phage contamination and to ensure stability of the escape mutation [485]. To corroborate that these bacteria were resistant to the phage of interest, spot tests on whole double overlay agar plates were performed on both WT PAO1 and generated mutants (refer to 2.7.2.5). Where phages were unable to form plaques on the mutant, it was considered completely resistant. All 10 generated mutants were cryopreserved at -80 °C (refer to 2.7.1.1).

3.2.2.10 Bacterial DNA Extraction

For simplicity one of the completely resistant escape mutants isolated above was randomly selected, initially cultured on LB agar and then as an overnight growth in LB broth (refer to 2.5.1.1 and 2.7.1.2). Genomic DNA was extracted from the bacteria in the broth using the DNeasy Tissue and Blood Extraction Kit (Qiagen, Hilden, Germany; refer to 2.7.1.6). Briefly, the overnight culture was centrifuged at 4,000 xg for 10 mins at room temperature to pellet the bacteria. This was then resuspended in 180 µL of the ATL buffer derived from the Qiagen DNeasy blood and tissue extraction kit (Qiagen, Hilden, Germany) and 20 µL of Proteinase K before incubation for one hour at 56 °C. Subsequently, 4 µL of RNase A was added (Invitrogen, Waltham, MA, USA) to the extractions, before incubation at room temperature for 15 mins. The process of washing and eluting the DNA was then performed as per manufacturer's instructions (Qiagen DNeasy Blood and Tissue kit, Qiagen, Hilden, Germany).

3.2.2.11 Bacterial Genome Analysis

The escape mutant's reads were quality controlled and assembled using a docker container created as part of this thesis called orange housed on Dockerhub

(<https://hub.docker.com/r/mantistobogan/orange>). Briefly, the assembly pipeline of this docker image uses a number of packages from BBmap v39.01 [421] to: trim reads with bbdduk, remove duplicate reads with dedupe, normalise coverage to 100X with bbnorm and merge reads to create longer ones with bbmerge. Reads were assembled by SPAdes v3.15.4 [422], and assembly gaps filled with Mind the Gap v2.3.0 [423] and utility scripts from Mine Your Symbiont v1.1 (MinYS) [424]. Species contamination was checked for by Kraken [425]. The annotation pipeline of orange determined the species of bacteria that was inputted via Kraken [425], annotated general genomic features with bakta v1.7.0 [433], phage resistance mechanisms by PADLOC v1.1.0 [434], multilocus sequence type (MLST) by the mlst package [435] using the PubMLST database [436]. It then used abricate v1.0.1 [437] to find antibiotic resistance genes and virulence genes by searching the Resfinder, Megares, VFDB, NCBI AMRFinder, CARD and ARG-annot databases [438-444] and finally searched for prophages using DBSCAN-SWA [445] which makes use of both diamond [446], prokka [447] and blast software [448]. Mutations were then detected using Snippy v4.6.0 [486] by mapping mutant reads to the WT PAO1 genome features file.

3.2.2.12 Thermal and pH Stability

Thermal stability for the phages that were sequenced, free of undesirable genes and were not contaminated with other phages were determined by storing 1 mL of propagated phage (refer to 2.7.2.6) at 25 °C (room temperature), 4 °C, -20 °C and -80 °C. Phages were enumerated after one week, one month, three months, six months, and a year of storage using their host *P. aeruginosa* (refer 2.7.2.7). Stability of phages at pH 3, 5, 7, 9 and 11 were also measured by changing the pH of SM buffer (refer to 2.5.2.2) to the desired level using 1M HCl (Univar, Ingleburn, NSW, Australia) or 1M NaOH (Sigma-Aldrich, St. Louis, MO, USA). Phages were then propagated, titred (refer to 2.7.2.6 and 2.7.2.7) and diluted 1 in 100 in each of the different pH SM buffers (refer to 2.5.2.2). These were left at 37 °C in a non-humidified incubator for 1 hour and 24 hrs before being enumerated (refer to 2.7.2.7). All experiments were performed in triplicate with duplicate enumerations at each time point.

3.2.2.13 One-step Growth Curve

A one-step growth curve was performed with minor modifications as previously described [466]. Briefly, an overnight culture of PAO1 was adjusted to an OD_{600nm} of 1.0 (refer to 2.7.1.3). PAO1 was then mixed with 10⁸ PFU/mL of each phage to achieve a multiplicity of infection (MOI) of 1. Phages were allowed to adsorb for five mins at 37 °C (non-humidified) with 50 rpm of shaking. A 100 µL aliquot was removed and used to enumerate phages (refer to 2.7.2.7) and the bacteria adsorbed phage solution was then diluted 1:10,000 and replaced in the incubator with 50 rpm of shaking. Every 10 mins, 100 µL was removed and used to enumerate phages (refer to 2.7.2.7). Plates were incubated overnight at 37 °C in a non-humidified incubator and plaques were counted. Plaque counts were used to determine the phages produced per infected bacterium (burst size) using the formula below:

$$\text{Burst size} = \left(\frac{\text{PFU}}{\text{mL}} \text{ at plateau of phage infection}\right) / \left(\frac{\text{PFU}}{\text{mL}} \text{ at during latent period}\right)$$

3.2.2.14 Statistical Analysis

Statistical analyses were conducted using GraphPad Prism v9.3.1 (GraphPad Software, La Jolla, CA). Data was tested for normality using the Shapiro-Wilk test. The temperature stability of phages over time was tested for significance using a repeated measures (RM) 2-way ANOVA with Tukey's multiple comparisons. The pH stability of phages was tested for significance using multiple t-test comparing pH 3, 5 and 9 to pH 7. In both tests, p<0.05 was considered statistically significant.

3.3 Results

3.3.1 Isolation, Purification and Macroscopic Characterisation

When enriched or unenriched wastewater was added to a whole plate agar overlay containing one of the *P. aeruginosa* isolates, plaques were visible (Figure 3.1 A). Several plaques per isolate were picked and subsequently purified by serially plating and picking plaques with the same morphology (Figure 3.1 A). Different combinations of size, halo, tails, shape, and plaque clarity were observed in purified phages (Figure 3.1 B; Table 3.1). In total, 252 phages were isolated (187 unenriched; 65 enriched). Of these, most were round (66%), medium in size (1-2mm; 44%), formed a clear plaque (67%) and did

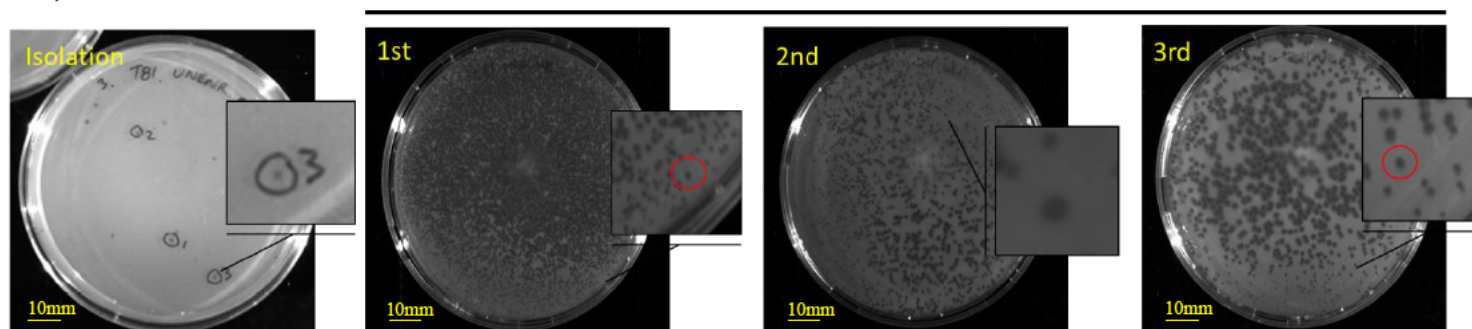
not have a halo (73%; Table 3.2; Table 3.2). Other isolated phages were found to be irregular (33%), pinpoint (18%), large (>2mm; 36%), exhibited a turbid zone of clearance (32%) or had a halo around the plaque (26%; Table 3.2).

Table 3.1: Macroscopic Characterisation of Phage Plaque Morphologies

Shape		Size			Zone of Clearing			Halo	
		< 1 mm	1-2 mm	> 2 mm					
Round	Irregular	Pinpoint	Medium	Large	Clear	Turbid	Negative	Present	Absent

A)

Purification



B)



Figure 3.1: Macroscopic Characterisation of Plaque Morphology. Overlay agar was inoculated with a *P. aeruginosa* isolate and enriched or unenriched, filtered wastewater samples. Plaques exhibiting different morphologies were picked, diluted, and inoculated into overlay agar containing a *P. aeruginosa* isolate. This process was repeated three times to get homogenous phage solutions. (A) Whole plate overlays were used to visualise the *P. aeruginosa* phages within the wastewater sample and several single plaques were picked. Each single plaque was then purified through three round of plaque purification where a similar plaque was picked and subcultured. (B) Representative plaque images of the various morphologies observed across the purified phages.

Table 3.2: Proportion of Phage Plaque Macroscopic Characteristics

Morphology		Number (% of total)
Shape	Round	168 (66)
	Irregular	84 (33)
Size	Pinpoint (<1mm)	47 (18)
	Medium (1-2mm)	113 (44)
	Large (>2mm)	92 (36)
Zone of Clearing	Clear	170 (67)
	Turbid	82 (32)
Halo	Present	68 (26)
	Absent	184 (73)

3.3.2 Phage Host Range

Phage infectivity (including partial and complete plaques) of the CF specific *P. aeruginosa* isolates (adult n=43 and paediatric n=30) ranged from 1-89% (Appendix Table C.1). This combined host range was then used to select the top 20 putative phages with the broadest profiles (Appendix Table C.1). These were then redesignated simplified identification names (numbers 1-20; Table 3.3) and assessed in more detail. The host range assay was repeated and expanded to include non-CF *P. aeruginosa* clinical isolates (total n=95) exhibiting various levels of lytic activity (59-85%; Table 3.3). Results illustrated that the putative phage samples did not appear to favour *P. aeruginosa* from specific infection types and any tropism in host range was *P. aeruginosa* isolate specific with some isolates highly permissible and others resistant regardless of their source (Figure 3.2). Putative phage samples 7 and 19 had a more restricted host range being only able to lyse 67 and 59% of isolates respectively (Table 3.3). The putative phage samples were confirmed to be *P. aeruginosa* specific since they were unable to lyse any other species including *Burkholderia cepacia* complex, *Escherichia coli*, *Enterococcus faecalis*, *Enterococcus faecium*, *Klebsiella pneumoniae* and *Staphylococcus aureus* (Appendix Table D.1).

Table 3.3 Host Range of the Top 20 Putative Phages Against the CF and Non-CF *P. aeruginosa* Isolates

		Lysis No. (%)				
		Negative	Positive			Total
			Clear	Partial	Total	
Phages	φ1	26 (27.7)	50 (53.2)	18 (19.2)	68 (72.3)	94 (100)
	φ2	18 (19.1)	55 (58.5)	21 (22.3)	76 (80.9)	94 (100)
	φ3	14 (14.9)	63 (67.0)	17 (18.1)	80 (85.1)	94 (100)
	φ4	13 (13.8)	64 (68.1)	17 (18.1)	81 (86.2)	94 (100)
	φ5	16 (17.0)	59 (62.8)	19 (20.2)	78 (83.0)	94 (100)
	φ6	15 (16.0)	54 (57.4)	25 (26.6)	79 (84.0)	94 (100)
	φ7	30 (31.9)	34 (36.2)	29 (30.9)	63 (67.0)	94 (100)
	φ8	9 (9.6)	72 (76.6)	13 (13.8)	85 (90.4)	94 (100)
	φ9	11 (11.7)	58 (61.7)	24 (25.5)	82 (87.2)	94 (100)
	φ10	16 (17.0)	55 (58.5)	23 (24.5)	78 (83.0)	94 (100)
	φ11	17 (18.1)	55 (58.5)	22 (23.4)	77 (81.9)	94 (100)
	φ12	19 (20.2)	45 (47.9)	30 (31.9)	75 (79.8)	94 (100)
	φ13	15 (16.0)	56 (59.6)	23 (24.5)	79 (84.0)	94 (100)
	φ14	20 (21.3)	54 (57.4)	20 (21.3)	74 (78.7)	94 (100)
	φ15	14 (14.9)	53 (56.4)	26 (27.7)	79 (84.0)	94 (100)
	φ16	15 (16.0)	60 (63.8)	19 (20.2)	79 (84.0)	94 (100)
	φ17	19 (20.2)	58 (61.7)	17 (18.1)	75 (79.8)	94 (100)
	φ18	21 (22.3)	58 (61.7)	15 (16.0)	73 (77.7)	94 (100)
	φ19	35 (37.2)	30 (31.9)	29 (30.9)	59 (62.8)	94 (100)
	φ20	12 (12.8)	64 (68.1)	18 (19.1)	82 (87.2)	94 (100)

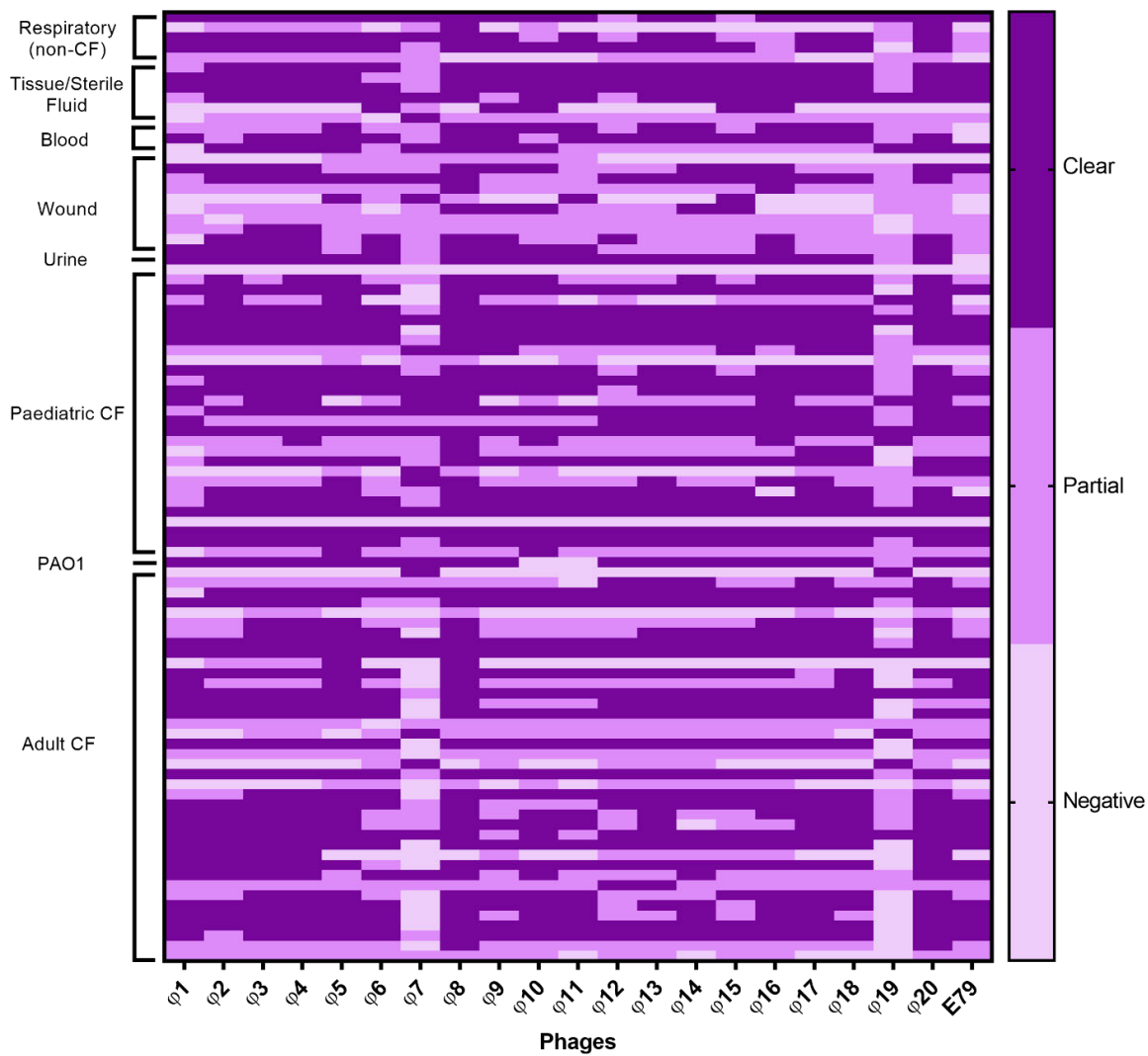


Figure 3.2: Host Range of the Top 20 Phages Against the Paediatric Derived CF *P. aeruginosa* Isolates. Phages were spot tested on overlay agar inoculated with the *P. aeruginosa* isolates and after overnight incubation complete, partial or no lysis visually inspected. Phages had broad host ranges against *P. aeruginosa* from a range of clinical origins.

3.3.3 Phage Genomic Analysis

Of the 20 putative phage samples sequenced, eighteen had genomes that were ~66 kbp long, 55% GC content and 90-95 coding sequences (CDS; Table 3.4). Putative phage samples 7 and 19 had much larger phage genomes, being ~270kbp, 36% GC content, 360 CDS and 6/7 tRNAs (Table 3.4). No known integrases, excisionases, transposases, antimicrobial or bacterial virulence genes were identified in the phage genomes after searching the Resfinder, Megares, VFDB, NCBI AMRFinder, CARD and ARG-annot databases (Table 3.4). Fourteen of the 20 sequenced putative phage samples had a single complete genome determined by CheckV. The remaining six putative phage samples contained secondary smaller genomes, which were likely temperate phages present in addition to the lytic phage genome (Table 3.5). These putative temperate phage genomes ~40kbp long, ~60% GC content and 60 CDS (Table 3.5). In addition, whilst none of the putative temperate phage genomes contained any antimicrobial or bacterial virulence genes, five genomes did have at least one integrase, excisionase or transposase indicating that they could integrate into the bacterial genome (Table 3.5). As a result, these six samples and that contained two phages' genomes were not included in any additional downstream characterisation studies performed.

Table 3.4: General Genomic Characteristics of the Top 20 Putative Phages

Phage No.	Genome Size (bp)	Coverage (X)	GC Content (%)	CDS	Genes	Hypothetical CDS	tRNAs	No. of Antibiotic Resistance Genes	No. of Bacterial Virulence Genes	Integrases, excisionases or transposases
φ1	66,160	118	55.64	91	91	54	0	0	0	0
φ2	66,628	118	55.60	92	92	55	0	0	0	0
φ3	66,622	118	55.60	93	93	55	0	0	0	0
φ4	66,622	118	55.60	92	92	55	0	0	0	0
φ5	66,420	118	55.67	93	93	57	0	0	0	0
φ6	66,379	118	55.71	91	91	54	0	0	0	0
φ7	278,796	118	36.91	362	368	275	6	0	0	0
φ8	66,284	118	55.67	95	95	59	0	0	0	0
φ9	66,372	118	55.62	91	91	56	0	0	0	0
φ10	66,516	118	55.47	94	94	57	0	0	0	0
φ11	66,124	118	55.72	91	91	54	0	0	0	0
φ12	62,577	118	55.59	80	80	46	0	0	0	0
φ13	66,622	118	55.60	93	93	56	0	0	0	0
φ14	65,645	118	55.18	93	93	56	0	0	0	0
φ15	62,576	118	55.58	81	81	46	0	0	0	0
φ16	66,033	118	55.04	91	91	55	0	0	0	0
φ17	66,393	118	55.64	90	90	54	0	0	0	0
φ18	66,393	118	55.61	90	90	54	0	0	0	0
φ19	277,192	118	36.81	357	364	272	7	0	0	0
φ20	66,600	118	54.76	93	93	55	0	0	0	0

CDS: coding sequences.

Table 3.5: General Genome Characteristics of the Putative Temperate Phage Contaminants






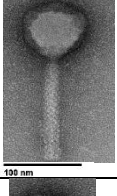
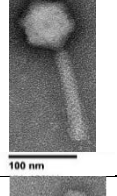
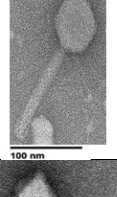

Phage	Smaller Contig Size (bp)	GC Content (%)	CDS	Genes	Hypothetical CDS	tRNAs	No. of Antibiotic Resistance Genes	No. of Bacterial Virulence Genes	Integrases, excisionases or transposases
φ6	43,237	53.89	55	55	20	0	0	0	0
φ8	40,741	61.78	68	68	41	0	0	0	1
φ10	37,300	64.35	57	57	26	0	0	0	2
φ11	39,582	61.73	63	63	39	0	0	0	2
φ15	39,894	62.73	56	56	23	0	0	0	2
φ16	40,708	61.96	60	60	36	0	0	0	2



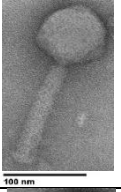


CDS: coding sequences.

3.3.4 Phage TEM Analysis

All 14 complete and lytic phages were then visualised by TEM (Table 3.6). All had an icosahedral head and a tail and met the criteria for belonging to the myovirus morphotype (Table 3.6). Twelve of the fourteen phages had similar dimensions (average head diameter; 71.76 ± 4.26 nm, head length; 81.82 ± 4.74 nm, tail width; 21.19 ± 2.31 nm and tail length; 142 ± 8.07 nm; Table 3.6). Phage 7 and 19 appeared much larger with an average head diameter 128.28 ± 7.28 nm, head length 129 ± 7.07 nm, tail width 26.22 ± 2.17 nm and a tail length 188.92 ± 5.95 nm (Table 3.6). Recognising the first nation ownership of the land of which these phages were sampled (Noongar Whadjuk Boodjar), all were given traditional nomenclature based on their appearance (refer to 2.7.2.13; ie Karamokiny 4, 5, 6, 7, 8, 11, 12, 13, 14, 15, 16 and 27 and Boorn-mokiny 1 and 2).

Table 3.6: Representative Phage TEM Images and Morphology

Previous Name	Phage	Representative Image	Head Diameter (nm ± SD)	Head length (nm ± SD)	Tail Diameter (nm ± SD)	Tail length (nm ± SD)	Morphotype
φ1	Kara-mokiny kep-wari Wadjak 4		75.02 ± 2.35	82.64 ± 5.02	20.32 ± 1.72	138.53 ± 1.52	Myovirus
φ2	Kara-mokiny kep-wari Wadjak 5		81.75 ± 3.73	84.73 ± 5.21	22.8 ± 2.97	146.36 ± 8.12	Myovirus
φ3	Kara-mokiny kep-wari Wadjak 6		79.01 ± 3.89	82.08 ± 3.72	21.10 ± 2.36	138.88 ± 3.37	Myovirus
φ4	Kara-mokiny kep-wari Wadjak 7		88.10 ± 5.10	89.54 ± 5.72	22.81 ± 2.53	149.66 ± 10.00	Myovirus
φ5	Kara-mokiny kep-wari Wadjak 8		72.05 ± 4.37	76.33 ± 4.11	22.02 ± 2.40	131.38 ± 4.20	Myovirus
φ9	Kara-mokiny 27		67.57 ± 7.66	72.64 ± 9.40	21.14 ± 1.69	138.53 ± 15.38	Myovirus
φ12	Kara-mokiny kep-wari Wadjak 11		81.12±5.55	89.32±2.16	20.68±0.64	153.20±10.95	Myovirus
φ13	Kara-mokiny kep-wari Wadjak 12		75.91 ± 2.72	77.87 ± 5.43	22.12 ± 2.17	130.47 ± 21.32	Myovirus
φ14	Kara-mokiny kep-wari Wadjak 13		80.85 ± 4.87	80.32 ± 3.03	22.10 ± 2.39	147.44 ± 6.50	Myovirus

$\phi 17$	Kara- mokino kep-wari Wadjak 14		79.06 ± 3.72	84.28 ± 4.55	19.5 ± 0.89	152.76 ± 7.79	Myovirus
$\phi 18$	Kara- mokino kep-wari Wadjak 15		69.95 ± 4.09	75.30 ± 2.82	17.84 ± 3.56	152.17 ± 4.79	Myovirus
$\phi 20$	Kara- mokino kep-wari Wadjak 16		72.85 ± 4.40	77.64 ± 3.14	21.80 ± 2.74	131.68 ± 5.82	Myovirus
$\phi 7$	Koomba boorn- mokino kep-wari Wadjak 1		120.47 ± 8.51	120.35 ± 7.97	24.24 ± 1.68	176.63 ± 5.39	Myovirus
$\phi 19$	Koomba boorn- mokino kep-wari Wadjak 2		136.10 ± 6.05	138.64 ± 6.16	28.20 ± 2.66	201.21 ± 6.50	Myovirus

3.3.5 Phage Phylogenetic Analysis

Phages were phylogenetically classified based on the consensus of Blast search results, with Kara-mokiny 4-16 putatively classified into the genus *Pbunavirus* and Boorn-mokiny 1 and 2 classified as *Phikzviruses*. These classifications correlated with the genomic and TEM results where the *Pbunaviruses* had smaller genomes (Table 3.4) and virions (Table 3.6), whilst the *Phikzviruses* were much larger morphologically (Table 3.6) and had larger genomes with tRNAs (Table 3.4). Both genera of phages are currently unclassified at sub-family and family phylogenetic levels due to the recent abolishment of old classifications [268].

Pairwise genome comparison of the isolated *Pbunaviruses* to each other found there was a high degree of similarity (Table 3.7). Analysis showed that there were at least five different species of phages in this group with no phages with >95% ANI (Table 3.7). Kara-mokiny 4, 5, 6, 7, 12, 14, 15 and 16 all had >95% ANI forming one cluster of highly similar phages (Table 3.7). Kara-mokiny 8, 11, 13 and 27 were not highly related to any of the other phages isolated with <95% ANI (Table 3.7). When compared to publicly available phages, ten of the eleven *Pbunaviruses* had similarity to at least one phage (ANI >95%) indicating that these were isolates of already identified species (Table 3.8). Kara-mokiny 4, 5, 6, 7, 11, 14 and 15 were most similar to Pseudomonas phage sortsol (MT119369; Table 3.8), Kara-mokiny 16 with Pseudomonas phage PA4 (MZ285878; Table 3.8) and Kara-mokiny 27 with Pseudomonas phage PASA16 (MT933737; Table 3.8). Kara-mokiny 8 was most similar to Pseudomonas phage PASA16 (MT933737; Table 3.8) and finally Kara-mokiny 11 with Kara-mokiny 1 and 2 (OP314870 and OP314871; Table 3.8). Of significance, Kara-mokiny 13 only had an ANI of 93.40% with Pseudomonas phage crassa (MT119377) indicating it is a new species of *Pbunavirus* (Table 3.8). Pairwise genome comparison of the two isolated *Phikzviruses* revealed that they were highly similar (ANI of ~97%) indicating that they were from the same species. When compared to publicly available *Phikzviruses*, both had multiple phages that had >95% ANI indicating that these two phages were isolates of an already discovered species of phage (Table 3.9). Boorn-mokiny 1 was most similar to Pseudomonas phage 30-1 phi30-1 (LC727696; Table 3.9) and Boorn-mokiny 2 with Pseudomonas phage PaSz-1_45_270k (MN871480; Table 3.10). Assembly of a phylogenetic tree supported generated genomic results and showed that the *Phikzviruses* and *Pbunaviruses* phages branched with publicly available phages from these genera on separate clades (Figure

3.3). Specifically, phages within the ANI cluster 1 (Table 3.7) were in proximity to each other within a single clade (Figure 3.3). Kara-mokiny 8, 11, 13 and 27, were all found in different clades and distinct from each other (Figure 3.3). Boorn-mokiny 1 and 2 were located within the same clade that contained publicly available *Phizviruses* (Figure 3.3). With diversity being the priority focus of this chapter, four phages from divergent clades, namely Kara-mokiny 8, 13, 16 (*Pbunaviruses*) and Boorn-mokiny 1 (a *Phikzvirus*) were then selected and characterised in more detail.

Table 3.7 Average Nucleotide Identity of Isolated Phages from the *Pbunavirus* Genus

		Cluster 1								Cluster 2	Cluster 3	Cluster 4	Cluster 5
		Kara-mokiny 4	Kara-mokiny 5	Kara-mokiny 6	Kara-mokiny 7	Kara-mokiny 12	Kara-mokiny 14	Kara-mokiny 15	Kara-mokiny 16	Kara-mokiny 27	Kara-mokiny 8	Kara-mokiny 11	Kara-mokiny 13
Cluster 1	Kara-mokiny 4	100	97.01	97.25	97.25	97.25	98.50	98.50	95.32	94.35	93.61	91.33	89.91
	Kara-mokiny 5	97.01	100	99.77	99.78	99.77	97.60	97.60	94.64	93.54	92.59	91.28	89.58
	Kara-mokiny 6	97.25	99.77	100	99.99	99.99	97.85	97.85	94.84	93.76	92.84	91.50	89.41
	Kara-mokiny 7	97.25	99.78	99.99	100	99.99	97.84	97.84	94.84	93.76	92.83	91.50	89.41
	Kara-mokiny 12	97.25	99.77	99.99	99.99	100	97.84	97.84	94.83	93.75	92.82	91.49	89.41
	Kara-mokiny 14	98.50	97.60	97.85	97.84	97.84	100	100	94.49	93.53	92.80	91.02	88.86
	Kara-mokiny 15	98.5	97.60	97.85	97.84	97.84	100	100	94.49	93.53	92.82	91.018	88.87
	Kara-mokiny 16	95.32	94.64	94.84	94.84	94.83	94.49	94.49	100	94.00	92.85	91.38	91.04
Cluster 2	Kara-mokiny 27	94.35	93.54	93.76	93.76	93.75	93.5	93.53	94.00	100	94.12	93.42	90.90
Cluster 3	Kara-mokiny 8	93.61	92.59	92.84	92.83	92.82	92.80	92.82	92.85	94.12	100	91.55	89.99
Cluster 4	Kara-mokiny 11	91.33	91.28	91.50	91.50	91.49	91.02	91.02	91.38	93.42	91.553	100	89.50
Cluster 5	Kara-mokiny 13	89.91	89.58	89.41	89.41	89.41	88.86	88.87	91.04	90.90	89.99	89.50	100

Values are represented as percentages. Colours are a gradient from yellow (lowest ANI) to green (highest ANI) for each phage row.

Table 3.8: Average Nucleotide Identity of Isolated Phages to Publicly Available *Pbunaviruses*

	Kara-mokiny 4	Kara-mokiny 5	Kara-mokiny 6	Kara-mokiny 7	Kara-mokiny 12	Kara-mokiny 14	Kara-mokiny 15	Kara-mokiny 16	Kara-mokiny 27	Kara-mokiny 8	Kara-mokiny 11	Kara-mokiny 13
MT1193 69	96.51	96.32	96.56	96.55	96.55	95.98	95.98	94.71	94.97	93.44	91.14	89.69
MZ2858 78	95.26	95.14	95.35	95.35	95.35	94.40	94.40	97.2	94.20	92.76	91.58	90.91
MN8714 66	93.80	92.87	93.11	93.11	93.10	93.10	93.10	93.50	97.22	94.31	94.41	90.91
MT9337 37	93.91	92.76	93.00	93.01	92.99	93.02	93.03	93.07	94.83	97.24	91.90	90.18
OP3148 70	92.57	92.09	92.27	92.27	92.26	91.81	91.81	92.94	95.95	93.91	96.61	91.21
OP3148 71	92.57	92.09	92.27	92.27	92.26	91.81	91.81	92.94	95.95	93.91	96.61	91.21
MT1193 77	88.92	88.81	88.65	88.65	88.64	88.29	88.29	89.89	90.87	88.90	87.69	93.40
MT1193 69	96.51	96.32	96.56	96.55	96.55	95.98	95.98	94.71	94.97	93.44	91.14	89.69

Values are represented as percentages. Colours are a gradient from yellow (lowest ANI) to green (highest ANI) for each phage row.

Table 3.9: *Phikzyviruses* Average Nucleotide Identity to Publicly Available Phage

	Boorn-mokiny 1	Boorn-mokiny 2
LC727696	97.50	97.10
MN563784	97.25	97.44
MN871480	97.23	97.45
KU521356	97.22	96.03
LC727699	97.17	96.94
AP019418	96.68	96.81
LC727701	96.41	96.26
AF399011	96.37	96.87
LC727695	96.15	96.47
MN871489	96.14	96.27
MT133560	95.94	94.48
MW057919	95.91	94.93
MT995926	95.75	95.02
MT995928	95.75	95.02
MT995927	95.72	95.02
OP953026	95.66	96.26
MZ444140	95.14	95.05
OM718002	94.89	95.03
JX233784	94.69	94.46
ON631220	94.54	93.36

Values are represented as percentages. Colours are a gradient from yellow (lowest ANI) to green (highest ANI) for each phage row.

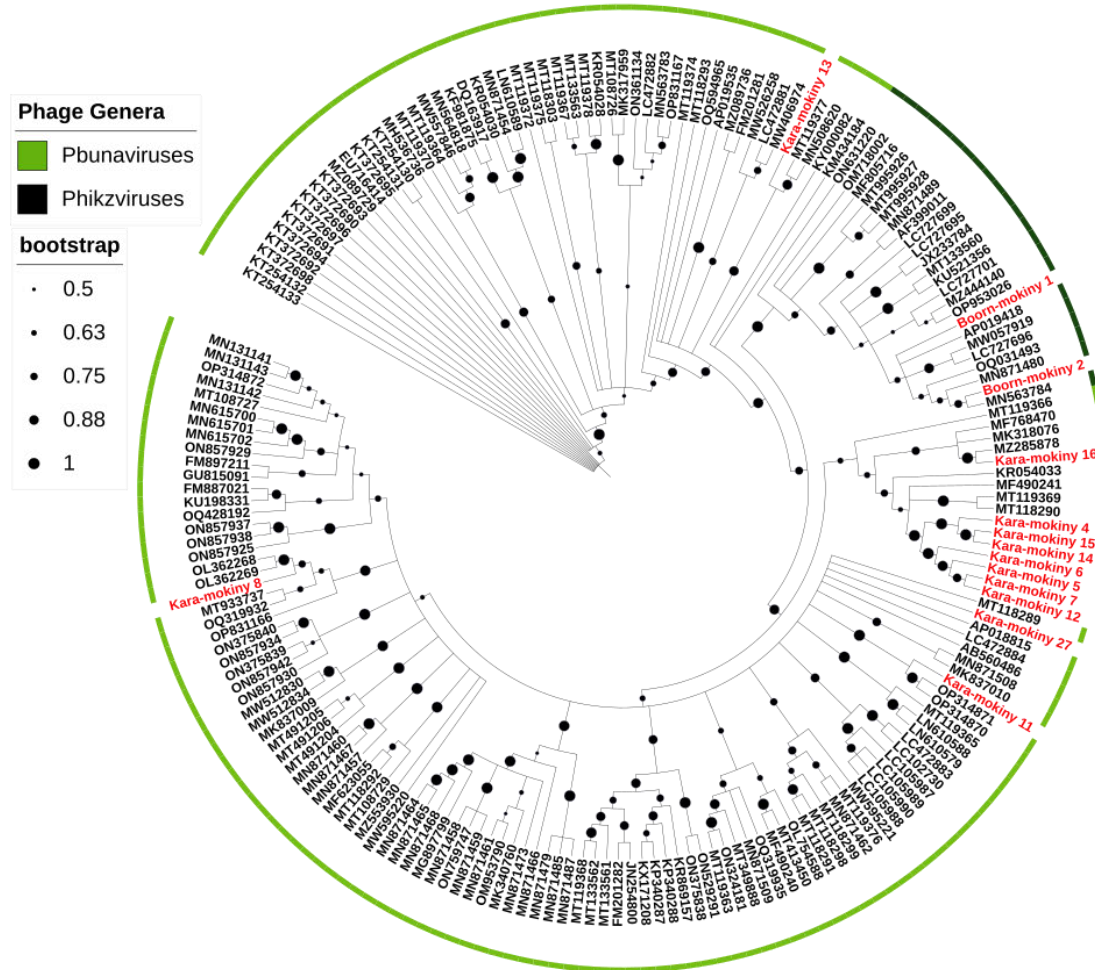


Figure 3.3: Phage Maximum Likelihood Phylogenetic Tree Calculated by MEGA v11 with 50 bootstraps and was annotated using iTOL. Phages Isolated in this study are highlighted in red, *Pbunaviruses* are surrounded by a green ring and the *Phikzviruses* are surrounded by a black ring. Bootstrap probabilities are represented by different size circles with the larger the circle the greater the probability.

3.3.6 Phage Receptor Determination

All four phages were infective against mPAO1 indicating that the WT expressed all the phages' receptors (Table 3.10). Kara-mokiny 8, 13 and 16 all were able to infect mutants missing pilus components (*pilA*, *pilB* and *pilY1*), efflux pumps (*oprM*, *oprN*, *oprH*, *oprD*, *oprJ* and *oprF*), flagella (*fliC*) and type VI secretion system (*clpVI*) (EOP \geq 0.1; Table 3.10). These three phages could also infect mutants with different components of the LPS biosynthesis cluster knocked out (*wzt*, *migA* and *rmlC*; EOP 0.6-2.2; Table 3.10). However, they were unable to infect the mutant missing the *galU* gene which also functions in LPS biosynthesis (EOP=0; Table 3.10). Collectively, results generated indicate that Kara-mokiny 8, 13 and 16 use LPS as their binding receptor, and require the *galU*-mediated modification of it to be able to attach to the *P. aeruginosa* cell.

Boorn-mokiny 1 was able to infect mutants defective in pilus formation/function (*pilA*, *pilB* and *pilY1*), efflux pumps (*oprM*, *oprN*, *oprH*, *oprD*, *oprJ* and *oprF*), type VI secretion system (*clpVI*) and LPS biosynthesis genes (*wzt*, *rmlC* and *migA*), including the *galU* mutant (EOP \geq 0.1; Table 3.10). Interestingly, it did have a weak infection of the mutant with disrupted flagella (*fliC*; EOP 0.005; Table 3.10). To confirm if flagella was the receptor, an escape mutant totally resistant to Boorn-mokiny 1 infection was derived, sequenced, and analysed. Data revealed seven mutations in the mutant when compared to the WT PAO1 (Table 3.11). Six mutations were SNPs and only two of these were in protein coding regions (Table 3.11). However, these proteins are not well annotated and are identified as hypothetical (FUSC family protein and NMT1 domain containing protein; Table 3.11). The final mutation was a large deletion in the *flgE* gene responsible for the flagellar hook protein, thus confirming that the flagella were the receptor for Boorn-mokiny 1 (Table 3.11).

Table 3.10: Efficiency of Plating of the Top 20 Phages Against a PAO1 Phage Receptor Mutant Library

	Wild Type	LPS Biosynthesis				Pilus Structure/Function			Type VI Secretion System	Outer Membrane Proteins						Flagella Structure
	mPAO1	<i>ΔgalU</i>	<i>ΔmigA</i>	<i>Δwzt</i>	<i>ΔrmlC</i>	<i>ΔpilA</i>	<i>ΔpilB</i>	<i>ΔpilY1</i>	<i>ΔclpVI</i>	<i>ΔoprM</i>	<i>ΔoprH</i>	<i>ΔoprJ</i>	<i>ΔoprF</i>	<i>ΔoprD</i>	<i>ΔoprN</i>	<i>ΔfliC</i>
Kara-mokiny 8	1	0	1.1	0.6	0.8	0.8	0.9	0.7	0.8	0.7	1.1	0.9	0.7	1	0.6	1.9
Boorn-mokiny 1	1	0.2	0.2	0.1	0.2	0.1	0.1	0.1	0.2	0.3	0.1	0.1	0.1	0.2	0.3	0.005
Kara-mokiny 13	1	0	1.2	0.6	1.7	1	1.2	1.1	1	1.2	1.1	1	1	1.1	1.2	0.7
Kara-mokiny 16	1	0	2.2	1	1	1.1	1.3	1.2	1	0.7	1.2	1.5	0.7	1	0.9	1.3
E79	1	0	1.1	0.7	0.8	0.9	0.9	0.9	1	0.9	1.1	0.9	0.5	0.7	0.8	0.8

EOP \geq 0.1 are normal infection, EOP \leq 0.1 are weak infection and EOP=0 is no infection. Values highlight in red are EOP values that show weak or no infection for each phage.

Table 3.11: Receptor Determination for Boorn-mokiny 1

Position (bp)	Variant Type	WT Allele	Mutant Allele	Allele Frequencies	Feature Affected	Strand	Nucleotide Position	Amino Acid Position	Effect	Gene Affected	Product Affected
207621	SNP	C	A	A:10 C:0	N/A	N/A	N/A	N/A	N/A	N/A	N/A
57	SNP	C	A	A:10 C:0	N/A	N/A	N/A	N/A	N/A	N/A	N/A
67	SNP	C	A	A:11 C:0	N/A	N/A	N/A	N/A	N/A	N/A	N/A
90663	SNP	G	C	C:20 G:0	CDS	+	1910/2040	637/679	Missense variant	N/A	FUSC family protein
123419	SNP	G	T	T:20 G:0	N/A	N/A	N/A	N/A	N/A	N/A	N/A
30686	SNP	C	A	A:20 C:0	CDS	+	1069/1407	357/468	Missense variant	N/A	NMT1 domain-containing protein
105296	Del	GACCTACGCCTGGAA CGGCGCGACCGGTGC CGCCAGCGGCATCTC CTTCGACATGCGCAA GACCACCC	G	G:10 GACCT...: 0	CDS	+	917/1389	306/462	Frameshift variant	<i>flgE</i>	flagellar hook protein FlgE

Note: SNP stands for single nucleotide polymorphism, Del stands for deletion, ‘...’ means that the allele continues as per the WT allele. CDS stands for coding sequence.

3.3.7 Phage Storage Stability Over a Range of Temperatures

Phage stability was tested over a range of temperatures over a 365-day (12-month) period. Results generated showed that phages were recoverable to varying degrees after 365-days at each of the temperatures tested (Figure 3.4). Kara-mokiny 8 titre only significantly decreased from propagated titre after 365-days of storage at room temperature ($p < 0.05$; Figure 3.4 A). Kara-mokiny 13 remained stable for the duration of the experiment at both 4 and $-80\text{ }^{\circ}\text{C}$, however, its titre was significantly reduced after 7 days of storage at $-20\text{ }^{\circ}\text{C}$ and was significantly reduced at every subsequent timepoint ($p < 0.05$; Figure 3.4 B). It was also significantly reduced when stored at room temperature after 30 days (1-month) of storage and at every subsequent timepoint ($p < 0.05$; Figure 3.4 B). Kara-mokiny 16 was stable for up to 365 days at $4\text{ }^{\circ}\text{C}$ (Figure 3.4 C). However, its titre was significantly reduced following 7-days of storage at room temperature and $-20\text{ }^{\circ}\text{C}$ and at every subsequent timepoint ($p < 0.05$; Figure 3.4 C). The titre of Kara-mokiny 16 was also significantly reduced after 180 and 365 days of storage at $-80\text{ }^{\circ}\text{C}$ ($p < 0.05$; Figure 3.4 C). Boorn-mokiny 1 was stable at 4, -20 and $-80\text{ }^{\circ}\text{C}$ for the duration of the experiment (Figure 3.4 D). However, its titre was statistically significantly reduced 100,000-fold after 180-days at room temperature ($p < 0.05$; Figure 3.4 D). No viable Boorn-mokiny 1 was recovered after 365-days of storage at room temperature ($p < 0.05$; Figure 3.4 D).

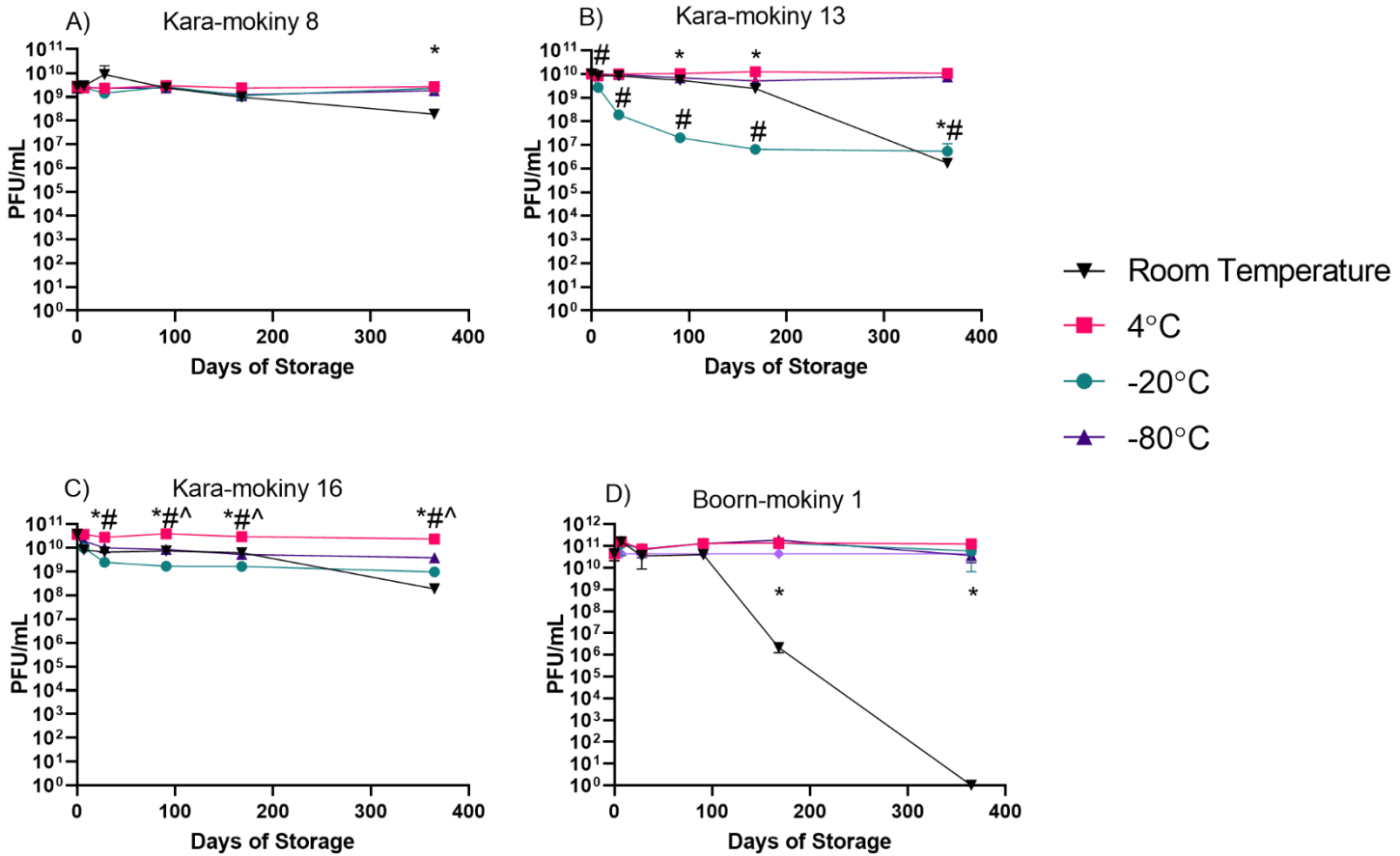


Figure 3.4: The Stability of the Top 4 Phages Across a Range of Temperatures. The stability of phage Kara-mokiny 8 (A), Kara-mokiny 13 (B), Kara-mokiny 16 (C) and Boorn-mokiny 1 (D) was tested by storing each of the phages at the defined temperatures for each of the defined periods where phages were enumerated in PFU/mL. Triplicate data is represented as mean \pm SD. A RM two-way ANOVA with Tukey's test for multiple comparisons was used to test for statistical significance. Symbols *, +, # and ^ denote statistically significant value ($p < 0.05$) for room temperature, 4 °C, -20 °C and -80 °C, respectively.

3.3.8 Phage pH Stability

After one hour of storage, Kara-mokiny 8 was found to be stable at all pHs tested (Figure 3.5 A). After 24 hrs, Kara-mokiny 8 was stable at pHs 5-9 but was not recoverable at pH 3 (Figure 3.5 A). Similarly, Kara-mokiny 13, Kara-mokiny 16 and Boorn-mokiny 1 were all stable at all pH after one hour of storage but were not recoverable after 24 hrs storage at pH 3 (Figure 3.5 B-D).

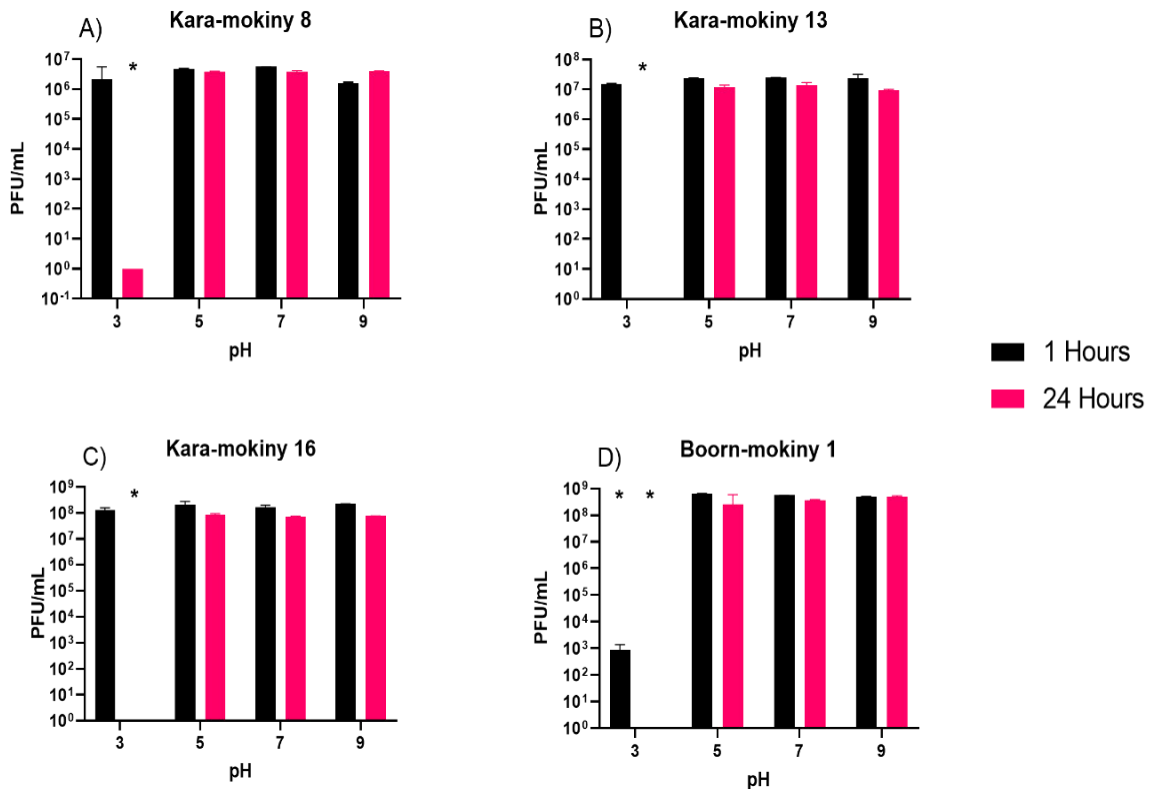


Figure 3.5: Stability of the Top 4 Phages at Different Acid-Base Concentrations (pH). The stability of Kara-mokiny 8 (A), Kara-mokiny 13 (B), Kara-mokiny 16 (C) and Boorn-mokiny 1 (D) tested after one and 24 hrs of incubation in SM buffer, adjusted to different pH levels, and enumerated using PFU/mL. All phages were stable at pH 5,7 and 9 after 1 and 24 hrs. Kara-mokiny 8, 13 and 16 were stable at a pH of 3 for one hour but significantly reduced after 24 hrs. Boorn-mokiny 1 was significantly reduced after one and 24 hrs of storage at a pH of 3. Experiments were performed in triplicate and data presented as median \pm range. A Wilcoxon test was used to test for statistical significance. Note: * $p < 0.05$.

3.3.9 One-Step Growth Curves

To determine the number of progeny phages produced from each phage infection, one step growth curves were performed to calculate the burst size of each phage. All phages demonstrated a latent period of approximately 40 mins prior to the lysis of their propagating host, resulting in the release of progeny phages. The burst size of Kara-mokiny 8 was ~136 phages/cell (Figure 3.5 A), Kara-mokiny 13 was ~132 phages/cell (Figure 3.5 B) and Kara-mokiny 16 was ~151 phages/cell (Figure 3.5 C). Boorn-mokiny 1 had a lower burst size of 59 phages/cell (Figure 3.5 D).

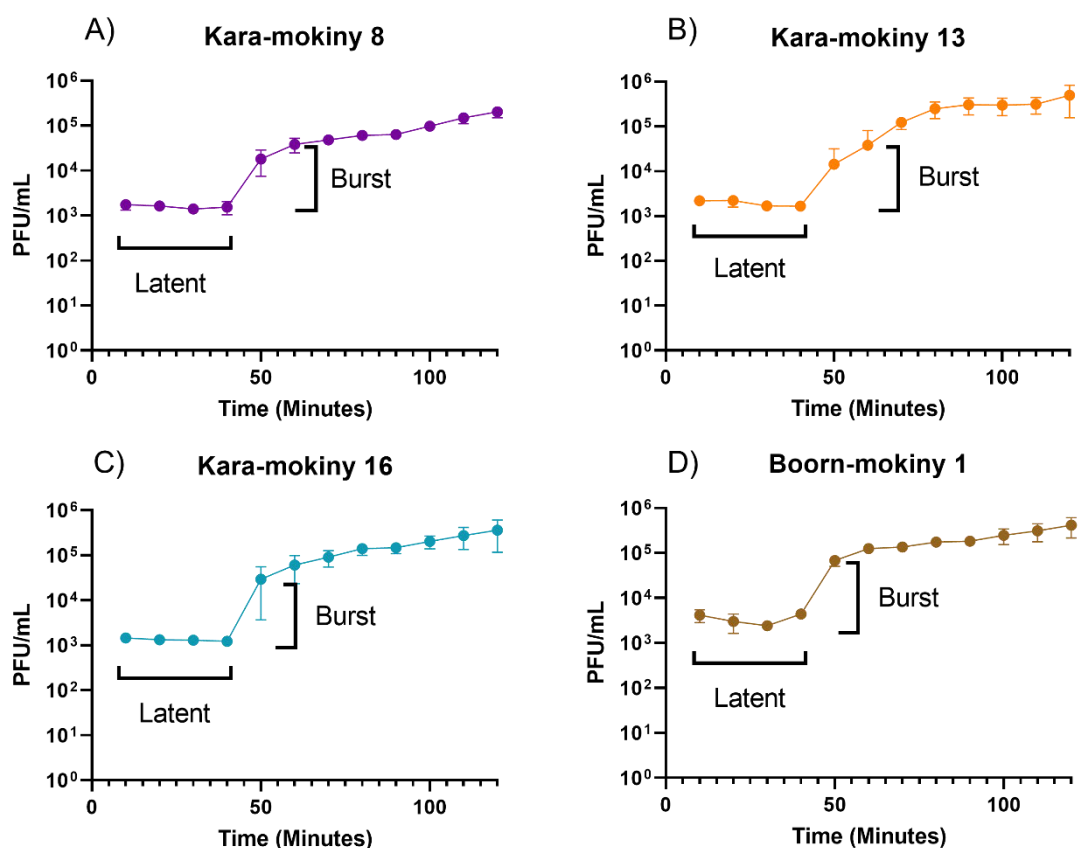


Figure 3.6: One-Step Growth Curves of Kara-mokiny 8, 13, 16 and Boorn-mokiny 1. Latent period and burst sizes were obtained after plaque enumeration from a one-step growth curve. (A) Kara-mokiny 8 had a burst size of 136 phages/cell (B) Kara-mokiny 13 had a burst size of 132 phages/cell (C) Kara-mokiny 16 had a burst size of 151 phages/cell and (D) Boorn-mokiny 1 had a burst size of 59 phages/cell. Experiments were repeated in triplicate and data plotted as mean \pm SD with burst and latent period indicated.

3.4 Discussion

Using a panel of 30 CF clinical *P. aeruginosa* isolates, 252 putative phages were successfully isolated from wastewater. Putative phages ranged from narrow to broad with their activity against the initial 30 *P. aeruginosa* and the 43 adult CF *P. aeruginosa* isolates. Twenty of the broadest acting putative phages were then selected and further characterised. These were found to be only infective against *P. aeruginosa* and, in addition to their broad activity against the isolates already tested, were also active against non-CF *P. aeruginosa* isolates. Whole genome sequencing analysis confirmed that in 18/20 putative phage samples there were phage genomes ~66,000 bp in length with ~90 CDS which classified into the genus *Pbunaviruses*. None of these genomes contained temperate phage associated genes. However, 6 of these 18 putative phage samples had secondary temperate phage contigs which contained integrase genes and thus these samples were removed from further analysis. The last 2 putative phage samples contained phage genomes that were ~270,000 bp long with ~360 CDS and were classified as *Phikzviruses*. None of the analysed genomes contained antimicrobial resistance or bacterial virulence genes. Morphological inspection revealed that all 14 remaining phages had a myovirus morphotype and there were clear differences between the *Pbunaviruses* and *Phikzviruses*. Comparison of the phage genomes identified ~ 4 different clades of *Pbunaviruses* and only one of the *Phikzviruses*. Four distinct phages were characterised further in terms of the receptor usage, acid-base stability, cryo-stability, and one-step growth kinetics.

Phages can be isolated from wherever their host bacteria are found. Wastewater has previously been found to be a rich source of *P. aeruginosa* phages, especially in the hospital catchments, where they can be isolated at high frequencies [265]. This was supported in this chapter, where over 250 phages were isolated as part of this study, the majority without the need for enrichment. Here, plaque morphology was initially used as a marker of phage diversity, and it indicated that there were different phages isolated. However, plaque morphology is affected by a range of phage, bacterial and environmental factors limiting the conclusions about phage diversity that can be made from it [487, 488]. Nevertheless, the putative phages exhibited a broad host range against paediatric and adult CF clinical isolates which facilitated the selection of 20 with the broadest activity that were then further characterised. Although isolated using CF *P. aeruginosa* isolates, these putative phages were capable of lysing *P. aeruginosa* isolates

from a range of clinical settings indicating they have broader applicability. A number of these isolates were from non-CF respiratory, burns, wounds, and blood where *P. aeruginosa* infections are also a particular problem indicating that they could provide another treatment option in other settings [489]. However, whilst phenotypic characteristics might indicate diversity, genomic analysis is needed in addition as the gold standard of phage characterisation.

Genomic analysis of the 20 putative phage samples revealed that six of the phage samples were unsuitable for therapy in their current state because they contained two phages' genomes and one typically had temperate phage-associated genes. Temperate phage contamination is an issue that the phage therapy field continually faces, and it was promising that the bioinformatic approach utilised here was able to identify and remove the samples early in characterisation [256, 298]. Interestingly, others have explored the potential of cell free phage production [490] or prophage removal from isolation hosts [491]. Data generated showed that the remaining samples contained a single phage each that fitted into one of two genera with two highly similar *Phikzviruses* and 12 *Pbunaviruses*. The *Pbunaviruses* were more diverse with five clusters of different phages and a completely novel species (Kara-mokiny 13 with <95% ANI). Importantly, none of the phages contained genes that would preclude their use for phage therapy. With a focus on diversity, four were selected and characterised further in terms of their stability over storage temperatures and pH ranges and their one-step growth.

Kara-mokiny 8, 13 and 16 (all *Pbunaviruses*) all had broad host ranges. Specifically, Kara-mokiny 8 formed clear and partial plaques on 90% of the *P. aeruginosa* strains tested, Kara-mokiny 13 on 72% of the *P. aeruginosa* strains and Kara-mokiny 16 on 75% of the bacteria. Such broad host ranges are preferred for therapeutic use since it increases the probability that a library will contain a phage active against a patient's isolate and be effective in the case of a multi-strain infection, therefore decreasing the chances of treatment failure [256, 471]. The genome of Kara-mokiny 8 was found to be 66,420 bp in length encoding 93 CDS, with 61% of these being hypothetical. Kara-mokiny 13 had a genome 65,645 bp in length and encoding 93 CDS, with 60% being hypothetical. Finally, Kara-mokiny 16 had a 66,600-bp long genome encoding 93 CDS, with 59% being hypothetical. Most phage genes are annotated as hypothetical due to the difficulties in experimentally verifying them [492]. Despite the large number of hypothetical genes, these phages did not contain known bacterial virulence or AMR genes or any that would

indicate it as temperate phage capable of integrating into bacteria which are essential considerations for therapeutical application [267].

All three *Pbunaviruses* (Kara-mokiny 8, 13 and 16) used the core of the LPS as their receptor since they were not capable of infecting a mutant missing the *galU* gene. The *galU* gene is responsible for the complete synthesis of the LPS core and without it a truncated version is created [493-495]. The core is an important precursor which other genes build sugars onto to form O-antigen specific, common polysaccharide antigen and uncapped LPS variants [494, 495]. Lipopolysaccharide is a common *P. aeruginosa* phage receptor and resistance to LPS core targeting phages is typically due to deletion of *galU* [275, 330, 485, 496]. Deletion of *galU* has also been associated with reduced antibiotic resistance and virulence [275, 330, 485, 496]. All three *Pbunaviruses* were found to be temperature and pH stable, key characteristics of stable active phage. Although, contentious, it has been suggested that the airways of people with CF are acidic which these phages would potentially need to survive to be effective [497-499]. Data generated in this chapter suggest that the three *Pbunaviruses* may be effective in the short term in acidic environments but may decrease in effectiveness as they degrade [476]. Storage stability of phages was also demonstrated, specifically over a 12-month period. This is important since prior works suggest a potentially long-time frame from request to administration of compassionate cases of phage therapy in USA (range 28-386 days with a median of 170.5 days; Aslam et al., 2020). Thus, a long phage shelf-life ensures stability of titre needed for infection elimination (Duyvejonck et al., 2021).

The *Phikzvirus* (Boorn-mokiny 1) formed clear and partial plaques on 74% of the *P. aeruginosa* isolates tested. Its genome was 278,796 bp long encoding 362 CDS, with 76% being hypothetical. Boorn-mokiny1 also encoded six of its own tRNAs. There are several hypotheses for the presence of tRNAs in phages with larger genomes [500-504]. Recent evidence has suggested that tRNAs allow phages to continue to replicate despite the host bacterial machinery (including tRNAs) degrading [500-502]. Of note, was the absence of any known bacterial virulence or AMR genes that would preclude its use in phage therapy [267]. Furthermore, Boorn-mokiny 1 used flagella as its surface receptor as indicated by its weak infection of the *fliC* mutant and a 67 bp deletion of the *flgE* gene found in a resistant PAO1 mutant derived from its treatment. The *fliC* gene encodes flagellin which is one of the main components of a flagellum and extends out from the bacterial cell [505]. Removal of flagellin through *fliC* mutation would leave the components more

proximal to the bacterial cell such as the flagellar hook (encoded by *flgE*) in a partially complete form of flagellum [505]. Mutation of *flgE* would completely truncate the flagellum as it is used to shuttle flagellin components to the growing flagellum tip [505]. This may explain why *fliC* weakened Boorn-mokiny 1 infection but *flgE* fully ablated it in results generated in this chapter. Whilst a common Gram-negative bacterial receptor [322], it has not been typically identified in *P. aeruginosa* phages [506]. Flagella are important for adhesion [507], pathogenesis [508] and biofilm formation [509, 510] but not integral to cell structure like the LPS core. Hence, *P. aeruginosa* may not constitutively express it [505] and it is commonly mutated especially in isolates chronically adapted to the CF airways, which may explain the narrower host range of Boorn-mokiny 1 compared to the *Pbunaviruses* [510-512]. Given the importance of flagella to virulence, some have postulated that phages targeting this receptor could drive advantageous bacterial phenotypes if resistance arises [506]. Many of the flagellotropic phages utilise more than one receptor [506] which cannot be discounted here with the use of only single gene mutants and in further gene knockout and complementation studies are required to confirm the findings. However, given that that flagella are often missing in *P. aeruginosa* isolates, it could indicate that this phage will have a more restricted host range. However, given the fitness trade-offs associated with losing the flagella, Boorn-mokiny 1 could be highly effective against bacteria it can infect [506]. The finding that there are phages that use two different receptors does open up the possibility of a phage cocktail that could be more effective, broader in host range, and suppress the emergence of resistance [372, 513-515]. Similar to the *Pbunaviruses*, Boorn-mokiny 1 was found to be temperature and pH stable.

One limitation to findings generated in this chapter was that isolation was performed with limited background knowledge of the *P. aeruginosa* isolates used as hosts and the use of a well characterised bacterial library for isolation may have increased the diversity of phages isolated [516]. Furthermore, only the phages with the greatest host range were selected for sequencing which probably reduced the diversity observed in this chapter. Despite this, phages spanning two genera were isolated, displaying intra-genus diversity that targeted two receptors.

In conclusion this chapter presents the isolation and characterisation of phages from wastewater. Purified phages had broad host range against *P. aeruginosa* arising from many types of infections. Phages unsuitable for therapy were identified by genomic

analyses and eliminated from further characterisation. The phages passing initial characterisation had qualities that make them suitable candidates for use in therapy. Four phages that represent the diversity of the isolated phages were storage and pH stable, highly lytic and targeted important bacterial surface molecules. This indicates that they could be very useful for therapy. However, phage treatment can lead to bacteria developing phage resistance [293, 298-302, 309]. Therefore, before these can be used in phage therapy more work needs to investigate the evolution of phage resistance and its prevention. There is a considerable lack of research on the development of phage resistance in *P. aeruginosa* isolated from people with CF [275, 282, 326-329]. These isolates are often distinct to those from other infection settings [308, 379, 380] due to prolonged adaptation to the host during chronic infection and often display diverse phenotypes [381, 382]. Hence, the four phages isolated and characterised in the most depth in this chapter will be used to treat distinct CF clinical isolates of *P. aeruginosa*. The evolution of phage resistance will be monitored, and resistant bacteria investigated in order to understand how it has occurred and ways to prevent it developing.

This page is intentionally left blank.

4. Phage Resistance Evolution in CF Isolates of *P. aeruginosa*

4.1 Introduction

Despite phage therapy being a promising alternative to antibiotics, resistance to phage-treatment, while rare, has been observed clinically [293, 296, 299-304, 307-309]. Bacterial resistance mechanisms exist for every stage of a phage's lifecycle and the type of resistance that evolves varies depending on the dose (multiplicity of infection; MOI) of phage used in the treatment, bacterial genomic features and bacterial growth altering factors [347-350]. However, adaptive resistance to phage treatment is predicted to occur either via CRISPR-cas systems or receptor mutation (Egido et al. 2021). In the setting of CF, *P. aeruginosa* isolates typically have hypermutability, defective quorum sensing and slower growth which impacts their ability to develop CRISPR-cas resistance [517-519] and receptor mutations have been found to be the primary form of resistance in recent cases investigated [303, 520].

P. aeruginosa phage receptor mutations are commonly associated with fitness trade-offs in virulence and/or antibiotic resistance [275, 282, 303, 308, 323, 326-330, 379, 516, 521-523]. However, this pleiotropy is difficult to predict as phage resistance has been found to simultaneously associated with increased sensitivity to colistin and increased resistance to tetracycline [524]. Similarly, pleiotropic effects on virulence have also been observed where phage-resistant bacteria simultaneously exhibit attenuated motility and greater biofilm formation [521]. Therefore, careful combination of phages that use different receptors, or pairing phages with antibiotics would need to be performed to leverage the desired pleiotropic effects that mitigate resistance emergence [258]. Antibiotic-phage combinations have been shown to work together to enhance killing of bacteria and prevent resistance evolving to either compound [274, 275, 279, 286, 307, 525-527]. Generally, it is thought phage resistance is prevented by combination treatment exploiting synergistic fitness trade-offs or antibiotics enhancing phage infection productivity [323, 528, 529]. Antibiotics can improve phage infection by delaying lysis as they activate the bacterial SOS stress response causing filamentation of the bacterium, which increases its surface area [528, 530]. However, the SOS response can also cause the upregulation of innate phage defence mechanisms, which may hinder some phage's infection [531]. In

the case where the antibiotic-mediated SOS response aided phage infection, the filamented bacteria had a larger surface area requiring more phage holins to have to accumulate at the inner membrane to facilitate lysis and allowed extended replication producing more phages [528]. However, most studies investigating phage resistance in *P. aeruginosa* have used the reference strain PAO1 [282, 326-330, 521-523] and growing evidence suggests that it shows both genotypic and phenotypic diversity across laboratories [532-534]. Furthermore, studies that have utilised clinical isolates to investigate phage resistance, have found that they do not experience the same fitness cost as PAO1 [379] or evolve resistance in similar ways [308, 379, 516]. Interestingly, CF isolates of *P. aeruginosa* are often genomically distinct where there are not only many genes under strong selection pressure to facilitate adaptation to the CF airways [535] but also geographic and intra-patient variation in isolates [154, 155, 536, 537]. Furthermore, few studies have investigated phage resistance by CF clinical isolates nor identified whether the mechanisms driving this are commonplace or specific to the isolate driving infection.

Thus, in this chapter resistance evolution to four phages' was investigated *in vitro* using three distinct CF isolates (two AUST-02 strains) of *P. aeruginosa*. Specifically, it was hypothesised that resistance would be affected by phage MOI, the type of phage used and the bacterial strain. It was also hypothesised that the development of resistance of *P. aeruginosa* to phages would result in enhanced susceptibility to antibiotics. To test these hypotheses, CF *P. aeruginosa* isolates were treated with different phages at a range of MOIs. Then OD_{600nm} was measured hourly, and bacteria and phages enumerated every six hrs before surviving *P. aeruginosa* were isolated, phenotyped, analysed bioinformatically and then had their antibiotic susceptibility tested.

4.2 Materials and Methods

4.2.1 Bacterial DNA Extraction, Quality Assessment and Sequencing

Wild-type (WT) reference *P. aeruginosa* DNA was both long and short read sequenced to facilitate hybrid assembly that would yield a complete high-quality chromosome that mutant reads could be mapped back to (Figure 4.1). Long bacterial reads were sequenced courtesy of Dr Samuel Montgomery (UWA, Perth Australia), where high molecular weight DNA was initially extracted [420] from overnight cultures of bacteria (refer to

2.7.1) and subsequently sequenced on Nanopore MinION flow cells using a Mk1C MinION sequencer (Oxford Nanopore Technologies, Oxford Science Park, Oxford, United Kingdom). In addition, phage treated mutants and WT *P. aeruginosa* DNA was extracted for Illumina short read sequencing as previously described (Figure 4.1; refer to 2.7.1.6). Briefly, bacteria were cultured on LB agar (refer to 2.5.1.2) overnight and then a single colony was cultured overnight in LB broth (refer to 2.5.1.1 and 2.7.1). Genomic DNA was then extracted using the DNeasy Tissue and Blood Extraction Kit (Qiagen, Hilden, Germany). Here, a 1 mL aliquot of the overnight culture was initially centrifuged at 4,000 xg for 10 mins at room temperature and resuspended in 180 µL of ATL buffer and 20 µL of Proteinase K (Qiagen, Hilden, Germany). Solutions were then incubated at 56 °C for 1 hour. Following this, 4 µL of RNase A (Invitrogen, Waltham, Massachusetts, United States of America) was added before a 15-minute incubation at room temperature. The process of washing and eluting the DNA was performed as per provided instructions in the kit (Qiagen, Hilden, Germany). DNA quality was assessed using a Nanodrop 2000c (Thermo Fisher Scientific, Waltham, Massachusetts, United States of America) to ensure the 260/280 ratio was between 1.8-2.0. Concentrations were then measured using a Qubit dsDNA High Sensitivity kit (Thermo Fisher Scientific, Waltham, Massachusetts, United States of America). Phage DNA libraries were prepared using the Nextera XT preparation kit and sequenced on the NovaSeq 6000 Illumina (Illumina, San-Diego, California, United States of America) next generation sequencing platform that generated 150 bp paired-end reads. Library preparation and sequencing was performed by the Australian Genomic Research Facility (Monash University, Melbourne, Victoria, Australia).

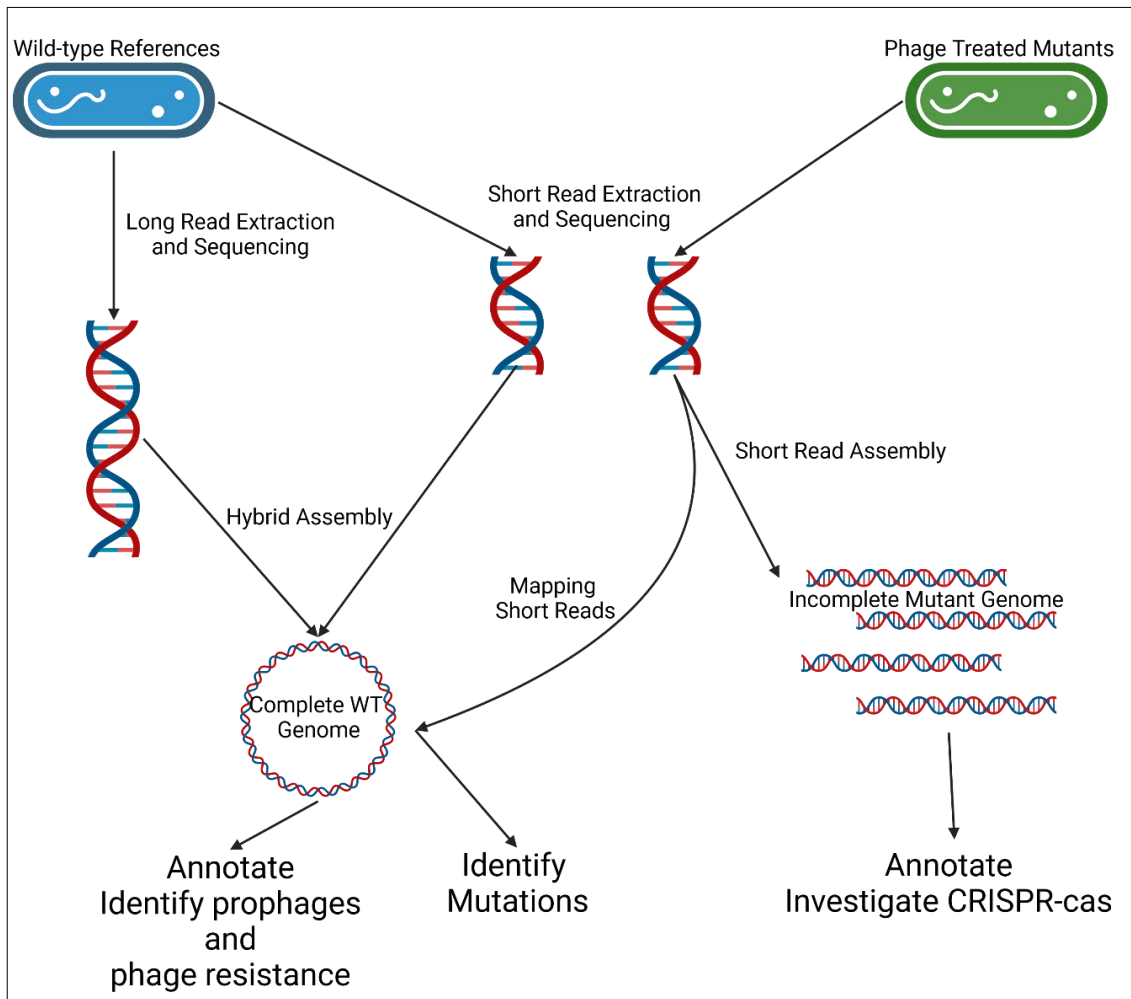


Figure 4.1 Bacterial Sequencing and Analysis. Wild-type *P. aeruginosa* was sequenced by both short and long read methodologies and used to hybrid assemble a single chromosome. Phage treated *P. aeruginosa* mutants were short read sequenced and the reads mapped to the complete WT genome to identify mutations.

4.2.2 Bacterial Short Paired-End Illumina Whole Genome Assembly

P. aeruginosa mutant short Illumina reads were quality controlled and assembled (Figure 4.1) using a docker container created as part of this thesis called Orange (<https://hub.docker.com/r/mantistobogan/orange>). Briefly, its assembly pipeline utilised a number of packages from BBmap v39.01 [421] to: trim reads with bbdduk, remove duplicate reads with dedupe, normalise coverage to 100X with bbnorm and merge reads to create longer ones with bbmerge. Reads were assembled with SPAdes v3.15.4 [422], and assembly gaps filled with Mind the Gap v2.3.0 [423] and utility scripts from Mine Your Symbiont v1.1 (MinYS) [424]. Species contamination was checked for by Kraken v1.0 [425].

4.2.3 Bacterial Long Read Nanopore and Short Paired-End Illumina Whole Genome Hybrid Assembly

Hybrid assemblies of wild-type (WT) *P. aeruginosa* isolates were performed to yield complete genomes using another Docker container created in this thesis called Magnum (Figure 4.1; <https://hub.docker.com/repository/docker/mantistobogan/magnum/general>). Briefly, short Illumina 150-bp paired end reads were quality controlled (refer to 4.2.2) along with the MinION Nanopore long reads before hybrid assembly was performed using a custom bash script. Long reads were filtered by length (>1000bp), quality (Q10), 140bp head cropped and 40bp tail cropped with chopper v0.6.0 [426]. Hybrid assemblies were then made using unicycler v0.4.8 [427]. Long read only assemblies were also created by unicycler v0.4.8 [427] and flye v2.8.1-b1676 [428]. A consensus assembly was then created from each of the long read drafts and the hybrid using tricycler v0.5.4 [429]. The assembly was then polished using the long reads with medaka v1.7.2 [430], BWA v 0.7.17-r1188 [431], and the short reads with polypolish v0.5.0 [432].

4.2.4 Bacterial Genome Annotation

The Orange docker image (<https://hub.docker.com/r/mantistobogan/orange>) included an annotation pipeline that; determined the species of bacteria via Kraken v1.0 [425], annotated general genomic features using Bakta v1.7.0 [433], identified phage resistance mechanisms by PADLOC v1.1.0 [434], multilocus sequence type (MLST) by the mlst

v2.23.0 package [435] which also used the PubMLST database [436]. It also included abricate v1.0.1 [437] to find antibiotic resistance genes and virulence genes by searching existing databases [438-444] and finally identified prophages using DBSCAN-SWA [445] which made use of both diamond [446], prokka v 1.14.6 [447] and blast software [448].

4.2.5 Phage Treatment of the Bacterial Isolates

The *P. aeruginosa* isolates (M1C79, AST154 and AST234) were treated with the phages Kara-mokiny 8, Kara-mokiny 13, Kara-mokiny 16 and Boorn-mokiny 1 (Figure 4.2). Briefly, each of the three *P. aeruginosa* isolates were grown in LB broth (refer to 2.5.1.1) in duplicate overnight (refer to 2.7.1.2) and their OD_{600nm} was read the following day (refer to 2.7.1.3). These values were used to adjust cultures to an OD_{600nm} value that corresponded to 10⁸ CFU/mL of each isolate (refer to 2.7.1.3). Each individual phage was then diluted in LB broth (refer to 2.5.1.1) to 10⁹, 10⁸, 10⁷ and 10⁶ PFU/mL. Equal volumes of each phage (100 µL) and the *P. aeruginosa* isolated were mixed in duplicate wells on five replicate 96 well plates. An OD_{600nm} reading was taken and repeated every hour using a CLARIOstar® Plus machine (BMG Labtech GmbH, Ortenberg, Germany). Between readings, the 96 well plates were incubated at 37 °C with 100 rpm of shaking. Phage titre and viable bacterial counts were also performed to ensure that the concentrations initially added were as calculated (i.e., 10⁸, 10⁷, 10⁶ and 10⁵ PFU/mL; refer to 2.7.2.7 and 2.7.1.4). Every six hrs, a plate was taken, and phage titre and viable bacterial counts performed from each well to monitor numbers of phages and bacteria over the course of treatment (refer to 2.7.2.7 and 2.7.1.4). After 24 hrs, a 10 µL loop was used to isolate bacteria surviving treatment which was then streaked onto LB agar plates (refer to 2.5.1.2). After overnight incubation, 5 randomly chosen single colonies of each isolates' duplicate populations (10 colonies total per isolate) were subcultured onto LB agar plates (refer to 2.5.1.2). This process was repeated three times to remove any phage contamination and ensure mutations were stable. Isolates were cryopreserved in 25% glycerol at -80 °C (refer to 2.7.1.1).

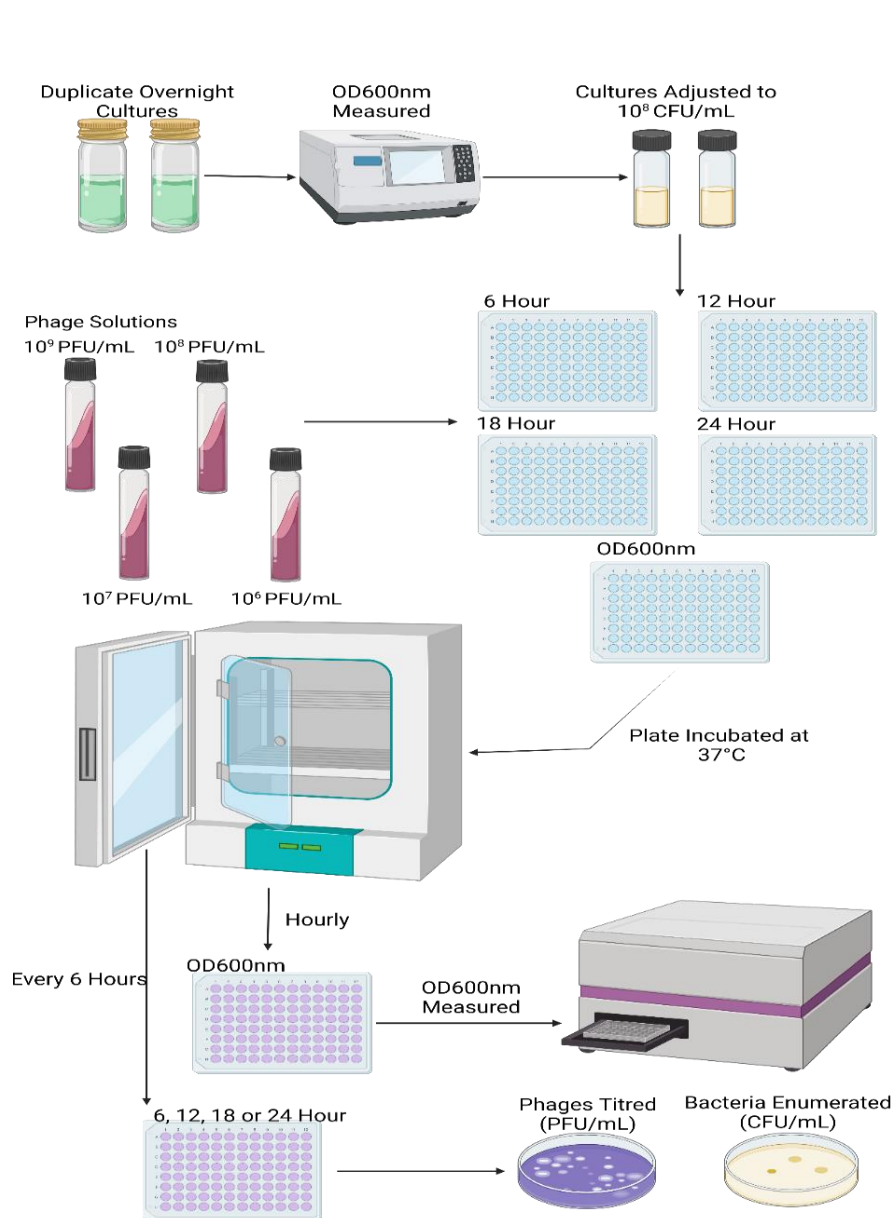


Figure 4.2 Overview of the Method used to Treat the *P. aeruginosa* Isolates with Each Phage. Duplicate overnight cultures were adjusted to 10^8 CFU/mL. Phages were diluted to 10^9 , 10^8 , 10^7 and 10^6 PFU/mL. Each of the duplicate bacterial cultures were seeded into five replicate 96 well plates. These were then treated with each of the different concentrations of the phages to represent MOI 10, 1, 0.1 and 0.01. The plates were incubated at 37 °C and every hour one of the plates was removed and the OD600nm measured. Every six hrs one of the plates was sacrificed and phages and bacteria enumerated (PFU/mL and CFU/mL).

4.2.6 Confirming Phage Resistance

Any resistance to phages used to treat mutants was determined via efficiency of plating (refer to 2.7.2.8). Briefly, phages were serially diluted (10-fold from 10^{-1} to 10^{-8}) and 10 μ L spotted in duplicate onto overlay agar imbued with 100 μ L of either one of the mutants, control, or WT. Spots were allowed to dry at room temperature and plates incubated overnight at 37 °C in a non-humidified incubator. Where present, plaques were counted, and phage titre determined on each of the mutant bacteria. Efficiency of plating was then determined by comparing the titres for each mutant to the corresponding *P. aeruginosa* isolate WT they had evolved from (refer to 2.7.2.8). Where a mutant was not resistant to the phage used to treat it, EOP was ≥ 0.1 , where a mutant was intermediately resistant to a phage, EOP was $0.1 \geq 0$ and where mutants were completely resistant EOP=0 [451].

4.2.7 Mutant Analysis

Mutations were predicted using snippy v4.6.0 by mapping mutant, control and WT bacterial short reads to the fully resolved WT genome [486]. Larger structural genomic changes were also searched for using breseq v0.36.0 [538]. Mutations were filtered out if they were present in that corresponding control, WT bacteria or susceptible phage-treated mutants. Mutated genes were classified according to the category assigned by the Cluster of Orthologous Genes (COGs) database [539]. CRISPR-cas resistance was also investigated in the M1C79-derived mutants because a system was annotated in this isolate. The Spacepharer v5.c2e680a package was utilised to predict phages that could be targeted by the M1C79 isolate's CRISPR by making a database of spacer sequences out of the phages' genomes and searching for them in the M1C79 and derived mutants' CRISPR systems [540].

4.2.8 Statistical Analyses

All statistical tests were performed in GraphPad Prism v9.3.1 (GraphPad Software, La Jolla, CA). Normality was tested for using the Shapiro-Wilk normality test. Microbiological data (OD_{600nm}, CFU/mL and PFU/mL) was performed and measured in biological duplicates and expressed as median \pm IQR. The Area Under the Curve (AUC) for the OD_{600nm} over time was calculated and compared between different phage's treatments using a 1-way ANOVA with Tukey's multiple comparison test. The CFU/mL

and PFU/mL data were compared between treatments via a repeated measures (RM) 2-way ANOVA with Tukey's multiple comparison test. Multiple comparisons were made between each treatment at each timepoint. Proportions of resistant *P. aeruginosa* after phage treatment were compared using multiple t-test. A $p < 0.05$ was considered statistically significant.

4.3 Results

4.3.1 Characteristics of *P. aeruginosa* Clinical isolates

For this study, three *P. aeruginosa* clinical isolates were chosen to represent the range seen in people with CF. M1C79, isolated from a child with CF, was non-mucoid and not resistant to any of the antibiotics commonly used to treat *P. aeruginosa* infections (Table 4.1). This isolate also did not share any alleles across those used to determine multilocus sequence type (MLST) with the other two isolates chosen for investigation (AST154 and AST234; Table 4.1). AST154 and 234 were both derived from adults with CF (Table 4.1) and shared more similarities, including the same alleles at 6/7 of the MLST sites, but differed in their alleles at the *mutL* locus (Table 4.1). Both isolates were also from the same strain, namely AUST-02 (Table 4.1), which is the most common epidemic strain infecting people with CF in Western Australia and Australia more broadly [148, 153, 154]. Despite being from the strain, AST154 and 234 differed in their colony morphology and antibiotic resistance (Table 4.1).

Genomically, AST154 and 234 were also found to be similar to each other compared to M1C79. M1C79, has a larger genome (~6.4mbp) and was found to have more coding sequences (~5,800; CDSs; Table 4.2). A cas type I-F1 CRISPR system was also identified and four prophages (Table 4.2). Isolates AST154 and 234 had smaller sized genomes (~6.2mbp), with fewer CDSs (~5,700), only two prophages, with both containing a type I restriction modification system (Table 4.2). In addition, AST154 had an *ietAS* toxin-antitoxin system which can cause abortive infection in response to specific phages (Table 4.2).

Table 4.1 General Characteristics of the Clinical Isolates of *P. aeruginosa*

Isolate	Origin	MLST							Strain	Colony Morphology	Antibiotic Resistance
		ascA	aroE	guaA	mutL	nuoD	ppsA	trpE			
M1C79	CF	71	15	9	93	62	57	281	N/A	NM	0/12
AST154	CF	28	5	11	5	4	4	7,321	AUST-02	NM	11/12
AST234	CF	28	5	11	303	4	4	7,321	AUST-02	M	5/12

Note: CF: Cystic Fibrosis, NM: non-mucoid, M: mucoid. Antibiotics that susceptibility was determined against included; gentamicin, imipenem, aztreonam, colistin, tobramycin, cefepime, ceftazidime, amikacin, tazobactam-piperacillin, ciprofloxacin, levofloxacin and meropenem.

Table 4.2 Genome Characteristics of the *P. aeruginosa* Clinical Isolates

Isolate	Genome Length (bp)	GC Content (%)	Coding Density (%)	tRNAs	tmRNAs	rRNAs	ncRNAs	CDSs	Hypotheticals	Phage Resistance Mechanisms	No. of Predicted Prophages
M1C79	6,440,852	66.1	90.1	64	1	12	50	5884	392	Cas type I-F1	4
AST154	6,285,712	66.5	90.30	63	1	12	47	5740	395	ietAS (abortive infection) and type I RM system	2
AST234	6,248,706	66.5	90.4	63	1	12	47	5714	406	Type I RM system	2

Note: RM: restriction modification system

4.3.2 Phage Infectivity Against Chosen *P. aeruginosa* Isolates

Results generated found that Kara-mokiny 8, 13 and 16 could infect all three *P. aeruginosa* isolates to varying degrees (EOPs>0; Table 4.3). In particular, Kara-mokiny 8 was observed to strongly infect all three isolates to a similar degree (EOP>0.1; Table 4.3), compared to both Kara-mokiny 13 and 16 which could strongly infect M1C79 and AST154 (EOP>0.1) but could only weakly infect AST234 (EOP<0.1; Table 4.3). Boorn-mokiny 1 could only infect M1C79 (EOP>0.1; Table 4.3). This phage's infection was resisted by AST154 and AST234 (EOP=0), although it did form partial plaques on the latter isolate (Table 4.3).

Table 4.3 Phage EOP Against the Clinical Isolates of *P. aeruginosa*

EOP			
Phage	M1C79	AST154	AST234
Kara-mokiny 8	1.11	0.75	0.93
Kara-mokiny 13	0.65	0.44	0.04
Kara-mokiny 16	1.46	1.21	0.01
Boorn-mokiny 1	0.69	0	0 (Partial Plaques)

4.3.3 Phage Treatment of the *P. aeruginosa* Clinical Isolate M1C79

The M1C79 isolate was treated with singular phage (MOIs 10, 1, 0.1 and 0.01) and effects on bacterial growth over time assessed by OD600nm. The AUC for each phage's treatment was then calculated and compared to other phages as well as the untreated control. For simplicity, only the highest and the lowest MOI (10 and 0.01) effects have been presented within the chapter (Figure 4.3 A and C), however, all results have been provided in the thesis appendices (Appendix Table E.1 and E.2). Treatment of M1C79 with Kara-mokiny 8 resulted in a significant reduction (39%) in AUC compared to the untreated control ($p<0.05$; Figure 4.3 A). This was also significantly higher than the effects seen with Kara-mokiny 13 (113%) and Kara-mokiny 16 (56%) treatments ($p<0.05$; Figure 4.3 A). Finally, the AUC was significantly elevated compared to Boorn-mokiny 1 (154% $p<0.05$; Figure 4.3 A). Differences in AUCs after Boorn-mokiny 1, Kara-mokiny 13 and Kara-mokiny 16 treatments of M1C79 for 24 hrs ranged from 16-38% but were not significant ($p>0.05$; Figure 4.3 A). Both Kara-mokiny 13 and 16 significantly reduced AUC compared to the untreated control (72 and 61% respectively; $p<0.05$; Figure 4.3 A). Boorn-mokiny 1 treatment also resulted in a significant reduction in AUC compared to the untreated control (76%; $p<0.05$; Figure 4.3 A). In summary,

each phage had a different effect on M1C79 OD_{600nm}. However, they all initially prevented M1C79 growth before eventual outgrowth (indicating the evolution of resistance) to different levels depending on the phage being used.

Every six hrs the number of viable bacteria (CFU/mL) after treatment with the phages at an MOI of 10 was also determined to corroborate OD_{600nm} results (Figure 4.3 B). Treatment of M1C79 with Kara-mokiny 8 at an MOI of 10 for 6 hrs resulted in significant reduction of viable bacteria (3.5 log-fold; $p < 0.05$; Figure 4.3 B). After 12 and 18 hrs the amount of viable M1C79 following Kara-mokiny 8 treatment at an MOI of 10 was not significantly altered ($p > 0.05$; Figure 4.3 B). However, following 24 hrs of treatment with Kara-mokiny 8 (MOI 10) viable M1C79 was significantly increased by compared to the untreated control (0.3 log-fold; $p < 0.05$; Figure 4.3 B). Treatment with Kara-mokiny 13 and an MOI of 10 for 6 hrs resulted in significant reduction in culturable M1C79 compared to the untreated control (2.8 log-fold; $p < 0.05$; Figure 4.3 B). However, treatment did not result in significant reductions in viable M1C79 after 12 and 18 hrs ($p > 0.05$; Figure 4.3 B). After 24 hrs, treatment with Kara-mokiny 13 (MOI of 10) caused a significant reduction in viable M1C79 compared to the control (0.6 log-fold; $p < 0.05$; Figure 4.3 B). Similarly, Kara-mokiny 16 treatment (MOI of 10) for 6 hrs resulted in significant reduction in viable M1C79 compared to the untreated control (4.3 log-fold; $p < 0.05$; Figure 4.3 B) but was not maintained after 12 or 18 hrs of treatment ($p > 0.05$; Figure 4.3 B). However, after 24 hrs of Kara-mokiny 16 treatment at an MOI of 10 the reduction in viable M1C79 was significant again (0.6 log-fold; $p < 0.05$; Figure 4.3 B). Treatment of M1C79 with Boorn-mokiny 1 at an MOI of 10 resulted in significant reductions in viable bacterial number after 6 hrs of treatment (2.8 log-fold; $p < 0.05$; Figure 4.3 B). This effect was not seen after 12 or 18 hrs of treatment of M1C79 ($p < 0.05$; Figure 4.3 B). Treatment with Boorn-mokiny 1 (MOI of 10) for 24 hrs resulted in significant reduction reductions in viable M1C79 compared to control again (0.8 log-fold; $p < 0.05$; Figure 4.3 B). Overall, phage treatment at an MOI of 10 caused a significant reduction in M1C79. but somewhat However, and apart from Kara-mokiny 8, surviving M1C79 did recover but remained significantly lower following phages treatments.

The OD_{600nm} of M1C79 was also assessed after treatment with each of the phages at an MOI of 0.01. Again, AUC for each phage's treatment was calculated and compared to the other phages and the untreated control. Treatment of M1C79 with Kara-mokiny 8 (MOI 0.01) resulted in a significant reduction in AUC compared to untreated control

bacterial growth (52%; $p < 0.05$; Figure 4.3 C). After 24 hrs of treatment with Kara-mokiny 8, AUC was significantly increased compared to Kara-mokiny 14 (148%; $p < 0.05$; Figure 4.3 C). However, when AUC of Kara-mokiny 8 treatment of M1C79 was compared to Kara-mokiny 16 and Boorn-mokiny 1, no differences were observed ($p > 0.05$; Figure 4.3 C). Kara-mokiny 13, 16 and Boorn-mokiny 1 treatments significantly reduced AUC compared to the M1C79 untreated control (81, 72 and 70%, respectively; $p < 0.05$; Figure 4.3 C). There was no significant difference in AUCs of Kara-mokiny 13, 16 and Boorn-mokiny 1 when compared to each other ($p > 0.05$; Figure 4.3 C). Similar to effects seen at the higher phage titre, effects at MOI 0.01 on bacterial growth were also phage specific. Again, each phage initially suppressed M1C79 growth before resistance evolved and bacterial growth resumed.

Every 6 hrs the number of viable M1C79 (CFU/mL) after treatment with the phages at an MOI of 0.01 was determined (Figure 4.3 D). Kara-mokiny 8 treatment of M1C79 at an MOI of 0.01 resulted in significant reduction of viable bacteria even after 6 hrs (4 log-fold; $p < 0.05$; Figure 4.3 D). This was not maintained after 12, 18 and 24 hrs of phage treatment ($p > 0.05$; Figure 4.3 D). Treatment with Kara-mokiny 13 (MOI 0.01) for 6 hrs resulted in a significant reduction in culturable M1C79 compared to the untreated control (2 log-fold; $p < 0.05$; Figure 4.3 D). However, treatment had no effect 12 and 18 hrs ($p > 0.05$; Figure 4.3 D). Treatment with Kara-mokiny 13 (MOI 0.01) for 24 hrs caused a significant reduction in viable M1C79 compared to the control (0.6 log-fold; $p < 0.05$; Figure 4.3 D). Similarly, Kara-mokiny 16 treatment (MOI 0.01) for 6 hrs resulted in 5 log-fold reduction in viable M1C79 compared to the untreated control ($p < 0.05$; Figure 4.3 D). This reduction was not maintained after 12, 18 or 24 hrs of treatment ($p > 0.05$; Figure 4.3 D). Treatment of M1C79 with Boorn-mokiny 1 at an MOI of 0.01 resulted in significant reduction in viable bacterial number after 6 hrs of treatment (2 log-fold; $p < 0.05$; Figure 4.3 D). This was not seen after 12 or 18 hrs of treatment ($p > 0.05$; Figure 4.3 D). Interestingly, treatment with Boorn-mokiny 1 at an MOI of 0.01 for 24 hrs resulted in a significant reduction in viable M1C79 compared to the control (1 log-fold; $p < 0.05$; Figure 4.3 D). Overall, any phage treatment at an MOI of 0.01 caused an initially significant reduction in surviving M1C79 but surviving bacteria were seen to recover and grew to varying levels at later sampling points.

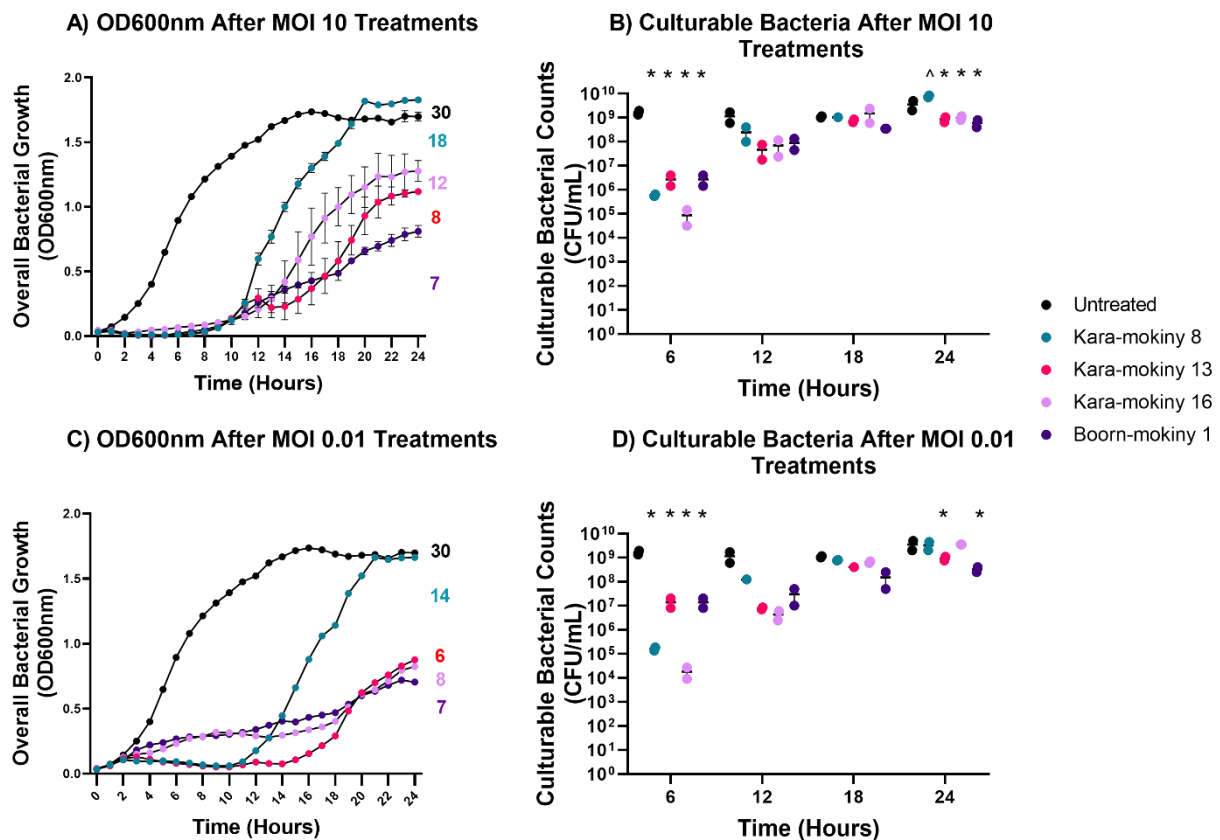


Figure 4.3 The Effects of Phage Treatment on M1C79 Growth (OD600nm) and Culturable Bacteria.

Kara-mokiny 8, 13, 16 and Boorn-mokiny 1 were used to treat M1C79 for 24 hrs at an MOI of 10 (A and B) or 0.01 (C and D) and OD600nm (A and C) or CFU/mL (B and D) measured every 6 hrs. Colours represent the phages used as the treatment as described in the legend. Different effects of phage treatment were observed depending on the phage and the MOI that was used. Duplicate values are represented as median±range. The OD600nm AUCs of each treatment (rounded to the whole number) are listed beside their 24-hour timepoint and are in the same colour as denoted in the legend. Each treatment's AUCs were compared using a 1-way with Tukey's multiple comparison test. The CFU/mL data was compared with a RM 2-way ANOVA with Tukey's multiple comparisons. A $p < 0.05$ was considered significant.

Phage titre was also determined to understand how it correlated with the different outcomes of phage treatment that were observed (Figure 4.4). When M1C79 was treated with Kara-mokiny 8 at an MOI of 10 for 6 hrs, phage titre was not significantly different to phage alone control ($p < 0.05$: Figure 4.4 A). Treatment with Kara-mokiny 8 (MOI 10, for 12 hrs) significantly increased the number of phages compared to the control ($p < 0.05$: Figure 4.4 A). However, Kara-mokiny 13, 16 and Boorn-mokiny 1 titres all did not significantly differ compared to their respective controls when used to treat M1C79 for 6, 12, 18 or 24 hrs ($p > 0.05$: Figure 4.4 A). When Kara-mokiny 8 was used to treat M1C79 (MOI 0.01 for 6 hrs) titre was not significantly different compared to the control ($p > 0.05$:

Figure 4.4 B). However, after 12, 18 and 24 hrs, Kara-mokiny 8 titre was significantly increased ($p < 0.05$: Figure 4.4 B). Similarly, when Kara-mokiny 13 was used to treat M1C79 (MOI 0.01 for 6 and 12 hrs) titre was significantly increased compared to the control ($p < 0.05$: Figure 4.4 B). Kara-mokiny 16 titre was not significantly altered when used to treat M1C79 for 6 hrs ($p > 0.05$: Figure 4.4 B). Over the longer term, (12, 18 and 24 hrs) Kara-mokiny 16 titre was significantly increased compared to the untreated control ($p < 0.05$: Figure 4.4 B). Finally, Boorn-mokiny 1 titre did not significantly differ to its control when used to treat M1C79 for 6, 12, 18 and 24 hrs ($p > 0.05$: Figure 4.4 B). In summary, each phages' titre rarely differed to the control when used to treat M1C79 at an MOI of 10. However, when used at an MOI of 0.01, phage titres were significantly increased compared to the control.

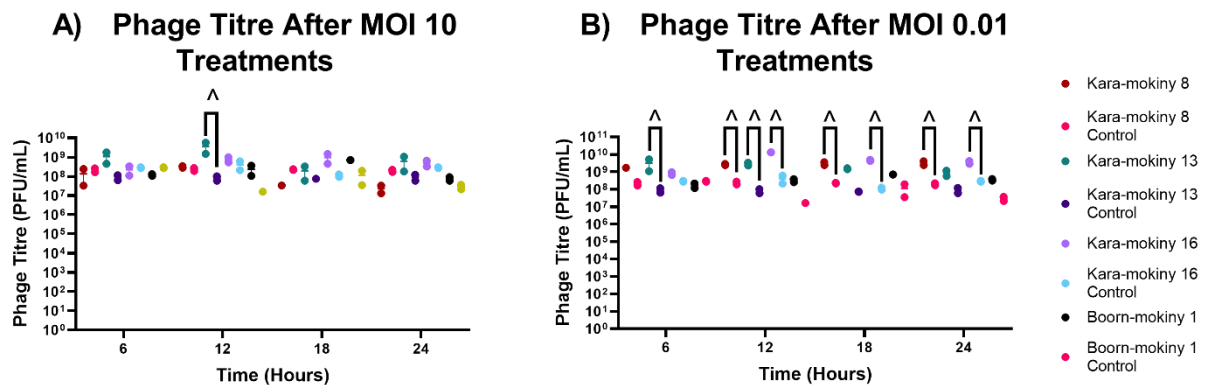


Figure 4.4 The Effects of Phage Treatment of M1C79 on Phage Titre. Kara-mokiny 8, 13, 16 and Boorn-mokiny 1 were used to treat M1C79 for 24 hrs at an MOI of 10 (A) or 0.01 (B) and phages were titrated every 6 hrs. Colours represent the phages used as the treatment as described in the legend. Each of the phage's titres was mostly not significantly different across the timepoints after treatment with an MOI of 10. There were many more phages' titres that were significantly increased after treatment of M1C79 with an MOI of 0.01. Data is represented as median±IQR. *denotes statistically significant reductions and ^ increase compared to control ($p < 0.05$) as tested by RM 2-way ANOVA with Tukey's multiple comparison test.

4.3.4 Phage Treatment of the *P. aeruginosa* Clinical Isolate AST154

Phages at various MOIs (10, 1, 0.1 and 0.01) were used to treat the *P. aeruginosa* isolate AST154 and effects on bacterial growth over time assessed by optical density at 600 nm (OD_{600nm}). From these, AUC was calculated and compared using a 1-way ANOVA. For simplicity, only the highest and the lowest MOI effects (10 and 0.01) have been presented (Figure 4.5 A and C) however all results have been supplied in the thesis appendices (Appendix Table E.3 and E.4). Treatment of AST154 with Kara-mokiny 8 for 24 hrs resulted in a significant reduction (68%) in the AUC compared to the untreated control ($p < 0.05$; Figure 4.5 A). Kara-mokiny 8 also significantly reduced (27%) the AUC compared to Kara-mokiny 13 ($p < 0.05$; Figure 4.5 A). However, the difference between Kara-mokiny 8 and Kara-mokiny 16 treatment (14%) was not significant ($p > 0.05$; Figure 4.5 A). Kara-mokiny 8 treatment caused a significant reduction (67%) in AUC compared to Boorn-mokiny 1 treatment ($p < 0.05$; Figure 4.5 A) and Kara-mokiny 13 treatment significantly reduced (72%) the AUC compared to the untreated control ($p < 0.05$; Figure 4.5 A). However, there was no significant difference between Kara-mokiny 13 and 16 treatments ($p > 0.05$; Figure 4.5 A). Kara-mokiny 13 treatment of AST 154 for 24 hrs significantly reduced (74%) the AUC compared to Boorn-mokiny 1 ($p < 0.05$; Figure 4.5 A). Kara-mokiny 16 significantly reduced the AUC compared to untreated control and Boorn-mokiny 1 treatment (72 and 71% respectively; $p < 0.05$; Figure 4.5 A). Finally, Boorn-mokiny 1 did not significantly reduce the AUC compared to the untreated control ($p > 0.05$; Figure 4.5 A). Overall, phages at an MOI of 10 had differential effects on AST154 growth, with Boorn-mokiny 1 having no effect which was expected from its EOP. The other three phages were found to reduce AST154 growth initially, but growth resumed indicating the evolution of resistance.

The amount of viable AST154 (CFU/mL) was also measured over the course of treatment with the phages at an MOI of 10 (Figure 4.5 B). Treatment with Kara-mokiny 8 did not result in significant reductions in culturable AST154 after 6, 12 or 18 hrs ($p > 0.05$; Figure 4.5 B). However, it did cause a significant reduction after 24 hrs of treatment (1.5 log-fold; $p < 0.05$; Figure 4.5 B). Kara-mokiny 13 treatment did not cause significant reductions in viable AST154 after 6, 12 or 18 hrs ($p > 0.05$; Figure 4.5 B). After 24 hrs of its treatment, Kara-mokiny 13 (MOI 10) resulted in a significant reduction in AST154 compared to the untreated control (1.2 log-fold; $p < 0.05$; Figure 4.5 B). Treatment of AST154 with Kara-mokiny 16 (MOI 10) did not result in significant reductions in

culturable AST154 after 6, 12 or 18 hrs ($p>0.05$; Figure 4.5 B). After 24 hrs, Kara-mokiny 16 MOI 10 treatment elicited a significant reduction in the amount of AST154 (1 log-fold; $p<0.05$; Figure 4.5 B). Boorn-mokiny 1 treatment of AST154 at an MOI of 10 did not result in significantly different amounts of viable bacteria across any of the timepoints sampled ($p>0.05$; Figure 4.5 B). Collectively, Boorn-mokiny1 had no effect on viable AST154, but the other three phages reduced culturable bacterial numbers at all subsequent time points which was significant at 24 hrs.

When AST154 was treated with Kara-mokiny 8 (MOI 0.01) the AUC was significantly reduced (76%) compared to the untreated control ($p<0.05$; Figure 4.5 C). However, Kara-mokiny 8, 13 and 16 treatments had no significant effect ($p>0.05$; Figure 4.5 C). Interestingly, Kara-mokiny 8 treatment significantly reduced (75%) the AUC compared to Boorn-mokiny 1 treatment ($p<0.05$; Figure 4.5 C). Compared to the untreated control, Kara-mokiny 8 (MOI 0.01) treatment significantly reduced (75%) the AUC ($p<0.05$; Figure 4.5 C). Furthermore, the same phage at the same MOI significantly reduced (74%) the AUC compared to Boorn-mokiny 1 ($p<0.05$; Figure 4.5 C). Kara-mokiny 16 also significantly reduced (78%) the AUC compared to the untreated control ($p<0.05$; Figure 4.5 C). Compared to Boorn-mokiny 1, Kara-mokiny 16 treatment significantly reduced the AUC (77%; $p<0.05$; Figure 4.5 C), but Boorn-mokiny 1 had no effect compared to the untreated control ($p>0.05$; Figure 4.5 C). To summarise, Boorn-mokiny 1 had no effect on AST154 growth, but the other phages' treatments at an MOI of 0.01 affected AST154 growth similarly.

The amount of viable AST154 (CFU/mL) was enumerated every six hrs during treatment with the phages at an MOI of 0.01 (Figure 4.5 D). Kara-mokiny 8 treatment at an MOI of 0.01 did not result in significant reductions in viable AST154 after 6, 12 or 18 hrs ($p>0.05$; Figure 4.5 D). However, after 24 hrs its treatment caused a significant reduction (1.7 log-fold) in viable AST154 ($p<0.05$; Figure 4.5 D). Kara-mokiny 13 treatment did not significantly alter the amount of viable AST154 after 6, 12 or 18 hrs ($p>0.05$; Figure 4.5 D). However, after 24 hrs of its treatment, it resulted in a significant reduction in viable AST154 compared to the untreated control (3 log-fold; $p<0.05$; Figure 4.5 D). The amount of viable AST154 was not significantly reduced by Kara-mokiny 16 treatment (MOI 0.01) after 6, 12 or 18 hrs ($p>0.05$; Figure 4.5 D). Yet, after 24 hrs, Kara-mokiny 16 treatment elicited a significant reduction in viable AST154 compared to the untreated control (1.9 log-fold; $p<0.05$; Figure 4.5 D). Boorn-mokiny 1

treatment (MOI 0.01) did not significantly alter culturable AST154 after 6, 12 or 18 hrs ($p>0.05$; Figure 4.5 D). After 24 hrs of Boorn-mokiny 1 treatment (MOI 0.01), viable AST154 was significantly reduced (0.7 log-fold) compared to untreated control ($p<0.05$; Figure 4.5 D). Overall, similar effects of phages were seen at low and high MOIs. Boorn-mokiny 1 had little effect on the amount of AST154, and Kara-mokiny 8, 13 and 16 reduced culturable AST154 becoming significant at 24 hrs.

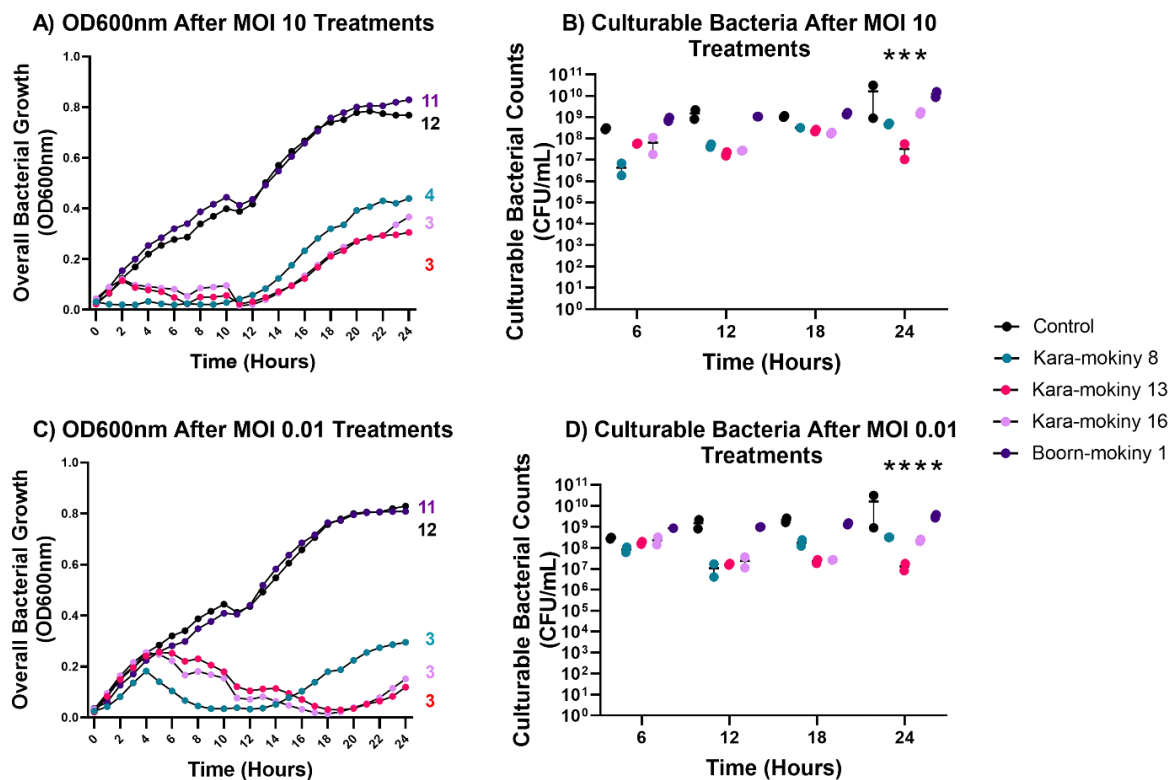


Figure 4.5 The Effects of Phage Treatment on AST154 Growth (OD600nm) and Culturable Bacteria. Kara-mokiny 8, 13, 16 and Boorn-mokiny 1 were used to treat AST154s for 24 hrs at an MOI of 10 (A and B) or 0.01 (C and D) and OD600nm (A and C) or CFU/mL (B and D) measured every 6 hrs. Colours represent the phages used as the treatment as described in the legend. Different effects of phage treatment were observed depending on the phage and the MOI that was used. Duplicate values are represented as median±range. The OD600nm AUCs of each treatment (rounded to the whole number) are listed beside their 24-hour timepoint and are in the same colour as denoted in the legend. Each treatment's AUCs were compared using a 1-way with Tukey's multiple comparison test. The CFU/mL data was compared with a RM 2-way ANOVA with Tukey's multiple comparison test. A $p<0.05$ was considered significant.

Phage titre was enumerated over the course of AST154 treatment (Figure 4.6). The titre of Kara-mokiny 8 was not significantly different compared to control after 6, 12, 18 or 24 hrs of treatment of AST154 at an MOI of 10 ($p>0.05$; Figure 4.6 A). After treatment of AST154 for 6, 12 and 18 hrs, the titre of Kara-mokiny 13 was not significantly different compared to the control ($p>0.05$; Figure 4.6 A). However, after 24 hrs, its titre was significantly reduced ($p<0.05$; Figure 4.6 A). The titre of Kara-mokiny 16 (MOI 0.01) was not significantly different compared to the control after it was used to treat AST154 for 6,12, 18 or 24 hrs ($p>0.05$; Figure 4.6 A). Likewise, the titre of Boorn-mokiny 1 (MOI 0.01) was not significantly different compared to the control after treatment of AST154 for 6, 12, 18 or 24 hrs ($p>0.05$; Figure 4.6 A). The titre of Kara-mokiny 8 (MOI 0.01) was not significantly different to control after it was used to treat AST154 for 6, 12, 18 or 24 hrs ($p>0.05$; Figure 4.6 B). Treatment of AST154 for 6, 12 and 18 hrs with Kara-mokiny 13 (MOI of 0.01) did not significantly alter the phage's titre compared to the control ($p>0.05$; Figure 4.6 B). However, after its treatment for 24 hrs its titre was significantly reduced ($p<0.05$; Figure 4.6 B). Treatment of AST154 with Kara-mokiny 16 (MOI 0.01) did not result in significant differences in the phage titre after 6, 12, 18 or 24 hrs ($p>0.05$; Figure 4.6 B). A similar observation was for Boorn-mokiny 1 at the same MOI ($p>0.05$; Figure 4.6 B). In summary, phage titres remained largely unchanged following treatment of AST154 at both MOIs.

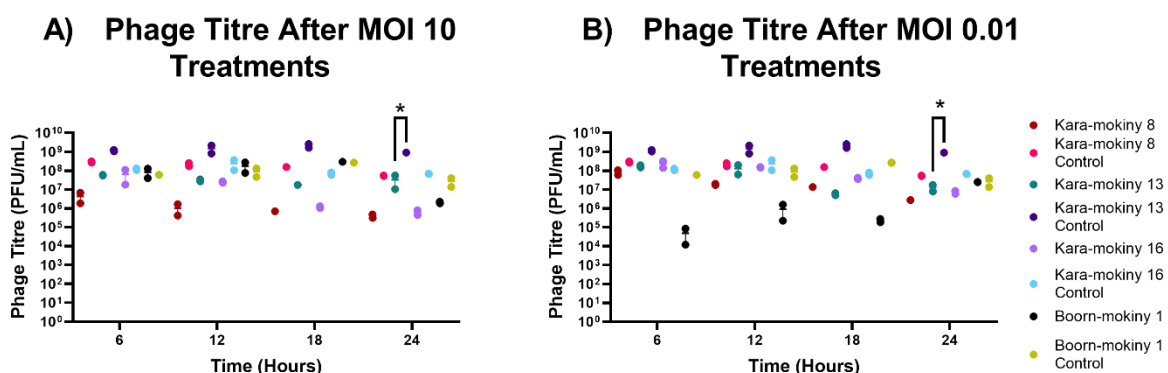


Figure 4.6 The Effects of Phage Treatment of AST154 on Phage Titre. Kara-mokiny 8, 13, 16 and Boorn-mokiny 1 were used to treat AST154 for 24 hrs at an MOI of 10 (A) or 0.01 (B) and phages were titrated every 6 hrs. Colours represent the phages used as the treatment as described in the legend. Each of the phage's titres was mostly not significantly different across the timepoints after treatment with an MOI of 10. There were many more phages' titres that were significantly increased after treatment of AST154 with an MOI of 0.01. Data is represented as median \pm IQR. *denotes statistically significant reductions and \wedge increase compared to control ($p<0.05$) as tested by RM 2-way ANOVA with Tukey's multiple comparison test.

4.3.5 Phage Treatment of the *P. aeruginosa* Clinical Isolate AST234

Phages at various MOIs (10, 1, 0.1 and 0.01) were used to treat *P. aeruginosa* isolate AST234 and effects on bacterial growth assessed over time by optical density at 600 nm (OD_{600nm}). For simplicity, only the highest and the lowest MOI (10 and 0.01) effects have been presented (Figure 4.7 A and C), however, all results have been supplied in the thesis appendices (Appendix Table E.5 and E.6). The AUCs of the OD_{600nm} plots following each phage's treatment were calculated and compared (Figure 4.7 A). Kara-mokiny 8 (MOI 10) treatment significantly reduced (93%) the AUC compared to the untreated control ($p < 0.05$; Figure 4.7 A). There were no significant differences between Kara-mokiny 8 and 13 treatments ($p > 0.05$; Figure 4.7 A), however, Kara-mokiny 8 significantly reduced the AUC compared to Kara-mokiny 16 and Boorn-mokiny 1 (74 and 88% respectively; $p < 0.05$; Figure 4.7 A). After 24 hrs of treatment, Kara-mokiny 13 (MOI 10) significantly reduced (86%) the AUC compared to the untreated control ($p < 0.05$; Figure 4.7 A). However, there was no differences seen between Kara-mokiny 13 and 16 treatments ($p > 0.05$; Figure 4.7 A). Additionally, Kara-mokiny 13 treatment (MOI 10) significantly reduced (76%) the AUC compared to Boorn-mokiny 1 ($p < 0.05$; Figure 4.7 A). Furthermore, Kara-mokiny 16 treatment of AST234 (MOI 10) significantly reduced the AUC compared to the untreated control and Boorn-mokiny 1 treatment (75 and 55% respectively; $p < 0.05$; Figure 4.7 A). Finally, Boorn-mokiny 1 treatment significantly reduced (43%) the AUC compared to the untreated control ($p < 0.05$; Figure 4.7 A). Overall, all phages had different effects on AST234 growth. Specifically, Boorn-mokiny 1 did not reduce AST234 growth, whereas the other three phages did with minimal re-growth observed.

Culturable AST234 was measured every six hrs during treatment with each of the phages at an MOI of 10 (Figure 4.7 B). Kara-mokiny 8 (MOI 10) did not impact culturable bacteria after 6 hrs ($p > 0.05$; Figure 4.7 B). However, after 12, 18 and 24 hrs, viable AST234 was significantly reduced when compared to the untreated control (2.2, 0.8 and 1.4 log-fold respectively; $p < 0.05$; Figure 4.7 B). After 6 hrs of treatment with Kara-mokiny 13 (MOI 10) there was not a significant decrease in viable AST234 ($p > 0.05$; Figure 4.7 B). However, after 12, 18 and 24 hrs of treatment significant reductions were seen compared to the control (1.2, 1.9 and 1.9 log-fold respectively; $p < 0.05$; Figure 4.7 B). Similarly, treatment of AST234 for 6 hrs with Kara-mokiny 16 (MOI 10) did not significantly impact viable bacteria compared to the untreated control ($p > 0.05$; Figure 4.7 B). After 12, 18 and 24 hrs, Kara-mokiny 16 treatment (MOI 10)

significantly reduced culturable AST234 compared to the control (1.3, 1.6 and 2.3 log-fold respectively; $p < 0.05$; Figure 4.7 B). Boorn-mokiny 1 (MOI 10) treatment of AST234 did not significantly decrease culturable bacteria after 6 hrs ($p > 0.05$; Figure 4.7 B). However, its treatment significantly reduced culturable AST234 after 12, 18 and 24 hrs compared to the control (0.2, 0.4 and 0.9 log-fold respectively; $p < 0.05$; Figure 4.7 B). To summarise, although all phages did not significantly reduce viable AST234 after 6 hrs, all were effective at reducing culturable AST234 at later time points tested.

Over the course of each of the phage's treatment (MOI 0.01) the OD_{600nm} of AST234 was measured, calculated, and compared (Figure 4.7 C). Treatment of AST234 with Kara-mokiny 8 resulted in a significant reduction in AUC compared to the untreated control (85%; $p < 0.05$; Figure 4.7 C). The difference in AUC between Kara-mokiny 8 and 13 (MOI 10) treatments of AST234 was not significant ($p > 0.05$; Figure 4.7 C). However, Kara-mokiny 8 treatment significantly reduced the AUC compared to Kara-mokiny 16 and Boorn-mokiny 1 (68% and 80% respectively; $p < 0.05$; Figure 4.7 C). Kara-mokiny 13 treatment (MOI 10) significantly reduced the AUC compared to the untreated control (64%; $p < 0.05$; Figure 4.7 C). However, it did not differ to AUC Kara-mokiny 16 treatment ($p > 0.05$; Figure 4.7 C). Compared to Boorn-mokiny 1 treatment, Kara-mokiny 13 (MOI 10) resulted in a significantly reduced AUC (55%; $p < 0.05$; Figure 4.7 C). After 24 hrs of treatment, Kara-mokiny 16 significantly reduced (51%) the AUC compared to the control ($p < 0.05$; Figure 4.7 C). It also resulted in a significant reduction (38%) in AUC compared to Boorn-mokiny 1 ($p < 0.05$; Figure 4.7 C). Finally, Boorn-mokiny (MOI 10) resulted in a significant reduction (21%) in the AUC compared to the untreated control ($p < 0.05$; Figure 4.7 C). To conclude, Boorn-mokiny 1 did not reduce AST234 growth, however the other phages significantly reduced bacterial growth, with minimal regrowth observed at 24 hrs.

Viable AST234 was enumerated every 6 hrs during treatment with each of the phages at an MOI of 0.01 (Figure 4.7 D). Treatment with Kara-mokiny 8 for 6 hrs did not significantly change the amount of culturable AST234 compared to the untreated control ($p > 0.05$; Figure 4.7 D). However, at 12, 18 and 24 hrs, treatment caused significant reductions in viable bacteria (2.6, 2.72 and 2.75 log-fold respectively; $p < 0.05$; Figure 4.7 D). Likewise, treatment with Kara-mokiny 13 (MOI 0.01) did not significantly reduce viable bacteria ($p > 0.05$; Figure 4.7 D), but was significant after 12, 18 and 24 hrs compared to the untreated control (1.1, 2.4 and 3 log-fold respectively; $p < 0.05$; Figure 4.7 D). Kara-mokiny 16 treatment (MOI 0.01) also did not

significantly affect viable AST234 after 6 hrs ($p>0.05$; Figure 4.7 D), but was significant after 12, 18 and 24 hrs of treatment (2.1, 2.4 and 2.5 log-fold respectively; $p<0.05$; Figure 4.7 D). Boorn-mokiny 1 treatment for 6 hrs did not significantly affect culturable AST234 ($p>0.05$; Figure 4.7 D). After 12 hrs viable AST234 was significantly increased (0.45 log-fold) following Boorn-mokiny 1 (MOI 0.01) treatment compared to the untreated control ($p<0.05$; Figure 4.7 D). Interestingly, Boorn-mokiny 1 treatment went on to significantly reduce viable AST234 after 18 and 24 hrs of treatment (0.4 and 0.9 log-fold respectively; $p<0.05$; Figure 4.7 D). Overall, AST234 was not affected by phage treatment up to 6 hrs but amounts significantly impacted culturable bacteria at all following time points.

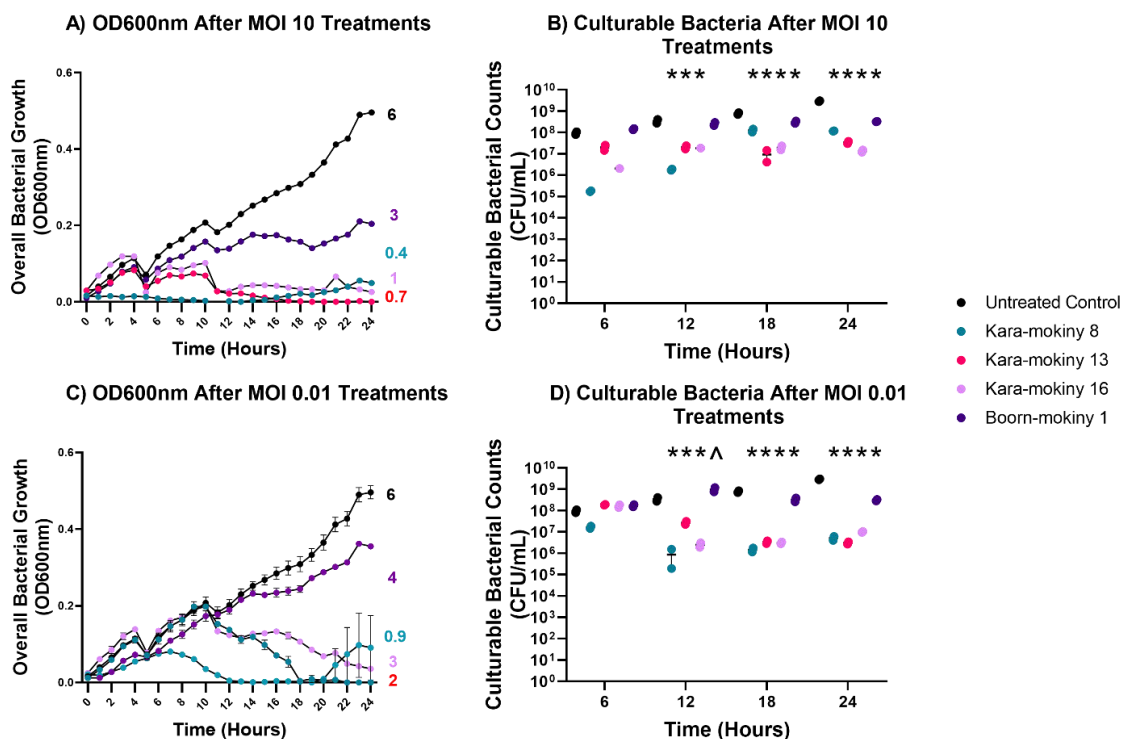


Figure 4.7 The Effects of Phage Treatment on AST234 Growth (OD600nm) and Culturable Bacteria. Kara-mokiny 8, 13, 16 and Boorn-mokiny 1 were used to treat AST234 for 24 hrs at an MOI of 10 (A and B) or 0.01 (C and D) and OD600nm (A and C) or CFU/mL (B and D) measured every 6 hrs. Colours represent the phages used as the treatment as described in the legend. Different effects of phage treatment were observed depending on the phage and the MOI that was used. Duplicate values are represented as median±range. The OD600nm AUCs of each treatment (rounded to the whole number) are listed beside their 24-hour timepoint and are in the same colour as denoted in the legend. Each treatment's AUCs were compared using a 1-way with Tukey's multiple comparison test. The CFU/mL data was compared with a RM 2-way ANOVA with Tukey's multiple comparisons. A $p<0.05$ was considered significant.

Each of the phage's titre was enumerated over the course of treating AST234 (Figure 4.8 A and B). Treatment of AST234 with Kara-mokiny 8 (MOI 10) resulted in a significant reduction in the phage's titre compared to the control after 6, 12, 18 and 24 hrs ($p < 0.05$; Figure 4.8 A). Kara-mokiny 13 (MOI 10) treatment did not result in significant change in phage titre after 6 hrs ($p > 0.05$; Figure 4.8 A), however, was significantly increased compared to control after 12 hrs ($p < 0.05$; Figure 4.8 A). At the subsequent timepoints (18 and 24 hrs) the titre of Kara-mokiny 13 was not significantly different compared to the control ($p > 0.05$; Figure 4.8 A). Kara-mokiny 16 titres were significantly reduced compared to the control after 6 hrs of treatment ($p < 0.05$; Figure 4.8 A) but did not significantly differ compared to the control after 12 hrs ($p > 0.05$; Figure 4.8 A). After treatment for 18 hrs (MOI 10), the titre of Kara-mokiny 16 was significantly increased ($p < 0.05$; Figure 4.8 A) but was significantly reduced compared to the control after 24 hrs of treatment ($p < 0.05$; Figure 4.8 A). The titre of Boorn-mokiny 1 was not significantly different compared to the control after it was used to treat AST234 at an MOI of 10 for 6, 12 or 18 hrs ($p > 0.05$; Figure 4.8 A). However, its titre was significantly increased after 24 hrs treatment ($p < 0.05$; Figure 4.8 A). Titres of Kara-mokiny 8 (MOI 0.01) were not significantly different compared to the control after 6 or 12 hrs of treatment ($p > 0.05$; Figure 4.8 B), became significant after 18 hrs ($p < 0.05$) before becoming non-significant after 24 hrs ($p > 0.05$; Figure 4.8 B). Titres of Kara-mokiny 13 (MOI 0.01) was not significantly different compared to the control at 6, 12, 18 or 24 hrs of treatment ($p > 0.05$; Figure 4.8 B). Finally, after treatment of AST234 for 6 and 12 hrs at an MOI of 0.01 the titre of Boorn-mokiny 1 did not significantly differ compared to the control ($p > 0.05$; Figure 4.8 B). However, after 18 and 24 hrs, its titre was significantly reduced compared to its control ($p < 0.05$; Figure 4.8 B). Collectively, there was no common trend in phages titres after treating AST234 at either MOI.

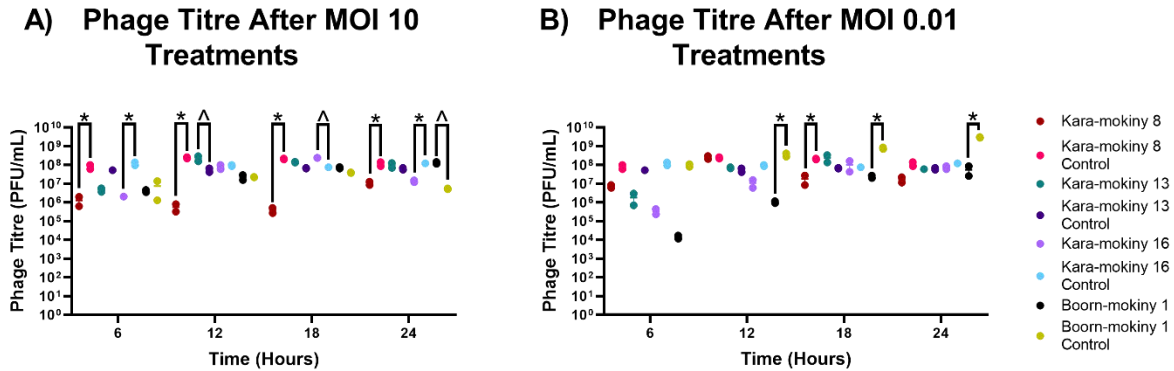


Figure 4.8 The Effects of Phage Treatment of AST234 on Phage Titre. Kara-mokiny 8, 13, 16 and Boorn-mokiny 1 were used to treat AST234 for 24 hrs at an MOI of 10 (A) or 0.01 (B) and phages were titrated every 6 hrs. Colours represent the phages used as the treatment as described in the legend. Each of the phage's titres was mostly not significantly different across the timepoints after treatment with an MOI of 10. There were many more phages' titres that were significantly increased after treatment of AST234 with an MOI of 0.01. Data is represented as median±IQR. *denotes statistically significant reductions and ^ increase compared to control ($p < 0.05$) as tested by RM 2-way ANOVA.

4.3.6 Frequency of Phage Resistance After Phage Treatment

Ten random colonies were selected, and subculture purified from each phage treatment and their resistance to the phage used to treat them determined (Table 4.4). Bacteria were then classified as either resistant, intermediately susceptible, or resistant and this was stratified according to the *P. aeruginosa* isolate they were derived from, the MOI and phage they were treated with (Table 4.4). Results generated showed that the number of MIC79-derived phage resistant mutants were significantly different to those derived from AST154 and AST234 ($p < 0.05$; Table 4.4). The number of AST154-derived phage resistant mutants was significantly different to the number derived from AST234 ($p < 0.05$; Table 4.4). The number of phage resistant mutants after treatment at MOIs of 10 were significantly different to the amount after treatment at an MOI of 0.1 ($p < 0.05$; Table 4.4). The number of phage resistant mutants were significantly different after treatments with MOIs 0.1 and 0.01 ($p < 0.05$; Table 4.4). The difference in the amount of phage resistant *P. aeruginosa* isolated was significant between those from Kara-mokiny 8 and 16 treatments ($p < 0.05$; Table 4.4). The amount of phage resistant *P. aeruginosa* isolated was significantly different between Kara-mokiny 8 and Boorn-mokiny 1 treatment ($p < 0.05$; Table 4.4). The Number of phage resistant *P. aeruginosa* isolated significantly differed between Kara-mokiny 13 and 16 treatments ($p < 0.05$; Table 4.4). The amount of phage resistant *P. aeruginosa* following Kara-mokiny 13 and Boorn-mokiny 1 treatment was significantly different ($p < 0.05$; Table 4.4). Furthermore, there was significantly

more phage-resistant mutants isolated after Kara-mokiny 16 treatment compared to Boorn-mokiny 1 ($p < 0.05$; Table 4.4). For subsequent sequencing of the phage-resistant mutants, 52 were selected across the three isolates that had been treated by the phages at an MOI of 10 or 0.01 as any effect of phage dosage on resistance would be expected to be most visible in the highest and lowest MOI. These were further subset based on diversity which was inferred through colony morphologies and phage susceptibilities (refer to Appendix Table F.1). Overall, AST154 had the highest proportion of resistant colonies isolated following treatment with any phage. Furthermore, few differences in the frequency of resistant bacteria isolated after treatments with the different MOIs (10-0.01) were found, indicating it may have limited influence on the evolution of phage resistance. Finally, of the phages (Kara-mokiny 8, 13 and 16) that could infect all three *P. aeruginosa* isolates, Kara-mokiny 16 induced significantly fewer resistant bacteria, highlighting its potential.

Table 4.4 Frequency of Resistance to Treating Phages in Surviving Bacteria

	No. (%) Susceptible ($1 \geq EOP \geq 0.1$)	No. (%) Intermediate ($0.1 > EOP > 0$)	No. (%) Resistant ($EOP = 0$)	Significance
Frequency by Isolate				
MIC79 (n=160)	36 (22.5)	20 (12.5)	104 (65)	* * *
AST154 (n=120 [#])	9 (7.5)	16 (13.33)	95 (79.16)	
AST234 (n=160)	71 (44.375)	15 (9.375)	74 (46.25)	
Frequency by MOI				
MOI 10 (n=110 [#])	36 (32.72)	9 (8.18)	65 (59.09)	* *
MOI 1 (n=110 [#])	28 (25.45)	16 (14.54)	66 (60)	
MOI 0.1 (n=110 [#])	19 (17.27)	17 (15.45)	74 (67.27)	
MOI 0.01 (n=110 [#])	33 (30)	9 (8.18)	68 (61.81)	
Frequency by Phage				
Kara-mokiny 8 (n=120)	16 (13.33)	11 (9.16)	93 (77.5)	* * * *
Kara-mokiny 13 (n=120)	14 (11.66)	6 (5)	100 (83.33)	
Kara-mokiny 16 (n=120)	12 (10)	34 (28.33)	74 (61.66)	
Boorn-mokiny 1 (n=80 [#])	74 (92.25)	0 (0)	6 (7.5)	

Note: MOI: multiplicity infection. [#] denotes where Boorn-mokiny 1 treated AST154 mutants were omitted from analysis as this isolate began resistant and all results were consistent with it remaining resistant. * denotes statistically significant reductions compared to control ($p < 0.05$) as tested by multiple t-test.

4.3.7 Mechanisms of Phage Resistance in *P. aeruginosa* Isolate M1C79

Since CRISPR-cas arrays were identified in the M1C79 genome, their contribution to phage resistance was investigated further by searching for phage targeting spacer sequences that belonged to the four phages used as treatments. Results generated showed that the same 20 spacers were predicted in both the control and mutant M1C79 genomes and the combined p-values were greater than 0.05 (Appendix Table G.1). Therefore, it was deemed unlikely that this was playing a role in phage resistance. Next, genomes of phage treated mutants were compared to the WT and control bacteria to identify any mutation/s that could confer phage resistance. Genomes of M1C79 phage treated bacteria were compared to the WT and control to find mutations that cause phage resistance. Mutations were removed if observed in the M1C79 control or WT or phage treated survivors that were still susceptible to phage infection. The mutations were then grouped based on the COGs classification of the gene they altered [539]. Analysis of M1C79-derived mutants following phage treatment identified 18 loci across the isolate's genome that were mutated (Appendix Table H.1), four were deletions, three were single nucleotide polymorphisms (SNPs) and four were insertions (Appendix Table H.1). The M1C79-derived mutants had mutations in genes involved in signal transduction mechanisms, cell motility, carbohydrate transport and metabolism, cell wall/membrane/envelope biogenesis and unknown function (Figure 4.9). All but one resistant mutant driven by Kara-mokiny phages' treatment, regardless of MOI, had mutations in genes involved in cell wall/membrane/envelope biogenesis (Figure 4.9). These mutations were all in the same *rfaB* gene that is a glycosyltransferase involved in cell wall biosynthesis (Figure 4.9). Interestingly, six out of the eight mutants with an altered *rfaB* had the same 207 bp deletion despite being derived from different Kara-mokiny phage treatment, indicating a conserved response (Figure 4.9). The final resistant mutant was the only M1C79-derived isolate sequenced that had multiple mutations after phage treatment (Figure 4.9). These mutations were in signal transduction mechanisms and carbohydrate transport and metabolism (Figure 4.9). Interestingly, two intermediately susceptible mutants also had mutations in the *rfaB* gene (Figure 4.9). A further two intermediately susceptible mutants derived from Kara-mokiny phages' treatments had mutations in *wzy* which is an O-antigen polysaccharide polymerase (Figure 4.9). The final intermediately susceptible mutant derived from Kara-mokiny phage treatment had a mutation in *wapR* which was classified as affecting cell motility, however, as an alpha-1,3-rhamnosyltransferase this could function in LPS biosynthesis (Figure 4.9).

The two intermediately susceptible mutants derived from Boorn-mokiny 1 treatment had mutations in genes affecting cell motility (Figure 4.9). These were both in flagella components and common between the two was alteration of *fliG*. However, one of the mutants had a large deletion that additionally disrupted *fliF*.

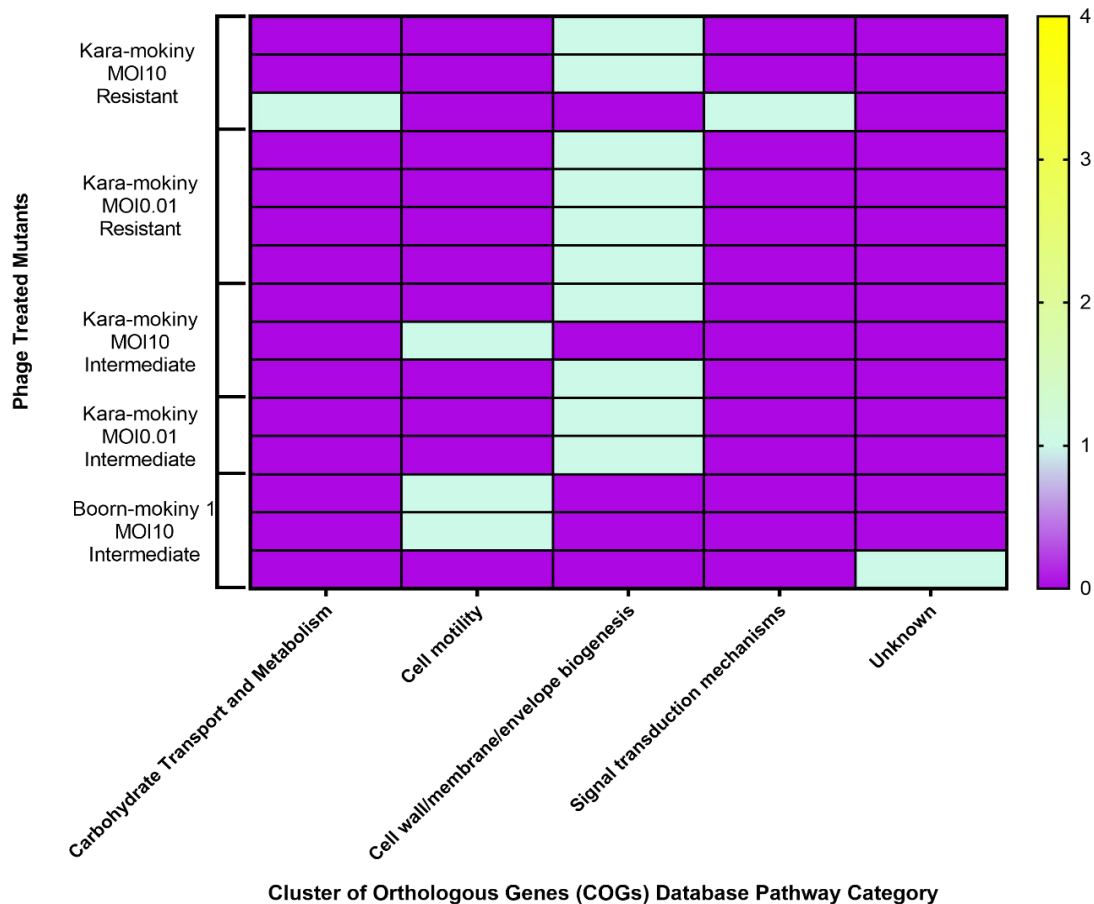
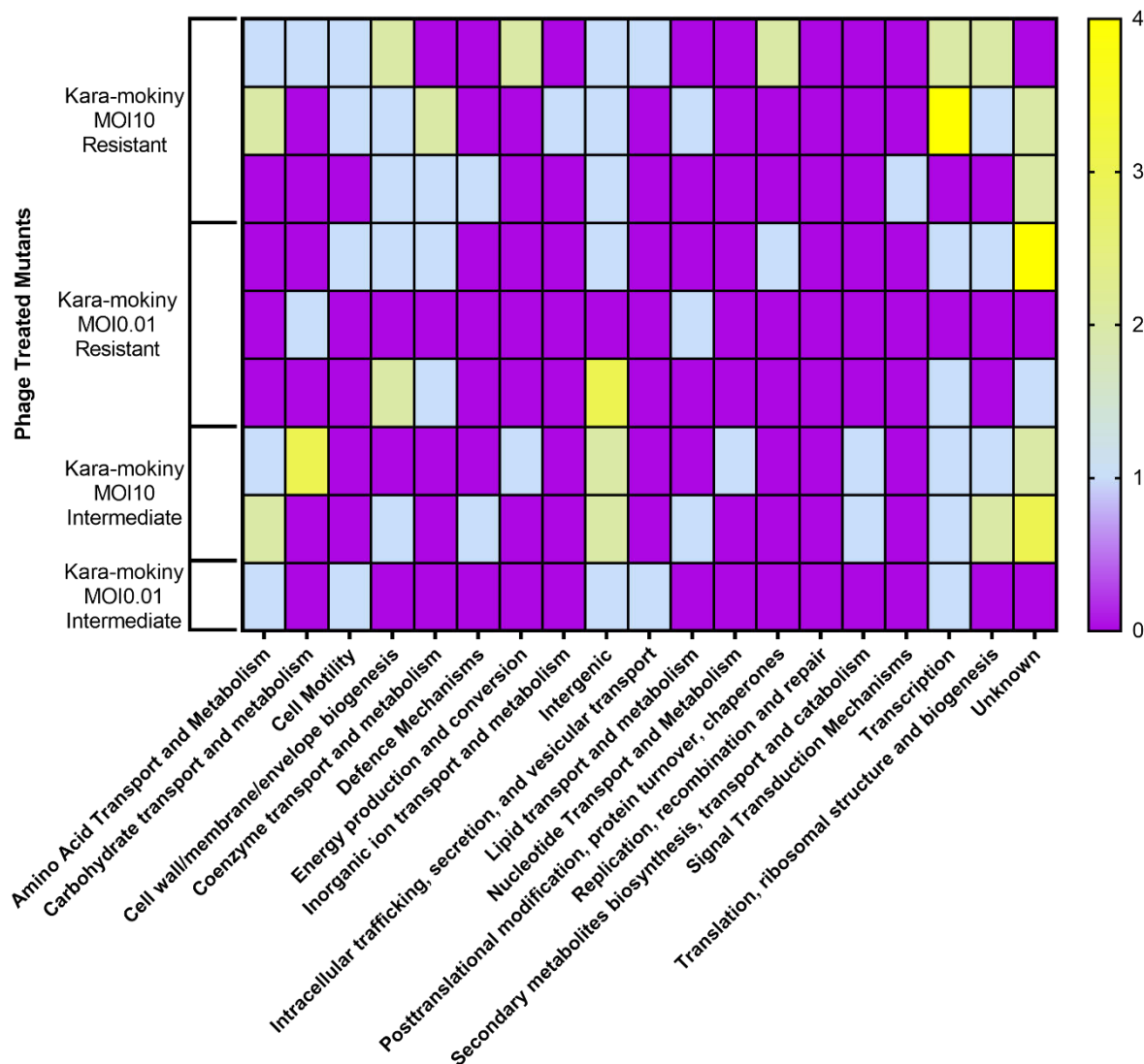


Figure 4.9 Mutations Identified in M1C79-Derived Mutants Surviving Phage Treatment. M1C79 was treated with the phages Kara-mokiny 8, 13, 16 and Boorn-mokiny 1 for 24 hrs before surviving bacteria were isolated and sequenced. Mutations in resistant bacteria were identified by mapping the mutants' reads to the WT. Mutations were filtered out if they were present in any *P. aeruginosa* susceptible to the phage such as the WT, control or susceptible treatment survivors. Mutations were then grouped based on the pathway that the gene they affected functioned in. Colours represent the number of mutations in the genes of that pathway.

4.3.8 Mechanisms of Phage Resistance in *P. aeruginosa* Isolate AST154

The genomes of AST154 phage treated bacteria were compared to the WT and control to find mutations that cause phage resistance. Boorn-mokiny 1 treated AST154 mutants were excluded from analysis since the isolate was resistant to the phage before and after treatment. Mutations were removed if observed in the AST154 control or WT or phage treated survivors that were still susceptible to phage infection. The mutations were then grouped based on the COGs classification of the gene they altered. Mutations across 103 different genomic loci were identified (Appendix Table H.2). Of these 10 were deletions, 76 were single nucleotide polymorphisms (SNPs) and 16 were insertions (Appendix Table H.2). Analysis identified 19 COG pathways affected by mutations in response to the phages' infections (Figure 4.10). Unlike, M1C79, AST154-derived mutants that were phage resistant or exhibited intermediate susceptibility to phage treatment each carried multiple mutations (Figure 4.10). The AST154-derived mutants had between 2 and 16 different mutations each (Figure 4.10). There did not seem to be a correlation between the number, type or pathways affected and the phage that was resisted (Figure 4.10). The most common type of mutation was intergenic variants whose impact is harder to discern (Figure 4.10). Most mutants also had mutations in genes encoding predicted proteins with unknown function (Figure 4.10). There were between 5 and 9 mutations observed across the different mutants in genes involved in transcription, amino acid transport and metabolism, translation, ribosomal structure and biogenesis, carbohydrate transport and metabolism, cell motility, post translation modification, protein turnover and chaperones, co-enzyme transport and metabolism and cell wall, membrane and envelope biogenesis (Figure 4.10). Interestingly, similar to M1C79-derived mutants *rfaB* was mutated in 6 mutants evolved from AST154. This includes all 5 sequenced mutants that were completely resistant to their respective treating phage's infection.

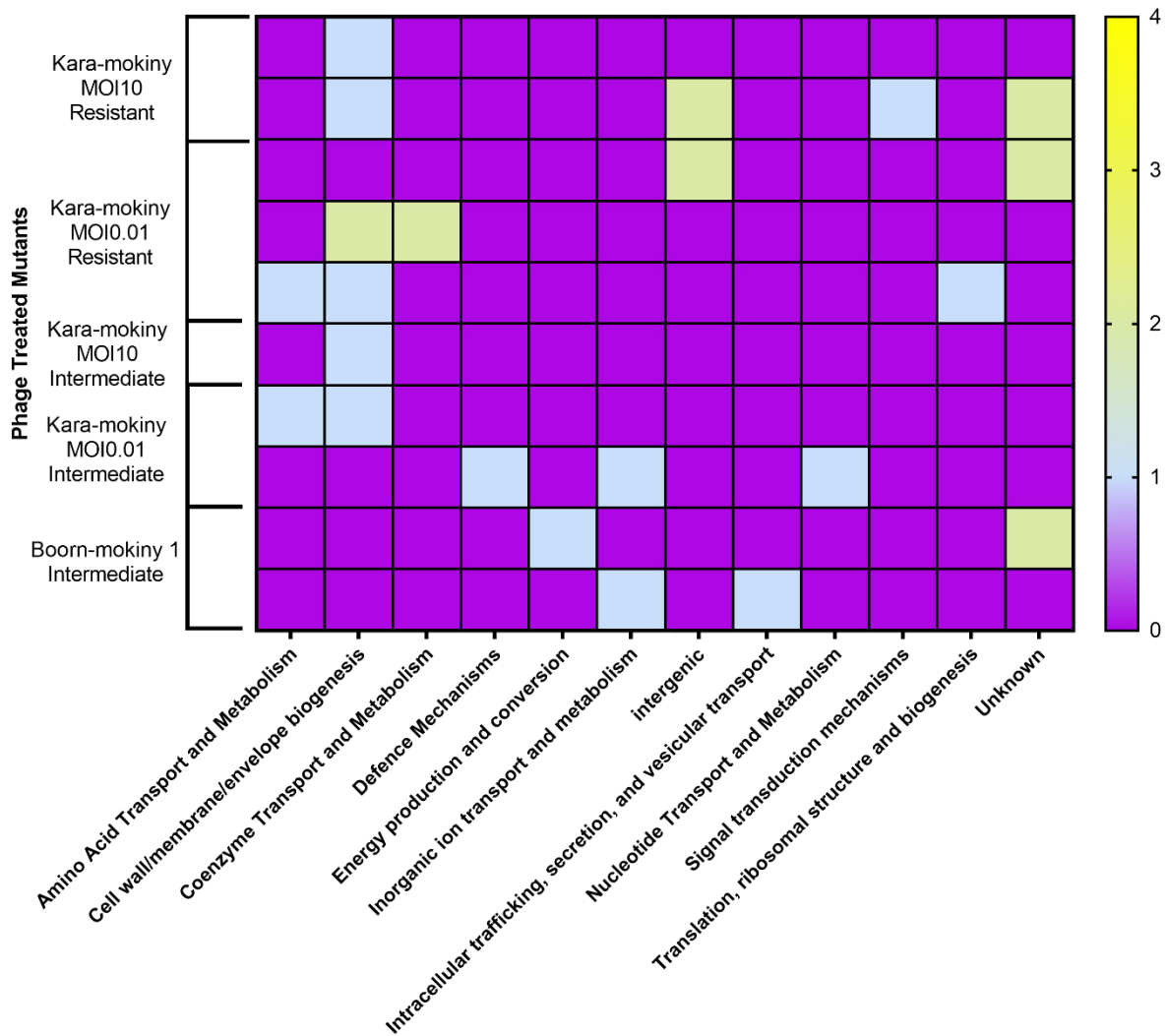


Cluster of Orthologous Genes (COGs) Database Pathway Category

Figure 4.10 Mutations identified in AST154-derived mutants surviving phage treatment. AST154 was exposed with singular phages (Kara-mokiny 8, 13, 16 and Boorn-mokiny 1) for 24 hrs before surviving bacteria were isolated and sequenced. Mutations in resistant bacteria were identified by mapping the mutants' reads to the WT. Mutations were filtered out if they were present in any *P. aeruginosa* susceptible to the phage such as the WT, control or susceptible treatment survivors. Mutations were then grouped based on the pathway that the gene they affected functioned in. Colours represent the number of mutations in the genes of that pathway.

4.3.9 Mechanisms of Phage Resistance in *P. aeruginosa* Isolate AST234

The genomes of AST234 phage treated bacteria were compared to the WT and control to find mutations that cause phage resistance. Mutations were removed if observed in the AST234 control or WT or phage treated survivors that were still susceptible to phage infection. The mutations were then grouped based on the COGs classification of the gene they altered [539]. Mutations were identified at 29 different loci across the AST234 genome (Appendix Table H.3). There were 22 SNPs, 3 deletions and 4 insertions identified (Appendix Table H.3). Analysis identified 12 pathways affected by mutations in the phage resistant mutants (Figure 4.11). Similar to AST154, AST234-derived mutants frequently (8/10) had multiple (2-6) mutations (Figure 4.11). Regardless of MOI the most common pathway affected in 6/10 AST234-derived mutants was cell (Figure 4.11). Apart from one mutation, all others in wall/membrane/envelope biogenesis, were specifically in the *rfaB* gene (Figure 4.11). The other mutation of the cell wall/membrane/envelope biogenesis pathway was in *galU*. Like AST154, in intergenic and unknown gene mutations were also frequent (Figure 4.11). Mutations affecting amino acid transport and metabolism, coenzyme transport and metabolism, inorganic ion transport and metabolism, intracellular trafficking, secretion, and vesicular transport, nucleotide transport and metabolism, signal transduction mechanisms, translation, ribosomal structure and biogenesis, energy production and conversion and defence mechanisms were also identified, although these only affected one to two mutants each (Figure 4.11).



Cluster of Orthologous Genes (COGs) Database Pathway Category

4.11 Mutations Identified in AST234-Derived Mutants Surviving Phage Treatment. AST234 was treated with the phages Kara-mokiny 8, 13, 16 and Boorn-mokiny 1 for 24 hrs before surviving bacteria were isolated and sequenced. Mutations that may be causing resistance were identified by mapping the mutants' reads to the WT. Mutations were filtered out if they were present in any *P. aeruginosa* susceptible to the phage such as the WT, control or susceptible treatment survivors. Mutations were then grouped based on the pathway that the gene they affected functioned in. The colours represent the number of mutations in the genes of that pathway

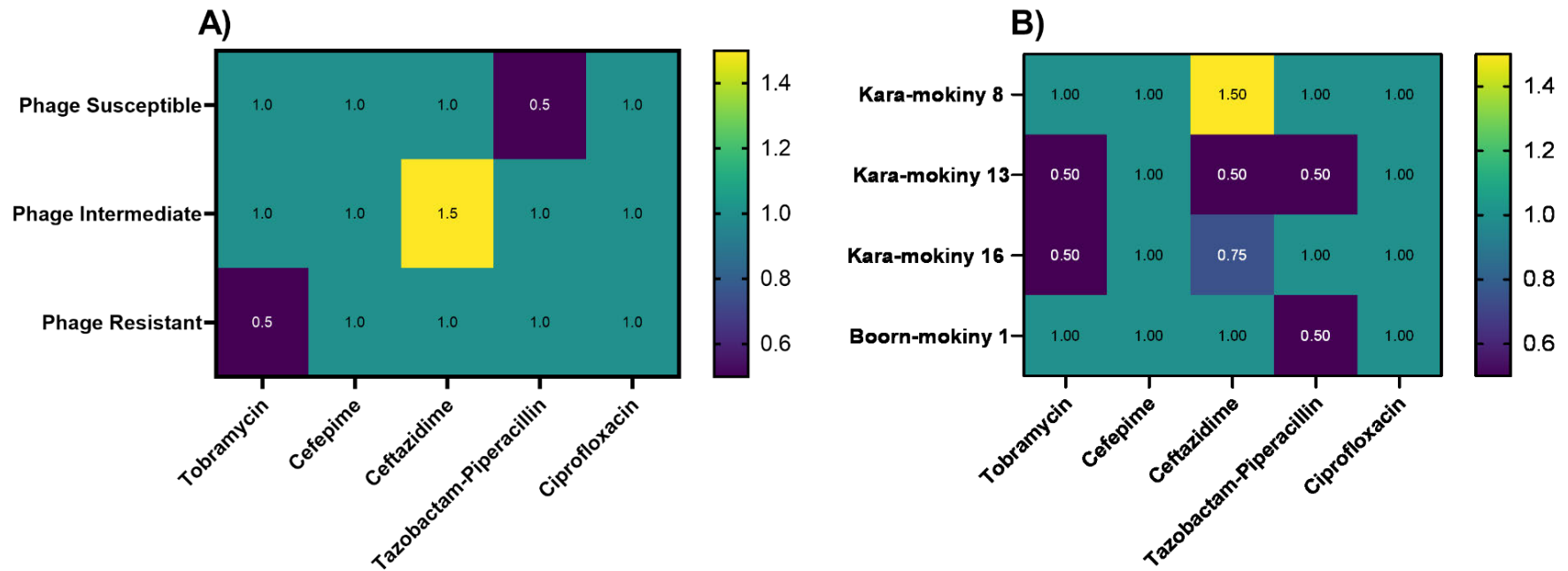


Figure 4.12 Fold-Change in Antibiotic Minimum Inhibitory (MIC) Concentrations in *P. aeruginosa* Surviving Phage Treatment. The phage treated mutants' susceptibilities to tobramycin, cefepime, ceftazidime, tazobactam-piperacillin and ciprofloxacin was determined by the broth microdilution method. Average fold-change of the antibiotic MICs relative to the mutants WT were stratified by **(A)** whether they were still susceptible, intermediate, or resistant to phages and **(B)** by what phage treatment the bacteria had survived. Phage resistant mutants had a 0.5-fold MIC to tobramycin, intermediately susceptible had a 1.5-fold MIC to ceftazidime and phage susceptible mutants had a 0.5-fold MIC to tazobactam-piperacillin. Furthermore, mutants treated with Kara-mokiny 8 had a 1.5-fold MIC to ceftazidime, those surviving Kara-mokiny 13 treatment had 0.5-fold MICs to tobramycin, ceftazidime and tazobactam-piperacillin, those treated with Kara-mokiny 16 had a 0.5-fold MIC to tobramycin and 0.75-fold MIC to ceftazidime and those treated with Boorn-mokiny 1 had a 0.5-fold MIC to tazobactam-piperacillin.

4.3.10 Antibiotic Susceptibility After Phage Treatment

Susceptibility of the *P. aeruginosa* that survived phage treatment was tested for five antibiotics commonly used to treat people with CF with this type of infection [541]. When the fold-change in antibiotic MIC was stratified by whether the surviving *P. aeruginosa* was still susceptible, intermediately susceptible, or completely resistant to the phage treatment, for the majority there was no change in antibiotic MIC (1.0-fold; Figure 4.12 A). In *P. aeruginosa* isolated after phage treatment that were still susceptible to phage therapy, the MIC to tazobactam-piperacillin was decreased (0.5-fold; Figure 4.12 A). Furthermore, intermediately susceptible *P. aeruginosa* had an elevated MIC to ceftazidime (1.5-fold; Figure 4.12 A). Phage-resistant *P. aeruginosa* isolated after treatment had a 0.5-fold MIC to tobramycin (Figure 4.12 A). When fold-changes in antibiotic MIC were stratified according to what phages the isolated bacteria were treated with, the majority were found to be unchanged (1.0-fold; Figure 4.12 B). Ceftazidime MIC of Kara-mokiny 8 treated *P. aeruginosa* increased by 1.5-fold (Figure 4.12 B). The MIC for tobramycin, ceftazidime and tazobactam-piperacillin following Kara-mokiny 13 treatment were reduced (0.5-fold; Figure 4.12 B). Kara-mokiny 16 treatment decreased *P. aeruginosa* MIC to tobramycin by 0.5-fold and ceftazidime 0.75-fold (Figure 4.12 B). Finally, Boorn-mokiny 1 treatment decreased the tazobactam-piperacillin MIC in *P. aeruginosa* by 0.5-fold (Figure 4.12 B).

4.4 Discussion

In this Chapter, the evolution of phage resistance in CF isolates of *P. aeruginosa*, the factors influencing its development and the associated fitness costs were tested. Three distinct *P. aeruginosa* isolates were treated with four diverse phages and kinetics monitored over 24 hrs. Treatment effectiveness differed between bacterial isolates and phages used. Phage dosage had limited effect on treatment kinetics. Despite often being significantly decreased compared to control after 24 hrs, bacteria were still recoverable. Randomly selected and purified colonies were tested for resistance to the phage used to treat them and it was observed that there were colonies still susceptible, intermediately susceptible, and completely resistant to treatment. The proportion of resistant colonies appeared affected by bacterial background and the phage that was used to treat it, however, was not affected by phage treatment dosage. Based on colony morphology and resistance, a subset of bacteria was selected, sequenced and analysed. Even though isolate

M1C79 had a CRISPR-cas system there was no bioinformatic evidence that this was involved in resistance to phages tested here. M1C79 resistance to Kara-mokiny 8, 13 and 16 appeared to be mediated via mutations that altered genes involved in cell wall/membrane/envelope biogenesis which could affect their attachment to bacterial cells. M1C79 appeared to become resistant to Boorn-mokiny 1 infection via mutation of a flagella component specifically *fliG*, as this was only found in resistant mutants. *P. aeruginosa* isolates. AST154 and 234 also evolved resistance to Kara-mokiny 8, 13 and 16 by evolving mutations in genes that also affected cell wall/membrane/envelope biogenesis. However, other mutations affecting transcription, translation, ribosomal structure and biogenesis, posttranslational modification, protein turnover and chaperones, amino acid transport and metabolism, carbohydrate transport and metabolism, cell motility and co-enzyme transport and metabolism. Of significance, some strains with resistance to Kara-mokiny 13 and 16 exhibited a reduction in tobramycin MIC. Collectively, data generated showed that evolution of resistance to the phages was varied greatly between CF *P. aeruginosa* isolates and was not largely affected by MOI of phage used. Furthermore, tobramycin combination with the phages could potentially limit the amount of resistance evolving and be a more effective treatment.

The genomic background of *P. aeruginosa* has been found to be an important factor driving the evolution of the phage resistance [308, 379]. To investigate how diversity in CF clinical isolates may affect phage resistance, three *P. aeruginosa* that were genomically and phenotypically distinct, were chosen and subsequently analysed. Phage treatment was much more efficient in the *P. aeruginosa* isolate derived from a child with CF (M1C79), however once resistance manifested, mutants were able to grow to similar levels as controls. In contrast, phage treatment of *P. aeruginosa* isolates derived from adults with CF, (AST154 and 234), seemed to take longer but reductions in bacteria were more prolonged. This could be due to the fact that chronic CF isolates of *P. aeruginosa* commonly have many mutations and a reduced growth rate which may reduce phage replication efficiency [154, 155, 535-537]. Fewer, resistant colonies were isolated following phage treatment of M1C79 which contrasts with previous findings that intermittent CF *P. aeruginosa* isolates evolve more resistance [542]. When assessed at the genomic level the childhood isolate M1C79, this strain had comparably fewer mutations and these were limited to genes that control receptor biosynthesis. The adult isolates AST154 and AST234, especially the former, had more mutations that were only in resistant mutants and not observed in susceptible phage-treated bacteria. AST154

appears to be a hypermutator that are commonly found in CF chronic isolates of *P. aeruginosa* [517]. The *mutL* DNA mismatch repair gene is a common cause of hypermutation and AST154 and 234 had different alleles of this gene [543]. The alterations in hypermutable isolates increase their mutation rate which is advantageous when faced with the selection pressures presented by the CF airways, including antibiotics [543, 544]. Future work should identify hypermutator *P. aeruginosa* and expose them to phages and antibiotics to identify if the increased mutation rates correlate with greater phage-resistance [543, 545-547]. Mutations observed in both the AST154 and AST234 isolates were associated with phage receptors, transcription, translation, metal ion acquisition and the cell surface more broadly. These could be more general changes that reduce phage replication efficiency, via altering protein synthesis [251, 253, 397, 548-550], oxidative stress responses [253], energy metabolism [251, 253], the cell surface to prevent attachment [252, 308, 379, 397, 550, 551] and the starvation of phages' of ions important for their structure [552, 553].

Phage dosage (specifically MOI) has been observed to influence the type of phage resistance that bacteria evolve [349]. Namely, lower MOI has been associated with CRISPR-cas resistance in a laboratory reference *P. aeruginosa* strain [349]. Work conducted in this chapter did not find any evidence of this, despite M1C79 having a CRISPR-cas system, it did not drive resistance even at the lowest MOI tested. Interestingly, all studies into *P. aeruginosa* CRISPR-cas have used the PA14 reference strain which behaves differently to clinical isolates [347-350]. Additionally, annotation of a CRISPR-cas system does not mean it is functional. Confirmation of the functionality of the CRISPR-cas system in M1C79 could be achieved by cloning a phage DNA sequence into the *P. aeruginosa* CRISPR spacer region and testing to see if it could then be used to resist the phage's infection [348]. Results generated showed that at both the highest and lowest phage MOIs tested (10 and 0.01), M1C79 favoured receptor altering mutations for both LPS and flagella targeting phages. Although, AST154 and 234 did not have CRISPR-cas systems, resistance to both phage MOIs was similar and in both cases favoured mutations of the phages' receptors. In fact, phage MOI overall had surprisingly little effect on treatment including its kinetics and proportion of resistance evolving to it. However, treatment kinetics were prone to the effect of variability due to only being performed in duplicate. Yet, this further highlights the need to study CRISPR-cas resistance in clinical isolates of *P. aeruginosa*.

The most important phage factor identified in this chapter influencing the evolution of resistance was the receptor that they used. Despite Kara-mokiny 8, 13 and 16 being genetically distinct, the bacterial genes that were mutated in response to their treatment were similar. This is in line with what has been found previously, where the bacterial response to distinct phages targeting the same receptor was in similar genes [379]. Mostly, the genes that were mutated were not shared across the different *P. aeruginosa* phage-resistant mutants. However, when the genes were classified according to their COGs categories there were some commonly altered pathways identified. These included cell wall/membrane/envelope biogenesis for Kara-mokiny phages and cell motility for Boorn-mokiny 1. This likely altered LPS which acts as the Kara-mokiny phages' receptor and prevented their binding. Likewise, the flagella functions in cell motility and is the receptor for Boorn-mokiny 1, so its alteration probably affected phage attachment. Other pathways commonly mutated included amino acid transport and metabolism, carbohydrate transport and metabolism, co-enzyme transport and metabolism, defence mechanisms, energy production and conversion, inorganic ion transport and metabolism, intracellular trafficking, secretion, and vesicular transport, nucleotide transport and metabolism, signal transduction mechanisms and translation, ribosomal structure and biogenesis. These likely represent more generalised phage resistance mechanisms that affect other stages of the phage lifecycle and reduce the efficiency of replication rather than prevent infection outright. The importance of generalised phage resistance mechanisms similar to what was found in this chapter is being realised more frequently [308]. Additionally, the growing number of transcriptomic studies of phage infection are elucidating the genes that are important for phage infection beyond the receptor binding stage [250, 251, 554]. These include genes involved in Energy production and conversion, Coenzyme transport and metabolism, amino acid transport and metabolism, transcription and translational, ribosomal structure and biogenesis [250, 251, 554]. Therefore, if these pathways are required during phage infection, it does support that the mutations in the genes found in this chapter could hinder viral replication. However, this would need to be validated by targeted mutation of these genes to see if they alone do impact phage resistance and whether subsequent complementation re-sensitises the bacteria to infection [327].

A gene that was mutated across all three *P. aeruginosa* isolates and was common amongst those that had become resistant to the Kara-mokiny phages was *rfaB*. This gene encodes a protein that was annotated as a glycosyltransferase involved in cell wall

biosynthesis. In future studies, clean *rfaB* knockout mutants paired with genetic complementation would be needed to confirm if the mutations observed in this thesis were sufficient to cause resistance alone. Previously, *rfaB* mutations were identified in clinical *P. aeruginosa* isolates that had evolved resistance to phage infection [516]. These authors observed a truncated LPS banding pattern in the *rfaB* mutants and concluded that this gene was necessary for proper LPS formation and its mutation prevented their phages binding to the bacteria [516]. Interestingly, studies of phage-resistant *P. aeruginosa* that have used PAO1 typically identify that the mutation that causes resistance is in *galU* and it is usually through a large (>200kbp) deletion [275, 326, 327, 330, 496, 555]. This gene was only mutated in one phage-resistant mutant in work here and large deletions were rare in our experiments. These differences between clinical *P. aeruginosa* responses to phage therapy and PAO1 highlight the importance of studying phage resistance in relevant isolates. As Boorn-mokiny 1 uses a different receptor, the mutations that its treatment induced differed to those elicited by Kara-mokiny 8, 13 and 16. This phage did not infect AST154 and only partially infected AST234. It was the most effective against MIC79, but high-level resistance evolution was not observed. This is an interesting observation since mutation or repression of the flagella is common in *P. aeruginosa* [510-512] so the difficulty experienced by this isolate should be investigated further. It is possible that Boorn-mokiny 1 has multiple receptors that it can use in the absence of flagella. Previously, a *P. aeruginosa* phage from a different genus but with a similar sized genome to Boorn-mokiny 1 was found to putatively use a combination of LPS, pili and flagella components [282]. Therefore, the potential receptors of Boorn-mokiny 1 requires further investigation with mutants that have double knockouts, using a pooled transposon library and insertion sequencing or *in silico* identification of the phages' receptor binding proteins (RBPs) before comparison to publicly available RBPs [282, 556-558].

Results generated also saw reductions in antibiotic resistance following phage treatment. This has been identified previously as a trade-off of phage resistance [275, 307, 323, 521]. However, in *P. aeruginosa*, this has been due to large deletions affecting an antibiotic resistance determinant or specific mutation of the phage's receptor which is an antibiotic resistance determinant [275, 307, 323, 521]. Results generated in this chapter saw that although there were reductions in antibiotic MIC, these were not associated with mutations to known antibiotic resistance determinants, which suggest a pleiotropic effect of alterations which has been shown to complicate phage-bacteria relationships [524]. In a similar study, mutations in LPS biosynthesis genes after phage infection, were also seen

to decrease antibiotic MIC without changing an antibiotic resistant determinant [516]. In this chapter the phages' treatments did not cause the same effect on antibiotic resistance trade-off, even when they targeted the same receptor. This is analogous to phages that use the same receptor but do not always induce mutations that cause cross resistance to each other [379] and is probably due to the unpredictability of pleiotropy [524]. The trade-offs in antibiotic resistance that were observed are either random or dependent on the Kara-mokiny 13 and 16 specific factors. To elucidate which of these is the case the development of resistance to these two phages should be repeated independently to investigate if the same reductions in antibiotic MIC occur. Furthermore, future work should consider other trade-offs associated with phage resistance such as growth rate, motility and virulence. However, findings generated in this chapter do indicate that although phages may target the same receptor and are from the same genus, some may be better suited for therapy than others. Specifically, experiments conducted identified Kara-mokiny 16 treatment of *P. aeruginosa* reduced its MIC to tobramycin but also had the lowest proportion of resistance arising from its treatment. This is important as tobramycin is commonly antibiotic prescribed to people with CF for *P. aeruginosa* infections [541] and as phages will not replace standard of care, they will need to complement existing therapies. Thus, this phage may be a primary candidate for cocktail formulation development.

In conclusion, results generated in this chapter, identified that resistance to phage infection by tested *P. aeruginosa* clinical isolates were due to alterations in phage receptors. This appeared not to be affected by MOI but was by both the bacteria, genetic background and the phage used as the treatment. Furthermore, and though not universally observed, developing phage resistance did come at a fitness cost to bacteria, namely in reduced antibiotic resistance. Results from this chapter found this was limited to tobramycin and Kara-mokiny 13 and 16 phages. Since Kara-mokiny 16 treatment elicited the least amount of resistance and significantly reduced *P. aeruginosa* MIC to tobramycin, its cocktail formulation and preclinical safety testing was assessed in the next chapter.

This page is intentionally left blank

5. Phage-Antibiotic Cocktail Efficacy and Effects on Primary Airway Epithelial Cells

5.1 Introduction

Phage therapy has been increasingly used on a compassionate basis, where few adverse events have been observed [290-294, 302-316]. Although, phage resistance has been a rare but observable side-effect [293, 299-302], cocktails can be formulated to prevent this from occurring [298]. However, before their translation *in vivo*, these formulations must be tested for their ability to inhibit bacterial growth over a prolonged period [524] as well as their ability to trigger a potentially dangerous inflammatory response [559]. In a respiratory context, airway epithelial cells are the first line of defence to bacteria, the site where infection, colonisation and biofilm manifests, and the initial innate immune responders to infections [58, 397, 560-562]. Thus, preclinical experimentation on a relevant airway model would offer insights into how such cocktail formulations may be tolerated [262].

The airway epithelium is a pseudostratified layer composed of basal, club, ciliated, goblet, tuft, hillock and microfold cells as well as ionocytes [563]. The abundance of these cells changes from the proximal to distal airways, but all perform important defensive functions against inhaled particles and pathogens [561, 563, 564]. In addition to being a physical barrier where tight junctions are formed between epithelial cell sub-populations, goblet cells also produce mucus that entrap particles/pathogens that are then removed via mucociliary transport performed by ciliated epithelial cells [561, 563, 564]. Airway epithelial cells also perform important immunological surveillance, by sensing microbial or allergen signals, producing antimicrobial peptides, undergoing cell death if infected, and releasing cytokines that then attract immune cells [565-570].

Most investigations that have assessed the airway epithelial response to phages have utilised immortalised cell lines [274, 395-397, 571]. However, due to this process, these cells have been shown to be less sensitive to stimuli, cannot be differentiated to the cell types found *in vivo* and exhibit limited diversity in their responses [125, 402-404, 572,

573]. In contrast, primary airway epithelial cells are a more relevant model as they differ in their behaviour based on the individual, they were isolated from [405, 411, 412] and can be terminally differentiated via air-liquid interface (ALI) culture which more reflective of the airway *in vivo* [405, 411-416]. Additionally, it has been established that differentiated primary airway epithelial cells mount a representative inflammatory response to pathogenic stimuli [262, 405, 408, 410-412, 416, 574-579]. This indicates that it would be an ideal model to study the *in vitro* inflammatory response to phage, however only a few studies have explored phage therapy using primary airway cell models [262, 578, 579].

Thus, in this chapter, we tested the hypothesis that phage and cocktail components identified in Chapter 4 (namely Kara-mokiny 16 and tobramycin) would not be cytotoxic or inflammatory to the host airway. Experiments were performed to assess the bactericidal effectiveness of this combination by checkerboard assays and resistance suppression via time-kill assays. Following this, a series of experiments were performed whereby purified Kara-mokiny 16 and tobramycin were added singularly or in combination to the apical surface of fully differentiated primary airway epithelial cells. After an exposure period, cells were then assessed for gross morphological changes, cytotoxicity via lactate dehydrogenase (LDH) and inflammatory cytokine production (i.e., IL-6 and IL-8) via ELISA.

5.2 Materials and Methods

5.2.1 Materials

All reagents and chemicals used in this chapter are listed in Chapter 2.

5.2.2 General Methodology

5.2.2.1 Microbiology

Bacterial culture was performed on the CF *P. aeruginosa* isolates used in the previous chapter (M1C79, AST154 and AST234) as described in Chapter 2 (refer to 2.7.1).

5.2.2.2 Phage Propagation

Kara-mokiny 16 was propagated as previously described (refer to 2.7.2.6) and diluted to desired titres (10^7 - 10^1 PFU/mL) in LB broth (refer to 2.5.1.1) for all antimicrobial testing (refer to 5.2.2.3 and 5.2.2.4).

5.2.2.3 Tobramycin

Tobramycin (Sigma-Aldrich, St. Louis, Missouri, United States of America) was prepared as previously described (refer to 2.4.31) and diluted in 1X PBS (refer to 2.4.25) to desired concentrations (128 - 0.25 $\mu\text{g/mL}$) for cell culture experiments and in LB broth for antimicrobial testing (refer to 2.5.1.1).

5.2.2.4 Synergism Checkerboard Assay

To assess the relationship between Kara-mokiny 16 and tobramycin, a checkerboard assay was performed (refer to 2.7.1.5). Briefly, 50 μL volume of 10^5 CFU of the most antibiotic resistant *P. aeruginosa* isolate (AST154) was added to individual wells of a 96 well plate. A 50 μL volume of ten-fold dilutions of Kara-mokiny 16 (10^7 - 10^1 PFU/mL) and two-fold dilutions of tobramycin (128 - 0.25 $\mu\text{g/mL}$) were then added to each well. Wells were topped up with LB broth (refer to 2.5.1.1) to a total volume of 200 μL and plates incubated for 24 hrs at 37 °C. Bacterial growth in all wells were then measured via turbidity (at OD600nm) using a CLARIOstar® Plus machine (BMG Labtech GmbH, Ortenberg, Germany). Where multiple antimicrobials were mixed, their fractional inhibitory concentration index (FICI) was calculated using the equation below. The antimicrobial relationship was then classified as synergistic (≤ 0.5), indifferent ($0.5 \leq 1$) or antagonistic (> 1).

$$\text{FICI} = \left(\frac{\text{Combination OD600nm}}{\text{Kara - mokiny 16 OD600nm}} \right) + \left(\frac{\text{Combination OD600nm}}{\text{Tobramycin OD600nm}} \right)$$

5.2.2.5 Evaluation of Suppression of Phage Resistance

To evaluate which combinations identified above (refer to 5.2.2.4) suppressed phage resistance, a time kill treatment was performed (refer to 2.7.2.9). Briefly, 50 μL of 10^8

CFU/mL of M1C79, AST154 or AST234 were added to individual wells of a 96 well plate, followed by 50 μ L of the desired concentrations of Kara-mokiny 16 and tobramycin in singularity or in combination. Each well was then topped up to 200 μ L with LB broth (refer to 2.5.1.1). Overall bacterial growth (OD_{600nm}) of biological duplicate wells were then taken at one hour time intervals on a CLARIOstar® Plus machine (BMG Labtech GmbH, Ortenberg, Germany). Lytic activity of phages was confirmed by enumerating viable bacterial load (CFU/mL; refer to 2.7.1.4) and phages (PFU/mL; refer to 2.7.2.7) every 6 hrs from biological duplicate wells.

5.2.2.6 Endotoxin Removal and Quantification

Prior to experimentation, endotoxin was removed from propagated Kara-mokiny 16 stocks (refer to 5.2.2.2) by passing it through Cytiva Acrodisc™ Units with Mustang E membranes twice (Cytiva, Marlborough, Massachusetts, United States of America). Endotoxin concentrations were quantified by the recombinant factor C ENDONEXT™ assay, performed as per the manufacturer's protocol (Biomerieux, Marcy-l'Étoile, France). Once endotoxin was depleted, the Kara-mokiny 16 stocks were diluted in 1X PBS (refer to 2.4.25) to 10⁶ PFU/mL so they could be exposed to the primary airway epithelial cells.

5.2.2.7 Cell Culture Ethics

Primary airway epithelial cells were collected by nasal brushing from patients undergoing elective non-respiratory surgery and was approved by St John of God Hospital (Subiaco; WAERP #901) and Curtin University Human Research Ethics Committee (2019-0086; refer to 2.7.3.2.1, 2.7.3.2.2 and Appendix A.1). Cells were processed in the laboratory and cryopreserved as previously described (refer to 2.7.3.2.2 and 2.7.3.2.4). For experiments conducted in this chapter, airway epithelial cells collected from six children (age range of 3.46-6.94 years; 3 males) of age were thawed, and cultures established and expanded (refer to 2.7.3.2.5, 2.7.3.2.6 and 2.7.3.2.7). Air-liquid interface cultures were then established and maintained as described (refer to 2.7.3.2.8). Trans-epithelial electrical resistance and mucus washing was performed every seven days post-airlift (refer to 2.7.3.2.9) until experiments were performed.

5.2.2.8 Treatment Conditions of Established Primary Airway Epithelial Cells

At 28 days post-airlift, ALI culture basal media was exchanged to Pneumacult™-ALI starvation medium (refer to 2.6.1.14) and primary cultures maintained for an additional 3 days. Following this, 200 µL 1X PBS (refer to 2.4.25) was added to the apical side and cultures incubated at 37°C in 5%CO₂/95% air for 5 mins. The PBS was then carefully aspirated off and the basal starvation medium (refer to 2.6.1.14) refreshed. Then, to triplicate inserts, 10 µL of Kara-mokiny 16 (10⁶ PFU/mL), tobramycin (2 µg/mL), Kara-mokiny 16 combined with of tobramycin (10⁶ PFU/mL, and 2 µg/mL respectively), heat killed PAO1 (10⁶ CFU/mL; refer to 2.7.1.10), or 1X PBS (refer to 2.4.25) was added to the apical surface of the cells and cultures incubated at 37 °C and 5%CO₂/95% air for 24 hrs. Primary airway epithelial cells that had been ALI cultured were exposed to a dose of 10⁶ PFU/mL and CFU/mL of Kara-mokiny 16 or heat killed PAO1 because this represented a 1:1 ratio of cells to microbe. Afterwards, 200 µL of 1X PBS (refer to 2.4.25) was added to the apical surface of the cells for 5 mins at room temperature. The 1X PBS (refer to 2.4.25) wash was then collected and 180 µL frozen at -80 °C to stabilise any IL6, IL8 and LDH for later measurement. The remaining 20 µL from the 1X PBS (refer to 2.4.25) wash was kept at 4 °C to be used to titre Kara-mokiny 16 (refer to 2.7.2.7). The basal media was equally divided between -80 °C and 4 °C storage. Once thawed, the -80 °C triplicate samples were pooled and then used to measure IL-6, IL-8, and cytotoxicity. The samples kept at 4 °C were not pooled and allowed triplicate measurement of Kara-mokiny 16 titre.

5.2.2.9 Primary Airway Epithelial Cell Histology

Culture inserts were prepared for histological staining and microscopy performed to identify any gross morphological effects of any of the various exposures had on primary airway epithelial cell cultures. Here, inserts were cut in half and placed in NBF (refer to 2.4.22) at 4 °C for 24 hrs and then 95% (v/v) ethanol at 4 °C for 24 hrs. Insert fixing and staining was performed by Mr Luke Berry (Telethon Kids Institute, Perth Western Australia). Inserts were then embedded in paraffin blocks, sliced into 5 µm sections and mounted on glass slides (Waldemar Knittel Glasbearbeitungs GmbH, Braunschweig, Germany). The slides were air-dried and then baked at 60 °C for 30 mins, before deparaffinisation (Leica autostainer XL, Leica, Mt Waverley, VIC, Australia). These were soaked in xylene twice and rehydrated in increasingly dilute ethanol solutions (100%, 95% (v/v), 70% (v/v) and 40% (v/v)). Slides were then stained for 5 mins with haematoxylin and eosin (Sigma-Aldrich, St. Louis, Missouri, United States of America) and rinsed twice for 5 mins with tap water. Then 2% acetic acid (v/v) was used to stain the slides for 10 sec, followed by 45 sec of bluing solution. The slides were rinsed twice under tap water for 5 mins again and dehydrated in increasingly concentrated ethanol solutions (40% (v/v) and 70% (v/v)). To assess mucus production slides were then stained with alcoholic eosin for 5 mins before further dehydration with 95% (v/v) and 100% ethanol. Deparaffinised sections were also stained with 8X alcian blue (Sigma-Aldrich, St. Louis, Missouri, United States of America) in 3% (v/v) acetic acid for 60 mins, followed by a 1-minute rinse with water. The slide was then stained with nuclear fast red for 5 mins before three rinses under tap water. Slides were then dehydrated in 70% (v/v) ethanol. Slides stained with either haematoxylin and eosin or alcian blue were both mounted with Permount (Thermo Fisher Scientific, Waltham, Massachusetts, United States of America) and a coverslip.

5.2.2.10 Primary Airway Epithelial Cell Cytotoxicity

Potential cytotoxicity caused by different stimuli to primary airway epithelial cells were measured by detecting LDH using the CytoTox 96® Non-Radioactive Cytotoxicity Assay (Promega Corporation, Madison, Wisconsin, United States of America) using supplied instructions. Here, 25 µL of thawed pooled triplicate samples were transferred to 96 half-area white plate (Perkin Elmer, Massachusetts, United States of America). Then, 25 µL of CytoTox 96® Reagent was added, plates covered with foil, and incubated

in the dark for 30 mins at room temperature. Afterwards, 25 μL of the kit's stop solution was added to each well and the absorbance read at 490nm on a CLARIOstar® Plus machine (BMG Labtech GmbH, Ortenberg, Germany). Cytotoxicity levels were measured in technical duplicate wells and normalised to 1X PBS (refer to 2.4.25) controls and expressed as fold-change.

5.2.2.11 Primary Airway Epithelial Cell IL-8 Cytokine Quantification

The inflammatory cytokine IL-8, secreted by primary airway epithelial cells was measured using a commercial kit (Becton Dickinson Biosciences, Franklin Lakes, New Jersey, United States of America). Briefly, 96 half-area white plates (PerkinElmer, Massachusetts, United States of America) were coated with 50 μL of capture antibody (Becton Dickinson Biosciences, Franklin Lakes, New Jersey, United States of America) 1:250 diluted with coating buffer (refer to 2.4.18) overnight at 4 °C. The coating solution was removed, and wells washed with 150 μL of IL-8 wash buffer (refer to 2.4.19) three times. Wells were then blocked with 50 μL of assay diluent (refer to 2.4.17) and incubated for one hour at room temperature. The blocking buffer was removed, and wells washed with 150 μL of IL-8 wash buffer (refer to 2.4.19) again three times. A volume of 50 μL of pooled triplicate samples, standards and blanks were then added to relevant wells before being incubated at room temperature for 2 hrs. Samples were then removed, and wells washed with 150 μL of IL-8 wash buffer (refer to 2.4.19) five times. To each well, 50 μL of working detector (refer to 2.4.20) was added and plates incubated at room temperature for 1 hour. The working detector was removed, and the wells washed with 150 μL of IL-8 wash buffer (refer to 2.4.19) seven times. Then, 50 μL of 1-Step™ Ultra TMB-ELISA solution (Thermo Fisher Scientific, Waltham, Massachusetts, United States of America) was added to each well and plates incubated in the dark for 30 mins at room temperature. Following this, 25 μL of the stop solution (2N H_2SO_4) was added to the wells and the absorbance read at 450 nm with wavelength correction at 570 nm on a CLARIOstar® Plus machine (BMG Labtech GmbH, Ortenberg, Germany). Inflammatory cytokine production was measured in technical duplicate wells and were normalised to 1X PBS (refer to 2.4.25) controls and expressed as fold-change.

5.2.2.12

Primary Airway Epithelial Cell IL-6 Cytokine Quantification

Interleukin-6 (IL-6) secreted by the primary airway epithelial cells was measured via ELISA [469]. This involved diluting the purified rat anti-human IL-6 primary antibody (Becton Dickinson Biosciences, Franklin Lakes, New Jersey, United States of America) 1:250 in IL-6 coating buffer (refer to 2.4.16), adding 50 μ L to each of the wells of a 96-well maxisorp plates (Thermo Fisher Scientific, Waltham, Massachusetts, United States of America) and incubating overnight at 4 °C. The coating solution was then discarded, and wells blocked with 300 μ L of blocking buffer (refer to 2.4.15) for 1 hour at room temperature. This was also then discarded, and wells washed with 300 μ L of time-resolved fluorescence (TRF) wash buffer (refer to 2.4.34) five times. Then, 50 μ L of pooled samples and the standards were added to the wells and plates incubated on a platform shaker with 300 rpm of shaking for 1 hour at room temperature. The biotin conjugated rat anti-human IL-6 secondary antibody (Becton Dickinson Biosciences, Franklin Lakes, New Jersey, United States of America) was initially diluted 1:500 in assay diluent (refer to 2.4.17) and 50 μ L added to each well for one hour at room temperature. Following this, any residual antibody was discarded, and wells washed with 300 μ L TRF wash buffer (refer to 2.4.34) five times. Secondary antibody (50 μ L) was added to each well and plates incubated on a platform shaker as described earlier for 1 hour at room temperature. The secondary antibody was then discarded, and wells washed with 300 μ L of TRF wash buffer (refer to 2.4.34) five times. Europium-labelled streptavidin (PerkinElmer, Waltham, Massachusetts, United States of America) was diluted 1:500 in DELFIA assay diluent (PerkinElmer, Waltham, Massachusetts, United States of America) and 50 μ L added to wells before incubation on the platform shaker for 30 mins. Following this, the liquid was removed, and wells washed with 300 μ L of TRF wash buffer (refer to 2.4.34) eight times. Then, 50 μ L of DELFIA enhancement solution (PerkinElmer, Waltham, Massachusetts, United States of America) was added to each well and plates incubated statically at room temperature for 5 mins. Time-resolved fluorescence was then measured at an excitation of 340 nm and emission of 615 nm on a CLARIOstar® Plus machine (BMG Labtech GmbH, Ortenberg, Germany). Inflammatory cytokine production was measured in technical duplicate wells and were normalised to 1X PBS (refer to 2.4.25) controls and expressed as fold-change.

5.2.2.13 Statistics

All statistical tests were performed in GraphPad Prism v9.3.1 (GraphPad Software, La Jolla, CA). Normality was tested for using the Shapiro-Wilk normality test. Microbiological data (OD600nm, CFU/mL and PFU/mL) was performed and measured in biological duplicates and expressed as median±IQR. The Area Under the Curve (AUC) for the OD600nm over time was calculated and compared between treatments using a 1-way ANOVA with Tukey's multiple comparison test. The CFU/mL and PFU/mL data were compared between treatments via a repeated measures (RM) 2-way ANOVA with Tukey's multiple comparison test. Multiple comparisons were made between each treatment at each timepoint. Primary cell experiments were performed in triplicate and pooled for downstream measurement. Technical duplicate wells of IL-6, IL-8 and cytotoxicity (LDH) were measured and averaged. These were expressed as fold-change over PBS control and compared to compared to heat-killed PAO1 via Kruskal-Wallis 1-way ANOVA with Dunn's multiple comparison test. A $p < 0.05$ was considered statistically significant.

5.3 Results

5.3.1 Kara-mokiny 16 and Tobramycin Combination Synergy

As an initial screen of the bactericidal relationship between Kara-mokiny 16 and tobramycin, different concentrations were mixed and used to treat the most antibiotic resistant isolate (AST154) out of the three used in the previous chapter. Treatment with the different concentration combinations was performed for 24 hrs before OD600nm values were used to calculate FICI. Results generated showed that combinations of Kara-mokiny 16 titres from 10^6 to 10^2 PFU/mL with tobramycin concentrations 16 to 128 $\mu\text{g/mL}$ were antagonistic ($\text{FICI} > 2$; Figure 5.1). In addition, Kara-mokiny 16 at 10^2 PFU/mL combined with tobramycin concentrations 8 to 2 $\mu\text{g/mL}$ was also antagonistic ($\text{FICI} > 2$; Figure 5.1). All other combinations of Kara-mokiny 16 and tobramycin were identified as indifferent ($2 > \text{FICI} \geq 1$; Figure 5.1). However, and of significance, combinations of Kara-mokiny 16 at 10^6 or 10^7 PFU/mL with 2 $\mu\text{g/mL}$ of tobramycin had an additive effect ($1 > \text{FICI} > 0.5$; Figure 5.1). There were no synergistic combinations of Kara-mokiny 16 and tobramycin ($\text{FICI} < 0.5$; Figure 5.1).

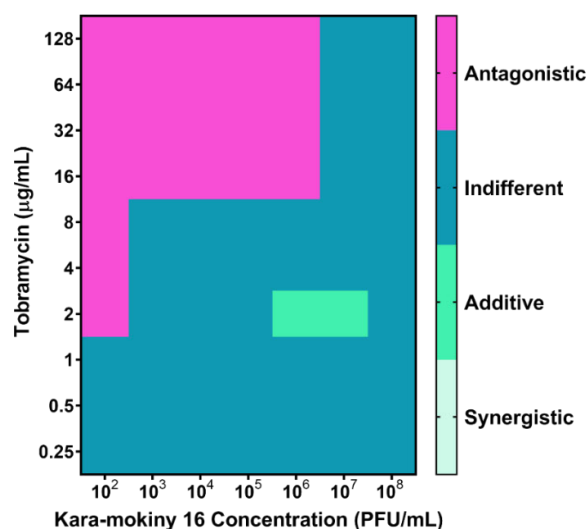


Figure 5.1 Synergistic Growth Suppression between Different Combinations of Kara-mokiny 16 and Tobramycin. *P. aeruginosa* isolate AST154 was treated with various combinations of tobramycin and Kara-mokiny 16 for 24 hrs and OD600nm measured. Values were used to calculate the FICI which was classified as Antagonistic (purple; $\text{FICI} > 2$), Indifferent (dark blue; $2 > \text{FICI} \geq 1$), Additive (turquoise; $1 > \text{FICI} > 0.5$) or Synergistic (pale green; $\text{FICI} < 0.5$). Combinations of Kara-mokiny 16 concentrations from 10^6 to 10^2 PFU/mL with 128 $\mu\text{g/mL}$ of tobramycin were antagonistic. Additionally, 10^2 PFU/mL of Kara-mokiny 16 with 2, 4 and 8 $\mu\text{g/mL}$ of tobramycin were also antagonistic. All other combinations of Kara-mokiny 16 and tobramycin were indifferent except 10^6 and 10^7 PFU/mL of Kara-mokiny 16 with 2 $\mu\text{g/mL}$ of tobramycin which were additive. There were no synergistic combinations identified. The results shown are the average of triplicate treatments.

5.3.2 M1C79 Resistance Suppression by Kara-mokiny 16 and Tobramycin Combinations

The combinations of 2 µg/mL of tobramycin 10^7 or 10^6 PFU/mL of Kara-mokiny 16, that additively suppressed AST154 growth in the checkerboard assay were then tested for their ability to prevent resistance in the isolates (M1C79, AST154 and AST234) used previously in this thesis. For the rest of this chapter 10^7 PFU/mL of Kara-mokiny 16 with 2 µg/mL of tobramycin will be referred to as high dose cocktail, whilst 10^6 PFU/mL of Kara-mokiny 16 with 2 µg/mL of tobramycin will be called low dose cocktail. Firstly, the combination of 2 µg/mL of tobramycin and 10^7 PFU/mL of Kara-mokiny 16 was used to treat M1C79 for 24 hrs and OD600nm and viable bacteria measured. For each treatment area under the curve (AUC) was calculated and the statistical significance between each was then assessed using a one-way ANOVA. Treatment for 24 hrs with 10^7 PFU/mL of Kara-mokiny 16 significantly reduced the OD600nm AUC compared to untreated M1C79 by ~70% ($p < 0.05$; Figure 5.2 A). Tobramycin also significantly reduced the OD600nm AUC compared to the M1C79 growth control by 84% ($p < 0.05$; Figure 5.2 A). Following treatment for 24 hrs with high dose cocktail the AUC was significantly reduced by ~91% compared to untreated M1C79 ($p < 0.05$; Figure 5.2 A). Kara-mokiny 16 treatment of M1C79 resulted in a ~79% significant increase in AUC compared to tobramycin treatment ($p < 0.05$; Figure 5.2 A). Treating M1C79 for 24 hrs with the high dose cocktail resulted in a non-significant ~45% reduction compared to tobramycin treatment ($p < 0.05$; Figure 5.2 A). Finally, the high dose cocktail caused a significant ~69% reduction in AUC compared to Kara-mokiny 16 treatment of M1C79 with 10^7 PFU/mL ($p < 0.05$; Figure 5.2 A). Overall, the high dose cocktail suppressed M1C79 growth more than Kara-mokiny 16 alone. Additionally, it showed greater suppression of growth compared to tobramycin alone initially but were similar after 24 hrs.

The number of culturable bacteria was also enumerated every 6 hrs after treatment and tested for significance using a 2-way ANOVA (Figure 5.2. B). For simplicity, only significance in the number of viable bacteria after 24 hrs of treatment are presented in this chapter, but all timepoints are presented in the appendices (Appendix Table I.1). After 24 hrs of treatment with 10^7 PFU/mL of Kara-mokiny 16, viable M1C79 was comparable (1.2 log-fold) to the untreated control ($p > 0.05$; Figure 5.2 B). However, 24 hrs of treatment with 2 µg/mL of tobramycin significantly reduced the amount of

culturable M1C79 (2.7 log-fold) compared to untreated control ($p < 0.05$; Figure 5.2 B). After 24 hrs of treatment with 2 $\mu\text{g}/\text{mL}$ of tobramycin the amount of culturable M1C79 was also significantly reduced (3.8 log-fold) compared to treatment with 10^7 PFU/mL of Kara-mokiny 16 ($p < 0.05$; Figure 5.2 B). Treatment with the high dose cocktail for 24 hrs significantly reduced the amount of culturable M1C79 (3.3 log-fold) compared to the untreated control ($p < 0.05$; Figure 5.2 B). After 24 hrs of treatment with the high dose cocktail the amount of culturable M1C79 was also significantly reduced (4.4 log-fold) compared to treatment with 10^7 PFU/mL of Kara-mokiny 16 ($p < 0.05$; Figure 5.2 B). However, there was no reduction in viable M1C79 (0.6 log-fold) caused by 24 hrs of treatment with the high dose cocktail compared to 2 $\mu\text{g}/\text{mL}$ of tobramycin ($p > 0.05$; Figure 5.2 B). In summary, the high dose cocktail and tobramycin alone both outperformed Kara-mokiny 16 and reduced the amount of M1C79 to similar levels after 24 hrs of treatment.

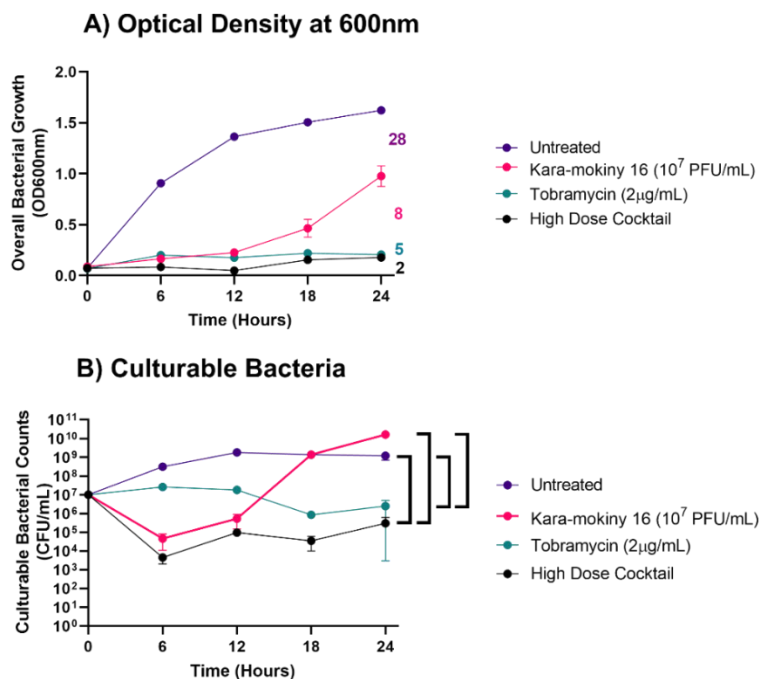


Figure 5.2 Isolate M1C79 resistance suppression by additive combination of tobramycin and Kara-mokiny 16. The clinical *P. aeruginosa* isolate, M1C79, was treated with 10^7 PFU/mL of Kara-mokiny 16 and 2 $\mu\text{g}/\text{mL}$ of tobramycin alone or in combination (high dose cocktail). Then **A)** OD600nm and **B)** M1C79 CFU/mL were measured. Treatment with the high dose cocktail and 2 $\mu\text{g}/\text{mL}$ of tobramycin alone reduced both OD600nm and viable M1C79 compared to 10^7 PFU/mL of Kara-mokiny 16 and untreated M1C79. However, there was no significant difference between the high dose cocktail treatment or 2 $\mu\text{g}/\text{mL}$ of tobramycin alone in terms of M1C79 growth or viable number. Duplicate values are represented as median \pm range. The OD600nm AUCs of each treatment (rounded to the whole number) are listed beside their 24-hour timepoint and are in the same colour as denoted in the legend. Each treatment's AUCs were compared using a 1-way with Tukey's multiple comparison test. The CFU/mL data was compared with a RM 2-way ANOVA with Tukey's multiple comparisons. A $p < 0.05$ was considered significant.

To test if the additive combination of 2 $\mu\text{g}/\text{mL}$ of tobramycin and 10^6 PFU/mL of Kara-mokiny 16 could prevent resistance evolving, they were used to treat M1C79 for 24 hrs and OD600nm and viable bacteria measured. Like the high dose cocktail above, the AUC for each OD600nm following the treatments were tested for significance using a one-way ANOVA. After 24 hrs of treatment with 10^6 PFU/mL of Kara-mokiny 16 the OD600nm AUC was reduced by ~68% compared to untreated control ($p < 0.05$; Figure 5.3 A). Treatment with 2 $\mu\text{g}/\text{mL}$ of tobramycin also significantly reduced the OD600nm AUC (~84%) compared to the untreated control ($p < 0.05$; Figure 5.3 A). Treatment for 24 hrs with 2 $\mu\text{g}/\text{mL}$ of tobramycin also significantly reduced the AUC (49%) compared to treatment with 10^6 PFU/mL of Kara-mokiny 16 ($p < 0.05$; Figure 5.3 A). After 24 hrs of treatment of M1C79 with the low dose cocktail, the AUC was significantly reduced by 91% compared to untreated control ($p < 0.05$; Figure 5.3 A). Treatment for 24 hrs with the low dose cocktail also significantly reduced the OD600nm of M1C79 compared to treatment with 10^6 PFU/mL of Kara-mokiny 16 (73%, $p < 0.05$; Figure 5.3 A). However, the reduction in AUC following low dose cocktail compared to 2 $\mu\text{g}/\text{mL}$ of tobramycin was not considered significant ($p > 0.05$; Figure 5.3 A). In summary, the low dose cocktail suppressed M1C79 growth for longer than Kara-mokiny 16 alone. It also suppressed bacterial growth more than tobramycin at earlier timepoints, but differences were negligible after 24 hrs.

At 6 hourly timepoints over the course of treatment of M1C79 the viable bacteria were measured (Figure 5.3 B). Like the high dose cocktail treatment of M1C79 only the significance after 24 hrs is shown and the other timepoints can be found in Appendix Table I.2. After 24 hrs of treatment with 10^6 PFU/mL of Kara-mokiny 16, the amount of culturable M1C79 was comparable to untreated control (0.1 log-fold, $p > 0.05$; Figure 5.3 B). Treatment for 24 hrs with 2 $\mu\text{g}/\text{mL}$ of tobramycin significantly reduced the amount of viable M1C79 (2.7 log-fold) compared to the untreated control ($p < 0.05$; Figure 5.3 B). It also significantly reduced the amount of viable M1C79 compared to treatment with 10^6 PFU/mL of Kara-mokiny 16 (2.6 log-fold, $p < 0.05$; Figure 5.3 B). Low dose cocktail treatment for 24 hrs reduced the amount of viable M1C79 (2.7 log-fold) compared to both the untreated control and treatment with 10^6 PFU/mL, but these differences were not significant ($p > 0.05$; Figure 5.3 B). There was also no difference between the amount of viable M1C79 after 24 hrs of treatment with the low dose cocktail compared to 2 $\mu\text{g}/\text{mL}$ of tobramycin alone ($p > 0.05$; Figure 5.3 B). To conclude, the low dose cocktail reduced viable M1C79 more than Kara-mokiny 16 alone after 24 hrs, indicating that it suppressed

the evolution of resistance more effectively than phage treatment alone. However, similar effects were observed between the cocktail and tobramycin alone indicating no difference in their suppression of resistance.

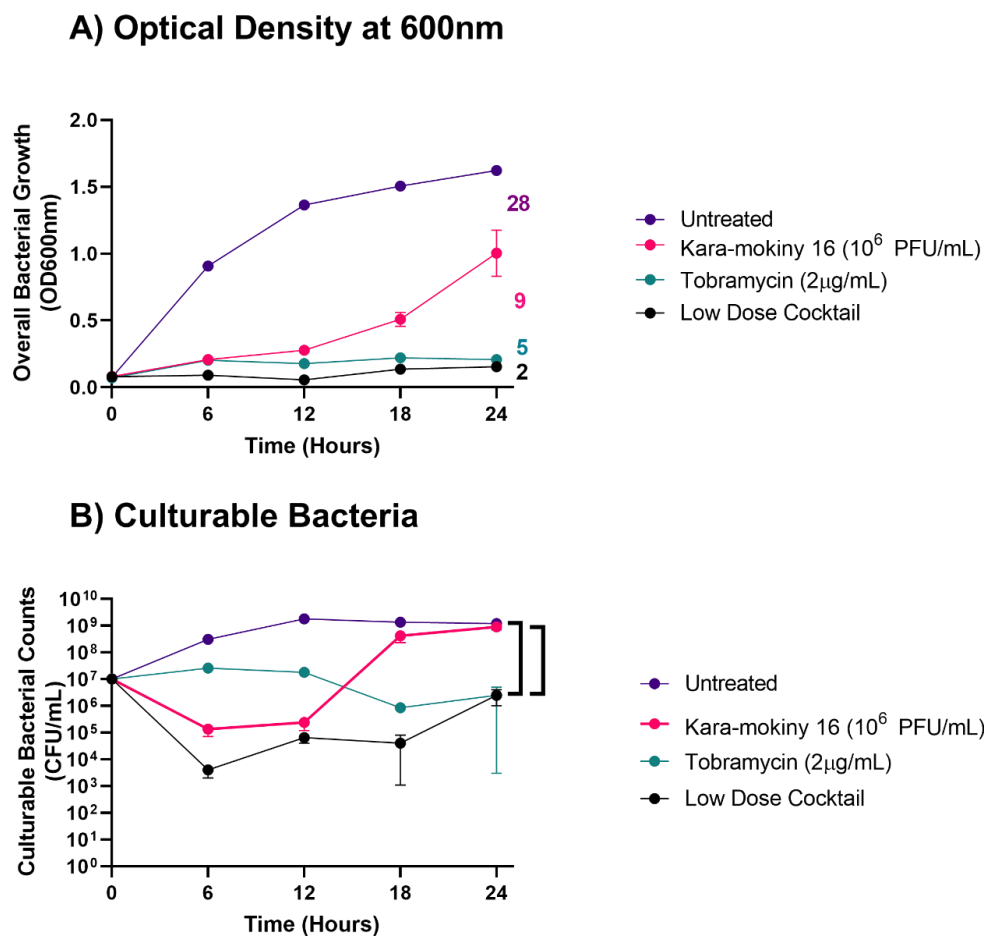


Figure 5.3 Isolate M1C79 resistance suppression by additive combination of tobramycin and Kara-mokiny 16. The *P. aeruginosa* isolate M1C79 was treated with 10⁶ PFU/mL of Kara-mokiny 16 and 2 µg/mL of tobramycin alone or in combination (low dose cocktail). Then **A)** bacterial growth and **B)** culturable bacteria were measured. Treatment with the low dose cocktail and 2 µg/mL of tobramycin alone reduced both OD600nm and viable M1C79 compared to 10⁶ PFU/mL of Kara-mokiny 16 and untreated M1C79. However, there was no significant difference between the low dose cocktail treatment or 2 µg/mL of tobramycin alone in terms of M1C79 growth or viable number. Duplicate values are represented as median±range. The OD600nm AUCs of each treatment (rounded to the whole number) are listed beside their 24-hour timepoint and are in the same colour as denoted in the legend. Each treatment's AUCs were compared using a 1-way with Tukey's multiple comparison test. The CFU/mL data was compared with a RM 2-way ANOVA with Tukey's multiple comparisons. A p<0.05 was considered significant.

5.3.3 AST154 Resistance Suppression by Kara-mokiny 16 and Tobramycin Combinations

To test if the additive combination of 2 µg/mL of tobramycin and 10⁷ PFU/mL of Kara-mokiny 16 could prevent resistance evolving, they were used to treat AST154 for 24 hrs and OD_{600nm} measured. As above for the M1C79 treatments, the AUC was calculated, and these compared between treatments using a one-way ANOVA. After 24 hrs of treatment with 10⁷ PFU/mL of Kara-mokiny 16 the AUC was significantly reduced (69%) compared to the untreated control (p<0.05; Figure 5.4 A). Treatment with 10⁷ PFU/mL of Kara-mokiny 16 for 24 hrs also significantly reduced the AUC (68%) compared to treatment with 2 µg/mL of tobramycin (p<0.05; Figure 5.4 A). The slight reduction in AUC caused by treatment with 2 µg/mL of tobramycin compared to untreated control (3%) was not significant (p>0.05; Figure 5.4 A). The high dose cocktail treatment for 24 hrs significantly reduced the AUC (64%) compared to the untreated control (p<0.05; Figure 5.4 A). Furthermore, the high dose cocktail's reduction in AUC (63%) compared to 2 µg/mL of tobramycin alone was significant (p<0.05; Figure 5.4 A). However, the high dose cocktail treatment AUC was higher comparable to Kara-mokiny 16 10⁷ PFU/mL (0.07%) which was not significant (p>0.05; Figure 5.4 A). In summary, tobramycin alone did not suppress AST154 growth. In addition, the high dose cocktail and Kara-mokiny 16 alone reduced AST154 growth to similar levels indicating comparable suppression of resistance development.

Every 6 hrs of treatment of AST15 the surviving bacteria were enumerated (Figure 5.4 B). Like the M1C79 treatments above only significant results at 24 hrs will be shown in the chapter with the full results in Appendix Table I.3. After 24 hrs of treatment with 10⁷ PFU/mL of Kara-mokiny 16 the amount of culturable AST154 was significantly reduced compared to untreated control (1.7 log-fold, p<0.05; Figure 5.4 B). Treatment with 10⁷ PFU/mL of Kara-mokiny 16 for 24 hrs also significantly reduced the amount of culturable AST154 compared to treatment with 2 µg/mL of tobramycin (1.0 log-fold, p<0.05; Figure 5.4 B). Treatment with 2 µg/mL of tobramycin only resulted in a 0.5 log-fold reduction in viable AST154 compared to the untreated control (p>0.05; Figure 5.4 B). However, the high dose cocktail treatment for 24 hrs significantly reduced the amount of viable AST154 compared to the untreated control (1.2 log-fold, p<0.05; Figure 5.4 B). High dose cocktail treatment for 24 hrs resulted in only 0.7 log-fold less viable AST154 compared to treatment with 2 µg/mL of tobramycin (p>0.05; Figure 5.4 B). Overall,

tobramycin alone had no effect on viable AST154. In addition, there was negligible differences in resistance suppression between the high dose cocktail and Kara-mokiny 16 alone.

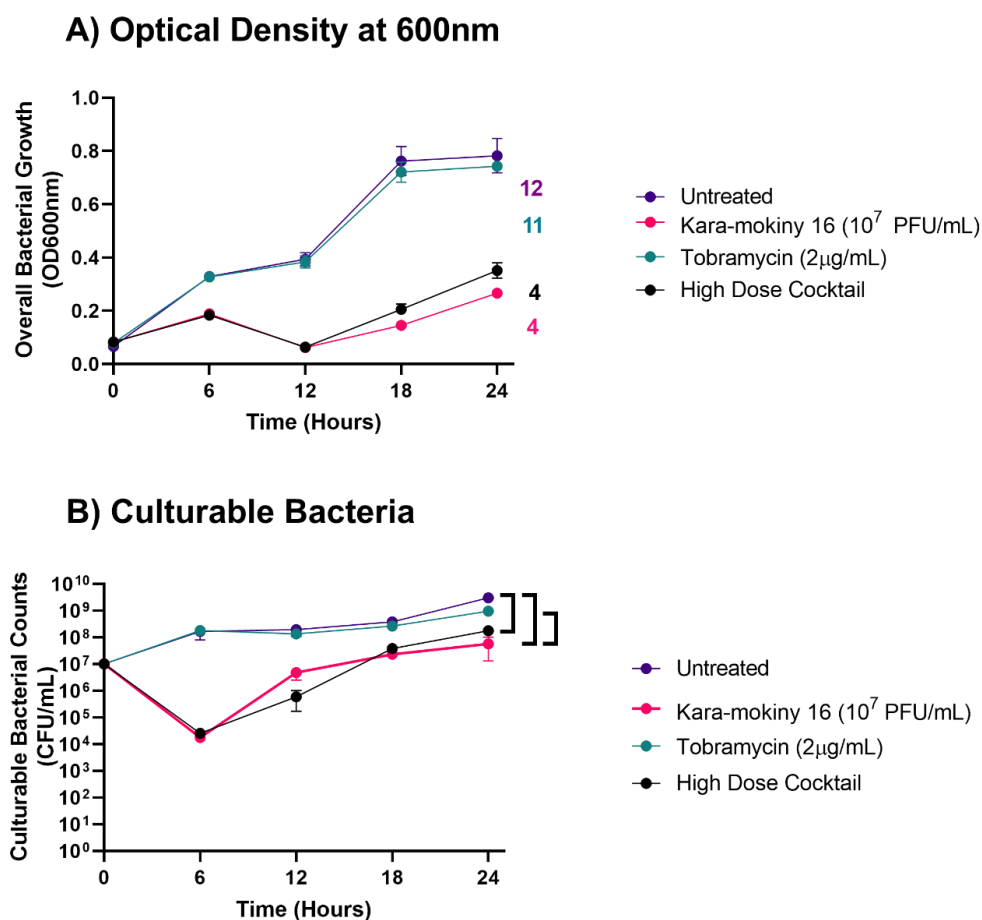


Figure 5.4 Isolate AST154 resistance suppression of additive combination of tobramycin and Kara-mokiny 16. The *P. aeruginosa* isolate AST154 was treated with 10⁷ PFU/mL of Kara-mokiny 16 and 2 μg/mL of tobramycin alone or in combination (high dose cocktail). Then **A)** OD600nm and **B)** AST154 CFU/mL were measured. Treatment with 2 μg/mL of tobramycin alone had little effect on AST154 growth or CFU/mL. Both treatment with 10⁷ PFU/mL of Kara-mokiny 16 and the high dose cocktail reduced both the OD600nm and viable amount of AST154 compared to untreated control and 2 μg/mL of tobramycin alone. However, there was no significant difference between the effect of the high dose cocktail and 10⁷ PFU/mL of Kara-mokiny 16 on growth and culturable bacteria. Duplicate values are represented as median±range. The OD600nm AUCs of each treatment (rounded to the whole number) are listed beside their 24-hour timepoint and are in the same colour as denoted in the legend. Each treatment's AUCs were compared using a 1-way with Tukey's multiple comparison test. The CFU/mL data was compared with a RM 2-way ANOVA with Tukey's multiple comparisons. A p<0.05 was considered significant.

To test if the additive combination of 2 µg/mL of tobramycin and 10⁶ PFU/mL of Kara-mokiny 16 could prevent resistance evolving, they were used to treat AST154 for 24 hrs and OD600nm. The AUC for each treatment was calculated and these were compared by one-way ANOVA. After 24 hrs of treatment with 10⁶ PFU/mL of Kara-mokiny 16 the AUC was significantly reduced compared to untreated control (67%; p<0.05; Figure 5.5 A). Treatment with 10⁶ PFU/mL of Kara-mokiny 16 also significantly reduced AUC (66%) compared to treatment with 2 µg/mL of tobramycin (p<0.05; Figure 5.5 A). After 24 hrs of treatment with 2 µg/mL of tobramycin the AUC was comparable to untreated control (p>0.05; Figure 5.5 A). The low dose cocktail treatment for 24 hrs significantly reduced the AUC (67%) compared to the untreated control (p<0.05; Figure 5.5 A). Treatment with the low dose cocktail for 24 hrs also significantly reduced AUC (66%) compared to treatment with 2 µg/mL of tobramycin (p<0.05; Figure 5.5 A). However, the difference between the low dose cocktail and 10⁶ PFU/mL Kara-mokiny 16 treatment (0.002%) was not significant (p>0.05; Figure 5.5 A). In summary, tobramycin alone had no effect on AST154 growth, corroborating prior work that identified it being resistant to this antibiotic. In addition, similar suppressive effects were observed between the high dose cocktail and Kara-mokiny 16 alone.

Over the course of treatment of AST154 the number of culturable bacteria was also measured (Figure 5.5 B). Only significance after 24 hrs of treatment is depicted and the full results statistics is in Appendix Table I.4. After 24 hrs of treatment with 10⁶ PFU/mL of Kara-mokiny 16 the amount of culturable AST154 was significantly reduced compared to the untreated control (1.7 log-fold, p<0.05; Figure 5.5 B). Treatment with 10⁶ PFU/mL of Kara-mokiny 16 for 24 hrs also significantly reduced the amount of culturable AST154 (1.2 log-fold) compared to treatment with 2 µg/mL of tobramycin (p<0.05; Figure 5.5 B). Treatment with 2 µg/mL of tobramycin only resulted in a non-significant reduction (0.5 log-fold) in viable AST154 compared to the untreated control (p>0.05; Figure 5.5 B). The low dose cocktail treatment for 24 hrs significantly reduced the amount of viable AST154 (1.6 log-fold) compared to the untreated control (p<0.05; Figure 5.5 B). Additionally, low dose cocktail treatment for 24 hrs significantly reduced the amount of viable AST154 (1.1 log-fold) compared to treatment with 2 µg/mL of tobramycin (p<0.05; Figure 5.5 B). Finally, there was only a 0.1 log-fold difference between the effect of the low dose cocktail and 10⁶ PFU/mL on viable AST154 after 24 hrs (p>0.05; Figure 5.5 B) To conclude, tobramycin alone did not affect viable AST154. Furthermore, similar

suppressive effects were observed between the high dose cocktail and Kara-mokiny 16 alone.

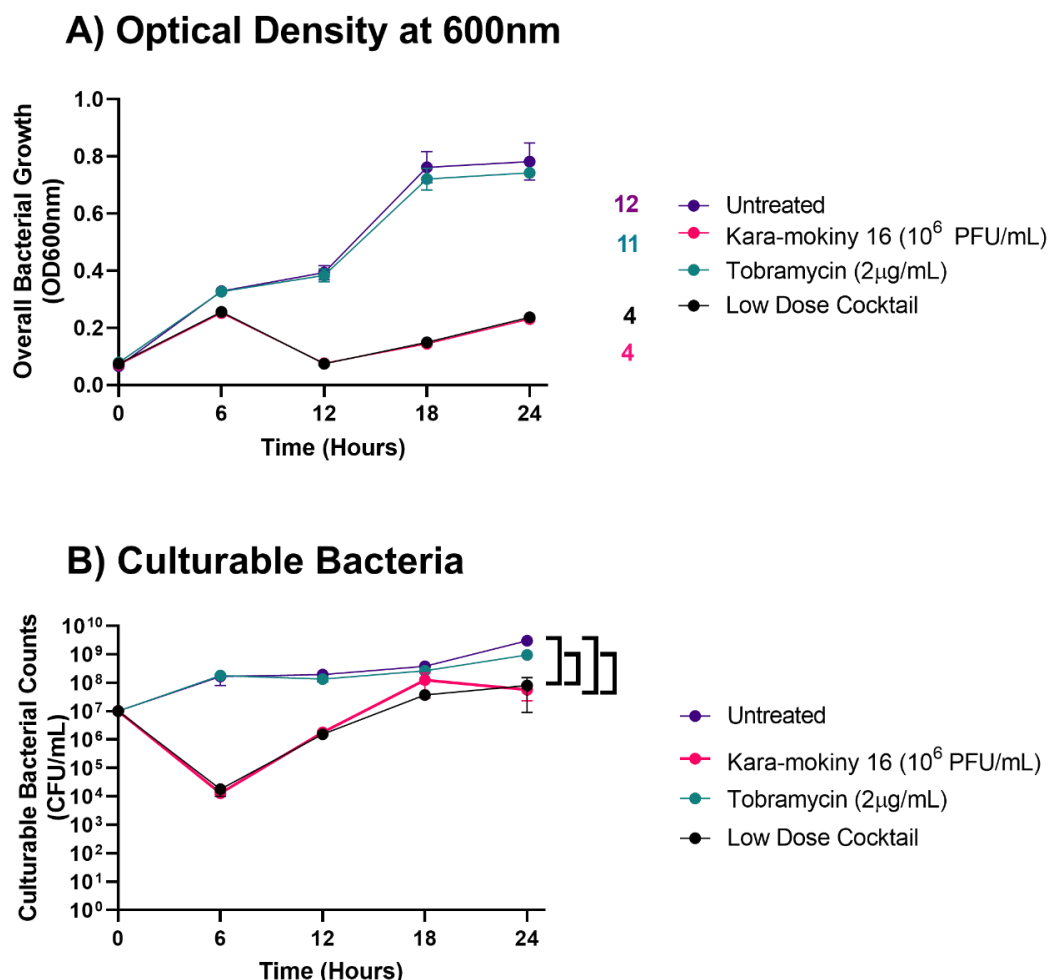


Figure 5.5 Isolate AST154 resistance suppression by additive combination of tobramycin and Kara-mokiny 16. The *P. aeruginosa* isolate AST154 was treated with 10⁶ PFU/mL of Kara-mokiny 16 and 2 μg/mL of tobramycin alone or in combination (low dose cocktail). Then **A)** OD600nm and **B)** AST154 CFU/mL were measured. Treatment with 2 μg/mL of tobramycin alone had little effect on AST154 growth or CFU/mL. Both treatment with the low dose cocktail and 10⁶ PFU/mL of Kara-mokiny 16 the reduced both the OD600nm and viable amount of AST154 compared to untreated control and 2 μg/mL of tobramycin alone. However, there was little difference between the effects of the low dose cocktail and 10⁶ PFU/mL of Kara-mokiny 16 on AST154. Duplicate values are represented as median±range. The OD600nm AUCs of each treatment (rounded to the whole number) are listed beside their 24-hour timepoint and are in the same colour as denoted in the legend. Each treatment's AUCs were compared using a 1-way with Tukey's multiple comparison test. The CFU/mL data was compared with a RM 2-way ANOVA with Tukey's multiple comparisons. A p<0.05 was considered significant.

5.3.4 AST234 Resistance Suppression by Kara-mokiny 16 and Tobramycin Combinations

To test if the additive combination of 2 µg/mL of tobramycin and 10⁷ PFU/mL of Kara-mokiny 16 could prevent resistance evolving, they were used to treat AST234 for 24 hrs and OD_{600nm} measured. The AUC for each treatment was calculated and these were compared by one-way ANOVA. Treatment of AST234 with Kara-mokiny 16 (10⁷ PFU/mL) for 24 hrs significantly reduced the AUC (40%) compared to the untreated control (p<0.05; Figure 5.6 A). Treatment of AST234 with Kara-mokiny 16 (10⁷ PFU/mL for 24 hrs) also significantly reduced the AUC (34%) compared to treatment with 2 µg/mL of tobramycin (p<0.05; Figure 5.6 A). Treatment for 24 hrs with 2 µg/mL of tobramycin resulted in a 9% reduction in the AUC which was not significant (p>0.05; Figure 5.6 A). After treatment of AST234 with the high dose cocktail for 24 hrs the AUC was significantly reduced (50%) compared to the untreated control (p<0.05; Figure 5.6 A). Furthermore, treatment of AST234 with the high dose cocktail for 24 hrs also significantly reduced the AUC (45%) compared to treatment with 2 µg/mL of tobramycin (p<0.05; Figure 5.6 A). Overall, tobramycin had a negligible effect on AST234 growth. There were also no differences seen between the high dose cocktail and Kara-mokiny 16 alone, suggesting that resistance was not more effectively suppressed by the combination.

Over the course of treatment of AST234 the number of viable bacteria was also measured (Figure 5.6 B). Only significance after 24 hrs of treatment is depicted in the chapter and full results are provided in Appendix Table I.5. After 24 hrs of treatment with 10⁷ PFU/mL of Kara-mokiny 16 the amount of viable AST234 was significantly reduced (2.5 log-fold) compared to the control (p<0.05; Figure 5.6 B). Treatment of AST234 for 24 hrs with 10⁷ PFU/mL of Kara-mokiny16 also significantly reduced the number of culturable bacteria (1.8 log-fold) compared to treatment with 2 µg/mL of tobramycin (p<0.05; Figure 5.6 B). There was only a 0.6 log-fold difference in the amount of viable AST234 between the untreated control and 24 hrs of 2 µg/mL of tobramycin treatment (p>0.05; Figure 5.6 B). Treatment with the high dose cocktail for 24 hrs significantly reduced the amount of viable AST234 (3.6 log-fold) compared to untreated control (p<0.05; Figure 5.6 B). Furthermore, after 24 hrs the high dose cocktail significantly reduced the amount of viable AST234 (3 log-fold) compared to 2 µg/mL of tobramycin (p<0.05; Figure 5.6 B). Additionally, treatment with the high dose cocktail for 24 hrs significantly reduced to the amount of culturable AST234 (1.1 log-fold) compared to treatment with 10⁷ PFU/mL of Kara-mokiny 16 (p<0.05; Figure 5.6 B). In summary, the

high dose cocktail reduced culturable AST234 more than tobramycin and Kara-mokiny 16 alone, indicating greater resistance suppression.

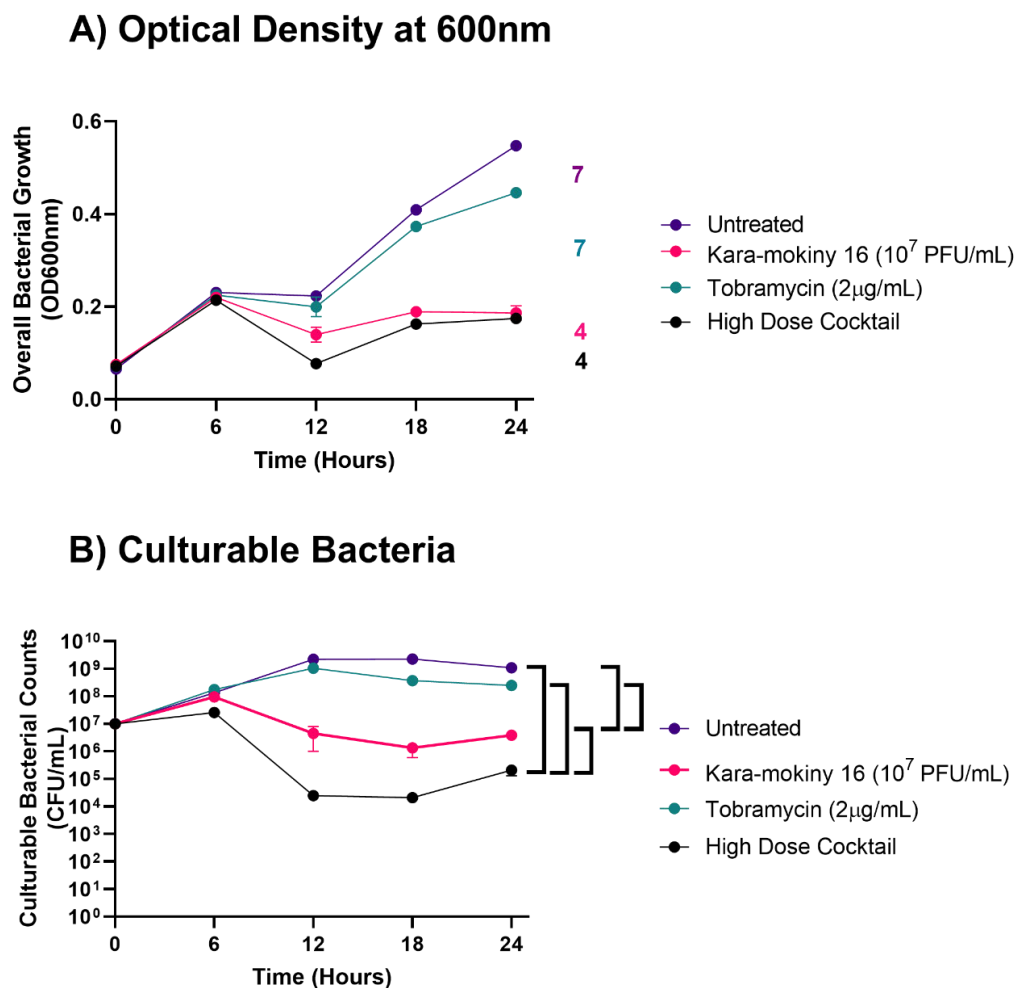


Figure 5.6 Isolate AST234 resistance suppression of additive combination of tobramycin and Kara-mokiny 16. The *P. aeruginosa* isolate AST234 was treated with 10⁷ PFU/mL of Kara-mokiny 16 and 2 µg/mL of tobramycin alone or in combination (high dose cocktail). Then **A)** OD600nm or **B)** viable AST234 was also enumerated. Treatment of AST234 with 2 µg/mL of tobramycin did not affect its growth or the CFU/mL. Both Kara-mokiny 16 10⁷ PFU/mL and the high dose cocktail reduced AST234 growth and viable number compared to untreated and tobramycin treatment. However, high dose cocktail treatment also significantly reduced viable AST234 compared to treatment with 10⁷ PFU/mL of Kara-mokiny 16. Data is represented as median±range. The OD600nm AUCs of each treatment (rounded to the whole number) are listed beside their 24-hour timepoint and are in the same colour as denoted in the legend. Each treatment's AUCs were compared using a 1-way with Tukey's multiple comparison test. The CFU/mL data was compared with a RM 2-way ANOVA with Tukey's multiple comparisons. A p<0.05 was considered significant.

To test if the additive combination of 2 $\mu\text{g}/\text{mL}$ of tobramycin and 10^6 PFU/mL of Kara-mokiny 16 could prevent resistance evolving, they were used to treat AST234 for 24 hrs and OD600nm measured. The AUC for each treatment was calculated and these were compared by one-way ANOVA. After 24 hrs of treatment with 10^6 PFU/mL of Kara-mokiny 16, the AUC was significantly reduced (32%) compared to untreated control ($p < 0.05$; Figure 5.7 A). After 24 hrs of treatment with 10^6 PFU/mL of Kara-mokiny 16, the AUC was significantly reduced (25%) compared to treatment with 2 $\mu\text{g}/\text{mL}$ of tobramycin ($p < 0.05$; Figure 5.7 A). Treatment with 2 $\mu\text{g}/\text{mL}$ of tobramycin for 24 hrs resulted in a non-significant decrease (9%) in AUC compared to the control ($p > 0.05$; Figure 5.7 A). Treatment of AST234 for 24 hrs with the low dose cocktail caused significant reduction in the AUC compared to untreated control (47%, $p < 0.05$; Figure 5.7 A). Furthermore, the low cocktail treatment for 24 hrs also resulted in a significant reduction (42%) in AUC compared to treatment with 2 $\mu\text{g}/\text{mL}$ of tobramycin ($p < 0.05$; Figure 5.7 A). Additionally, low dose cocktail treatment for 24 hrs significantly reduced the AUC (23%) compared to treatment with 10^6 PFU/mL of Kara-mokiny 16 ($p < 0.05$; Figure 5.7 A). In conclusion, the low dose cocktail reduced AST234 growth more than either tobramycin or Kara-mokiny 16 alone, suggesting it was more effectively suppresses resistance.

Every 6 hrs of treatment of AST234 the number of viable bacteria was enumerated (Figure 5.7 B). Only significance after 24 hrs of treatment is depicted and the full results statistics are presented in Appendix Table I.6. After 24 hrs of treatment with 10^6 PFU/mL of Kara-mokiny 16 the amount of viable AST234 was significantly reduced (2.4 log-fold) compared to the untreated control ($p < 0.05$; Figure 5.7 B). Treatment of AST234 for 24 hrs with 10^6 PFU/mL of Kara-mokiny 16 also significantly reduced the number of culturable bacteria (1.8 log-fold) compared to treatment with 2 $\mu\text{g}/\text{mL}$ of tobramycin ($p < 0.05$; Figure 5.7 B). The amount of viable AST234 was not significantly reduced by 2 $\mu\text{g}/\text{mL}$ of tobramycin compared to control after 24 hrs (0.6 log-fold, $p > 0.05$; Figure 5.7 B). Treatment with the low dose cocktail for 24 hrs significantly reduced the amount of viable AST234 (2.8 log-fold) compared to untreated control ($p < 0.05$; Figure 5.7 B). After 24 hrs of treatment with the low dose cocktail the amount of viable AST234 was also significantly reduced compared to treatment with 2 $\mu\text{g}/\text{mL}$ of tobramycin (2.1 log-fold, $p < 0.05$; Figure 5.7 B). The low dose cocktail reduced the amount of AST234 compared to Kara-mokiny 16 10^6 PFU/mL treatment but was not considered significant (0.4 log-fold, $p > 0.05$; Figure 5.7 B). After 24 hrs there was no difference in the reductions seen in

viable AST234 between Kara-mokiny 16 alone and the low dose cocktail suggesting that resistance suppression was not enhanced by the combination.

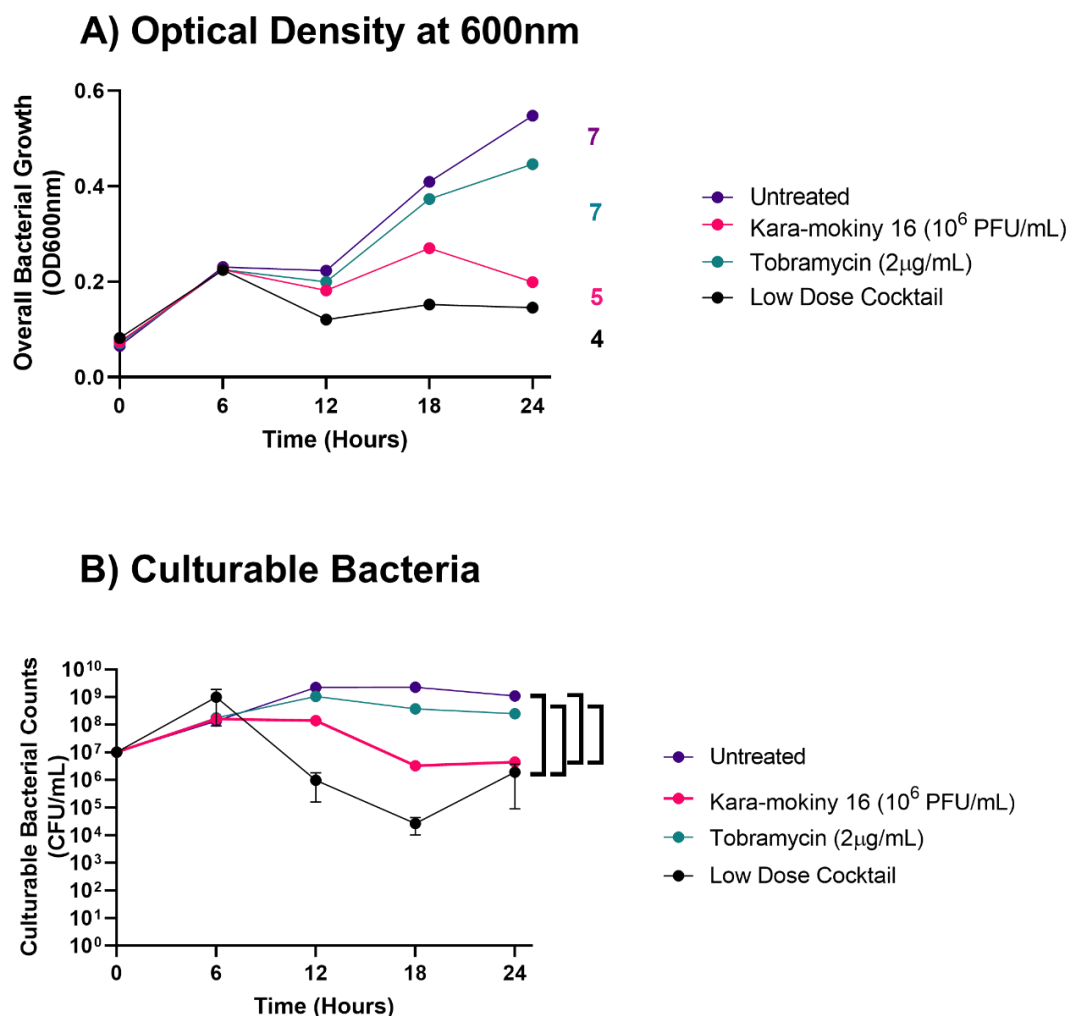


Figure 5.7 Isolate AST234 resistance suppression of additive combination of tobramycin and Kara-mokiny 16. The *P. aeruginosa* isolate AST234 was treated with 10⁶ PFU/mL of Kara-mokiny 16 and 2 μg/mL of tobramycin alone or in combination (low dose cocktail). **A)** OD600nm or **B)** viable AST234 was also enumerated. Treatment of AST234 with 2 μg/mL of tobramycin did not affect its growth or the CFU/mL. Both Kara-mokiny 16 10⁶ PFU/mL and the low dose cocktail reduced AST234 growth and viable number compared to untreated and tobramycin treatment. However, there was no difference in the effects of the low dose cocktail and Kara-mokiny 10⁶ PFU/mL treatments on AST234. Data is represented as median±range. The OD600nm AUCs of each treatment (rounded to the whole number) are listed beside their 24-hour timepoint and are in the same colour as denoted in the legend. Each treatment's AUCs were compared using a 1-way with Tukey's multiple comparison test. The CFU/mL data was compared with a RM 2-way ANOVA with Tukey's multiple comparisons. A p<0.05 was considered significant.

5.3.5 Comparison of Phage Titres During Combination Treatments of the *P. aeruginosa* Isolates

Every six hrs, during Kara-mokiny 16 and tobramycin combination treatments of M1C79, Kara-mokiny 16 titres were measured. Titres were then compared between each treatment using a two-way ANOVA and for simplicity only significance at 24 hrs will be referred to and shown within this chapter (refer to Appendix Table I.7 for statistical analysis performed). No Kara-mokiny 16 was detected in the untreated control after 24 hrs (Figure 5.8 A). Following 24 hrs of treatment of M1C79 with 10^7 PFU/mL of Kara-mokiny 16, phage titre was significantly increased (2.5 log-fold) compared to the low dose cocktail ($p < 0.05$; Figure 5.8 A). Phage titre was also significantly increased (3.2 log-fold) after 24 hrs of 10^7 PFU/mL treatment of M1C79 compared to the high dose cocktail ($p < 0.05$; Figure 5.8 A). Kara-mokiny 16 titre after 10^7 PFU/mL treatment was comparable to 10^6 PFU/mL treatment (0.1 log-fold higher, $p > 0.05$; Figure 5.8 A). Following 24 hrs of treatment of M1C79 with 10^6 PFU/mL of Kara-mokiny 16, phage titre was significantly increased (2.4 log-fold) compared to the low dose cocktail ($p < 0.05$; Figure 5.8 A). Kara-mokiny 16 titre was also significantly increased (3.1 log-fold) after 24 hrs of 10^6 PFU/mL treatment of M1C79 compared to the high dose cocktail ($p < 0.05$; Figure 5.8 A). After 24 hrs, no Kara-mokiny 16 was detected in the M1C79 treated with $2\mu\text{g/mL}$ of tobramycin (Figure 5.8 A). There was also significantly more Kara-mokiny 16 following 24 hrs of treatment of M1C79 with the low dose cocktail compared to the treatment with the high dose cocktail (0.7 log-fold, $p < 0.05$; Figure 5.8 A). In summary, Kara-mokiny 16 titre was lower when used in the combination treatment with tobramycin compared to when used alone.

Every six hrs, during Kara-mokiny 16 and tobramycin combination treatments of AST154, Kara-mokiny 16 titres were measured. Titres were then compared between each treatment using a two-way ANOVA and for simplicity only significance at 24 hrs will be referred to and shown in the figures (Figure 5.8 B) and the full statistics are provided in Appendix Table I.7. After 24 hrs there was no Kara-mokiny 16 detected in the untreated control (Figure 5.8 B). There were only minimal differences in the titres of Kara-mokiny 16 after 24 hrs of treatment of AST154 with 10^6 PFU/mL, 10^7 PFU/mL, low dose and high dose cocktail (range 0.1-0.2 log-fold, $p > 0.05$; Figure 5.8 B). Kara-mokiny 16 was not detectable after 24 hrs of treatment of AST154 with $2\mu\text{g/mL}$ of tobramycin (Figure

5.8 B). To conclude, no differences in Kara-mokiny 16 titres were seen when used in either combination treatment or on its own.

Every six hrs, during Kara-mokiny 16 and tobramycin combination treatments of AST234, phage titre was measured. These were then compared between each treatment using a two-way ANOVA and for simplicity only significance at 24 hrs will be shown in the figures (Figure 5.8 C) and the full statistics have been provided in Appendix Table I.7. After 24 hrs, no Kara-mokiny 16 was detected in the untreated control (Figure 5.8 C). There was no significant difference in Kara-mokiny 16 after 24 hrs of treatment of AST234 with 10^7 PFU/mL compared to 10^6 PFU/mL of Kara-mokiny 16 (0.2 log-fold, $p>0.05$; Figure 5.8 C). Treatment of AST234 with 10^6 PFU/mL of Kara-mokiny 16 for 24 hrs resulted in 2.1 log-fold more Kara-mokiny 16 compared to treatment with the low dose cocktail ($p<0.05$; Figure 5.8 C). Treatment of AST234 with 10^6 PFU/mL of Kara-mokiny 16 for 24 hrs also resulted in higher titres of Kara-mokiny 16 compared to treatment with the high dose cocktail (1.9 log-fold, $p<0.05$; Figure 5.8 C). Treatment of AST234 with 10^7 PFU/mL of Kara-mokiny 16 for 24 hrs resulted in significantly increased titres of Kara-mokiny 16 (2.3 log-fold) compared to treatment with the low dose cocktail ($p<0.05$; Figure 5.8 C). Treatment of AST234 with 10^7 PFU/mL of Kara-mokiny 16 for 24 hrs also resulted in a significant increase titre of Kara-mokiny 16 (2.1 log-fold) compared to treatment with the high dose cocktail ($p<0.05$; Figure 5.8 C). After 24 hrs of treatment of AST234 with 2 $\mu\text{g/mL}$ of tobramycin, no Kara-mokiny 16 detected (Figure 5.8 C). Finally, titres of Kara-mokiny 16 following 24 hrs of treatment of AST234 with low and high dose cocktail were similar (0.1 log-fold, $p>0.05$; Figure 5.8 C). Overall, when Kara-mokiny 16 was used in combination with tobramycin its titre was lower than when it was used alone.

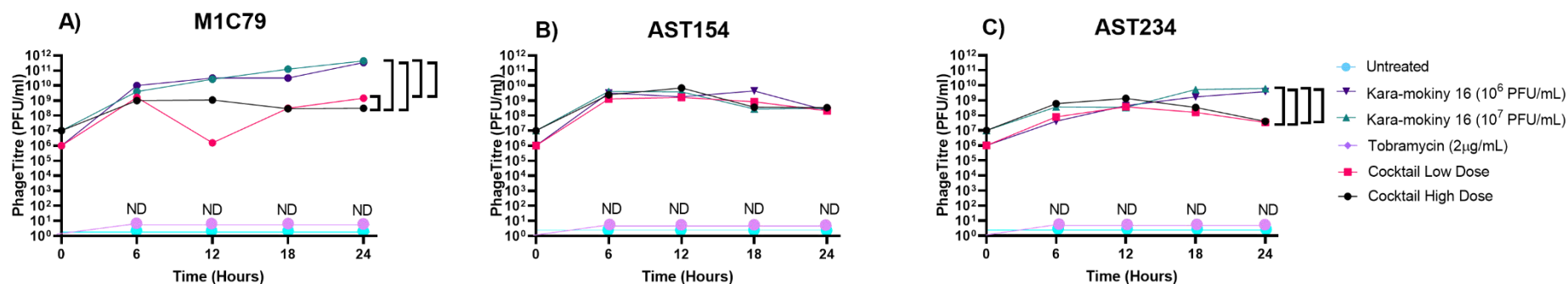


Figure 5.8 Titre of Kara-mokiny 16 over time after different treatments of the *P. aeruginosa* isolates. The *P. aeruginosa* isolate (A) M1C79, (B) AST154 and (C) AST234 was treated with 10⁶ or 10⁷ PFU/mL of Kara-mokiny 16 and 2 µg/mL of tobramycin alone or in combination. Every 6 hrs Kara-mokiny 16 was enumerated and PFU/mL calculated for each treatment. No Kara-mokiny 16 was detected in the untreated controls or 2 µg/mL of tobramycin alone treatments. There was more Kara-mokiny 16 after treatment of M1C79 with either dose (10⁶ or 10⁷ PFU/mL) of Kara-mokiny 16 compared to the high and low dose cocktails. There was also more Kara-mokiny 16 following the low dose cocktail compared to its high dose counterpart. There was no difference in Kara-mokiny 16 following any of the treatments of AST154 for 24 hrs. Finally, there was significantly more Kara-mokiny 16 after 24 hrs of treating AST234 with Kara-mokiny 16 alone (10⁶ or 10⁷ PFU/mL) compared to either the low or high dose cocktails. Data is represented as median±range and RM 2-way ANOVA was used with Tukey's multiple comparisons between each treatment to test for significance (p<0.05). ND denotes not detectable Kara-mokiny 16.

5.3.6 Endotoxin Levels in Phage Preparations for Primary Airway Epithelial Exposures

Filtrated stocks of 1×10^{10} PFU/mL Kara-mokiny 16 were found to have 23.4 EU/mL of measurable endotoxin. When diluted to the delivery titre of 1×10^6 PFU/mL, this meant that primary airway epithelial cells were exposed to 0.0234 EU/mL, well below the Food and Drug Administration standard for therapeutics which is <5 EU per kilogram of a person's body weight per hour [580].

5.3.7 Morphological Assessment of Differentiated Primary Airway Epithelial Cells

Gross morphologies of primary airway epithelial ALI cultures after 24 hrs of exposure to different stimuli, were assessed by histological staining and compared to the vehicle control (1X PBS; Figure 5.9 A-E). Results illustrated that all primary cultures exhibited a multilayered, pseudostratified structure (Figure 5.9 A-E) and that exposure to heat killed PAO1 did not cause gross changes compared to the PBS control (Figures 5.9 A and B). Importantly, exposure to 10^6 PFU/mL Kara-mokiny 16 did not affect epithelial structural morphology (Figure 5.9 C) nor did exposure to 2 μ g/mL tobramycin (Figure 5.9 D). Structural morphology was also maintained after exposure to the combination of 10^6 PFU/mL Kara-mokiny 16 and 2 μ g/mL tobramycin (Figure 5.9 E).

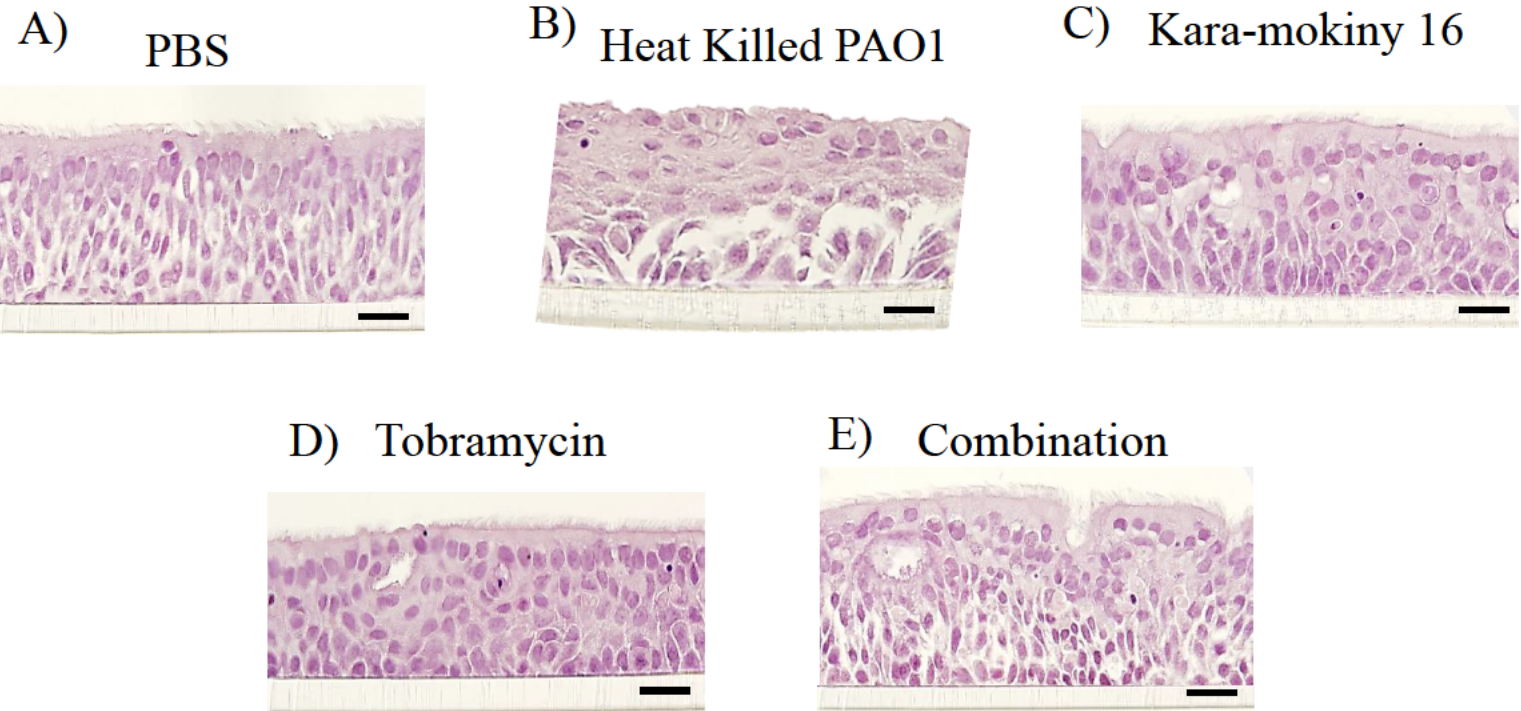


Figure 5.9 Morphological assessment of treated ALI primary airway epithelial cell cultures. Primary airway epithelial cells collected from children, were cultured for 28 days, exposed to 10^6 PFU/mL of Kara-mokiny 16 and $2 \mu\text{g/mL}$ of tobramycin alone or in combination, fixed with 10% NBF and embedded in paraffin prior to sectioning. Sections were stained with H&E to visualise the multilayered pseudostratified epithelium and cilia formation after exposure to **A)** 1X PBS control, **B)** Heat killed PAO1 **C)** Kara-mokiny 16 (10^6 PFU/mL), **D)** Tobramycin ($2 \mu\text{g/mL}$) and **E)** Combination (Kara-mokiny 16/ Tobramycin (10^6 PFU/mL/ $2 \mu\text{g/mL}$)). There was no difference in the cell structures in the ALI cultures after any of the exposures when compared to the untreated (PBS) control (A). Stained sections also showed a fully intact, multi-layered, and ciliated cellular layer after 24 hrs of exposure. Scale bar for reference at $50 \mu\text{m}$.

5.3.8 Assessment of Mucus Production by the Differentiated Primary Airway Epithelial Cells Following 24 Hrs of Exposure to Different Stimuli

Mucus on the apical surface and within goblet cells after 24 hrs of exposure to the different stimuli, was assessed via alcian blue staining (Figure 5.10 A-E) and visually compared to the vehicle control (1X PBS; Figure 5.10 A). Exposure to heat killed PAO1 did not appear to cause mucus hyperproduction, as the intensity of alcian blue staining appeared comparable to PBS (Figure 5.10 B). Similarly, exposure to 10^6 PFU/mL Karamokiny 16 (Figure 5.10 C) or 2 $\mu\text{g/mL}$ tobramycin did not alter the alcian blue staining intensity (Figure 5.10 D). Finally, similar staining intensities were observed between the combined formulation and the PBS control (Figure 5.10 E).

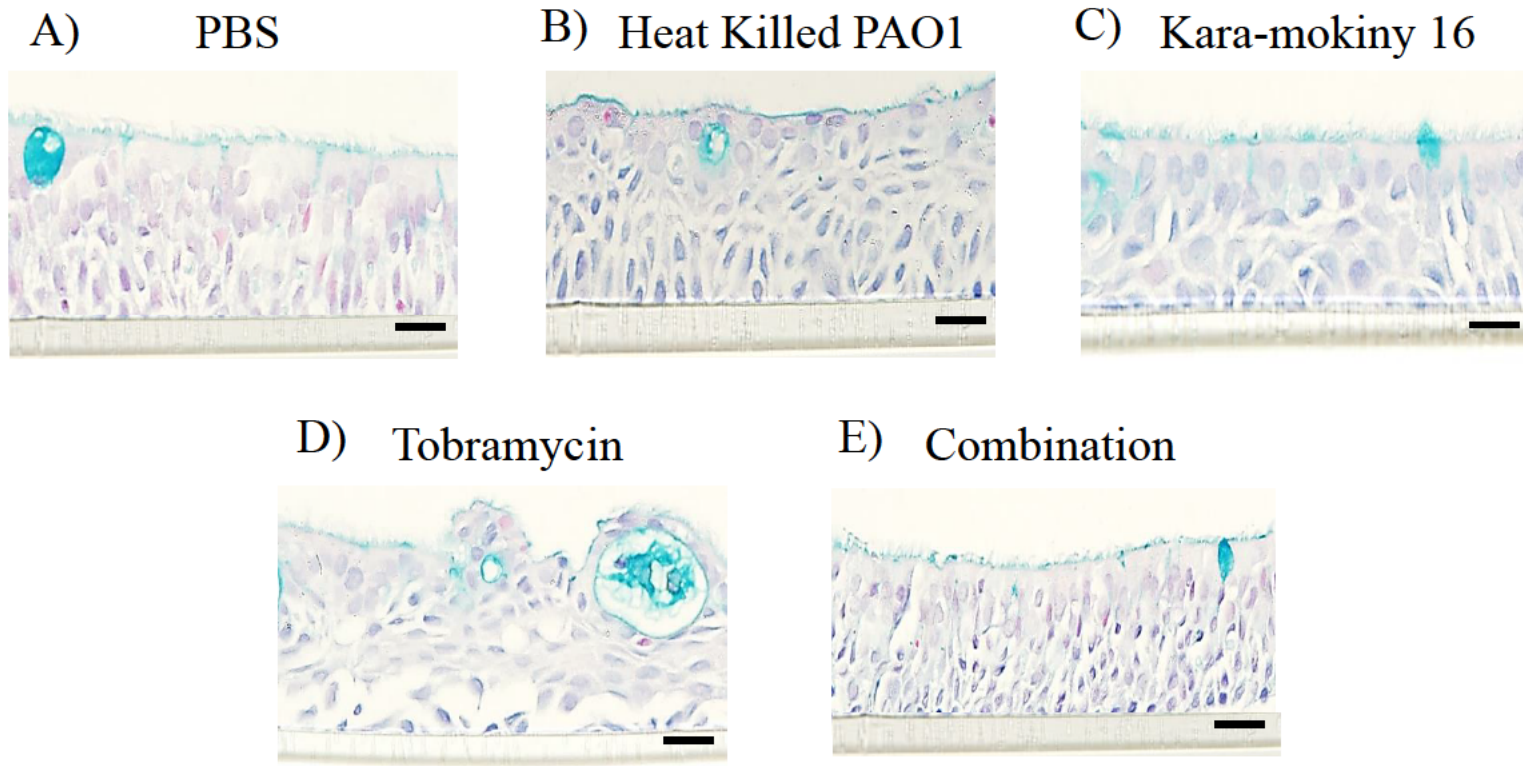


Figure 5.10 Mucus production visualisation after treatment of ALI primary airway epithelial cell cultures. Primary airway epithelial cells collected from children, were cultured for 28 days, exposed to 10^6 PFU/mL of Kara-mokiny 16 and $2 \mu\text{g/mL}$ of tobramycin alone or in combination, fixed with 10% NBF and embedded in paraffin prior to sectioning. Sections were stained with alcian blue to visualise mucus on the apical surface and within goblet cells after exposure to **A)** 1X PBS control, **B)** Heat killed PAO1 **C)** Kara-mokiny 16 (10^6 PFU/mL), **D)** Tobramycin ($2 \mu\text{g/mL}$) and **E)** Combination (Kara-mokiny 16/ Tobramycin (10^6 PFU/mL/ $2 \mu\text{g/mL}$)). There was no visible difference in the alcian blue staining of the ALI cultures that would indicate mucus hyperproduction after any of the exposures when compared to the untreated (PBS) control (A). Stained sections also showed a fully intact, multi-layered, and ciliated cellular layer after 24 hrs of exposure. Scale bar for reference at $50 \mu\text{m}$.

5.3.9 Primary Airway Cytotoxicity Stimulated by Different Exposures

Cytotoxicity in the basal (indicative of the systemic pulmonary environment) and apical (indicative of the luminal airway surface) compartments of ALI cultured primary airway epithelial cells were measured after 24 hrs of exposure to different treatments and compared to heat-killed PAO1 (Figure 5.11 A and B). Apically released LDH post exposure to heat killed PAO1 was not significantly different compared to the PBS vehicle control ($p>0.05$; Figure 5.11 A). In addition, no significant cytotoxicity was observed when primary airway cells were stimulated with 10^6 PFU/mL of Kara-mokiny 16, nor when cells were exposed $2 \mu\text{g/mL}$ of tobramycin ($p>0.05$; Figure 5.11 A). Importantly, exposure to the combination of 10^6 PFU/mL of Kara-mokiny 16 and $2 \mu\text{g/mL}$ of tobramycin did not stimulate significant cytotoxicity at the apical layer of the culture ($p>0.05$; Figure 5.11 A). Basolaterally released LDH after exposure to heat killed PAO1 did not significantly differ to the PBS vehicle control ($p>0.05$; Figure 5.11 B). Additionally, there was no significant cytotoxicity in the basal compartment supernatant stimulated by 10^6 PFU/mL of Kara-mokiny 16, $2 \mu\text{g/mL}$ of tobramycin or the combination of 10^6 PFU/mL of Kara-mokiny 16 and $2 \mu\text{g/mL}$ of tobramycin ($p>0.05$; Figure 5.11 B).

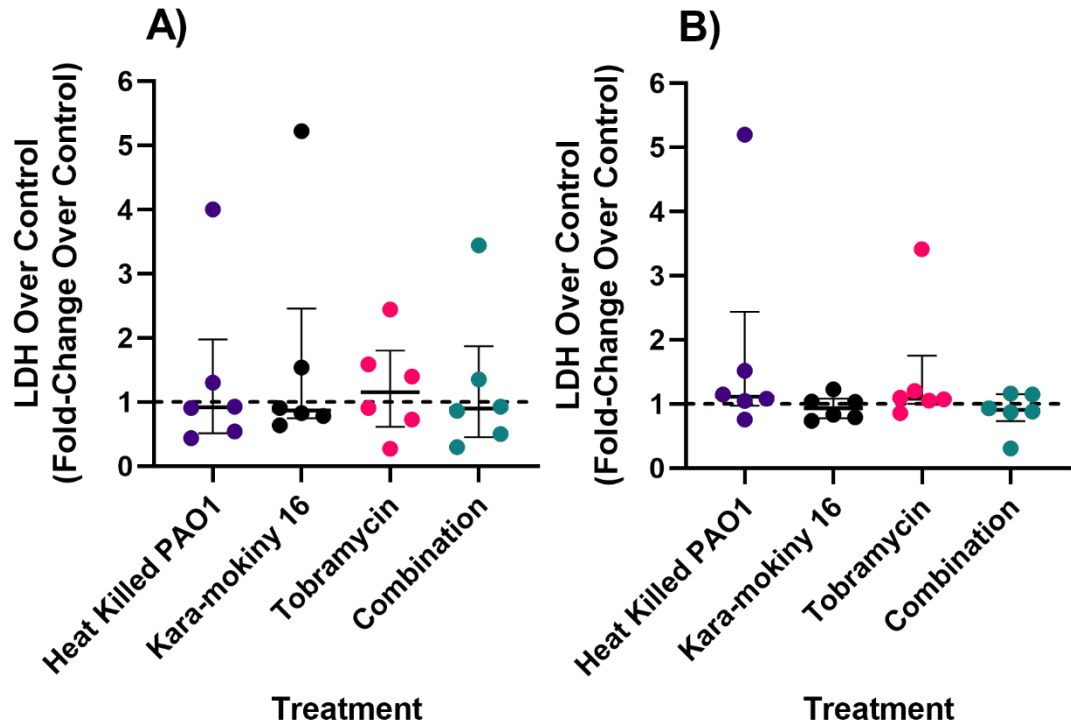


Figure 5.11 Measurable LDH levels in apical (A) washings and basolateral (B) supernatants following 24 hrs exposure to phage, antibiotics and cocktail combinations. Primary airway epithelial cells were cultured and differentiated at ALI for 30 days before being exposed for 24 hrs to heat killed PAO1, 10^6 PFU/mL of Kara-mokiny 16, 2 μ g/mL of tobramycin or Combination (10^6 PFU/mL Kara-mokiny 16 and 2 μ g/mL tobramycin). Triplicate cell culture basal supernatants or apical washings were collected and pooled and used to measure cytotoxicity via a commercially available LDH assay. No increased cytotoxicity was detected in the apical or basal compartments of the ALI cultures after exposure to any of the stimuli compared to heat killed PAO1. Data is represented as median \pm IQR and expressed as fold-change over uninfected PBS controls (dashed lines). Significance was tested by Kruskal-Wallis 1-way ANOVA with Dunn's multiple comparison tests and comparisons made to heat killed PAO1. A $p < 0.05$ was considered significant.

5.3.10 Assessment of IL-8 Produced by Primary Airway Cells Following Exposures to Different Treatments

The sentinel inflammatory cytokine, IL-8 was measured in both the apical and basolateral compartments following exposure to different phage and cocktail component treatments and compared to the heat killed PAO1 (Figure 5.12 A and B). Apically released IL-8 was not significantly elevated by exposure to heat killed PAO1 (28.61 ± 13.58 ng/mL) compared to the 1X PBS vehicle control (36.25 ± 9.01 ng/mL; $p > 0.05$; Figure 5.12 A). In addition, exposure to 10^6 PFU/mL of Kara-mokiny 16 did not stimulate significant IL-8 release apically (33.09 ± 6.92 ng/mL; $p > 0.05$; Figure 5.12 A). Furthermore, exposure to 2 μ g/mL of tobramycin did not stimulate significant IL-8 production (30.34 ± 10.96 ng/mL; $p > 0.05$; Figure 5.12 A). Importantly, the combination of 10^6 PFU/mL of Kara-mokiny 16 and 2 μ g/mL of tobramycin did not stimulate IL-8 production (37.56 ± 12.91 ng/mL; $p > 0.05$; Figure 5.12 A). Similar observations were made for corresponding basolateral compartments exposures. Specifically, IL-8 was not significantly elevated by exposure to heat killed PAO1 (42.29 ± 19.85 ng/mL) compared to the 1X PBS vehicle control (44.68 ± 20.21 ng/mL; $p > 0.05$; Figure 5.12 B). Exposure to 10^6 PFU/mL of Kara-mokiny 16 alone (45.34 ± 15.15 ng/mL; $p > 0.05$; Figure 5.12 B) or 2 μ g/mL of tobramycin did not stimulate significant IL-8 production in the basolateral compartment (38.12 ± 15.38 ng/mL; $p > 0.05$; Figure 5.12 B). Importantly, exposure to the combination of 10^6 PFU/mL of Kara-mokiny 16 and 2 μ g/mL of tobramycin did not induce IL-8 release into the basolateral compartment (42.35 ± 19.85 ng/mL; $p > 0.05$; Figure 5.12 B).

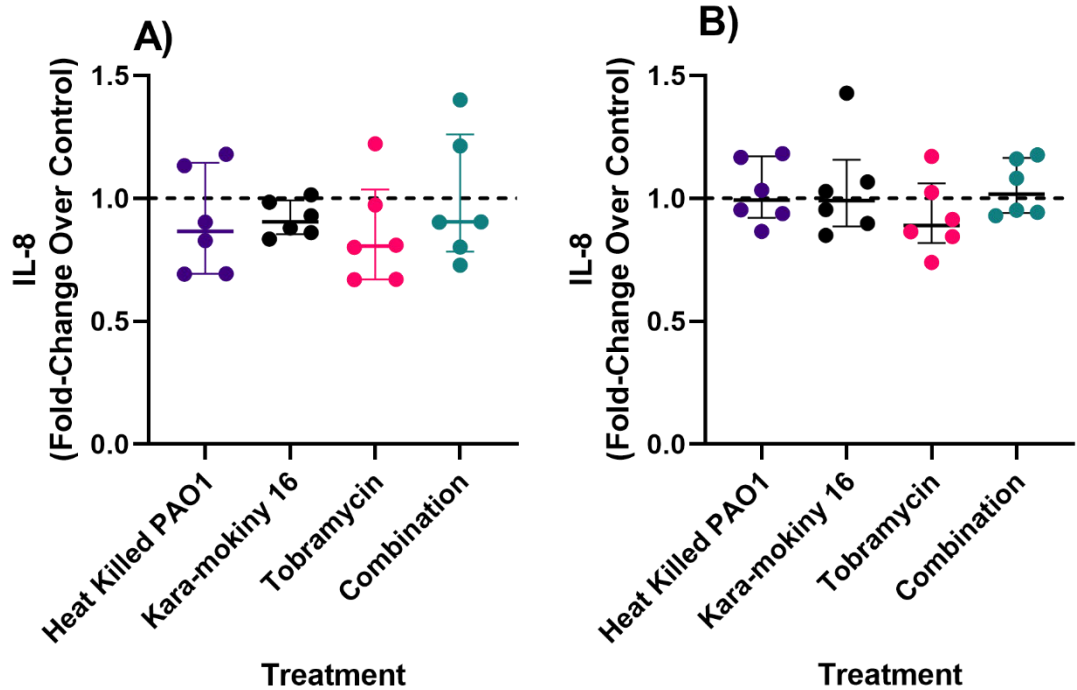


Figure 5.12 IL-8 produced ALI-cultured primary airway epithelial cells after 24 hrs of exposure to different treatments. Primary airway epithelial cells were cultured and differentiated at ALI for 30 days before being exposed to heat killed PAO1, 10^6 PFU/mL of Kara-mokiny 16, 2 μ g/mL of tobramycin or Combination (10^6 PFU/mL Kara-mokiny 16 and 2 μ g/mL tobramycin). Triplicate cell culture (A) apical washings or (B) basal supernatants were collected and pooled and used to measure IL-8 via an IL-8 ELISA. There was not any significant increase in IL-8 production apically or basolaterally after exposure to any of the stimuli for 24 hrs compared to heat killed PAO1. Data is represented as median \pm IQR and expressed as fold-change over uninfected PBS controls (dashed lines). Significance was tested by Kruskal-Wallis 1-way ANOVA with Dunn's multiple comparison tests and comparisons made to heat killed PAO1. A $p < 0.05$ was considered significant.

5.3.11 Assessment of IL-6 Produced by Primary Airway Cells Following Exposures to Different Treatments

Another sentinel inflammatory cytokine, IL-6 was also measured in both the apical and basolateral compartments following exposure to different phage and cocktail component treatments and compared to heat killed PAO1 (Figure 5.13 A and B). Apically released IL-6 was not significantly elevated by exposure to heat killed PAO1 (3.57 ± 0.66 ng/mL) compared to the 1X PBS vehicle control (3.95 ± 0.46 ng/mL; $p>0.05$; Figure 5.13 A). Additionally, exposure to 10^6 PFU/mL of Kara-mokiny 16 (3.92 ± 0.46 ng/mL) or 2 μ g/mL of tobramycin for 24 hrs did not stimulate significant apical IL-6 production (3.73 ± 0.98 ng/mL; $p>0.05$; Figure 5.13 A). Importantly, exposure to the combination of 10^6 PFU/mL of Kara-mokiny 16 and 2 μ g/mL of tobramycin for 24 hrs did not stimulate significant apical production of IL-6 (3.62 ± 0.55 ng/mL; $p>0.05$; Figure 5.13 A). Similar to the apical findings, basally released IL-6 was not significantly elevated by exposure to heat killed PAO1 (3.58 ± 0.38 ng/mL) compared to the 1X PBS vehicle control (3.61 ± 0.35 ng/mL; $p>0.05$; Figure 5.13 B). Exposure to 10^6 PFU/mL of Kara-mokiny 16 for 24 hrs did not stimulate significant IL-6 release basolaterally either (3.67 ± 0.48 ng/mL; $p>0.05$; Figure 5.13 B). Additionally, exposure to 2 μ g/mL of tobramycin (3.58 ± 0.44 ng/mL) or the combination of 10^6 PFU/mL of Kara-mokiny 16 and 2 μ g/mL of tobramycin for 24 hrs did not stimulate significant basal production of IL-6 (3.60 ± 0.39 ng/mL; $p>0.05$; Figure 5.13 B)

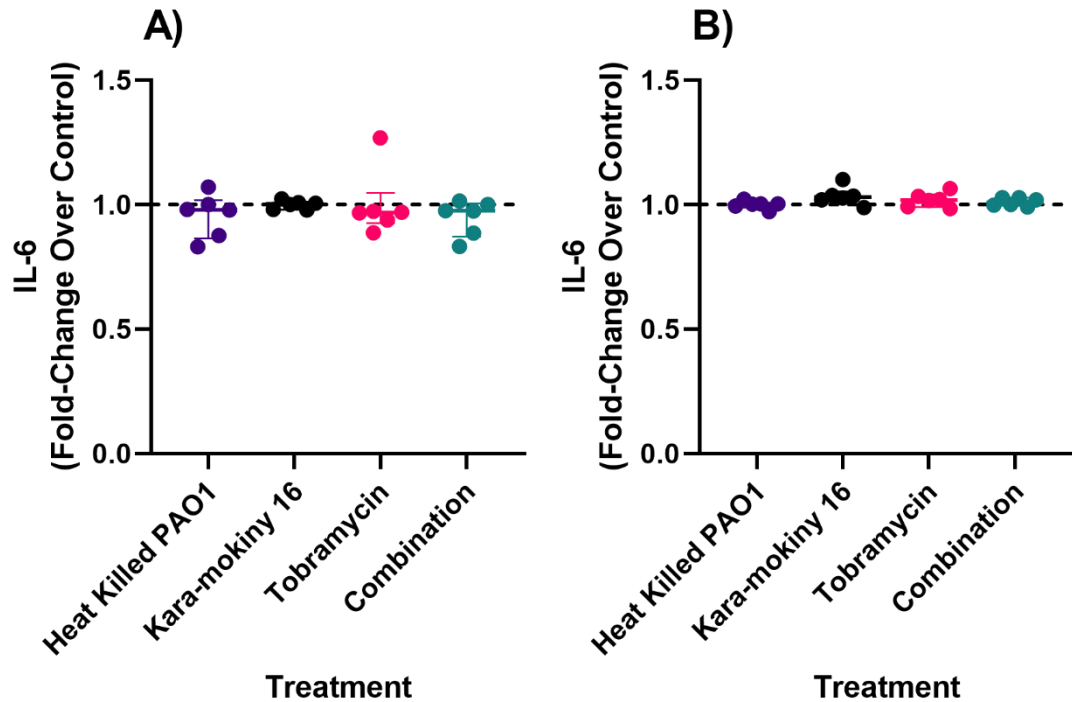


Figure 5.13 IL-6 produced ALI-cultured primary airway epithelial cells after 24 hrs of exposure to different treatments. Primary airway epithelial cells were cultured and differentiated at ALI for 30 days before being exposed to heat killed PAO1, 10^6 PFU/mL of Kara-mokiny 16, 2 μ g/mL of tobramycin or Combination (10^6 PFU/mL Kara-mokiny 16 and 2 μ g/mL tobramycin). Triplicate cell culture (A) apical washings or (B) basal supernatants were collected and pooled and used to measure IL-6 via an IL-6 ELISA. There was not any significant increase in IL-6 production apically after exposure to any of the stimuli for 24 hrs compared to heat killed PAO1. Furthermore, there was not any significant increase in the IL-6 produced and secreted basolaterally following exposure to any of the stimuli for 24 hrs. Data is represented as median \pm IQR and expressed as fold-change over uninfected PBS controls (dashed lines). Significance was tested by Kruskal-Wallis 1-way ANOVA with Dunn's multiple comparison tests and comparisons made to heat killed PAO1. A $p < 0.05$ was considered significant.

5.3.12 Phage Titres Following Exposure to ALI Cultured Primary Airway Epithelial Cells

To determine the fate of phages applied to the primary airway epithelial cells, apical washes and basal supernatants were collected after 24 hrs of exposure to different stimuli and used to enumerate Kara-mokiny 16. There was no Kara-mokiny 16 detected in the apical washing of cultures exposed to the 1X PBS vehicle control (Figure 5.14 A). No phages were detected in apical washings of cultures exposed to heat killed PAO1 (Figure 5.14 A). However, phages were recovered from the apical washes of inserts exposed to Kara-mokiny 16 but was not significantly different when compared to the amount originally exposed to the cells ($p>0.05$; Figure 5.14 A). Phages were also not detected in apical washings of cultures exposed to 2 $\mu\text{g/mL}$ of tobramycin (Figure 5.14 A). Phages were detected in the apical washings of cultures exposed to the combination of 10^6 PFU/mL Kara-mokiny 16 and 2 $\mu\text{g/mL}$ tobramycin but again, this was not significantly different to the original concentration exposed to the cells ($p>0.05$; Figure 5.14 A). When the amount of Kara-mokiny 16 was measured in the basal supernatants there was not any detected in the cultures exposed to the 1X PBS vehicle control (Figure 5.14 B). No phages were detected in the basal media of cultures exposed to heat killed PAO1 (Figure 5.14 B). Phages were also not recovered from the basal media of inserts exposed to Kara-mokiny 16 (Figure 5.14 B) nor when exposed to 2 $\mu\text{g/mL}$ of tobramycin (Figure 5.14 B). Finally, Kara-mokiny 16 was also not detected in the basal media of cultures exposed to the combination of 10^6 PFU/mL Kara-mokiny 16 and 2 $\mu\text{g/mL}$ (Figure 5.14 A). Therefore, phages were only recovered from the inserts that were exposed to Kara-mokiny 16. Furthermore, there was no loss of Kara-mokiny 16 compared to the amount originally added and no phages migrated through the cell layers.

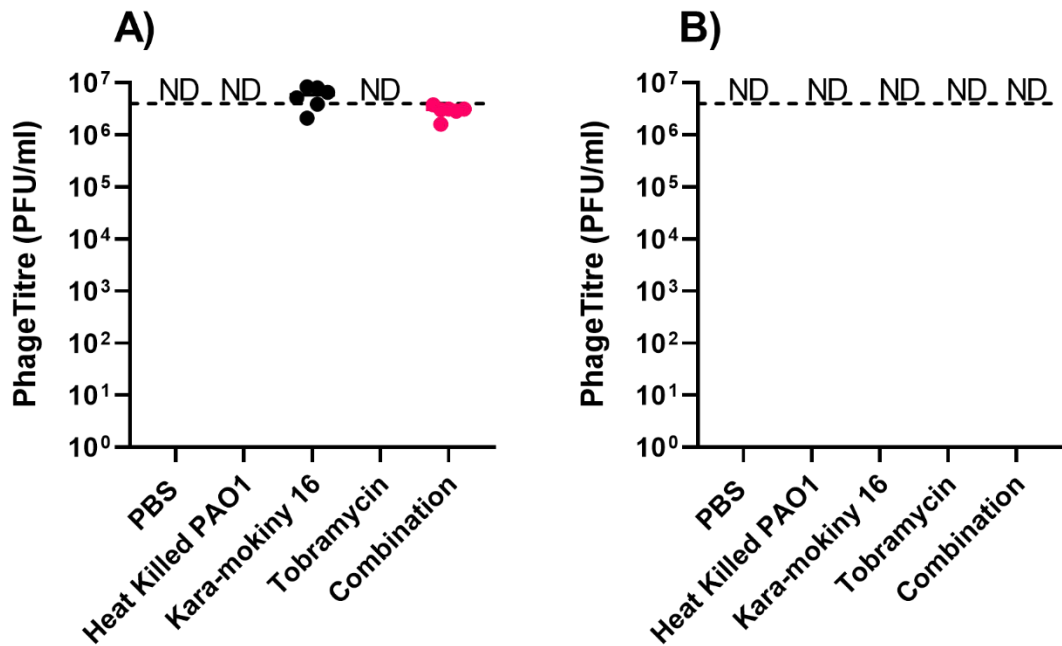


Figure 5.14 Phage titres in ALI-cultured primary airway epithelial cell cultures after 24 hrs of exposure to different treatments. Primary airway epithelial cells were cultured and differentiated at ALI for 30 days before being exposed to 1X PBS, heat killed PAO1, 10^6 PFU/mL of Kara-mokiny 16, 2 μ g/mL of tobramycin or Combination (10^6 PFU/mL Kara-mokiny 16/2 μ g/mL tobramycin). Triplicate cell culture **A)** apical washings or **B)** basal supernatants were collected and used to titre Kara-mokiny 16. Kara-mokiny 16 was only detected from the apical surface of the ALI cultured cells exposed to 10^6 PFU/mL of Kara-mokiny 16 or when it was combined with 2 μ g/mL tobramycin. These titres were not significantly different to those that were initially applied to the cells. There was not any Kara-mokiny 16 detected in the basal supernatants of ALI cultures exposed to 10^6 PFU/mL of Kara-mokiny alone or when it was combined with 2 μ g/mL tobramycin. There was no Kara-mokiny 16 detected on the apical surface or basal supernatants of the ALI cultures exposed to PBS, heat killed PAO1 or 2 μ g/mL of tobramycin alone. Data is represented as median; each point represents a different primary cell donor, and the dashed line is the phage concentration added to the cells. Significance was tested by Kruskal-Wallis 1-way ANOVA with Dunn's multiple comparison tests and comparisons made to original concentration added to the cells. ND denotes not detectable Kara-mokiny 16. A $p < 0.05$ was considered significant.

5.4 Discussion

In this chapter, the potential bactericidal effects of a cocktail combination comprising of Kara-mokiny 16, and tobramycin was explored, followed by its preclinical safety assessment using a 3-dimensional model of the lung. Firstly, results generated identified that 10^7 or 10^6 PFU/mL Kara-mokiny 16 combined with 2 $\mu\text{g/mL}$ of tobramycin had an additive bactericidal effect on AST154. When these combinations were used to treat M1C79, AST154 and AST234 and compared to the components alone, the combination performed better for M1C79 and AST234 but had a similar effect to Kara-mokiny 16 alone when used against AST154. Safety assessment of singular components as well as the combination of 10^6 PFU/mL and 2 $\mu\text{g/mL}$ of tobramycin was then tested using a primary airway epithelial ALI culture model. Results showed that neither Kara-mokiny 16 or the combination treatment induced, morphological alterations, cytotoxicity, IL-6 or IL-8 production. Collectively, work performed in this chapter has utilised CF clinical bacterial isolates to investigate the combination of phages and antibiotics to suppress resistance. Furthermore, it is the first to establish a preclinical safety profile for Kara-mokiny 16 in singularity or in combination with antibiotics, when exposed to primary airway epithelial cells cultured at the air-liquid interface.

Results from Chapter 4 identified that the combination of Kara-mokiny 16 and tobramycin had potential to prevent phage resistance occurring. As a result, this combination was investigated in more detail within this chapter. Checkerboard assays were initially performed to identify concentrations of Kara-mokiny 16 and tobramycin that would work together against the most antibiotic resistant *P. aeruginosa* isolate AST154. Results identified two additive concentrations of Kara-mokiny 16 with 2 $\mu\text{g/mL}$ of tobramycin, which was well below the minimum inhibitory concentration (MIC) of 16 $\mu\text{g/mL}$ for AST154. Previous work conducted has reported phage-antibiotic pairing that can reduce bacterial MIC to antibiotics [323, 525, 581-584]. Relevant to this study, it has previously been demonstrated that phages and tobramycin can prevent resistance occurring and be used at a reduced MIC [279, 285]. Reductions in MIC are perceived as beneficial since in order to achieve clinical improvement in over 90% of patients, aminoglycoside peak serum concentrations 8-10 times higher than the pathogen's MIC must be attained [585]. With results generated in this chapter showing efficacy at a reduced MIC, it suggests that peak serum concentrations of tobramycin required to ensure reliable clinical improvement may be lowered. Lower tobramycin concentrations will

reduce the risks of side effects such as ototoxicity as well as nephrotoxicity that can result from prolonged high dose aminoglycoside therapy [586, 587]. However, there were only marginal improvements in suppression of M1C79 and AST234 after combination treatment and no improvement over Kara-mokiny 16 alone in the treatment of AST154. The difference in response to the combination treatment could be related to initial *P. aeruginosa* isolate susceptibility to tobramycin, as M1C79 and AST234 were sensitive and intermediately sensitive whereas AST154 was resistant. Perhaps, this could be improved by increasing the concentration of tobramycin closer to the *P. aeruginosa* MIC. In support of this it has been previously demonstrated that synergistic effects of phages and tobramycin are observed at the MIC of the *P. aeruginosa* isolate being treated [279, 285]. Additionally, a stepwise treatment could be utilised where phages are used initially and then followed by tobramycin to eradicate any surviving *P. aeruginosa* [326, 588]. Whilst there is optimisation of the combination still required, given that 60-70% of people with CF are given inhaled tobramycin [589], its safety with concurrent phage therapy was still investigated.

In this chapter, safety of singular phage and tobramycin treatments as well as their combination, was evaluated. This required the removal of endotoxin from preparations since phage propagation lyses bacteria releasing Lipopolysaccharide (LPS), the potent inflammatory component of the *P. aeruginosa* cell membrane [590, 591] and exposure to high levels can lead to septic shock [592]. Beyond the immediate detrimental effects of endotoxin exposure, inhalation of lower levels of LPS over a longer period is associated with lung function decline and respiratory diseases like chronic bronchitis and asthma [593-595]. Therefore, to mitigate any detrimental effects endotoxin can have on the human body many methods including chromatography, organic extraction and cesium chloride density centrifugation have been used in the case studies applying phages to humans [290-294, 302-316, 596]. Whilst fevers and other self-limiting minor side effects are common in phage therapy it is often thought that this is a result of the phage-mediated bacterial lysis [293, 294, 302, 304, 309, 315, 596]. However, in one case study that recognised phage therapy was not adequately purified, fever, wheezing, and shortness of breath were observed shortly after treatment was administered [293]. Once treatment was diluted, symptoms stopped and the authors postulated that either other pyrogens or chemical solvents from the production process were contaminating the preparation [293]. Other pyrogens from bacterial lysis like DNA, peptidoglycan and toxins can be present in phage preparations and stimulate the human immune system [597-600]. As shown in

a review of the reported characteristics of phage preparations that were used in both *in vitro* and *in vivo* studies, pyrogens other than endotoxin are not part of routine screening [601]. Given no inflammation or cytotoxicity was observed after exposure to phages in this chapter, it appears that these were sufficiently depleted. However, in the future it would be important to check for these by running the phage preparations on DNA and protein electrophoresis gels to identify bands that suggest contamination [601]. Furthermore, organic chemicals are often used to remove endotoxin from phage therapy preparations and subsequently need to be eliminated [602, 603]. The issue of organic solvent contamination was circumvented in this chapter by endotoxin depletion using a simple commercially available syringe filter that was able to purify the phage preparation to below the Food and Drug Administration standard for therapeutics of <5 EU/kg [580]. However, in the future the purification of phage treatments will need to be scaled up using a different method to be used in people. The purification performed here ensured that any inflammatory response was not due to endotoxin contamination of the phage sample.

Viral and bacterial infection of the airways cause cell death via several apoptotic pathways [125, 410, 604-607]. These pathways are commonly dysregulated in chronic respiratory conditions like CF or chronic obstructive pulmonary disease (COPD) occurring more frequently or aberrantly leading to heightened inflammation [125, 410, 606]. AMR infections are frequent in people with these chronic respiratory conditions and therefore have the greatest need for phage therapy, so it is necessary that the treatment does not lead to more cell death and inflammation [125, 410, 606]. Importantly, Karamokiny 16 alone or combined with tobramycin did not elicit any cytotoxicity from the primary airway epithelial cells which are known to undergo cell death in response to stimuli [125, 410, 579]. Whilst this is promising, the airway epithelium is also capable of signalling immune system while alive.

An important sentinel cytokine produced by the airway epithelium in response to infections is IL-8 [125, 408, 410, 608, 609]. Like cytotoxicity, IL-8 is also elevated in people with CF or COPD, and it is often a factor contributing to their disease progression [114, 117, 610, 611]. In these conditions prolonged high levels of IL-8 attract neutrophils which fail to clear the cause of the signals and instead release tissue damaging proteases [114, 117, 612, 613]. Therefore, it is important that phages do not elicit IL-8 so that they do not contribute to the lung damaging processes. Although it has been demonstrated that ALI-cultured primary airway epithelial cells produce IL-8 in response to stimuli [262,

408, 410, 574, 578, 579], Kara-mokiny 16 alone or combined with tobramycin did not elicit an increase IL-8 production either systemically (basolaterally) or luminally (apically). However, IL-8 is only one of the cytokines produced by the epithelium, so IL-6 was also measured. The expression of IL-6 is also increased within the airways upon infection [408, 574, 575, 614]. It has also been implicated in asthma, CF and COPD where it is elevated in the airways [572, 615-617]. Given that the prevalence of asthma is between 5 and 10% globally it is likely that at some point in the future someone with this condition will receive phage therapy for an unrelated infection [618]. Thus, in order to not exacerbate either asthma, CF or COPD phages should not cause production of IL-6 in the airways. Results here suggested that exposure to phage or combination do not cause IL-6 to be secreted onto the apical side of the primary airway epithelial cell cultures which represents the airway lumen. Likewise, there was not any significant increase in IL-6 production and secretion basolaterally from the ALI-cultured airway epithelial cells indicating that there would not be systemic inflammation either. This is encouraging as it is well established that ALI-cultured primary airway epithelial cells produce IL-6 in response to stimuli [408, 574-577, 579]. Beyond an innate immune response, there is the potential for an adaptive response to be mounted which is more likely to occur if phages can pass from the lungs into the bloodstream and circulate systemically. Therefore, it becomes important to assess whether phages can pass through the airway epithelium.

There was no passage of phages through the epithelial barrier over the course of exposure indicating that barrier integrity was not affected by the phages. An intact airway epithelial barrier is important to protect against both allergens and pathogens [562, 619-621]. The lack of passage of phages through the epithelium also suggests that there may be no systemic circulation if administered via nebulisation. This supports previous data where nebulised phage therapy in a pig infection model of *P. aeruginosa* did not return systemically circulating virions [622]. Although not specifically assessed here, given that there was not a significant loss of phage titre over 24 hrs there does not appear to be large scale endocytosis of phages into the epithelial cells, which could limit their effectiveness [571]. This is contrary to previous studies which have shown phages are internalised into epithelial cells via micropinocytosis which can lead to their degradation, transcytosis across cell layers and activation of the innate immune system [623, 624]. Interestingly, in these studies it was the airway cell lines that were amongst those that most readily internalise phages [571, 623]. The differences in findings could be due to the use of primary and immortalised cells, which it has been well established behave differently

[125, 402-404, 572, 573]. Additionally, it could be that Kara-mokiny 16 is not internalised because the amount of endocytosis occurring has been observed to differ between phages [571]. Therefore, further sensitive testing with a labelled phage to visualise its localisation would be required to elucidate the differences in findings [571]. Whether phages are internalised into airway epithelial cells or transported across the cell layer may determine the utility of nebulised phage therapy. If phages are indeed restricted to the airway lumen when nebulised it would be beneficial for therapy because it is the site of bacterial colonisation during respiratory infections. It also limits the ability of the adaptive immune system to mount a response that could prevent phage therapy efficacy by neutralising virions with an antibodies [316, 625-628]. Together, these results indicate that when phages are nebulised, they will remain in the airway lumen and provides rationale for testing in a more complex model such as an *in vivo* rodent model. An *in vivo* model would allow several of the findings about phage localisation, antibody response and safety to be further investigated.

This study was limited by the lack of induction of inflammatory cytokines or cytotoxicity in the presence of a positive control. Whilst it was assumed that heat killed PAO1, should contain many inflammatory molecules and therefore stimulate cytotoxicity, IL-6 or IL-8 this has since been found to not be the case and it did not stimulate inflammation as was found in this chapter [629-633]. Due to the airways being exposed to bacteria with every breath, the body discriminates between threats and undertakes a heightened response to live *P. aeruginosa*, which does not occur when the bacteria are heat killed [633]. The paucity of a positive LPS inflammatory response therefore limits the conclusions that can be drawn for the primary airway epithelial cell model regarding the safety of phages. However, it has been well established that differentiated primary airway epithelial cells produce cytokines and undergo cell death in response to stimuli so the lack of stimulation by the phage treatments is still promising [262, 405, 408, 410-412, 416, 574-579]. In the future, stimulation could be achieved by phage treatment of a live *P. aeruginosa* infection of the airway. Such a study would allow simultaneous assessment of phage efficacy and safety as well as the evolution of phage resistance within a more complex environment that would provide greater selection pressures. Assessing phage resistance evolution after an infection of cells or animals has been treated constrains how resistance can arise [308, 330, 396, 634]. Additionally, in the present study safety was evaluated using primary cells collected from healthy individuals; in the future phages should be exposed to cells collected from people with CF [405]. Airway epithelial cells collected from people with

CF have been shown to react with heightened inflammation and cell death to pathogens and it would be important to determine whether phages are still safe in a disease setting [125, 410]. Once phage safety has been demonstrated in the targeted population, they could be applied to an animal model such as the mouse chronic lung *P. aeruginosa* infection model [277]. This model allows *P. aeruginosa* to become adapted to the host airways and form biofilms, mimicking what occurs in people with CF [277]. Furthermore, utilising an *in vivo* model would allow phage therapy's interaction with other cell types, any adaptive immune response to the virions, safety and efficacy to also be investigated.

In summary, this chapter assessed two Kara-mokiny 16-tobramycin combinations for their ability to suppress phage resistance in three *P. aeruginosa* clinical isolates. Whilst some resistance suppression was observed, further work is needed to optimise the concentration of tobramycin to improve the observed effect. Importantly, work conducted here is one of the first studies to measure the ALI-cultured primary airway epithelial cell inflammation and cytotoxicity stimulated by exposure to phages. There was no cell death or inflammation observed and the phages did not penetrate the epithelial barrier. Collectively, these results suggest that Kara-mokiny 16 combined with tobramycin has promise in effectively treating *P. aeruginosa* and will be tolerated by the airways.

This page is intentionally left blank.

6. Chapter 6: General Discussion

6.1 Summary of Findings

In this thesis we set out to isolate novel bacteriophage active against clinically relevant *P. aeruginosa* isolated for potential use in phage therapy treatment of cystic fibrosis. We isolated over 250 phages and sequenced the genomes of the 20 most broad acting. We further characterised the 20 phages at a genomic level using short-read sequencing. We selected four diverse phages and identified their receptors, stability at different temperatures and pHs as well as their burst size. These phages (Kara-mokiny 8, 13, 16 and Boorn-mokiny 1) were found to have potential to be used therapeutically. In one of the first studies of its kind to be conducted (Chapter 4) these phages were then used to treat three CF clinical isolates of *P. aeruginosa* to assess the evolution of phage resistance. It was found that resistance in these isolates was mediated by genetic mutations that affected the phage's receptor, however, the number that each clinical CF isolate acquired in response to phage treatment differed. Overall, phage resistance was associated with a decreased MIC to tobramycin. This result implied that combination of phages with tobramycin could prevent phage resistance. Therefore, in Chapter 5, the bactericidal relationship between different combinations of tobramycin with Kara-mokiny 16 was tested and results generated showed that 10^6 or 10^7 PFU/mL with 2 μ g/mL of tobramycin additively reduced *P. aeruginosa* growth. These combinations were then tested for their ability to suppress the evolution of phage resistance over 24 hrs of treatment and compared to treatment components alone. In support of the second hypothesis, suppression of resistance was observed in 2 out of the 3 CF *P. aeruginosa* isolates. Subsequent preclinical safety studies showed that 10^6 PFU/mL with 2 μ g/mL of tobramycin on ALI cultured primary airway epithelial cells did not induce any cytotoxicity or inflammation (IL-8 or IL6). Collectively, findings from this thesis indicate that the phages as well as the combinations investigated have the potential to be used therapeutically to treat *P. aeruginosa* infections.

As the concern around AMR infections grows, so does the use of phages to treat people on a compassionated basis [290-294, 302-316]. Most of these have been successful, with few minor side effects and often resolution of infections. Despite this, phage therapy has yet to be broadly applied [635, 636]. This discussion will outline several pertinent questions about the challenges faced in making phage therapy a widespread treatment.

6.2 Is phage resistance a significant problem?

Bacteria readily become resistant to phages *in vitro* but this is often accompanied by reduced virulence [275, 282, 323, 325-330, 379]. However, it has been previously shown that the evolution of phage resistance is different between bacteria growing *in vitro* and in their natural environment [637, 638]. It has been suggested that these differences are due to selection pressures in the bacteria's natural environment that increase the fitness costs of phage resistance mutations and make them non-viable [637, 638]. However, a recent study of phage resistance evolution against *P. aeruginosa* *in vitro* and *in vivo*, illustrated similarities at the molecular level, and the authors concluded that laboratory assays could in fact be used to predict phage treatment outcomes [308]. However, important caveat observations were made, namely that the bacteria was not eradicated and phenotypic changes were exaggerated *in vitro*, whereas complete decolonisation was achieved after four days *in vivo* [308]. Again, this was attributed to the existence of greater selection pressures such as the microbiota that outcompeted phage-resistant *P. aeruginosa* and immune system clearance of any avirulent phage-resistant variants [308]. In support of this assertion, the importance of the immune system in removing bacteria that have become phage-resistant has been demonstrated in rodent model studies and supported by mathematical modelling [276, 639, 640]. AMR infections are predominantly a secondary morbidity in people with underlying conditions, hence the immune system and microbiota may not be capable of eradicating the phage-resistant bacteria [10]. Yet, in compassionate cases to date, phage-resistant bacteria have rarely occurred and where identified, phages have been exchanged for others that are still active [293, 299-302]. As phage therapy becomes more widespread and routine, the number of treatments resulting in resistance may also increase. However, given their abundance [232] it is likely there will be phages with activity against the bacteria that evolve phage resistance. Therefore, if resistance is recognised early, phages can be exchanged in a timely manner thus overcoming phage resistance. Timing is critical with current estimates of phage identification/matching to clinical treatment being ~170 days in America [293]. With many patients suffering from life-threatening infections, a short turnaround time to treatment is essential. Thus, preventing phage resistance may be one approach that would mitigate having to go through the phage identification/matching and production process where there is significant lag time, more than once. Although phage resistance is not a significant issue currently, it may become more frequently recognised as phage therapy

becomes more widespread. Therefore, it needs to be studied more extensively so that strategies to prevent it when treating patients are available.

6.3 Is the model used to investigate phage resistance representative?

In this thesis, resistance to phages was investigated in planktonically growing pure cultures of *P. aeruginosa*. Outside the laboratory, bacteria rarely exist in this state and are frequently part of polymicrobial communities, often biofilms, and these can offer a range of fitness advantages including antibiotic resistance [641-647]. It is often observed that despite *in vitro* susceptibility to antibiotics, treatments fail or underperform, which is attributed to biofilm formation and multispecies interactions [648, 649]. Therefore, planktonic phage resistance may not reflect that occurring when the same bacteria are growing in a biofilm and are able to interact with other species. Currently, there have been only a few studies exploring phage resistance evolution during treatments of biofilms, and none when polymicrobial [379, 650, 651]. Findings identified a complex interaction between phage-susceptible and -resistant bacteria influenced by nutrient availability, frequency of resistant cells and phage diffusion through the matrix [650, 651]. A study that mimicked CF airway *P. aeruginosa* aggregate formation *in vitro*, found that the biofilm matrix occluded phage infection although bacteria were in fact susceptible [652]. Instead, phages were found to target the planktonically *P. aeruginosa* that shed from the aggregates, preventing dispersal and further communities to be established [652]. However, in another study, numerous mutations were observed following phage treatment of *P. aeruginosa* biofilms grown on abiotic surfaces, suggesting that the phages exerted a selection pressure on the bacteria [379]. These mutations were similar to those from this thesis and often in genes responsible for the phages' receptors, affecting LPS, type IV pili and flagella [379]. The similarity between resistance formed by planktonic bacteria in this thesis compared to that from sessile *P. aeruginosa* is promising, yet it is unclear how representative the biofilms grown on plastic are of those found *in vivo*. The lack of investigation of phage resistance using models of biofilms and/or polymicrobial infections likely stems from the complexities in establishing these models and determining the mechanisms of resistance from them. However, polymicrobial infections do not just impact the development of phage resistance but also increase the complexities of therapy by compounding the number of bacteria that must be targeted.

The prevalence of polymicrobial infections differs depending on the patient population but in general they account for ~11-15% of blood stream, 5-52% of urinary tract, 22% of diabetic foot ulcer and 60% of CF airway infections [653-658] and phages have already been used to treat these types of infections [659-661]. In this setting, a phage cocktail targeting numerous pathogens would understandably be required in order to prevent a bacteria not being targeted from dominating. This assertion is supported by a study that attempted to treat a polymicrobial chronic bone infection consisting of *Clostridium hathewayi*, *Proteus mirabilis*, *Finnegoldia magna* and *S. aureus* [660] using a phage cocktail targeting only *S. aureus* [660]. Despite some improvement, treatment failed, and it was suggested that incomplete coverage of the pathogens involved was responsible [660]. In contrast, a number of polymicrobial diabetic foot infections have been successfully treated with only a *S. aureus* phage, with the authors concluding that this was due to it being the main pathogen in this infection setting [661]. Thus, it remains unknown whether all pathogens in a polymicrobial infection need to be targeted by a phage cocktail. In the setting of CF, the focus of this thesis, *P. aeruginosa* and *S. aureus* co-infection occur in ~60% of individuals [657, 658]. Given both *S. aureus* and *P. aeruginosa* are recognised pathogens in CF and impact lung disease future work should focus on a phage cocktail that can treat these pathogens in a polymicrobial setting [134, 662-667]. The increasing complexity of the models required to investigate phage resistance evolution will need to be facilitated by new methods that allow quicker and more sensitive analyses.

6.4 Increasing Phage Screening Throughput

Methods utilised to investigate phage resistance are extremely time consuming and require a lot of resources. Additionally, many methodologies used lack sensitivity. As a result, several novel approaches are being explored that could modernise phage research methodologies allowing greater sensitivity which could lead to improvements in the investigations of resistance.

6.4.1 Transposon Insertion Sequencing Libraries

Transposon insertion sequencing is a relatively new method that allows high-throughput screening of the effects of every bacterial genomic component on a selection pressure, such as phage infection [668]. There are four main kinds of insertion sequencing,

transposon-directed sequencing (TraDIS), insertion sequencing (INSeq) and high-throughput insertion tracking (HITS) [557, 558, 668]. While there are differences between each technique, they follow a similar approach of inserting transposons with selectable markers into the genomes of the bacteria within a population [558, 668], with those containing transposons being selected and pooled [558, 668]. Genomes are then fragmented, and adaptors added to each end of the transposons, before PCR and sequencing allows the position of each to be determined [558, 668]. The outcome is a population of bacteria with transposons in different genes that prevent their functioning [550, 558, 668]. Thus, when selection pressures, like phages are applied to the bacterial population, only those with transposons (knocked out genes) that increase their fitness will survive [550, 558, 668]. Sequencing the transposons and determining those that have increased abundance compared to controls then allows which genes are important for bacterial fitness in the presence of the selection pressure [550, 558, 668]. Transposon insertion sequencing has only been used by a few studies to investigate phage resistance [550, 557, 558, 669]. This has the benefit that it can identify genes that are important for phage infection beyond the receptor binding stage and may not be observed through normal phage treatment and isolation of surviving mutants [550, 557, 558, 669]. In one of the most comprehensive studies of phage resistance using insertion sequencing, random-barcode transposon sequencing (RB-TnSeq) [670] was used alongside CRISPR interference (CRISPRi) [671] and dual-barcoded shotgun expression library sequencing (Dub-seq) [550, 672], allowing complimentary information regarding host bacterial factors that were important for phage infection to be obtained. Specifically, RB-TnSeq allowed the effect of gene loss of function to be measured [550]. However, it is limited to genes that are non-essential for bacterial survival to be evaluated [550]. The CRISPRi method allowed the partial loss of function of genes to be evaluated and therefore could identify genes that were either essential or non-essential genes to bacterial survival [550]. Finally, the Dub-seq technique measured the effects of gene gain of function and dosage on phage infection [550]. Collectively, the three complimentary techniques enabled host bacterial factors required for phage infection to be comprehensively determined, such as genes encoding phage receptor, protein synthesis and regulatory mechanisms [550]. In the future, these methods could be employed to replace those currently used (Chapter 4) to identify more genes that are important for phage infection and reduce the noise of off-target mutations. As insertion sequencing techniques become more widespread, they will be important in comprehensively determining bacterial genes required for phage infection and therefore indicate potential mechanisms of phage resistance.

6.4.2 Flow Cytometry

One rapid method recently developed for determining bacterial antibiotic susceptibility using flow cytometry could be easily adapted to phage therapy [673]. Briefly, this uses a dye that binds to DNA and a viability stain to tell if bacteria pre-incubated with antibiotics are susceptible to them [673]. This method was able to correctly classify the antibiotic susceptibility of five different bacterial pathogens, almost 95% of the time and produced results within 3-6 hrs compared to the conventional time of 1-3 days with culturing and broth microdilution susceptibility testing [673]. Flow cytometry for phage therapy has been trialled previously and measured by looking at changes in cell shape and cell wall density or staining with live/dead dyes [674, 675]. However, these methodologies do not seem as sophisticated and there does not appear to be concordance between culture and flow cytometry methodologies [674]. Flow cytometry could be used to study phage resistance and would allow earlier detection of resistance with greater sensitivity than current optical density-based methods. Optical density can be affected by a number of technical factors and bacterial factors that can influence its performance and its reproducibility [676]. The use of stains and measurement with lasers is more specific for what it is measuring and would therefore overcome many of these limitations. In the future if this technique is developed, then potentially more stains could be added for other components of the bacteria allowing more insight to be gained from its use. For example, a stain for CRISPR components could be added that would allow bacteria that were resistant via this system to be differentiated from those that were resistant due to receptor mutations. In addition, sampling a phage infected bacterial culture at different timepoints could allow the shift in the population to be visualised. In the past, stains have been developed to investigate different bacterial characteristics via flow cytometry [677]. However, this is complicated by the fact that bacteria are small which affects the signal that can be derived as well as the fact that bacteria have mechanisms that enable them to occlude or extrude molecules that are recognised as toxic (e.g., stains) [677]. Thus, the use of flow cytometry remains promising for phage research and warrants further development.

6.4.3 Artificial Intelligence Algorithms

Another exciting field that could revolutionise phage research is artificial intelligence (AI). This is currently used in phage research to classify phage lifecycles based on

genomic sequences [678, 679], identify phage receptor binding proteins [556], determine the host specificity of a phage [680] and predict phage activity against a bacteria based on sequencing [681]. Potentially, an AI model could be trained on data similar to that contained in Chapter 4, describing how a diverse set of bacteria become resistant to a distinct set of phages and the associated fitness costs. Then, given a phage and bacteria the AI could predict the likely mechanism of resistance and the fitness cost. This would mean that phage resistance experiments would only need to be done on a representative dataset of phage and bacteria in order to train the model. However, this model is not feasible yet and efforts are initially being focused on using AI to predict if a phage can infect a bacterial strain/isolate [681, 682].

Using AI to match bacteria to an active phage has the potential to revolutionise phage therapy because it eliminates the need to culture bacteria and perform phage susceptibility testing [681, 682]. A functional AI model could determine a phage's activity against a bacteria based solely on their genomic sequences. [681, 682]. Hence, the time required for selection of phages would only be the time it takes to perform sequencing. Platforms currently used, vary in the time it takes to sequence samples [683]. For example, short read Illumina sequencing takes up to four days [683], whereas PacBio long read sequencing takes ~30 hrs and a complete nanopore run only takes 48 hrs [683]. However, with improvements in nanopore technologies and real time sequencing, a complete bacteria can actually be sequenced and assembled in a couple of hrs [683, 684]. This would facilitate a more rapid administration of phage therapy which has previously taken a median time of 170 days in America [293]. It would also enable more phages to be screened for activity because there would no longer be a need to carry out manual microbiology testing. An AI model that has been developed recently for this purpose, relied on a well-defined phage and host (*Klebsiella pneumoniae*) interaction [681]. Here, phages use the *K. pneumoniae* capsule as their receptor which is well understood [685], and programs exist for classifying, typing and identifying the genes that are responsible for its biosynthesis in the bacteria [686]. However, it may not be as easy for *P. aeruginosa* phages which can target multiple receptors (LPS, pili and antibiotic efflux pumps) and the biosynthesis genes are complicated or poorly defined due to horizontal gene transfer and high levels of variability [323, 379, 687]. It is likely that whilst AI models will start with phage receptors they will be enhanced to account for additional layers of complexity [682]. For example, programs exist to predict innate phage resistance mechanisms in bacteria [434, 688] and this could be incorporated into an AI model to further enhance

prediction. Eventually, the growing amount of gene expression/protein interaction data could also be used to improve the predictive capacity if necessary [682]. Whilst this could improve predictions of phage effectiveness against target bacteria, there is still work required to understand the impact of therapy on humans.

6.5 How can phage preclinical safety be evaluated to be relevant to CF

In Chapter 5, the preliminary safety of the Kara-mokiny 16 and tobramycin combination was evaluated using non-CF primary airway epithelial cells. As this was one of the first to use primary airway epithelial cells to study phage safety, using non-CF cells is an important first step in determining the effects on a non-diseased cohort. However, cells from people with CF exhibit abnormal apoptosis, a heightened inflammatory response and greater production of dehydrated and compositionally different mucus that influence how response to pathogens [125, 405, 408-410, 689-691]. Thus, it would be important to determine that these innate differences in cells from people with CF do not also influence their response to phages. However, even with ALI-culturing to enable the CF epithelial cells to differentiate into cell types found *in vivo* [405], there are still many other cell types that phages may interact with *in vivo*. Therefore, it is important to investigate the interactions of phages with other types of cells by using more complex models.

One such model uses organ on a chip technology. This technology aims to recapitulate the cell types, *in vivo* architecture, biochemical and biophysical factors of different human organs *in vitro* [692]. This would allow high throughput investigation of different treatments or stimuli on small-scale mimics of human anatomy and physiology [692]. To date, chips for the liver [693-695], pancreas [696, 697], kidney [698-700], heart [701-705], intestine [706-708], brain [709, 710], bone (including marrow) [711-713] and lung [714] have been developed. These can be combined in different configurations to allow the effects of drugs or stimuli on multiple organs to be investigated [715, 716]. With the advent of multi-organ chips it is now possible to investigate pharmacokinetics and pharmacodynamics of a treatment under investigation [695, 700, 704, 708, 715, 716]. Theoretically it may become possible to connect enough organs to form a body on a chip that would allow the investigation of a drug on the whole human body. Furthermore, since the cells that are used in the organ on chip can be taken from a person, this technology ushers in a new era of personalised medicine, where an individual's response to a treatment can be determined. In the case of CF, only the pancreas and lung have been

modelled on a chip [697, 717, 718]. The CF airway model displays many of the characteristics that are observed *in vivo* including greater mucus accumulation, higher baseline inflammation (including IL-8) and higher levels of neutrophil migration to the luminal side of lung [718]. *P. aeruginosa* growth also appears enhanced on the CF lung on a chip which subsequently increased inflammation and neutrophil recruitment [718]. Therefore, this model could provide a more comprehensive investigation of phage therapy pulmonary safety to both the airways and potentially other organs through multi-organ technology. However, as this technology is still advancing, investigating new treatments still requires the use of relevant animal models.

There have been many animal models of CF developed which all have their own advantages and disadvantages. In general, mouse models are the most widely used animal because they are small, animal husbandry is cost effective and there are resources widely available to facilitate their use in research [383]. However, mice make poor models of CF disease because the cellular composition of their trachea is highly divergent from humans [391]. Furthermore, their CFTR channel is different in terms of expression, structure and function [390]. They also do not exhibit many of the symptoms observed in CF, with the most important being lung disease [390, 392]. Rat models of CF overcome some of the issues that exist with mouse CF models. Rats have an airway cellular composition more closely resembling humans [719] but they still do not exhibit CF lung disease that is the major symptom in humans [398, 399, 720]. Other rodent models of CF have also been developed with more success including ferrets [388]. The ferret model of CF recapitulates the lung disease and spontaneous infections observed in people with CF [721, 722]. It also manifests many of the symptoms of CF across other organs including the intestine, pancreas, liver, gallbladder, and reproductive organs [722-724]. However, the feasibility of this model is impacted by its severe gastrointestinal disease-causing mortality unless further interventions are made [722]. Larger animals like sheep or pigs are arguably the best models of CF because they have airway structures most similar to humans and recapitulate almost every important feature of human CF such as pancreatic deficiency, meconium ileus (MI), lung disease and spontaneous airway infections [384, 386, 387, 725]. However, their use is limited by their size and animal husbandry costs and high mortality rate due to severe gastrointestinal symptoms that require intervention [383, 384, 725]. There are still many outstanding questions around phages and immunological interactions, dosage and the correlation between *in vitro* susceptibility testing with *in vivo* efficacy that cannot be studied in humans. Therefore, even with their limitations, *in vitro*

and animal CF models are still relevant to utilise to answer such questions. However, the fact remains that phages have been used in a growing number of humans with few side effects. Therefore, even with the unknown aspects of phage therapy they are safe and effective. Thus, the bottleneck for their widespread use does not appear to be due to research but rather the regulatory agencies that govern therapeutic approvals.

6.6 Regulatory Roadblocks to Phage Therapy

The main roadblock to phage therapy efficiency are the various regulatory pathways that must be traversed to administer treatment. Problems with regulating phage therapy stem from both the biology of the phages themselves and the governing agencies trying to classify phages according to traditional schemes [726-730]. Firstly, unlike antibiotics, phages are highly specific for the bacteria they can kill [728]. This means that treating an infection empirically is not feasible and therapy will likely progress down a personalised pathway [726-730]. Yet, there is currently no regulatory framework specifically for personalised phage therapy that would enable it to be a non-experimental medicine, thus phages are relegated to small scale compassionate use [729]. The regulatory schemes that enable last line treatments are different around the World [726-730]. In America, Australia and some parts of Europe, phage therapy is administered under compassionate use schemes, whereby experimental treatments can be used once all traditional methods are exhausted [293, 729, 731]. Whilst there are requirements for successful compassionate use applications the process has a significant lag time and the cost of producing a therapeutic-grade phage therapy is high [293, 731]. In America, the FDA recognises phages as a drug [636, 732] but use of a single treatment still requires notification of an institutional review board and the FDA [293, 635, 636]. However, the FDA has approved a company's (Adaptive Phage Therapeutic's) phage bank as an investigational new drug therefore allowing their library of phages to be used as treatments more easily [635]. In Western Europe, different countries have individualised approaches to phage therapy administration. In the United Kingdom phage therapy must be manufactured according to good manufacturing principles (GMP) [635, 733] and whilst there is no regulatory barrier to using phages, to produce them according to the required standards is expensive and the UK does not have this infrastructural capacity at present [733]. However, a recent parliamentary enquiry into phage therapy was conducted to address these challenges and how these may be overcome [635]. In Belgium, regulation of phage therapy has been implemented under magistral preparations [729]. Here,

individual phages are prepared according to the required standards and mixed by a pharmacist as per a doctor's prescription [636, 729]. This allows a more personalised therapy approach to be taken but is still not adequate to allow the demand for phages to be met [729]. In Australia, the Therapeutic Goods Administration (TGA) have not made a ruling on how phages should be classified and are considered investigational drugs [636]. Therefore, phage therapy is limited to the special access scheme pathway, meaning that the TGA and local ethics committees must approve each treatment on a case-by-case basis [636]. The regulation around the use of phage therapy around the World are far from perfect and contribute to the significant lag time from infection to treatment administration and prevent wide-spread use. However, issues also stem from the fact that phages do not fit the existing model of a therapy and so regulations must be changed to support their use. Therefore, it may be easier to identify antibacterial compounds from phages that more can be regulated more similarly to existing antibiotics.

6.7 Use phage products instead of whole phages

Phages produce antimicrobials that they use to kill the bacteria as part of their lifecycle which can be extracted and used, instead of using whole phages [734, 735]. The primary phage antimicrobials being investigated are called endolysins [736]. These are hydrolytic enzymes that target different peptidoglycan bonds of the bacterial cell wall [736]. Like phages these have demonstrated low toxicity to eukaryotes (including humans) because they target a specific bacterial component [735, 737-741]. However, unlike phages they can target multiple bacteria and be given as a concentration similar to antibiotics, with no need to consider infection dynamics [742-748]. This would mean that endolysins could be regulated more similarly to other biological drugs [749]. This has already been demonstrated with clinical trials of endolysin treatment of Gram-positive bacteria occurring and endolysin treatment being approved [737, 749-755]. For Gram-negative bacteria it is not as simple because the cell wall is beneath the outer membrane so for a long time it was thought endolysins had to be modified to increase their permeability [756]. However, some endolysins exist that have an amphipathic tail and can pass through the Gram-negative bacterial outer membrane to cleave the cell wall [744-748, 757, 758]. There are reports of these kinds of endolysins being able to treat both Gram-negative and positive pathogens, opening the possibility of empirical treatment similar to antibiotics [742, 743]. Unlike antibiotics (and phages) there is limited resistance able to be evolved to endolysin treatment due to the highly conserved cell wall structure [759]. Furthermore,

endolysins have high commercialisation potential and there have been platforms and techniques developed that have formed the foundation of companies [760, 761]. This makes them a lot more attractive as an alternative to antibiotics and companies are frequently being formed to develop endolysin therapy [762]. Ultimately, phages and endolysins both have different benefits and disadvantages, but both will likely form parts of the solution to the AMR crisis.

6.8 Conclusion

In summary the studies described in this thesis show that phages have potential to effectively treat *P. aeruginosa* in CF, without phage resistance evolving and causing harmful effects to the human airways. Data generated support the project hypothesis that effective *P. aeruginosa* phages that have characteristics that make them suitable for therapy can be isolated from wastewater. For the first time, it also demonstrated how three distinct CF isolates gain resistance to four diverse phages' treatment and that this came at the cost of resistance to tobramycin. Testing of a phage with tobramycin showed that there was some suppression of phage resistance however this requires further optimisation. In addition, novel experiments performed, show that the phage-tobramycin combination could be applied to a highly representative epithelial cell model without eliciting potentially detrimental inflammation or cytotoxicity. The results from this thesis have added further support that phages are safe and will contribute to their recognition as a conventional therapy. Furthermore, it lays the foundation for future studies investigating phage resistance in clinical isolates of *P. aeruginosa* and formulating phage cocktails.

Appendix

Appendix A.1



Research Office at Curtin

GPO Box U1987
Perth Western Australia 6845

Telephone +61 8 9266 7863
Facsimile +61 8 9266 3793
Web research.curtin.edu.au

26-Feb-2019

Name: Anthony Kicic
Department/School: School of Public Health
Email: Anthony.Kicic@curtin.edu.au

Dear Anthony Kicic

RE: Reciprocal ethics approval
Approval number: HRE2019-0086

Thank you for your application submitted to the Human Research Ethics Office for the project WA Epithelial Research Program for Childhood Respiratory Diseases.

Your application has been approved by the Curtin University Human Research Ethics Committee (HREC) through a reciprocal approval process with the lead HREC.

The lead HREC for this project has been identified as St John of God Health Care Human Research Ethics Committee.

Approval number from the lead HREC is noted as 901.

The Curtin University Human Research Ethics Office approval number for this project is **HRE2019-0086**. Please use this number in all correspondence with the Curtin University Ethics Office regarding this project.

Approval is granted for a period of one year from to **22-Jan-2028**. Continuation of approval will be granted on an annual basis following submission of an annual report.

Personnel authorised to work on this project:

Name	Role
Kicic, Anthony	CI

You must comply with the lead HREC's reporting requirements and conditions of approval. You must also:

- Keep the Curtin University Ethics Office informed of submissions to the lead HREC, and of the review outcomes for those submissions
- Conduct your research according to the approved proposal
- Report to the lead HREC anything that might warrant review of the ethics approval for the project
- Submit an annual progress report to the Curtin University Ethics Office on or before the anniversary of approval, and a completion report on completion of the project. These can be the same reports submitted to the lead HREC.
- Personnel working on this project must be adequately qualified by education, training and experience for their role, or supervised
- Personnel must disclose any actual or potential conflicts of interest, including any financial or other interest or affiliation, that bears on this project
- Data and primary materials must be managed in accordance with the [Western Australian University Sector Disposal Authority \(WAUSDA\)](#) and the [Curtin University Research Data and Primary Materials policy](#)
- Where practicable, results of the research should be made available to the research participants in a timely and clear manner
- The Curtin University Ethics Office may conduct audits on a portion of approved projects.

This letter constitutes ethical approval only. This project may not proceed until you have met all of the Curtin University research governance requirements.

Should you have any queries regarding consideration of your project, please contact the Ethics Support Officer for your faculty or the Ethics Office at hrec@curtin.edu.au or on 9266 2784.

Yours sincerely

A solid black rectangular box used to redact the signature of Amy Bowater.

Amy Bowater
Ethics, Team Lead

Appendix Table B.1 *P. aeruginosa* Receptor Mutations Conferring Phage-Resistance

Phage Treatment	Mutation Type	Gene/s	Receptor	Role of Gene	Cost to Fitness	Bacterial Genetic Background	Reference
Sequential 2 phages	80 bp deletion	<i>galU</i>	LPS	LPS core biosynthesis	N/A	PAO1	[326]
Sequential 2 phages	Nonsense	<i>galU</i>	LPS	LPS core biosynthesis	N/A	PAO1	[326]
Single Phage	Frameshift	<i>Ssg</i>	LPS	OSA biosynthesis	N/A	PAO1	[326]
Sequential 2 phages	91bp deletion	<i>wapH</i>	LPS	Probable outer core biosynthesis	N/A	PAO1	[326]
Sequential 2 phages	Missense	<i>rmlA</i>	LPS	LPS core biosynthesis	N/A	PAO1	[326]
2 phage cocktail	Frameshift	<i>wbpL</i>	LPS	LPS CPA and OSA biosynthesis	N/A	PAO1	[326]
Sequential 2 phages	Nonsense	<i>wzy</i>	LPS	LPS OSA biosynthesis	N/A	PAO1	[326]
2 phage cocktail	Frameshift	<i>wzy</i>	LPS	LPS OSA biosynthesis	N/A	PAO1	[326]
Sequential 2 phages	Missense	<i>pilB</i>	T4P	Pilus extension	N/A	PAO1	[326]
Sequential 2 phages	12 bp insertion	<i>pilE</i>	T4P	Minor pilin	N/A	PAO1	[326]
Sequential 2 phages	Missense	<i>pilN</i>	T4P	Pilus assembly	N/A	PAO1	[326]
Sequential 2 phages	Missense	<i>pilR</i>	T4P	Interacts with sensor to regulate the production of the pilus	N/A	PAO1	[326]

Sequential 2 phages	1,192 bp deletion	<i>pilT and pilU</i>	T4P	Twitching motility	N/A	PAO1	[326]
Sequential 2 phages	Nonsense	<i>pilY1</i>	T4P	Pilus anti-retraction	N/A	PAO1	[326]
2 phage cocktail	Frameshift	<i>pilY1</i>	T4P	Pilus anti-retraction	N/A	PAO1	[326]
2 phage cocktail	250 kbp deletion	<i>galU</i> and 200 other genes	LPS	N/A	N/A	PAO1	[326]
Single Phage	1 bp Substitution	<i>wzy</i>	LPS	LPS OSA biosynthesis	Reduced biofilm formation	PA1	[327]
Single Phage	1 bp insertion	<i>wbpL</i>	LPS	LPS CPA and OSA biosynthesis	N/A	PAO1	[325]
Single Phage	1 bp insertion	<i>wzy</i>	LPS	LPS OSA biosynthesis	N/A	PAO1	[325]
Single Phage	4 bp deletion	<i>pilB</i>	T4P	Motor protein powering pilus extension	N/A	PAO1	[325]
Single Phage	Nonsense	<i>pilB</i>	T4P	Motor protein powering pilus extension	N/A	PAO1	[325]
Single Phage	Missense	<i>pilT</i>	T4P	Motor protein powering pilus retraction	N/A	PAO1	[325]
Single Phage	1200 bp deletion	<i>pilT</i>	T4P	Motor protein powering pilus retraction	N/A	PAO1	[325]
Single Phage	12 bp deletion	<i>pilT</i>	T4P	Motor protein powering pilus retraction	N/A	PAO1	[325]
Single Phage	1 bp deletion	<i>pilY1</i>	T4P	Pilus anti-retraction	N/A	PAO1	[325]

Single Phage	Missense	<i>pilJ</i>	T4P	Transduction of signals to system regulating type IV pilus motility	N/A	PAO1	[325]
Single Phage	Nonsense	<i>pilD</i>	T4P	Processing T4P prepilins	N/A	PAO1	[325]
Single Phage	183 bp deletion	<i>pilQ</i>	T4P	Pilus outer membrane secretin pore	N/A	PAO1	[325]
Single Phage	35 bp deletion	<i>fimV</i>	T4P	Involved in pilus assembly	N/A	PAO1	[325]
Single Phage	1 bp deletion	<i>rpoN</i>	T4P	Regulates expression of major pilin protein	N/A	PAO1	[325]
Single Phage	Missense	<i>rpoN</i>	T4P	Regulates expression of major pilin protein	N/A	PAO1	[325]
Single Phage	1 bp deletion	<i>pilR</i>	T4P	Interacts with sensor to regulate the production of the pilus	N/A	PAO1	[325]
Single Phage	Missense	<i>pilR</i>	T4P	Interacts with sensor to regulate the production of the pilus	N/A	PAO1	[325]
Single Phage	Nonsense	<i>pilS</i>	T4P	Sensor that interacts with regulator to produce the pilus	N/A	PAO1	[325]

Single Phage	Missense	PA1875	Putative Efflux Pump	N/A	N/A	PAO1	[325]
Single Phage	220 kbp deletion	<i>galU</i>	LPS	LPS core biosynthesis	Less virulent in mouse model	PA1	[330]
13 Phage Cocktail	15 bp deletion	<i>pilT</i>	T4P	Motor protein for pilus retraction	Twitching motility	CHA	[275]
13 Phage Cocktail	362 kbp deletion	<i>galU</i>	LPS	LPS core biosynthesis	Decreased resistance to ciprofloxacin	CHA	[275]
3 Phage Cocktail	1 bp insertion	Pseudogene	N/A	N/A	Reduced swimming, swarming and twitching motility	PAO1	(Pires et al. 2017)
	1 bp substitution	<i>ldhA</i>	N/A	Cell metabolism			
	1 bp substitution	<i>galU</i>	LPS	LPS core biosynthesis			
	1bp deletion	Hypothetical protein	N/A	N/A			
	3 bp insertion	<i>mexT</i>	N/A	Transcriptional regulator			
	1 bp substitution	Probable transcriptional regulator	N/A	N/A			
	1 bp insertion	Hypothetical protein	N/A	N/A			
1 bp substitution	<i>pilE</i>	T4P	Type 4 fimbrial biogenesis				
3 Phage Cocktail	1 bp insertion	Pseudogene	N/A	N/A	Reduced swimming,	PAO1	(Pires et al. 2017)

	1 bp substitution	<i>ldhA</i>	N/A	Cell metabolism	swarming and twitching motility		
	1 bp substitution	<i>galU</i>	LPS	LPS core biosynthesis			
	1bp deletion	Hypothetical protein	N/A	N/A			
	3 bp insertion	<i>mexT</i>	N/A	Transcriptional regulator			
	1 bp substitution	Probable transcriptional regulator	N/A	N/A			
	1 bp insertion	Hypothetical protein	N/A	N/A			
	1 bp substitution	<i>pilO</i>	T4P	Type 4 fimbrial biogenesis			
3 Phage Cocktail	1 bp insertion	Pseudogene	N/A	N/A	Reduced swimming, swarming and twitching motility	PAO1	(Pires et al. 2017)
	1 bp substitution	<i>ldhA</i>	N/A	Cell metabolism			
	1 bp substitution	<i>galU</i>	LPS	LPS core biosynthesis			
	1 bp deletion	Hypothetical protein	N/A	N/A			
	3 bp insertion	<i>mexT</i>	N/A	Transcriptional regulator			
	1 bp substitution	Probable transcriptional regulator	N/A	N/A			

	1 bp insertion 1 bp insertion	Hypothetical protein <i>pilC</i>	N/A T4P	N/A Type 4 fimbrial biogenesis			
3 Phage Cocktail	1 bp insertion	Pseudogene	N/A	N/A	Reduced swimming, swarming and twitching motility	PAO1	(Pires et al. 2017)
	1 bp substitution	<i>ldhA</i>	N/A	Cell metabolism			
	1 bp substitution	<i>galU</i>	LPS	LPS core biosynthesis			
	1 bp deletion	Hypothetical protein	N/A	N/A			
	3 bp insertion	<i>mexT</i>	N/A	Transcriptional regulator			
	1 bp substitution	Probable transcriptional regulator	N/A	N/A			
1 bp insertion 1 bp insertion	Hypothetical protein <i>pilM</i>	N/A T4P	N/A Type 4 fimbrial biogenesis				
5 Cocktail	1 bp insertion	<i>wzy</i>	LPS	LPS OSA biosynthesis	N/A	PA1	[372]
	1 bp substitution	<i>migA</i>	LPS	LPS core biosynthesis			
5 Cocktail	1 bp substitution	<i>migA</i>	LPS	LPS core biosynthesis	N/A	PA1	[372]
	6 bp insertion	<i>fimL</i>	Unknown	Unknown			

	1 bp substitution 3 bp substitution	<i>wzy</i> <i>gmd</i>	LPS LPS	LPS OSA biosynthesis LPS CPA biosynthesis			
5 Cocktail	1 bp substitution 1 bp substitution 1 bp substitution	<i>migA</i> <i>wzy</i> <i>rmd</i>	LPS LPS LPS	LPS core biosynthesis LPS OSA biosynthesis LPS CPA biosynthesis	N/A	PA1	[372]
5 Cocktail	1 bp substitution 1 bp substitution 1 bp substitution	<i>migA</i> <i>wzy</i> <i>PA5455</i>	LPS LPS Unknown	LPS core biosynthesis LPS OSA biosynthesis Unknown	N/A	PA1	[372]
2 Phage Cocktail	1 bp insertion	<i>wzy</i>	LPS	LPS OSA biosynthesis	N/A	PA01	[328]
2 Phage Cocktail	1 bp insertion	<i>wzy</i>	LPS	LPS OSA biosynthesis	N/A	PA01	[328]
	1 bp substitution	<i>migA</i>	LPS	LPS core biosynthesis	N/A	PA01	[328]
Single Phage	1 bp insertion	<i>wzy</i>	LPS	LPS OSA biosynthesis	N/A	PA01	[328]
Single Phage	1 bp insertion	<i>wzy</i>	LPS	LPS OSA biosynthesis	N/A	PA01	[328]
Single Phage	1 bp insertion	<i>wbpL</i>	LPS	LPS CPA and OSA biosynthesis	N/A	PA01	[328]
Single Phage	1 bp substitution	<i>wapH</i>	LPS	Probable outer core biosynthesis	N/A	PA01	[328]
2 Phage Cocktail	1 bp substitution	<i>dnpA</i>	N/A	LPS core biosynthesis	N/A	PA01	[328]

4 Phage Cocktail	1 bp insertion	<i>wzy</i>	LPS	LPS OSA biosynthesis	N/A	PA01	[328]
2 Phage Cocktail	1 bp insertion	<i>mucA</i>	N/A	Anti-sigma factor; alginate regulation	N/A	PA01	[328]
2 Phage Cocktail	1 bp insertion	<i>wzz2</i>	LPS	LPS OSA biosynthesis	N/A	PA01	[328]
2 Phage Cocktail	1 bp insertion	<i>mucA</i>	N/A	Anti-sigma factor; alginate regulation	N/A	PA01	[328]
Single Phage	1 bp substitution	<i>pgi</i>	N/A	Cell metabolism	N/A	PA01	[328]
Single Phage	1 bp substitution	<i>mucA</i> intergenic <i>algU</i>	N/A	N/A	N/A	PA01	[328]
Single Phage	1 bp substitution	<i>wzy</i>	LPS	LPS OSA biosynthesis	N/A	PA01	[328]
Single Phage	19 bp deletion	<i>pilQ</i>	T4P	Outer membrane secretin pore within pilus structure	N/A	PA01	[328]
4 Phage Cocktail	1 bp insertion 1 bp substitution	<i>wzy</i> <i>pilR</i>	LPS T4P	LPS OSA biosynthesis Motility two-component response regulator	N/A	PA01	[328]
2 Phage Cocktail	10 bp deletion 1 bp substitution	<i>pilY1</i> <i>wzy</i>	T4P LPS	Pilus anti-retraction factor LPS OSA biosynthesis	N/A	PA01	[328]
4 Phage Cocktail	555 bp deletion	<i>pilQ</i>	T4P	Pilus outer membrane secretin pore	N/A	PA01	[328]
4 Phage Cocktail	1 bp deletion	<i>pilR</i>	T4P	Two-component response regulator	N/A	PA01	[328]

	213 bp deletion	<i>algC</i>	LPS	O antigen and alginate biosynthesis			
2 Phage Cocktail	1 bp insertion	<i>wzy</i>	LPS	LPS OSA biosynthesis	N/A	PA01	[328]
	1 bp deletion	<i>wzy</i>	LPS	LPS OSA biosynthesis			
	109 bp deletion	<i>pilY1</i>	T4P	Pilus anti-retraction factor			
2 Phage Cocktail	11 bp insertion	<i>pilJ</i>	T4P	Motility two-component response signal transduction	N/A	PA01	[328]
	1 bp insertion	<i>wzy</i>	LPS	LPS OSA biosynthesis			

Note: Where a row contains more than one mutation it is because a single escape mutant contained multiple mutations

Appendix Table C.1 Ranked Host Range of all the Phages Isolated in this Thesis

Phage Original Name	Number	Lysis	Partial	No Lysis	Total Lysis (%)
T81.M79.U2.1.1.1	116	38	27	8	89.04%
T81.M77.U5.1.1.1	67	35	29	9	87.67%
T81.M100.U6.1.1.1	130	40	22	11	84.93%
T81.PAO1.U3.1.1.1	92	29	32	12	83.56%
T81.PAO1.U8.1.1.1	97	37	23	13	82.19%
T81.M34.E3.1.1.1	110	34	26	13	82.19%
T81.PAO1.U2.1.1.1	91	29	31	13	82.19%
T81.M108.U4.1.1.1	39	34	24	15	79.45%
T81.M130.U2.1.1.1	20	33	25	15	79.45%
T81.M34.E2.1.1.1	109	28	30	15	79.45%
T81.M79.U3.1.1.1	117	33	24	16	78.08%
T81.M34.U1.1.1.1	111	25	32	16	78.08%
T81.M108.U8.1.1.1	43	31	25	17	76.71%
T81.M130.U3.1.1.1	21	29	27	17	76.71%
T81.PAO1.U4.1.1.1	93	10	46	17	76.71%
T81.M37.U1.1.1.1	172	41	14	18	75.34%
T81.M66.U4.1.1.1	13	31	24	18	75.34%
T81.M34.E1.1.1.1	108	35	19	19	73.97%
T81.M108.U2.1.1.1	37	23	30	20	72.60%
T81.M90.U7.1.1.1	163	23	30	20	72.60%
T81.M74.U8.1.1.1	138	16	37	20	72.60%
T81.M4.U1.1.1.1	249	32	20	21	71.23%
T81.M123.U9.1.1.1	80	30	22	21	71.23%
T81.M4.U7.1.1.1	251	28	24	21	71.23%
T81.M90.U8.1.1.1	164	25	26	22	69.86%
T81.M90.U1.1.1.1	157	24	27	22	69.86%
T81.M123.U1.1.1.1	72	34	16	23	68.49%
T81.M34.U3.1.1.1	113	28	22	23	68.49%
T81.PAO1.U6.1.1.1	95	20	30	23	68.49%
T81.M81.E4.1.1.1	155	18	32	23	68.49%
T81.M108.U9.1.1.1	44	11	39	23	68.49%
T81.M108.U1.1.1.1	36	25	24	24	67.12%
T81.M52.U6.1.1.1	203	19	30	24	67.12%
T81.M123.U6.1.1.1	77	16	33	24	67.12%
T81.M79.U4.1.1.1	118	15	34	24	67.12%
T81.M77.U3.1.1.1	65	24	24	25	65.75%
T81.M79.U5.1.1.1	119	23	25	25	65.75%
T81.M39.U5.1.1.1	85	19	29	25	65.75%
T81.M52.U8.1.1.1	205	18	30	24	65.75%
T81.M130.U4.1.1.1	22	15	33	25	65.75%
T81.M108.U5.1.1.1	40	1	47	26	65.75%
T81.M93.U4.1.1.1	57	31	16	25	64.38%

T81.M73.U4.1.1.1	192	22	25	25	64.38%
T81.M123.U2.1.1.1	73	14	33	26	64.38%
T81.M39.U6.1.1.1	86	22	24	27	63.01%
T81.M39.U7.1.1.1	87	22	24	27	63.01%
T81.PAO1.U7.1.1.1	96	13	33	26	63.01%
T81.M130.U1.1.1.1	19	12	34	27	63.01%
T81.M39.U2.1.1.1	82	23	22	28	61.64%
T81.M77.U1.1.1.1	63	22	23	28	61.64%
T81.M39.U1.1.1.1	81	22	23	28	61.64%
T81.M39.U3.1.1.1	83	22	23	28	61.64%
T81.M52.U4.1.1.1	201	19	26	28	61.64%
T81.M130.E3.1.1.1	27	25	19	28	60.27%
T81.M130.E2.1.1.1	26	20	24	28	60.27%
T81.M34.U2.1.1.1	112	19	25	29	60.27%
T81.M81.E3.1.1.1	154	16	28	29	60.27%
T81.M52.U5.1.1.1	202	12	31	30	58.90%
T81.M37.U3.1.1.1	174	17	25	30	57.53%
T81.M90.U3.1.1.1	159	3	39	31	57.53%
T81.M37.E1.1.1.1	171	16	25	32	56.16%
T81.PAO1.U1.1.1.1	90	10	31	32	56.16%
T81.M74.U5.1.1.1	135	1	40	32	56.16%
T81.M123.U7.1.1.1	78	17	23	32	54.79%
T81.M81.E5.1.1.1	156	17	23	32	54.79%
T81.M81.E2.1.1.1	153	16	24	33	54.79%
T81.M64.U2.1.1.1	31	15	25	33	54.79%
T81.M64.U3.1.1.1	32	15	25	33	54.79%
T81.M34.U4.1.1.1	114	12	28	33	54.79%
T81.M39.U4.1.1.1	84	11	29	33	54.79%
T81.M93.U9.1.1.1	62	2	38	33	54.79%
T81.M108.U7.1.1.1	42	1	39	34	54.79%
T81.M90.U5.1.1.1	161	1	39	33	54.79%
T81.M108.U6.1.1.1	41	0	40	33	54.79%
T81.M52.U1.1.1.1	198	18	21	34	53.42%
T81.M37.U2.1.1.1	173	15	24	34	53.42%
T81.M64.U1.1.1.1	30	14	25	34	53.42%
T81.M130.U5.1.1.1	23	10	29	34	53.42%
T81.PAO1.U9.1.1.1	98	9	30	34	53.42%
T81.M73.U8.1.1.1	196	2	36	34	52.05%
T81.M64.E1.1.1.1	28	12	25	35	50.68%
T81.M64.U6.1.1.1	35	11	26	35	50.68%
T81.M74.U4.1.1.1	134	2	35	35	50.68%
T81.M74.U6.1.1.1	136	2	35	35	50.68%
T81.M73.U9.1.1.1	197	2	35	35	50.68%
T81.M64.E2.1.1.1	29	12	24	36	49.32%
T81.M54.U3.1.1.1	47	12	23	37	47.95%
T81.M123.U4.1.1.1	75	12	23	38	47.95%

T81.M52.U9.1.1.1	206	4	31	37	47.95%
T81.M74.U1.1.1.1	131	2	32	38	46.58%
T81.M90.U6.1.1.1	162	1	33	39	46.58%
T81.M74.U7.1.1.1	137	2	31	39	45.21%
T81.M52.U3.1.1.1	200	9	23	40	43.84%
T81.M64.U4.1.1.1	33	8	23	42	42.47%
T81.M74.U3.1.1.1	133	0	31	41	42.47%
T81.M73.U6.1.1.1	194	2	27	43	39.73%
T81.M37.U7.1.1.1	178	13	15	44	38.36%
T81.M131.U1.1.1.1	240	13	15	45	38.36%
T81.M93.U3.1.1.1	56	3	25	45	38.36%
T81.M74.U2.1.1.1	132	1	27	45	38.36%
T81.PA01.U5.1.1.1	94	2	24	46	35.62%
T81.M94.E5.1.1.1	237	1	25	47	35.62%
T81.M108.U3.1.1.1	38	0	25	46	34.25%
T81.M90.U4.1.1.1	160	0	25	47	34.25%
T81.M94.E3.1.1.1	235	0	25	47	34.25%
T81.M50.U1.1.1.1	216	14	10	48	32.88%
T81.M130.U6.1.1.1	24	4	20	49	32.88%
T81.M141.E6.1.1.1	229	1	23	49	32.88%
T81.M94.E4.1.1.1	236	1	23	49	32.88%
T81.M90.U2.1.1.1	158	0	24	48	32.88%
T81.M66.U2.1.1.1	11	8	15	50	31.51%
T81.M54.U1.1.1.1	45	6	17	49	31.51%
T81.M54.U4.1.1.1	48	5	18	49	31.51%
T81.M73.U1.1.1.1	189	2	20	50	30.14%
T81.M94.U5.1.1.1	239	1	21	51	30.14%
T81.M50.E1.1.1.1	218	15	6	52	28.77%
T81.M50.E5.1.1.1	222	11	10	51	28.77%
T81.M54.U7.1.1.1	51	5	16	51	28.77%
T81.M52.U7.1.1.1	204	1	20	52	28.77%
T81.M50.E2.1.1.1	219	15	5	53	27.40%
T81.M50.E3.1.1.1	220	14	6	53	27.40%
T81.M50.E4.1.1.1	221	14	6	53	27.40%
T81.M50.E6.1.1.1	223	14	6	53	27.40%
T81.M66.U5.1.1.1	14	7	13	53	27.40%
T81.M141.E4.1.1.1	227	3	17	52	27.40%
T81.M52.U2.1.1.1	199	2	18	52	27.40%
T81.M141.E8.1.1.1	231	1	19	53	27.40%
T81.M93.U6.1.1.1	59	0	20	53	27.40%
T81.M54.U5.1.1.1	49	4	15	53	26.03%
T81.M54.U6.1.1.1	50	2	17	53	26.03%
T81.M93.U7.1.1.1	60	0	19	53	26.03%
T81.M54.U9.1.1.1	53	4	14	54	24.66%
T81.M54.U8.1.1.1	52	3	15	54	24.66%
T81.M58.E9.1.1.1	188	4	13	55	23.29%

T81.M66.U8.1.1.1	17	3	14	55	23.29%
T81.M77.U4.1.1.1	66	3	14	55	23.29%
T81.M141.E9.1.1.1	232	1	16	56	23.29%
T81.M81.E1.1.1.1	152	9	7	56	21.92%
T81.M81.U5.1.1.1	151	4	12	56	21.92%
T81.M54.U2.1.1.1	46	2	14	56	21.92%
T81.M77.U6.1.1.1	68	2	14	56	21.92%
T81.M58.E3.1.1.1	182	2	14	56	21.92%
T81.M58.E4.1.1.1	183	2	14	56	21.92%
T81.M73.U3.1.1.1	191	2	14	56	21.92%
T81.M64.U5.1.1.1	34	1	15	57	21.92%
T81.M124.U1.1.1.1	170	5	10	57	20.55%
T81.M39.U8.1.1.1	88	3	12	57	20.55%
T81.M100.U5.1.1.1	129	3	12	58	20.55%
T81.M58.E6.1.1.1	185	3	12	57	20.55%
T81.M4.U8.1.1.1	252	3	12	57	20.55%
T81.M94.E1.1.1.1	233	1	14	58	20.55%
T81.M94.U3.1.1.1	238	0	15	57	20.55%
T81.M100.U4.1.1.1	128	3	11	59	19.18%
T81.M77.U7.1.1.1	69	2	12	58	19.18%
T81.M58.E8.1.1.1	187	2	12	58	19.18%
T81.M73.U5.1.1.1	193	2	12	58	19.18%
T81.M14.U1.1.1.1	99	1	13	59	19.18%
T81.M14.E5.1.1.1	104	0	14	58	19.18%
T81.M14.E6.1.1.1	105	0	14	58	19.18%
T81.M77.U2.1.1.1	64	3	10	59	17.81%
T81.M39.U9.1.1.1	89	3	10	59	17.81%
T81.M66.U1.1.1.1	10	2	11	59	17.81%
T81.M77.U8.1.1.1	70	2	11	59	17.81%
T81.M58.E2.1.1.1	181	2	11	59	17.81%
T81.M14.E4.1.1.1	103	1	12	60	17.81%
T81.M14.E7.1.1.1	106	1	12	60	17.81%
T81.M58.E1.1.1.1	180	3	9	60	16.44%
T81.M58.E7.1.1.1	186	2	10	60	16.44%
T81.M73.U7.1.1.1	195	2	10	60	16.44%
T81.M14.E1.1.1.1	100	1	11	61	16.44%
T81.M14.E2.1.1.1	101	1	11	61	16.44%
T81.M14.E8.1.1.1	107	1	11	61	16.44%
T81.M124.U3.1.1.1	169	1	11	61	16.44%
T81.M141.E2.1.1.1	225	0	12	60	16.44%
T81.M79.U1.1.1.1	115	3	8	62	15.07%
T81.M124.U5.1.1.1	168	3	8	61	15.07%
T81.M141.E5.1.1.1	228	1	10	62	15.07%
T81.M141.E1.1.1.1	224	0	11	61	15.07%
T81.M141.E3.1.1.1	226	0	11	61	15.07%
T81.M79.U9.1.1.1	123	3	7	63	13.70%

T81.M81.U3.1.1.1	149	3	7	62	13.70%
T81.M79.U6.1.1.1	120	2	8	63	13.70%
T81.M67.U7.1.1.1	7	1	9	63	13.70%
T81.M14.E3.1.1.1	102	1	9	63	13.70%
T81.M94.E2.1.1.1	234	1	9	63	13.70%
T81.M73.U2.1.1.1	190	0	10	62	13.70%
T81.M79.U8.1.1.1	122	3	6	64	12.33%
T81.M124.E2.1.1.1	166	2	7	63	12.33%
T81.M141.E7.1.1.1	230	0	9	63	12.33%
T81.M123.U5.1.1.1	76	3	5	65	10.96%
T81.M79.U7.1.1.1	121	3	5	65	10.96%
T81.M86.E1.1.1.1	207	2	6	64	10.96%
T81.M50.U2.1.1.1	217	2	6	64	10.96%
T81.M10.U1.1.1.1	139	0	8	64	10.96%
T81.M58.E5.1.1.1	184	0	8	64	10.96%
T81.M67.U4.1.1.1	4	3	4	65	9.59%
T81.M66.U6.1.1.1	15	2	5	66	9.59%
T81.M81.U4.1.1.1	150	2	5	65	9.59%
T81.M67.U1.1.1.1	1	1	6	67	9.59%
T81.M67.U2.1.1.1	2	1	6	66	9.59%
T81.M67.U8.1.1.1	8	1	6	66	9.59%
T81.M67.U9.1.1.1	9	1	6	66	9.59%
T81.M130.E1.1.1.1	25	1	6	66	9.59%
T81.M77.U9.1.1.1	71	0	7	65	9.59%
T81.M37.U6.1.1.1	177	0	7	65	9.59%
T81.M86.E2.1.1.1	208	0	7	65	9.59%
T81.M86.E3.1.1.1	209	0	7	65	9.59%
T81.M131.U9.1.1.1	248	0	7	65	9.59%
T81.M66.U7.1.1.1	16	2	4	67	8.22%
T81.M123.U3.1.1.1	74	2	4	67	8.22%
T81.M131.U4.1.1.1	243	1	5	67	8.22%
T81.M37.U5.1.1.1	176	0	6	66	8.22%
T81.M66.U3.1.1.1	12	2	3	68	6.85%
T81.M10.E4.1.1.1	143	2	3	67	6.85%
T81.M81.U2.1.1.1	148	1	4	68	6.85%
T81.M100.U2.1.1.1	127	0	5	67	6.85%
T81.M10.E1.1.1.1	140	0	5	67	6.85%
T81.M10.E2.1.1.1	141	0	5	67	6.85%
T81.M10.E3.1.1.1	142	0	5	67	6.85%
T81.M86.E4.1.1.1	210	0	5	67	6.85%
T81.M131.U8.1.1.1	247	0	5	67	6.85%
T81.M66.U9.1.1.1	18	2	2	69	5.48%
T81.M67.U3.1.1.1	3	0	4	68	5.48%
T81.M93.U5.1.1.1	58	0	4	68	5.48%
T81.M100.E2.1.1.1	125	0	4	68	5.48%
T81.M10.E8.1.1.1	147	0	4	68	5.48%

T81.M37.U4.1.1.1	175	0	4	68	5.48%
T81.M37.U8.1.1.1	179	0	4	68	5.48%
T81.M131.U3.1.1.1	242	0	4	68	5.48%
T81.M131.U5.1.1.1	244	0	4	68	5.48%
T81.M131.U7.1.1.1	246	0	4	68	5.48%
T81.M4.U2.1.1.1	250	0	4	68	5.48%
T81.M67.U6.1.1.1	6	2	1	69	4.11%
T81.M93.U8.1.1.1	61	0	3	69	4.11%
T81.M123.U8.1.1.1	79	0	3	69	4.11%
T81.M100.E1.1.1.1	124	0	3	69	4.11%
T81.M100.E3.1.1.1	126	0	3	69	4.11%
T81.M10.E7.1.1.1	146	0	3	69	4.11%
T81.M86.E6.1.1.1	212	0	3	69	4.11%
T81.M86.E7.1.1.1	213	0	3	69	4.11%
T81.M86.E8.1.1.1	214	0	3	69	4.11%
T81.M86.E9.1.1.1	215	0	3	69	4.11%
T81.M131.U2.1.1.1	241	0	3	69	4.11%
T81.M131.U6.1.1.1	245	0	3	69	4.11%
T81.M67.U5.1.1.1	5	1	1	71	2.74%
T81.M93.U1.1.1.1	54	0	2	70	2.74%
T81.M10.E6.1.1.1	145	0	2	70	2.74%
T81.M124.E4.1.1.1	167	0	2	70	2.74%
T81.M86.E5.1.1.1	211	0	2	70	2.74%
T81.M93.U2.1.1.1	55	0	1	71	1.37%
T81.M10.E5.1.1.1	144	0	1	71	1.37%
T81.M124.E1.1.1.1	165	0	1	71	1.37%

Appendix Table D.1 The Top 20 Phages Host Specificity

Activity/Any Lysis (%)						
	<i>Staphylococcus aureus</i> (n=20)	<i>Burkholderia cepacia</i> complex (n=20)	<i>Escherichia coli</i> (n=1)	<i>Klebsiella pneumoniae</i> (n=3)	<i>Enterococcus faecalis</i> (n=1)	<i>Enterococcus faecium</i> (n=2)
φ1	0(0)	0(0)	0(0)	0(0)	0(0)	0(0)
φ2	0(0)	0(0)	0(0)	0(0)	0(0)	0(0)
φ3	0(0)	0(0)	0(0)	0(0)	0(0)	0(0)
φ4	0(0)	0(0)	0(0)	0(0)	0(0)	0(0)
φ5	0(0)	0(0)	0(0)	0(0)	0(0)	0(0)
φ6	0(0)	0(0)	0(0)	0(0)	0(0)	0(0)
φ7	0(0)	0(0)	0(0)	0(0)	0(0)	0(0)
φ8	0(0)	0(0)	0(0)	0(0)	0(0)	0(0)
φ9	0(0)	0(0)	0(0)	0(0)	0(0)	0(0)
φ10	0(0)	0(0)	0(0)	0(0)	0(0)	0(0)
φ11	0(0)	0(0)	0(0)	0(0)	0(0)	0(0)
φ12	0(0)	0(0)	0(0)	0(0)	0(0)	0(0)
φ13	0(0)	0(0)	0(0)	0(0)	0(0)	0(0)
φ14	0(0)	0(0)	0(0)	0(0)	0(0)	0(0)
φ15	0(0)	0(0)	0(0)	0(0)	0(0)	0(0)
φ16	0(0)	0(0)	0(0)	0(0)	0(0)	0(0)
φ17	0(0)	0(0)	0(0)	0(0)	0(0)	0(0)
φ18	0(0)	0(0)	0(0)	0(0)	0(0)	0(0)
φ19	0(0)	0(0)	0(0)	0(0)	0(0)	0(0)
φ20	0(0)	0(0)	0(0)	0(0)	0(0)	0(0)

Appendix Table E.1 Effects of Phage Treatments at MOI 1 on M1C79 OD600nm and CFU/mL

OD600nm AUC					
Tukey's multiple comparisons test	Mean Diff.	95.00% CI of diff.	Significant ?	Summary	Adjusted P Value
Kara-mokiny 8 vs. Boorn-mokiny 1	10.51	5.964 to 15.07	Yes	**	0.0013
Kara-mokiny 8 vs. Kara-mokiny 13	10.07	5.521 to 14.62	Yes	**	0.0016
Kara-mokiny 8 vs. Kara-mokiny 16	7.108	2.557 to 11.66	Yes	**	0.008
Kara-mokiny 8 vs. Untreated Control	-11.9	-16.45 to -7.349	Yes	***	0.0007
Boorn-mokiny 1 vs. Kara-mokiny 13	-0.443	-4.994 to 4.108	No	ns	0.9935
Boorn-mokiny 1 vs. Kara-mokiny 16	-3.407	-7.958 to 1.144	No	ns	0.135
Boorn-mokiny 1 vs. Untreated Control	-22.41	-26.97 to -17.86	Yes	****	<0.0001
Kara-mokiny 13 vs. Kara-mokiny 16	-2.964	-7.515 to 1.587	No	ns	0.2025
Kara-mokiny 13 vs. Untreated Control	-21.97	-26.52 to -17.42	Yes	****	<0.0001
Kara-mokiny 16 vs. Untreated Control	-19.01	-23.56 to -14.46	Yes	****	<0.0001
CFU/mL					
Dunnett's multiple comparisons test	Mean Diff.	95.00% CI of diff.	Significant ?	Summary	Adjusted P Value
6 Hrs					
Untreated Control vs. Kara-mokiny 8	1.65E+09	-784846537 to 4084016537	No	ns	0.2486
Untreated Control vs. Kara-mokiny 13	1.65E+09	-784559037 to 4084304037	No	ns	0.2483
Untreated Control vs. Kara-mokiny 16	1.65E+09	-784460787 to 4084402287	No	ns	0.2483
Untreated Control vs. Boorn-mokiny 1	1.65E+09	-785281537 to 4083581537	No	ns	0.2487
12 Hrs					
Untreated Control vs. Kara-mokiny 8	7.75E+08	-1659431537 to 3209431537	No	ns	0.8135
Untreated Control vs. Kara-mokiny 13	1.13E+09	-1299681537 to 3569181537	No	ns	0.5561
Untreated Control vs. Kara-mokiny 16	1.12E+09	-1312931537 to 3555931537	No	ns	0.5658
Untreated Control vs. Boorn-mokiny 1	1.09E+09	-1341931537 to 3526931537	No	ns	0.5869
18 Hrs					
Untreated Control vs. Kara-mokiny 8	-1.80E+08	-2609431537 to 2259431537	No	ns	0.9989
Untreated Control vs. Kara-mokiny 13	1.00E+08	-2334431537 to 2534431537	No	ns	0.9999
Untreated Control vs. Kara-mokiny 16	50000000	-2384431537 to 2484431537	No	ns	>0.9999
Untreated Control vs. Boorn-mokiny 1	9.25E+08	-1509431537 to 3359431537	No	ns	0.71
24 Hrs					
Untreated Control vs. Kara-mokiny 8	-1.00E+09	-3434431537 to 1434431537	No	ns	0.655

Untreated Control vs. Karamokiny 13	2.30E+09	-134431537 to 4734431537	No	ns	0.0673
Untreated Control vs. Karamokiny 16	- 2.30E+08	-2659431537 to 2209431537	No	ns	0.9972
Untreated Control vs. Boornmokiny 1	3.20E+09	765568463 to 5634431537	Yes	**	0.0082

Appendix Table E.2 Effects of Phage Treatments at MOI 0.1 on M1C79 OD600nm and CFU/mL

OD600nm AUC					
Tukey's multiple comparisons test	Mean Diff.	95.00% CI of diff.	Significant ?	Summary	Adjusted P Value
Kara-mokiny 8 vs. Boorn-mokiny 1	6.723	2.254 to 11.19	Yes	**	0.0094
Kara-mokiny 8 vs. Kara-mokiny 13	8.521	4.052 to 12.99	Yes	**	0.0033
Kara-mokiny 8 vs. Kara-mokiny 16	6.372	1.903 to 10.84	Yes	*	0.0119
Kara-mokiny 8 vs. Untreated Control	-14.14	-18.61 to -9.671	Yes	***	0.0003
Boorn-mokiny 1 vs. Kara-mokiny 13	1.798	-2.671 to 6.267	No	ns	0.5467
Boorn-mokiny 1 vs. Kara-mokiny 16	-0.3505	-4.819 to 4.118	No	ns	0.9971
Boorn-mokiny 1 vs. Untreated Control	-20.86	-25.33 to -16.39	Yes	****	<0.0001
Kara-mokiny 13 vs. Kara-mokiny 16	-2.149	-6.617 to 2.320	No	ns	0.4077
Kara-mokiny 13 vs. Untreated Control	-22.66	-27.13 to -18.19	Yes	****	<0.0001
Kara-mokiny 16 vs. Untreated Control	-20.51	-24.98 to -16.04	Yes	****	<0.0001
CFU/mL					
Dunnett's multiple comparisons test	Mean Diff.	95.00% CI of diff.	Significant ?	Summary	Adjusted P Value
6 Hrs					
Untreated Control vs. Kara-mokiny 8	1.65E+09	-2260151956 to 5559861956	No	ns	0.635
Untreated Control vs. Kara-mokiny 13	1.65E+09	-2260099456 to 5559914456	No	ns	0.635

Untreated Control vs. Karamokiny 16	1.65E+09	-2260037956 to 5559975956	No	ns	0.635
Untreated Control vs. Boornmokiny 1	1.64E+09	-2266006956 to 5554006956	No	ns	0.6377
12 Hrs					
Untreated Control vs. Karamokiny 8	1E+09	-2910006956 to 4910006956	No	ns	0.9006
Untreated Control vs. Karamokiny 13	1.14E+09	-2768006956 to 5052006956	No	ns	0.853
Untreated Control vs. Karamokiny 16	1.14E+09	-2770756956 to 5049256956	No	ns	0.8539
Untreated Control vs. Boornmokiny 1	8.1E+08	-3100006956 to 4720006956	No	ns	0.9494
18 Hrs					
Untreated Control vs. Karamokiny 8	1.25E+08	-3785006956 to 4035006956	No	ns	0.9999
Untreated Control vs. Karamokiny 13	2.25E+08	-3685006956 to 4135006956	No	ns	0.9997
Untreated Control vs. Karamokiny 16	4E+08	-3510006956 to 4310006956	No	ns	0.9961
Untreated Control vs. Boornmokiny 1	9.53E+08	-2957506956 to 4862506956	No	ns	0.9144
24 Hrs					
Untreated Control vs. Karamokiny 8	2.5E+08	-3660006956 to 4160006956	No	ns	0.9991
Untreated Control vs. Karamokiny 13	1.93E+09	-1985006956 to 5835006956	No	ns	0.5107
Untreated Control vs. Karamokiny 16	-6.8E+09	-10660006956 to -2839993044	Yes	***	0.0007
Untreated Control vs. Boornmokiny 1	3.3E+09	-610006956 to 7210006956	No	ns	0.1135

Appendix Table E.3 Effects of Phage Treatments at MOI 1 on AST154 OD600nm and CFU/mL

OD600nm AUC					
Tukey's multiple comparisons test	Mean Diff.	95.00% CI of diff.	Significant ?	Summary	Adjusted P Value
Kara-mokiny 8 vs. Boorn-mokiny 1	-7.288	-7.720 to -6.856	Yes	****	<0.0001
Kara-mokiny 8 vs. Kara-mokiny 13	2.213	1.780 to 2.645	Yes	****	<0.0001
Kara-mokiny 8 vs. Kara-mokiny 16	1.709	1.276 to 2.141	Yes	****	<0.0001
Kara-mokiny 8 vs. Untreated Control	-7.613	-8.045 to -7.181	Yes	****	<0.0001
Boorn-mokiny 1 vs. Kara-mokiny 13	9.501	9.068 to 9.933	Yes	****	<0.0001
Boorn-mokiny 1 vs. Kara-mokiny 16	8.997	8.564 to 9.429	Yes	****	<0.0001
Boorn-mokiny 1 vs. Untreated Control	-0.325	-0.7573 to 0.1073	No	ns	0.1332
Kara-mokiny 13 vs. Kara-mokiny 16	-0.504	-0.9363 to -0.07174	Yes	*	0.0275
Kara-mokiny 13 vs. Untreated Control	-9.826	-10.26 to -9.393	Yes	****	<0.0001
Kara-mokiny 16 vs. Untreated Control	-9.322	-9.754 to -8.889	Yes	****	<0.0001
CFU/mL					
Dunnnett's multiple comparisons test	Mean Diff.	95.00% CI of diff.	Significant ?	Summary	Adjusted P Value
6 Hrs					
Untreated Control vs. Kara-mokiny 8	1.15E+09	-11846227317 to 14144027317	No	ns	0.9977
Untreated Control vs. Kara-mokiny 13	1.15E+09	-11845689817 to 14144564817	No	ns	0.9976

Untreated Control vs. Karamokiny 16	1.15E+09	-11845344817 to 14144909817	No	ns	0.9976
Untreated Control vs. Boornmokiny 1	5.75E+08	-12420127317 to 13570127317	No	ns	0.9998
12 Hrs					
Untreated Control vs. Karamokiny 8	1.43E+09	-11560877317 to 14429377317	No	ns	0.9949
Untreated Control vs. Karamokiny 13	1.47E+09	-11522352317 to 14467902317	No	ns	0.9943
Untreated Control vs. Karamokiny 16	1.46E+09	-11530377317 to 14459877317	No	ns	0.9944
Untreated Control vs. Boornmokiny 1	7E+08	-12295127317 to 13695127317	No	ns	0.9997
18 Hrs					
Untreated Control vs. Karamokiny 8	1.82E+09	-11177627317 to 14812627317	No	ns	0.9873
Untreated Control vs. Karamokiny 13	2E+09	-11000127317 to 14990127317	No	ns	0.9821
Untreated Control vs. Karamokiny 16	1.92E+09	-11077627317 to 14912627317	No	ns	0.9846
Untreated Control vs. Boornmokiny 1	1.25E+09	-11745127317 to 14245127317	No	ns	0.9969
24 Hrs					
Untreated Control vs. Karamokiny 8	1.55E+10	2499872683 to 28490127317	Yes	*	0.0168
Untreated Control vs. Karamokiny 13	1.55E+10	2537372683 to 28527627317	Yes	*	0.0165
Untreated Control vs. Karamokiny 16	1.52E+10	2154872683 to 28145127317	Yes	*	0.0196
Untreated Control vs. Boornmokiny 1	1.01E+10	-2945127317 to 23045127317	No	ns	0.1603

Appendix Table E.4 Effects of Phage Treatments at MOI 0.1 on AST154 OD600nm and CFU/mL

AUC					
Tukey's multiple comparisons test	Mean Diff.	95.00% CI of diff.	Significant ?	Summary	Adjusted P Value
Kara-mokiny 8 vs. Boorn-mokiny 1	-8.433	-8.809 to -8.056	Yes	****	<0.0001
Kara-mokiny 8 vs. Kara-mokiny 13	0.606	0.2299 to 0.9821	Yes	**	0.007
Kara-mokiny 8 vs. Kara-mokiny 16	0.6235	0.2474 to 0.9996	Yes	**	0.0061
Kara-mokiny 8 vs. Untreated Control	-8.823	-9.199 to -8.446	Yes	****	<0.0001
Boorn-mokiny 1 vs. Kara-mokiny 13	9.039	8.662 to 9.415	Yes	****	<0.0001
Boorn-mokiny 1 vs. Kara-mokiny 16	9.056	8.680 to 9.432	Yes	****	<0.0001
Boorn-mokiny 1 vs. Untreated Control	-0.39	-0.7661 to -0.01391	Yes	*	0.0436
Kara-mokiny 13 vs. Kara-mokiny 16	0.0175	-0.3586 to 0.3936	No	ns	0.9996
Kara-mokiny 13 vs. Untreated Control	-9.429	-9.805 to -9.052	Yes	****	<0.0001
Kara-mokiny 16 vs. Untreated Control	-9.446	-9.822 to -9.070	Yes	****	<0.0001
CFU/mL					
Dunnett's multiple comparisons test	Mean Diff.	95.00% CI of diff.	Significant ?	Summary	Adjusted P Value
6 Hrs					
Untreated Control vs. Kara-mokiny 8	1.15E+09	-11493935057 to 13788585057	No	ns	0.9974
Untreated Control vs. Kara-mokiny 13	1.12E+09	-11516760057 to 13765760057	No	ns	0.9976

Untreated Control vs. Karamokiny 16	1.15E+09	-11494335057 to 13788185057	No	ns	0.9974
Untreated Control vs. Boornmokiny 1	4.5E+08	-12191260057 to 13091260057	No	ns	0.9999
12 Hrs					
Untreated Control vs. Karamokiny 8	1.46E+09	-11183010057 to 14099510057	No	ns	0.9939
Untreated Control vs. Karamokiny 13	1.45E+09	-11187510057 to 14095010057	No	ns	0.994
Untreated Control vs. Karamokiny 16	1.47E+09	-11167885057 to 14114635057	No	ns	0.9936
Untreated Control vs. Boornmokiny 1	7.5E+08	-11891260057 to 13391260057	No	ns	0.9994
18 Hrs					
Untreated Control vs. Karamokiny 8	1.83E+09	-10808760057 to 14473760057	No	ns	0.9855
Untreated Control vs. Karamokiny 13	2.03E+09	-10613010057 to 14669510057	No	ns	0.9792
Untreated Control vs. Karamokiny 16	1.98E+09	-10661260057 to 14621260057	No	ns	0.9808
Untreated Control vs. Boornmokiny 1	1.18E+09	-11466260057 to 13816260057	No	ns	0.9972
24 Hrs					
Untreated Control vs. Karamokiny 8	1.56E+10	2993739943 to 28276260057	Yes	*	0.013
Untreated Control vs. Karamokiny 13	1.57E+10	3061239943 to 28343760057	Yes	*	0.0126
Untreated Control vs. Karamokiny 16	1.55E+10	2901239943 to 28183760057	Yes	*	0.0135
Untreated Control vs. Boornmokiny 1	1.41E+10	1483739943 to 26766260057	Yes	*	0.0259

Appendix Table E.5 Effects of Phage Treatments at MOI 1 on AST234 OD600nm and CFU/mL

AUC					
Tukey's multiple comparisons test	Mean Diff.	95.00% CI of diff.	Significant?	Summary	Adjusted P Value
Kara-mokiny 8 vs. Boorn-mokiny 1	-3.109	-4.068 to -2.150	Yes	***	0.0003
Kara-mokiny 8 vs. Kara-mokiny 13	-0.5997	-1.559 to 0.3593	No	ns	0.2257
Kara-mokiny 8 vs. Kara-mokiny 16	-1.686	-2.645 to -0.7271	Yes	**	0.0047
Kara-mokiny 8 vs. Untreated Control	-5.164	-6.123 to -4.205	Yes	****	<0.0001
Boorn-mokiny 1 vs. Kara-mokiny 13	2.509	1.550 to 3.468	Yes	***	0.0007
Boorn-mokiny 1 vs. Kara-mokiny 16	1.423	0.4640 to 2.382	Yes	*	0.01
Boorn-mokiny 1 vs. Untreated Control	-2.055	-3.014 to -1.096	Yes	**	0.0019
Kara-mokiny 13 vs. Kara-mokiny 16	-1.086	-2.045 to -0.1274	Yes	*	0.0309
Kara-mokiny 13 vs. Untreated Control	-4.564	-5.523 to -3.605	Yes	****	<0.0001
Kara-mokiny 16 vs. Untreated Control	-3.478	-4.437 to -2.519	Yes	***	0.0001
CFU/mL					
Dunnett's multiple comparisons test	Mean Diff.	95.00% CI of diff.	Significant?	Summary	Adjusted P Value
6 Hrs					
Untreated Control vs. Kara-mokiny 8	7825000	-68216634 to 224716634	No	ns	0.4414
Untreated Control vs. Kara-mokiny 13	-1.5E+07	-161466634 to 131466634	No	ns	0.9961
Untreated Control vs. Kara-mokiny 16	7950000	-66966634 to 225966634	No	ns	0.428

Untreated Control vs. Boorn-mokiny 1	- 7.8E+07	-223966634 to 68966634	No	ns	0.4497
12 Hrs					
Untreated Control vs. Kara-mokiny 8	3.18E+08	171783366 to 464716634	Yes	****	<0.0001
Untreated Control vs. Kara-mokiny 13	3.4E+08	193958366 to 486891634	Yes	****	<0.0001
Untreated Control vs. Kara-mokiny 16	3.23E+08	176533366 to 469466634	Yes	****	<0.0001
Untreated Control vs. Boorn-mokiny 1	7250000	-73966634 to 218966634	No	ns	0.5062
18 Hrs					
Untreated Control vs. Kara-mokiny 8	7.72E+08	625783366 to 918716634	Yes	****	<0.0001
Untreated Control vs. Kara-mokiny 13	7.72E+08	625808366 to 918741634	Yes	****	<0.0001
Untreated Control vs. Kara-mokiny 16	7.64E+08	617033366 to 909966634	Yes	****	<0.0001
Untreated Control vs. Boorn-mokiny 1	4.95E+08	348533366 to 641466634	Yes	****	<0.0001
24 Hrs					
Untreated Control vs. Kara-mokiny 8	2.92E+09	2770083366 to 3063016634	Yes	****	<0.0001
Untreated Control vs. Kara-mokiny 13	2.9E+09	2757533366 to 3050466634	Yes	****	<0.0001
Untreated Control vs. Kara-mokiny 16	2.91E+09	2761533366 to 3054466634	Yes	****	<0.0001
Untreated Control vs. Boorn-mokiny 1	2.62E+09	2473533366 to 2766466634	Yes	****	<0.0001

Appendix Table E.6 Effects of Phage Treatments at MOI 0.1 on AST234 OD600nm and CFU/mL

AUC					
Tukey's multiple comparisons test	Mean Diff.	95.00% CI of diff.	Significant?	Summary	Adjusted P Value
Kara-mokiny 8 vs. Boorn-mokiny 1	-3.541	-4.710 to -2.373	Yes	***	0.0004
Kara-mokiny 8 vs. Kara-mokiny 13	-0.9181	-2.087 to 0.2504	No	ns	0.1159
Kara-mokiny 8 vs. Kara-mokiny 16	-2.093	-3.262 to -0.9246	Yes	**	0.0043
Kara-mokiny 8 vs. Untreated Control	-5.114	-6.283 to -3.946	Yes	****	<0.0001
Boorn-mokiny 1 vs. Kara-mokiny 13	2.623	1.454 to 3.792	Yes	**	0.0015
Boorn-mokiny 1 vs. Kara-mokiny 16	1.448	0.2795 to 2.617	Yes	*	0.0215
Boorn-mokiny 1 vs. Untreated Control	-1.573	-2.742 to -0.4045	Yes	*	0.0152
Kara-mokiny 13 vs. Kara-mokiny 16	-1.175	-2.344 to -0.006471	Yes	*	0.049
Kara-mokiny 13 vs. Untreated Control	-4.196	-5.365 to -3.027	Yes	***	0.0002
Kara-mokiny 16 vs. Untreated Control	-3.021	-4.190 to -1.852	Yes	***	0.0008
CFU/mL					
Dunnett's multiple comparisons test	Mean	95.00% CI of diff.	Significant?	Summary	Adjusted P Value
	Diff.		t?		
6 Hrs					
Untreated Control vs. Kara-mokiny 8	9310000	-95957843 to 282157843	No	ns	0.5106
Untreated Control vs. Kara-mokiny 13	-8.5E+07	-274057843 to 104057843	No	ns	0.5854
Untreated Control vs. Kara-mokiny 16	2750000	-161557843 to 216557843	No	ns	0.9853

Untreated Control vs. Boorn-mokiny 1	- 7.8E+07	-266557843 to 111557843	No	ns	0.6566
12 Hrs					
Untreated Control vs. Kara-mokiny 8	3.41E+08	152267157 to 530382843	Yes	***	0.0004
Untreated Control vs. Kara-mokiny 13	3.36E+08	146992157 to 525107843	Yes	***	0.0005
Untreated Control vs. Kara-mokiny 16	3.41E+08	151517157 to 529632843	Yes	***	0.0004
Untreated Control vs. Boorn-mokiny 1	20000000	-169057843 to 209057843	No	ns	0.9956
18 Hrs					
Untreated Control vs. Kara-mokiny 8	7.73E+08	583542157 to 961657843	Yes	****	<0.0001
Untreated Control vs. Kara-mokiny 13	7.75E+08	585649657 to 963765343	Yes	****	<0.0001
Untreated Control vs. Kara-mokiny 16	7.63E+08	573942157 to 952057843	Yes	****	<0.0001
Untreated Control vs. Boorn-mokiny 1	5.18E+08	328442157 to 706557843	Yes	****	<0.0001
24 Hrs					
Untreated Control vs. Kara-mokiny 8	2.91E+09	2717692157 to 3095807843	Yes	****	<0.0001
Untreated Control vs. Kara-mokiny 13	2.92E+09	2730967157 to 3109082843	Yes	****	<0.0001
Untreated Control vs. Kara-mokiny 16	2.91E+09	2722192157 to 3100307843	Yes	****	<0.0001
Untreated Control vs. Boorn-mokiny 1	2.76E+09	2568692157 to 2946807843	Yes	****	<0.0001

Appendix Table F.1 Selected Phage Treated Mutants EOP and Colony Morphology

Mutant ID	Phage	Wild-Type Bacteria	Treatment MOI	EOP	Colony Morphology	Plaquing Morphology
PAEM1	Kara-mokiny 8	M1C79	10	0	2mm, Circular, Green, Flat	No Plaques
PAEM2	Kara-mokiny 8	M1C79	10	0	2mm, Circular, Green, Flat	Partial Plaques at 10 ⁻¹
PAEM3	Kara-mokiny 8	M1C79	10	0	2mm, Circular, Green, Flat	Partial Plaques at 10 ⁻²
PAEM4	Kara-mokiny 8	M1C79	0.01	0	2mm, Circular, Green, Flat	Partial Plaques at 10 ⁻¹
PAEM5	Kara-mokiny 8	M1C79	0.01	0.2038835	2mm, Circular, Green, Flat	Single Plaques
PAEM6	Boorn-mokiny 1	M1C79	10	0.9081633	2mm, Circular, Green	Single Plaques
PAEM7	Boorn-mokiny 1	M1C79	10	0.5714286	1mm, Yellow/green, Round	Single Plaques
PAEM9	Boorn-mokiny 1	M1C79	10	0	2mm, Circular, Green, Pinpoint centre	Partial Plaques at 10 ⁻⁴
PAEM10	Boorn-mokiny 1	M1C79	10	0	2mm, Circular, Green, Flat	Partial Plaques at 10 ⁻⁵
PAEM8	Boorn-mokiny 1	M1C79	10	0.6530612	2mm, Circular, Green, Pinpoint centre	Single Plaques
PAEM11	Boorn-mokiny 1	M1C79	10	0	>2mm, Irregular, Green/Grey, Dry	Partial Plaques at 10 ⁻⁴
PAEM12	Boorn-mokiny 1	M1C79	0.01	0.9591837	2mm, Circular, Green, Flat	Single Plaques
PAEM13	Boorn-mokiny 1	M1C79	0.01	0.3163265	2mm, Circular, Blue/Metallic, Flat	Single Plaques
PAEM14	Boorn-mokiny 1	M1C79	0.01	0.5102041	1mm, Yellow/green, Round	Single Plaques
PAEM15	Kara-mokiny 13	M1C79	10	0.00E+00	2mm, Circular, Green, Flat	No Plaques
PAEM16	Kara-mokiny 13	M1C79	0.01	0.00E+00	2mm, Circular, Green, Flat	No Plaques
PAEM17	Kara-mokiny 13	M1C79	0.01	0.00E+00	1mm, Circular, Green, Round	No Plaques
PAEM18	Kara-mokiny 16	M1C79	10	2.03E-06	2mm, Circular, Green, Flat	Single Plaques
PAEM19	Kara-mokiny 16	M1C79	10	0	2mm, Circular, Green, Flat	No Plaques
PAEM22	Kara-mokiny 16	M1C79	0.01	2.51E-06	2mm, Circular, Green, Flat	Single Plaques
PAEM21	Kara-mokiny 16	M1C79	0.01	0	2mm, Circular, Green, Flat	No Plaques
PAEM20	Kara-mokiny 16	M1C79	0.01	0	Green, 2mm, Circular	No Plaques
PAEM23	Kara-mokiny 8	AST154	10	0	WT Morphology	No Plaques
PAEM24	Kara-mokiny 8	AST154	10	0.4576271	WT Morphology with partial/faint plaques	Single Plaques
PAEM25	Kara-mokiny 8	AST154	0.01	0	WT Morphology	No Plaques
PAEM26	Kara-mokiny 8	AST154	0.01	0.5254237	WT Morphology	Single Plaques
PAEM27	Kara-mokiny 8	AST154	0.01	0.0055932	WT Morphology	Single Plaques
PAEM28	Boorn-mokiny 1	AST154	10	0	WT Morphology	Partial Plaques at 10 ⁻²
PAEM29	Boorn-mokiny 1	AST154	0.01	0	WT Morphology	Partial Plaques at 10 ⁻²
PAEM30	Kara-mokiny 13	AST154	10	0	WT Morphology	No Plaques
PAEM31	Kara-mokiny 13	AST154	10	0	WT Morphology	Partial Plaques at 10 ⁻⁴
PAEM32	Kara-mokiny 13	AST154	0.01	0	WT Morphology	No Plaques

PAEM33	Kara-mokiny 13	AST154	0.01	0.3533333	WT Morphology	Single Plaques
PAEM34	Kara-mokiny 16	AST154	10	0	WT Morphology	No Plaques
PAEM35	Kara-mokiny 16	AST154	10	0.3488372	WT Morphology with faint plaques	Single Plaques
PAEM36	Kara-mokiny 16	AST154	10	3.49E-06	faint plaques WT	Single Plaques
PAEM37	Kara-mokiny 16	AST154	0.01	0	WT Morphology with faint plaques	No Plaques
PAEM38	Kara-mokiny 8	AST234	10	0.3373333	WT Morphology	Single Plaques
PAEM39	Kara-mokiny 8	AST234	0.01	0	WT Morphology	No Plaques
PAEM40	Kara-mokiny 8	AST234	0.01	0	WT Morphology	Partial Plaques at 10 ⁻²
PAEM41	Kara-mokiny 8	AST234	0.01	0.0306667	WT Morphology	Single Plaques
PAEM42	Kara-mokiny 8	AST234	0.01	0	Dry yellow colonies	No Plaques
PAEM43	Boorn-mokiny 1	AST234	10	0	WT Morphology	Partial at neat
PAEM44	Boorn-mokiny 1	AST234	0.01	0	WT Morphology	Partial at neat
PAEM45	Kara-mokiny 13	AST234	10	4.9019608	WT Morphology	Single Plaques
PAEM46	Kara-mokiny 13	AST234	10	0	WT Morphology	No Plaques
PAEM47	Kara-mokiny 13	AST234	10	0.000451	WT Morphology	Single Plaques
PAEM48	Kara-mokiny 13	AST234	0.01	0	WT Morphology	No Plaques
PAEM49	Kara-mokiny 16	AST234	10	0	WT Morphology	No Plaques
PAEM50	Kara-mokiny 16	AST234	10	0.6923077	WT Morphology	Single Plaques
PAEM51	Kara-mokiny 16	AST234	0.01	0	WT Morphology	No Plaques
PAEM52	Kara-mokiny 16	AST234	0.01	2.3846154	WT Morphology	Single Plaques

Appendix Table G.1 Predicted Phage Spacers in M1C79 CRISPR-cas System

Bacterial ID	phage ID	Combined p-value	Number of Hits
M1C79 WT	Boorn-mokiny 1	181.8	9
M1C79 WT	Kara-mokiny 13	37.43	2
M1C79 WT	Kara-mokiny 16	31.84	3
M1C79 WT	Kara-mokiny 8	45.89	3
M1C79 Control	Boorn-mokiny 1	203.4	10
M1C79 Control	Kara-mokiny 13	37.45	2
M1C79 Control	Kara-mokiny 16	34.93	4
M1C79 Control	Kara-mokiny 8	48.98	4
PAEM1	Boorn-mokiny 1	203.4	10
PAEM1	Kara-mokiny 13	37.45	2
PAEM1	Kara-mokiny 16	34.95	4
PAEM1	Kara-mokiny 8	49	4
PAEM2	Boorn-mokiny 1	203.4	10
PAEM2	Kara-mokiny 13	37.45	2
PAEM2	Kara-mokiny 16	34.94	4
PAEM2	Kara-mokiny 8	48.99	4
PAEM3	Boorn-mokiny 1	203.4	10
PAEM3	Kara-mokiny 13	37.45	2
PAEM3	Kara-mokiny 16	34.94	4
PAEM3	Kara-mokiny 8	48.99	4

PAEM4	Boorn-mokiny 1	203.4	10
PAEM4	Kara-mokiny 13	37.45	2
PAEM4	Kara-mokiny 16	34.94	4
PAEM4	Kara-mokiny 8	48.99	4
PAEM5	Boorn-mokiny 1	203.4	10
PAEM5	Kara-mokiny 13	37.45	2
PAEM5	Kara-mokiny 16	34.94	4
PAEM5	Kara-mokiny 8	48.99	4
PAEM6	Boorn-mokiny 1	203.4	10
PAEM6	Kara-mokiny 13	37.45	2
PAEM6	Kara-mokiny 16	34.95	4
PAEM6	Kara-mokiny 8	49	4
PAEM7	Boorn-mokiny 1	203.4	10
PAEM7	Kara-mokiny 13	37.45	2
PAEM7	Kara-mokiny 16	34.94	4
PAEM7	Kara-mokiny 8	48.99	4
PAEM8	Boorn-mokiny 1	203.4	10
PAEM8	Kara-mokiny 13	37.45	2
PAEM8	Kara-mokiny 16	34.94	4
PAEM8	Kara-mokiny 8	48.99	4
PAEM9	Boorn-mokiny 1	203.4	10

PAEM9	Kara-mokiny 13	37.45	2
PAEM9	Kara-mokiny 16	34.94	4
PAEM9	Kara-mokiny 8	48.99	4
PAEM10	Boorn-mokiny 1	203.4	10
PAEM10	Kara-mokiny 13	37.45	2
PAEM10	Kara-mokiny 16	34.94	4
PAEM10	Kara-mokiny 8	48.99	4
PAEM11	Boorn-mokiny 1	203.4	10
PAEM11	Kara-mokiny 13	37.45	2
PAEM11	Kara-mokiny 16	34.93	4
PAEM11	Kara-mokiny 8	48.98	4
PAEM12	Boorn-mokiny 1	203.4	10
PAEM12	Kara-mokiny 13	37.45	2
PAEM12	Kara-mokiny 16	34.94	4
PAEM12	Kara-mokiny 8	48.99	4
PAEM13	Boorn-mokiny 1	203.4	10
PAEM13	Kara-mokiny 13	37.45	2
PAEM13	Kara-mokiny 16	34.95	4
PAEM13	Kara-mokiny 8	49	4
PAEM14	Boorn-mokiny 1	203.4	10
PAEM14	Kara-mokiny 13	37.45	2

PAEM14	Kara-mokiny 16	34.95	4
PAEM14	Kara-mokiny 8	49	4
PAEM15	Boorn-mokiny 1	203.4	10
PAEM15	Kara-mokiny 13	37.45	2
PAEM15	Kara-mokiny 16	34.93	4
PAEM15	Kara-mokiny 8	48.98	4
PAEM16	Boorn-mokiny 1	203.4	10
PAEM16	Kara-mokiny 13	37.45	2
PAEM16	Kara-mokiny 16	34.94	4
PAEM16	Kara-mokiny 8	48.99	4
PAEM17	Boorn-mokiny 1	203.4	10
PAEM17	Kara-mokiny 13	37.45	2
PAEM17	Kara-mokiny 16	34.94	4
PAEM17	Kara-mokiny 8	48.99	4
PAEM18	Boorn-mokiny 1	203.4	10
PAEM18	Kara-mokiny 13	37.45	2
PAEM18	Kara-mokiny 16	34.94	4
PAEM18	Kara-mokiny 8	48.99	4
PAEM19	Boorn-mokiny 1	203.4	10
PAEM19	Kara-mokiny 13	37.45	2
PAEM19	Kara-mokiny 16	34.94	4

PAEM19	Kara-mokiny 8	48.99	4
PAEM20	Boorn-mokiny 1	203.4	10
PAEM20	Kara-mokiny 13	37.45	2
PAEM20	Kara-mokiny 16	34.94	4
PAEM20	Kara-mokiny 8	48.99	4
PAEM21	Boorn-mokiny 1	203.4	10
PAEM21	Kara-mokiny 13	37.45	2
PAEM21	Kara-mokiny 16	34.94	4
PAEM21	Kara-mokiny 8	48.99	4
PAEM22	Boorn-mokiny 1	203.4	10
PAEM22	Kara-mokiny 13	37.45	2
PAEM22	Kara-mokiny 16	34.93	4
PAEM22	Kara-mokiny 8	48.98	4

Note: The mutant names are denoted as PAEM (*P. aeruginosa* Escape Mutant) followed by a number.

Appendix Table H.1 Filtered Mutations Identified in the M1C79 Mutants Following Phage Treatment

Mutation Type	Reference Allele	Alternative Allele	Ftype	Effect	Gene	Product	I	I	I	I	I	I	I	I	R	R	R	R	R	R	R	COG		
							PAE M2	PAE M3	PAE M4	PAE M9	PAE M10	PAE M11	PAE M18	PAE M22	PAE M1	PAE M15	PAE M16	PAE M17	PAE M19	PAE M20	PAE M21	COG		
del	CTGGCTGTGGCTGTGGCTGTGGCTGTGGCTG	C	CD S	conservative_inframe_deletion p.Gln286_Pro295del	<i>flaI</i>	type VI secretion system forkhead-associated protein FlaI																	TU	
ins	A	AG	CD S	frameshift_variant p.Phe248fs	<i>Wzy</i>	O-antigen polysaccharide polymerase Wzy																		M
snp	T	G	CD S	missense_variant p.Phe248Val	<i>Wzy</i>	O-antigen polysaccharide polymerase Wzy																		M
snp	G	A	CD S	missense_variant p.Gly221Arg		Glycosyl transferase																		
ins	TACCG	TACCGTACCG	CD S	frameshift_insertion p.300Pro	<i>flaG</i>	flagellar motor switch protein G																		N
del	+650bp	Δ650 bp	CD S	disruptive_frameshift_deletion	<i>flaG</i> - <i>flaH</i>	flagellar motor switch protein G and flagellar assembly protein H																		N/N U
ins	G	GCTGCTCGGC	CD S	conservative_inframe_insertion p.Leu323_Gly325dup	<i>pgi</i>	glucose-6-phosphate isomerase																		G
snp	G	A	CD S	missense_variant p.Ala123Val	<i>wapA</i>	alpha-1,3-rhamnosyltransferase																		N
snp	G	T	CD S	stop_gained p.Tyr136*	<i>rfaB</i>	Glycosyltransferase involved in cell wall biosynthesis																		M
del	+207bp	Δ207 bp	CD S	disruptive_inframe_deletion p.Glyc153_Cys222del	<i>rfaB</i>	Glycosyltransferase involved in cell wall biosynthesis																		M
del	GA	G	CD S	frameshift_variant p.Phe90fs	<i>rfaB</i>	Glycosyltransferase involved in cell wall biosynthesis																		M

Note: In the mutation type column del: deletion, ins: insertion and snp: single nucleotide polymorphism. Ftype is the type of sequence that was affected by the mutation and CDS stands for coding sequence. Phage Susceptibility is stated as I: intermediately susceptible or R: completely resistant. The mutant names are denoted as PAEM (*P. aeruginosa* Escape Mutant) followed by a number. COG stands for Cluster of Orthologous Genes which is a database that classifies genes into categories. The letters in the COG column correspond to a category within this database. Blue indicates where the mutant had the reference allele and red where it had the mutant allele.

Appendix Table H.2 Filtered Mutations Identified in the AST154 Mutants Following Phage Treatment

Mutation Type	Reference Allele	Alternative Allele	Type	Effect	Gene	Product	Phage Susceptibilities										COG					
							I PAEM2 7	I PAEM2 8	I PAEM2 9	I PAEM3 1	I PAEM3 6	R PAEM2 3	R PAEM2 5	R PAEM3 2	R PAEM3 4	R PAEM3 7						
snp	C	T	CDS	missense_variant p.Ala74Val	<i>mupP</i>	ABC-type guanosine uptake system NupNOPQ, permease component NupP															F	
snp	A	G	CDS	missense_variant p.Thr100Ala	<i>pcbC</i>	Isopenicillin N synthase and related dioxygenases																Q
ins	T	TG	CDS	frameshift_variant p.Val103fs	<i>iclR</i>	DNA-binding transcriptional regulator, IclR family																K
del	TA	T	intergenic		<i>hcpA</i> ← / → <i>ornR</i>	Hcp family type VI secretion system effector (RNA-Arg(ccg))																Intergenic
snp	C	T	CDS	synonymous_variant p.Pro209Pro		putative membrane transporter protein																Unknown
snp	A	G	CDS	missense_variant p.Thr319Ala	<i>spuD</i>	Putrescine-binding periplasmic protein SpuD																H
snp	C	T	intergenic		<i>pitA</i> ← / → <i>ηfD</i>	Phosphate/sulfate permease/Membrane-bound serine protease NfeD, ClpP class UPP0229 protein PSPA7_0730																Intergenic
snp	C	T	CDS	missense_variant p.Ala382Thr	<i>yaaH</i>	UPP0229 protein PSPA7_0730																Unknown
snp	A	G	CDS	missense_variant p.Thr264Ala	<i>rplB</i>	50S ribosomal protein L2																J
snp	T	C	CDS	missense_variant p.Val50Ala	<i>rplV</i>	50S ribosomal protein L22																J
snp	C	T	CDS	missense_variant p.Pro497Leu	<i>pchH</i>	ABC transporter ATP-binding protein PchH																V
snp	A	G	CDS	synonymous_variant p.Arg196Arg	<i>nmoR</i>	HTH-type transcriptional regulator NmoR																K
snp	C	T	CDS	missense_variant p.Arg30His		Ribosomal protein S3AE																J
snp	T	C	CDS	missense_variant p.Val245Ala	<i>fhaB</i>	Large exoprotein involved in heme utilization or adhesion																U
snp	T	C	intergenic		<i>rimI</i> ← / → <i>eutC</i>	Ribosomal protein S18 acetylase RimI and related acetyltransferases/ethanolamine ammonia-lyase subunit EurC																Intergenic
snp	G	A	CDS	missense_variant p.Pro322Ser	<i>eutB</i>	Ethanolamine ammonia-lyase, large subunit																E
snp	A	G	CDS	missense_variant p.Phe39Ser		Bifunctional lytic transglycosylase/aminic acid ABC transporter substrate-binding protein																Unknown
snp	C	T	CDS	missense_variant p.Gly374Ser	<i>opuBA</i>	ABC-type proline/glycine betaine transport system, ATPase component																E
snp	C	T	intergenic		<i>leuA</i> ← / → <i>BLBJND_01950</i>	2-isopropylmalate synthase/DUF2946 domain-containing protein																Intergenic
snp	A	G	CDS	missense_variant p.Val207Ala	<i>yhjE</i>	Inner membrane metabolite transport protein yhjE																Unknown
snp	C	T	CDS	synonymous_variant p.Leu145Leu		Rha family transcriptional regulator																K
snp	C	T	CDS	synonymous_variant p.Leu82Leu	<i>fhpA</i>	FKBP-type peptidyl-prolyl cis-trans isomerase																O
ins	T	TC	CDS	frameshift_variant p.Lys40fs		hypothetical protein																Unknown
snp	T	C	CDS	missense_variant p.Gln130Arg	<i>cheY</i>	CheY-like REC (receiver) domain, includes chemotaxis protein CheY and sporulation regulator SpoF																T
del	GC	G	intergenic		<i>hasA</i> / <i>arpD</i>	heme acquisition protein HasA/ABC-type protease/lipase transport system, ATPase and permease components																Intergenic
snp	A	G	CDS	missense_variant p.Ser100Pro	<i>rhaT</i>	Permease of the drug/metabolite transporter (DMT) superfamily																GER
snp	T	C	CDS	missense_variant p.Val76Ala	<i>lhr</i>	Lhr-like helicase																L
snp	T	C	CDS	missense_variant p.Val244Ala	<i>araC</i>	AraC-type DNA-binding domain and AraC-containing proteins																K
ins	C	CG	CDS	frameshift_variant p.Val336fs		Glycosyltransferase family 2 protein																K
ins	T	TG	CDS	frameshift_variant p.Gln246fs		Flippase																M

Appendix Table H.3 Filtered Mutations Identified in the AST234 Mutants Following Phage Treatment

Mutation Type	Reference Allele	Alternative Allele	Ftype	Effect	Gene	Product	Phage Susceptibilities										COG	
							I PAEM40	I PAEM43	I PAEM44	I PAEM41	I PAEM47	R PAEM39	R PAEM46	R PAEM48	R PAEM49	R PAEM51		
snp	C	T	CDS	synonymous_variant p.Leu132Leu		Hemolysin												Unknown
snp	A	G	CDS	missense_variantc.745T>C p.Phe249Leu	<i>pdxA</i>	4-hydroxythreonine-4-phosphate dehydrogenase PdxA												H
snp	G	A	CDS	synonymous_variant p.Ala127Ala	<i>pchI</i>	ABC transporter ATP-binding protein PchI												V
ins	T	TG	intergenic		<i>PLFKEE_05050 / brp</i>	DUF2788 domain-containing protein/DNA-binding transcriptional regulator, Lrp family												Unknown
ins	T	TG	CDS	frameshift_variant p.Gln167fs		Flippase												M
snp	C	T	CDS	missense_variant p.Arg109Cys	<i>mkk</i>	dTMP kinase												F
del	CG	C	intergenic		<i>caiD / deaD</i>	Enoyl-CoA hydratase/carnithine racemase/ATP-dependent RNA helicase DeaD												intergenic
snp	T	C	CDS	missense_variant p.Asn211Ser		Quercetin 2,3-dioxygenase												Unknown
del	AG	A	CDS	frameshift_variant p.Pro150fs		hypothetical protein												Unknown
snp	T	C	intergenic		<i>cymI / cymS</i>	carbonic anhydrase CymI/cyanase												intergenic
snp	G	A	CDS	missense_variant p.Pro18Leu	<i>galU</i>	UTP-glucose-1-phosphate uridylyltransferase GalU												M
snp	G	A	CDS	missense_variant c.574G>A p.Gly192Ser	<i>brnQ</i>	branched-chain amino acid transport system II carrier protein												E
snp	G	A	CDS	missense_variant p.Arg424Cys	<i>cobN</i>	cobalochelatase subunit CobN												H
snp	G	A	CDS	missense_variant p.Arg45Tyr	<i>rimI</i>	Ribosomal protein S18 acetylase RimI and related acetyltransferases												J
snp	T	C	CDS	missense_variant p.Leu363Pro	<i>acnB</i>	bifunctional aconitate hydratase 2/2-methylisocitrate dehydratase												C
ins	A	AG	intergenic															intergenic
ins	GGGGGGG	GGGGGGGG	intergenic		<i>casT / exsD</i>	CesT family type III secretion system chaperone/T3SS regulon anti-activator ExsD												intergenic
snp	T	C	CDS	missense_variant p.Phe19Leu	<i>vgrG</i>	type VI secretion system tip protein VgrG												UXR
snp	G	A	CDS	missense_variant p.Arg328Gln	<i>mntH2</i>	Nramp family divalent metal transporter												P
snp	A	G	CDS	missense_variant p.Asp127Gly	<i>retS</i>	hybrid sensor histidine kinase/response regulator RetS												TK
snp	C	T	CDS	stop_gained p.Trp100*		Uncharacterized conserved protein, contains a phytase-like domain												Unknown
snp	T	C	CDS	missense_variant p.Tyr163Cys	<i>rfaB</i>	Glycosyltransferase involved in cell wall biosynthesis												M
snp	G	A	CDS	missense_variant p.Arg110Tyr	<i>rfaB</i>	Glycosyltransferase involved in cell wall biosynthesis												M
snp	A	G	CDS	missense_variant p.Leu287Pro	<i>rfaB</i>	Glycosyltransferase involved in cell wall biosynthesis												M
snp	A	G	CDS	missense_variant p.Leu333Pro	<i>aroB</i>	3-dehydroquinate synthase												E

snp	A	G	CDS	missense_variant p.Asn111Ser	<i>rfbA</i>	glucose-1-phosphate thymidyltransferase <i>RfbA</i>	Blue	Blue	Blue	Blue	Blue	Red	Blue	Blue	Blue	Blue	Blue	M
snp	T	C	CDS	missense_variant p.Leu232Pro	<i>rfbA</i>	glucose-1-phosphate thymidyltransferase <i>RfbA</i>	Blue	Blue	Blue	Blue	Red	Blue	Blue	Blue	Blue	Blue	Blue	M
del	GC	G	CDS	frameshift_variant p.Ala104fs	<i>cyaY</i>	Iron-sulfur cluster assembly protein CyaY	Blue	Red	Blue	Blue	Blue	Blue	Blue	Blue	Blue	Blue	Blue	P
snp	T	C	CDS	missense_variant p.Gln211Arg		DctA-YdbH domain- containing protein	Blue	Blue	Red	Blue	Blue	Blue	Blue	Blue	Blue	Blue	Blue	Unknown

Note: In the mutation type column del: deletion, ins: insertion and snp: single nucleotide polymorphism. Ftype is the type of sequence that was affected by the mutation and CDS stands for coding sequence. Intergenic mutations do not have a gene associated with them but instead have the genes that are either side of them depicted (ie: gene1 / gene2). Phage Susceptibility is stated as I: intermediately susceptible or R: completely resistant. The mutant names are denoted as PAEM (*P. aeruginosa* Escape Mutant) followed by a number. COG stands for Cluster of Orthologous Genes which is a database that classifies genes into categories. The letters in the COG column correspond to a category within this database. Blue indicates where the mutant had the reference allele and red where it had the mutant allele.

Appendix Table I.1 Statistics of 2-way ANOVA for Viable M1C79 at 6,12, 18 and 24 Hrs After the High Dose Combination Treatments

Tukey's multiple comparisons test	Mean Diff.	95.00% CI of diff.	Significant?	Summary	Adjusted P Value
6 Hrs					
Cocktail High Dose vs. Cocktail Low Dose	0.035	-3.159 to 3.229	No	ns	>0.9999
Cocktail High Dose vs. Kara-mokiny 16 10 ⁷	-0.895	-4.089 to 2.299	No	ns	0.9509
Cocktail High Dose vs. Kara-mokiny 16 10 ⁶	-1.5	-4.694 to 1.694	No	ns	0.6962
Cocktail High Dose vs. Tobramycin (2µg/mL)	-3.84	-7.034 to -0.6459	Yes	*	0.0121
Cocktail High Dose vs. Untreated	-4.915	-8.109 to -1.721	Yes	***	0.001
Kara-mokiny 16 10 ⁷ vs. Kara-mokiny 16 10 ⁶	-0.605	-3.799 to 2.589	No	ns	0.9911
Kara-mokiny 16 10 ⁷ vs. Tobramycin (2µg/mL)	-2.945	-6.139 to 0.2491	No	ns	0.0829
Kara-mokiny 16 10 ⁷ vs. Untreated	-4.02	-7.214 to -0.8259	Yes	**	0.008
Tobramycin (2µg/mL) vs. Untreated	-1.075	-4.269 to 2.119	No	ns	0.8993
12 Hrs					
Cocktail High Dose vs. Cocktail Low Dose	0.195	-2.999 to 3.389	No	ns	>0.9999
Cocktail High Dose vs. Kara-mokiny 16 10 ⁷	-0.595	-3.789 to 2.599	No	ns	0.9917
Cocktail High Dose vs. Kara-mokiny 16 10 ⁶	-0.35	-3.544 to 2.844	No	ns	0.9993
Cocktail High Dose vs. Tobramycin (2µg/mL)	-2.285	-5.479 to 0.9091	No	ns	0.269
Cocktail High Dose vs. Untreated	-4.26	-7.454 to -1.066	Yes	**	0.0046

Kara-mokiny 16 10⁷ vs. Kara-mokiny 16 10⁶	0.245	-2.949 to 3.439	No	ns	0.9999
Kara-mokiny 16 10⁷ vs. Tobramycin (2µg/mL)	-1.69	-4.884 to 1.504	No	ns	0.5842
Kara-mokiny 16 10⁷ vs. Untreated	-3.665	-6.859 to -0.4709	Yes	*	0.018
Tobramycin (2µg/mL) vs. Untreated	-1.975	-5.169 to 1.219	No	ns	0.4194
18 Hrs					
Cocktail High Dose vs. Cocktail Low Dose	0.42	-2.774 to 3.614	No	ns	0.9984
Cocktail High Dose vs. Kara-mokiny 16 10⁷	-4.74	-7.934 to -1.546	Yes	**	0.0015
Cocktail High Dose vs. Kara-mokiny 16 10⁶	-4.18	-7.374 to -0.9859	Yes	**	0.0055
Cocktail High Dose vs. Tobramycin (2µg/mL)	-1.535	-4.729 to 1.659	No	ns	0.676
Cocktail High Dose vs. Untreated	-4.74	-7.934 to -1.546	Yes	**	0.0015
Kara-mokiny 16 10⁷ vs. Kara-mokiny 16 10⁶	0.56	-2.634 to 3.754	No	ns	0.9937
Kara-mokiny 16 10⁷ vs. Tobramycin (2µg/mL)	3.205	0.01095 to 6.399	Yes	*	0.0489
Kara-mokiny 16 10⁷ vs. Untreated	0	-3.194 to 3.194	No	ns	>0.9999
Tobramycin (2µg/mL) vs. Untreated	-3.205	-6.399 to -0.01095	Yes	*	0.0489
24 Hrs					
Cocktail High Dose vs. Cocktail Low Dose	-3.41	-6.604 to -0.2159	Yes	*	0.0316
Cocktail High Dose vs. Kara-mokiny 16 10⁷	-7.28	-10.47 to -4.086	Yes	****	<0.0001
Cocktail High Dose vs. Kara-mokiny 16 10⁶	-6.06	-9.254 to -2.866	Yes	****	<0.0001
Cocktail High Dose vs. Tobramycin (2µg/mL)	-2.2	-5.394 to 0.9941	No	ns	0.3063

Cocktail High Dose vs. Untreated	-6.15	-9.344 to -2.956	Yes	****	<0.0001
Kara-mokiny 16 10⁷ vs. Kara-mokiny 16 10⁶	1.22	-1.974 to 4.414	No	ns	0.8414
Kara-mokiny 16 10⁷ vs. Tobramycin (2µg/mL)	5.08	1.886 to 8.274	Yes	***	0.0007
Kara-mokiny 16 10⁷ vs. Untreated	1.13	-2.064 to 4.324	No	ns	0.879
Tobramycin (2µg/mL) vs. Untreated	-3.95	-7.144 to -0.7559	Yes	**	0.0094

Appendix Table I.2 Statistics of 2-way ANOVA for Viable M1C79 at 6,12, 18 and 24 Hrs After Low Dose Combination Treatment

Tukey's multiple comparisons test	Mean Diff.	95.00% CI of diff.	Significant?	Summary	Adjusted P Value
6 Hrs					
Cocktail Low Dose vs. Kara-mokiny 16 10 ⁷	-0.93	-4.124 to 2.264	No	ns	0.9427
Cocktail Low Dose vs. Kara-mokiny 16 10 ⁶	-1.535	-4.729 to 1.659	No	ns	0.676
Cocktail Low Dose vs. Tobramycin (2µg/mL)	-3.875	-7.069 to -0.6809	Yes	*	0.0112
Cocktail Low Dose vs. Untreated	-4.95	-8.144 to -1.756	Yes	***	0.0009
Kara-mokiny 16 10 ⁶ vs. Tobramycin (2µg/mL)	-2.34	-5.534 to 0.8541	No	ns	0.2466
Kara-mokiny 16 10 ⁶ vs. Untreated	-3.415	-6.609 to -0.2209	Yes	*	0.0313
Tobramycin (2µg/mL) vs. Untreated	-1.075	-4.269 to 2.119	No	ns	0.8993
12 Hrs					
Cocktail Low Dose vs. Kara-mokiny 16 10 ⁷	-0.79	-3.984 to 2.404	No	ns	0.9709
Cocktail Low Dose vs. Kara-mokiny 16 10 ⁶	-0.545	-3.739 to 2.649	No	ns	0.9945
Cocktail Low Dose vs. Tobramycin (2µg/mL)	-2.48	-5.674 to 0.7141	No	ns	0.1956
Cocktail Low Dose vs. Untreated	-4.455	-7.649 to -1.261	Yes	**	0.0029
Kara-mokiny 16 10 ⁶ vs. Tobramycin (2µg/mL)	-1.935	-5.129 to 1.259	No	ns	0.4415
Kara-mokiny 16 10 ⁶ vs. Untreated	-3.91	-7.104 to -0.7159	Yes	*	0.0104
Tobramycin (2µg/mL) vs. Untreated	-1.975	-5.169 to 1.219	No	ns	0.4194
18 Hrs					
Cocktail Low Dose vs. Kara-mokiny 16 10 ⁷	-5.16	-8.354 to -1.966	Yes	***	0.0005

Cocktail Low Dose vs. Kara-mokiny 16 10⁶	-4.6	-7.794 to -1.406	Yes	**	0.0021
Cocktail Low Dose vs. Tobramycin (2µg/mL)	-1.955	-5.149 to 1.239	No	ns	0.4304
Cocktail Low Dose vs. Untreated	-5.16	-8.354 to -1.966	Yes	***	0.0005
Kara-mokiny 16 10⁶ vs. Tobramycin (2µg/mL)	2.645	-0.5491 to 5.839	No	ns	0.1464
Kara-mokiny 16 10⁶ vs. Untreated	-0.56	-3.754 to 2.634	No	ns	0.9937
Tobramycin (2µg/mL) vs. Untreated	-3.205	-6.399 to -0.01095	Yes	*	0.0489
24 Hrs					
Cocktail Low Dose vs. Kara-mokiny 16 10⁷	-3.87	-7.064 to -0.6759	Yes	*	0.0113
Cocktail Low Dose vs. Kara-mokiny 16 10⁶	-2.65	-5.844 to 0.5441	No	ns	0.1451
Cocktail Low Dose vs. Tobramycin (2µg/mL)	1.21	-1.984 to 4.404	No	ns	0.8458
Cocktail Low Dose vs. Untreated	-2.74	-5.934 to 0.4541	No	ns	0.1229
Kara-mokiny 16 10⁶ vs. Tobramycin (2µg/mL)	3.86	0.6659 to 7.054	Yes	*	0.0116
Kara-mokiny 16 10⁶ vs. Untreated	-0.09	-3.284 to 3.104	No	ns	>0.9999
Tobramycin (2µg/mL) vs. Untreated	-3.95	-7.144 to -0.7559	Yes	**	0.0094

Appendix Table I.3 Statistics of 2-way ANOVA for Viable AST154 at 6,12, 18 and 24 Hrs After the High Dose Combination Treatments

Tukey's multiple comparisons test	Mean Diff.	95.00% CI of diff.	Significant?	Summary	Adjusted P Value
6 Hrs					
Cocktail High Dose vs. Cocktail Low Dose	0.19	-0.8274 to 1.207	No	ns	0.9916
Cocktail High Dose vs. Kara-mokiny 16 10 ⁷	0.155	-0.8624 to 1.172	No	ns	0.9967
Cocktail High Dose vs. Kara-mokiny 16 10 ⁶	0.28	-0.7374 to 1.297	No	ns	0.9544
Cocktail High Dose vs. Tobramycin (2µg/mL)	-3.855	-4.872 to -2.838	Yes	****	<0.0001
Cocktail High Dose vs. Untreated	-3.755	-4.772 to -2.738	Yes	****	<0.0001
Kara-mokiny 16 10 ⁷ vs. Kara-mokiny 16 10 ⁶	0.125	-0.8924 to 1.142	No	ns	0.9988
Kara-mokiny 16 10 ⁷ vs. Tobramycin (2µg/mL)	-4.01	-5.027 to -2.993	Yes	****	<0.0001
Kara-mokiny 16 10 ⁷ vs. Untreated	-3.91	-4.927 to -2.893	Yes	****	<0.0001
Tobramycin (2µg/mL) vs. Untreated	0.1	-0.9174 to 1.117	No	ns	0.9996
12 Hrs					
Cocktail High Dose vs. Cocktail Low Dose	-0.575	-1.592 to 0.4424	No	ns	0.5159
Cocktail High Dose vs. Kara-mokiny 16 10 ⁷	-1.01	-2.027 to 0.007405	No	ns	0.0525
Cocktail High Dose vs. Kara-mokiny 16 10 ⁶	-0.62	-1.637 to 0.3974	No	ns	0.4351
Cocktail High Dose vs. Tobramycin (2µg/mL)	-2.515	-3.532 to -1.498	Yes	****	<0.0001
Cocktail High Dose vs. Untreated	-2.63	-3.647 to -1.613	Yes	****	<0.0001
Kara-mokiny 16 10 ⁷ vs. Kara-mokiny 16 10 ⁶	0.39	-0.6274 to 1.407	No	ns	0.8395
Kara-mokiny 16 10 ⁷ vs. Tobramycin (2µg/mL)	-1.505	-2.522 to -0.4876	Yes	**	0.0015
Kara-mokiny 16 10 ⁷ vs. Untreated	-1.62	-2.637 to -0.6026	Yes	***	0.0006

Tobramycin (2µg/mL) vs. Untreated	-0.115	-1.132 to 0.9024	No	ns	0.9992
18 Hrs					
Cocktail High Dose vs. Cocktail Low Dose	0.015	-1.002 to 1.032	No	ns	>0.9999
Cocktail High Dose vs. Kara-mokiny 16 10⁷	0.245	-0.7724 to 1.262	No	ns	0.974
Cocktail High Dose vs. Kara-mokiny 16 10⁶	-0.32	-1.337 to 0.6974	No	ns	0.9222
Cocktail High Dose vs. Tobramycin (2µg/mL)	-0.83	-1.847 to 0.1874	No	ns	0.1571
Cocktail High Dose vs. Untreated	-0.995	-2.012 to 0.02241	No	ns	0.0578
Kara-mokiny 16 10⁷ vs. Kara-mokiny 16 10⁶	-0.565	-1.582 to 0.4524	No	ns	0.5344
Kara-mokiny 16 10⁷ vs. Tobramycin (2µg/mL)	-1.075	-2.092 to -0.05759	Yes	*	0.0341
Kara-mokiny 16 10⁷ vs. Untreated	-1.24	-2.257 to -0.2226	Yes	*	0.0108
Tobramycin (2µg/mL) vs. Untreated	-0.165	-1.182 to 0.8524	No	ns	0.9956
24 Hrs					
Cocktail High Dose vs. Cocktail Low Dose	0.67	-0.3474 to 1.687	No	ns	0.3524
Cocktail High Dose vs. Kara-mokiny 16 10⁷	0.68	-0.3374 to 1.697	No	ns	0.337
Cocktail High Dose vs. Kara-mokiny 16 10⁶	0.58	-0.4374 to 1.597	No	ns	0.5067
Cocktail High Dose vs. Tobramycin (2µg/mL)	-0.74	-1.757 to 0.2774	No	ns	0.2533
Cocktail High Dose vs. Untreated	-1.22	-2.237 to -0.2026	Yes	*	0.0124
Kara-mokiny 16 10⁷ vs. Kara-mokiny 16 10⁶	-0.1	-1.117 to 0.9174	No	ns	0.9996
Kara-mokiny 16 10⁷ vs. Tobramycin (2µg/mL)	-1.42	-2.437 to -0.4026	Yes	**	0.0029
Kara-mokiny 16 10⁷ vs. Untreated	-1.9	-2.917 to -0.8826	Yes	****	<0.0001
Tobramycin (2µg/mL) vs. Untreated	-0.48	-1.497 to 0.5374	No	ns	0.6922

Appendix Table I.4 Statistics of 2-way ANOVA for Viable AST154 at 6,12, 18 and 24 Hrs After Low Dose Combination Treatment

Tukey's multiple comparisons test	Mean Diff.	95.00% CI of diff.	Significant ?	Summary	Adjusted P Value
6 Hrs					
Cocktail Low Dose vs. Kara-mokiny 16 10 ⁷	-0.035	-1.052 to 0.9824	No	ns	>0.9999
Cocktail Low Dose vs. Kara-mokiny 16 10 ⁶	0.09	-0.9274 to 1.107	No	ns	0.9998
Cocktail Low Dose vs. Tobramycin (2µg/mL)	-4.045	-5.062 to -3.028	Yes	****	<0.0001
Cocktail Low Dose vs. Untreated	-3.945	-4.962 to -2.928	Yes	****	<0.0001
Kara-mokiny 16 10 ⁶ vs. Tobramycin (2µg/mL)	-4.135	-5.152 to -3.118	Yes	****	<0.0001
Kara-mokiny 16 10 ⁶ vs. Untreated	-4.035	-5.052 to -3.018	Yes	****	<0.0001
Tobramycin (2µg/mL) vs. Untreated	0.1	-0.9174 to 1.117	No	ns	0.9996
12 Hrs					
Cocktail Low Dose vs. Kara-mokiny 16 10 ⁷	-0.435	-1.452 to 0.5824	No	ns	0.7703
Cocktail Low Dose vs. Kara-mokiny 16 10 ⁶	-0.045	-1.062 to 0.9724	No	ns	>0.9999
Cocktail Low Dose vs. Tobramycin (2µg/mL)	-1.94	-2.957 to -0.9226	Yes	****	<0.0001
Cocktail Low Dose vs. Untreated	-2.055	-3.072 to -1.038	Yes	****	<0.0001
Kara-mokiny 16 10 ⁶ vs. Tobramycin (2µg/mL)	-1.895	-2.912 to -0.8776	Yes	****	<0.0001
Kara-mokiny 16 10 ⁶ vs. Untreated	-2.01	-3.027 to -0.9926	Yes	****	<0.0001
Tobramycin (2µg/mL) vs. Untreated	-0.115	-1.132 to 0.9024	No	ns	0.9992
18 Hrs					
Cocktail Low Dose vs. Kara-mokiny 16 10 ⁷	0.23	-0.7874 to 1.247	No	ns	0.9803
Cocktail Low Dose vs. Kara-mokiny 16 10 ⁶	-0.335	-1.352 to 0.6824	No	ns	0.9073

Cocktail Low Dose vs. Tobramycin (2µg/mL)	-0.845	-1.862 to 0.1724	No	ns	0.1443
Cocktail Low Dose vs. Untreated	-1.01	-2.027 to 0.007405	No	ns	0.0525
Kara-mokiny 16 10⁶ vs. Tobramycin (2µg/mL)	-0.51	-1.527 to 0.5074	No	ns	0.6371
Kara-mokiny 16 10⁶ vs. Untreated	-0.675	-1.692 to 0.3424	No	ns	0.3446
Tobramycin (2µg/mL) vs. Untreated	-0.165	-1.182 to 0.8524	No	ns	0.9956
24 Hrs					
Cocktail Low Dose vs. Kara-mokiny 16 10⁷	0.01	-1.007 to 1.027	No	ns	>0.9999
Cocktail Low Dose vs. Kara-mokiny 16 10⁶	-0.09	-1.107 to 0.9274	No	ns	0.9998
Cocktail Low Dose vs. Tobramycin (2µg/mL)	-1.41	-2.427 to -0.3926	Yes	**	0.0031
Cocktail Low Dose vs. Untreated	-1.89	-2.907 to -0.8726	Yes	****	<0.0001
Kara-mokiny 16 10⁶ vs. Tobramycin (2µg/mL)	-1.32	-2.337 to -0.3026	Yes	**	0.006
Kara-mokiny 16 10⁶ vs. Untreated	-1.8	-2.817 to -0.7826	Yes	***	0.0002
Tobramycin (2µg/mL) vs. Untreated	-0.48	-1.497 to 0.5374	No	ns	0.6922

Appendix Table I.5 Statistics of 2-way ANOVA for Viable AST234 at 6,12, 18 and 24 Hrs After the High Dose Combination Treatments

Tukey's multiple comparisons test	Mean Diff.	95.00% CI of diff.	Significant ?	Summary	Adjusted P Value
6 Hrs					
Cocktail High Dose vs. Cocktail Low Dose	-1.23	-2.462 to 0.001964	No	ns	0.0505
Cocktail High Dose vs. Kara-mokiny 16 (10 ⁷ PFU/mL)	-0.59	-1.822 to 0.6420	No	ns	0.6791
Cocktail High Dose vs. Kara-mokiny 16 (10 ⁶ PFU/mL)	-0.82	-2.052 to 0.4120	No	ns	0.3413
Cocktail High Dose vs. Tobramycin (2µg/mL)	-0.86	-2.092 to 0.3720	No	ns	0.2929
Cocktail High Dose vs. Untreated	-0.745	-1.977 to 0.4870	No	ns	0.4434
Kara-mokiny 16 (10 ⁷ PFU/mL) vs. Kara-mokiny 16 (10 ⁶ PFU/mL)	-0.23	-1.462 to 1.002	No	ns	0.9916
Kara-mokiny 16 (10 ⁷ PFU/mL) vs. Tobramycin (2µg/mL)	-0.27	-1.502 to 0.9620	No	ns	0.9828
Kara-mokiny 16 (10 ⁷ PFU/mL) vs. Untreated	-0.155	-1.387 to 1.077	No	ns	0.9987
Tobramycin (2µg/mL) vs. Untreated	0.115	-1.117 to 1.347	No	ns	0.9997
12 Hrs					
Cocktail High Dose vs. Cocktail Low Dose	-1.335	-2.567 to -0.1030	Yes	*	0.0283
Cocktail High Dose vs. Kara-mokiny 16 (10 ⁷ PFU/mL)	-2.055	-3.287 to -0.8230	Yes	***	0.0004
Cocktail High Dose vs. Kara-mokiny 16 (10 ⁶ PFU/mL)	-3.72	-4.952 to -2.488	Yes	****	<0.0001
Cocktail High Dose vs. Tobramycin (2µg/mL)	-4.61	-5.842 to -3.378	Yes	****	<0.0001
Cocktail High Dose vs. Untreated	-4.945	-6.177 to -3.713	Yes	****	<0.0001

Kara-mokiny 16 (10⁷ PFU/mL) vs. Kara-mokiny 16 (10⁶ PFU/mL)	-1.665	-2.897 to -0.4330	Yes	**	0.004
Kara-mokiny 16 (10⁷ PFU/mL) vs. Tobramycin (2µg/mL)	-2.555	-3.787 to -1.323	Yes	****	<0.0001
Kara-mokiny 16 (10⁷ PFU/mL) vs. Untreated	-2.89	-4.122 to -1.658	Yes	****	<0.0001
Tobramycin (2µg/mL) vs. Untreated	-0.335	-1.567 to 0.8970	No	ns	0.9566
18 Hrs					
Cocktail High Dose vs. Cocktail Low Dose	-0.015	-1.247 to 1.217	No	ns	>0.9999
Cocktail High Dose vs. Kara-mokiny 16 (10⁷ PFU/mL)	-1.75	-2.982 to -0.5180	Yes	**	0.0024
Cocktail High Dose vs. Kara-mokiny 16 (10⁶ PFU/mL)	-2.195	-3.427 to -0.9630	Yes	***	0.0002
Cocktail High Dose vs. Tobramycin (2µg/mL)	-4.27	-5.502 to -3.038	Yes	****	<0.0001
Cocktail High Dose vs. Untreated	-5.05	-6.282 to -3.818	Yes	****	<0.0001
Kara-mokiny 16 (10⁷ PFU/mL) vs. Kara-mokiny 16 (10⁶ PFU/mL)	-0.445	-1.677 to 0.7870	No	ns	0.8696
Kara-mokiny 16 (10⁷ PFU/mL) vs. Tobramycin (2µg/mL)	-2.52	-3.752 to -1.288	Yes	****	<0.0001
Kara-mokiny 16 (10⁷ PFU/mL) vs. Untreated	-3.3	-4.532 to -2.068	Yes	****	<0.0001
Tobramycin (2µg/mL) vs. Untreated	-0.78	-2.012 to 0.4520	No	ns	0.3941
24 Hrs					
Cocktail High Dose vs. Cocktail Low Dose	-0.475	-1.707 to 0.7570	No	ns	0.8362
Cocktail High Dose vs. Kara-mokiny 16 (10⁷ PFU/mL)	-1.305	-2.537 to -0.07304	Yes	*	0.0335
Cocktail High Dose vs. Kara-mokiny 16 (10⁶ PFU/mL)	-1.355	-2.587 to -0.1230	Yes	*	0.0252

Cocktail High Dose vs. Tobramycin (2µg/mL)	-3.1	-4.332 to -1.868	Yes	****	<0.0001
Cocktail High Dose vs. Untreated	-3.755	-4.987 to -2.523	Yes	****	<0.0001
Kara-mokiny 16 (10⁷ PFU/mL) vs. Kara-mokiny 16 (10⁶ PFU/mL)	-0.05	-1.282 to 1.182	No	ns	>0.9999
Kara-mokiny 16 (10⁷ PFU/mL) vs. Tobramycin (2µg/mL)	-1.795	-3.027 to -0.5630	Yes	**	0.0018
Kara-mokiny 16 (10⁷ PFU/mL) vs. Untreated	-2.45	-3.682 to -1.218	Yes	****	<0.0001
Tobramycin (2µg/mL) vs. Untreated	-0.655	-1.887 to 0.5770	No	ns	0.5793

Appendix Table I.6 Statistics of 2-way ANOVA for Viable AST234 at 6,12, 18 and 24 Hrs After Low Dose Combination Treatment

Tukey's multiple comparisons test	Mean Diff.	95.00% CI of diff.	Significant?	Summary	Adjusted P Value
6 Hrs					
Cocktail Low Dose vs. Kara-mokiny 16 (10 ⁷ PFU/mL)	0.64	-0.5920 to 1.872	No	ns	0.6025
Cocktail Low Dose vs. Kara-mokiny 16 (10 ⁶ PFU/mL)	0.41	-0.8220 to 1.642	No	ns	0.9035
Cocktail Low Dose vs. Tobramycin (2µg/mL)	0.37	-0.8620 to 1.602	No	ns	0.9351
Cocktail Low Dose vs. Untreated	0.485	-0.7470 to 1.717	No	ns	0.8243
Kara-mokiny 16 (10 ⁶ PFU/mL) vs. Tobramycin (2µg/mL)	-0.04	-1.272 to 1.192	No	ns	>0.9999
Kara-mokiny 16 (10 ⁶ PFU/mL) vs. Untreated	0.075	-1.157 to 1.307	No	ns	>0.9999
Tobramycin (2µg/mL) vs. Untreated	0.115	-1.117 to 1.347	No	ns	0.9997
12 Hrs					
Cocktail Low Dose vs. Kara-mokiny 16 (10 ⁷ PFU/mL)	-0.72	-1.952 to 0.5120	No	ns	0.4801
Cocktail Low Dose vs. Kara-mokiny 16 (10 ⁶ PFU/mL)	-2.385	-3.617 to -1.153	Yes	****	<0.0001
Cocktail Low Dose vs. Tobramycin (2µg/mL)	-3.275	-4.507 to -2.043	Yes	****	<0.0001
Cocktail Low Dose vs. Untreated	-3.61	-4.842 to -2.378	Yes	****	<0.0001
Kara-mokiny 16 (10 ⁶ PFU/mL) vs. Tobramycin (2µg/mL)	-0.89	-2.122 to 0.3420	No	ns	0.2597
Kara-mokiny 16 (10 ⁶ PFU/mL) vs. Untreated	-1.225	-2.457 to 0.006964	No	ns	0.0519
Tobramycin (2µg/mL) vs. Untreated	-0.335	-1.567 to 0.8970	No	ns	0.9566

18 Hrs					
Cocktail Low Dose vs. Kara-mokiny 16 (10⁷ PFU/mL)	-1.735	-2.967 to -0.5030	Yes	**	0.0026
Cocktail Low Dose vs. Kara-mokiny 16 (10⁶ PFU/mL)	-2.18	-3.412 to -0.9480	Yes	***	0.0002
Cocktail Low Dose vs. Tobramycin (2µg/mL)	-4.255	-5.487 to -3.023	Yes	****	<0.0001
Cocktail Low Dose vs. Untreated	-5.035	-6.267 to -3.803	Yes	****	<0.0001
Kara-mokiny 16 (10⁶ PFU/mL) vs. Tobramycin (2µg/mL)	-2.075	-3.307 to -0.8430	Yes	***	0.0003
Kara-mokiny 16 (10⁶ PFU/mL) vs. Untreated	-2.855	-4.087 to -1.623	Yes	****	<0.0001
Tobramycin (2µg/mL) vs. Untreated	-0.78	-2.012 to 0.4520	No	ns	0.3941
24 Hrs					
Cocktail Low Dose vs. Kara-mokiny 16 (10⁷ PFU/mL)	-0.83	-2.062 to 0.4020	No	ns	0.3288
Cocktail Low Dose vs. Kara-mokiny 16 (10⁶ PFU/mL)	-0.88	-2.112 to 0.3520	No	ns	0.2704
Cocktail Low Dose vs. Tobramycin (2µg/mL)	-2.625	-3.857 to -1.393	Yes	****	<0.0001
Cocktail Low Dose vs. Untreated	-3.28	-4.512 to -2.048	Yes	****	<0.0001
Kara-mokiny 16 (10⁶ PFU/mL) vs. Tobramycin (2µg/mL)	-1.745	-2.977 to -0.5130	Yes	**	0.0025
Kara-mokiny 16 (10⁶ PFU/mL) vs. Untreated	-2.4	-3.632 to -1.168	Yes	****	<0.0001
Tobramycin (2µg/mL) vs. Untreated	-0.655	-1.887 to 0.5770	No	ns	0.5793

Appendix Table I.7 Statistics of 2-way ANOVA for Phage Titres After Combination Treatments of M1C79, AST154 and AST234 at 6,12, 18 and 24 Hrs

M1C79 Treatment					
Tukey's multiple comparisons test	Mean Diff.	95.00% CI of diff.	Significant ?	Summary	Adjusted P Value
6 Hrs					
Cocktail High Dose vs. Cocktail Low Dose	-0.22	-0.7124 to 0.2724	No	ns	0.5889
Cocktail High Dose vs. Kara-mokiny 16 (10 ⁷ PFU/mL)	-0.605	-1.097 to -0.1126	Yes	*	0.0137
Cocktail High Dose vs. Kara-mokiny 16 (10 ⁶ PFU/mL)	-0.995	-1.487 to -0.5026	Yes	***	0.0001
Cocktail Low Dose vs. Kara-mokiny 16 (10 ⁷ PFU/mL)	-0.385	-0.8774 to 0.1074	No	ns	0.1555
Cocktail Low Dose vs. Kara-mokiny 16 (10 ⁶ PFU/mL)	-0.775	-1.267 to -0.2826	Yes	**	0.0018
Kara-mokiny 16 (10 ⁷ PFU/mL) vs. Kara-mokiny 16 (10 ⁶ PFU/mL)	-0.39	-0.8824 to 0.1024	No	ns	0.148
12 Hrs					
Cocktail High Dose vs. Cocktail Low Dose	2.8	2.308 to 3.292	Yes	****	<0.0001
Cocktail High Dose vs. Kara-mokiny 16 (10 ⁷ PFU/mL)	-1.425	-1.917 to -0.9326	Yes	****	<0.0001
Cocktail High Dose vs. Kara-mokiny 16 (10 ⁶ PFU/mL)	-1.42	-1.912 to -0.9276	Yes	****	<0.0001
Cocktail Low Dose vs. Kara-mokiny 16 (10 ⁷ PFU/mL)	-4.225	-4.717 to -3.733	Yes	****	<0.0001
Cocktail Low Dose vs. Kara-mokiny 16 (10 ⁶ PFU/mL)	-4.22	-4.712 to -3.728	Yes	****	<0.0001
Kara-mokiny 16 (10 ⁷ PFU/mL) vs. Kara-mokiny 16 (10 ⁶ PFU/mL)	0.005	-0.4874 to 0.4974	No	ns	>0.9999
18 Hrs					
Cocktail High Dose vs. Cocktail Low Dose	-0.04	-0.5324 to 0.4524	No	ns	0.9954

Cocktail High Dose vs. Kara-mokiny 16 (10 ⁷ PFU/mL)	-2.64	-3.132 to -2.148	Yes	****	<0.0001
Cocktail High Dose vs. Kara-mokiny 16 (10 ⁶ PFU/mL)	-2.045	-2.537 to -1.553	Yes	****	<0.0001
Cocktail Low Dose vs. Kara-mokiny 16 (10 ⁷ PFU/mL)	-2.6	-3.092 to -2.108	Yes	****	<0.0001
Cocktail Low Dose vs. Kara-mokiny 16 (10 ⁶ PFU/mL)	-2.005	-2.497 to -1.513	Yes	****	<0.0001
Kara-mokiny 16 (10 ⁷ PFU/mL) vs. Kara-mokiny 16 (10 ⁶ PFU/mL)	0.595	0.1026 to 1.087	Yes	*	0.0154
24 Hrs					
Cocktail High Dose vs. Cocktail Low Dose	-0.655	-1.147 to 0.1626	Yes	**	0.0076
Cocktail High Dose vs. Kara-mokiny 16 (10 ⁷ PFU/mL)	-3.125	-3.617 to -2.633	Yes	****	<0.0001
Cocktail High Dose vs. Kara-mokiny 16 (10 ⁶ PFU/mL)	-3.045	-3.537 to -2.553	Yes	****	<0.0001
Cocktail Low Dose vs. Kara-mokiny 16 (10 ⁷ PFU/mL)	-2.47	-2.962 to -1.978	Yes	****	<0.0001
Cocktail Low Dose vs. Kara-mokiny 16 (10 ⁶ PFU/mL)	-2.39	-2.882 to -1.898	Yes	****	<0.0001
Kara-mokiny 16 (10 ⁷ PFU/mL) vs. Kara-mokiny 16 (10 ⁶ PFU/mL)	0.08	-0.4124 to 0.5724	No	ns	0.9657
AST154 Treatment					
Tukey's multiple comparisons test	Mean Diff.	95.00% CI of diff.	Significant?	Summary	Adjusted P Value
6 Hrs					
Cocktail High Dose vs. Cocktail Low Dose	0.165	-0.6514 to 0.9814	No	ns	0.9372
Cocktail High Dose vs. Kara-mokiny 16 (10 ⁷ PFU/mL)	-0.33	-1.146 to 0.4864	No	ns	0.6615
Cocktail High Dose vs. Kara-mokiny 16 (10 ⁶ PFU/mL)	-0.19	-1.006 to 0.6264	No	ns	0.9084
Cocktail Low Dose vs. Kara-mokiny 16 (10 ⁷ PFU/mL)	-0.495	-1.311 to 0.3214	No	ns	0.3391

Cocktail Low Dose vs. Kara-mokiny 16 (10⁶ PFU/mL)	-0.355	-1.171 to 0.4614	No	ns	0.6093
Kara-mokiny 16 (10⁷ PFU/mL) vs. Kara-mokiny 16 (10⁶ PFU/mL)	0.14	-0.6764 to 0.9564	No	ns	0.9601
12 Hrs					
Cocktail High Dose vs. Cocktail Low Dose	0.53	-0.2864 to 1.346	No	ns	0.2844
Cocktail High Dose vs. Kara-mokiny 16 (10⁷ PFU/mL)	0.165	-0.6514 to 0.9814	No	ns	0.9372
Cocktail High Dose vs. Kara-mokiny 16 (10⁶ PFU/mL)	0.425	-0.3914 to 1.241	No	ns	0.4662
Cocktail Low Dose vs. Kara-mokiny 16 (10⁷ PFU/mL)	-0.365	-1.181 to 0.4514	No	ns	0.5885
Cocktail Low Dose vs. Kara-mokiny 16 (10⁶ PFU/mL)	-0.105	-0.9214 to 0.7114	No	ns	0.9824
Kara-mokiny 16 (10⁷ PFU/mL) vs. Kara-mokiny 16 (10⁶ PFU/mL)	0.26	-0.5564 to 1.076	No	ns	0.7993
18 Hrs					
Cocktail High Dose vs. Cocktail Low Dose	-0.345	-1.161 to 0.4714	No	ns	0.6302
Cocktail High Dose vs. Kara-mokiny 16 (10⁷ PFU/mL)	0.135	-0.6814 to 0.9514	No	ns	0.9639
Cocktail High Dose vs. Kara-mokiny 16 (10⁶ PFU/mL)	-1.025	-1.841 to -0.2086	Yes	*	0.0117
Cocktail Low Dose vs. Kara-mokiny 16 (10⁷ PFU/mL)	0.48	-0.3364 to 1.296	No	ns	0.3645
Cocktail Low Dose vs. Kara-mokiny 16 (10⁶ PFU/mL)	-0.68	-1.496 to 0.1364	No	ns	0.1208
Kara-mokiny 16 (10⁷ PFU/mL) vs. Kara-mokiny 16 (10⁶ PFU/mL)	-1.16	-1.976 to -0.3436	Yes	**	0.0045
24 Hrs					
Cocktail High Dose vs. Cocktail Low Dose	0.245	-0.5714 to 1.061	No	ns	0.8257
Cocktail High Dose vs. Kara-mokiny 16 (10⁷ PFU/mL)	0.065	-0.7514 to 0.8814	No	ns	0.9957

Cocktail High Dose vs. Kara-mokiny 16 (10 ⁶ PFU/mL)	0.195	-0.6214 to 1.011	No	ns	0.9019
Cocktail Low Dose vs. Kara-mokiny 16 (10 ⁷ PFU/mL)	-0.18	-0.9964 to 0.6364	No	ns	0.9206
Cocktail Low Dose vs. Kara-mokiny 16 (10 ⁶ PFU/mL)	-0.05	-0.8664 to 0.7664	No	ns	0.998
Kara-mokiny 16 (10 ⁷ PFU/mL) vs. Kara-mokiny 16 (10 ⁶ PFU/mL)	0.13	-0.6864 to 0.9464	No	ns	0.9676
AST234 Treatment					
Tukey's multiple comparisons test	Mean Diff.	95.00% CI of diff.	Significant?	Summary	Adjusted P Value
6 Hrs					
Cocktail High Dose vs. Cocktail Low Dose	0.875	0.3744 to 1.376	Yes	***	0.0007
Cocktail High Dose vs. Kara-mokiny 16 (10 ⁷ PFU/mL)	0.205	-0.2956 to 0.7056	No	ns	0.6524
Cocktail High Dose vs. Kara-mokiny 16 (10 ⁶ PFU/mL)	1.165	0.6644 to 1.666	Yes	****	<0.0001
Cocktail Low Dose vs. Kara-mokiny 16 (10 ⁷ PFU/mL)	-0.67	-1.171 to -0.1694	Yes	**	0.0072
Cocktail Low Dose vs. Kara-mokiny 16 (10 ⁶ PFU/mL)	0.29	-0.2106 to 0.7906	No	ns	0.3767
Kara-mokiny 16 (10 ⁷ PFU/mL) vs. Kara-mokiny 16 (10 ⁶ PFU/mL)	0.96	0.4594 to 1.461	Yes	***	0.0003
12 Hrs					
Cocktail High Dose vs. Cocktail Low Dose	0.565	0.06445 to 1.066	Yes	*	0.0243
Cocktail High Dose vs. Kara-mokiny 16 (10 ⁷ PFU/mL)	0.62	0.1194 to 1.121	Yes	*	0.0129
Cocktail High Dose vs. Kara-mokiny 16 (10 ⁶ PFU/mL)	0.555	0.05445 to 1.056	Yes	*	0.0272
Cocktail Low Dose vs. Kara-mokiny 16 (10 ⁷ PFU/mL)	0.055	-0.4456 to 0.5556	No	ns	0.9888
Cocktail Low Dose vs. Kara-mokiny 16 (10 ⁶ PFU/mL)	-0.01	-0.5106 to 0.4906	No	ns	>0.9999

Kara-mokiny 16 (10⁷ PFU/mL) vs. Kara-mokiny 16 (10⁶ PFU/mL)	-0.065	-0.5656 to 0.4356	No	ns	0.9819
18 Hrs					
Cocktail High Dose vs. Cocktail Low Dose	0.25	-0.2506 to 0.7506	No	ns	0.5005
Cocktail High Dose vs. Kara-mokiny 16 (10⁷ PFU/mL)	-1.26	-1.761 to -0.7594	Yes	****	<0.0001
Cocktail High Dose vs. Kara-mokiny 16 (10⁶ PFU/mL)	-0.775	-1.276 to -0.2744	Yes	**	0.0021
Cocktail Low Dose vs. Kara-mokiny 16 (10⁷ PFU/mL)	-1.51	-2.011 to -1.009	Yes	****	<0.0001
Cocktail Low Dose vs. Kara-mokiny 16 (10⁶ PFU/mL)	-1.025	-1.526 to -0.5244	Yes	***	0.0001
Kara-mokiny 16 (10⁷ PFU/mL) vs. Kara-mokiny 16 (10⁶ PFU/mL)	0.485	-0.01555 to 0.9856	No	ns	0.0592
24 Hrs					
Cocktail High Dose vs. Cocktail Low Dose	0.07	-0.4306 to 0.5706	No	ns	0.9776
Cocktail High Dose vs. Kara-mokiny 16 (10⁷ PFU/mL)	-2.19	-2.691 to -1.689	Yes	****	<0.0001
Cocktail High Dose vs. Kara-mokiny 16 (10⁶ PFU/mL)	-1.985	-2.486 to -1.484	Yes	****	<0.0001
Cocktail Low Dose vs. Kara-mokiny 16 (10⁷ PFU/mL)	-2.26	-2.761 to -1.759	Yes	****	<0.0001
Cocktail Low Dose vs. Kara-mokiny 16 (10⁶ PFU/mL)	-2.055	-2.556 to -1.554	Yes	****	<0.0001
Kara-mokiny 16 (10⁷ PFU/mL) vs. Kara-mokiny 16 (10⁶ PFU/mL)	0.205	-0.2956 to 0.7056	No	ns	0.6524

Reference List

1. Murray, C.J.L., et al., *Global burden of bacterial antimicrobial resistance in 2019: a systematic analysis*. The Lancet, 2022.
2. O'Neill, J., *Tackling drug-resistant infections globally: final report and recommendations*. Review on Antimicrobial Resistance, 2016.
3. Munita, J.M. and C.A. Arias, *Mechanisms of Antibiotic Resistance*. Microbiology spectrum, 2016. **4**(2): p. 10.1128/microbiolspec.VMBF-0016-2015.
4. Reygaert, W.C., *An overview of the antimicrobial resistance mechanisms of bacteria*. AIMS microbiology, 2018. **4**(3): p. 482-501.
5. Breijyeh, Z., B. Jubeh, and R. Karaman, *Resistance of Gram-Negative Bacteria to Current Antibacterial Agents and Approaches to Resolve It*. Molecules, 2020. **25**(6).
6. Hall-Stoodley, L. and P. Stoodley, *Developmental regulation of microbial biofilms*. Current Opinion in Biotechnology, 2002. **13**(3): p. 228-233.
7. Flemming, H.-C., et al., *Biofilms: an emergent form of bacterial life*. Nature Reviews Microbiology, 2016. **14**(9): p. 563-575.
8. Hall, C.W. and T.-F. Mah, *Molecular mechanisms of biofilm-based antibiotic resistance and tolerance in pathogenic bacteria*. FEMS Microbiology Reviews, 2017. **41**(3): p. 276-301.
9. Ciofu, O. and T. Tolker-Nielsen, *Tolerance and Resistance of Pseudomonas aeruginosa Biofilms to Antimicrobial Agents—How P. aeruginosa Can Escape Antibiotics*. Frontiers in Microbiology, 2019. **10**.
10. CDC, *Antibiotic resistance threats in the United States, 2019*. 2019, Department of Health and Human Services, Centre for Disease Control: Atlanta, GA: U.S.
11. Laxminarayan, R., et al., *Antibiotic resistance—the need for global solutions*. The Lancet Infectious Diseases, 2013. **13**(12): p. 1057-1098.
12. WHO, *Prioritization of pathogens to guide discovery, research and development of new antibiotics for drug-resistant bacterial infections, including tuberculosis*. 2017, World Health Organisation: Geneva (Switzerland).
13. Boucher, H.W., et al., *Bad Bugs, No Drugs: No ESKAPE! An Update from the Infectious Diseases Society of America*. Clinical Infectious Diseases, 2009. **48**(1): p. 1-12.
14. Llor, C. and L. Bjerrum, *Antimicrobial resistance: risk associated with antibiotic overuse and initiatives to reduce the problem*. Therapeutic advances in drug safety, 2014. **5**(6): p. 229-241.
15. Lambert, M.-L., et al., *Clinical outcomes of health-care-associated infections and antimicrobial resistance in patients admitted to European intensive-care units: a cohort study*. The Lancet Infectious Diseases, 2011. **11**(1): p. 30-38.
16. Wolkewitz, M., et al., *Mortality associated with in-hospital bacteraemia caused by Staphylococcus aureus: a multistate analysis with follow-up beyond hospital discharge*. Journal of Antimicrobial Chemotherapy, 2010. **66**(2): p. 381-386.
17. de Kraker, M.E.A., et al., *Mortality and Hospital Stay Associated with Resistant Staphylococcus aureus and Escherichia coli Bacteremia: Estimating the Burden of Antibiotic Resistance in Europe*. PLOS Medicine, 2011. **8**(10): p. e1001104.
18. Theuretzbacher, U., et al., *Analysis of the clinical antibacterial and antituberculosis pipeline*. Lancet Infect. Dis., 2018. **19**.
19. WHO, *Antibacterial agents in clinical development: an analysis of the antibacterial clinical development pipeline, including tuberculosis*. 2019, World Health Organisation: Geneva (Switzerland).
20. O'Neill, J., *Review on antimicrobial resistance: tackling a crisis for the health and wealth of nations*. 2014: London.
21. Wozniak, T.M., et al., *Disease burden, associated mortality and economic impact of antimicrobial resistant infections in Australia*. Lancet Reg Health West Pac, 2022. **27**: p. 100521.
22. Reyes, J., et al., *Global epidemiology and clinical outcomes of carbapenem-resistant Pseudomonas aeruginosa and associated carbapenemases (POP): a prospective cohort study*. The Lancet Microbe, 2023. **4**(3): p. e159-e170.

23. Sheng, W.H., R.E. Badal, and P.R. Hsueh, *Distribution of extended-spectrum β -lactamases, AmpC β -lactamases, and carbapenemases among Enterobacteriaceae isolates causing intra-abdominal infections in the Asia-Pacific region: results of the study for Monitoring Antimicrobial Resistance Trends (SMART)*. *Antimicrob Agents Chemother*, 2013. **57**(7): p. 2981-8.
24. Stewart, A.G., et al., *Molecular Epidemiology of Third-Generation-Cephalosporin-Resistant Enterobacteriaceae in Southeast Queensland, Australia*. *Antimicrob Agents Chemother*, 2021. **65**(6).
25. Bell, J.M., et al., *Australian Group on Antimicrobial Resistance (AGAR) Australian Gram-negative Sepsis Outcome Programme (GNSOP) Annual Report 2018*, T. Farmer, Editor. 2020, Australian Government Department of Health.
26. ACSQHC, *AURA 2021: fourth Australian report on antimicrobial use and resistance in human health*. 2021, Australian Commission on Safety and Quality in Health Care: Sydney.
27. WHO, *2020 Antibacterial agents in clinical and preclinical development: an overview and analysis*. 2021: Geneva.
28. Theuretzbacher, U., et al., *Critical analysis of antibacterial agents in clinical development*. *Nature Reviews Microbiology*, 2020. **18**(5): p. 286-298.
29. Tacconelli, E., et al., *Discovery, research, and development of new antibiotics: the WHO priority list of antibiotic-resistant bacteria and tuberculosis*. *The Lancet Infectious Diseases*, 2018. **18**(3): p. 318-327.
30. Thaden, J.T., et al., *Results from a 13-Year Prospective Cohort Study Show Increased Mortality Associated with Bloodstream Infections Caused by Pseudomonas aeruginosa Compared to Other Bacteria*. *Antimicrob Agents Chemother*, 2017. **61**(6).
31. Moore, N.M. and M.L. Flaws, *Introduction: Pseudomonas aeruginosa*. *Clinical Laboratory Science*, 2011. **24**(1): p. 41-2.
32. Moore, N.M. and M.L. Flaws, *Epidemiology and Pathogenesis of Pseudomonas aeruginosa Infections*. *Clinical Laboratory Science*, 2011. **24**(1): p. 43-6.
33. Barbier, F., et al., *Hospital-acquired pneumonia and ventilator-associated pneumonia: recent advances in epidemiology and management*. *Curr Opin Pulm Med*, 2013. **19**(3): p. 216-28.
34. Klockgether, J., et al., *Pseudomonas aeruginosa Genomic Structure and Diversity*. *Frontiers in microbiology*, 2011. **2**: p. 150-150.
35. Pang, Z., et al., *Antibiotic resistance in Pseudomonas aeruginosa: mechanisms and alternative therapeutic strategies*. *Biotechnology Advances*, 2019. **37**(1): p. 177-192.
36. Sugawara, E., et al., *Pseudomonas aeruginosa porin OprF exists in two different conformations*. *The Journal of biological chemistry*, 2006. **281**(24): p. 16220-16229.
37. Yoneyama, H. and T. Nakae, *Mechanism of efficient elimination of protein D2 in outer membrane of imipenem-resistant Pseudomonas aeruginosa*. *Antimicrobial Agents and Chemotherapy*, 1993. **37**(11): p. 2385.
38. Bell, A., M. Bains, and R.E. Hancock, *Pseudomonas aeruginosa outer membrane protein OprH: expression from the cloned gene and function in EDTA and gentamicin resistance*. *Journal of Bacteriology*, 1991. **173**(21): p. 6657.
39. Macfarlane, E.L., et al., *PhoP-PhoQ homologues in Pseudomonas aeruginosa regulate expression of the outer-membrane protein OprH and polymyxin B resistance*. *Mol Microbiol*, 1999. **34**(2): p. 305-16.
40. Llanes, C., et al., *Role of the MexEF-OprN efflux system in low-level resistance of Pseudomonas aeruginosa to ciprofloxacin*. *Antimicrobial agents and chemotherapy*, 2011. **55**(12): p. 5676-5684.
41. Okamoto, K., N. Gotoh, and T. Nishino, *Extrusion of penem antibiotics by multicomponent efflux systems MexAB-OprM, MexCD-OprJ, and MexXY-OprM of Pseudomonas aeruginosa*. *Antimicrobial agents and chemotherapy*, 2002. **46**(8): p. 2696-2699.
42. Masuda, N., et al., *Substrate specificities of MexAB-OprM, MexCD-OprJ, and MexXY-oprM efflux pumps in Pseudomonas aeruginosa*. *Antimicrobial agents and chemotherapy*, 2000. **44**(12): p. 3322-3327.

43. Zhao, W.-H. and Z.-Q. Hu, *β -Lactamases identified in clinical isolates of Pseudomonas aeruginosa*. 2010. p. 245-258.
44. Poole, K., *Aminoglycoside Resistance in Pseudomonas aeruginosa*. Antimicrobial Agents and Chemotherapy, 2005. **49**(2): p. 479.
45. Wolter, D.J., N.D. Hanson, and P.D. Lister, *Insertional inactivation of oprD in clinical isolates of Pseudomonas aeruginosa leading to carbapenem resistance*. FEMS Microbiology Letters, 2004. **236**(1): p. 137-143.
46. Boll, M., et al., *4-Amino-4-deoxy-L-arabinose in LPS of enterobacterial R-mutants and its possible role for their polymyxin reactivity*. FEMS Immunology and Medical Microbiology, 1994. **8**(4): p. 329-341.
47. Mandsberg, L.F., et al., *Antibiotic resistance in Pseudomonas aeruginosa strains with increased mutation frequency due to inactivation of the DNA oxidative repair system*. Antimicrob Agents Chemother, 2009. **53**(6): p. 2483-91.
48. Poonsuk, K., C. Tribuddharat, and R. Chuanchuen, *Simultaneous overexpression of multidrug efflux pumps in Pseudomonas aeruginosa non-cystic fibrosis clinical isolates*. Can J Microbiol, 2014. **60**(7): p. 437-43.
49. Juan, C., et al., *Molecular mechanisms of beta-lactam resistance mediated by AmpC hyperproduction in Pseudomonas aeruginosa clinical strains*. Antimicrob Agents Chemother, 2005. **49**(11): p. 4733-8.
50. Berrazeg, M., et al., *Mutations in β -Lactamase AmpC Increase Resistance of Pseudomonas aeruginosa Isolates to Antipseudomonal Cephalosporins*. Antimicrob Agents Chemother, 2015. **59**(10): p. 6248-55.
51. Bruchmann, S., et al., *Quantitative contributions of target alteration and decreased drug accumulation to Pseudomonas aeruginosa fluoroquinolone resistance*. Antimicrob Agents Chemother, 2013. **57**(3): p. 1361-8.
52. El'Garch, F., et al., *Cumulative effects of several nonenzymatic mechanisms on the resistance of Pseudomonas aeruginosa to aminoglycosides*. Antimicrob Agents Chemother, 2007. **51**(3): p. 1016-21.
53. Moyá, B., et al., *Pan- β -lactam resistance development in Pseudomonas aeruginosa clinical strains: molecular mechanisms, penicillin-binding protein profiles, and binding affinities*. Antimicrob Agents Chemother, 2012. **56**(9): p. 4771-8.
54. Ciofu, O. and T. Tolker-Nielsen, *Tolerance and Resistance of Pseudomonas aeruginosa Biofilms to Antimicrobial Agents-How P. aeruginosa Can Escape Antibiotics*. Frontiers in microbiology, 2019. **10**: p. 913-913.
55. Peña, C., et al., *Influence of virulence genotype and resistance profile in the mortality of Pseudomonas aeruginosa bloodstream infections*. Clin Infect Dis, 2015. **60**(4): p. 539-48.
56. Henry, R.L., C.M. Mellis, and L. Petrovic, *Mucoid Pseudomonas aeruginosa is a marker of poor survival in cystic fibrosis*. Pediatr. Pulmonol., 1992. **12**(3): p. 158-61.
57. Feldman, M., et al., *Role of Flagella in Pathogenesis of Pseudomonas aeruginosa Pulmonary Infection*. Infection and Immunity, 1998. **66**(1): p. 43.
58. Bucior, I., J.F. Pielage, and J.N. Engel, *Pseudomonas aeruginosa pili and flagella mediate distinct binding and signaling events at the apical and basolateral surface of airway epithelium*. PLoS pathogens, 2012. **8**(4): p. e1002616-e1002616.
59. Sampedro, I., et al., *Pseudomonas chemotaxis*. FEMS Microbiology Reviews, 2014. **39**(1): p. 17-46.
60. Ozer, E., et al., *An inside look at a biofilm: Pseudomonas aeruginosa flagella biotracking*. Science Advances, 2021. **7**(24): p. eabg8581.
61. Whitchurch, C.B., et al., *Characterization of a complex chemosensory signal transduction system which controls twitching motility in Pseudomonas aeruginosa*. Molecular Microbiology, 2004. **52**(3): p. 873-893.
62. Overhage, J., et al., *Swarming of Pseudomonas aeruginosa Is a Complex Adaptation Leading to Increased Production of Virulence Factors and Antibiotic Resistance*. Journal of Bacteriology, 2008. **190**(8): p. 2671-2679.
63. Pier, G.B., *Pseudomonas aeruginosa lipopolysaccharide: A major virulence factor, initiator of inflammation and target for effective immunity*. International Journal of Medical Microbiology, 2007. **297**(5): p. 277-295.

64. Goldberg, J.B. and G.B. Pier, *Pseudomonas aeruginosa lipopolysaccharides and pathogenesis*. Trends in Microbiology, 1996. **4**(12): p. 490-494.
65. Wells, T.J., et al., *Increased severity of respiratory infections associated with elevated anti-LPS IgG2 which inhibits serum bactericidal killing*. J Exp Med, 2014. **211**(9): p. 1893-904.
66. Filloux, A., *Protein Secretion Systems in Pseudomonas aeruginosa: An Essay on Diversity, Evolution, and Function*. Front Microbiol, 2011. **2**: p. 155.
67. Laarman, A.J., et al., *Pseudomonas aeruginosa alkaline protease blocks complement activation via the classical and lectin pathways*. J Immunol, 2012. **188**(1): p. 386-93.
68. Bardoel, B.W., et al., *Pseudomonas Evades Immune Recognition of Flagellin in Both Mammals and Plants*. PLOS Pathogens, 2011. **7**(8): p. e1002206.
69. Liao, C., et al., *Virulence Factors of Pseudomonas Aeruginosa and Antivirulence Strategies to Combat Its Drug Resistance*. Frontiers in Cellular and Infection Microbiology, 2022. **12**.
70. Iglewski, B.H. and D. Kabat, *NAD-dependent inhibition of protein synthesis by Pseudomonas aeruginosa toxin*. Proceedings of the National Academy of Sciences, 1975. **72**(6): p. 2284.
71. Döring, G., et al., *Role of Pseudomonas aeruginosa exoenzymes in lung infections of patients with cystic fibrosis*. Infection and immunity, 1985. **49**(3): p. 557-562.
72. Gellatly, S.L. and R.E.W. Hancock, *Pseudomonas aeruginosa : new insights into pathogenesis and host defenses*. Pathogens and Disease, 2013. **67**(3): p. 159-173.
73. Jaeger, K.E., et al., *Bacterial lipases*. FEMS Microbiol Rev, 1994. **15**(1): p. 29-63.
74. Martínez, A., P. Ostrovsky, and D.N. Nunn, *LipC, a second lipase of Pseudomonas aeruginosa, is LipB and Xcp dependent and is transcriptionally regulated by pilus biogenesis components*. Mol Microbiol, 1999. **34**(2): p. 317-26.
75. Lu, H.M., S. Mizushima, and S. Lory, *A periplasmic intermediate in the extracellular secretion pathway of Pseudomonas aeruginosa exotoxin A*. J Bacteriol, 1993. **175**(22): p. 7463-7.
76. Ochoa, C.D., et al., *Pseudomonas aeruginosa Exotoxin Y Is a Promiscuous Cyclase That Increases Endothelial Tau Phosphorylation and Permeability*. J. Biol. Chem., 2012. **287**(30): p. 25407-25418.
77. Engel, J. and P. Balachandran, *Role of Pseudomonas aeruginosa type III effectors in disease*. Current Opinion in Microbiology, 2009. **12**(1): p. 61-66.
78. He, J., et al., *The broad host range pathogen Pseudomonas aeruginosa strain PA14 carries two pathogenicity islands harboring plant and animal virulence genes*. Proc Natl Acad Sci U S A, 2004. **101**(8): p. 2530-5.
79. Yahr, T.L., et al., *Identification of type III secreted products of the Pseudomonas aeruginosa exoenzyme S regulon*. J Bacteriol, 1997. **179**(22): p. 7165-8.
80. Juhas, M., *Type IV secretion systems and genomic islands-mediated horizontal gene transfer in Pseudomonas and Haemophilus*. Microbiological Research, 2015. **170**: p. 10-17.
81. Cornelis, P. and J. Dingemans, *Pseudomonas aeruginosa adapts its iron uptake strategies in function of the type of infections*. Frontiers in cellular and infection microbiology, 2013. **3**: p. 75-75.
82. Kang, D., et al., *Pyoverdine-Dependent Virulence of Pseudomonas aeruginosa Isolates From Cystic Fibrosis Patients*. Frontiers in Microbiology, 2019. **10**(2048).
83. Bonneau, A., B. Roche, and I.J. Schalk, *Iron acquisition in Pseudomonas aeruginosa by the siderophore pyoverdine: an intricate interacting network including periplasmic and membrane proteins*. Scientific Reports, 2020. **10**(1): p. 120.
84. Rada, B. and T.L. Leto, *Pyocyanin effects on respiratory epithelium: relevance in Pseudomonas aeruginosa airway infections*. Trends Microbiol, 2013. **21**(2): p. 73-81.
85. Hocquet, D., et al., *Pyomelanin-producing Pseudomonas aeruginosa selected during chronic infections have a large chromosomal deletion which confers resistance to pyocins*. Environmental microbiology, 2016. **18**(10): p. 3482-3493.
86. Inchingolo, R., et al., *Antimicrobial Resistance in Common Respiratory Pathogens of Chronic Bronchiectasis Patients: A Literature Review*. Antibiotics (Basel), 2021. **10**(3).

87. Smith, D., et al., *Prevalence, Pattern, Risks Factors and Consequences of Antibiotic Resistance in COPD: A Systematic Review*. COPD: Journal of Chronic Obstructive Pulmonary Disease, 2021. **18**(6): p. 672-682.
88. Ahern, S., et al., *The ACFDR Registry Annual Report, 2021*. 2022, Monash University, Department of Epidemiology and Preventive Medicine.
89. Foundation, C.F., *Cystic fibrosis foundation patient registry 2018 annual data report*. 2019: Bethesda, Maryland.
90. Foundation, C.F., *Cystic Fibrosis Foundation Patient Registry 2021 Annual Data Report*. 2022: Bethesda, Maryland.
91. Durda-Masny, M., et al., *The determinants of survival among adults with cystic fibrosis—a cohort study*. Journal of Physiological Anthropology, 2021. **40**(1): p. 19.
92. Guo, J., A. Garratt, and A. Hill, *Worldwide rates of diagnosis and effective treatment for cystic fibrosis*. Journal of Cystic Fibrosis, 2022. **21**(3): p. 456-462.
93. Scotet, V., C. L'Hostis, and C. Férec, *The Changing Epidemiology of Cystic Fibrosis: Incidence, Survival and Impact of the CFTR Gene Discovery*. Genes (Basel), 2020. **11**(6).
94. Susannah Ahern, G.S., Mark Tacey, Michael Esler, John Oldroyd, Joanna Dean, Scott Bell on behalf of the Australian Cystic Fibrosis Data Registry, *The Australian cystic fibrosis data registry annual report, 2015*. 2017, Monash University, Department of Epidemiology and Preventive Medicine.
95. Elborn, J.S., *Cystic fibrosis*. Lancet, 2016. **388**(10059): p. 2519-2531.
96. Quinton, P.M., *Chloride impermeability in cystic fibrosis*. Nature, 1983. **301**(5899): p. 421-2.
97. Boucher, R.C., et al., *Na⁺ transport in cystic fibrosis respiratory epithelia. Abnormal basal rate and response to adenylate cyclase activation*. J Clin Invest, 1986. **78**(5): p. 1245-52.
98. Stutts, M.J., et al., *CFTR as a cAMP-dependent regulator of sodium channels*. Science, 1995. **269**(5225): p. 847.
99. Matsui, H., et al., *Evidence for periciliary liquid layer depletion, not abnormal ion composition, in the pathogenesis of cystic fibrosis airways disease*. Cell, 1998. **95**(7): p. 1005-15.
100. Henderson, A.G., et al., *Cystic fibrosis airway secretions exhibit mucin hyperconcentration and increased osmotic pressure*. J Clin Invest, 2014. **124**(7): p. 3047-60.
101. Worlitzsch, D., et al., *Effects of reduced mucus oxygen concentration in airway Pseudomonas infections of cystic fibrosis patients*. J Clin Invest, 2002. **109**(3): p. 317-25.
102. Hisert, K.B., et al., *Restoring Cystic Fibrosis Transmembrane Conductance Regulator Function Reduces Airway Bacteria and Inflammation in People with Cystic Fibrosis and Chronic Lung Infections*. Am J Respir Crit Care Med, 2017. **195**(12): p. 1617-1628.
103. Rowe, S.M., et al., *Clinical mechanism of the cystic fibrosis transmembrane conductance regulator potentiator ivacaftor in G551D-mediated cystic fibrosis*. Am J Respir Crit Care Med, 2014. **190**(2): p. 175-84.
104. Sheikh, S., et al., *Impact of elexacaftor-tezacaftor-ivacaftor on bacterial colonization and inflammatory responses in cystic fibrosis*. Pediatr Pulmonol, 2023. **58**(3): p. 825-833.
105. Gushue, C., et al., *Impact of Elexacaftor–Tezacaftor–Ivacaftor on lung disease in cystic fibrosis*. Pediatric Pulmonology, 2023. **58**(8): p. 2308-2316.
106. Heltshe, S.L., et al., *Pseudomonas aeruginosa in Cystic Fibrosis Patients With G551D-CFTR Treated With Ivacaftor*. Clinical Infectious Diseases, 2015. **60**(5): p. 703-712.
107. Nichols, D.P., et al., *Pharmacologic improvement of CFTR function rapidly decreases sputum pathogen density, but lung infections generally persist*. The Journal of Clinical Investigation, 2023. **133**(10).
108. Ledger, E.L., et al., *Impact of CFTR Modulation on Pseudomonas aeruginosa Infection in People With Cystic Fibrosis*. The Journal of Infectious Diseases, 2024: p. jiae051.
109. Marieke van, H., et al., *Risk factors for lung disease progression in children with cystic fibrosis*. European Respiratory Journal, 2018. **51**(6): p. 1702509.

110. Döring, G., et al., *Treatment of lung infection in patients with cystic fibrosis: current and future strategies*. J Cyst Fibros, 2012. **11**(6): p. 461-79.
111. Sly, P.D., et al., *Lung disease at diagnosis in infants with cystic fibrosis detected by newborn screening*. Am J Respir Crit Care Med, 2009. **180**(2): p. 146-52.
112. Pillarisetti, N., et al., *Infection, inflammation and lung function decline in infants with cystic fibrosis*. Am. J. Respir. Crit. Care Med., 2011. **184**(1): p. 75-81.
113. Rosenow, T., et al., *PRAGMA-CF. A Quantitative Structural Lung Disease Computed Tomography Outcome in Young Children with Cystic Fibrosis*. Am J Respir Crit Care Med, 2015. **191**(10): p. 1158-65.
114. Sly, P.D., et al., *Risk factors for bronchiectasis in children with cystic fibrosis*. N Engl J Med, 2013. **368**(21): p. 1963-70.
115. Thornton, C.S., et al., *Exploring the Cystic Fibrosis Lung Microbiome: Making the Most of a Sticky Situation*. J Pediatric Infect Dis Soc, 2022. **11**(Supplement_2): p. S13-s22.
116. Cuthbertson, L., et al., *Lung function and microbiota diversity in cystic fibrosis*. Microbiome, 2020. **8**(1): p. 45.
117. Stick, S.M., et al., *Bronchiectasis in infants and preschool children diagnosed with cystic fibrosis after newborn screening*. J Pediatr, 2009. **155**(5): p. 623-8.e1.
118. Turcios, N.L., *Cystic Fibrosis Lung Disease: An Overview*. Respiratory Care, 2020. **65**(2): p. 233.
119. van Ewijk, B.E., et al., *Prevalence and impact of respiratory viral infections in young children with cystic fibrosis: prospective cohort study*. Pediatrics, 2008. **122**(6): p. 1171-6.
120. Deschamp, A.R., et al., *Early respiratory viral infections in infants with cystic fibrosis*. Journal of cystic fibrosis : official journal of the European Cystic Fibrosis Society, 2019. **18**(6): p. 844-850.
121. Eymery, M., et al., *Viral respiratory tract infections in young children with cystic fibrosis: a prospective full-year seasonal study*. Virology Journal, 2019. **16**(1): p. 111.
122. Armstrong, D., et al., *Severe viral respiratory infections in infants with cystic fibrosis*. Pediatr Pulmonol, 1998. **26**(6): p. 371-9.
123. Hiatt, P.W., et al., *Effects of viral lower respiratory tract infection on lung function in infants with cystic fibrosis*. Pediatrics, 1999. **103**(3): p. 619-26.
124. Smyth, A.R., et al., *Effect of respiratory virus infections including rhinovirus on clinical status in cystic fibrosis*. Archives of disease in childhood, 1995. **73**(2): p. 117-120.
125. Sutanto, E.N., et al., *Innate inflammatory responses of pediatric cystic fibrosis airway epithelial cells: effects of nonviral and viral stimulation*. Am J Respir Cell Mol Biol, 2011. **44**(6): p. 761-7.
126. Kieninger, E., et al., *High rhinovirus burden in lower airways of children with cystic fibrosis*. Chest, 2013. **143**(3): p. 782-790.
127. Breuer, O., et al., *Changing Prevalence of Lower Airway Infections in Young Children with Cystic Fibrosis*. American Journal of Respiratory and Critical Care Medicine, 2019. **200**(5): p. 590-599.
128. Delfino, E., et al., *Respiratory Fungal Diseases in Adult Patients With Cystic Fibrosis*. Clinical medicine insights. Circulatory, respiratory and pulmonary medicine, 2019. **13**: p. 1179548419849939-1179548419849939.
129. Poore, T.S., et al., *Clinical characteristics of people with cystic fibrosis and frequent fungal infection*. Pediatric Pulmonology, 2022. **57**(1): p. 152-161.
130. Hector, A., et al., *Microbial colonization and lung function in adolescents with cystic fibrosis*. Journal of Cystic Fibrosis, 2016. **15**(3): p. 340-349.
131. Smith, K., et al., *Aspergillus fumigatus enhances elastase production in Pseudomonas aeruginosa co-cultures*. Med Mycol, 2015. **53**(7): p. 645-55.
132. Schwarz, C., et al., *Respiratory Fungal Infections in Cystic Fibrosis: Diagnostic and Therapeutic Challenges*. Current Fungal Infection Reports, 2023. **17**(3): p. 202-213.
133. Gangell, C., et al., *Inflammatory responses to individual microorganisms in the lungs of children with cystic fibrosis*. Clin. Infect. Dis., 2011. **53**(5): p. 425-32.

134. Douglas, T.A., et al., *Acquisition and eradication of P. aeruginosa in young children with cystic fibrosis*. Eur. Respir. J., 2009. **33**(2): p. 305.
135. Scoffone, V.C., et al., *Burkholderia cenocepacia Infections in Cystic Fibrosis Patients: Drug Resistance and Therapeutic Approaches*. Front Microbiol, 2017. **8**: p. 1592.
136. Lambiase, A., et al., *Achromobacter xylosoxidans respiratory tract infection in cystic fibrosis patients*. Eur J Clin Microbiol Infect Dis, 2011. **30**(8): p. 973-80.
137. Firmida, M.C., et al., *Clinical impact of Achromobacter xylosoxidans colonization/infection in patients with cystic fibrosis*. Braz J Med Biol Res, 2016. **49**(4): p. e5097.
138. Waters, V., et al., *Stenotrophomonas maltophilia in cystic fibrosis: serologic response and effect on lung disease*. Am J Respir Crit Care Med, 2011. **183**(5): p. 635-40.
139. Skolnik, K., G. Kirkpatrick, and B.S. Quon, *Nontuberculous Mycobacteria in Cystic Fibrosis*. Curr Treat Options Infect Dis, 2016. **8**(4): p. 259-274.
140. Nixon, G.M., et al., *Clinical outcome after early Pseudomonas aeruginosa infection in cystic fibrosis*. J. Pediatr., 2001. **138**(5): p. 699-704.
141. Rosenfeld, M., et al., *Early pulmonary infection, inflammation, and clinical outcomes in infants with cystic fibrosis*. Pediatr. Pulmonol., 2001. **32**(5): p. 356-66.
142. Emerson, J., et al., *Pseudomonas aeruginosa and other predictors of mortality and morbidity in young children with cystic fibrosis*. Pediatr. Pulmonol., 2002. **34**(2): p. 91-100.
143. Li, Z., et al., *Longitudinal development of mucoid Pseudomonas aeruginosa infection and lung disease progression in children with cystic fibrosis*. JAMA, 2005. **293**(5): p. 581-8.
144. Saiman, L., *Microbiology of early CF lung disease*. Paediatr. Respir. Rev., 2004. **5**: p. S367-S369.
145. Ranganathan, S.C., et al., *Geographical differences in first acquisition of Pseudomonas aeruginosa in cystic fibrosis*. Ann. Am. Thorac. Soc, 2013. **10**(2): p. 108-114.
146. Burns, J.L., et al., *Longitudinal assessment of Pseudomonas aeruginosa in young children with cystic fibrosis*. J. Infect. Dis., 2001. **183**(3): p. 444-452.
147. Kidd, T.J., et al., *Pseudomonas aeruginosa genotypes acquired by children with cystic fibrosis by age 5-years*. J. Cyst. Fibros., 2015. **14**(3): p. 361-9.
148. Tai, A.S., et al., *Molecular surveillance for carbapenemase genes in carbapenem-resistant Pseudomonas aeruginosa in Australian patients with cystic fibrosis*. Pathology, 2015. **47**(2): p. 156-60.
149. Al-Aloul, M., et al., *Increased morbidity associated with chronic infection by an epidemic Pseudomonas aeruginosa strain in CF patients*. Thorax, 2004. **59**(4): p. 334-6.
150. Aaron, S.D., et al., *Infection with transmissible strains of Pseudomonas aeruginosa and clinical outcomes in adults with cystic fibrosis*. Jama, 2010. **304**(19): p. 2145-53.
151. Jones, A.M., et al., *Clinical outcome for cystic fibrosis patients infected with transmissible Pseudomonas aeruginosa: an 8-year prospective study*. Chest, 2010. **137**(6): p. 1405-9.
152. Ashish, A., et al., *Increasing resistance of the Liverpool Epidemic Strain (LES) of Pseudomonas aeruginosa (Psa) to antibiotics in cystic fibrosis (CF)--a cause for concern?* J. Cyst. Fibros., 2012. **11**(3): p. 173-9.
153. Kidd, T.J., et al., *Shared Pseudomonas aeruginosa genotypes are common in Australian cystic fibrosis centres*. Eur. Respir. J., 2013. **41**(5): p. 1091.
154. Tai, A.S., et al., *Genotypic diversity within a single Pseudomonas aeruginosa strain commonly shared by Australian patients with cystic fibrosis*. PloS one, 2015. **10**(12): p. e0144022-e0144022.
155. Wee, B.A., et al., *Whole genome sequencing reveals the emergence of a Pseudomonas aeruginosa shared strain sub-lineage among patients treated within a single cystic fibrosis centre*. BMC genomics, 2018. **19**(1): p. 644-644.
156. Valerius, N.H., C. Koch, and N. Højby, *Prevention of chronic Pseudomonas aeruginosa colonisation in cystic fibrosis by early treatment*. Lancet, 1991. **338**(8769): p. 725-6.

157. Wiesemann, H.G., et al., *Placebo-controlled, double-blind, randomized study of aerosolized tobramycin for early treatment of Pseudomonas aeruginosa colonization in cystic fibrosis*. Pediatric Pulmonology, 1998. **25**(2): p. 88-92.
158. Gibson, R.L., et al., *Significant microbiological effect of inhaled tobramycin in young children with cystic fibrosis*. Am. J. Respir. Crit. Care Med., 2003. **167**(6): p. 841-849.
159. Ratjen, F., et al., *Treatment of early Pseudomonas aeruginosa infection in patients with cystic fibrosis: the ELITE trial*. Thorax, 2010. **65**(4): p. 286.
160. Treggiari, M.M., et al., *Comparative efficacy and safety of 4 randomized regimens to treat early Pseudomonas aeruginosa infection in children with cystic fibrosis*. Arch. Pediatr. Adolesc. Med., 2011. **165**(9): p. 847-856.
161. Taccetti, G., et al., *Early antibiotic treatment for Pseudomonas aeruginosa eradication in patients with cystic fibrosis: a randomised multicentre study comparing two different protocols*. Thorax, 2012. **67**(10): p. 853-9.
162. Proesmans, M., et al., *Comparison of two treatment regimens for eradication of Pseudomonas aeruginosa infection in children with cystic fibrosis*. J. Cyst. Fibros., 2013. **12**(1): p. 29-34.
163. Ruseckaite, R., et al., *The Australian cystic fibrosis data registry annual report, 2017*. 2019, Monash University, Department of Epidemiology and Preventive Medicine.
164. Singh, P.K., et al., *Quorum-sensing signals indicate that cystic fibrosis lungs are infected with bacterial biofilms*. Nature, 2000. **407**(6805): p. 762-4.
165. Winstanley, C., S. O'Brien, and M.A. Brockhurst, *Pseudomonas aeruginosa evolutionary adaptation and diversification in cystic fibrosis chronic lung infections*. Trends Microbiol., 2016. **24**(5): p. 327-337.
166. Maciá, M.D., et al., *Hypermutation Is a key factor in development of multiple-antimicrobial resistance in Pseudomonas aeruginosa strains causing chronic lung infections*. Antimicrob. Agents Chemother., 2005. **49**(8): p. 3382.
167. Smith, E.E., et al., *Genetic adaptation by Pseudomonas aeruginosa to the airways of cystic fibrosis patients*. Proc. Natl. Acad. Sci. USA, 2006. **103**(22): p. 8487-8492.
168. Chung, J.C.S., et al., *Genomic variation among contemporary Pseudomonas aeruginosa isolates from chronically infected cystic fibrosis patients*. J. bacteriol., 2012. **194**(18): p. 4857-4866.
169. Workentine, M.L., et al., *Phenotypic heterogeneity of Pseudomonas aeruginosa populations in a cystic fibrosis patient*. PloS one, 2013. **8**(4): p. e60225-e60225.
170. Fegan, M., et al., *Phenotypic conversion of Pseudomonas aeruginosa in cystic fibrosis*. J. Clin. Microbiol., 1990. **28**(6): p. 1143-1146.
171. Szaff, M., N. Højby, and E.W. Flensburg, *Frequent antibiotic therapy improves survival of cystic fibrosis patients with chronic Pseudomonas aeruginosa infection*. Acta Paediatr Scand, 1983. **72**(5): p. 651-7.
172. Moss, R.B., *Long-term benefits of inhaled tobramycin in adolescent patients with cystic fibrosis*. Chest, 2002. **121**(1): p. 55-63.
173. Ramsey, B.W., et al., *Intermittent administration of inhaled tobramycin in patients with cystic fibrosis*. Cystic Fibrosis Inhaled Tobramycin Study Group. N Engl J Med, 1999. **340**(1): p. 23-30.
174. Lenoir, G., et al., *Efficacy, safety, and local pharmacokinetics of highly concentrated nebulized tobramycin in patients with cystic fibrosis colonized with Pseudomonas aeruginosa*. Paediatr Drugs, 2007. **9 Suppl 1**: p. 11-20.
175. Chuchalin, A., et al., *A formulation of aerosolized tobramycin (Bramitob) in the treatment of patients with cystic fibrosis and Pseudomonas aeruginosa infection: a double-blind, placebo-controlled, multicenter study*. Paediatr Drugs, 2007. **9 Suppl 1**: p. 21-31.
176. Konstan, M.W., et al., *Tobramycin inhalation powder for P. aeruginosa infection in cystic fibrosis: the EVOLVE trial*. Pediatric pulmonology, 2011. **46**(3): p. 230-238.
177. Konstan, M.W., et al., *Safety, efficacy and convenience of tobramycin inhalation powder in cystic fibrosis patients: The EAGER trial*. Journal of cystic fibrosis : official journal of the European Cystic Fibrosis Society, 2011. **10**(1): p. 54-61.

178. West, N.E., et al., *Standardized Treatment of Pulmonary Exacerbations (STOP) study: Physician treatment practices and outcomes for individuals with cystic fibrosis with pulmonary Exacerbations*. J Cyst Fibros, 2017. **16**(5): p. 600-606.
179. Emerson, J., et al., *Changes in cystic fibrosis sputum microbiology in the United States between 1995 and 2008*. Pediatr Pulmonol, 2010. **45**(4): p. 363-70.
180. Smith, D.J., et al., *Pseudomonas aeruginosa antibiotic resistance in Australian cystic fibrosis centres*. Respirology, 2016. **21**(2): p. 329-337.
181. Conway, S., et al., *Antibiotic treatment of multidrug-resistant organisms in cystic fibrosis*. Am. J. Respir. Crit. Care Med., 2003. **2**(4): p. 321-332.
182. Sordé, R., A. Pahissa, and J. Rello, *Management of refractory Pseudomonas aeruginosa infection in cystic fibrosis*. Infect. Drug. Resist., 2011. **4**: p. 31-41.
183. Rachel, M., et al., *Renal Function in Patients with Cystic Fibrosis: A Single-Center Study*. Int J Environ Res Public Health, 2022. **19**(9).
184. Harruff, E.E., et al., *Ototoxicity in cystic fibrosis patients receiving intravenous tobramycin for acute pulmonary exacerbation: Ototoxicity following tobramycin treatment*. J Cyst Fibros, 2021. **20**(2): p. 288-294.
185. Piccolo, F., et al., *Clostridium difficile infection in cystic fibrosis: an uncommon but life-threatening complication*. Respirol Case Rep, 2017. **5**(1): p. e00204.
186. Wiesemann, H.G., et al., *Placebo-controlled, double-blind, randomized study of aerosolized tobramycin for early treatment of Pseudomonas aeruginosa colonization in cystic fibrosis*. Pediatr. Pulmonol., 1998. **25**(2): p. 88-92.
187. Ratjen, F., et al., *Treatment of early Pseudomonas aeruginosa infection in patients with cystic fibrosis: the ELITE trial*. Thorax, 2010. **65**(4): p. 286-91.
188. Gibson, R.L., J.L. Burns, and B.W. Ramsey, *Pathophysiology and Management of Pulmonary Infections in Cystic Fibrosis*. American Journal of Respiratory and Critical Care Medicine, 2003. **168**(8): p. 918-951.
189. McCoy, K.S., et al., *Inhaled aztreonam lysine for chronic airway Pseudomonas aeruginosa in cystic fibrosis*. Am J Respir Crit Care Med, 2008. **178**(9): p. 921-8.
190. Jensen, T., et al., *Colistin inhalation therapy in cystic fibrosis patients with chronic Pseudomonas aeruginosa lung infection*. Journal of Antimicrobial Chemotherapy, 1987. **19**(6): p. 831-838.
191. Tümmler, B., *Emerging therapies against infections with Pseudomonas aeruginosa*. F1000Research, 2019. **8**: p. F1000 Faculty Rev-1371.
192. Tamma, P.D., et al., *The use of intravenous colistin among children in the United States: results from a multicenter, case series*. Pediatr Infect Dis J, 2013. **32**(1): p. 17-22.
193. Jeannot, K., et al., *Detection of Colistin Resistance in Pseudomonas aeruginosa Using the MALDIxin Test on the Routine MALDI Biotyper Sirius Mass Spectrometer*. Frontiers in Microbiology, 2021. **12**.
194. Garazzino, S., et al., *Ceftolozane/Tazobactam for Treating Children With Exacerbations of Cystic Fibrosis Due to Pseudomonas aeruginosa: A Review of Available Data*. Frontiers in pediatrics, 2020. **8**: p. 173-173.
195. Drawz, S.M. and R.A. Bonomo, *Three decades of beta-lactamase inhibitors*. Clin Microbiol Rev, 2010. **23**(1): p. 160-201.
196. Zhanel, G.G., et al., *Imipenem-Relebactam and Meropenem-Vaborbactam: Two Novel Carbapenem-β-Lactamase Inhibitor Combinations*. Drugs, 2018. **78**(1): p. 65-98.
197. Thomson, K.S., et al., *Activity of Cefepime-Zidebactam against Multidrug-Resistant (MDR) Gram-Negative Pathogens*. Antibiotics (Basel), 2019. **8**(1).
198. Okujava, R., et al., *1359. Activity of Meropenem/Nacubactam Combination Against Gram-Negative Clinical Isolates: ROSCO Global Surveillance 2017*. Open Forum Infectious Diseases, 2018. **5**(suppl_1): p. S416-S416.
199. Daigle, D., et al., *1370. Cefepime/VNRX-5133 Broad-Spectrum Activity Is Maintained Against Emerging KPC- and PDC-Variants in Multidrug-Resistant K. pneumoniae and P. aeruginosa*. Open Forum Infectious Diseases, 2018. **5**(suppl_1): p. S419-S420.
200. Zhanel, G.G., et al., *Cefiderocol: A Siderophore Cephalosporin with Activity Against Carbapenem-Resistant and Multidrug-Resistant Gram-Negative Bacilli*. Drugs, 2019. **79**(3): p. 271-289.

201. Sader, H.S., et al., *Murepavadin activity tested against contemporary (2016-17) clinical isolates of XDR Pseudomonas aeruginosa*. J Antimicrob Chemother, 2018. **73**(9): p. 2400-2404.
202. Gorr, S.-U., C.M. Flory, and R.J. Schumacher, *In vivo activity and low toxicity of the second-generation antimicrobial peptide DGL13K*. PloS one, 2019. **14**(5): p. e0216669-e0216669.
203. Beaudoin, T., et al., *Activity of a novel antimicrobial peptide against Pseudomonas aeruginosa biofilms*. Scientific reports, 2018. **8**(1): p. 14728-14728.
204. Molchanova, N., et al., *Antimicrobial Activity of α -Peptide/ β -Peptoid Lysine-Based Peptidomimetics Against Colistin-Resistant Pseudomonas aeruginosa Isolated From Cystic Fibrosis Patients*. Frontiers in microbiology, 2019. **10**: p. 275-275.
205. De Soyza, A., et al., *RESPIRE 1: a phase III placebo-controlled randomised trial of ciprofloxacin dry powder for inhalation in non-cystic fibrosis bronchiectasis*. Eur Respir J, 2018. **51**(1).
206. Aksamit, T., et al., *RESPIRE 2: a phase III placebo-controlled randomised trial of ciprofloxacin dry powder for inhalation in non-cystic fibrosis bronchiectasis*. Eur Respir J, 2018. **51**(1).
207. Haworth, C.S., et al., *Inhaled liposomal ciprofloxacin in patients with non-cystic fibrosis bronchiectasis and chronic lung infection with Pseudomonas aeruginosa (ORBIT-3 and ORBIT-4): two phase 3, randomised controlled trials*. Lancet Respir Med, 2019. **7**(3): p. 213-226.
208. Derbali, R.M., et al., *Tailored Nanocarriers for the Pulmonary Delivery of Levofloxacin against Pseudomonas aeruginosa: A Comparative Study*. Mol Pharm, 2019. **16**(5): p. 1906-1916.
209. Clancy, J.P., et al., *Phase II studies of nebulised Arikace in CF patients with Pseudomonas aeruginosa infection*. Thorax, 2013. **68**(9): p. 818-25.
210. Riethmüller, J., et al., *Sequential Inhalational Tobramycin-Colistin-Combination in CF-Patients with Chronic P. Aeruginosa Colonization - an Observational Study*. Cell Physiol Biochem, 2016. **39**(3): p. 1141-51.
211. Rojo-Moliner, E., et al., *Sequential Treatment of Biofilms with Aztreonam and Tobramycin Is a Novel Strategy for Combating Pseudomonas aeruginosa Chronic Respiratory Infections*. Antimicrob Agents Chemother, 2016. **60**(5): p. 2912-22.
212. Soares, A., et al., *Efficacy of a ciprofloxacin/amikacin combination against planktonic and biofilm cultures of susceptible and low-level resistant Pseudomonas aeruginosa*. Journal of Antimicrobial Chemotherapy, 2019. **74**(11): p. 3252-3259.
213. Zemke, A.C., et al., *Nitrite modulates bacterial antibiotic susceptibility and biofilm formation in association with airway epithelial cells*. Free Radic Biol Med, 2014. **77**: p. 307-16.
214. Major, T.A., et al., *Sodium nitrite-mediated killing of the major cystic fibrosis pathogens Pseudomonas aeruginosa, Staphylococcus aureus, and Burkholderia cepacia under anaerobic planktonic and biofilm conditions*. Antimicrob Agents Chemother, 2010. **54**(11): p. 4671-7.
215. Banin, E., K.M. Brady, and E.P. Greenberg, *Chelator-induced dispersal and killing of Pseudomonas aeruginosa cells in a biofilm*. Appl Environ Microbiol, 2006. **72**(3): p. 2064-9.
216. Puvvadi, R., et al., *Role of Tris-CaEDTA as an adjuvant with nebulised tobramycin in cystic fibrosis patients with Pseudomonas aeruginosa lung infections: A randomised controlled trial*. J Cyst Fibros, 2021. **20**(2): p. 316-323.
217. Cryz, S.J., Jr., et al., *Immunization of cystic fibrosis patients with a Pseudomonas aeruginosa O-polysaccharide-toxin A conjugate vaccine*. Behring Inst Mitt, 1997(98): p. 345-9.
218. Pennington, J.E., et al., *Use of a Pseudomonas Aeruginosa vaccine in pateints with acute leukemia and cystic fibrosis*. Am J Med, 1975. **58**(5): p. 629-36.
219. Döring, G., et al., *A double-blind randomized placebo-controlled phase III study of a Pseudomonas aeruginosa flagella vaccine in cystic fibrosis patients*. Proceedings of the National Academy of Sciences of the United States of America, 2007. **104**(26): p. 11020-11025.

220. Baumann, U., E. Mansouri, and B.U. von Specht, *Recombinant OprF-OprI as a vaccine against Pseudomonas aeruginosa infections*. Vaccine, 2004. **22**(7): p. 840-7.
221. Johansen, H.K. and P.C. Gøtzsche, *Vaccines for preventing infection with Pseudomonas aeruginosa in cystic fibrosis*. Cochrane Database Syst Rev, 2008(4): p. Cd001399.
222. Defoirdt, T., *Quorum-Sensing Systems as Targets for Antivirulence Therapy*. Trends Microbiol, 2018. **26**(4): p. 313-328.
223. Tateda, K., et al., *Azithromycin inhibits quorum sensing in Pseudomonas aeruginosa*. Antimicrob Agents Chemother, 2001. **45**(6): p. 1930-3.
224. Goss, C.H., et al., *Gallium disrupts bacterial iron metabolism and has therapeutic effects in mice and humans with lung infections*. Sci Transl Med, 2018. **10**(460).
225. Ali, S.O., et al., *Phase I study of MEDI3902, an investigational anti-Pseudomonas aeruginosa PcrV and Psl bispecific human monoclonal antibody, in healthy adults*. Clin Microbiol Infect, 2019. **25**(5): p. 629.e1-629.e6.
226. Jain, R., et al., *KB001-A, a novel anti-inflammatory, found to be safe and well-tolerated in cystic fibrosis patients infected with Pseudomonas aeruginosa*. J Cyst Fibros, 2018. **17**(4): p. 484-491.
227. Kutter, E., et al., *Phage therapy in clinical practice: treatment of human infections*. Curr Pharm Biotechnol, 2010. **11**(1): p. 69-86.
228. Loc-Carrillo, C. and S.T. Abedon, *Pros and cons of phage therapy*. Bacteriophage, 2011. **1**(2): p. 111-114.
229. Pires, D.P., et al., *Genetically Engineered Phages: a Review of Advances over the Last Decade*. Microbiology and Molecular Biology Reviews, 2016. **80**(3): p. 523.
230. Maciejewska, B., T. Olszak, and Z. Drulis-Kawa, *Applications of bacteriophages versus phage enzymes to combat and cure bacterial infections: an ambitious and also a realistic application?* Applied microbiology and biotechnology, 2018. **102**(6): p. 2563-2581.
231. Roach, D.R. and D.M. Donovan, *Antimicrobial bacteriophage-derived proteins and therapeutic applications*. Bacteriophage, 2015. **5**(3): p. e1062590-e1062590.
232. Øivind, B., et al., *High abundance of viruses found in aquatic environments*. Nature, 1989. **340**(6233): p. 467.
233. Felix, D.H., *On an invisible microbe antagonistic toward dysenteric bacilli: brief note by Mr. F. D'Herelle, presented by Mr. Roux*. Research in Microbiology, 2007. **158**(7): p. 553-554.
234. Twort, F.W., *AN INVESTIGATION ON THE NATURE OF ULTRA-MICROSCOPIC VIRUSES*. The Lancet, 1915. **186**(4814): p. 1241-1243.
235. Kutateladze, M. and R. Adamia, *Phage therapy experience at the Eliava Institute*. Med. Mal. Infect., 2008. **38**(8): p. 426-30.
236. Sulakvelidze, A., Z. Alavidze, and J.G. Morris, Jr., *Bacteriophage therapy*. Antimicrob. Agents Chemother., 2001. **45**(3): p. 649-659.
237. Ofir, G. and R. Sorek, *Contemporary Phage Biology: From Classic Models to New Insights*. Cell, 2018. **172**(6): p. 1260-1270.
238. Dion, M.B., F. Oechslin, and S. Moineau, *Phage diversity, genomics and phylogeny*. Nature Reviews Microbiology, 2020. **18**(3): p. 125-138.
239. Cook, R., et al., *Infrastructure for a PHAge REference Database: Identification of large-scale biases in the current collection of phage genomes*. bioRxiv, 2021: p. 2021.05.01.442102.
240. Ackermann, H.-W., *Chapter 1 - Bacteriophage Electron Microscopy*, in *Advances in Virus Research*, M. Łobocka and W.T. Szybalski, Editors. 2012, Academic Press. p. 1-32.
241. Huss, P., et al., *Mapping the functional landscape of the receptor binding domain of T7 bacteriophage by deep mutational scanning*. eLife, 2021. **10**: p. e63775.
242. Maghsoodi, A., et al., *How the phage T4 injection machinery works including energetics, forces, and dynamic pathway*. Proceedings of the National Academy of Sciences, 2019. **116**(50): p. 25097-25105.
243. Hobbs, Z. and S.T. Abedon, *Diversity of phage infection types and associated terminology: the problem with 'Lytic or lysogenic'*. FEMS Microbiol. Lett., 2016. **363**(7).

244. Cortes, M.G., et al., *From Bench to Keyboard and Back Again: A Brief History of Lambda Phage Modeling*. Annual Review of Biophysics, 2021. **50**(1): p. 117-134.
245. Casjens, S.R. and R.W. Hendrix, *Bacteriophage lambda: Early pioneer and still relevant*. Virology, 2015. **479-480**: p. 310-30.
246. Fry, B.A., *Conditions for the Infection of Escherichia coli with Lambda Phage and for the Establishment of Lysogeny*. Microbiology, 1959. **21**(3): p. 676-684.
247. Lieb, M., *Studies on lysogenization in Escherichia coli*. Cold Spring Harb Symp Quant Biol, 1953. **18**: p. 71-3.
248. Thomas, R. and L. Lambert, *On the occurrence of bacterial mutations permitting lysogenization by clear variants of temperate bacteriophages*. J Mol Biol, 1962. **5**: p. 373-4.
249. Tsao, Y.F., et al., *Phage Morons Play an Important Role in Pseudomonas aeruginosa Phenotypes*. J Bacteriol, 2018. **200**(22).
250. Zhao, X., et al., *Transcriptomic and Metabolomics Profiling of Phage-Host Interactions between Phage PaP1 and Pseudomonas aeruginosa*. Frontiers in Microbiology, 2017. **8**.
251. Zhao, X., et al., *Global Transcriptomic Analysis of Interactions between Pseudomonas aeruginosa and Bacteriophage PaP3*. Sci Rep, 2016. **6**: p. 19237.
252. Katarzyna, D.-W., et al., *Genomic, transcriptomic, and structural analysis of Pseudomonas virus PA5oct highlights the molecular complexity among Jumbo phages*. bioRxiv, 2018: p. 406421.
253. Zhong, Q., et al., *Transcriptomic Analysis Reveals the Dependency of Pseudomonas aeruginosa Genes for Double-Stranded RNA Bacteriophage phiYY Infection Cycle*. iScience, 2020. **23**(9): p. 101437.
254. Finstrlová, A., et al., *Global Transcriptomic Analysis of Bacteriophage-Host Interactions between a Kayvirus Therapeutic Phage and Staphylococcus aureus*. Microbiol Spectr, 2022. **10**(3): p. e0012322.
255. Young, R., *Phage lysis: three steps, three choices, one outcome*. J Microbiol, 2014. **52**(3): p. 243-58.
256. Hyman, P., *Phages for phage therapy: Isolation, characterization, and host range breadth*. Pharmaceuticals, 2019. **12**(1): p. 35.
257. Gordillo Altamirano, F.L. and J.J. Barr, *Phage Therapy in the Postantibiotic Era*. Clinical microbiology reviews, 2019. **32**(2): p. e00066-18.
258. Abedon, S.T., K.M. Danis-Wlodarczyk, and D.J. Wozniak, *Phage Cocktail Development for Bacteriophage Therapy: Toward Improving Spectrum of Activity Breadth and Depth*. Pharmaceuticals (Basel), 2021. **14**(10).
259. Molina, F., et al., *A New Pipeline for Designing Phage Cocktails Based on Phage-Bacteria Infection Networks*. Frontiers in Microbiology, 2021. **12**.
260. Forti, F., et al., *Design of a Broad-Range Bacteriophage Cocktail That Reduces Pseudomonas aeruginosa Biofilms and Treats Acute Infections in Two Animal Models*. Antimicrobial Agents and Chemotherapy, 2018. **62**(6): p. 10.1128/aac.02573-17.
261. Fernández, L., et al., *The perfect bacteriophage for therapeutic applications-a quick guide*. Antibiotics, 2019. **8**(3): p. 126.
262. Trend, S., et al., *Use of a primary epithelial cell screening tool to investigate phage therapy in cystic fibrosis*. Frontiers in Pharmacology, 2018. **9**(1330).
263. Latz, S., et al., *Preliminary survey of local bacteriophages with lytic activity against multi-drug resistant bacteria*. J Basic Microbiol, 2016. **56**(10): p. 1117-1123.
264. Mattila, S., P. Ruotsalainen, and M. Jalasvuori, *On-demand isolation of bacteriophages against drug-resistant bacteria for personalized phage therapy*. Front. Microbiol., 2015. **6**: p. 1271-1271.
265. Mattila, S., P. Ruotsalainen, and M. Jalasvuori, *On-Demand Isolation of Bacteriophages Against Drug-Resistant Bacteria for Personalized Phage Therapy*. Frontiers in microbiology, 2015. **6**: p. 1271-1271.
266. Millard, A.S.a.A., *Phage Genome Annotation: Where to Begin and End*. PHAGE, 2021. **2**(4): p. 183-193.
267. Philipson, C.W., et al., *Characterizing Phage Genomes for Therapeutic Applications*. Viruses, 2018. **10**(4): p. 188.

268. Turner, D., A.M. Kropinski, and E.M. Adriaenssens, *A Roadmap for Genome-Based Phage Taxonomy*. *Viruses*, 2021. **13**(3).
269. Debarbieux, L., et al., *Bacteriophages Can Treat and Prevent Pseudomonas aeruginosa Lung Infections*. *J. Infect. Dis.*, 2010. **201**(7): p. 1096-1104.
270. Morello, E., et al., *Pulmonary bacteriophage therapy on Pseudomonas aeruginosa cystic fibrosis strains: first steps towards treatment and prevention*. *PLoS one*, 2011. **6**(2): p. e16963-e16963.
271. Alemayehu, D., et al., *Bacteriophages phiMR299-2 and phiNH-4 can eliminate Pseudomonas aeruginosa in the murine lung and on cystic fibrosis lung airway cells*. *mBio*, 2012. **3**(2): p. e00029-12.
272. Kim, S., et al., *Pseudomonas aeruginosa bacteriophage PA1Ø requires type IV pili for infection and shows broad bactericidal and biofilm removal activities*. *Appl. Environ. Microbiol.*, 2012. **78**(17): p. 6380-6385.
273. Hosseini Doust, Z., N. Tufenkji, and T.G. van de Ven, *Formation of biofilms under phage predation: considerations concerning a biofilm increase*. *Biofouling*, 2013. **29**(4): p. 457-68.
274. Danis-Włodarczyk, K., et al., *A proposed integrated approach for the preclinical evaluation of phage therapy in Pseudomonas infections*. *Sci. Rep.*, 2016. **6**(1): p. 28115.
275. Oechslin, F., et al., *Synergistic interaction between phage therapy and antibiotics clears Pseudomonas aeruginosa infection in endocarditis and reduces virulence*. *J. Infect. Dis.*, 2016. **215**(5): p. 703-712.
276. Roach, D.R., et al., *Synergy between the host immune system and bacteriophage is essential for successful phage therapy against an acute respiratory pathogen*. *Cell Host & Microbe*, 2017. **22**(1): p. 38-47.e4.
277. Waters, E.M., et al., *Phage therapy is highly effective against chronic lung infections with Pseudomonas aeruginosa*. *Thorax*, 2017. **72**(7): p. 666-667.
278. Fong, S.A., et al., *Activity of bacteriophages in removing biofilms of Pseudomonas aeruginosa isolates from chronic rhinosinusitis patients*. *Front. Cell. Infect. Microbiol.*, 2017. **7**: p. 418-418.
279. Chaudhry, W.N., et al., *Synergy and order effects of antibiotics and phages in killing Pseudomonas aeruginosa biofilms*. *PLoS One*, 2017. **12**(1): p. e0168615.
280. Forti, F., et al., *Design of a broad-range bacteriophage cocktail that reduces Pseudomonas aeruginosa biofilms and treats acute infections in two animal models*. *Antimicrob. Agents Chemother.*, 2018. **62**(6): p. e02573-17.
281. Cafora, M., et al., *Phage therapy against Pseudomonas aeruginosa infections in a cystic fibrosis zebrafish model*. *Sci. Rep.*, 2019. **9**(1): p. 1527.
282. Olszak, T., et al., *Pseudomonas aeruginosa PA5oct Jumbo Phage Impacts Planktonic and Biofilm Population and Reduces Its Host Virulence*. *Viruses*, 2019. **11**(12): p. 1089.
283. Malhotra, S., D. Hayes, Jr., and D.J. Wozniak, *Cystic Fibrosis and Pseudomonas aeruginosa: the Host-Microbe Interface*. *Clin Microbiol Rev*, 2019. **32**(3).
284. Tai, A.S., et al., *Antibiotic perturbation of mixed-strain Pseudomonas aeruginosa infection in patients with cystic fibrosis*. *BMC Pulm Med*, 2017. **17**(1): p. 138.
285. Coulter, L.B., et al., *Effect of bacteriophage infection in combination with tobramycin on the emergence of resistance in Escherichia coli and Pseudomonas aeruginosa biofilms*. *Viruses*, 2014. **6**(10): p. 3778-3786.
286. Torres-Barceló, C., et al., *A window of opportunity to control the bacterial pathogen Pseudomonas aeruginosa combining antibiotics and phages*. *PLoS One*, 2014. **9**(9): p. e106628.
287. Gu Liu, C., et al., *Phage-Antibiotic Synergy Is Driven by a Unique Combination of Antibacterial Mechanism of Action and Stoichiometry*. *mBio*. **11**(4): p. e01462-20.
288. Pons, B.J., et al., *Antibiotics that affect translation can antagonize phage infectivity by interfering with the deployment of counter-defenses*. *Proceedings of the National Academy of Sciences*, 2023. **120**(4): p. e2216084120.
289. Ma, D., et al., *The antagonistic interactions between a polyvalent phage SaP7 and β -lactam antibiotics on combined therapies*. *Veterinary Microbiology*, 2022. **266**: p. 109332.

290. Rubalskii, E., et al., *Bacteriophage Therapy for Critical Infections Related to Cardiothoracic Surgery*. *Antibiotics*, 2020. **9**(5): p. 232.
291. Tan, X., et al., *Clinical Experience of Personalized Phage Therapy Against Carbapenem-Resistant Acinetobacter baumannii Lung Infection in a Patient With Chronic Obstructive Pulmonary Disease*. *Frontiers in Cellular and Infection Microbiology*, 2021. **11**.
292. Wu, N., et al., *Pre-optimized phage therapy on secondary Acinetobacter baumannii infection in four critical COVID-19 patients*. *Emerging Microbes & Infections*, 2021. **10**(1): p. 612-618.
293. Aslam, S., et al., *Lessons Learned From the First 10 Consecutive Cases of Intravenous Bacteriophage Therapy to Treat Multidrug-Resistant Bacterial Infections at a Single Center in the United States*. *Open forum infectious diseases*, 2020. **7**(9): p. ofaa389-ofaa389.
294. Petrovic Fabijan, A., et al., *Safety of bacteriophage therapy in severe Staphylococcus aureus infection*. *Nature Microbiology*, 2020. **5**(3): p. 465-472.
295. Wright, A., et al., *A controlled clinical trial of a therapeutic bacteriophage preparation in chronic otitis due to antibiotic-resistant Pseudomonas aeruginosa; a preliminary report of efficacy*. *Clin. Otolaryngol.*, 2009. **34**(4): p. 349-357.
296. Jault, P., et al., *Efficacy and tolerability of a cocktail of bacteriophages to treat burn wounds infected by Pseudomonas aeruginosa (PhagoBurn): a randomised, controlled, double-blind phase 1/2 trial*. *Lancet Infect. Dis.*, 2019. **19**(1): p. 35-45.
297. Ng, R.N., et al., *Overcoming Challenges to Make Bacteriophage Therapy Standard Clinical Treatment Practice for Cystic Fibrosis*. *Front Microbiol*, 2020. **11**: p. 593988.
298. Rohde, C., et al., *Expert opinion on three phage therapy related topics: bacterial phage resistance, phage training and prophages in bacterial production strains*. *Viruses*, 2018. **10**(4).
299. Schooley, R.T., et al., *Development and use of personalized bacteriophage-based therapeutic cocktails to treat a patient with a disseminated resistant Acinetobacter baumannii infection*. *Antimicrob. Agents Chemother.*, 2017. **61**(10): p. e00954-17.
300. Zhvania, P., et al., *Phage Therapy in a 16-Year-Old Boy with Netherton Syndrome*. *Front. Med.*, 2017. **4**: p. 94-94.
301. Duplessis, C., et al., *Refractory Pseudomonas bacteremia in a 2-year-old sterilized by bacteriophage therapy*. *J. Pediatric. Infect. Dis. Soc.*, 2018. **7**(3): p. 253-256.
302. Aslam, S., et al., *Early clinical experience of bacteriophage therapy in 3 lung transplant recipients*. *Am. J. Transplant.*, 2019. **19**(9): p. 2631-2639.
303. Chan, B.K., et al., *Personalized Inhaled Bacteriophage Therapy Decreases Multidrug-Resistant Pseudomonas aeruginosa*. *medRxiv*, 2023: p. 2023.01.23.22283996.
304. Law, N., et al., *Successful adjunctive use of bacteriophage therapy for treatment of multidrug-resistant Pseudomonas aeruginosa infection in a cystic fibrosis patient*. *Infection*, 2019. **47**(4): p. 665-668.
305. Maddocks, S., et al., *Bacteriophage Therapy of Ventilator-associated Pneumonia and Empyema Caused by Pseudomonas aeruginosa*. *American Journal of Respiratory and Critical Care Medicine*, 2019. **200**(9): p. 1179-1181.
306. Ferry, T., et al., *Personalized bacteriophage therapy to treat pandrug-resistant spinal Pseudomonas aeruginosa infection*. *Nature Communications*, 2022. **13**(1): p. 4239.
307. Chan, B.K., et al., *Phage treatment of an aortic graft infected with Pseudomonas aeruginosa*. *Evolution, Medicine, and Public Health*, 2018. **2018**(1): p. 60-66.
308. Castledine, M., et al., *Parallel evolution of Pseudomonas aeruginosa phage resistance and virulence loss in response to phage treatment in vivo and in vitro*. *eLife*, 2022. **11**: p. e73679.
309. Blasco, L., et al., *Case report: Analysis of phage therapy failure in a patient with a Pseudomonas aeruginosa prosthetic vascular graft infection*. *Frontiers in Medicine*, 2023. **10**.
310. Hoyle, N., et al., *Phage therapy against Achromobacter xylosoxidans lung infection in a patient with cystic fibrosis: a case report*. *Research in Microbiology*, 2018. **169**(9): p. 540-542.

311. Gainey, A.B., et al., *Combining bacteriophages with cefiderocol and meropenem/vaborbactam to treat a pan-drug resistant Achromobacter species infection in a pediatric cystic fibrosis patient*. *Pediatric Pulmonology*, 2020. **55**(11): p. 2990-2994.
312. Lebeaux, D., et al., *A Case of Phage Therapy against Pandrug-Resistant Achromobacter xylosoxidans in a 12-Year-Old Lung-Transplanted Cystic Fibrosis Patient*. *Viruses*, 2021. **13**(1): p. 60.
313. Nick, J.A., et al., *Host and pathogen response to bacteriophage engineered against *Mycobacterium abscessus* lung infection*. *Cell*, 2022. **185**(11): p. 1860-1874.e12.
314. Dedrick, R.M., et al., *Engineered bacteriophages for treatment of a patient with a disseminated drug-resistant Mycobacterium abscessus*. *Nature Medicine*, 2019. **25**(5): p. 730-733.
315. Rao, S., et al., *Critically Ill Patient with Multidrug-Resistant Acinetobacter baumannii Respiratory Infection Successfully Treated with Intravenous and Nebulized Bacteriophage Therapy*. *Antimicrob Agents Chemother*, 2022. **66**(1): p. e0082421.
316. Dedrick, R.M., et al., *Potent antibody-mediated neutralization limits bacteriophage treatment of a pulmonary Mycobacterium abscessus infection*. *Nature Medicine*, 2021. **27**(8): p. 1357-1361.
317. Labrie, S.J., J.E. Samson, and S. Moineau, *Bacteriophage resistance mechanisms*. *Nat. Rev. Microbiol.*, 2010. **8**(5): p. 317-27.
318. Bernheim, A. and R. Sorek, *The pan-immune system of bacteria: antiviral defence as a community resource*. *Nat. Rev. Microbiol.*, 2020. **18**(2): p. 113-119.
319. Stern, A. and R. Sorek, *The phage-host arms race: shaping the evolution of microbes*. *BioEssays*, 2011. **33**(1): p. 43-51.
320. Broniewski, J.M., et al., *The effect of phage genetic diversity on bacterial resistance evolution*. *ISME J.*, 2020. **14**(3): p. 828-836.
321. Johnson, M.C., et al., *Core defense hotspots within Pseudomonas aeruginosa are a consistent and rich source of anti-phage defense systems*. *Nucleic Acids Research*, 2023. **51**(10): p. 4995-5005.
322. Bertozzi Silva, J., Z. Storms, and D. Sauvageau, *Host receptors for bacteriophage adsorption*. *FEMS Microbiol. Lett.*, 2016. **363**(4).
323. Chan, B.K., et al., *Phage selection restores antibiotic sensitivity in MDR Pseudomonas aeruginosa*. *Sci. Rep.*, 2016. **6**(1): p. 26717.
324. Bradley, D.E., *Evidence for the retraction of Pseudomonas aeruginosa RNA phage pili*. *Biochem. Biophys. Res. Commun.*, 1972. **47**(1): p. 142-149.
325. Wright, R.C.T., et al., *Cross-resistance is modular in bacteria-phage interactions*. *PLoS Biol.*, 2018. **16**(10): p. e2006057.
326. Wright, R.C.T., et al., *Resistance evolution against phage combinations depends on the timing and order of exposure*. *mBio*, 2019. **10**(5): p. e01652-19.
327. Li, G., et al., *Adaptation of Pseudomonas aeruginosa to phage PaPI predation via O-antigen polymerase mutation*. *Front. Microbiol.*, 2018. **9**(1170).
328. Latino, L., et al., *Pseudolysogeny and sequential mutations build multiresistance to virulent bacteriophages in Pseudomonas aeruginosa*. *Microbiol.*, 2016. **162**(5): p. 748-763.
329. Pires, D.P., et al., *A Genotypic Analysis of Five P. aeruginosa Strains after Biofilm Infection by Phages Targeting Different Cell Surface Receptors*. *Frontiers in microbiology*, 2017. **8**: p. 1229-1229.
330. Le, S., et al., *Chromosomal DNA deletion confers phage resistance to Pseudomonas aeruginosa*. *Sci. Rep.*, 2014. **4**: p. 4738-4738.
331. Burgener, E.B., et al., *Filamentous bacteriophages are associated with chronic Pseudomonas lung infections and antibiotic resistance in cystic fibrosis*. *Sci. Transl. Med.*, 2019. **11**(488): p. eaau9748.
332. Secor, P.R., et al., *Filamentous Bacteriophage Promote Biofilm Assembly and Function*. *Cell host & microbe*, 2015. **18**(5): p. 549-559.

333. Winstanley, C., et al., *Newly introduced genomic prophage islands are critical determinants of in vivo competitiveness in the Liverpool Epidemic Strain of Pseudomonas aeruginosa*. *Genome Res.*, 2009. **19**(1): p. 12-23.
334. Ismail, M.H., et al., *The Repressor C Protein, Pf4r, Controls Superinfection of Pseudomonas aeruginosa PAO1 by the Pf4 Filamentous Phage and Regulates Host Gene Expression*. *Viruses*, 2021. **13**(8).
335. Bondy-Denomy, J., et al., *Prophages mediate defense against phage infection through diverse mechanisms*. *ISME J.*, 2016. **10**(12): p. 2854-2866.
336. Newton, G.J., et al., *Three-component-mediated serotype conversion in Pseudomonas aeruginosa by bacteriophage D3*. *Mol. Microbiol.*, 2001. **39**(5): p. 1237-47.
337. Chung, I.-Y., et al., *A phage protein that inhibits the bacterial ATPase required for type IV pilus assembly*. *Proc. Natl. Acad. Sci. USA*, 2014. **111**(31): p. 11503.
338. Tsao, Y.-F., et al., *Phage morons play an important role in Pseudomonas aeruginosa phenotypes*. *J. Bacteriol.*, 2018. **200**(22): p. e00189-18.
339. Hanjeong, H., et al., *Pseudomonas aeruginosa defends against phages through type IV pilus glycosylation*. *Nature Microbiol.*, 2018. **3**(1): p. 47-52.
340. Doolittle, M., J. Cooney, and D. Caldwell, *Tracing the interaction of bacteriophage with bacterial biofilms using fluorescent and chromogenic probes*. *J. Indust. Microbiol.*, 1996. **16**(6): p. 331-341.
341. Hanlon, G.W., et al., *Reduction in exopolysaccharide viscosity as an aid to bacteriophage penetration through Pseudomonas aeruginosa biofilms*. *Appl. Environ. Microbiol.*, 2001. **67**(6): p. 2746-2753.
342. Augustyniak, D., T. Olszak, and Z. Drulis-Kawa, *Outer Membrane Vesicles (OMVs) of Pseudomonas aeruginosa Provide Passive Resistance but Not Sensitization to LPS-Specific Phages*. *Viruses*, 2022. **14**(1): p. 121.
343. Cady, K.C., et al., *Prevalence, conservation and functional analysis of Yersinia and Escherichia CRISPR regions in clinical Pseudomonas aeruginosa isolates*. *Microbiol.*, 2011. **157**(2): p. 430-437.
344. Cady, K.C., et al., *The CRISPR/Cas adaptive immune system of Pseudomonas aeruginosa mediates resistance to naturally occurring and engineered phages*. *J. Bacteriol.*, 2012. **194**(21): p. 5728.
345. Bondy-Denomy, J., et al., *Bacteriophage genes that inactivate the CRISPR/Cas bacterial immune system*. *Nature*, 2013. **493**(7432): p. 429-432.
346. Pawluk, A., et al., *A new group of phage anti-CRISPR genes inhibits the type I-E CRISPR-Cas system of Pseudomonas aeruginosa*. *mBio*, 2014. **5**(2): p. e00896-e00896.
347. Dimitriu, T., et al., *Bacteriostatic antibiotics promote CRISPR-Cas adaptive immunity by enabling increased spacer acquisition*. *Cell Host & Microbe*, 2022.
348. Høyland-Kroghsbo, N.M., K.A. Muñoz, and B.L. Bassler, *Temperature, by Controlling Growth Rate, Regulates CRISPR-Cas Activity in Pseudomonas aeruginosa*. *mBio*, 2018. **9**(6).
349. Westra, Edze R., et al., *Parasite Exposure Drives Selective Evolution of Constitutive versus Inducible Defense*. *Current Biology*, 2015. **25**(8): p. 1043-1049.
350. Chevallereau, A., et al., *The effect of bacterial mutation rate on the evolution of CRISPR-Cas adaptive immunity*. *Philos Trans R Soc Lond B Biol Sci*, 2019. **374**(1772): p. 20180094.
351. Broniewski, J.M., et al., *The effect of Quorum sensing inhibitors on the evolution of CRISPR-based phage immunity in Pseudomonas aeruginosa*. *The ISME Journal*, 2021. **15**(8): p. 2465-2473.
352. Tock, M.R. and D.T.F. Dryden, *The biology of restriction and anti-restriction*. *Curr. Opin. Microbiol.*, 2005. **8**(4): p. 466-472.
353. Wang, L., et al., *Phosphorothioation of DNA in bacteria by dnd genes*. *Nat. Chem. Biol.*, 2007. **3**(11): p. 709-710.
354. Dy, R.L., et al., *A widespread bacteriophage abortive infection system functions through a Type IV toxin-antitoxin mechanism*. *Nucleic Acids Res*, 2014. **42**(7): p. 4590-605.
355. Gao, L., et al., <https://www.biorxiv.org/content/10.1101/2022.08.12.503731v2.full>. *Science*, 2020. **369**(6507): p. 1077-1084.

356. Adi, M., et al., *An expanding arsenal of immune systems that protect bacteria from phages*. bioRxiv, 2022: p. 2022.05.11.491447.
357. Goldfarb, T., et al., *BREX is a novel phage resistance system widespread in microbial genomes*. Embo j, 2015. **34**(2): p. 169-83.
358. Millman, A., et al., *Diversity and classification of cyclic-oligonucleotide-based anti-phage signalling systems*. Nature Microbiology, 2020. **5**(12): p. 1608-1615.
359. LeRoux, M., et al., *The DarTG toxin-antitoxin system provides phage defence by ADP-ribosylating viral DNA*. Nature microbiology, 2022. **7**(7): p. 1028-1040.
360. Tal, N., et al., *Bacteria deplete deoxynucleotides to defend against bacteriophage infection*. Nat Microbiol, 2022. **7**(8): p. 1200-1209.
361. Ofir, G., et al., *DISARM is a widespread bacterial defence system with broad anti-phage activities*. Nat Microbiol, 2018. **3**(1): p. 90-98.
362. Xu, T., et al., *A novel host-specific restriction system associated with DNA backbone S-modification in Salmonella*. Nucleic Acids Res, 2010. **38**(20): p. 7133-41.
363. Doron, S., et al., *Systematic discovery of antiphage defense systems in the microbial pangenome*. Science, 2018. **359**(6379): p. eaar4120.
364. Guo, L., et al., *A Bacterial Dynamin-Like Protein Confers a Novel Phage Resistance Strategy on the Population Level in Bacillus subtilis*. mBio, 2021. **13**(1): p. e0375321.
365. Rousset, F., et al., *Prophage-encoded hotspots of bacterial immune systems*. bioRxiv, 2021: p. 2021.01. 21.427644.
366. Xiong, X., et al., *SspABCD-SspE is a phosphorothioation-sensing bacterial defence system with broad anti-phage activities*. Nat Microbiol, 2020. **5**(7): p. 917-928.
367. Ka, D., et al., *Structural and functional evidence of bacterial antiphage protection by Thoeris defense system via NAD⁺ degradation*. Nature Communications, 2020. **11**(1): p. 2816.
368. Le, S., et al., *Mapping the tail fiber as the receptor binding protein responsible for differential host specificity of Pseudomonas aeruginosa bacteriophages PaP1 and JG004*. PLoS ONE, 2013. **8**(7): p. e68562.
369. Burrowes, B.H., I.J. Molineux, and J.A. Fralick, *Directed in vitro evolution of therapeutic bacteriophages: The Appelmans protocol*. Viruses, 2019. **11**(3): p. 241.
370. Betts, A., et al., *Back to the future: evolving bacteriophages to increase their effectiveness against the pathogen Pseudomonas aeruginosa PAO1*. Evolutionary applications, 2013. **6**(7): p. 1054-1063.
371. Friman, V.P., et al., *Pre-adapting parasitic phages to a pathogen leads to increased pathogen clearance and lowered resistance evolution with Pseudomonas aeruginosa cystic fibrosis bacterial isolates*. Journal of Evolutionary Biology, 2016. **29**(1): p. 188-198.
372. Yang, Y., et al., *Development of a bacteriophage cocktail to constrain the emergence of phage-resistant Pseudomonas aeruginosa*. Front. Microbiol., 2020. **11**(327).
373. Trasanidou, D., et al., *Keeping crisper in check: diverse mechanisms of phage-encoded anti-crisprs*. FEMS Microbiology Letters, 2019. **366**(9).
374. Landsberger, M., et al., *Anti-CRISPR Phages Cooperate to Overcome CRISPR-Cas Immunity*. Cell, 2018. **174**(4): p. 908-916.e12.
375. Chevallereau, A., et al., *Exploitation of the Cooperative Behaviors of Anti-CRISPR Phages*. Cell Host & Microbe, 2020. **27**(2): p. 189-198.e6.
376. Shah, M., et al., *A phage-encoded anti-activator inhibits quorum sensing in Pseudomonas aeruginosa*. Molecular Cell, 2021. **81**(3): p. 571-583.e6.
377. Flores, V., et al., *Comparative genomic analysis of Pseudomonas aeruginosa phage PaMx25 reveals a novel siphovirus group related to phages infecting hosts of different taxonomic classes*. Arch. Virol., 2017. **162**(8): p. 2345-2355.
378. Lee, Y.-J., et al., *Identification and biosynthesis of thymidine hypermodifications in the genomic DNA of widespread bacterial viruses*. PNAS, 2018. **115**(14): p. E3116.
379. Markwitz, P., et al., *Genome-driven elucidation of phage-host interplay and impact of phage resistance evolution on bacterial fitness*. The ISME Journal, 2022. **16**(2): p. 533-542.

380. Cullen, L., et al., *Phenotypic characterization of an international Pseudomonas aeruginosa reference panel: strains of cystic fibrosis (CF) origin show less in vivo virulence than non-CF strains*. Microbiology, 2015. **161**(10): p. 1961-1977.
381. Kidd, T.J., et al., *Shared Pseudomonas aeruginosa genotypes are common in Australian cystic fibrosis centres*. Eur Respir J, 2013. **41**(5): p. 1091-100.
382. Clark, S.T., D.S. Guttman, and D.M. Hwang, *Diversification of Pseudomonas aeruginosa within the cystic fibrosis lung and its effects on antibiotic resistance*. FEMS Microbiology Letters, 2018. **365**(6).
383. McCarron, A., D. Parsons, and M. Donnelley, *Animal and Cell Culture Models for Cystic Fibrosis: Which Model Is Right for Your Application?* The American Journal of Pathology, 2021. **191**(2): p. 228-242.
384. Stoltz, D.A., et al., *Cystic fibrosis pigs develop lung disease and exhibit defective bacterial eradication at birth*. Sci Transl Med, 2010. **2**(29): p. 29ra31.
385. Rogers, C.S., et al., *Disruption of the CFTR gene produces a model of cystic fibrosis in newborn pigs*. Science, 2008. **321**(5897): p. 1837-41.
386. Ostedgaard, L.S., et al., *The $\Delta F508$ mutation causes CFTR misprocessing and cystic fibrosis-like disease in pigs*. Sci Transl Med, 2011. **3**(74): p. 74ra24.
387. Fan, Z., et al., *A sheep model of cystic fibrosis generated by CRISPR/Cas9 disruption of the CFTR gene*. JCI Insight, 2018. **3**(19).
388. Sun, X., et al., *Gastrointestinal pathology in juvenile and adult CFTR-knockout ferrets*. Am J Pathol, 2014. **184**(5): p. 1309-22.
389. Darrah, R., et al., *Cystic Fibrosis Mice Develop Spontaneous Chronic Bordetella Airway Infections*. J Infect Pulm Dis, 2017. **3**(2).
390. Wilke, M., et al., *Mouse models of cystic fibrosis: phenotypic analysis and research applications*. J Cyst Fibros, 2011. **10** Suppl 2: p. S152-71.
391. Plopper, C.G., et al., *Comparison of nonciliated tracheal epithelial cells in six mammalian species: ultrastructure and population densities*. Exp Lung Res, 1983. **5**(4): p. 281-94.
392. Grubb, B.R. and R.C. Boucher, *Pathophysiology of gene-targeted mouse models for cystic fibrosis*. Physiol Rev, 1999. **79**(1 Suppl): p. S193-214.
393. Mall, M., et al., *Increased airway epithelial Na⁺ absorption produces cystic fibrosis-like lung disease in mice*. Nature Medicine, 2004. **10**(5): p. 487-493.
394. Brao Kristen, J., et al., *Scnn1b-Transgenic BALB/c Mice as a Model of Pseudomonas aeruginosa Infections of the Cystic Fibrosis Lung*. Infection and Immunity, 2020. **88**(9): p. 10.1128/iai.00237-20.
395. Alemayehu, D., et al., *Bacteriophages ϕ MR299-2 and ϕ NH-4 Can Eliminate Pseudomonas aeruginosa in the Murine Lung and on Cystic Fibrosis Lung Airway Cells*. mBio, 2012. **3**(2): p. 10.1128/mbio.00029-12.
396. Luscher, A., et al., *Combined Bacteriophage and Antibiotic Treatment Prevents Pseudomonas aeruginosa Infection of Wild Type and cftr- Epithelial Cells*. Frontiers in Microbiology, 2020. **11**.
397. Brandão, A.C., et al., *Impact of phage predation on P. aeruginosa adhered to human airway epithelium: major transcriptomic changes in metabolism and virulence-associated genes*. RNA Biol, 2023. **20**(1): p. 235-247.
398. Birket, S.E., et al., *Development of an airway mucus defect in the cystic fibrosis rat*. JCI Insight, 2018. **3**(1).
399. Tuggle, K.L., et al., *Characterization of defects in ion transport and tissue development in cystic fibrosis transmembrane conductance regulator (CFTR)-knockout rats*. PLoS One, 2014. **9**(3): p. e91253.
400. Zabner, J., et al., *Development of cystic fibrosis and noncystic fibrosis airway cell lines*. Am J Physiol Lung Cell Mol Physiol, 2003. **284**(5): p. L844-54.
401. Hermanns, M.I., et al., *Lung epithelial cell lines in coculture with human pulmonary microvascular endothelial cells: development of an alveolo-capillary barrier in vitro*. Lab Invest, 2004. **84**(6): p. 736-52.
402. Ehrhardt, C., et al., *Towards an in vitro model of cystic fibrosis small airway epithelium: characterisation of the human bronchial epithelial cell line CFBE41o*. Cell Tissue Res, 2006. **323**(3): p. 405-15.

403. Gruenert, D.C., et al., *Established cell lines used in cystic fibrosis research*. Journal of Cystic Fibrosis, 2004. **3**: p. 191-196.
404. Lundberg, A.S., et al., *Immortalization and transformation of primary human airway epithelial cells by gene transfer*. Oncogene, 2002. **21**(29): p. 4577-86.
405. Martinovich, K.M., et al., *Conditionally reprogrammed primary airway epithelial cells maintain morphology, lineage and disease specific functional characteristics*. Scientific Reports, 2017. **7**(1): p. 17971.
406. Schögler, A., et al., *Characterization of pediatric cystic fibrosis airway epithelial cell cultures at the air-liquid interface obtained by non-invasive nasal cytology brush sampling*. Respiratory Research, 2017. **18**(1): p. 215.
407. Aldallal, N., et al., *Inflammatory Response in Airway Epithelial Cells Isolated from Patients with Cystic Fibrosis*. American Journal of Respiratory and Critical Care Medicine, 2002. **166**(9): p. 1248-1256.
408. Ling, K.M., et al., *Rhinovirus Infection Drives Complex Host Airway Molecular Responses in Children With Cystic Fibrosis*. Front Immunol, 2020. **11**: p. 1327.
409. Agudelo-Romero, P., et al., *Using integrated omics to assess the effects of rhinovirus infection in children with Cystic Fibrosis (CF)*. European Respiratory Journal, 2020. **56**(suppl 64): p. 4342.
410. Montgomery, S.T., et al., *Rhinovirus Infection Is Associated With Airway Epithelial Cell Necrosis and Inflammation via Interleukin-1 in Young Children With Cystic Fibrosis*. Frontiers in Immunology, 2020. **11**.
411. Looi, K., et al., *Effect of human rhinovirus infection on airway epithelium tight junction protein disassembly and transepithelial permeability*. Exp Lung Res, 2016. **42**(7): p. 380-395.
412. Looi, K., et al., *Effects of human rhinovirus on epithelial barrier integrity and function in children with asthma*. Clin Exp Allergy, 2018. **48**(5): p. 513-524.
413. Pezzulo, A.A., et al., *The air-liquid interface and use of primary cell cultures are important to recapitulate the transcriptional profile of in vivo airway epithelia*. American Journal of Physiology-Lung Cellular and Molecular Physiology, 2011. **300**(1): p. L25-L31.
414. Wang, H., et al., *Establishment and comparison of air-liquid interface culture systems for primary and immortalized swine tracheal epithelial cells*. BMC Cell Biology, 2018. **19**(1): p. 10.
415. Nahar, K., et al., *In vitro, in vivo and ex vivo models for studying particle deposition and drug absorption of inhaled pharmaceuticals*. European Journal of Pharmaceutical Sciences, 2013. **49**(5): p. 805-818.
416. Upadhyay, S. and L. Palmberg, *Air-Liquid Interface: Relevant In Vitro Models for Investigating Air Pollutant-Induced Pulmonary Toxicity*. Toxicological Sciences, 2018. **164**(1): p. 21-30.
417. Dunn, N.W. and B.W. Holloway, *Pleiotrophy of p-fluorophenylalanine-resistant and antibiotic hypersensitive mutants of Pseudomonas aeruginosa*. Genet Res, 1971. **18**(2): p. 185-97.
418. Jacobs, M.A. and C. Manoil, *A Genome-Wide Mutant Library of Pseudomonas aeruginosa*, in *Pseudomonas: Volume 4 Molecular Biology of Emerging Issues*, J.-L. Ramos and R.C. Levesque, Editors. 2006, Springer US: Boston, MA. p. 121-138.
419. Held, K., et al., *Sequence-verified two-allele transposon mutant library for Pseudomonas aeruginosa PAO1*. Journal of bacteriology, 2012. **194**(23): p. 6387-6389.
420. Montgomery, S., *Extraction of high molecular weight DNA from nasal lining fluid*. protocols.io, 2023.
421. Bushnell, B., *BBmap*. 2020, sourceforge.
422. Bankevich, A., et al., *SPAdes: a new genome assembly algorithm and its applications to single-cell sequencing*. Journal of computational biology : a journal of computational molecular cell biology, 2012. **19**(5): p. 455-477.
423. Rizk, G., et al., *MindTheGap: integrated detection and assembly of short and long insertions*. Bioinformatics, 2014. **30**(24): p. 3451-3457.
424. Guyomar, C., et al., *MinYS: mine your symbiont by targeted genome assembly in symbiotic communities*. NAR Genomics and Bioinformatics, 2020. **2**(3): p. lqaa047.

425. Wood, D.E. and S.L. Salzberg, *Kraken: ultrafast metagenomic sequence classification using exact alignments*. *Genome Biology*, 2014. **15**(3): p. R46.
426. De Coster, W. and R. Rademakers, *NanoPack2: population-scale evaluation of long-read sequencing data*. *Bioinformatics*, 2023. **39**(5).
427. Wick, R.R., et al., *Unicycler: Resolving bacterial genome assemblies from short and long sequencing reads*. *PLOS Computational Biology*, 2017. **13**(6): p. e1005595.
428. Kolmogorov, M., et al., *Assembly of long, error-prone reads using repeat graphs*. *Nature Biotechnology*, 2019. **37**(5): p. 540-546.
429. Wick, R.R., et al., *Tricycler: consensus long-read assemblies for bacterial genomes*. *Genome Biology*, 2021. **22**(1): p. 266.
430. Nanopore, O., *Medaka*. 2023: Github.
431. Li, H. and R. Durbin, *Fast and accurate short read alignment with Burrows–Wheeler transform*. *Bioinformatics*, 2009. **25**(14): p. 1754-1760.
432. Wick, R.R. and K.E. Holt, *Polypolish: Short-read polishing of long-read bacterial genome assemblies*. *PLOS Computational Biology*, 2022. **18**(1): p. e1009802.
433. Schwengers, O., et al., *Bakta: rapid and standardized annotation of bacterial genomes via alignment-free sequence identification*. *Microbial Genomics*, 2021. **7**(11).
434. Payne, L.J., et al., *Identification and classification of antiviral defence systems in bacteria and archaea with PADLOC reveals new system types*. *Nucleic Acids Research*, 2021. **49**(19): p. 10868-10878.
435. Seemann, T., *mlst*. 2022, Github
436. Jolley, K.A. and M.C.J. Maiden, *BIGSdb: Scalable analysis of bacterial genome variation at the population level*. *BMC Bioinformatics*, 2010. **11**(1): p. 595.
437. Seemann, T., *Abricate*. 2020: Github.
438. Alcock, B.P., et al., *CARD 2020: antibiotic resistome surveillance with the comprehensive antibiotic resistance database*. *Nucleic Acids Research*, 2019. **48**(D1): p. D517-D525.
439. Feldgarden, M., et al., *Validating the AMRFinder Tool and Resistance Gene Database by Using Antimicrobial Resistance Genotype-Phenotype Correlations in a Collection of Isolates*. *Antimicrob Agents Chemother*, 2019. **63**(11).
440. Zankari, E., et al., *Identification of acquired antimicrobial resistance genes*. *Journal of Antimicrobial Chemotherapy*, 2012. **67**(11): p. 2640-2644.
441. Gupta, S.K., et al., *ARG-ANNOT, a new bioinformatic tool to discover antibiotic resistance genes in bacterial genomes*. *Antimicrob Agents Chemother*, 2014. **58**(1): p. 212-20.
442. Chen, L., et al., *VFDB 2016: hierarchical and refined dataset for big data analysis--10 years on*. *Nucleic Acids Res*, 2016. **44**(D1): p. D694-7.
443. Carattoli, A., et al., *In Silico Detection and Typing of Plasmids using PlasmidFinder and Plasmid Multilocus Sequence Typing*. *Antimicrobial Agents and Chemotherapy*, 2014. **58**(7): p. 3895-3903.
444. Doster, E., et al., *MEGARes 2.0: a database for classification of antimicrobial drug, biocide and metal resistance determinants in metagenomic sequence data*. *Nucleic Acids Res*, 2020. **48**(D1): p. D561-d569.
445. Gan, R., et al., *DBSCAN-SWA: An Integrated Tool for Rapid Prophage Detection and Annotation*. *Frontiers in Genetics*, 2022. **13**.
446. Buchfink, B., K. Reuter, and H.-G. Drost, *Sensitive protein alignments at tree-of-life scale using DIAMOND*. *Nature Methods*, 2021. **18**(4): p. 366-368.
447. Seemann, T., *Prokka: rapid prokaryotic genome annotation*. *Bioinformatics*, 2014. **30**(14): p. 2068-9.
448. Camacho, C., et al., *BLAST+: architecture and applications*. *BMC Bioinformatics*, 2009. **10**(1): p. 421.
449. Bonilla, N., et al., *Phage on tap—a quick and efficient protocol for the preparation of bacteriophage laboratory stocks*. *PeerJ*, 2016. **4**: p. e2261-e2261.
450. Ng, R.N., et al., *Development and validation of a miniaturized host range screening assay for bacteriophages*. *bioRxiv*, 2021: p. 2021.02.18.431904.
451. Gibson, S.B., et al., *Constructing and Characterizing Bacteriophage Libraries for Phage Therapy of Human Infections*. *Frontiers in Microbiology*, 2019. **10**(2537).

452. Jakočiūnė, D. and A. Moodley, *A Rapid Bacteriophage DNA Extraction Method*. *Methods Protoc*, 2018. **1**(3).
453. Iszatt, J., *Phanatic*. 2023, Github.
454. Nayfach, S., et al., *CheckV assesses the quality and completeness of metagenome-assembled viral genomes*. *Nature Biotechnology*, 2021. **39**(5): p. 578-585.
455. Iszatt, J., *PhageOrder*. 2023, Github.
456. Terzian, P., et al., *PHROG: families of prokaryotic virus proteins clustered using remote homology*. *NAR Genomics and Bioinformatics*, 2021. **3**(3).
457. Cock, P.J.A., et al., *Biopython: freely available Python tools for computational molecular biology and bioinformatics*. *Bioinformatics*, 2009. **25**(11): p. 1422-1423.
458. Lowe, T.M. and S.R. Eddy, *tRNAscan-SE: a program for improved detection of transfer RNA genes in genomic sequence*. *Nucleic Acids Res*, 1997. **25**(5): p. 955-64.
459. Iszatt, J., *PhindersKeepers*. 2023: Github.
460. Katoh, K., et al., *MAFFT: a novel method for rapid multiple sequence alignment based on fast Fourier transform*. *Nucleic Acids Res*, 2002. **30**(14): p. 3059-66.
461. Tamura K, S.G., and Kumar S, *MEGA11: Molecular Evolutionary Genetics Analysis version 11*. *Molecular Biology and Evolution* 2021. **38**: p. 3022-3027.
462. Letunic, I. and P. Bork, *Interactive Tree Of Life (iTOL) v5: an online tool for phylogenetic tree display and annotation*. *Nucleic Acids Research*, 2021. **49**(W1): p. W293-W296.
463. Iszatt, J., *Phusion*. 2023: Github.
464. Moraru, C., A. Varsani, and A.M. Kropinski, *VIRIDIC-A Novel Tool to Calculate the Intergenomic Similarities of Prokaryote-Infecting Viruses*. *Viruses*, 2020. **12**(11).
465. Rasband, W., *ImageJ*. 1997-2012: Bethesda, Maryland, USA.
466. Kropinski, A.M., *Practical Advice on the One-Step Growth Curve*. *Methods Mol Biol*, 2018. **1681**: p. 41-47.
467. Todaro, G.J. and H. Green, *Quantitative studies of the growth of mouse embryo cells in culture and their development into established lines*. *J Cell Biol*, 1963. **17**(2): p. 299-313.
468. Jainchill, J.L., S.A. Aaronson, and G.J. Todaro, *Murine sarcoma and leukemia viruses: assay using clonal lines of contact-inhibited mouse cells*. *J Virol*, 1969. **4**(5): p. 549-53.
469. Taylor, A.L., et al., *FOXP3 mRNA expression at 6 months of age is higher in infants who develop atopic dermatitis, but is not affected by giving probiotics from birth*. *Pediatric Allergy and Immunology*, 2007. **18**(1): p. 10-19.
470. Suttle, C.A., *Viruses in the sea*. *Nature*, 2005. **437**(7057): p. 356-361.
471. Ross, A., S. Ward, and P. Hyman, *More Is Better: Selecting for Broad Host Range Bacteriophages*. *Frontiers in Microbiology*, 2016. **7**.
472. Shen, A. and A. Millard, *Phage Genome Annotation: Where to Begin and End*. *PHAGE*, 2021. **2**(4): p. 183-193.
473. Turner, D., et al., *Phage Annotation Guide: Guidelines for Assembly and High-Quality Annotation*. *PHAGE*, 2021. **2**(4): p. 170-182.
474. Fillol-Salom, A., et al., *Bacteriophages benefit from generalized transduction*. *PLoS Pathog*, 2019. **15**(7): p. e1007888.
475. Fong, K., et al., *How Broad Is Enough: The Host Range of Bacteriophages and Its Impact on the Agri-Food Sector*. *PHAGE*, 2021. **2**(2): p. 83-91.
476. Blazanin, M., et al., *Decay and damage of therapeutic phage OMK01 by environmental stressors*. *PLoS One*, 2022. **17**(2): p. e0263887.
477. Jończyk-Matysiak, E., et al., *Factors determining phage stability/activity: challenges in practical phage application*. *Expert Rev Anti Infect Ther*, 2019. **17**(8): p. 583-606.
478. Jacobs, M.A., et al., *Comprehensive transposon mutant library of Pseudomonas aeruginosa*. *Proc Natl Acad Sci U S A*, 2003. **100**(24): p. 14339-44.
479. LaBauve, A.E. and M.J. Wargo, *Growth and Laboratory Maintenance of Pseudomonas aeruginosa*. *Current Protocols in Microbiology*, 2012. **25**(1): p. 6E.1.1-6E.1.8.
480. Missiakas, D.M. and O. Schneewind, *Growth and laboratory maintenance of Staphylococcus aureus*. *Curr Protoc Microbiol*, 2013. **Chapter 9**: p. Unit 9C.1.
481. Tuttle, A.R., N.D. Trahan, and M.S. Son, *Growth and Maintenance of Escherichia coli Laboratory Strains*. *Curr Protoc*, 2021. **1**(1): p. e20.

482. Kumar, V., et al., *Comparative genomics of Klebsiella pneumoniae strains with different antibiotic resistance profiles*. Antimicrob Agents Chemother, 2011. **55**(9): p. 4267-76.
483. Garcia, E.C. and P.A. Cotter, *Burkholderia thailandensis: Growth and Laboratory Maintenance*. Current Protocols in Microbiology, 2016. **42**(1): p. 4C.1.1-4C.1.7.
484. Peters, D.L., et al., *Bacteriophage Isolation, Purification, and Characterization Techniques Against Ubiquitous Opportunistic Pathogens*. Current Protocols, 2022. **2**(11): p. e594.
485. Wannasrichan, W., et al., *Phage-resistant Pseudomonas aeruginosa against a novel lytic phage JJ01 exhibits hypersensitivity to colistin and reduces biofilm production*. Frontiers in Microbiology, 2022. **13**.
486. Seeman, T., *Snippy*. 2020, Github.
487. Jurczak-Kurek, A., et al., *Biodiversity of bacteriophages: morphological and biological properties of a large group of phages isolated from urban sewage*. Scientific Reports, 2016. **6**(1): p. 34338.
488. Gallet, R., S. Kannoly, and I.-N. Wang, *Effects of bacteriophage traits on plaque formation*. BMC Microbiology, 2011. **11**(1): p. 181.
489. Reynolds, D. and M. Kollef, *The Epidemiology and Pathogenesis and Treatment of Pseudomonas aeruginosa Infections: An Update*. Drugs, 2021. **81**(18): p. 2117-2131.
490. Emslander, Q., et al., *Cell-free production of personalized therapeutic phages targeting multidrug-resistant bacteria*. Cell Chemical Biology, 2022. **29**(9): p. 1434-1445.e7.
491. Shmidov, E., et al., *An Efficient, Counter-Selection-Based Method for Prophage Curing in Pseudomonas aeruginosa Strains*. Viruses, 2021. **13**(2).
492. Van den Bossche, A., et al., *Systematic Identification of Hypothetical Bacteriophage Proteins Targeting Key Protein Complexes of Pseudomonas aeruginosa*. Journal of Proteome Research, 2014. **13**(10): p. 4446-4456.
493. Choudhury, B., R.W. Carlson, and J.B. Goldberg, *The structure of the lipopolysaccharide from a galU mutant of Pseudomonas aeruginosa serogroup-O11*. Carbohydrate Research, 2005. **340**(18): p. 2761-2772.
494. Huszczyński, S.M., J.S. Lam, and C.M. Khursigara, *The Role of Pseudomonas aeruginosa Lipopolysaccharide in Bacterial Pathogenesis and Physiology*. Pathogens, 2019. **9**(1).
495. Lam, J., et al., *Genetic and Functional Diversity of Pseudomonas aeruginosa Lipopolysaccharide*. Frontiers in Microbiology, 2011. **2**(118).
496. Nakamura, K., et al., *Fluctuating Bacteriophage-induced galU Deficiency Region is Involved in Trade-off Effects on the Phage and Fluoroquinolone Sensitivity in Pseudomonas aeruginosa*. Virus Res, 2021. **306**: p. 198596.
497. Schultz, A., et al., *Airway surface liquid pH is not acidic in children with cystic fibrosis*. Nature Communications, 2017. **8**(1): p. 1409.
498. Stick, S.M., A. Kicic, and S. Ranganathan, *Of Pigs, Mice, and Men: Understanding Early Triggers of Cystic Fibrosis Lung Disease*. Am J Respir Crit Care Med, 2016. **194**(7): p. 784-785.
499. McShane, D., et al., *Airway surface pH in subjects with cystic fibrosis*. European Respiratory Journal, 2003. **21**(1): p. 37.
500. Yang, J.Y., et al., *Degradation of host translational machinery drives tRNA acquisition in viruses*. Cell Systems, 2021. **12**(8): p. 771-779.e5.
501. van den Berg, D.F., et al., *Phage tRNAs evade tRNA-targeting host defenses through anticodon loop mutations*. eLife, 2023. **12**: p. e85183.
502. Bailly-Bechet, M., M. Vergassola, and E. Rocha, *Causes for the intriguing presence of tRNAs in phages*. Genome Research, 2007. **17**: p. 1486-1495.
503. Cowe, E. and P.M. Sharp, *Molecular evolution of bacteriophages: Discrete patterns of codon usage in T4 genes are related to the time of gene expression*. Journal of Molecular Evolution, 1991. **33**(1): p. 13-22.
504. Scherberg, N.H. and S.B. Weiss, *T4 Transfer RNAs: Codon Recognition and Translational Properties*. Proceedings of the National Academy of Sciences, 1972. **69**(5): p. 1114-1118.

505. Bouteiller, M., et al., *Pseudomonas Flagella: Generalities and Specificities*. International Journal of Molecular Sciences, 2021. **22**(7): p. 3337.
506. Esteves, N.C. and B.E. Scharf, *Flagellotropic Bacteriophages: Opportunities and Challenges for Antimicrobial Applications*. Int J Mol Sci, 2022. **23**(13).
507. Bucior, I., J.F. Pielage, and J.N. Engel, *Pseudomonas aeruginosa Pili and Flagella Mediate Distinct Binding and Signaling Events at the Apical and Basolateral Surface of Airway Epithelium*. PLOS Pathogens, 2012. **8**(4): p. e1002616.
508. Garcia, M., et al., *Pseudomonas aeruginosa flagellum is critical for invasion, cutaneous persistence and induction of inflammatory response of skin epidermis*. Virulence, 2018. **9**(1): p. 1163-1175.
509. Toutain, C.M., et al., *Roles for flagellar stators in biofilm formation by Pseudomonas aeruginosa*. Research in Microbiology, 2007. **158**(5): p. 471-477.
510. Harrison, J.J., et al., *Elevated exopolysaccharide levels in Pseudomonas aeruginosa flagellar mutants have implications for biofilm growth and chronic infections*. PLoS Genet, 2020. **16**(6): p. e1008848.
511. Smith, E.E., et al., *Genetic adaptation by Pseudomonas aeruginosa to the airways of cystic fibrosis patients*. Proc Natl Acad Sci U S A, 2006. **103**(22): p. 8487-92.
512. Wolfgang, M.C., et al., *Pseudomonas aeruginosa regulates flagellin expression as part of a global response to airway fluid from cystic fibrosis patients*. Proceedings of the National Academy of Sciences, 2004. **101**(17): p. 6664-6668.
513. Borin, J.M., et al., *Comparison of bacterial suppression by phage cocktails, dual-receptor generalists, and coevolutionarily trained phages*. Evolutionary Applications, 2023. **16**(1): p. 152-162.
514. Camens, S., et al., *Preclinical Development of a Bacteriophage Cocktail for Treating Multidrug Resistant Pseudomonas aeruginosa Infections*. Microorganisms, 2021. **9**(9).
515. Li, M., et al., *Phage cocktail powder for Pseudomonas aeruginosa respiratory infections*. Int J Pharm, 2021. **596**: p. 120200.
516. Nordstrom, H.R., et al., *Genomic characterization of lytic bacteriophages targeting genetically diverse Pseudomonas aeruginosa clinical isolates*. iScience, 2022. **25**(6): p. 104372.
517. Oliver, A., et al., *High Frequency of Hypermutable Pseudomonas aeruginosa in Cystic Fibrosis Lung Infection*. Science, 2000. **288**(5469): p. 1251-1253.
518. Smith, E.E., et al., *Genetic adaptation by Pseudomonas aeruginosa to the airways of cystic fibrosis patients*. Proceedings of the National Academy of Sciences, 2006. **103**(22): p. 8487-8492.
519. La Rosa, R., et al., *Compensatory evolution of Pseudomonas aeruginosa's slow growth phenotype suggests mechanisms of adaptation in cystic fibrosis*. Nature Communications, 2021. **12**(1): p. 3186.
520. Egido, J.E., et al., *Mechanisms and clinical importance of bacteriophage resistance*. FEMS Microbiology Reviews, 2021. **46**(1).
521. Li, N., et al., *Characterization of Phage Resistance and Their Impacts on Bacterial Fitness in Pseudomonas aeruginosa*. Microbiol Spectr, 2022. **10**(5): p. e0207222.
522. Markwitz, P., et al., *Emerging Phage Resistance in Pseudomonas aeruginosa PAO1 Is Accompanied by an Enhanced Heterogeneity and Reduced Virulence*. Viruses, 2021. **13**(7): p. 1332.
523. Menon, N.D., et al., *Increased Innate Immune Susceptibility in Hyperpigmented Bacteriophage-Resistant Mutants of Pseudomonas aeruginosa*. Antimicrob Agents Chemother, 2022. **66**(8): p. e0023922.
524. Burmeister, A.R., et al., *Pleiotropy complicates a trade-off between phage resistance and antibiotic resistance*. Proceedings of the National Academy of Sciences, 2020. **117**(21): p. 11207-11216.
525. Chang, R.Y.K., et al., *Bacteriophage PEV20 and Ciprofloxacin Combination Treatment Enhances Removal of Pseudomonas aeruginosa Biofilm Isolated from Cystic Fibrosis and Wound Patients*. Aaps j, 2019. **21**(3): p. 49.
526. Knezevic, P., et al., *Phage-antibiotic synergism: a possible approach to combatting Pseudomonas aeruginosa*. Res Microbiol, 2013. **164**(1): p. 55-60.

527. Uchiyama, J., et al., *Piperacillin and ceftazidime produce the strongest synergistic phage-antibiotic effect in Pseudomonas aeruginosa*. Arch Virol, 2018. **163**(7): p. 1941-1948.
528. Kim, M., et al., *Phage-Antibiotic Synergy via Delayed Lysis*. Appl Environ Microbiol, 2018. **84**(22).
529. Comeau, A.M., et al., *Phage-Antibiotic Synergy (PAS): beta-lactam and quinolone antibiotics stimulate virulent phage growth*. PLoS One, 2007. **2**(8): p. e799.
530. Bulsico, J., et al., *Phage-antibiotic synergy: Cell filamentation is a key driver of successful phage predation*. PLOS Pathogens, 2023. **19**(9): p. e1011602.
531. Singletary, L.A., et al., *An SOS-regulated type 2 toxin-antitoxin system*. Journal of bacteriology, 2009. **191**(24): p. 7456-7465.
532. Liu, Y., et al., *Microevolution of the mexT and lasR Reinforces the Bias of Quorum Sensing System in Laboratory Strains of Pseudomonas aeruginosa PAO1*. Frontiers in Microbiology, 2022. **13**.
533. Chandler, C.E., et al., *Genomic and Phenotypic Diversity among Ten Laboratory Isolates of Pseudomonas aeruginosa PAO1*. J Bacteriol, 2019. **201**(5).
534. Klockgether, J., et al., *Genome diversity of Pseudomonas aeruginosa PAO1 laboratory strains*. J Bacteriol, 2010. **192**(4): p. 1113-21.
535. Dettman, J.R. and R. Kassen, *Evolutionary Genomics of Niche-Specific Adaptation to the Cystic Fibrosis Lung in Pseudomonas aeruginosa*. Molecular Biology and Evolution, 2020. **38**(2): p. 663-675.
536. De Soyza, A., et al., *Developing an international Pseudomonas aeruginosa reference panel*. MicrobiologyOpen, 2013. **2**(6): p. 1010-1023.
537. Moore, M.P., et al., *Transmission, adaptation and geographical spread of the Pseudomonas aeruginosa Liverpool epidemic strain*. Microb Genom, 2021. **7**(3).
538. Deatherage, D.E. and J.E. Barrick, *Identification of mutations in laboratory-evolved microbes from next-generation sequencing data using breseq*. Methods Mol Biol, 2014. **1151**: p. 165-88.
539. Galperin, M.Y., et al., *COG database update: focus on microbial diversity, model organisms, and widespread pathogens*. Nucleic Acids Research, 2020. **49**(D1): p. D274-D281.
540. Zhang, R., et al., *SpacePHARER: sensitive identification of phages from CRISPR spacers in prokaryotic hosts*. Bioinformatics, 2021. **37**(19): p. 3364-3366.
541. Currie, G., et al., *Variation in treatment preferences of pulmonary exacerbations among Australian and New Zealand cystic fibrosis physicians*. BMJ Open Respiratory Research, 2021. **8**(1): p. e000956.
542. Friman, V.-P., et al., *Pseudomonas aeruginosa Adaptation to Lungs of Cystic Fibrosis Patients Leads to Lowered Resistance to Phage and Protist Enemies*. PLOS ONE, 2013. **8**(9): p. e75380.
543. Rees, V.E., et al., *Characterization of Hypermutator Pseudomonas aeruginosa Isolates from Patients with Cystic Fibrosis in Australia*. Antimicrob Agents Chemother, 2019. **63**(4).
544. Oliver, A. and A. Mena, *Bacterial hypermutation in cystic fibrosis, not only for antibiotic resistance*. Clinical Microbiology and Infection, 2010. **16**(7): p. 798-808.
545. Dulanto Chiang, A., et al., *Hypermutator strains of Pseudomonas aeruginosa reveal novel pathways of resistance to combinations of cephalosporin antibiotics and beta-lactamase inhibitors*. PLOS Biology, 2022. **20**(11): p. e3001878.
546. Maciá, M.D., et al., *Hypermutation is a key factor in development of multiple-antimicrobial resistance in Pseudomonas aeruginosa strains causing chronic lung infections*. Antimicrob Agents Chemother, 2005. **49**(8): p. 3382-6.
547. Smania, A.M., et al., *Emergence of phenotypic variants upon mismatch repair disruption in Pseudomonas aeruginosa*. Microbiology, 2004. **150**(5): p. 1327-1338.
548. Lavigne, R., et al., *A multifaceted study of Pseudomonas aeruginosa shutdown by virulent podovirus LUZ19*. mBio, 2013. **4**(2): p. e00061-13.
549. Chevallereau, A., et al., *Next-Generation "-omics" Approaches Reveal a Massive Alteration of Host RNA Metabolism during Bacteriophage Infection of Pseudomonas aeruginosa*. PLoS Genet, 2016. **12**(7): p. e1006134.

550. Mutalik, V.K., et al., *High-throughput mapping of the phage resistance landscape in E. coli*. PLoS Biol, 2020. **18**(10): p. e3000877.
551. Garbe, J., et al., *Sequencing and characterization of Pseudomonas aeruginosa phage JG004*. BMC Microbiol, 2011. **11**: p. 102.
552. Cui, X., et al., *Characterization of Pseudomonas aeruginosa Phage C11 and Identification of Host Genes Required for Virion Maturation*. Sci Rep, 2016. **6**: p. 39130.
553. Maynard, N.D., et al., *A forward-genetic screen and dynamic analysis of lambda phage host-dependencies reveals an extensive interaction network and a new anti-viral strategy*. PLoS Genet, 2010. **6**(7): p. e1001017.
554. Brandão, A., et al., *Differential transcription profiling of the phage LUZ19 infection process in different growth media*. RNA Biol, 2021. **18**(11): p. 1778-1790.
555. Pires, D.P., et al., *A genotypic analysis of five P. aeruginosa strains after biofilm infection by phages targeting different cell surface receptors*. Front. Microbiol., 2017. **8**(1229).
556. Boeckaerts, D., et al., *Identification of Phage Receptor-Binding Protein Sequences with Hidden Markov Models and an Extreme Gradient Boosting Classifier*. Viruses, 2022. **14**(6).
557. Kortright, K.E., B.K. Chan, and P.E. Turner, *High-throughput discovery of phage receptors using transposon insertion sequencing of bacteria*. Proc Natl Acad Sci U S A, 2020. **117**(31): p. 18670-18679.
558. Dunstan, R.A., et al., *Epitopes in the capsular polysaccharide and the porin OmpK36 receptors are required for bacteriophage infection of Klebsiella pneumoniae*. Cell Rep, 2023. **42**(6): p. 112551.
559. Khatami, A., et al., *Bacterial lysis, autophagy and innate immune responses during adjunctive phage therapy in a child*. EMBO Mol Med, 2021. **13**(9): p. e13936.
560. Chatteraj, S.S., et al., *Rhinovirus infection liberates planktonic bacteria from biofilm and increases chemokine responses in cystic fibrosis airway epithelial cells*. Thorax, 2011. **66**(4): p. 333.
561. Knight, D.A. and S.T. Holgate, *The airway epithelium: Structural and functional properties in health and disease*. Respirology, 2003. **8**(4): p. 432-446.
562. Sajjan, U., et al., *Rhinovirus disrupts the barrier function of polarized airway epithelial cells*. Am J Respir Crit Care Med, 2008. **178**(12): p. 1271-81.
563. Davis, J.D. and T.P. Wypych, *Cellular and functional heterogeneity of the airway epithelium*. Mucosal Immunology, 2021. **14**(5): p. 978-990.
564. Pieter, S.H., Paul B. McCray, Jr., and B. Robert, *The innate immune function of airway epithelial cells in inflammatory lung disease*. European Respiratory Journal, 2015. **45**(4): p. 1150.
565. Hillyer, P., et al., *Differential Responses by Human Respiratory Epithelial Cell Lines to Respiratory Syncytial Virus Reflect Distinct Patterns of Infection Control*. J Virol, 2018. **92**(15).
566. Wei, H., et al., *Suppression of interferon lambda signaling by SOCS-1 results in their excessive production during influenza virus infection*. PLoS Pathog, 2014. **10**(1): p. e1003845.
567. Wang, J., et al., *Differentiated human alveolar type II cells secrete antiviral IL-29 (IFN-lambda 1) in response to influenza A infection*. J Immunol, 2009. **182**(3): p. 1296-304.
568. Diamond, G., D.E. Jones, and C.L. Bevins, *Airway epithelial cells are the site of expression of a mammalian antimicrobial peptide gene*. Proceedings of the National Academy of Sciences, 1993. **90**(10): p. 4596-4600.
569. Vernooij, J.H., et al., *Intratracheal instillation of lipopolysaccharide in mice induces apoptosis in bronchial epithelial cells: no role for tumor necrosis factor-alpha and infiltrating neutrophils*. Am J Respir Cell Mol Biol, 2001. **24**(5): p. 569-76.
570. Brydon, E.W.A., H. Smith, and C. Sweet, *Influenza A virus-induced apoptosis in bronchiolar epithelial (NCI-H292) cells limits pro-inflammatory cytokine release*. J Gen Virol, 2003. **84**(Pt 9): p. 2389-2400.
571. Bichet, M.C., et al., *Bacteriophage uptake by mammalian cell layers represents a potential sink that may impact phage therapy*. iScience, 2021. **24**(4): p. 102287.

572. Kicic, A., et al., *Intrinsic biochemical and functional differences in bronchial epithelial cells of children with asthma*. Am J Respir Crit Care Med, 2006. **174**(10): p. 1110-8.
573. Aldallal, N., et al., *Inflammatory response in airway epithelial cells isolated from patients with cystic fibrosis*. Am J Respir Crit Care Med, 2002. **166**(9): p. 1248-56.
574. Endres, A., et al., *Pseudomonas aeruginosa Affects Airway Epithelial Response and Barrier Function During Rhinovirus Infection*. Frontiers in Cellular and Infection Microbiology, 2022. **12**.
575. Barnett, K.C., et al., *An epithelial-immune circuit amplifies inflammasome and IL-6 responses to SARS-CoV-2*. Cell Host Microbe, 2023. **31**(2): p. 243-259.e6.
576. Ramezanzpour, M., et al., *Primary human nasal epithelial cells: a source of poly (I:C) LMW-induced IL-6 production*. Scientific Reports, 2018. **8**(1): p. 11325.
577. Qi, L., et al., *Adenovirus 7 Induces Interleukin-6 Expression in Human Airway Epithelial Cells via p38/NF- κ B Signaling Pathway*. Frontiers in Immunology, 2020. **11**.
578. Medeea, C.P., et al., *A filamentous phage triggers antiviral responses in cystic fibrosis basal airway epithelial cells*. bioRxiv, 2022: p. 2022.09.27.509771.
579. Tzani-Tzanopoulou, P., et al., *Development of an in vitro homeostasis model between airway epithelial cells, bacteria and bacteriophages: a time-lapsed observation of cell viability and inflammatory response*. Journal of General Virology, 2022. **103**(12).
580. FDA. *Bacterial Endotoxins/Pyrogens | FDA. Inspection Technical Guides*. 2014 [cited 2023].
581. Engeman, E., et al., *Synergistic Killing and Re-Sensitization of Pseudomonas aeruginosa to Antibiotics by Phage-Antibiotic Combination Treatment*. Pharmaceuticals (Basel), 2021. **14**(3).
582. Akturk, E., et al., *Synergistic Action of Phage and Antibiotics: Parameters to Enhance the Killing Efficacy Against Mono and Dual-Species Biofilms*. Antibiotics (Basel), 2019. **8**(3).
583. Lopes, A., C. Pereira, and A. Almeida, *Sequential Combined Effect of Phages and Antibiotics on the Inactivation of Escherichia coli*. Microorganisms, 2018. **6**(4).
584. Blasco, L., et al., *Combined Use of the Ab105-2 ϕ ACI Lytic Mutant Phage and Different Antibiotics in Clinical Isolates of Multi-Resistant Acinetobacter baumannii*. Microorganisms, 2019. **7**(11).
585. Moore, R.D., P.S. Lietman, and C.R. Smith, *Clinical response to aminoglycoside therapy: importance of the ratio of peak concentration to minimal inhibitory concentration*. J Infect Dis, 1987. **155**(1): p. 93-9.
586. Smyth, A.R., *Minimizing the toxicity of aminoglycosides in cystic fibrosis*. J R Soc Med, 2010. **103** Suppl 1(Suppl 1): p. S3-5.
587. Garinis, A., et al., *Prospective cohort study of ototoxicity in persons with cystic fibrosis following a single course of intravenous tobramycin*. Journal of Cystic Fibrosis, 2021. **20**(2): p. 278-283.
588. Hall, A.R., et al., *Effects of sequential and simultaneous applications of bacteriophages on populations of Pseudomonas aeruginosa in vitro and in wax moth larvae*. Applied and environmental microbiology, 2012. **78**(16): p. 5646-5652.
589. Foundation, C.F., *Cystic Fibrosis Foundation Patient Registry 2022 Annual Data Report*. 2023, Cystic Fibrosis Foundation Bethesda, Maryland.
590. Raoust, E., et al., *Pseudomonas aeruginosa LPS or Flagellin Are Sufficient to Activate TLR-Dependent Signaling in Murine Alveolar Macrophages and Airway Epithelial Cells*. PLOS ONE, 2009. **4**(10): p. e7259.
591. Yun, M., et al., *Inhibition of Pseudomonas aeruginosa LPS-Induced airway inflammation by RIPK3 in human airway*. J Cell Mol Med, 2022. **26**(21): p. 5506-5516.
592. Galanos, C. and M.A. Freudenberg, *Mechanisms of endotoxin shock and endotoxin hypersensitivity*. Immunobiology, 1993. **187**(3-5): p. 346-56.
593. Farokhi, A., D. Heederik, and L.A.M. Smit, *Respiratory health effects of exposure to low levels of airborne endotoxin – a systematic review*. Environmental Health, 2018. **17**(1): p. 14.
594. Eduard, W., N. Pearce, and J. Douwes, *Chronic bronchitis, COPD, and lung function in farmers: the role of biological agents*. Chest, 2009. **136**(3): p. 716-725.

595. Bolund, A.C., et al., *The effect of occupational farming on lung function development in young adults: a 15-year follow-up study*. Occup Environ Med, 2015. **72**(10): p. 707-13.
596. Onallah, H., et al., *Refractory Pseudomonas aeruginosa infections treated with phage PASA16: A compassionate use case series*. Med, 2023. **4**(9): p. 600-611.e4.
597. Fries, B.C. and A.K. Varshney, *Bacterial Toxins-Staphylococcal Enterotoxin B*. Microbiol Spectr, 2013. **1**(2).
598. Proft, T. and J.D. Fraser, *Bacterial superantigens*. Clin Exp Immunol, 2003. **133**(3): p. 299-306.
599. Seo, H.S., S.M. Michalek, and M.H. Nahm, *Lipoteichoic acid is important in innate immune responses to gram-positive bacteria*. Infect Immun, 2008. **76**(1): p. 206-13.
600. Pisetsky, D.S., *The origin and properties of extracellular DNA: from PAMP to DAMP*. Clin Immunol, 2012. **144**(1): p. 32-40.
601. Liu, D., et al., *The Safety and Toxicity of Phage Therapy: A Review of Animal and Clinical Studies*. Viruses, 2021. **13**(7).
602. Hietala, V., et al., *The Removal of Endo- and Enterotoxins From Bacteriophage Preparations*. Front Microbiol, 2019. **10**: p. 1674.
603. Szermer-Olearnik, B. and J. Boratyński, *Removal of endotoxins from bacteriophage preparations by extraction with organic solvents*. PLoS One, 2015. **10**(3): p. e0122672.
604. Tripathi, S., et al., *Influenza A virus nucleoprotein induces apoptosis in human airway epithelial cells: implications of a novel interaction between nucleoprotein and host protein Clusterin*. Cell Death & Disease, 2013. **4**(3): p. e562-e562.
605. Simpson, J., et al., *Respiratory Syncytial Virus Infection Promotes Necroptosis and HMGB1 Release by Airway Epithelial Cells*. American Journal of Respiratory and Critical Care Medicine, 2020. **201**(11): p. 1358-1371.
606. David, M.C., et al., *Airway epithelial cell apoptosis and inflammation in COPD, smokers and nonsmokers*. European Respiratory Journal, 2013. **41**(5): p. 1058.
607. Singhera, G.K., et al., *Apoptosis of viral-infected airway epithelial cells limit viral production and is altered by corticosteroid exposure*. Respiratory Research, 2006. **7**(1): p. 78.
608. Yoshimura, T., et al., *Purification of a human monocyte-derived neutrophil chemotactic factor that has peptide sequence similarity to other host defense cytokines*. Proc Natl Acad Sci U S A, 1987. **84**(24): p. 9233-7.
609. Schröder, J.M., et al., *Purification and partial biochemical characterization of a human monocyte-derived, neutrophil-activating peptide that lacks interleukin 1 activity*. J Immunol, 1987. **139**(10): p. 3474-83.
610. Pesci, A., et al., *Inflammatory cells and mediators in bronchial lavage of patients with chronic obstructive pulmonary disease*. Eur Respir J, 1998. **12**(2): p. 380-6.
611. Peleman, R.A., et al., *The cellular composition of induced sputum in chronic obstructive pulmonary disease*. Eur Respir J, 1999. **13**(4): p. 839-43.
612. Margaroli, C., et al., *Elastase Exocytosis by Airway Neutrophils Is Associated with Early Lung Damage in Children with Cystic Fibrosis*. American Journal of Respiratory and Critical Care Medicine, 2019. **199**(7): p. 873-881.
613. Garratt, L.W., et al., *Changes in airway inflammation with pseudomonas eradication in early cystic fibrosis*. J Cyst Fibros, 2021. **20**(6): p. 941-948.
614. Pestrak, M.J., et al., *Pseudomonas aeruginosa rugose small-colony variants evade host clearance, are hyper-inflammatory, and persist in multiple host environments*. PLoS Pathog, 2018. **14**(2): p. e1006842.
615. Tillie-Leblond, I., et al., *Balance between proinflammatory cytokines and their inhibitors in bronchial lavage from patients with status asthmaticus*. Am J Respir Crit Care Med, 1999. **159**(2): p. 487-94.
616. Neveu, W.A., et al., *Elevation of IL-6 in the allergic asthmatic airway is independent of inflammation but associates with loss of central airway function*. Respir Res, 2010. **11**(1): p. 28.
617. Eickmeier, O., et al., *Sputum biomarker profiles in cystic fibrosis (CF) and chronic obstructive pulmonary disease (COPD) and association between pulmonary function*. Cytokine, 2010. **50**(2): p. 152-7.

618. Dharmage, S.C., J.L. Perret, and A. Custovic, *Epidemiology of Asthma in Children and Adults*. *Front Pediatr*, 2019. **7**: p. 246.
619. Wan, H., et al., *Der p 1 facilitates transepithelial allergen delivery by disruption of tight junctions*. *J Clin Invest*, 1999. **104**(1): p. 123-33.
620. Lehmann, A.D., et al., *Diesel exhaust particles modulate the tight junction protein occludin in lung cells in vitro*. *Part Fibre Toxicol*, 2009. **6**: p. 26.
621. Kim, J.Y., et al., *Disruption of tight junctions during traversal of the respiratory epithelium by Burkholderia cenocepacia*. *Infect Immun*, 2005. **73**(11): p. 7107-12.
622. Guillon, A., et al., *Inhaled bacteriophage therapy in a porcine model of pneumonia caused by Pseudomonas aeruginosa during mechanical ventilation*. *British Journal of Pharmacology*, 2021. **178**(18): p. 3829-3842.
623. Nguyen, S., et al., *Bacteriophage Transcytosis Provides a Mechanism To Cross Epithelial Cell Layers*. *mBio*, 2017. **8**(6): p. 10.1128/mbio.01874-17.
624. Sweere, J.M., et al., *Bacteriophage trigger antiviral immunity and prevent clearance of bacterial infection*. *Science (New York, N.Y.)*, 2019. **363**(6434): p. eaat9691.
625. Archana, A., et al., *Neutralizing antibody response against subcutaneously injected bacteriophages in rabbit model*. *Virusdisease*, 2021. **32**(1): p. 38-45.
626. Łusiak-Szelachowska, M., et al., *Phage neutralization by sera of patients receiving phage therapy*. *Viral Immunol*, 2014. **27**(6): p. 295-304.
627. Kaźmierczak, Z., et al., *Immune Response to Therapeutic Staphylococcal Bacteriophages in Mammals: Kinetics of Induction, Immunogenic Structural Proteins, Natural and Induced Antibodies*. *Frontiers in Immunology*, 2021. **12**.
628. Dedrick, R.M., et al., *Phage Therapy of Mycobacterium Infections: Compassionate Use of Phages in 20 Patients With Drug-Resistant Mycobacterial Disease*. *Clinical Infectious Diseases*, 2022. **76**(1): p. 103-112.
629. Kolbe, U., et al., *Early Cytokine Induction Upon Pseudomonas aeruginosa Infection in Murine Precision Cut Lung Slices Depends on Sensing of Bacterial Viability*. *Front Immunol*, 2020. **11**: p. 598636.
630. Borthwick, L.A., et al., *Pseudomonas aeruginosa Induced Airway Epithelial Injury Drives Fibroblast Activation: A Mechanism in Chronic Lung Allograft Dysfunction*. *Am J Transplant*, 2016. **16**(6): p. 1751-65.
631. Sweere, J.M., et al., *The Immune Response to Chronic Pseudomonas aeruginosa Wound Infection in Immunocompetent Mice*. *Adv Wound Care (New Rochelle)*, 2020. **9**(2): p. 35-47.
632. Clatworthy, A.E., et al., *Pseudomonas aeruginosa infection of zebrafish involves both host and pathogen determinants*. *Infect Immun*, 2009. **77**(4): p. 1293-303.
633. Kolbe, U., et al., *Early Cytokine Induction Upon Pseudomonas aeruginosa Infection in Murine Precision Cut Lung Slices Depends on Sensing of Bacterial Viability*. *Frontiers in Immunology*, 2020. **11**.
634. Markwitz, P., et al., *Emerging Phage Resistance in Pseudomonas aeruginosa PAO1 Is Accompanied by an Enhanced Heterogeneity and Reduced Virulence*. *Viruses*, 2021. **13**(7).
635. Yang, Q., et al., *Regulations of phage therapy across the world*. *Frontiers in Microbiology*, 2023. **14**.
636. Georgia, M., et al., *Phage therapy for pulmonary infections: lessons from clinical experiences and key considerations*. *European Respiratory Review*, 2022. **31**(166): p. 220121.
637. Gómez, P. and A. Buckling, *Bacteria-Phage Antagonistic Coevolution in Soil*. *Science*, 2011. **332**(6025): p. 106-109.
638. Hernandez, C.A. and B. Koskella, *Phage resistance evolution in vitro is not reflective of in vivo outcome in a plant-bacteria-phage system**. *Evolution*, 2019. **73**(12): p. 2461-2475.
639. Rodriguez-Gonzalez, R.A., et al., *Quantitative Models of Phage-Antibiotic Combination Therapy*. *mSystems*, 2020. **5**(1): p. 10.1128/msystems.00756-19.
640. Leung, C.Y.J. and J.S. Weitz, *Modeling the synergistic elimination of bacteria by phage and the innate immune system*. *J Theor Biol*, 2017. **429**: p. 241-252.

641. Jean-Pierre, F., et al., *Community composition shapes microbial-specific phenotypes in a cystic fibrosis polymicrobial model system*. eLife, 2023. **12**: p. e81604.
642. Beaudoin, T., et al., *Staphylococcus aureus interaction with Pseudomonas aeruginosa biofilm enhances tobramycin resistance*. npj Biofilms and Microbiomes, 2017. **3**(1): p. 25.
643. Bottery, M.J., et al., *Inter-species interactions alter antibiotic efficacy in bacterial communities*. The ISME Journal, 2022. **16**(3): p. 812-821.
644. O'Brien, T.J., W. Figueroa, and M. Welch, *Decreased efficacy of antimicrobial agents in a polymicrobial environment*. The ISME Journal, 2022. **16**(7): p. 1694-1704.
645. Orazi, G., F. Jean-Pierre, and G.A. O'Toole, *Pseudomonas aeruginosa PA14 Enhances the Efficacy of Norfloxacin against Staphylococcus aureus Newman Biofilms*. J Bacteriol, 2020. **202**(18).
646. Orazi, G. and G.A. O'Toole, *Pseudomonas aeruginosa Alters Staphylococcus aureus Sensitivity to Vancomycin in a Biofilm Model of Cystic Fibrosis Infection*. mBio, 2017. **8**(4).
647. Orazi, G., K.L. Ruoff, and G.A. O'Toole, *Pseudomonas aeruginosa Increases the Sensitivity of Biofilm-Grown Staphylococcus aureus to Membrane-Targeting Antiseptics and Antibiotics*. mBio, 2019. **10**(4).
648. Waters, V.J., et al., *Reconciling Antimicrobial Susceptibility Testing and Clinical Response in Antimicrobial Treatment of Chronic Cystic Fibrosis Lung Infections*. Clinical Infectious Diseases, 2019. **69**(10): p. 1812-1816.
649. Doern, G.V. and S.M. Brecher, *The Clinical Predictive Value (or Lack Thereof) of the Results of In Vitro Antimicrobial Susceptibility Tests*. 2011: J Clin Microbiol. 2011 Sep;49(9 Suppl):S11-4. doi: 10.1128/JCM.00580-11.
650. Matthew, S., et al., *Evolutionary dynamics of phage resistance in bacterial biofilms*. bioRxiv, 2019: p. 552265.
651. Simmons, E.L., et al., *Phage mobility is a core determinant of phage–bacteria coexistence in biofilms*. The ISME Journal, 2018. **12**(2): p. 531-543.
652. Darch, S.E., et al., *Phage Inhibit Pathogen Dissemination by Targeting Bacterial Migrants in a Chronic Infection Model*. mBio, 2017. **8**(2): p. 10.1128/mbio.00240-17.
653. Mitchell, K.F., M.L. Yarbrough, and C.D. Burnham, *More than Just Contaminants: Frequency and Characterization of Polymicrobial Blood Cultures from a Central Clinical Microbiology Laboratory Serving a Large Healthcare System*. J Appl Lab Med, 2021. **6**(6): p. 1433-1440.
654. Zheng, C., et al., *Clinical characteristics and risk factors of polymicrobial Staphylococcus aureus bloodstream infections*. Antimicrobial Resistance & Infection Control, 2020. **9**(1): p. 76.
655. Du, F., et al., *Microbial Infection and Antibiotic Susceptibility of Diabetic Foot Ulcer in China: Literature Review*. Front Endocrinol (Lausanne), 2022. **13**: p. 881659.
656. Gaston Jordan, R., et al., *Polymicrobial Interactions in the Urinary Tract: Is the Enemy of My Enemy My Friend?* Infection and Immunity, 2021. **89**(4): p. 10.1128/iai.00652-20.
657. Hubert, D., et al., *Association between Staphylococcus aureus alone or combined with Pseudomonas aeruginosa and the clinical condition of patients with cystic fibrosis*. Journal of Cystic Fibrosis, 2013. **12**(5): p. 497-503.
658. Fischer, A.J., et al., *Sustained Coinfections with Staphylococcus aureus and Pseudomonas aeruginosa in Cystic Fibrosis*. American Journal of Respiratory and Critical Care Medicine, 2021. **203**(3): p. 328-338.
659. Nir-Paz, R., et al., *Successful Treatment of Antibiotic-resistant, Poly-microbial Bone Infection With Bacteriophages and Antibiotics Combination*. Clinical Infectious Diseases, 2019. **69**(11): p. 2015-2018.
660. Van Nieuwenhuysse, B., et al., *A Case of In Situ Phage Therapy against Staphylococcus aureus in a Bone Allograft Polymicrobial Biofilm Infection: Outcomes and Phage-Antibiotic Interactions*. Viruses, 2021. **13**(10).
661. Young, M.J., et al., *Phage Therapy for Diabetic Foot Infection: A Case Series*. Clinical Therapeutics, 2023. **45**(8): p. 797-801.

662. Gangell, C., et al., *Inflammatory responses to individual microorganisms in the lungs of children with cystic fibrosis*. Clin. Infect. Dis., 2011. **53**(5): p. 425-432.
663. Sagel, S.D., et al., *Impact of Pseudomonas and Staphylococcus infection on inflammation and clinical status in young children with cystic fibrosis*. J Pediatr, 2009. **154**(2): p. 183-8.
664. Junge, S., et al., *Factors Associated with Worse Lung Function in Cystic Fibrosis Patients with Persistent Staphylococcus aureus*. PLoS One, 2016. **11**(11): p. e0166220.
665. Armstrong, D.S., et al., *Lower airway inflammation in infants with cystic fibrosis detected by newborn screening*. Pediatr Pulmonol, 2005. **40**(6): p. 500-10.
666. Ramsey, K.A., et al., *Early respiratory infection Is associated with reduced spirometry in children with cystic fibrosis*. American Journal of Respiratory and Critical Care Medicine, 2014. **190**(10): p. 1111-6.
667. Malhotra, S., D. Hayes, Jr., and D.J. Wozniak, *Mucoid Pseudomonas aeruginosa and regional inflammation in the cystic fibrosis lung*. J Cyst Fibros, 2019. **18**(6): p. 796-803.
668. Cain, A.K., et al., *A decade of advances in transposon-insertion sequencing*. Nature Reviews Genetics, 2020. **21**(9): p. 526-540.
669. McKitterick, A.C. and T.G. Bernhardt, *Phage resistance profiling identifies new genes required for biogenesis and modification of the corynebacterial cell envelope*. eLife, 2022. **11**: p. e79981.
670. Price, M.N., et al., *Mutant phenotypes for thousands of bacterial genes of unknown function*. Nature, 2018. **557**(7706): p. 503-509.
671. Harneet, S.R., et al., *Systematic genome-wide querying of coding and non-coding functional elements in E. coli using CRISPRi*. bioRxiv, 2020: p. 2020.03.04.975888.
672. Mutalik, V.K., et al., *Dual-barcoded shotgun expression library sequencing for high-throughput characterization of functional traits in bacteria*. Nat Commun, 2019. **10**(1): p. 308.
673. Mulrone, K., et al., *Same-day confirmation of infection and antimicrobial susceptibility profiling using flow cytometry*. eBioMedicine, 2022. **82**.
674. Melo, L.D.R., et al., *Phage-Host Interaction Analysis by Flow Cytometry Allows for Rapid and Efficient Screening of Phages*. Antibiotics, 2022. **11**(2): p. 164.
675. Michelsen, O., et al., *Detection of bacteriophage-infected cells of Lactococcus lactis by using flow cytometry*. Appl Environ Microbiol, 2007. **73**(23): p. 7575-81.
676. Mira, P., P. Yeh, and B.G. Hall, *Estimating microbial population data from optical density*. PLoS One, 2022. **17**(10): p. e0276040.
677. Müller, S. and G. Nebe-von-Caron, *Functional single-cell analyses: flow cytometry and cell sorting of microbial populations and communities*. FEMS Microbiology Reviews, 2010. **34**(4): p. 554-587.
678. Tynecki, P., et al., *PhageAI - Bacteriophage Life Cycle Recognition with Machine Learning and Natural Language Processing*. 2020, bioRxiv.
679. Hockenberry, A.J. and C.O. Wilke, *BACPHLIP: predicting bacteriophage lifestyle from conserved protein domains*. PeerJ, 2021. **9**: p. e11396.
680. Boeckaerts, D., et al., *Predicting bacteriophage hosts based on sequences of annotated receptor-binding proteins*. Scientific Reports, 2021. **11**(1): p. 1467.
681. Briers, Y., et al., *Actionable prediction of Klebsiella phage-host specificity at the subspecies level*. 2023.
682. Lood, C., et al., *Digital phagograms: predicting phage infectivity through a multilayer machine learning approach*. Current Opinion in Virology, 2022. **52**: p. 174-181.
683. Meslier, V., et al., *Benchmarking second and third-generation sequencing platforms for microbial metagenomics*. Scientific Data, 2022. **9**(1): p. 694.
684. Ferreira, F.A., et al., *Rapid nanopore-based DNA sequencing protocol of antibiotic-resistant bacteria for use in surveillance and outbreak investigation*. Microb Genom, 2021. **7**(4).
685. Beamud, B., et al., *Genetic determinants of host tropism in Klebsiella phages*. Cell Rep, 2023. **42**(2): p. 112048.

686. Lam, M.M.C., et al., *Kaptive 2.0: updated capsule and lipopolysaccharide locus typing for the Klebsiella pneumoniae species complex*. Microb Genom, 2022. **8**(3).
687. Kung, V.L., E.A. Ozer, and A.R. Hauser, *The accessory genome of Pseudomonas aeruginosa*. Microbiol Mol Biol Rev, 2010. **74**(4): p. 621-41.
688. Tesson, F., et al., *Systematic and quantitative view of the antiviral arsenal of prokaryotes*. Nature Communications, 2022. **13**(1): p. 2561.
689. Matsui, H., et al., *Evidence for Periciliary Liquid Layer Depletion, Not Abnormal Ion Composition, in the Pathogenesis of Cystic Fibrosis Airways Disease*. Cell, 1998. **95**(7): p. 1005-1015.
690. Matsui, H., et al., *A physical linkage between cystic fibrosis airway surface dehydration and Pseudomonas aeruginosa biofilms*. Proceedings of the National Academy of Sciences, 2006. **103**(48): p. 18131-18136.
691. Worlitzsch, D., et al., *Effects of reduced mucus oxygen concentration in airway Pseudomonas infections of cystic fibrosis patients*. J. Clin. Invest., 2002. **109**(3): p. 317-25.
692. Leung, C.M., et al., *A guide to the organ-on-a-chip*. Nature Reviews Methods Primers, 2022. **2**(1): p. 33.
693. Weng, Y.S., et al., *Scaffold-Free Liver-On-A-Chip with Multiscale Organotypic Cultures*. Adv Mater, 2017. **29**(36).
694. Jang, K.J., et al., *Reproducing human and cross-species drug toxicities using a Liver-Chip*. Sci Transl Med, 2019. **11**(517).
695. Ma, C., et al., *On-Chip Construction of Liver Lobule-like Microtissue and Its Application for Adverse Drug Reaction Assay*. Anal Chem, 2016. **88**(3): p. 1719-27.
696. Glieberman, A.L., et al., *Synchronized stimulation and continuous insulin sensing in a microfluidic human Islet on a Chip designed for scalable manufacturing*. Lab Chip, 2019. **19**(18): p. 2993-3010.
697. Shik Mun, K., et al., *Patient-derived pancreas-on-a-chip to model cystic fibrosis-related disorders*. Nat Commun, 2019. **10**(1): p. 3124.
698. Mu, X., et al., *Engineering a 3D vascular network in hydrogel for mimicking a nephron*. Lab Chip, 2013. **13**(8): p. 1612-8.
699. Musah, S., et al., *Mature induced-pluripotent-stem-cell-derived human podocytes reconstitute kidney glomerular-capillary-wall function on a chip*. Nat Biomed Eng, 2017. **1**.
700. Yin, L., et al., *Efficient Drug Screening and Nephrotoxicity Assessment on Co-culture Microfluidic Kidney Chip*. Scientific Reports, 2020. **10**(1): p. 6568.
701. Ahn, S., et al., *Mussel-inspired 3D fiber scaffolds for heart-on-a-chip toxicity studies of engineered nanomaterials*. Anal Bioanal Chem, 2018. **410**(24): p. 6141-6154.
702. Marsano, A., et al., *Beating heart on a chip: a novel microfluidic platform to generate functional 3D cardiac microtissues*. Lab Chip, 2016. **16**(3): p. 599-610.
703. Ugolini, G.S., et al., *Generation of functional cardiac microtissues in a beating heart-on-a-chip*. Methods Cell Biol, 2018. **146**: p. 69-84.
704. Zhang, X., et al., *High-Throughput Assessment of Drug Cardiac Safety Using a High-Speed Impedance Detection Technology-Based Heart-on-a-Chip*. Micromachines (Basel), 2016. **7**(7).
705. Sheehy, S.P., et al., *Toward improved myocardial maturity in an organ-on-chip platform with immature cardiac myocytes*. Exp Biol Med (Maywood), 2017. **242**(17): p. 1643-1656.
706. Shim, K.Y., et al., *Microfluidic gut-on-a-chip with three-dimensional villi structure*. Biomed Microdevices, 2017. **19**(2): p. 37.
707. Pocevicute, R. and R.F. Ismagilov, *Human-gut-microbiome on a chip*. Nat Biomed Eng, 2019. **3**(7): p. 500-501.
708. Guo, Y., et al., *A Biomimetic Human Gut-on-a-Chip for Modeling Drug Metabolism in Intestine*. Artif Organs, 2018. **42**(12): p. 1196-1205.
709. Wevers, N.R., et al., *A perfused human blood-brain barrier on-a-chip for high-throughput assessment of barrier function and antibody transport*. Fluids Barriers CNS, 2018. **15**(1): p. 23.

710. Koo, Y., B.T. Hawkins, and Y. Yun, *Three-dimensional (3D) tetra-culture brain on chip platform for organophosphate toxicity screening*. *Sci Rep*, 2018. **8**(1): p. 2841.
711. Marturano-Kruik, A., et al., *Human bone perivascular niche-on-a-chip for studying metastatic colonization*. *Proc Natl Acad Sci U S A*, 2018. **115**(6): p. 1256-1261.
712. Hao, S., et al., *A Spontaneous 3D Bone-On-a-Chip for Bone Metastasis Study of Breast Cancer Cells*. *Small*, 2018. **14**(12): p. e1702787.
713. Torisawa, Y.S., et al., *Modeling Hematopoiesis and Responses to Radiation Countermeasures in a Bone Marrow-on-a-Chip*. *Tissue Eng Part C Methods*, 2016. **22**(5): p. 509-15.
714. Zamprogno, P., et al., *Second-generation lung-on-a-chip with an array of stretchable alveoli made with a biological membrane*. *Communications Biology*, 2021. **4**(1): p. 168.
715. Pires de Mello, C.P., et al., *Microphysiological heart-liver body-on-a-chip system with a skin mimic for evaluating topical drug delivery*. *Lab Chip*, 2020. **20**(4): p. 749-759.
716. Maschmeyer, I., et al., *A four-organ-chip for interconnected long-term co-culture of human intestine, liver, skin and kidney equivalents*. *Lab Chip*, 2015. **15**(12): p. 2688-99.
717. Ogden, H.L., et al., *Cystic Fibrosis Human Organs-on-a-Chip*. *Micromachines (Basel)*, 2021. **12**(7).
718. Plebani, R., et al., *Modeling pulmonary cystic fibrosis in a human lung airway-on-a-chip*. *Journal of Cystic Fibrosis*, 2022. **21**(4): p. 606-615.
719. Widdicombe, J.H., et al., *Distribution of tracheal and laryngeal mucous glands in some rodents and the rabbit*. *J Anat*, 2001. **198**(Pt 2): p. 207-21.
720. Dreano, E., et al., *Characterization of two rat models of cystic fibrosis-KO and F508del CFTR-Generated by Crispr-Cas9*. *Animal Model Exp Med*, 2019. **2**(4): p. 297-311.
721. Sun, X., et al., *Lung phenotype of juvenile and adult cystic fibrosis transmembrane conductance regulator-knockout ferrets*. *Am J Respir Cell Mol Biol*, 2014. **50**(3): p. 502-12.
722. Sun, X., et al., *Disease phenotype of a ferret CFTR-knockout model of cystic fibrosis*. *J Clin Invest*, 2010. **120**(9): p. 3149-60.
723. Olivier, A.K., et al., *Abnormal endocrine pancreas function at birth in cystic fibrosis ferrets*. *J Clin Invest*, 2012. **122**(10): p. 3755-68.
724. Sun, X., et al., *Gastrointestinal Pathology in Juvenile and Adult CFTR-Knockout Ferrets*. *The American Journal of Pathology*, 2014. **184**(5): p. 1309-1322.
725. Meyerholz, D.K., et al., *Pathology of Gastrointestinal Organs in a Porcine Model of Cystic Fibrosis*. *The American Journal of Pathology*, 2010. **176**(3): p. 1377-1389.
726. Pires, D.P., et al., *Current challenges and future opportunities of phage therapy*. *FEMS Microbiology Reviews*, 2020. **44**(6): p. 684-700.
727. Vázquez, R., et al., *Essential Topics for the Regulatory Consideration of Phages as Clinically Valuable Therapeutic Agents: A Perspective from Spain*. *Microorganisms*, 2022. **10**(4).
728. Petrovic Fabijan, A., et al., *Translating phage therapy into the clinic: Recent accomplishments but continuing challenges*. *PLOS Biology*, 2023. **21**(5): p. e3002119.
729. Pirnay, J.-P., T. Ferry, and G. Resch, *Recent progress toward the implementation of phage therapy in Western medicine*. *FEMS Microbiology Reviews*, 2021. **46**(1).
730. Furfaro, L.L., M.S. Payne, and B.J. Chang, *Bacteriophage Therapy: Clinical Trials and Regulatory Hurdles*. *Frontiers in cellular and infection microbiology*, 2018. **8**: p. 376-376.
731. McCallin, S., et al., *Current State of Compassionate Phage Therapy*. *Viruses*, 2019. **11**(4).
732. Naureen, Z., et al., *Comparison between American and European legislation in the therapeutical and alimentary bacteriophage usage*. *Acta Biomed*, 2020. **91**(13-s): p. e2020023.
733. Jones, J.D., et al., *The Future of Clinical Phage Therapy in the United Kingdom*. *Viruses*, 2023. **15**(3).
734. Maxted, W.R., *The active agent in nascent phage lysis of streptococci*. *J Gen Microbiol*, 1957. **16**(3): p. 584-95.

735. Nelson, D., L. Loomis, and V.A. Fischetti, *Prevention and elimination of upper respiratory colonization of mice by group A streptococci by using a bacteriophage lytic enzyme*. Proc Natl Acad Sci U S A, 2001. **98**(7): p. 4107-12.
736. Young, R., *Bacteriophage lysis: mechanism and regulation*. Microbiol Rev, 1992. **56**(3): p. 430-81.
737. Jun, S.Y., et al., *Pharmacokinetics and Tolerance of the Phage Endolysin-Based Candidate Drug SAL200 after a Single Intravenous Administration among Healthy Volunteers*. Antimicrob Agents Chemother, 2017. **61**(6).
738. Jun, S.Y., et al., *Pharmacokinetics of the phage endolysin-based candidate drug SAL200 in monkeys and its appropriate intravenous dosing period*. Clin Exp Pharmacol Physiol, 2016. **43**(10): p. 1013-6.
739. Jun, S.Y., et al., *Preclinical safety evaluation of intravenously administered SAL200 containing the recombinant phage endolysin SAL-1 as a pharmaceutical ingredient*. Antimicrob Agents Chemother, 2014. **58**(4): p. 2084-8.
740. Zhang, L., et al., *LysGH15 kills Staphylococcus aureus without being affected by the humoral immune response or inducing inflammation*. Scientific Reports, 2016. **6**(1): p. 29344.
741. Loeffler, J.M., S. Djurkovic, and V.A. Fischetti, *Phage lytic enzyme Cpl-1 as a novel antimicrobial for pneumococcal bacteremia*. Infect Immun, 2003. **71**(11): p. 6199-204.
742. Wang, F., et al. *TSPphg Lysin from the Extremophilic Thermus Bacteriophage TSP4 as a Potential Antimicrobial Agent against Both Gram-Negative and Gram-Positive Pathogenic Bacteria*. Viruses, 2020. **12**, DOI: 10.3390/v12020192.
743. Yuan, Y., et al., *The endolysin of the Acinetobacter baumannii phage vB_AbaP_D2 shows broad antibacterial activity*. Microbial Biotechnology, 2021. **14**(2): p. 403-418.
744. Guo, M., et al., *A Novel Antimicrobial Endolysin, LysPA26, against Pseudomonas aeruginosa*. Frontiers in Microbiology, 2017. **8**.
745. Antonova, N.P., et al., *Broad Bactericidal Activity of the Myoviridae Bacteriophage Lysins LysAm24, LysECD7, and LysSi3 against Gram-Negative ESKAPE Pathogens*. Viruses, 2019. **11**(3).
746. Kim, S., et al., *Antimicrobial activity of LysSS, a novel phage endolysin, against Acinetobacter baumannii and Pseudomonas aeruginosa*. J Glob Antimicrob Resist, 2020. **22**: p. 32-39.
747. Lim, J., et al., *Bactericidal Effect of Cecropin A Fused Endolysin on Drug-Resistant Gram-Negative Pathogens*. Journal of Microbiology and Biotechnology, 2022. **32**(6): p. 816-823.
748. Khan, F.M., et al., *A Novel Acinetobacter baumannii Bacteriophage Endolysin LysAB54 With High Antibacterial Activity Against Multiple Gram-Negative Microbes*. Front Cell Infect Microbiol, 2021. **11**: p. 637313.
749. Abdelkader, K., et al., *The Preclinical and Clinical Progress of Bacteriophages and Their Lytic Enzymes: The Parts are Easier than the Whole*. Viruses, 2019. **11**(2).
750. Cassino, C., et al. *Results of the first in human study of lysin CF-301 evaluating the safety, tolerability and pharmacokinetic profile in healthy volunteers*. in *Proceedings of the 26th European Congress of Clinical Microbiology and Infectious Diseases, Amsterdam, The Netherlands*. 2016.
751. Jandourek, A., et al., *Long term immunology results of a phase 1 placebo controlled dose escalating study to examine the safety of CF-301 in human volunteers*. Proceedings of the 27th ECCMID, Vienna, Austria, 2017: p. 22-25.
752. Jandourek, A., et al., *Inflammatory markers in a phase 1 placebo controlled dose escalating study of intravenous doses of CF-301 in human subjects*. Proceedings of the ASM Microbe, New Orleans, LA, USA, 2017. **2**.
753. Ghahramani, P., et al., *Population pharmacokinetic-pharmacodynamic assessment of cardiac safety endpoints for CF-301, a first-in-class antibacterial lysin*. Proceedings of the ASM Microbe, New Orleans, LA, USA, 2017. **3**.
754. Rotolo, J.A., et al., *PK-PD driver of efficacy for CF-301, a novel anti-staphylococcal lysin: Implications for human target dose*. Proceedings of the ASM Microbe, Boston, MA, USA, 2016: p. 16-20.

755. Totté, J., et al., *Targeted anti-staphylococcal therapy with endolysins in atopic dermatitis and the effect on steroid use, disease severity and the microbiome: study protocol for a randomized controlled trial (MAAS trial)*. *Trials*, 2017. **18**(1): p. 404.
756. Gutiérrez, D. and Y. Briers, *Lysins breaking down the walls of Gram-negative bacteria, no longer a no-go*. *Current Opinion in Biotechnology*, 2021. **68**: p. 15-22.
757. Wu, M., et al., *A Novel Phage PD-6A3, and Its Endolysin Ply6A3, With Extended Lytic Activity Against Acinetobacter baumannii*. *Frontiers in Microbiology*, 2019. **9**.
758. Chu, J.J.K., et al., *Novel Phage Lysin Abp013 against Acinetobacter baumannii*. *Antibiotics (Basel)*, 2022. **11**(2).
759. Grishin, A.V., et al., *Resistance to peptidoglycan-degrading enzymes*. *Critical Reviews in Microbiology*, 2020. **46**(6): p. 703-726.
760. Briers, Y., et al., *Engineered endolysin-based "Artilysins" to combat multidrug-resistant gram-negative pathogens*. *mBio*, 2014. **5**(4): p. e01379-14.
761. Gerstmans, H., et al., *A VersaTile-driven platform for rapid hit-to-lead development of engineered lysins*. *Science Advances*, 2020. **6**(23): p. eaaz1136.
762. Abdelrahman, F., et al., *Phage-Encoded Endolysins*. *Antibiotics (Basel)*, 2021. **10**(2).